JULIANA ALMEIDA BARROS DA SILVA

Regulação da biossíntese da vitamina E em tomateiro (*Solanum lycopersicum* L.): da diversidade natural à manipulação do metabolismo

Tese apresentada ao Instituto de Biociências da Universidade de São Paulo para a obtenção de Título de Doutor em Ciências, na área de Botânica.

Orientadora: Profa. Dra. Maria Magdalena Rossi
Laboratório de Genética Molecular de Plantas

São Paulo
2015

FICHA CATALOGRÁFICA

Almeida, Juliana

Regulação da biossíntese da vitamina E em tomateiro (*Solanum lycopersicum* L.): da diversidade natural à manipulação do metabolismo

247 p

Tese (Doutorado) - Instituto de Biociências da Universidade de São Paulo. Departamento de Botânica.

1. Tomate 2. *Solanum lycopersicum* 3. Tocoferol 4. Vitamina E 5. Clorofila 6. Fitol 7. Metabolismo.

Universidade de São Paulo. Instituto de Biociências. Departamento de Botânica.

COMISSÃO JULGADORA

_____ _____

Prof (a). Dr (a). Prof (a). Dr (a).

_____ _____

Prof (a). Dr (a). Prof (a). Dr (a).

_____

Profa. Dra. Maria Magdalena Rossi
Orientadora

Aos meus pais, Manoel e Cida,
dedico

"[...] quem elegeu a busca não pode recusar a travessia."

Alfredo Bosi

Céu, inferno
(análise de Primeiras Estórias de Guimarães Rosa)

AGRADECIMENTOS

Tomo a oportunidade da gratidão para expressar a satisfação por finalizar esta etapa. Assim registro meus agradecimentos:

Ao Departamento de Botânica do Instituto de Biociências da Universidade de São Paulo pelo suporte acadêmico e estrutural.

À FAPESP pelas bolsas concedidas no país e no exterior. Ao Programa EU-SOL pelo auxílio financeiro para estágio internacional.

À Magdalena Rossi por confiar-me tal trabalho; pela possibilidade das escolhas de ir e vir e, fundamentalmente, por suportá-las. Pela contínua intercessão de ideias; pela sua generosa e presente orientação ao longo desses anos. Pela amizade e incentivo. Por todos ensinamentos que contribuíram tanto para minha formação humana quanto científica.

Ao Fernando Carrari pelas valiosas contribuições metodológicas e conceituais que enriqueceram esse trabalho; pelas intervenções perspicazes na elaboração dos artigos; pela oportunidade de colaboração em parcerias tão frutíferas. Ao Leandro Quadrana, pela parceria, inquietude e boas discussões; pela introdução às ferramentas estatísticas e ao VIGS. A Luisa Bermudez pela cooperação e acolhimento.

Ao Rámon Asis pelos ensinamentos sobre química analítica, pela colaboração e prontidão nas análises bioquímicas; pelo recebimento. À Andrea Carranza pelo "otro par de manos" para os ensaios de atividade antioxidante. À Romina pelo auxílio nas análises em HPLC.

Ao Lázaro Peres pelo suporte para obtenção das linhagens transgênicas RNAi; pelas proveitosas contribuições que acrescentaram a esta tese as análises de mutantes de amadurecimento e senescência; pela infraestrutura para seleção e retrocruza dos mutantes TILLING. Por abrir gentilmente às portas de seu grupo de pesquisa. À Mariana Azevedo e ao Ivan Sestari pela parceria mais do que fundamental.

Ao Christophe Rothan pela colaboração para obtenção de mutantes EMS; pelo suporte para a realização do estágio no INRA-Bordeaux; pela cuidadosa revisão do manuscrito vte5. A Cecile Brès e Jean-Philippe Mauxion por introduzir-me à técnica do TILLING.

Ao Stefan Hörtensteiner pelo oportuno auxílio na quantificação de clorofila; pela supervisão de estágio na UZH; pela solicitude. Pelas contribuições valiosas para discussão dos resultados; pela leitura generosa e competente. À Luzia Guyer pelos ensinamentos na preparação e análise das amostras; pela sua inestimável ajuda em Zürich.

Ao Félix Kessler pela colaboração nas análises lipidômicas; pelas boas ideias e seu entusiasmo pelo tema. Ao Gáetan Glauser pela parceria nas análises UHPLC. À Livia Spicher pela ajuda na preparação das amostras e análise dos resultados; pelo envolvimento e todo suporte em Neuchâtel.

Ao Peter Dörmann pela oportunidade de colaboração nas análises de lipídeos. À Katharina vom Dorp pela cuidadosa análise das amostras.

À Eny Floh, ao Luciano Freschi, ao Marcos Buckeridge e à Marie Anne van Sluys pelo provimento de infraestrutura e de equipamentos para realização de experimentos no IBUSP.

Aos colegas do laboratório de Genética de Molecular Plantas: Andy, Bruno Lira, Daniele, Fabiana, Gabriela, Junia, Leandro Salles e Silvia, parceiros em tantos sítios. Obrigada pelos anos de convivência que muito contribuiram para minha formação. À Fabi pelos ensinamentos de qPCR; pelo auxílio com as clonagens e por tudo mais. À Silvia, pela ajuda técnica indispensável.

Aos colegas do laboratório de Biologia Celular: Amanda Macedo, André, Augusto Tomba, Bruno Navarro, Caroline, Fernanda, Igor, Leandro, Paula e Roberta Martins. Pela prestativa ajuda e boas conversas para além de tomate.

A todos do laboratório de Controle Hormonal do Desenvolvimento Vegetal (ESALQ) pela convivência, ajuda e descontração: Ariadne, Cássia, Eloísa, Frederico, Guilherme, João Pedro, Jonata, Lucas, Marcela, Maísa, Matheus e Stevan.

À Adriana, Eglee, Eveline e Viviane do laboratório de Fisiologia Ecológica de Plantas (LAFIECO) pelo convívio, auxílio nas análises laboratoriais (nitrogênio!) e trâmites internacionais. À Amanda de Souza pela maratona de medidas de fotossíntese; pela valiosa ajuda nas quantificações de açúcares e discussão dos resultados.

A Julien, Kentaro e Natsuko do INRA-Bordeaux, pela convivência e ajuda. Às queridas colegas de La Rouquette: Julia, Ilinka, Carolina, Elizabeth, Fah, Tamara e Regiane pelo convívio aconchegante; por compartir tantas boas experiências de suas culturas.

A Celine, Cyrille, Monica, Veronique do Laboratoire de Physiologie Végétale, pelo acolhimento e suporte durante a estadia em Neuchâtel. Aos colegas Deneb, Manu e Alaleh pela boa vizinhança no Jardin Botanique; pela generosa ajuda com o cotidiano franco-suíço.

A Aditi, Noemi, Song, Kathrin do grupo Molecular Plant Physiology UZH, pela solicitude; pelo interesse sincero na cultura brasileira.

Aos colegas do GaTE, Érika, Kleber e Mayra, pela ajuda oportuna; à Tatiana Côrrea pela presteza costumeira; pelo suporte de reagentes/protocolos, equipamentos e pelos incontáveis cafés.

Ao André Nakasato do LAM pelo suporte no sequenciamento.

Ao Homelhan pela solicitude; por tanto me ajudar com a manutenção das plantas.

Ao Waldir (IBUSP) e Mário (CEFAP) pelo suporte na obtenção das imagens de microscopia confocal.

À Carol, Mari e Sil, novamente, por ir além do razoável. Tanto e tanto.

Aos meus pais, Manoel e Cida, por todo apoio e torcida reconfortante; às minhas irmãs, Andréia e Nadia. Ao Miguel pela animação com os tomates.

Ao Bruno, por ser e estar, sempre.

"A felicidade aparece para aqueles que choram, para aqueles que se machucam, para aqueles que buscam e tentam sempre. E para aqueles que reconhecem a importância das pessoas que passam por suas vidas"

Clarice Lispector

ABREVIATURAS E NEOLOGISMOS

aa – aminoácidos
BLAST – ferramenta básica de busca de alinhamentos locais (do inglês *Basic Local Alignment Search Tool*)
bp – pares de bases (o mesmo que pb)
cDNA – DNA complementar
cM – centimorgan
Ct – ciclo limiar (do inglês *treshold cycle*)
DEPC – dietilpirocarbonato
DNA – ácido desoxirribonucléico
DNAse – desoxirribonuclease
dNTP – desorribonucleotídeos trifosfatado
EDTA – ácido etilenodiamonotetracético
GFP – proteína fluorescente verde (do inglês *Green Fluorescent Protein*)
GOI – gene de interesse (do inglês *Gene of Interest*)
IL – linhagens introgredidas (do inglês *introgressed line*)
Kb – kilo pares de base
LB – meio de crescimento Luria-Bertani
Mb – mega pares de bases
MES – ácido 2-morfolinoetanosulfónico monohidratado
NADP – nicotinamida adenina dinucleotídeo fosfato
NADPH - nicotinamida adenina dinucleótido fosfato reduzido
nt – nucleotídeos
PCR – reação em cadeia da polimerasa (do inglês *Polymerase Chain Reaction*)
ppm - partes por milhão
qPCR - reação em cadeia da polimerasa quantitativa (do inglês *Quantitative Polymerase Chain Reaction*)
QTL – *locus* para caráter quantitativo (do inglês *Quantitative Trait Locus*)
RNA – ácido ribonucléico
RNAi – RNA de interferência
RNAm – RNA mensageiro
rpm – revoluções por minuto
SGN – *Solanaceae Genome Network*
unigene – consenso de sequências de cDNA segundo a Solanaceae Genomics Network
U.V. - ultravioleta
5´UTR – região 5´ não traduzida do RNAm
3´UTR – região 3´ não traduzida do RNAm

SUMÁRIO

RESUMO 15
ABSTRACT 17
INTRODUÇÃO GERAL 19
1. A vitamina E: estrutura e importância nutricional 19
2. A biossíntese de tocoferol 21
3. A importância do tocoferol para o organismo vegetal 22
4. Melhoramento das espécies cultivadas: a exploração da diversidade natural e manipulação genética 24
5. O tomateiro: modelo de estudo com importância agronômica 27
6. A regulação da vitamina E em tomateiro: antecedentes e construção das hipóteses de trabalho 31
7. Referências bibliográficas 35
OBJETIVOS 43
CAPÍTULO I. ESTUDO DA REGULAÇÃO TRANSCRICIONAL DA ROTA BIOSSINTÉTICA DE TOCOFERÓIS EM TOMATEIRO 45
CAPÍTULO II. ANÁLISE DO PERFIL TRANSCRICIONAL DOS GENES ASSOCIADOS À BIOSSÍNTESE DE VITAMINA E EM LINHAGENS INTROGREDIDAS (IL) QUE APRESENTAM AUMENTO NO CONTEÚDO DE TOCOFERÓIS 65
1. Introdução 65
2. Objetivos específicos 68
3. Material e métodos 69
3.1. Material vegetal 69
3.2. Análise da expressão gênica 69
3.2.1. Extração de RNA total e síntese de cDNA 69
3.2.2. PCR quantitativa em tempo real (qPCR) 70
4. Resultados e discussão 72
4.1. Perfil transcricional das IL6-1 e 6-2 72
4.2. Perfil transcricional das IL9-2 e 9-2-6 74
4.3. Perfil da IL9-1 76
5. Conclusão 81
6. Referências bibliográficas 82
CAPÍTULO III. ESTUDO DO EFEITO DOS GENES *CLOROFILASE1, FARNESOL QUINASE* E *FITOL QUINASE* NA BIOSSÍNTESE DE TOCOFERÓIS EM FRUTOS DE TOMATE VIA SILENCIAMENTO GÊNICO POR INDUZIDO VÍRUS 85
1. Introdução 85
2. Objetivos específicos 87

3. Material e métodos 88
3.1. Material vegetal 88
3.2. Cepas bacterianas e vetores 88
3.2.1. *Escherichia coli* 88
3.2.2. *Agrobacterium tumefaciens* 89
3.2.3. Plasmídeos 89
3.3. Extração de RNA total e síntese de cDNA 90
3.4. Construção dos vetores de VIGS 91
3.4.1. Clonagem do fragmento do gene de interesse (*GOI*) para VIGS 91
3.4.2. Clonagem do fragmento *GFP-GOI* 92
3.4.3. Obtenção da construção pTRV2*GFP-GOI* 92
3.4.4. Transformação de *A. tumefaciens* e seleção de clones pTRV2*GFP-GOI* 93
3.4.5. Agroinfiltração de botões florais e de folhas com TRV 93
3.5. Análise da expressão gênica 94
3.6. Quantificação do conteúdo de tocoferóis por cromatografia líquida de alta eficiência (HPLC) 94
3.6.1. Preparação dos extratos 94
3.6.2. Determinação por HPLC 94
3.7. Quantificação de clorofila 95
4. Resultados 96
5. Discussão 101
6. Conclusão 103
7. Referências Bibliográficas 104
CAPÍTULO IV. AVALIAÇÃO DO CONTEÚDO DE TOCOFERÓIS EM MUTANTES DE TOMATEIRO DEFICIENTES NO AMADURECIMENTO DE FRUTO, NA SENESCÊNCIA E NA PERCEPÇÃO DE ÁCIDO JASMÔNICO 107
CAPÍTULO V. CARACTERIZAÇÃO FUNCIONAL DO GENE *CLOROFILASE1* EM TOMATEIRO 121
1. Introdução 121
2. Objetivos específicos 124
3. Material e métodos 125
3.1. Material vegetal 125
3.2. Cepas bacterianas e vetores 125
3.2.1. *Escherichia coli* 125
3.2.2. *Agrobacterium tumefaciens* 125

3.2.3. Plasmídeos 126
3.3. Extração de RNA total e síntese de cDNA 126
3.4. Obtenção da construção para estudo da localização subcelular da proteína SlCLH(1) 126
3.5. Transformação transiente de folhas de *Nicotiana benthamiana* por agroinfiltração 127
3.6. Construção dos vetores para silenciamento gênico por RNAi 128
3.7. Transformação genética estável 128
3.8. Verificação da presença do transgene 129
3.9. Análise de expressão gênica nas linhagens RNAi transgênicas 129
3.10. Caracterização fenotípica das linhagens *SlCLH(1)*-RNAi transgênicas 130
3.10.1. Quantificação de prenilipídeos por cromatografia líquida de ultra eficiência acoplada à espectrometria de massas 130
3.10.2. Clorofila e carotenóides 130
3.10.3. Quantificação de açúcares solúveis e amido 131
3.10.4. Parâmetros de fluorescência e trocas gasosas 132
4. Resultados 133
4.1. Verificação da localização subcelular 133
4.2. Obtenção de linhagens transgênicas estáveis silenciadas para *CLH(1)* 134
4.3. Caracterização fenotípica de plantas de tomateiro silenciadas para *CLH(1)* 135
4.3.1. Quantificação de clorofila e catabólitos verdes 136
4.3.2. Conteúdo de tocoferol 137
4.3.3. Perfil de prenilipídeos 138
4.3.4. Parâmetros fotossintéticos e determinação dos carboidratos foliares 138
4.3.5. Perfil de expressão 141
5. Discussão 143
6. Conclusão 145
7. Referências Bibliográficas 146
CAPÍTULO VI. CARACTERIZAÇÃO FUNCIONAL DO GENE *FITOL QUINASE* EM TOMATEIRO 149
CONSIDERAÇÕES FINAIS 201
Referências bibliográficas 205
ARTIGOS PUBLICADOS 206
ANEXO I 207
ANEXO II 223
ANEXO III 237
ANEXO IV 241

RESUMO

Tocoferóis, compostos com atividade de vitamina E (VTE), são antioxidantes lipofílicos sintetizados exclusivamente por organismos fotossintetizantes. A produção desses compostos ocorre a partir da ligação de um grupo cromanol a uma cadeia isoprênica, esta originada a partir de duas vias metabólicas possíveis: pela síntese *de novo* ou pela ativação do fitol liberado durante a quebra da clorofila, esta dependente de fitol quinase (VTE5). Conhecer os mecanismos responsáveis pela síntese e pelo acúmulo de vitamina VTE em plantas cultivadas é de grande interesse devido sua importância para a fisiologia vegetal e para a saúde humana. Frutos de tomate e seus derivados constituem fonte significativa de VTE na dieta humana. Para além da importância nutricional, o tomateiro emerge como um interessante modelo de estudo dos mecanismos regulatórios subjacentes à biossíntese de tocoferóis, visto que seu fruto combina uma ativa síntese *de novo* de isoprenóides juntamente com a degradação de clorofila durante o amadurecimento. Em estudo anterior, *loci* para caracteres quantitativos (QTL) para tocoferol em frutos foram identificados a partir da determinação dos níveis das isoformas α, β, μ e δ em uma população de linhagens introgredidas (ILs) de *Solanum pennellii*. Genes candidatos dentro dos intervalos dos QTL foram propostos, incluindo alguns relacionados à defitilação da clorofila e ao metabolismo fitol, *CLOROFILASE* (*CLH*) e um homólogo à *VTE5*, nomeado *FARNESOL QUINASE* (*FOLK*). Nesse contexto, o presente trabalho apresenta contribuições para o entendimento da regulação da biossíntese de VTE em tomateiro. Para tanto, adotaram-se diferentes abordagens, as quais incluem: a caracterização inicial da regulação transcricional dos genes envolvidos na biossíntese de tocoferóis ao longo do desenvolvimento de tomateiro; a exploração dos determinantes genéticos envolvidos no QTL para tocoferol a partir da análise do perfil transcricional de ILs; a análise integrada das mudanças do metabolismo de tocoferóis e outros isoprenóides em mutantes de tomateiro deficientes no amadurecimento e na degradação de clorofila; e, por fim, o estudo detalhado do metabolismo do fitol por meio da caracterização funcional dos genes codificantes para VTE5, *FOLK* e *CLH(1)*. Os resultados obtidos fornecem valiosas informações sobre os mecanismos que controlam o acúmulo de VTE, além de expor inúmeras conexões entre o metabolismo de tocoferol e outras vias metabólicas que, em última análise, impactam a fisiologia de tomateiro.

ABSTRACT

Tocopherols, compounds with vitamin E activity, are lipid-soluble antioxidants exclusively synthesized by photosynthetic organisms. The formation of tocopherol involves the condensation of a chromanol group with an isoprenoid chain, derived from two possible metabolic pathways: from the *de novo* biosynthesis or from chlorophyll phytol tail recycling, which depends on phytol kinase (VTE5) activity. Understanding the mechanisms underlying synthesis and accumulation of vitamin E in crops is of great interest because of its implications for plant physiology and human health. Tomato fruit and its derivatives constitute a significant dietary source of VTE for humans. Beyond the nutritional value, tomato emerges as an interesting study model of the regulatory mechanisms underlying tocopherol biosynthesis, since fruit couples an active *de novo* synthesis of isoprenoids together with chlorophyll degradation along ripening. In a previous work, quantitative trait *loci* (QTL) for VTE content were identified in ripe fruits by tocopherol determination of α, β, μ e δ isoform levels in a population of *Solanum pennellii* introgression lines (IL). Candidate genes within QTL intervals were proposed, including some related to chlorophyll dephytylation and phytol metabolism, a *CHLOROPHYLLASE* (CLH) and a *VTE5* homolog, named *FARNESOL KINASE* (*FOLK*). In this context, this work presents contributions to understanding the regulation of VTE biosynthesis in tomato. For this, different approachs were taken including: an initial characterization of transcriptional regulation of the genes involved in tocopherol biosynthesis along tomato development; the exploitation of genetic determinants involved in QTL for tocopherol from the transcriptional profile analyses of ILs; the integrated analyses of tocopherols metabolism changes and other isoprenoids in ripening impaired and chlorophyll degraded tomato mutants; and, finally, the detailed study of phytol metabolism by means of functional characterization of the genes encoding for *VTE5*, *FOLK* and *CLH(1).* Our results provide valuable insights into the mechanisms that control the VTE accumulation and also expose several cross-talks between the tocopherol metabolism and other metabolic pathways that, ultimately, impact on tomato physiology.

INTRODUÇÃO GERAL

1. A vitamina E: estrutura e importância nutricional

A evolução dos processos metabólicos aeróbios, tais como a respiração e a fotossíntese, promoveu inevitavelmente a produção de espécies reativas de oxigênio (ROS) em mitocôndrias, cloroplastos e peroxissomos. Ânions superóxidos ($O2^{\bullet-}$), radicais lipídicos peroxil ($ROO^{\bullet}$), peróxido de hidrogênio (H_2O_2), radicais hidroxil ($OH^{\bullet}$), oxigênio singleto ($^1O_2$) são continuamente produzidos durante o metabolismo aeróbico dos organismos. Embora atuem como sinalizadores em diversos processos celulares, o desequilíbrio na produção de ROS é capaz de causar danos oxidativos significativos às proteínas, ao DNA e aos lipídeos. A detoxificação de ROS é feita por uma rede antioxidante dinâmica, interconectada e redundante, que inclui mecanismos enzimáticos – superóxido dismutase, ascobarto peroxidase, glutationa peroxidase, catalase – e não-enzimáticos – ascorbato (VTC), glutationa, flavonóides, carotenóides e tococromanóis (VTE) (Apel & Hirt, 2004).

O termo VTE abrange uma classe de compostos lipossolúveis antioxidantes, tocoferóis e tocotrienóis, fundamentais para saúde humana, e coletivamente conhecidos como tococromanóis (Kamal-Eldin & Appelqvist, 1996; DellaPenna & Pogson, 2006). O valor nutricional desses compostos em animais foi descoberto há mais de um século, descrito inicialmente como fator da dieta importante para a reprodução animal (Evans & Bishop, 1922). Exclusivamente sintetizados por organismos fotossintetizantes, tocoferóis e tocotrienóis podem ocorrer naturalmente como quatro espécies diferencialmente metiladas (α, β, γ e δ) (Grusak & DellaPenna, 1999). O prefixo grego refere-se ao grau de metilação do grupo aromático; enquanto α-tocoferol e α-tocotrienol representam os tococromanóis com maior número de metilações, as respectivas formas δ são aquelas com menor grau. Tocoferóis, mais abundante em plantas, têm cadeia lateral saturada derivada do fitil-difosfato, enquanto tocotrienóis, abundantes nas sementes de monocotiledôneas, possuem cauda insaturada derivada do geranilgeranil difosfato (Figura 1). Embora todos análogos apresentem atividade antioxidante *in vitro*, α-tocoferol é a forma biológica mais ativa, em parte, devido a sua retenção seletiva no corpo humano pela proteína transportadora de α-tocoferol (α-TTP) (Traber & Sies, 1996; Ricciarelli *et al.*, 2001).

Como para todos os nutrientes essenciais, níveis mínimos de VTE são necessários na dieta humana. A deficiência clínica de VTE é rara e resulta em anemia hemolítica em bebês prematuros e alterações neurológicas diversas, incluindo a ataxia (impedimento no balanço e coordenação) e miopatia (fraqueza muscular). A baixa ingestão de VTE tem sido associada com aumento do risco a doenças vasculares, alguns tipos de câncer, além da diminuição da função imunológica (Kushi *et al.*, 1996; Wright *et al.*, 2006). Por sua vez, os estudos utilizando suplementação terapêutica têm

produzido efeitos ainda inconclusivos em virtude das inúmeras variáveis envolvidas como a diferença na biodisponibilidade, no transporte por proteínas específicas e no metabolismo das isoformas de VTE (Cardenas & Gosh, 2014). Na criação de gado, a suplementação da dieta com VTE tem grande importância para a indústria alimentar, pois melhora a qualidade e prolonga o tempo de prateleira da carne (Sander *et al.*, 1997). Além disso, a vida de prateleira de óleos vegetais e alimentos ricos em lipídeos também é influenciada pelo conteúdo e pela composição de tococromanóis (Kamal-Eldin & Appelqvist, 1996).

Os óleos de sementes constituem a principal fonte de VTE da dieta humana, porém, nestes alimentos α-tocoferol está presente com frequência como espécie minoritária. Por outro lado, tecidos fotossintéticos de hortaliças e frutos, por exemplo, brócolis, espinafre e tomate, apresentam altos teores de α-tocoferol. Em estudo comparativo, Chun *et al.* (2006) reportou valores de α-tocoferol que variam de 0,53 a 4,66 mg/100 g de peso comestível no tomate *in natura* e seus produtos derivados (pasta em conserva), respectivamente. O índice recomendado de ingestão diária é de 15 mg/dia da isoforma α pura ou 22.4 IU (*National Institute of Health*, http://ods.od.nih.gov/factsheets/list-all/VitaminE/).

Grande parte das propriedades benéficas de tocoferóis como VTE é atribuída a sua função como antioxidante, baseada na habilidade desses compostos em sequestrar (*scavenging*) radicais peroxil, prevenindo a propagação da peroxidação de ácidos graxos poliinsaturados que compõem as membranas celulares (Serbinova *et al.*, 1991; Traber & Atkinson, 2008). Um segundo mecanismo de proteção observado em tocoferóis é a capacidade de eliminar (*quenching*) oxigênio singleto ($^1O_2$) (Kaiser *et al.*, 1990; Di Mascio *et al.*, 1990; Fukuzawa *et al.*, 1997), função que tem relevância na manutenção do aparato fotossintético em plantas (Krieger-Liszkay & Trebst, 2006; Triantaphylidès & Havaux, 2009).

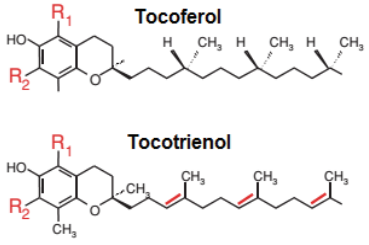

Atividade versus α-tocoferol

Tococromanol	R_1	R_2	ligação com α-TPP	Atividade vitamina E
α-tocopherol	CH_3	CH_3	100	100
α-tocotrienol	CH_3	CH_3	12.5	21-50
β-tocopherol	CH_3	H	38	25-50
β-tocotrienol	CH_3	H	nd	nm
γ-tocopherol	H	CH_3	9	8-19
γ-tocotrienol	H	CH_3	nd	nm
δ-tocopherol	H	H	1.5	<3
δ-tocotrienol	H	H	nd	nm

Figura 1: Estrutura química dos tococromanóis e atividade de VTE. A tabela indica (i) o número e posição do radical metil no anel em α, β, γ e δ- tocoferol e tocotrienol (R1 e R2), (ii) a ligação de cada tococromanol à proteína transportadora de α-tocoferol humana (α-TTP), (iii) a atividade VTE de acordo com o ensaio de gestação-reabsorção em ratos, expresso como porcentagem relativa ao α-tocoferol (100%). Em vermelho, as diferenças estruturais. nm: não mensurável. Adaptado de Dellapenna & Pogson (2006)

2. A biossíntese de tocoferol

A síntese de tocoferol ocorre somente em organismos fotossintetizantes e produz as moléculas anfipáticas compostas por um anel hidroxicromanol, derivado do homogentisato, e uma cadeia prenílica, produtos da via do chiquimato (SK) e metil-eritritrol-fosfato (MEP), respectivamente (Munné-Bosch & Alegre, 2002). A condensação de ambos precursores inicia as reações que compõem a rota central da VTE, na qual as seguintes enzimas estão envolvidas: homogentisato fitil transferase (VTE2), dimetil-fitil-quinol metil transferase (VTE3), γ-tocoferol metiltransferase (VTE4), tocoferol ciclase (VTE1), além da fitol quinase (VTE5) (Dellapenna & Last, 2006). Após a ligação do fitil difosfato ao homogentisato pela VTE2 e posterior metilação, catalisada pela VTE3, o intermediário formado - 2,3-dimetil-5-fitil-1,4-hidroquinol (DMPQ) - é convertido em γ-tocoferol pela VTE1. O α-tocoferol é então produzido pela ação da VTE4. Para produção do fitil difosfato, além da síntese *de novo*, existe uma via alternativa dependente da fitol quinase (VTE5), que fosforila o fitol liberado durante a degradação da clorofila para incorporação subsequente na síntese de tocoferóis (Valentin *et al.*, 2006; Ischebeck *et al.*, 2006) (Figura 2A).

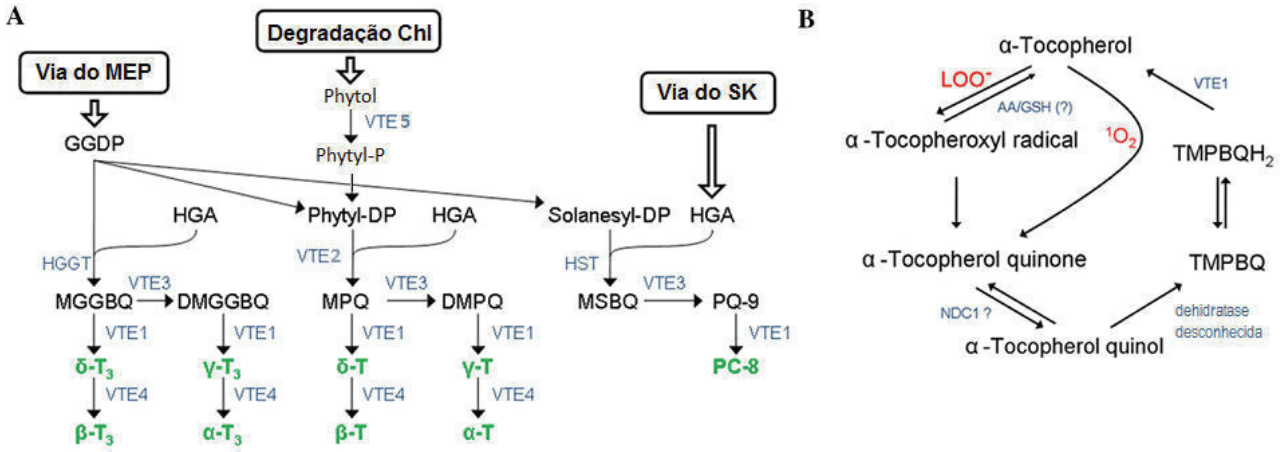

Figura 2. Visão geral da biossíntese de tococromanóis em plantas e do ciclo de oxidação e reciclagem de α-tocoferol. (A) Biossíntese. T, tocoferol; T_3, tocotrienol; PC-8, plastocromanol-8; PQ-9, plastoquinona-9; MPQ, 2-methyl-6-fitil-1,4-hidroquinol; DMPQ, 2,3-dimetil-5-fitil-1,4-benzoquinol; MGGBQ, 2-metil-6-geranilgeranil benzoquinol; DMGGBQ, 2,3-dimetil-6-geranilgeranil benzoquinol; MSBQ, 2-metil-6-solanesil-1,4-benzoquinol; DMSBQ, 2,3-dimetil-6-solanesil-1,4-benzoquinol; HST, homogentisato solanesil transferase; GGDP, geranilgeranil difosfato; HGA, homogentisato; Chl, clorofila; MEP, metil eritritol fosfato; SK, chiquimato. (B) Ciclo de oxidação e reciclagem de α-tocoferol. AA/GSH, ciclo do ascorbato/glutationa; NDC1, oxiredutase de quinona dependente de NAD(P)Hase; TMPBQ, 2,3,5-trimetil-6-fitil-1,4-benzoquinona; TMPBQH2, 2,3,5-trimetil-6-fitil-1,4-benzoquinol. Além do sequestro de radicais peroxil lipídicos (LOO·) e oxigênio singleto ($^1O_2$); tocoferol pode fisicamente desativar $^1O_2$ na membrana dos tilacóides (não representado). ?: denota possíveis fatores envolvidos na conversão representada. Adaptado de Miret & Munne-Bosch (2015).

VTE1, VTE3 e VTE4 são igualmente responsáveis pela formação de tocotrienóis e, nas espécies que acumulam significativamente esses compostos, há uma preniltransferase específica para cadeia insaturada, a homogentisato geranilgeranil transferase (HGGT) (Cahoon *et al.*, 2003; Hunter & Cahoon, 2007) (Figura 2A). Para além da síntese *de novo,* VTE1 também atua no ciclo redox de tocoferóis. Após a reação com radical peroxil, o radical α-tocoferoxil formado é logo reduzido por outros antioxidantes (*i.e.* ascorbato e glutationa); o intermediário produzido, α-tocoferolquinol (α-TQH_2), pode ser convertido novamente a tocoferol por uma sequência de reações que depende da atividade de VTE1 (Kobayashi & DellaPenna, 2008; Eugeni-Piller *et al.*, 2014) (Figura 2B).

Outra peculiaridade da biossíntese de VTE em plantas é sua estreita relação com a formação de outras prenilquinonas (Block *et al.*, 2013). Primeiro, o anel cromanol de plastoquinona-9 (PQ-9), transportador de elétrons que atua no fotossistema II (PSII), também é originado do homogentisato. Segundo, VTE3 também atua como metiltransferase no intermediário quinol produzido na síntese de PQ-9. Finalmente, PQ-9 serve como substrato para a síntese de outro tococromanol nos plastoglóbulos, o plastocromanol (PC-8), reação catalisada pela VTE1 (Figura 2A). Embora pouco estudado comparado ao tocoferol, PC-8 também atua como antioxidante em plantas (Kruk *et al.*, 2014).

Nas células vegetais, enquanto as atividades de VTE2, VTE3, VTE4 e VTE5 estão associadas à membrana interna do plastídeo (Soll *et al.*, 1985; Cheng *et al.*, 2003; Ischebeck *et al.*, 2006; Zbierzak *et al.*, 2010), a VTE1 está compartimentalizada em inclusões lipídicas conhecidas como plastoglóbulos (Vidi *et al.*, 2006; Lundquist *et al.*, 2012). Tais observações sugerem um intenso tráfego de intermediários dentro do plastídeo para síntese desses compostos (Brehélin *et al.*, 2007; Besagni & Kessler, 2013). Coincidentemente, em tecidos fotossintéticos, tococromanóis estão presentes em grande quantidade em todas as membranas plastidiais: envelope, tilacóides fotossinteticamente ativos e plastoglóbulos (Lichtenthaler, 2007). Fora do cloroplasto, também podem ser encontrados nos corpos oleosos, derivados do retículo endoplasmático, de sementes como girassol e aveia (DellaPena & Mène-Saffrané, 2011).

3. A importância do tocoferol para o organismo vegetal

A presença marcante de tococromanóis nos cloroplastos está intimamente relacionada a algumas das principais funções atribuídas para esses antioxidantes em plantas. Durante a fotossíntese, tanto o vazamento de elétrons da cadeia de transporte de elétrons, quanto a fotorreatividade da clorofila favorecem a formação de ROS (Foyer & Noctor, 2005). Como parte da maquinaria de fotoproteção, tocoferóis atuam particularmente no controle (i) dos níveis de $^1O_2$ no PSII, que possibilita o contínuo *turnover* da proteína D_1, necessário para manutenção dos centros de reação

(Krieger-Liszkay & Trebst 2006), (ii) da extensão da peroxidação lipídica nos tilacóides, especialmente durante condições de estresse (Triantaphylidès & Havaux, 2009; Rastogi *et al.*, 2014; Miret & Munné-Bosch, 2015).

A caracterização de mutantes para VTE e plantas transgênicas tem contribuído de maneira significativa para o conhecimento da função de tocoferóis em plantas (revisto por Falk & Munné-Bosch, 2010; DellaPenna & Mène-Saffrané, 2011). Estes estudos sugerem que além de funções associadas à fotoproteção, VTE desempenha um papel em diversos processos fisiológicos como germinação e estabelecimento da plântula, senescência foliar, resposta aos estresses abióticos, crescimento e particionamento de fotoassimilados (Falk & Munné-Bosch, 2010; Mène-Saffrané *et al.*, 2010; Asensi-Fabado *et al.*, 2014; Eugeni-Piller *et al.*, 2014; Maeda *et al.*, 2014).

Curiosamente, plantas adultas deficientes em tocoferol apresentam fenótipo discrepante sob condições ótimas de crescimento. Enquanto plantas de batata (*Solanum tuberosum*) e de milho (*Zea mays*) deficientes em *VTE1* exibem folhas fonte com prejuízo na exportação de açúcares e déficit no crescimento em condições normais (Provencher *et al.*, 2001; Hofius *et al.*, 2004), tal fenótipo não é observado em plantas de tabaco (*Nicotiana tabacum*) e ocorre em mutantes de *Arabidopsis thaliana vte2* apenas sob condições de estresse causado por baixa temperatura (Maeda *et al.* 2006; 2008). Tais diferenças observadas na partição de açúcares poderiam ser explicadas considerando as demandas fisiológicas das espécies em questão: batata e milho, diferentemente de *Arabidopsis* e tabaco, possuem órgãos drenos fortes que demandam alta taxa de exportação de açúcares das folhas fonte (Asensi-Fabado *et al.*, 2014). Todavia, a falta de fenótipos óbvios em plantas adultas aparentemente contradiz as funções de fotoproteção atribuídas ao tocoferol no cloroplasto. Esse fenômeno, porém, pode ser entendido à luz da rede de detoxificação que atua nos cloroplastos, na qual outros antioxidantes lipossolúveis podem compensar a ausência de VTE nas membranas de plantas deficientes. Vários trabalhos que caracterizam mutantes desprovidos de componentes do sistema antioxidante apontam a indução de vias alternativas de defesa (Miret & Munné-Bosch, 2015). No entanto, o estudo de duplos mutantes - por exemplo, deficientes tanto em tocoferóis quanto em componentes do ciclo da xantofila - assinalam que a rede de antioxidantes do cloroplasto tolera a deficiência de um componente, mas efeitos severos serão observados quando mais de uma via é acometida (Munné-Bosch & Falk, 2004; Havaux *et al.*, 2005).

O acúmulo de tocoferóis nos tecidos vegetais é um processo altamente controlado. Por um lado, está sujeito à modulação ambiental; em resposta a estresses, incluindo seca, baixa temperatura, alta luminosidade e osmótico, os níveis de tocoferóis aumentam em geral (Munné-Bosch, 2005). Tais observações estão de acordo com a responsividade dos genes envolvidos na síntese de VTE a hormônios como etileno, jasmonato, ácido salicílico e ácido abscísico (revisto por Havaux & García-

Plazaola, 2014). Além disso, fatores internos também determinam a regulação do conteúdo de tocoferol, especialmente durante o processo de senescência, em que os níveis de tocoferol aumentam gradativamente (Hormaetxe *et al.*, 2005). Da relação coordenada entre os níveis de clorofila e de tocoferóis durante a senescência, ambas moléculas derivadas da cadeia isoprênica fitil difosfato, depreendeu-se que o tocoferol poderia ser um dreno do fitol gerado pela quebra da clorofila (Rise *et al.*, 1989). Contudo, para ser incorporado na síntese de tocoferol, o fitol deveria ser ativado por subsequentes fosforilações. A demonstração de uma via de reciclagem específica para este álcool prenílico juntamente com a clonagem do gene codificante para uma das quinases, a enzima VTE5, reforçou a hipótese de tocoferóis como dreno do fitol (Figura 2). Mutantes de *Arabidopsis vte5* apresentam redução de aproximadamente 80% e 65% do conteúdo de tocoferóis em sementes e folhas maduras, respectivamente (Valentin *et al.*, 2006). Evidências adicionais foram obtidas no estudo com plântulas de *Arabidopsis* supridas com fitol exógeno marcado; estas exibiram não só aumento de tocoferóis, mas também de ésteres de fitol, compostos igualmente induzidos sob condições de estresses e que se acumulam nos plastoglóbulos (Ischebeck *et al.*, 2006). Considerando a possível toxicidade atribuída ao fitol livre nas células, tocoferóis e ésteres do fitol formariam um mecanismo de detoxificação que atuaria no cloroplasto associado aos plastoglóbulos (Dörmann, 2007).

4. Melhoramento das espécies cultivadas: a exploração da diversidade natural e manipulação genética

Em virtude da sua importância na fisiologia vegetal e para a nutrição humana, muitos esforços têm sido feitos para entender os mecanismos responsáveis pela biossíntese e acúmulo de VTE em plantas, especialmente nas espécies cultivadas, com o objetivo de melhorar a produtividade e a qualidade nutricional.

A exploração da diversidade natural constitui uma das possíveis abordagens para o melhoramento do conteúdo de VTE nas plantas cultivadas. Até o momento, inúmeros *loci* para caracteres quantitativos (QTL) que explicam a variação no conteúdo total e na composição de VTE foram identificados, utilizando populações de mapeamento de *Arabidopsis*, soja (*Glicine max*), colza (*Brassica napus*), girassol (*Helianthus annuus*), milho e tomate (*Solanum lycopersicum*) (Gilliland *et al.* 2006; Schauer *et al.*, 2006; Almeida *et al.*, 2011; Dwiyanti *et al.* 2011; Haddadi *et al.* 2012; Lipka *et al.*, 2013; Shutu *et al.* 2012; Wang *et al.* 2012). Em alguns desses estudos, genes da rota central de tocoferol colocalizam com os QTL, embora o tamanho do intervalo tenha limitado a demonstração definitiva de sua base molecular (Fitzpatrick *et al.*, 2012).

A elucidação da rota biossintética da VTE permitiu substancial progresso na manipulação genética dessa via, permitindo a obtenção de plantas transgênicas em várias espécies cultivadas com

altos teores VTE, destacando-se milho, soja e canola (Fitzpatrick *et al.*, 2012). Desde a primeira demonstração que a composição de VTE poderia ser alterada em favor da síntese de α-tocoferol (Shintani & DellaPenna, 1998), vários esforços têm sido feitos para aumentar o conteúdo e/ou biodisponilidade de VTE. Dos resultados obtidos pelos estudos subsequentes, depreende-se que VTE3 e VTE4 representam pontos chaves no controle da composição de tocoferol em diferentes espécies (Collakova & DellaPenna, 2003a; Van Eenennaam *et al.*, 2003; Quadrana *et al.*, 2011), enquanto HGGT e VTE2 são limitantes para os níveis totais de tocotrienóis e tocoferóis, respectivamente (Cahoon *et al.*, 2003; Collakova & DellaPenna, 2003b; Sattler *et al.*, 2004; Karunanandaa *et al.*, 2005; Seo *et al.*, 2011). Com efeito, a sobrexpressão de VTE2 resultou apenas em modesto aumento no conteúdo VTE, particularmente, em soja, canola e tomate. Uma explicação plausível para esses resultados apoia-se na complexa regulação do *pool* de fitil difosfato no plastídeo, proveniente tanto da síntese *de novo* - a partir da via do MEP - quanto da degradação da clorofila; de fato, a disponibilidade de cadeia isoprênica constitui um dos importantes gargalos para o aumento de tocoferóis.

Outro limitante, todavia, é o *pool* de homogentisato. Tentativas de manipulação do conteúdo de VTE em plantas transgênicas por meio da sobrexpressão da hidroxifenil piruvato (HPPD), que catalisa o passo final na produção do homogentisato, produziram apenas incrementos modestos (Tsegaye *et al.*, 2002; Falk *et al.*, 2003; Karunanandaa *et al.*, 2005). Nesse caso, o gargalo metabólico para produção do homogentisato decorre do forte *feedback* negativo exercido pela tirosina nas reações finais da via do SK que levam à síntese do hidrofenil piruvato, impedindo, portanto, o aumento da disponibilidade desse precursor para a produção de tocoferóis (Rippert & Matringe, 2002; Tzin & Galili, 2010). A introdução de genes bacterianos e de leveduras em plantas sobrepuseram essa regulação negativa (Figura 3). Plantas transgênicas de *Arabidopsis* e de soja, que sobrexpressam uma corismato mutase/prefenato desidratase (CM/PDT) bifuncional bacteriana insensível ao *feedback* negativo da tirosina mostraram um considerável acúmulo de tococromanóis, especialmente de tocotrienóis (Karunanandaa *et al.*, 2005; Zhang *et al.*, 2013). De forma semelhante, plantas de tabaco sobrexpressando uma prefenato dehidrogenase (PDH) de levedura capaz de converte prefenato em hidrofenil piruvato diretamente – rota identificada também em leguminosas (Schenk *et al.*, 2015) – também resultou no incremento no conteúdo de tocotrienóis (Rippert *et al.*, 2004).

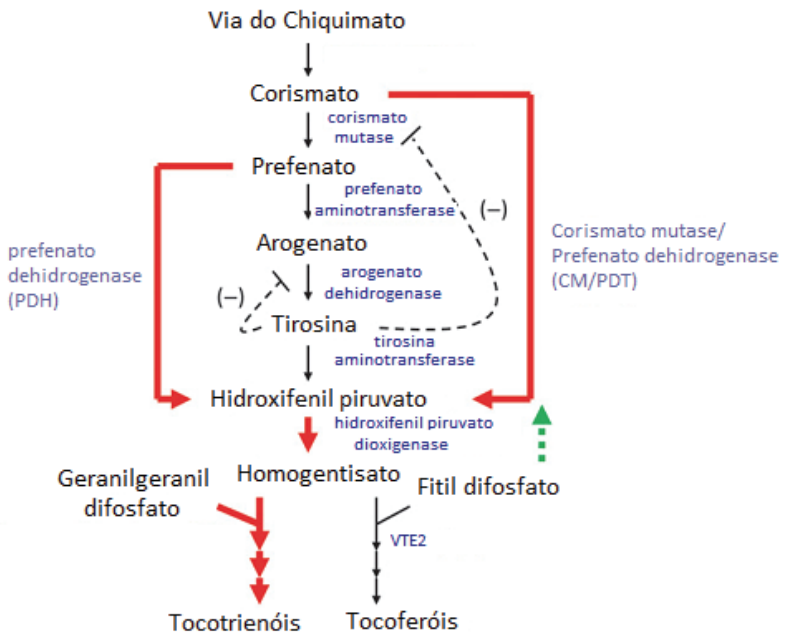

Figura 3: Biossíntese do homogentisato e regulação pós-transcricional da via do chiquimato. O nível de homogentisato é altamente regulado pela concentração de tirosina por meio de feedback negativo nas enzimas da rota (linhas tracejadas). Pontos regulatórios sobrepostos em plantas pela expressão de genes de microrganismos estão destacados em vermelho. O desbalanço eficiente na produção de homogentisato é atingido juntamente com a sobrexpressão da hidroxigenil piruvato dioxigenase, que resulta no aumento de VTE, principalmente de tocotrienóis. Adaptado de Zhang *et al.* (2013).

Os trabalhos descritos acima revelam que o acúmulo de VTE é influenciado por perturbações das vias precursoras tanto do MEP quanto do SK. Tais observação implicam uma maior complexidade para a manipulação do conteúdo desse nutracêutico em plantas, visto que ambas são vias centrais no metabolismo do plastídeos. Enquanto a rota do MEP é responsável pela formação de isoprenóides, precursores da síntese de clorofilas, carotenóides e prenilquinonas (DellaPenna & Pogson, 2006), a rota do SK produz intermediários para a síntese de folato (vitamina B_9), prenilquinonas, aminoácidos aromáticos e seus derivados, como fenilpropanóides e alcalóides (Tzin *et al.*, 2010).

Nessa perspectiva, manipulações de fatores genéticos que influenciem o metabolismo e desenvolvimento plastidial poderiam afetar o conteúdo de VTE. Com efeito, em tomateiro, a alteração de fatores de transcrição envolvidos no desenvolvimento e amadurecimento dos frutos (Enfissi *et al.*, 2010; Karlova *et al.*, 2011) e na formação da cutícula de frutos (Adato *et al.*, 2009) modificaram o conteúdo de tocoferóis. Notavelmente, plantas transgênicas de *S. lycopersicum* que sobrexpressam em fruto o gene *FITOENO SINTASE* (*PSY*), que codifica para enzima chave da biossíntese de carotenóides, apresentaram incremento nos níveis de carotenóides e também de tocoferol (Fraser *et al.*, 2007). Em contrapartida, modificações na atividade do complexo NAD(P)H dehidrogenase plastidial, que catalisa a redução das PQ-9, favoreceu o acúmulo de tocoferóis em detrimento de licopeno em tomate (Nashilevitz *et al.*, 2010).

5. O tomateiro: modelo de estudo com importância agronômica

O tomateiro (*Solanum lycopersicum* L., antigo *Lycopersicon esculentum*) desponta atualmente como uma das horticulturas de maior importância econômica mundial além de ser organismo modelo para estudo dos aspectos relacionados ao desenvolvimento e fisiologia dos frutos carnosos.

Sob a perspectiva agronômica, o tomateiro é uma das hortaliças mais cultivadas mundialmente, cuja produção ultrapassa 160 milhões de toneladas anualmente. China, Índia e Estados Unidos destacam-se na produção mundial, enquanto o Brasil consolida-se na oitava posição com um volume de 4,2 milhões de toneladas ao ano (*Food and Agriculture Organization of the United Nations*, FAO, http://faostat.fao.org). O destino da produção é, principalmente, o consumo humano na forma *in natura* ou de produtos processados pela indústria. O fruto de tomate e seus derivados constituem fonte importante de aminoácidos essenciais, fibras, flavonóides, vitaminas C (VTC), (VTE) e carotenóides para a dieta humana (Abushita *et al.*, 1997; Beecher, 1998).

S. lycopersicum é uma das espécies domesticadas da família Solanaceae da qual também fazem parte batata, berinjela (*Solanum melongena*), pimenta (*Capsicum* ssp) e tabaco (várias espécies). Dentro dessa família, o tomateiro é a espécie mais profundamente estudada, sendo o modelo primário para o estudo da biologia de frutos carnosos e climatéricos (Giovannoni, 2004).

O fruto do tomateiro é constituído de uma epiderme, de um espesso pericarpo - derivado da parede do ovário - e de tecido placentário que envolve as sementes. Ao longo do desenvolvimento do fruto, distinguem-se quatro fases (Figura 4A): (i) o desenvolvimento da flor, desde a iniciação floral até antese; (ii) o período de intensa divisão celular que começa após fertilização; (iii) o período de expansão celular, que se estende desde o fim da fase de divisão até o início do amadurecimento, no qual o fruto atinge seu tamanho máximo, e passa por sucessivos processos de endoreduplicação gerando células altamente polissomáticas (256C); e (iv) o amadurecimento, marcado por alterações bioquímicas, incluindo o acúmulo de açúcares, ácidos, pigmentos e voláteis, que afetam a aparência, a textura e o teor nutricional atraindo organismos dispersores de sementes (Gillaspy *et al.*, 1993; Giovannoni, 2004). Sob a perspectiva agronômica, o valor nutricional, o sabor, o aroma, as características de processamento e o tempo de prateleira determinam a qualidade do fruto (Osorio *et al.*, 2013).

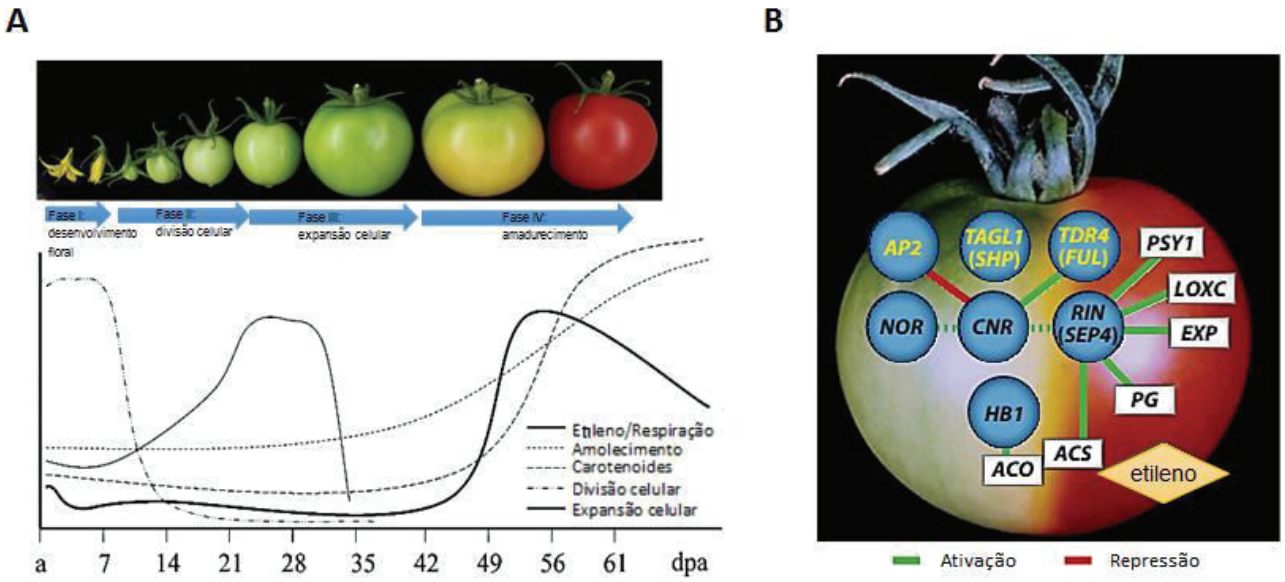

Figura 4. Desenvolvimento do fruto de tomateiro. (A) Aspecto do fruto desde a antese até o amadurecimento e principais alterações bioquímicas e fisiológicas. a: antese. dpa: dias pós-antese. Adaptado de Giovannoni (2004) e Karlova *et al.* (2014). (B) Rede molecular de regulação do amadurecimento de frutos carnosos com os principais reguladores conhecidos. Os círculos azuis são fatores de transcrição; os genes em amarelo são os ortólogos também encontrados em frutos deiscentes como de *Arabidopsis*. Alguns dos genes regulados pelos fatores são mostrados em caixas brancas. Precisamente, o modo de interação entre NOR, CNR e RIN ainda é desconhecido e representado por linhas pontilhadas. As abreviaturas correspondem a: gene homeótico floral *APETALA2* (*AP2*); gene *MADS-box TOMATO AGAMOUS LIKE1* (*TAGL1*); gene *MADS box* (*TDR4/FUL*); gene da proteína com *HOMEODOMÍNIO DE ZÍPER DE LEUCINA* (*HB1*); genes envolvidos na síntese de etileno *ACC OXIDASE* (*ACO*) e *ACC SINTASE* (*ACS*), de carotenóides *FITOENO SINTASE* (*PSY1*), de parede celular *EXPANSINA* (*EXP*) e *POLIGALACTURONASE* (*PG*), e de compostos voláteis *13-LIPOXIGENASE* (*LoxC*). Adaptado de Seymour *et al.* (2013).

O amadurecimento em frutos climatéricos coincide com a maturação da semente e está intimamente relacionado com o aumento da respiração e biossíntese de etileno, desencadeando uma complexa, coordenada e rápida alteração no perfil metabólico (Giovannoni, 2004). Um dos processos importantes nessa fase de desenvolvimento dos frutos é a conversão de cloroplastos a cromoplastos (Figura 5). Ao longo do amadurecimento, os tilacóides dos cloroplastos se desorganizam; os plastoglóbulos, por sua vez, aumentam de tamanho. Simultaneamente, enquanto a clorofila é degradada, a síntese de carotenóides é dramaticamente estimulada e resulta no acúmulo de predominante de licopeno, determinando, assim, a mudança de cor (Klee & Giovannoni 2011). O impressivo avanço na compreensão dos aspectos moleculares que regulam o amadurecimento foi alcançado, em parte, por meio da caracterização de mutantes monogênicos de tomateiro deficientes nesse processo, tais como *ripening-inhibitor* (*rin*), *non-ripening* (*nor*), *colorless non-ripening* (*Cnr*) e *never-ripe* (*Nr*; Giovannoni, 2006). Enquanto a proteína Nr corresponde a um dos receptores de etileno, NOR, CNR e RIN são fatores de transcrição que regulam globalmente o amadurecimento. Detalhados estudo de imunoprecipitação de cromatina demonstraram que RIN modula a expressão de centenas de genes envolvidos em vias ativas durante a transição de frutos verdes para maduros,

i.e. carotenogênese, degradação da clorofila, síntese e percepção de etileno, remodelamento da parede celular (Klee & Giovannoni 2011; Martel *et al.*, 2011; Fujisawa *et al.*, 2013) (Figura 4B).

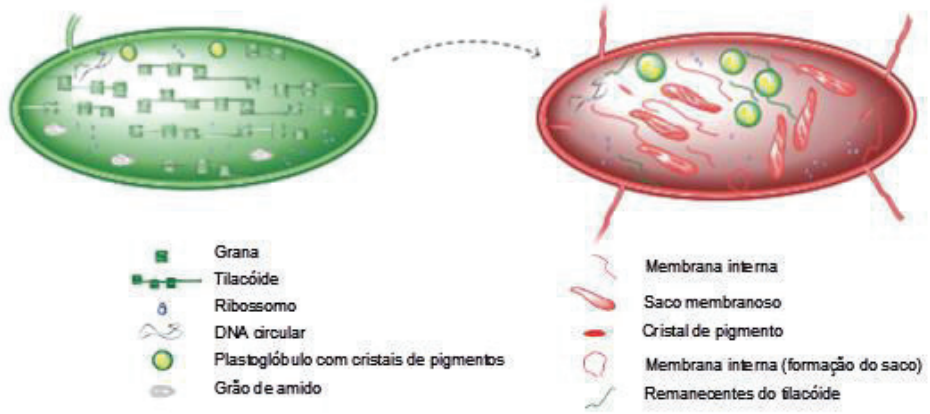

Figura 5. Representação esquemática das mudanças que ocorrem na diferenciação de cloroplastos em cromoplastos. Adaptado de Bian *et al.* (2011).

A utilização do tomateiro como modelo de estudo é decorrente das diversas características intrínsecas da espécie, como genoma diplóide de tamanho reduzido (900 Mb), curto tempo de geração e reprodução por autofecundação (Shibata, 2005). Além disso, importantes ferramentas para análise genética são aplicadas com sucesso em tomateiro como, por exemplo, a transformação genética estável e o silenciamento gênico induzido por vírus (VIGS) (Barone *et al.*, 2008; Quadrana *et al.*, 2011). Finalmente, nas últimas duas décadas, uma vasta diversidade de recursos genéticos e genômicos foram desenvolvidos, os quais incluem: (i) mapas genéticos de alta densidade; (ii) caracterização do germoplasma selvagem; (iii) populações de mapeamento de QTL; (iv) coleções de mutantes e plataformas para TILLING (*Targeted Induced Local Lesions in Genomes*); (iv) genoma sequenciado tanto da espécie cultivada *S. lycopersicum* (*cv*. Heinz 1706) quanto de espécies selvagens correlatas como *Solanum pennellii* e *Solanum pimpinellifolioum* (The Tomato Genome Consortium, 2012; Bolger *et al.*, 2014), todos de acesso público (*Solanaceae Genomics Network,* http://solgenomics.net/). Com o advento das tecnologias de sequenciamento da nova geração (*next-generation sequencing*), para além das sequências genômicas altamente curadas, também estão disponíveis o transcriptoma de *S. lycopersicum* em diferentes tecidos e condições, que incluem tanto dados de RNA codificante (mRNA) quanto de RNAs regulatórios - pequenos RNA (sRNA) e micro RNA (miRNA) - além da caracterização do epigenoma (Zhong *et al.*, 2013). Dos 34.727 genes codificantes para proteínas preditos no genoma de referência (ITAG Release 2.3), 30.855 são suportados pelos dados de sequenciamento de RNA (The Tomato Genome Consortium, 2012).

Dentro da seção Lycopersicon existem 12 espécies selvagens, as quais exibem grande diversidade fenotípica (Peralta *et al.*, 2005), incluindo variações no conteúdo de metabólitos em folhas e frutos (Schauer *et al.,* 2005). Essas espécies são portadoras de valiosos genes que podem contribuir para o melhoramento nutricional e industrial do cultivar de elite (Zamir, 2001; Fernie & Klee, 2011). A maioria dos caracteres de interesse agronômico é de herança quantitativa, sendo determinada por QTL (Fernie & Schauer, 2009; Stitt *et al.,* 2010). Partindo da exploração da variação natural, uma das abordagens para estudo genético das características de heranças complexas, é o mapeamento de QTL, que utiliza populações experimentais produzidas a partir do cruzamentos de linhagens geneticamente divergentes e com fenótipo contrastante (Rothan & Causse, 2007; Stitt *et al.*, 2010). Dentre elas, as populações de linhagens introgredidas (ILs) constituem uma poderosa ferramenta para espécies autógamas. Isso porque são geradas por retrocruzamentos sucessivos da progênie F_1 com um dos genitores e, ao final, os indivíduos contêm apenas um único fragmento introgredido do genótipo doador que se contrapõem ao fundo genético isogênico (Figura 6A). Por conseguinte, qualquer diferença fenotípica observada entre a IL e o parental recorrente é atribuída, exclusivamente, ao fragmento genômico introgredido. De fato, outra vantagem dessa população experimental é a homozigose da introgressão, permitindo a manutenção por autofecundação e, portanto, a utilização em diversas situações experimentais (Zamir, 2001; Lippman *et al.*, 2007; Rothan & Causse, 2007).

No caso do tomateiro, uma população de ILs que combina fragmentos genômicos da espécie selvagem *S. pennellii* (LA716) no fundo genético da espécie domesticada *S. lycopersicum* (*cv*. M82) (Eshed & Zamir, 1995) tem sido extensivamente caracterizada. Ao todo, os fragmentos introgredidos das ILs de *S. pennellii* cobrem por completo o genoma do tomateiro sendo bem delimitados por marcadores moleculares (http://www.sgn.cornell.edu/maps/pe.pl) (Figura 6B). A caracterização fenotípica das ILs de *S. pennellii* permitiu a identificação de milhares de QTL que afetam desde morfologia da planta, produtividade, atividade enzimática e metabolismo do fruto (Lippman *et al.*, 2007; Fernie & Schauer, 2009; Steinhauser *et al.*, 2011; Chitwood *et al.*, 2013; Alseekh *et al.*, 2015; Perez-Fons *et al.*, 2014), incluindo o conteúdo de VTE.

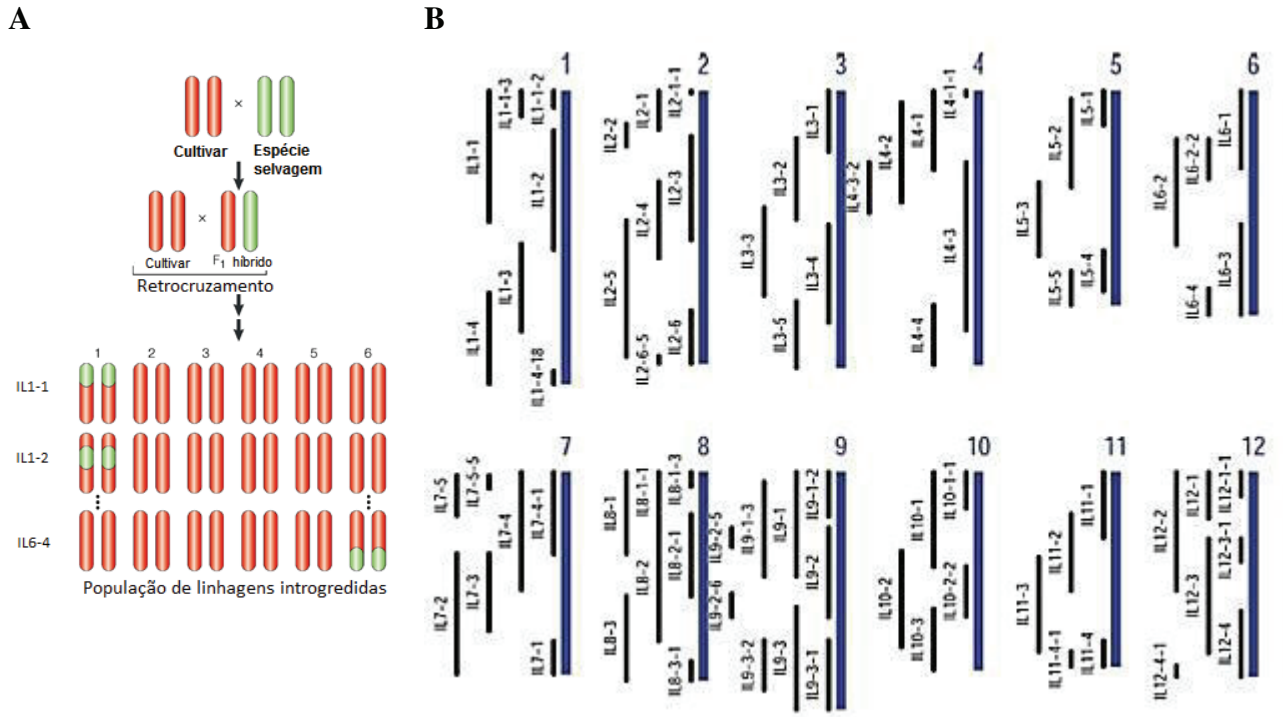

Figura 6: Representação esquemática da população de ILs de *S. pennellii* desenvolvidas por Eshed & Zamir (1995). (A) Obtenção das ILs. O esquema mostra um exemplo de três IL para os cromossomos 1 e 6. As ILs foram obtidas por meio de sucessivos retrocruzamentos e seleção assistida por marcadores moleculares, seguido de duas gerações de autofecundação para obtenção dos fragmentos em homozigose. Adaptado de Zamir (2001). (B) Coleção das ILs que recobrem o genoma de *S. lycopersicum* em linhas pretas. As linhas azuis correspondem aos cromossomos. Adaptado de Lippman *et al.* (2007).

6. A regulação da vitamina E em tomateiro: antecedentes e construção das hipóteses de trabalho

Diferentemente dos estudos que realizaram perfis metabólicos extensivos em frutos das ILs por técnicas de alto rendimento mapeando dezenas de metabólitos simultaneamente (Schauer *et al.*, 2006; Perez-Fons *et al.*, 2014), nosso grupo investigou detalhadamente o perfil das quatro espécies genômica dos *loci* relacionados à biossíntese de tocoferol. As variações encontradas permitiram mapear 12 QTL para o conteúdo de tocoferol em tomateiro. A análise integrada dos dados metabólicos, genômicos e genéticos levou a proposição de 16 *loci* candidatos que poderiam explicar as mudanças no conteúdo de tocoferóis observadas (Almeida *et al.*, 2011) (Figura 7). Em conjunto, os resultados obtidos pelo grupo representam uma vasta plataforma de dados para exploração dos componentes genéticos envolvidos na determinação da variação natural do conteúdo de VTE.

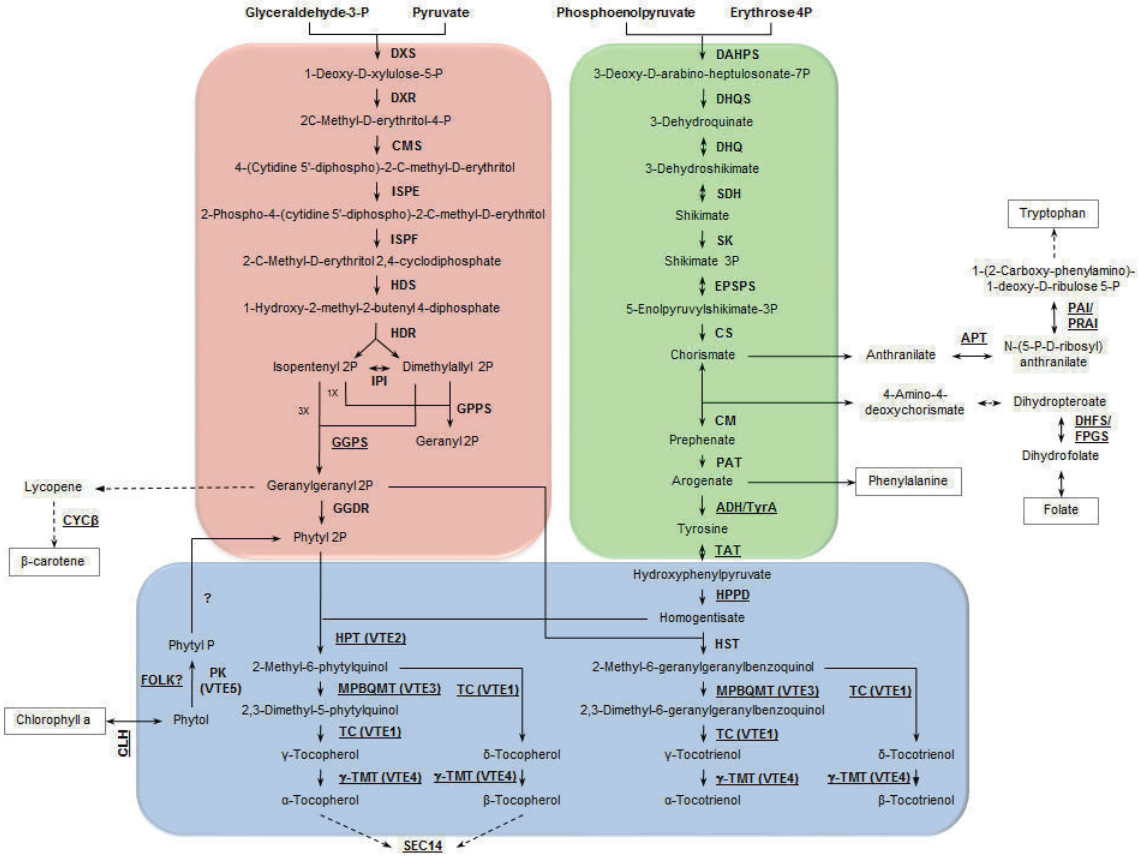

Figura 7: Mapa da biossíntese de VTE e genes candidatos identificados para QTL associados ao conteúdo de VTE em frutos de tomate. As rotas de síntese de MEP, SK e central de tocoferol estão destacadas em vermelho, verde e azul, respectivamente. Genes candidatos encontram-se sublinhados. Os genes que codificam para as enzimas estão nomeados de acordo às seguintes abreviações: *1-DEOXI-D-XILULOSE-5-P SINTASE (DXS), 2-C-METIL-D- ERITRITOL 4-FOSFATO SINTASE (DXR), 2-C-METIL-D- ERITRITOL 4-FOSFATO CITIDILILTRANSFERASE (CMS), 4-(CITIDINA 5'-DIFOSFO)-2-C-METIL-D-ERITRITOL QUINASE (ISPE), 2-C-METIL-D-ERITRITOL 2,4-CICLODIFOSFATO SINTASE (ISPF), 4-HIDROXI-3-METILBUT-2-ENIL- DIFOSFATO SINTASE (HDS), 4-HIDROXI-3-METILBUT-2-ENIL- DIFOSFATO REDUTASE (HDR), ISOPENTENIL DIFOSFATO ISOMERASE (IPI), GERANIL DIFOSFATO SINTASE (GPPS), GERANILGERANIL DIFOSFATO SINTASE (GGPS), GERANILGERANIL REDUTASE (GGDR), 3-DEOXI-D-ARABINO-HEPTULOSONATO-7-P SINTASE (DAHPS), 3-DEHIDROQUINATO SINTASE (DHQS), CHIQUIMATO DEHIDROGENASE (SDH)/ 3-DEHIDROQUINATO DEHIDRATSE (DHQ), CHIQUIMATO QUINASE (SK), 5-ENOLPIRUVILCHIQUIMATO-3-P SINTASE (EPSPS), CORISMATO SINTASE (CS), CORISMATO MUTASE (CM), PREFENATO AMINOTRANSFERASE (PAT), AROGENATO DEHIDROGENASE (ADH), TIROSINA AMINOTRANSFERASE (TAT),* 4*-HIDROXIFENILPIRUVATO DIOXIGENASE1* (*HPPD*), *TOCOFEROL CICLASE* (*VTE1*), *HOMOGENTISATO FITIL TRANSFERASE (VTE2), DIMETIL-FITILQUINOL METIL TRANSFERASE (VTE3), γ-TOCOFEROL C-METIL TRANSFERASE (VTE4), FITOL QUINASE (VTE5), FARNESOL QUINASE (FOLK), CLOROFILASE (CLH), LICOPENO β CICLASE* (*CYCβ*), *FOSFORIBOSILANTRANILATO ISOMERASE* (*PAI*), *DIHIDROFOLATO SINTASE* (*DHFS*), *ANTRANILATO FOSFORRIBOSILTRANSFERASE (APT)*. Adaptado de Almeida *et al.* (2011).

Considerando a intensa degradação de clorofila que o fruto de tomate sofre durante o amadurecimento, os genes codificantes para clorofilase (CLH, Solyc06g053980) e a farnesol quinase (FOLK, antigo VTE5, Solyc09g018510), que são enzimas envolvidas no metabolismo do fitol, destacaram-se como interessantes candidatos associados aos QTL dos cromossomos 6 e 9, respectivamente.

Até recentemente, a CLH era a única enzima conhecida responsável pela defitilação da clorofila, evento inicial da degradação do pigmento. No entanto, ausência de correlação dos

transcritos e da atividade enzimática durante o processo de senescência em várias espécies, incluindo *Arabidopsis*, além um cenário incoerente quanto à localização subcelular sugeriam a existência de vias alternativas para degradação da clorofila (Amir-Shapira et al., 1987; Yamauchi et al., 1991; Matile et al., 1996; Fang et al., 1998; Takamiya et al., 2000; Schenk et al., 2007). A identificação da feofitinase (PPH), enzima defitiladora protagonista durante o processo de senescência foliar, resolveu a questão parcialmente (Schelbert *et al.*, 2009). Não obstante, a regulação do catabolismo de clorofila ainda não foi completamente elucidada e o cenário emergente aponta para um processo complexo. Em contrapartida à *Arabidopsis*, outros trabalhos suportam o envolvimento das CLHs na defitilação da clorofila em outras espécies, como *Brassica oleracea* e *Citrus,* durante o processo de desverdecimento de inflorescência e do amadurecimento de frutos induzido por etileno (Harpaz-Saad *et al.*, 2007; Chen *et al.*, 2008). Em tomateiro, Guyer *et al.* (2014) recentemente mostraram que, em linhagens transgênicas silenciadas para *PPH,* embora a degradação de clorofila esteja comprometida durante a foliar senescência, os frutos ainda são capazes de degradar clorofila durante o amadurecimento. Os resultados sugerem a participação de outras hidrolases na defitilação da clorofila em frutos como as clorofilases ou outra(s) hidrolase(s) ainda não identificada(s) (Guyer *et al.*, 2014). Com a finalização do genoma de *S. lycopersicum,* nosso grupo identificou quatro genes parálogos codificantes para CLHs (Lira *et al.*, 2014) localizados no cromossomo 6 (*SlCLH1*), 9 (*SlCLH2* e *SlCLH3*) e 12 (*SlCLH4*). O gene candidato do cromossomo 6 descrito por Almeida *et al.* (2011) corresponde a *SlCLH1*; por sua vez, *SlCLH2* colocaliza com o QTL descrito para VTE no cromossomo 9. A relevância biológica dessas enzimas para a fisiologia de tomateiro ainda não está esclarecida. Ainda que sua atividade seja prescindível para o processo de senescência foliar, CLHs poderiam participar da quebra da clorofila durante o amadurecimento ou, ainda, estariam envolvidas no *turnover* da clorofila em tecidos fotossinteticamente ativos.

Valentin *et al.* (2006) caracterizaram funcionalmente o gene At5g04490 como uma VTE5 e identificaram um putativo parálogo, At5g58560. Baseado na homologia com esse último, o *locus* candidato FARNESOL QUINASE (*FOLK*, Solyc09g018510) do cromossomo 9 foi inicialmente anotado como *VTE5* em Almeida *et al.* (2011). Diante de evidências experimentais posteriores, que demonstraram que At5g58560 codifica para FOLK em *Arabidopsis* (Fitzpatrick *et al.*, 2011), a anotação do gene candidato de tomateiro foi atualizada, assim como identificado o respectivo gene codificante para VTE5 no genoma de *S. lycopersicum* (Solyc03g071720). Entretanto, vale ressaltar que a predição *in silico* da localização subcelular da proteína FOLK de *S. lycopersicum* sugere o direcionamento para o cloroplasto (Almeida *et al.*, 2011). Tal constatação diverge das evidências reportadas na literatura; a atividade farnesol kinase é verificada, principalmente, na fração microsomal da célula vegetal (Thai *et al.*, 1999). Dessa maneira, se FOLK é direcionada ao

cloroplasto em tomateiro, eventualmente, poderia contribuir para fosforilação do fitol e, consequemente com a síntese de tocoferóis.

É na perspectiva de melhor compreender como ocorre a regulação da da biossíntese de VTE em tomateiro que esta tese se insere. Apresenta-se, primeiramente, uma análise detalhada do perfil transcricional dos genes associados à biossíntese de VTE nas seguintes condições: ao longo do desenvolvimento de folhas e frutos de tomateiro, nas ILs de *S. pennellii* que apresentam aumento no conteúdo de tocoferóis, e nos frutos de mutantes de tomateiro deficientes nos processos de amadurecimento e de degradação da clorofila. Tal proposta sustenta-se sob a hipótese de que alterações na abundância desses transcritos, causadas tanto pelo controle endógeno, quanto pela presença de variantes alélicas, modulam o acúmulo de VTE em tomateiro. Por fim, um estudo aprofundado do metabolismo do fitol é apresentado por meio da caracterização funcional dos genes codificantes para *VTE5, CLH1* e *FOLK*. Neste caso, considera-se que tais fatores são relevantes para o controle dos níveis de tocoferol, principalmente em fruto, uma vez que neste órgão ocorre significativa quebra de clorofila durante o processo de amadurecimento. Os resultados obtidos constituem um avanço expressivo no conhecimento dos mecanismos que regulam o acúmulo de VTE, além de expor inúmeras conexões entre o metabolismo de tocoferol e outras vias metabólicas que impactam a fisiologia de *S. lycopersicum*.

7. Referências bibliográficas

Abushita, A. A., Hebshi, E. A., Daood, H. G., Biacs, P. A. (1997) Determination of antioxidant vitamins in tomatoes. *Food Chemistry,* 60, 207–212.

Adato, A., Mandel, T., Mintz-Oron, S., Venger, I., Levy, D., Yativ, M., *et al.* (2009) Fruit-surface flavonoid accumulation in tomato is controlled by a SLMYB12-regulated transcriptional network. *PLoS Genetics*, 5, e1000777.

Almeida, J., Quadrana, L., Asis, R., Setta, N., de Godoy, F., Bermudez, L., Otaiza, S., *et al.* (2011) Genetic dissection of vitamin E biosynthesis in tomato. *Journal of Experimental Botany,* 62, 3781–3798.

Alseekh, S., Tohge, T., Wendenberg, R., Scossa, F., Omranian, N., Li, J., *et al.* (2015) Identification and Mode of Inheritance of Quantitative Trait Loci for Secondary Metabolite Abundance in Tomato. *The Plant Cell*, 27, 485-512.

Amir-Shapira, D., Goldschmidt, E. E., Altman, A. (1987) Chlorophyll catabolism in senescing plant tissues: *In vivo* breakdown intermediates suggest different degradative pathways for *Citrus* fruit and parsley leaves. *Proceedings of the National Academy of Sciences of the United States of America*, *84*, 1901–1905.

Asensi-Fabado, M. A., Ammon, A., Sonnewald, U., Munné-Bosch, S., Voll, L.M. (2014) Tocopherol deficiency reduces sucrose export from salt-stressed potato leaves independently of oxidative stress and symplastic obstruction by callose. *Journal of Experimental Botany*, 66, 957–971.

Barone, A., Chiusano, M. L., Ercolano, M. R., Giuliano, G., Grandillo, S., Frusciante, L. (2008) Structural and functional genomics of tomato. *International Journal of Plant Genomics*, 2008, 820274.

Beecher, G. R. (1998) Nutrient content of tomatoes and tomato products. *Proceedings of the Society for Experimental Biology and Medicine*, 218, 98-100.

Besagni, C., Kessler, F. (2013) A mechanism implicating plastoglobules in thylakoid disassembly during senescence and nitrogen starvation. *Planta*, 237, 463–470.

Bian, W., Barsan, C., Egea, I., Purgatto, E., Chervin, C., Zouine, M., Latché, A., *et al*. (2011) Metabolic and molecular events occurring during chromoplast biogenesis. *Journal of Botany*, 11, 1-13.

Block, A., Fristedt, R., Rogers, S., Kumar, J., Barnes, B., Barnes, J., *et al*. (2013) Functional Modeling Identifies Paralogous Solanesyl Diphosphate Synthases that Assemble the Side Chain of Plastoquinone-9 in Plastids. *The Journal of Biological Chemistry*, 288, 27594–27606.

Bolger, A., Scossa, F., Bolger, M. E., Lanz, C., Maumus, F., Tohge, T., Quesneville, H., *et al*. (2014) The genome of the stress-tolerant wild tomato species *Solanum pennellii. Nature Genetics*, 46, 1034–1038.

Bréhélin C., Kessler F., van Wijk, K.J. (2007) Plastoglobules: versatile lipoprotein particles in plastids. *Trends in Plant Science*, 12, 260–266.

Cardenas, E., Ghosh, R. (2013) Vitamin E: a dark horse at the crossroad of cancer management. *Biochemical Pharmacology*, 86, 845-852.

Chen, L. F. O., Lin, C. H., Kelkar, S. M., Chang, Y. M., Shaw, J. F. (2008) Transgenic broccoli (*Brassica oleracea* var. *italica*) with antisense chlorophyllase (BoCLH1) delays postharvest yellowing. *Plant Science,* 174, 25–31.

Cheng, Z., Sattler, S., Maeda, H., Sakuragi, Y., Bryant, D. A., DellaPenna, D. (2003) Highly divergent methyltransferases catalyze a conserved reaction in tocopherol and plastoquinone synthesis in cyanobacteria and photosynthetic eukaryotes. *The Plant Cell*, 15, 2343–2356.

Chitwood, D. H., Kumar, R., Headland, L. R., Ranjan, A., Covington, M. F., Ichihashi, Y., *et al*. (2013) A quantitative genetic basis for leaf morphology in a set of precisely defined tomato introgression lines. *Plant Cell*, 25, 2465–2481.

Chun, J., Lee, J., Ye, L., Exler, J., Eitenmiller, R.R. (2006) Tocopherol and tocotrienol contents of raw and processed fruits and vegetables in the United States diet. *Journal of Food Composition and Analysis*, 19, 196–204.

Collakova, E., DellaPenna, D. (2003a) The role of homogentisate phytyltransferase and other tocopherol pathway enzymes in the regulation of tocopherol synthesis during abiotic stress. *Plant Physiology*, 133, 930–940.

Collakova, E., DellaPenna, D. (2003b) Homogentisate phytyltransferase activity is limiting for tocopherol biosynthesis in Arabidopsis. *Plant Physiology,* 131, 632–642.

DellaPenna, D., Last, R.L. (2006) Progress in the dissection and manipulation of plant vitamin E biosynthesis. *Physiologia Plantarum*, 126, 356–368.

DellaPenna, D., Pogson, B.J. (2006) Vitamin synthesis in plants: tocopherols and carotenoids. *Annual Review of Plant Biology*, 57, 711–738.

DellaPenna, D., Mène-Saffrané, L. (2011).Vitamin E in Biosynthesis of vitamins in plants. *Advances in Botanical Research,* 59, 179-227.

Di Mascio, P., Devasagayam, T.P., Kaiser, S., Sies, H. (1990) Carotenoids, tocopherols and thiols as biological singlet molecular oxygen quenchers. *Biochemical Society Transactions*, 18, 1054–1056.

Dörmann, P. (2007) Functional diversity of tocochromanols in plants. *Planta*, 225, 269–276.

Dwiyanti, M. S., Yamada, T., Sato, M., Abe, J., Kitamura, K. (2011) Genetic variation of γ-tocopherol methyltransferase gene contributes to elevated α-tocopherol content in soybean seeds. *BMC Plant Biology*, 11, 152.

Enfissi, E. M. A., Barneche, F., Ahmed, I., Lichtlé, C., Gerrish, C., McQuinn, R. P., *et al*. (2010) Integrative transcript and metabolite analysis of nutritionally enhanced DE-ETIOLATED1 downregulated tomato fruit. *The Plant Cell*, 22, 1190–1215.

Eshed, Y., Zamir, D. (1995) An introgression line population of Lycopersicon pennellii in the cultivated tomato enables the identification and fine mapping of yield-associated QTL. *Genetics*, 141, 1147-1162.

Eugeni-Piller, L., Glauser, G., Kessler, F., Besagni, C. (2014) Role of plastoglobules in metabolite repair in the tocopherol redox cycle. *Frontiers in Plant Science*, 5, 298.

Evans, H. M., Bishop, K. S. (1922) On the existence of a hitherto unrecognized dietary factor essential for reproduction. *Science*, 56, 650–651.

Falk, J., Andersen, G., Kernebeck, B., Krupinska, K. (2003) Constitutive overexpression of barley 4–hydroxyphenylpyruvate dioxygenase in tobacco results in elevation of the vitamin E content in seeds but not in leaves. *FEBS Letters*, 540, 35–40.

Falk, J., Munne-Bosch, S. (2010) Tocochromanol functions in plants: antioxidation and beyond. *Journal of Experimental Botany,* 61, 1549–1566.

Fang, Z., Bouwkamp, J. C., Solomos, T. (1998) Chlorophyllase activities and chlorophyll degradation during leaf senescence in non-yellowing mutant and wild type of *Phaseolus vulgaris* L. *Journal of Experimental Botany*, 49, 503–510.

Fernie, A. R., Schauer, N. (2009) Metabolomics-assisted breeding: A viable option for crop improvement? *Trends Genetics*, 25, 39–48.

Fernie, A. R., Klee, H. J. (2011) The use of natural genetic diversity in the understanding of metabolic organization and regulation. *Frontiers in Plant Science*, 2, 59.

Food and Agriculture Organization of the United Nations. Tomato production. http://faostat.fao.org/ (2013). Data de acesso 20/05/15.

Fitzpatrick, A. H., Bhandari, J., Crowell, D. N. (2011) Farnesol kinase is involved in farnesol metabolism, ABA signaling and flower development in Arabidopsis. *The Plant Journal*, 66, 1078–1088.

Fitzpatrick, T. B., Basset, G. J. C., Borel, P., Carrari, F., DellaPenna, D., Fraser, P. D., *et al*. (2012) Vitamin Deficiencies in Humans: Can Plant Science Help? *The Plant Cell Online*, 24, 395–414.

Fraser, P. D., Enfissi, E. M. A, Halket, J. M., Truesdale, M. R., Yu, D., Gerrish, C., Bramley, P. M. (2007) Manipulation of phytoene levels in tomato fruit: effects on isoprenoids, plastids, and intermediary metabolism. *The Plant Cell*, 19, 3194–3211.

Foyer, C.H., Noctor, G. (2005) Redox homeostasis and antioxidant signaling: a metabolic interface between stress perception and physiological responses. *Plant Cell*, 17, 1866–1875.

Fujisawa, M., Nakano, T., Shima, Y., Ito, Y. (2013) A large-scale identification of direct targets of the tomato MADS Box transcription factor RIPENING INHIBITOR reveals the regulation of fruit ripening. *The Plant Cell*, 25, 371–386.

Fukuzawa, K., Matsuura, K., Tokumura, A., Suzuki, A., Terao, J. (1997) Kinetics and dynamics of singlet oxygen scavenging by alpha-tocopherol in phospholipid model membranes. *Free Radical Biology and Medicine*, 22, 923–930.

Gillaspy, G., Ben-David, H., Gruissem, W. (1993) Fruits: a developmental perspective. *The Plant Cell*, 5, 1439–1451.

Gilliland, L. U., Magallanes-Lundback, M., Hemming, C., Supplee, A., Koornneef, M., Bentsink, L., Dellapenna, D. (2006) Genetic basis for natural variation in seed vitamin E levels in Arabidopsis thaliana. *Proceedings of the National Academy of Sciences of the United States of America*, 103, 18834–18841.

Giovannoni, J. J. (2004) Genetic Regulation of Fruit Development and Ripening. *The Plant Cell,* 16, 170–181.

Giovannoni, J. J. (2007). Fruit ripening mutants yield insights into ripening control. *Current Opinion in Plant Biology*, 10, 283–289.

Grusak, M. A., DellaPenna, D. (1999) Improving the nutrient composition of plants to enhance human nutrition and health. *Annual Review of Plant Physiology and Plant Molecular Biology*, 50, 133–161.

Guyer, L., Schelbert H. S., Christ, B., Lira, B. S., Rossi, M., Hörtensteiner, S. (2014) Different mechanisms are responsible for chlorophyll dephytylation during fruit ripening and leaf senescence in tomato. *Plant Physiology,* 166, 44-56.

Haddadi, P., Ebrahimi, A., Langlade, N. B., Yazdi-samadi, B., Berger, M., Calmon, A., *et al*. (2012) Genetic dissection of tocopherol and phytosterol in recombinant inbred lines of sunflower through quantitative trait locus analysis and the candidate gene approach. *Molecular Breeding*, 29, 717–729.

Harpaz-Saad, S., Azoulay, T., Arazi, T., Ben-Yaakov, E., Mett, A., Shiboleth, Y.M., *et al*. (2007) Chlorophyllase is a rate-limiting enzyme in chlorophyll catabolism and is posttranslationally regulated. *The Plant Cell*, 19, 1007–1022.

Havaux, M., Eymery, F., Porfirova, S., Rey, P., Dörmann, P. (2005) Vitamin E protects against photoinhibition and photooxidative stress in Arabidopsis thaliana. *The Plant Cell*, 17, 3451–3469.

Havaux, M., García-Plazaola, J.I. (2014). Beyond non-photochemical fluorescence quenching: the overlapping antioxidant functions of zeaxanthin and tocopherols. Non-Photochemical Quenching and Energy Dissipation in Plants, Algae and Cyanobacteria. *Advances in Photosynthesis and Respiration*. *Springer Netherlands*, 583-603.

Hofius, D., Hajirezaei, M.-R., Geiger, M., Tschiersch, H., Melzer, M., Sonnewald, U. (2004) RNAi-mediated tocopherol deficiency impairs photoassimilate export in transgenic potato plants. *Plant Physiology*, 135, 1256–1268.

Hormaetxe, K., Esteban, R., Becerril, J. M., García-Plazaola, J. I. (2005) Dynamics of the α-tocopherol pool as affected by external (environmental) and internal (leaf age) factors in Buxus sempervirens leaves. *Physiologia Plantarum*, 125, 333–344.

Hunter, S. C., Cahoon, E. B. (2007) Enhancing vitamin E in oilseeds: Unraveling tocopherol and tocotrienol biosynthesis. *Lipids*, 42, 97–108.

Ischebeck, T., Zbierzak, A. M., Kanwischer, M., Dörmann, P. (2006) A salvage pathway for phytol metabolism in Arabidopsis. *The Journal of Biological Chemistry*, 281, 2470–2477.

Kaiser, S., Di Mascio, P., Murphy, M. E., Sies, H. (1990) Physical and chemical scavenging of singlet molecular oxygen by tocopherols. *Archives of Biochemistry and Biophysics*, 277, 101–108.

Kamal-Eldin, A., Appelqvist, L. A. (1996) The chemistry and antioxidant properties of tocopherols and tocotrienols. *Lipids*, 31, 671–701.

Karunanandaa, B., Qi, Q., Hao, M., Baszis, S. R., Jensen, P. K., Wong, Y. H. H., *et al*. (2005) Metabolically engineered oilseed crops with enhanced seed tocopherol. *Metabolic Engineering*, 7, 384–400.

Karlova, R., Rosin, F. M., Busscher-Lange, J., Parapunova, V., Do, P. T., Fernie, A. R., et al. (2011) Transcriptome and metabolite profiling show that APETALA2a is a major regulator of tomato fruit ripening. *The Plant Cell*, 23, 923–941.

Klee, H. J., Giovannoni, J. J. (2011) Genetics and control of tomato fruit ripening and quality attributes. *Annual Review of Genetics*, 45, 41–59.

Kobayashi, N., DellaPenna, D. (2008) Tocopherol metabolism, oxidation and recycling under high light stress in Arabidopsis. *The Plant Journal*, 55, 607–618.

Krieger-Liszkay, A., Trebst, A. (2006) Tocopherol is the scavenger of singlet oxygen produced by the triplet states of chlorophyll in the PSII reaction centre. *Journal of Experimental Botany*, 57, 1677–1684.

Kruk, J., Szymańska, R., Cela, J., Munne-Bosch, S. (2014) Plastochromanol-8: Fifty years of research. *Phytochemistry*, 108, 9–16.

Kushi, L. H., Folsom, A. R., Prineas, R. J., Mink, P. J., Wu, Y., Bostic, R. M. (1996) Dietary antioxidant vitamins and death from coronary heart disease in postmenopausal women. *New England Journal of Medicine*, 334, 1156–1162.

Lichtenthaler, H.K. (2007) Biosynthesis, accumulation and emission of carotenoids, a-tocopherol, plastoquinone, and isoprene in leaves under high photosynthetic irradiance. *Photosynthesis Research*, 92, 163–179.

Lira, B. S., de Setta, N., Rosado, D., Almeida, J., Freschi, L., Rossi, M. (2014) Plant degreening: evolution and expression of tomato (*Solanum lycopersicum*) dephytylation enzymes. *Gene*, 546, 359-366.

Lipka, A. E., Gore, M. A., Magallanes-Lundback, M., Mesberg, A., Lin, H., Tiede, T., *et al*. (2013) Genome-wide association study and pathway-level analysis of tocochromanol levels in maize grain. *G3: Genes| Genomes| Genetics*, 3, 1287-1299.

Lippman, Z. B., Semel, Y., Zamir, D. (2007) An integrated view of quantitative trait variation using tomato interspecific introgression lines. *Current Opinion in Genetics & Development*, 17, 545–552.

Lundquist, P. K., Poliakov, A., Bhuiyan, N. H., Zybailov, B., Sun, Q., van Wijk, K. J. (2012) The Functional Network of the Arabidopsis Plastoglobule Proteome Based on Quantitative Proteomics and Genome-Wide Coexpression Analysis. *Plant Physiology*, 158, 1172-1192.

Maeda, H., Song, W., Sage, T. L., DellaPenna, D. (2006) Tocopherols play a crucial role in low-temperature adaptation and Phloem loading in Arabidopsis. *Plant Cell*, 18, 2710–2732.

Maeda, H., Sage, T. L., Isaac, G., Welti, R., Dellapenna, D. (2008) Tocopherols modulate extraplastidic polyunsaturated fatty acid metabolism in Arabidopsis at low temperature. *Plant Cell*, 20, 452–470.

Martel, C., Vrebalov, J., Tafelmeyer, P., Giovannoni, J. J. (2011) The tomato MADS-box transcription factor RIPENING INHIBITOR interacts with promoters involved in numerous ripening processes in a COLORLESS NONRIPENING-dependent manner. *Plant Physiology*, 157, 1568–1579.

Matile, P., Hortensteiner, S., Thomas, H., Krautler, B. (1996). Chlorophyll Breakdown in Senescent Leaves. *Plant Physiology*, 112, 1403–1409.

Miret, J. A., Munné-Bosch, S. (2015) Redox signaling and stress tolerance in plants: a focus on vitamin E. *Annals of the New York Academy of Sciences*, 1340, 29-38.

Munné-Bosch, S., Alegre, L. (2002) The function of tocopherols and tocotrienols in plants. *Critical Reviews in Plant Sciences*, 21, 31–57.

Munné-Bosch, S., Falk, J. (2004) New insights into the function of tocopherols in plants. *Planta*, 218, 323–326.

Munné-Bosch, S. (2005) The role of α-tocopherol in plant stress tolerance. *Journal of Plant Physiology*, 162, 743–748.

Nashilevitz, S., Melamed-Bessudo, C., Izkovich, Y., Rogachev, I., Osorio, S., Itkin, M., *et al*. (2010) An orange ripening mutant links plastid NAD(P)H dehydrogenase complex activity to central and specialized metabolism during tomato fruit maturation. *The Plant Cell*, 22, 1977–97.

Osorio, S., Scossa, F., Fernie, A. R. (2013) Molecular regulation of fruit ripening. *Frontiers in Plant Science*, 4, 198.

Peralta, I. E., Knapp, S. K., Spooner, D. M. (2005) New species of wild tomatoes (Solanum section Lycopersicon: Solanaceae) from Northern Peru. *Systematic Botany*, 30, 424–434.

Perez-Fons, L., Wells, T., Corol, D. I., Ward, J. L., Gerrish, C., Beale, M. H., *et al*. (2014) A genome-wide metabolomic resource for tomato fruit from Solanum pennellii. *Scientific Reports*, 4, 3859.

Provencher, L. M., Miao, L., Sinha, N., Lucas, W. J. (2001) Sucrose export defective1 encodes a novel protein implicated in chloroplast-to-nucleus signaling. *The Plant Cell*, 13, 1127–1141.

Quadrana, L., Rodriguez, M. C., Lopez, M., Bermudez, L. M., Nunes-Nesi, A., Fernie, A. R., *et al*. (2011) Coupling virus induced gene silencing to exogenous green fluorescence protein expression provides a highly efficient system for functional genomics, in Arabidopsis and across all stages of tomato fruit development. *Plant Physiology*, 56, 1278–1291.

Rastogi, A., Yadav, D. K., Szymanska, R., Kruk, J., Sedlárová, M., Pospíšil, P. (2014) Singlet oxygen scavenging activity of tocopherol and plastochromanol in Arabidopsis thaliana: relevance to photooxidative stress. *Plant, Cell & Environment*, 37, 392–401.

Ricciarelli, R., Zingg, J., Azzi, A. (2002) The 80 th Anniversary of Vitamin E: Beyond Its Antioxidant Properties. *Biological Chemistry*, 383, 457-465.

Rippert, P., Matringe, M. (2002) Purification and kinetic analysis of the two recombinant arogenate dehydrogenase isoforms of Arabidopsis thaliana. *European Journal of Biochemistry*, 269, 4753–4761.

Rippert, P., Scimemi, C., Dubald, M. and Matringe, M. (2004) Engineering plant shikimate pathway for production of tocotrienol and improving herbicide resistance. *Plant Physiology*, 134, 92–100.

Rise, M., Cojocaru, M., Gottlieb, H. E., Goldschmidt, E. E. (1989) Accumulation of a-Tocopherol in Senescing Organs as Related to Chlorophyll Degradation. *Plant Physiology*, 89, 1028-1030.

Rothan, C., Causse, M. (2007) Natural and artificially induced genetic variability in crop and model plant species for plant systems biology. *Plant Systems Biology*, 97, 21-53.

Sanders, S. K., Morgan, J. B., Wulf, D. M., Tatum, J. D., Williams, S. N., Smith, G. C. (1997) Vitamin E supplementation of cattle and shelf-life of beef for the Japanese market. *Journal of Animal Science*, 75, 2634–2640.

Sattler, S. E., Gilliland, L. U., Magallanes-lundback, M., Pollard, M., Dellapenna, D. (2004) Vitamin E Is Essential for Seed Longevity and for Preventing Lipid Peroxidation during Germination. *The Plant Cell*, 16, 1419–1432.

Schauer, N., Zamir, D., Fernie, A. R. (2005) Metabolic profiling of leaves and fruit of wild species tomato: a survey of the Solanum lycopersicon complex. *Journal of Experimental Botany*, 56, 297–307.

Schauer, N., Semel, Y., Roessner, U., Gur, A., Balbo, I., Carrari, F., *et al*. (2006) Comprehensive metabolic profiling and phenotyping of interspecific introgression lines for tomato improvement. *Nature Biotechnology*, 24, 447–54.

Schenck, C. A., Chen, S., Siehl, D. L., Maeda, H. A. (2014) Non-plastidic, tyrosine-insensitive prephenate dehydrogenases from legumes. *Nature Chemical Biology*, 11, 52–57.

Schenk, N., Schelbert, S., Kanwischer, M., Goldschmidt, E. E., Dörmann, P., Hörtensteiner, S. (2007). The chlorophyllases AtCLH1 and AtCLH2 are not essential for senescence-related chlorophyll breakdown in Arabidopsis thaliana. *FEBS Letters*, 581, 5517–5525.

Serbinova, E., Kagan, V., Han, D., Packer, L. (1991) Free radical recycling and intramembrane mobility in the antioxidant properties of alpha-tocopherol and alpha-tocotrienol. *Free Radical Biology and Medicine*, 10, 263–275.

Seo, Y. S., Kim, S. J., Harn, C. H., Kim, W. T. (2011) Ectopic expression of apple fruit homogentisate phytyltransferase gene (MdHPT1) increases tocopherol in transgenic tomato (*Solanum lycopersicum* cv. Micro-Tom) leaves and fruits. *Phytochemistry*, 72, 321–329.

Seymour, G. B., Østergaard, L., Chapman, N. H., Knapp, S., Martin, C. (2013) Fruit development and ripening. *The Annual Review of Plant Biology*, 64, 219–241.

Schelbert, S., Aubry, S., Burla, B., Agne, B., Kessler, F., Krupinska, K., Hörtensteiner, S. (2009) Pheophytin pheophorbide hydrolase (pheophytinase) is involved in chlorophyll breakdown during leaf senescence in Arabidopsis. *The Plant Cell*, 21, 767–785.

Shibata, D. (2005) Genome sequencing and functional genomics approaches in tomato. *Journal of General Plant Pathology*, 71, 1–7.

Shintani, D., DellaPenna, D. (1998) Elevating the vitamin E contente of plants through metabolic engineering. *Science*, 282, 2098–2100.

Shutu, X., Dalong, Z., Ye, C., Yi, Z., Shah, T., Ali, F., *et al*. (2012) Dissecting tocopherols content in maize (Zea mays L.), using two segregating populations and high-density single nucleotide polymorphism markers. *BMC Plant Biology*, 12, 201.

Soll, J., Schultz, G., Joyard, J., Douce, R., Block, M.A. (1985) Localization and synthesis of prenylquinones in isolated outer and inner envelope membranes from spinach chloroplasts. *Archives of Biochemistry and Biophysics*, 238, 290–299.

Steinhauser, M., Steinhauser, D., Gibon, Y., Bolger, M., Arrivault, S., Usadel, B., *et al*. (2011) Identification of enzyme activity quantitative trait loci in a *Solanum lycopersicum* x *Solanum pennellii* introgression line population. *Plant Physiology*, 157, 998–1014.

Stitt, M., Sulpice, R., Keurentjes, J. (2010) Metabolic networks: how to identify key components in the regulation of metabolism and growth? *Plant Physiology*, 152, 428–444.

Thai, L., Rush, J. S., Maul, J. E., Devarenne, T., Rodgers, D. L., Chappell, J., Waechter, C. J. (1999) Farnesol is utilized for isoprenoid biosynthesis in plant cells via farnesyl pyrophosphate formed by successive monophosphorylation reactions. *Proceedings of the National Academy of Sciences of the United States of America*, 96, 13080–13085.

Takamiya, K. I., Tsuchiya, T., Ohta, H. (2000) Degradation pathway(s) of chlorophyll: what has gene cloning revealed? *Trends in Plant Science*, 5, 426–43.

Tomato Genome Consortium. (2012). The tomato genome sequence provides insights into fleshy fruit evolution. *Nature*, 485, 635-641

Traber, M. G., Atkinson, J. (2008). Vitamin E, antioxidant and nothing more. *Free Radical Biology and Medicine*, 43, 4-15.

Traber, M. G., Sies, H. (1996) Vitamin E in humans: demand and delivery. *Annual Review of Nutrition*, 16, 321–347.

Triantaphylidès, C., Havaux, M. (2009) Singlet oxygen in plants: production, detoxification and signaling. *Trends in Plant Science*, 14, 219–228.

Tsegaye, Y., Shintani, D. K., DellaPenna, D. (2002) Overexpression of the enzyme p–hydroxyphenolpyruvate dioxygenase in Arabidopsis and its relation to tocopherol biosynthesis. *Plant Physiology and Biochemistry*, 40, 913–920.

Tzin, V., Galili, G. (2010) New insights into the shikimate and aromatic amino acids biosynthesis pathways in plants. *Molecular Plant*, 3, 956–972.

Valentin, H. E., Lincoln, K., Moshiri, F., Jensen, P. K., Qi, Q., Venkatesh, T. V., *et al*. (2006) The Arabidopsis vitamin E pathway gene5-1 mutant reveals a critical role for phytol kinase in seed tocopherol biosynthesis. *The Plant Cell*, 18, 212–224.

Van Eenennaam, A. L., Lincoln, K., Durrett, T. P., Valentin, H. E., Shewmaker, C. K., Thorne, G. M., *et al*. (2003) Engineering vitamin E content: From Arabidopsis mutant to soy oil. *The Plant Cell*, 15, 3007–3019.

Vidi, P. A., Kanwischer, M., Baginsky, S., Austin, J. R., Csucs, G., Dörmann, P., *et al*. (2006) Tocopherol cyclase (VTE1) localization and vitamin E accumulation in chloroplast plastoglobule lipoprotein particles. *Journal of Biological Chemistry*, 281, 11225–11234.

Wang, X., Zhang, C., Li, L., Fritsche, S., Endrigkeit, J., Zhang, W., *et al*. (2012) Unraveling the Genetic Basis of Seed Tocopherol Content and Composition in Rapeseed (*Brassica napus* L.). *Plos One*, 7, 8–14.

Wright, M. E., Lawson, K. A., Weinstein, S. J., Pietinen, P., Taylor, P. R., Virtamo, J., *et al.* (2006) Higher baseline serum concentrations of vitamin E are associated with lower total and cause-specific mortality in the Alpha-Tocopherol, Beta-Carotene Cancer Prevention Study. *The American Journal of Clinical Nutrition*, 84, 1200–1207.

Yamauchi, N., Watada, A. E. (1991). Regulated Chlorophyll Degradation in Spinach Leaves during Storage. *Journal of the America Society for Horticultural Science*, 116, 58–62.

Zamir, D. (2001) Improving plant breeding with exotic genetic libraries. *Nature Reviews Genetics*, 2, 983–989.

Zbierzak, A. M., Kanwischer, M., Wille, C., Vidi, P. A., Giavalisco, P., Lohmann, A., *et al*. (2010) Intersection of the tocopherol and plastoquinol metabolic pathways at the plastoglobule. *Biochemical Journal*, 425, 389–399.

Zhang, C., Cahoon, R. E., Hunter, S. C., Chen, M., Han, J., Cahoon, E. B. (2013) Genetic and biochemical basis for alternative routes of tocotrienol biosynthesis for enhanced vitamin E antioxidant production. *The Plant Journal*, 73, 628–39.

Zhong, S., Fei, Z., Chen, Y.-R., Zheng, Y., Huang, M., Vrebalov, J., *et al.* (2013) Single-base resolution methylomes of tomato fruit development reveal epigenome modifications associated with ripening. *Nature Biotechnology*, 31, 154–159.

OBJETIVOS

O presente trabalho visa aprofundar o conhecimento sobre a regulação da rota biossintética de vitamina E em tomateiro. Para tanto, elegeram-se duas estratégias, em essência, com base no conjunto de dados prévios estabelecidos por Almeida *et al.* (2011). Na primeira, investigou-se a associação entre a regulação transcricional dos genes envolvidos na biossíntese de tocoferol e o acúmulo desse antioxidante a partir de duas perspectivas: à luz do desenvolvimento de tomateiro e da variação alélica natural presente tanto nas linhagens introgredidas de *S. pennellii,* quanto em mutantes de tomateiro deficientes nos processos de amadurecimento e de degradação da clorofila. Na segunda abordagem, elegeu-se o metabolismo do fitol como foco para a manipulação metabólica, circunscrevendo, em particular, os papéis desempenhados por VTE5, FOLK e CLH(1). Dessa maneira, buscou-se compreender o papel da reciclagem do fitol provindo da degradação de clorofila no suprimento da cadeia isoprênica para síntese de tocoferóis e sua relação com as demais vias metabólicas plastidiais em folhas e em frutos de tomateiro. Formulado nesses termos, para o desenvolvimento deste trabalho foram propostos os seguintes objetivos:

i. Estudar a regulação transcricional da rota biossintética de tocoferóis (Capítulo I).
ii. Analisar o perfil transcricional dos genes associados à biossíntese de VTE em linhagens introgredidas (IL) que apresentam aumento no conteúdo de tocoferóis (Capítulo II).
iii. Estudar a contribuição dos genes *CLOROFILASE 1*, *FARNESOL QUINASE* e *FITOL QUINASE* no conteúdo de tocoferóis em frutos de tomateiro via silenciamento gênico induzido por vírus (Capítulo III).
iv. Avaliar o conteúdo de tocoferóis em mutantes de tomateiro deficientes no amadurecimento de fruto, na degradação de clorofila e na percepção de ácido jasmônico (Capítulo IV).
v. Caracterizar funcionalmente o gene *CLOROFILASE 1* (Capítulo V).
vi. Caracterizar funcionalmente o gene *FITOL QUINASE* (Capítulo VI).

CAPÍTULO I. ESTUDO DA REGULAÇÃO TRANSCRICIONAL DA ROTA BIOSSINTÉTICA DE TOCOFERÓIS EM TOMATEIRO

Os resultados, material e métodos e discussão deste capítulo são apresentados na forma de artigo publicado no periódico *Plant Molecular Biology*. O material suplementar corresponde ao Anexo I.

Quadrana L*, **Almeida J***, Otaiza S, Duffy T, Correa-Silva JV, de Godoy F, Asís R, Bermudez L, Fernie A, Carrari F, Rossi M. (2013). Transcriptional regulation of vitamin E biosynthesis in tomato. *Plant Molecular Biology,* 81, 309-325.

* *Contribuição equivalente.*

Resumo

Tocoferóis, compostos com atividade de vitamina E (VTE), são potentes antioxidantes lipossolúveis produzidos exclusivamente por organismos fotossintetizantes. A biossíntese desses compostos ocorre a partir da condensação dos precursores fitil-difosfato e homogentisato provenientes das vias do metil-eritritol fosfato (MEP) e chiquimato (SK), respectivamente. Tais vias metabólicas são centrais no metabolismo do cloroplasto e estão envolvidas na biossíntese de moléculas importantes como clorofilas, carotenóides, aminoácidos aromáticos e prenilquinonas. Na última década, alguns estudos evidenciaram aspectos relacionados à regulação e ao acúmulo de VTE em plantas. Entretanto, os mecanismos regulatórios dessa via nos níveis de mRNA permanecem não esclarecidos. Recentemente, nosso grupo identificou uma coleção de genes envolvidos na biossíntese de tocoferol em tomateiro. No presente trabalho, por meio de uma plataforma de *array* para PCR quantitativa (qPCR), os níveis dos transcritos de 47 genes, incluindo parálogos, foram determinados em folhas e ao longo do desenvolvimento do fruto. A correlação dos dados de expressão com os perfis de tocoferóis foi analisada por meio de abordagens de agrupamentos neurais e redes de corregulação. Os resultados mostraram que a biossíntese de tocoferol é controlada tanto temporalmente quanto espacialmente, contudo os níveis desse composto permanecem constantes. Estas análises expuseram 18 genes chaves envolvidos nas vias do MEP, SK, reciclagem do fitol e rota central de tocoferol, os quais estão altamente associados ao conteúdo de tocoferóis em folhas e frutos. Além disso, análises genômicas das regiões promotoras sugerem que a expressão dos genes da rota central do tocoferol é corregulada transcricionalmente com genes específicos das vias precursoras. Enquanto em frutos, os perfis transcricionais dos genes das vias precursoras sugerem um aumento do conteúdo de VTE ao longo do desenvolvimento, os dados indicam que no cultivar M82, o suprimento de fitil-difosfato

limita a síntese de tocoferol nos estádios avançados do fruto. Isto ocorre, em parte, devido à redução nos níveis de transcritos de *GERANILGERANIL REDUTASE* (*GGDR*) que restringe a disponibilidade do precursor isoprenóide. Como prova de conceito, por meio da análise de uma coleção de cultivares locais andinos, a função dos genes identificados na determinação do conteúdo de tocoferol pode ser confirmada. Esses resultados revelaram uma regulação bem sintonizada capaz de alterar as vias precursoras, controlando o influxo de substrato para biossíntese de VTE e superando a competição endógena por intermediários. Finalmente, o conjunto completo de dados permite propor que os genes codificantes para as enzimas 1-DEOXI-D-XILULOSE-5-FOSFATO SINTASE (DXS) e GGDR, os quais determinam a disponibilidade de fitil-difosfato, juntamente com os genes envolvidos no metabolismo de fitol derivado da clorofila aparecem como possíveis alvos de manipulação, visando melhorar os valores nutricionais do fruto de tomate.

Plant Mol Biol (2013) 81:309–325
DOI 10.1007/s11103-012-0001-4

Transcriptional regulation of tocopherol biosynthesis in tomato

Leandro Quadrana · Juliana Almeida · Santiago N. Otaiza · Tomas Duffy · Junia V. Corrêa da Silva · Fabiana de Godoy · Ramon Asís · Luisa Bermúdez · Alisdair R. Fernie · Fernando Carrari · Magdalena Rossi

Received: 11 September 2012 / Accepted: 10 December 2012 / Published online: 18 December 2012
© Springer Science+Business Media Dordrecht 2012

Abstract Tocopherols, compounds with vitamin E (VTE) activity, are potent lipid-soluble antioxidants synthesized only by photosynthetic organisms. Their biosynthesis requires the condensation of phytyl-diphosphate and homogentisate, derived from the methylerythritol phosphate (MEP) and shikimate pathways (SK), respectively. These metabolic pathways are central in plant chloroplast metabolism and are involved in the biosynthesis of important molecules such as chlorophyll, carotenoids, aromatic amino-acids and prenylquinones. In the last decade, few studies have provided insights into the regulation of VTE biosynthesis and its accumulation. However, the pathway regulatory mechanism/s at mRNA level remains unclear. We have recently identified a collection of tomato genes involved in tocopherol biosynthesis. In this work, by a dedicated qPCR array platform, the transcript levels of 47 genes, including paralogs, were determined in leaves and across fruit development. Expression data were analyzed for correlation with tocopherol profiles by coregulation network and neural clustering approaches. The results showed that tocopherol biosynthesis is controlled both temporally and spatially however total tocopherol content remains constant. These analyses exposed 18 key genes from MEP, SK, phytol recycling and VTE-core pathways highly associated with VTE content in leaves and fruits. Moreover, genomic analyses of promoter regions suggested that the expression of the tocopherol-core pathway genes is trancriptionally coregulated with specific genes of

Leandro Quadrana, Juliana Almeida, Fernando Carrari and Magdalena Rossi contributed equally to this work.

Electronic supplementary material The online version of this article (doi:10.1007/s11103-012-0001-4) contains supplementary material, which is available to authorized users.

L. Quadrana · T. Duffy · F. Carrari
Instituto de Biotecnología, Instituto Nacional de Tecnología Agropecuaria and Consejo Nacional de Investigaciones Científicas y Técnicas, PO Box 25, B1712WAA Castelar, Argentina
e-mail: lquadrana@cnia.inta.gov.ar

T. Duffy
e-mail: tduffy@cnia.inta.gov.ar

F. Carrari
e-mail: fcarrari@cnia.inta.gov.ar

J. Almeida · J. V. Corrêa da Silva · F. de Godoy · L. Bermúdez · M. Rossi (✉)
Departamento de Botânica, Instituto de Biociências, Universidade de São Paulo, Rua do Matão 277, São Paulo, SP 05508-900, Brazil
e-mail: mmrossi@usp.br

J. Almeida
e-mail: juliana.almeida.silva@usp.br

J. V. Corrêa da Silva
e-mail: juniavcs@gmail.com

F. de Godoy
e-mail: fabidegodoy@hotmail.com

L. Bermúdez
e-mail: lubhe0@gmail.com

S. N. Otaiza · R. Asís
CIBICI, Facultad de Ciencias Químicas, Universidad Nacional de Córdoba, CC 5000 Córdoba, Argentina
e-mail: santiagootaiza@hotmail.com

R. Asís
e-mail: rasis@mail.fcq.unc.edu.ar

A. R. Fernie
Max Planck Institute for Molecular Plant Physiology, Wissenschaftspark Gölm, Am Mühlenberg 1, 14476 Potsdam-Golm, Germany
e-mail: fernie@mpimp-golm.mpg.de

the upstream pathways. Whilst the transcriptional profiles of the precursor pathway genes would suggest an increase in VTE content across fruit development, the data indicate that in the M82 cultivar phytyl diphosphate supply limits tocopherol biosynthesis in later fruit stages. This is in part due to the decreasing transcript levels of geranylgeranyl reductase (*GGDR*) which restricts the isoprenoid precursor availability. As a proof of concept, by analyzing a collection of Andean landrace tomato genotypes, the role of the pinpointed genes in determining fruit tocopherol content was confirmed. The results uncovered a finely tuned regulation able to shift the precursor pathways controlling substrate influx for VTE biosynthesis and overcoming endogenous competition for intermediates. The whole set of data allowed to propose that 1-deoxy-D-xylulose-5-phosphate synthase and *GGDR* encoding genes, which determine phytyl-diphosphate availability, together with enzyme encoding genes involved in chlorophyll-derived phytol metabolism appear as the most plausible targets to be engineered aiming to improve tomato fruit nutritional value.

Keywords Tomato · Metabolism · Tocopherol · Vitamin E · Transcriptional regulation

Introduction

Plants, like all aerobic organisms, have evolved a complex antioxidant system to regulate the intracellular redox status while avoiding the deleterious oxidation of cellular components caused by reactive oxygen species (ROS) (Apel and Hirt 2004). Tocopherols and tocotrienols, collectively referred to as vitamin E (VTE), are non-enzymatic lipid-soluble antioxidants synthesized only by photosynthetic organisms. Beside other roles, VTE compounds inhibit lipid peroxidation and protect photosystem II from oxidative damage by scavenging lipid peroxyl radicals and singlet oxygen. (Munné-Bosch and Alegre 2002; Falk and Munné-Bosch 2010; Takahashi and Badger 2011; Loyola et al. 2012). VTE compounds are tocochromanols; thus, they contain a polar chromanol group originated from homogentisate which derives from shikimate (SK) pathway and an isoprenoid-derived chain which results from the plastidial methylerythritol phosphate (MEP) pathway. The first step of the tocopherol-core pathway, catalyzed by 4-hydroxyphenylpyruvate dioxygenase (HPPD), involves reduction of 4-hydroxyphenylpyruvate to homogentisate, which further is decarboxylated and then condensated with a prenyl donor by a specific prenyltransferase; homogentisate phytyl transferase (VTE2) (reviewed by Munné-Bosch and Alegre 2002). It has been demonstrated that the prenyl donor for tocopherol biosynthesis, phytyl diphosphate, can also be originated from phytol recycling after chlorophyll degradation by a phytol kinase (VTE5) (Valentin et al. 2006). There are four natural forms of tocopherol (α, β, γ and δ) which differ in the position and number of methyl groups on the chromanol ring and are products of the reactions catalyzed by 2-methyl-6-phytyl-1,4-benzoquinol methyltransferase (VTE3), tocopherol cyclase (VTE1) and γ-tocopherol methyl transferase (VTE4) (Munné-Bosch and Alegre 2002). Despite all tocochromanols are potent antioxidants in vitro, α-tocopherol presents the highest VTE activity in humans and animals (Traber and Sies 1996).

Although a considerable amount of information has been accumulated, the knowledge concerning the molecular mechanisms regulating tocopherol biosynthesis remains fragmentary. Enzyme encoding genes involved in the MEP pathway have been found to be transcriptionally activated during plant development in Arabidopsis, suggesting the presence of common transcription factor binding motifs in the promoter regions of these genes (Guevara-García et al. 2005). In this sense, it has been demonstrated that MEP pathway genes are coordinately upregulated by light in Arabidopsis seedlings (Córdoba et al. 2009). On the other hand, regulation of carbon flux through the SK pathway is much less well understood. Recently, 3-deoxy-D-arabino-heptulosonate 7-phosphate synthase (DAHPS) has showed to be a rate-limiting factor in this pathway (Tzin et al. 2012). Besides, some transcription factors have been revealed to influence MEP and SK pathways but the mechanism by which this is achieved remains unclear. In tomato, the overexpression of the MYB transcription factor *ODORANT1* led to a significant increase in phenylpropanoid content concomitantly with transcriptional upregulation of several SK pathway genes (Dal Cin et al. 2011). Furthermore, downregulation of *DET1,* which is involved in the suppression of light responses in the absence of light in tomato fruit, resulted in increased contents of carotenoids, flavonoids and tocopherol (Enfissi et al. 2010). Regarding the last steps in tocopherol biosynthesis, several reports have described the effect of gene overexpression on tocopherol profiles, highlighting the role of *HPPD* and *VTE2* in determining total tocopherol content, and *VTE1*, *VTE3* and *VTE4* in shaping tocopherol composition (reviewed by Dellapenna and Mène-Saffrané 2011). However, systematic studies about the spatio-temporal regulatory network of gene expression and VTE contents have not been boarded. Nor a comparative analysis of the *cis*-regulatory motifs in the promoter regions of the MEP, SK and tocopherol-core pathway genes have been studied to date.

Cultivated tomato (*Solanum lycopersicum*) is one of the most globally consumed vegetables and has been intensively used as model system of plants bearing fleshy fruits (Yelle et al. 1991; Rose et al. 2004; Alba et al. 2005; Carrari et al. 2006; Klee 2010). Measurements of tocopherol in ripe tomatoes (Moco et al. 2007; Meléndez-Martínez et al. 2010) suggest that this vegetable is an important source of VTE. Likewise, genes involved in the MEP, SK

and tocopherol-core pathways have been recently identified and mapped onto the tomato genome. In addition, quantitative trait loci (QTL) for tocopherol content have been identified and some of them co-localize with tocochromanol biosynthetic genes, emerging as strong candidates for exploring the allelic natural variation present in this plant species (Almeida et al. 2011). This will not only represent an important resource for biotechnological applications but also likely prove instrumental in improving our understanding of the intricate regulation circuit that operates in these pathways (Fitzpatrick et al. 2012).

In this work, we developed a dedicated qPCR array for a global analysis of the transcript profiles of all tocopherol biosynthetic genes in photosynthetic tissues and across tomato fruit development. Results were analyzed in parallel with tocopherol and pigment profiles. Network analyses provided insights into the relationship between tocopherol content and spatio-temporal mRNA accumulation of the biosynthetic pathway genes, exposing key regulatory points that were confirmed in Andean landrace genotypes. Furthermore, bioinformatics tools allowed the identification of *cis*-regulatory motifs in the promoter regions of coregulated genes which could be acting as binding sites for shared transcription factors. In sum, the results allowed to suggest possible targets for metabolic engineering of this important nutraceutical trait in tomato.

Results

Vitamin E and pigment contents in tomato

To study the spatial and temporal variation of tocopherol levels in tomato (cv M82), the quantitative profile of α, β, γ and δ forms was determined in source and sink leaves, and in pericarp along fruit development (in green, mature green, breaker and ripe stages). Additionally, the levels of total carotene, lycopene and chlorophylls were determined at the same stages of fruit development (Table 1). Since only traces of tocotrienols were detected in these samples, as in agreement with previous reports (Horvath et al. 2006a), these compounds were not considered here.

Total tocopherol was approximately twofold more abundant in leaves than in fruits and; all the samples analyzed showed detectable amounts of each tocopherol form, although at variable levels. The main VTE-active molecule, α-tocopherol, was the most abundant species both in leaves and fruits, contributing up to 97 % of the total VTE in the mature green fruits but essentially being invariant across tissues. While the profile of the least abundant tocopherol forms kept invariant between source and sink leaves, it varied along fruit development (Table 1).

As expected, whereas total carotene and lycopene displayed a massive increase at the fruit ripe stage, 6- and 29-fold higher than that observed at the mature green stage, respectively; the chlorophyll contents decreased during fruit development down to undetectable levels, reflecting the transition from chloroplasts to chromoplasts and the consequent metabolic changes during the ripening of tomato fruit (Table 1).

Expression profile of the genes encoding vitamin E biosynthesis enzymes

Almeida et al. (2011) identified, characterized and mapped the enzyme encoding genes involved in VTE biosynthetic pathways of tomato. On the basis of this information, a qPCR array was developed to address the variation of

Table 1 Tocopherol, lycopene, total carotene and chlorophylls content in tomato

	Leaves			Fruits		
	Source	Sink	Green	Mature green	Breaker	Ripe
α-tocopherol	17.92 ± 2.99^{a}	$15.45 \pm 2.83^{(a,b)}$	$9.11 \pm 1.55^{(b)}$	$7.43 \pm 1.01^{(b)}$	$10.54 \pm 0.44^{(b)}$	$9.74 \pm 0.65^{(b)}$
β-tocopherol	$0.60 \pm 0.12^{(a)}$	$0.63 \pm 0.15^{(a)}$	$1.13 \pm 0.44^{(a)}$	$0.13 \pm 0.05^{(b)}$	$0.14 \pm 0.00^{(b)}$	$0.15 \pm 0.01^{(b)}$
δ-tocopherol	$2.62 \pm 0.77^{(a)}$	$4.43 \pm 1.04^{(a)}$	$0.26 \pm 0.04^{(a)}$	$0.02 \pm 0.00^{(b)}$	$0.02 \pm 0.01^{(b)}$	$0.11 \pm 0.03^{(a)}$
γ-tocopherol	$0.79 \pm 0.17^{(a)}$	$1.26 \pm 0.21^{(a)}$	$0.17 \pm 0.05^{(b)}$	$0.09 \pm 0.03^{(b)}$	$0.72 \pm 0.10^{(a)}$	$1.64 \pm 0.49^{(a)}$
Total tocopherol	$21.93 \pm 2.49^{(a)}$	$21.77 \pm 10.10^{(a)}$	$10.67 \pm 1.46^{(b)}$	$7.67 \pm 1.07^{(b)}$	$11.42 \pm 0.55^{(b)}$	$11.64 \pm 0.28^{(b)}$
Lycopene	–	–	$3.02 \pm 1.12^{(a)}$	$1.86 \pm 0.56^{(a)}$	$4.60 \pm 1.28^{(a)}$	$54.02 \pm 11.32^{(b)}$
Total carotene	–	–	$6.76 \pm 0.79^{(a)}$	$2.43 \pm 0.35^{(a,b)}$	$3.41 \pm 0.16^{(b)}$	$15.26 \pm 2.29^{(c)}$
Chlorophyll a	$532.98 \pm 29.99^{(a)}$	$426.18 \pm 22.80^{(b)}$	$12.16 \pm 0.95^{(c)}$	$9.08 \pm 1.22^{(c)}$	$3.57 \pm 1.39^{(d)}$	nd
Chlorophyll b	$142.89 \pm 21.99^{(a)}$	$110.77 \pm 11.73^{(a)}$	$3.76 \pm 0.38^{(b)}$	$4.05 \pm 0.88^{(b)}$	$3.76 \pm 2.29^{(b)}$	nd

Tomato plant samples (cv. M82) were grown in greenhouse under controlled conditions as described in "Materials and methods". Values are expressed in μg gFW^{-1} and are means ± SE from 4 to 6 replicates. Different letters indicate statistically significant differences between tissues detected by the Tukey tests ($p < 0.05$)

nd non detected, – non measured

mRNA levels of these genes along with the fluctuation in tocopherol and pigment contents. For this purpose, specific primer pairs were designed for 16 MEP, 16 SK, 9 tocopherol-core, and 6 tocopherol-related pathway genes. Figure 1 displays a heat map presenting a global view of the normalized expression patterns for all VTE biosynthetic pathway genes in source and sink leaves as well as in green, mature green, breaker and ripe fruits from the *S. lycopersicum* cv M82. It can be observed that, with the exception of *DXS(2)* and *TYRA(2)* at the breaker and mature green stages, respectively, the complete set of genes were expressed in all the samples analyzed (Table S1). Interestingly, paralogous genes showed differences in expression profiles, suggesting a spatio-temporal specificity. In this sense, for five pairs of paralogs (*IPI*, *GGPS*, *CS*, *CM* and *TAT*) the correlation analysis displayed opposite patterns of expression (Fig. S1).

It is worth mentioning that both precursor pathways of VTE synthesis, MEP and SK, also provide intermediates for a plethora of plastid-synthesized compounds whose levels are tightly controlled during plant development (Vranová et al. 2012). Thus, it is expected that the contents of the end-products depend, at least in part, on the control of mRNA levels of the enzyme encoding genes that supply the needed precursor metabolites. This is suggested by the principal component analysis (PCA) of the gene expression data, where the first two dimensions explained 67.8 % of the data variance for all the samples analyzed and separated both organs and developmental stages (Fig. 2).

In summary, the results presented here clearly reveal that there are several steps along the carbon flux through tocopherol biosynthesis that are both temporally and spatially regulated at the mRNA levels of the enzyme encoding gene.

Coordinated changes in gene transcript levels and tocopherol contents in tomato leaves and fruits

To better understand the impact of the variation in gene mRNA levels on VTE content, two different approaches were taken. First, a weighted coregulation network analysis including mRNA and metabolites quantification data from leaves and fruits was performed (Zhang and Horvath 2005). This approach assigns a connection weight to each gene/metabolite pair showing a coordinated expression and allowed the identification of one well defined cluster consisting of genes highly associated to pigments and VTE content (Fig. 3). This cluster showed a median number of neighbors of 6 (Table S2) and, as expected, chlorophyll a and b were centrally positioned in the network. Eleven genes (out of those 18 weighted by the analysis) showed at least 6 links. Interestingly, *VTE3(2)* gene resulted in the most interconnected node with 20 directed edges. Furthermore, it was highly linked to tocopherol, but neither with lycopene nor with total carotene thus, exposing this gene as the major hub in the regulatory circuit of VTE contents in tomato tissues. *VTE4* and *HPPD(1)* of the tocopherol core-pathway; *DXR, GGDR* and *GGPS(1)* of the MEP; *CM(2), TAT(2)* and *PAT* of the SK pathway as well as *CLH* and *FPGS* also showed a number of links above the median. Hence, these results would suggest that these genes are key players of the VTE content modulation when considering both photosynthetic and fruit tissues.

The second approach to link gene expression patterns with tocopherol variations entailed the application of a neural clustering model through a self-organizing map (*omeSOM; Milone et al. 2010) that grouped genes and metabolites according to their variations exclusively across fruit development and ripening. Three main patterns were identified (Fig. S2). The first group included 13 genes, whose expression varied from early developmental stages until breaker stage and kept constant afterwards. In contrast, the second group clustered 19 genes, γ-tocopherol and chlorophylls, showing fairly constant expression patterns until mature green or breaker stages, increasing or decreasing drastically later on. Finally, the third cluster included 13 genes peaking at breaker and decreased towards ripe stage. Although no pathway-specific pattern was detected, some interesting observations could be made when the expression profiles of the individual pathways were analyzed across fruit development (Fig. S2 and Table S1). Most of the MEP genes were upregulated from green fruits to their breaker stage. The exceptions were *CMS* and *GGDR*. For the latter, the reduction in transcript levels from green fruit onwards coincided temporally with the decrease in chlorophyll biosynthesis at later stages of fruit development. By contrast, the transcript profiles of SK genes were more variable. Remarkably, the genes encoding enzymes downstream of shikimate-3P were upregulated at least until breaker stage, with the only exception of the *PAT* gene, which remained constant. Despite no significant alterations were detected in total tocopherol content throughout fruit development, the core pathway genes showed altered mRNA levels. While *VTE*1, *VTE3(2)*, *VTE*4 and *VTE*5 were downregulated, *VTE*2 was upregulated. Additionally, *HPPD* and *VTE*3*(1)* reached the highest mRNA accumulation at breaker stage. Finally, it is worth pinpointing the decrease of *GGDR* and *VTE5* expression across fruit ripening, both of which directly limits phytol diphosphate input supply towards VTE biosynthesis.

Identification of common *cis*-regulatory elements in VTE biosynthetic pathway gene promoters

Having demonstrated that VTE biosynthesis genes are modulated at transcript level in tomato in a spatial and

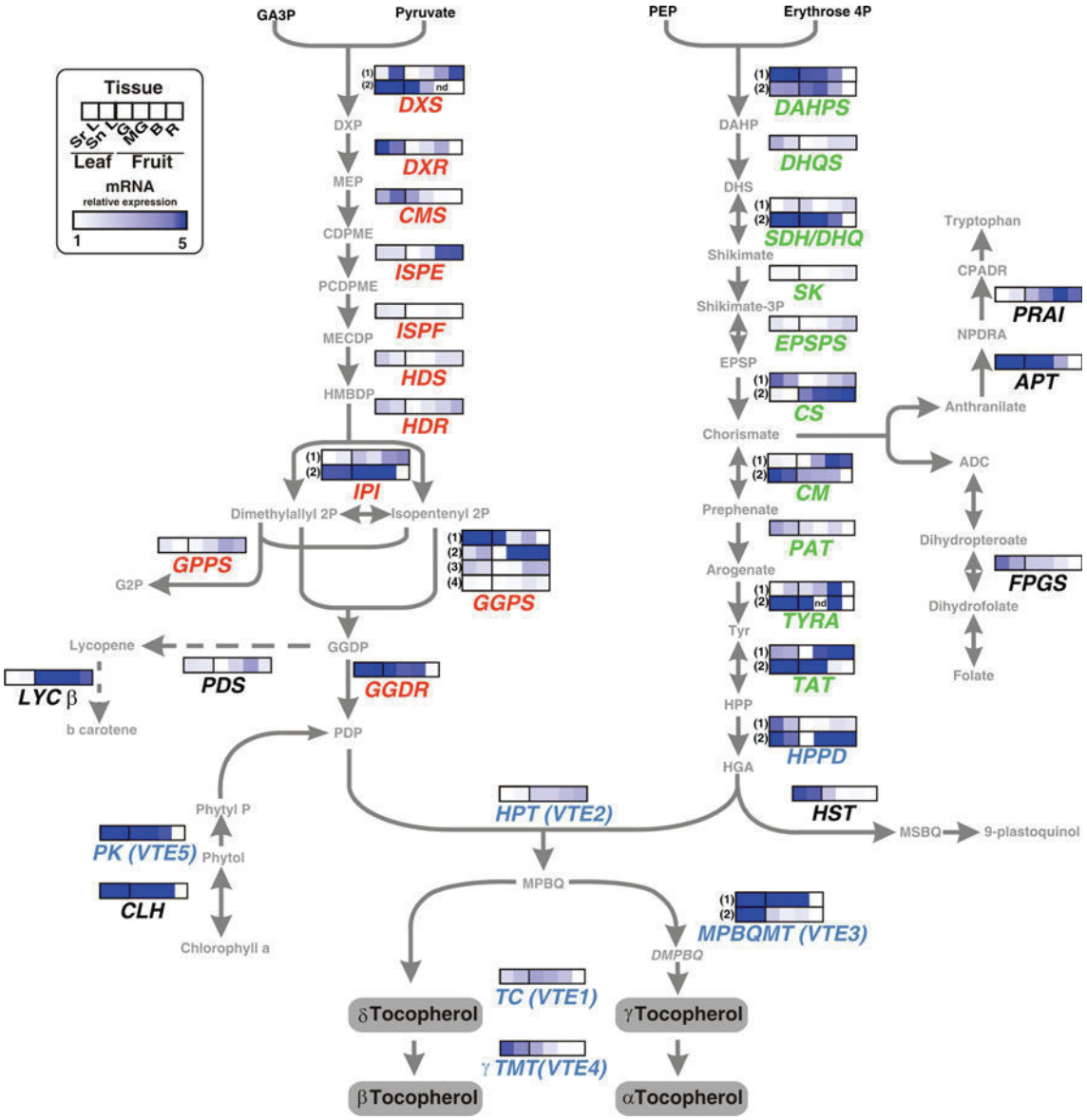

Fig. 1 Expression profile of VTE biosynthetic pathway genes in tomato. Schematic view of the methyl erythritol (MEP), shikimate (SK), vitamin E-core and -related pathways with the corresponding enzymes indicated in *red*, *green*, *blue* and *black*, respectively. Intermediate compounds are indicated in *gray*. Gene expression profiles of each enzyme-encoding gene were measured by qPCR in samples from source (SrL) and sink (SnL) leaves, and green (G), mature green (MG), breaker (B) and ripe (R) fruits (n = 3). Relative gene expressions are indicated above the name of each enzyme by a *color scale* representing the median expression normalized to the sample showing the lowest relative expression. Enzyme encoding genes are named according to the following abbreviations: 1-deoxy-D-xylulose-5-P synthase (*DXS*); 2-C-methyl-D-erythritol 4-phosphate synthase (*DXR*); 2-C-methyl-D-erythritol 4-phosphate cytidylyltransferase (*CMS*); 4-(cytidine 5′-diphospho)-2-C-methyl-D-erythritol kinase (*ISPE*); 2-C-methyl-D-erythritol 2,4-cyclodiphosphate synthase (*ISPF*); 4-hydroxy-3-methylbut-2-enyl- diphosphatesynthase (*HDS*); 4-hydroxy-3-methylbut-2-enyl- diphosphate reductase (*HDR*); isopentenyl diphosphate d–isomerase (*IPI*); geranyl pyrophosphate synthase (*GPPS*); geranylgeranyl pyrophosphate synthase (*GGPS*); geranylgeranyl reductase (*GGDR*); 3-deoxy-D-arabino-heptulosonate-7-P synthase (*DAHPS*); 3-dehydroquinate synthase (*DHQS*); shikimate dehydrogenase/3-dehydroquinate dehydratase (*SDH/DHQ*); shikimate kinase (*SK*); 5-enolpyruvylshikimate-3-P synthase (*EPSPS*); chorismate synthase (*CS*); chorismate mutase (*CM*); prephenate aminotransferase (*PAT*); arogenate dehydrogenase (*TYRA*); tyrosine aminotransferase (*TAT*) 4-hydroxyphenylpyruvate dioxygenase (*HPPD*); homogentisate solanesyl transferase (*HST*); homogentisate phytyl transferase (*VTE2*); 2,3-dimethyl-5-phytylquinol methyltransferase (*VTE3*); tocopherol cyclase (*VTE1*); c -tocopherol C-methyl transferase (*VTE4*); phytol kinase (*VTE5*); anthranilate phosphoribosyltransferase (*APT*); phosphoribosylanthranilate isomerase (*PRAI*); folylpolyglutamate synthase (*FPGS*); chlorophyllase (*CLH*); lycopeno β-cyclase (*LYCβ*); phytoene desaturase (*PDS*). Paralogous genes are indicated by *different numbers*

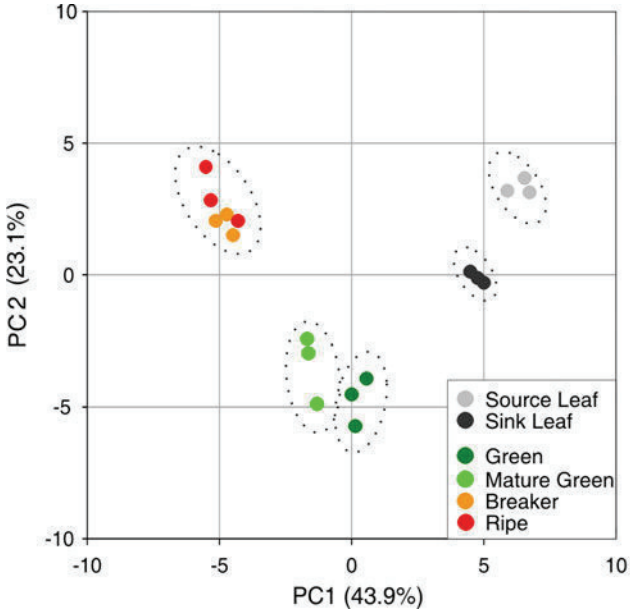

Eigenvector 1		Eigenvector 2	
APT	0.209	*GGPS(3)*	0.289
VTE3(2)	0.202	*HDS*	0.284
TAT(2)	0.200	*HDR*	0.261
CM(2)	0.200	*CS(1)*	0.256
GGDR	0.197	*DHQS*	0.237
VTE4	0.197	*DXS(1)*	0.220
FPGS	0.191	*EPSPS*	0.218
DAHPS(1)	0.190	*HPPD(2)*	0.202
VTE5	0.184	*ISPE*	0.200
HST	0.183	*TAT(1)*	0.187
SDH/DHQ(2)	0.181	*HPPD(1)*	0.175
GGPS(1)	0.180	*SK*	0.173
DXR	0.179	*VTE1*	-0.170
PAT	0.176	*DAHPS(2)*	-0.178
DXS(2)	0.174	*IPI(2)*	-0.251
CLH	0.173		
PRAI	-0.178		
CM(1)	-0.188		
IPI(1)	-0.191		
CS(2)	-0.207		

Fig. 2 PCA of the expression profile of VTE biosynthetic pathway genes in tomato leaves and fruits. A principal component analysis was performed with the expression data of the 47 VTE biosynthetic genes assayed in different developmental stages of tomato leaves and fruits. The highest coefficients (cut off |0.170|) of the first two eigenvectors are shown on the *right*

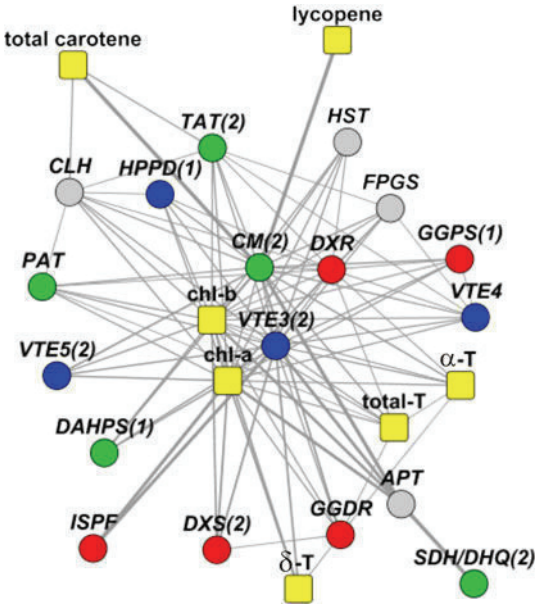

Fig. 3 Gene expression and tocopherol content co-variation network. *Circles and boxes* represent gene and metabolite nodes, respectively. *Red*, *green*, *blue* and *gray circles* indicate MEP, SK, VTE-core and VTE-related genes, respectively. Chl-a and chl–b indicate chlorophyll a and b, respectively. Total-T, δ-T, and α-T indicate total, α and δ-tocopherol, respectively. *Thickness of the lines* is proportional to nodes relative interconnectedness. The network was constructed by using the WGCNA R package and parameters selected as described in "Materials and methods". Cytoscape software (Shannon et al. 2003) was used for network drawing

temporal manner, we next proceeded *(i)* to identify *cis*-regulatory motifs overrepresented in promoter regions of the 47 genes analyzed and *(ii)* to evaluate the conservation of *bona fide* transcription factor-binding sites in orthologous sequences. Out of 38 consensus motifs found in these gene promoter regions, 20 were found to be significantly overrepresented ($p < 0.001$) in the VTE genes promoters when compared to 10,000 randomly selected groups of 47 *S. lycopersicum* promoters (Table S3). Among these overrepresented motifs, 18 showed high similarity (e value <1e−4) to previously reported *cis*-regulatory elements annotated in public databases (AGRIS, Yilmaz et al. 2011; AthaMap, Bülow et al. 2009 and; PLACE, Higo et al. 1999), whereas two, VTE12MEME6 and VTE15Av_12, had not been previously described. The two top MNCP scoring motifs (VTE14Av_28 and VTE14MEME5) showed high similarity to described MYB transcription factor binding sites found in phenylpropanoid biosynthetic gene promoters, while the third highest scoring motifs (VTE12MEME9) was similar to a bZIP binding site (Table S3).

Some of the motifs were found in a high number of gene promoters from the three biosynthetic pathways analyzed (VTE10MS10, VTE10Av_27, VTE10Av_29), while others were restricted to a relative few number of genes (VTE14MEME5, VTE15Av_12 and VTE12Av_46). On the other hand, some other motifs were overrepresented in the MEP (VTE12MS7, VTE14MEME8), SK (VTE14Av_42) or the tocopherol core (VTE12MS2) pathway genes, whereas VTE12MEME4, VTE14MEME6 and VTE14Av_47 were found exclusively in MEP gene promoters (*IPI(1)*, *HDS*, *IPI(2)*, *HDR*, *GPPS*) (Fig. 4a).

In agreement with the fact that most of the paralogous genes showed different expression profiles, they displayed at least four motifs distinct between each other, suggesting potential spatio-temporal specificity (Fig. 1 and Fig. S1).

Since it is well known that the regulation of gene expression may occur through the coordinated action of

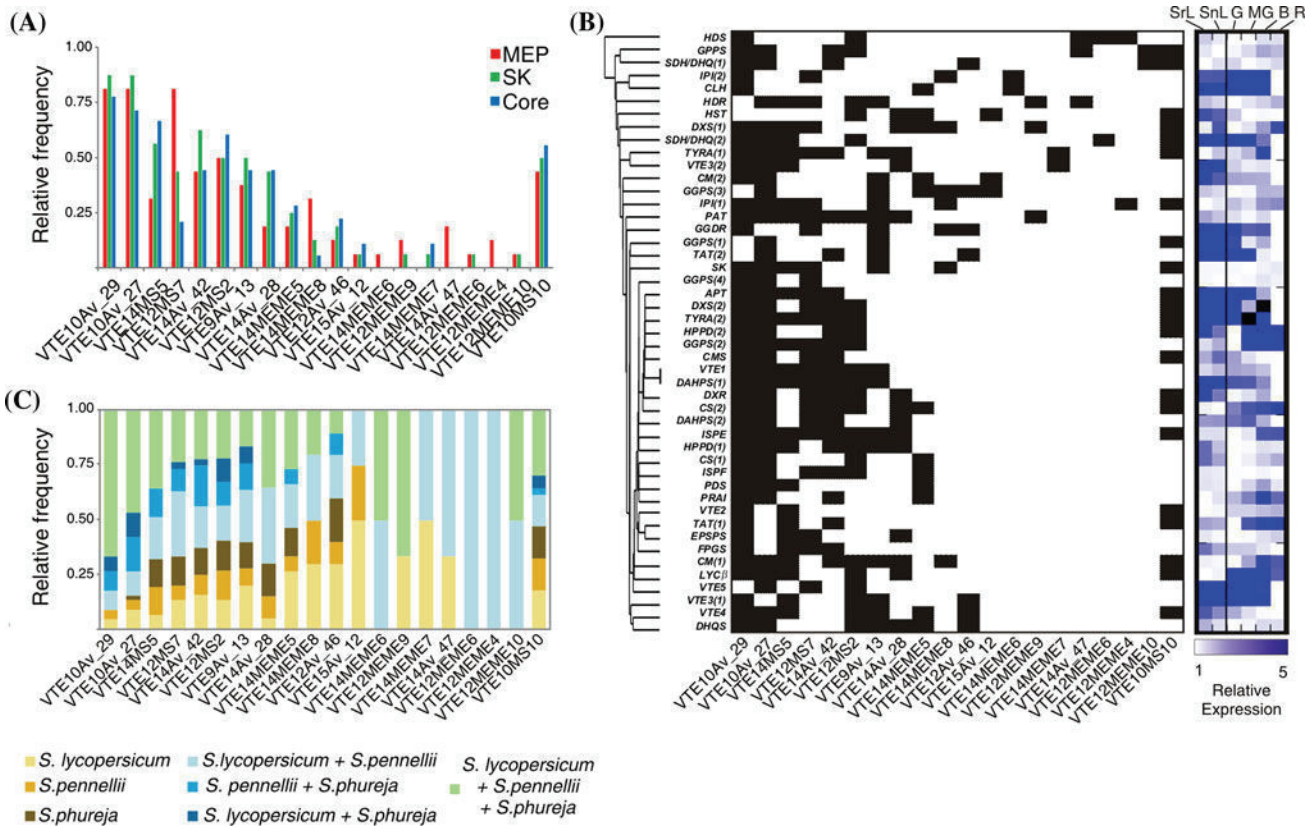

Fig. 4 *Cis*-consensus motifs identified in MEP, SK, VTE-core and VTE-related pathway genes. **a** Relative frequency distribution of the *cis*-consensus motifs identified in promoter regions of MEP- (*red*), SK- (*green*) and VTE core-pathway (*blue*) *S. lycopersicum* genes. **b** Concurrency of consensus motifs in VTE co-expressed genes. Black boxes indicate motif presence, and the expression profile of each gene is indicated by the heat map presented on the right. **c** Relative frequency distribution of the conservation of the identified *cis*-motifs in *S. lycopersicum*, *S. pennellii* and *S. phureja*

multiple transcription factors, a single linkage clustering analysis was performed to group promoters sharing the same motifs (Fig. 4b). Overall it is possible to identify that closely related genes in the cladogram displayed similar transcript patterns. An interesting example is that of *VTE1* and *DAHPS(1)* carrying the same seven motifs in their promoters and both genes displaying similar mRNA accumulation profiles, decreasing along ripening. The *CLH* and *IPI(2)* genes pair shares the ubiquitous VTE10Av_29 and the exclusive VTE14MEME6 motifs and their mRNA levels showed a gradual decrease across fruit development (Fig. 4b and Table S1).

Phylogenetic conservation of the above-mentioned elements was investigated by mapping all motifs on the orthologous promoter regions from *Solanum pennellii* and *Solanum phureja*. All motifs were found in the wild tomato species, while 15 were also found in the potato orthologs, in agreement with the phylogenetic distance between species. The most widely distributed motifs were VTE10Av_29, VTE10Av_27 and VTE12MEME9, which were found in the three species analyzed in over 40 % of the genes in which they occur. In contrast, a subset of motifs including VTE15Av_12, VTE14MEME7, VTE14Av_47, VTE12_-MEME6 and VTE12_MEME4, occurs exclusively in genes from the two species of the Lycopersicon section (Fig. 4c).

Positional preference is a variable determining biological functionality in evaluations of transcription factor-binding motifs (Tharakaraman et al. 2005). Out of the 20 overrepresented motifs, VTE14Av_28, VTE9Av_13 and VTE14MEME6 showed strong positional preference ($p < 0.0001$) when mapped along the first 750 bp on the VTE gene promoters (Table S3). These motifs displayed the highest frequency in the first 200 bp upstream of the putative translation start site. The fact that VTE14Av_28 and VTE9Av_13 also displayed significant p values when mapped on all annotated gene promoters of the *S. lycopersicum* genome reinforces the positional preference of these motifs.

Tocopherol content and qPCR profiles in Andean tomato land-races

To evaluate the variation in the transcript levels of the key genes that regulate fruit VTE contents, 16 genotypes of the

section Lycopersicon from different geographic origins and evolutionary history were analyzed: eleven *S. lycopersicum* Andean landrace genotypes, two wild tomato species (*Solanum habrochaites,* LA407 and *Solanum pimpinellifolium,* LA1589), and four commercial reference cultivars (Fig. 5a). Tocopherol forms, lycopene and total carotene were also quantified in ripe fruits of these genotypes. Six genotypes (LA1589, CHMI, CMP, STUF, C526 and GPEA) displayed increased total tocopherol levels, whereas none showed a statistically reduction with respect to the reference cultivar (M82). By contrast, six other accessions presented decreased lycopene levels and, as expected, the high-lycopene-containing LA1589 accession showed the highest pigment contents (Fig. 5b).

Taking an advantage of the diversity revealed concerning tocopherols and carotenoids content in the analyzed genotypes, we next applied the above-described qPCR array for the 19 enzyme encoding genes whose expression levels might limit tocopherol synthesis in ripe fruit. Although this qPCR platform was established for the M82 cultivar, mRNA levels were reliable detected for most of the genes and genotypes tested. The only exceptions were *DXS(1), VTE2* and *VTE1* for LA407, *VTE1* for CZBU and *DXS(2)* for C525, most likely due to the existence of polymorphisms in the amplicon sequences. Interestingly, all the six high-tocopherol-containing genotypes showed increased amounts of mRNA for tocopherol core-encoding genes (Fig. 5c and Table S4). In particular, these genotypes exhibited higher level of the *VTE3(2)* mRNA, while five of them also displayed increased amount of *HPPD(2)* transcript. Moreover, *VTE*4, *VTE*2 and *VTE3(1)* mRNA levels were also high in at least two of the high-tocopherol-containing genotypes. Focusing on the MEP pathway, *DXS(2)* and *GGDR* were upregulated in five and two out of the six genotypes of the VTE elite, respectively. LA1589, the only genotype with high content of both quantified metabolite

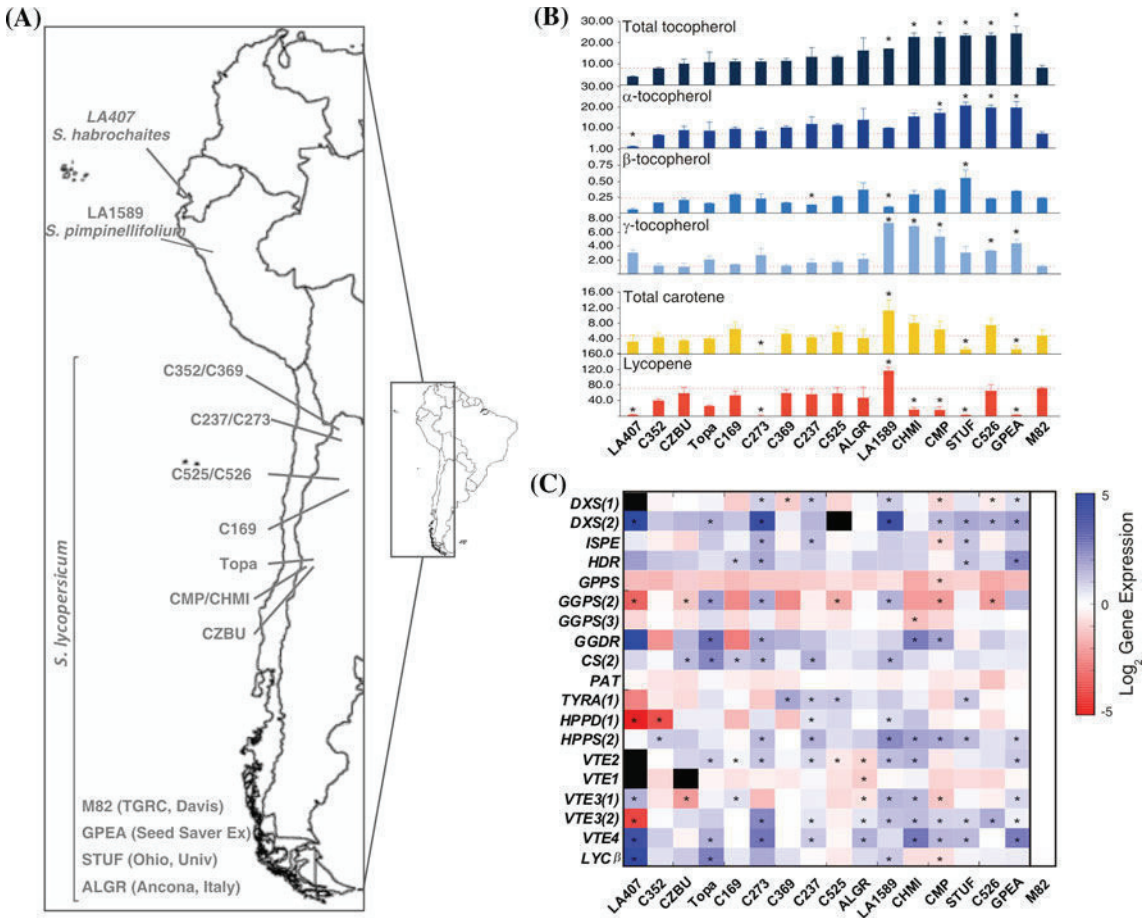

Fig. 5 Natural variation in VTE content regulation in tomato fruits. **a** Geographic distribution of the tomato Andean landrace of *S. lycopersicum* and the wild species *S. habrochaites* and *S. pimpinellifolium* used in this study. **b** Tocopherol and pigment contents in pericarps of ripe fruits. **c** Relative gene expression levels ($\log_2$ median) are shown in a *color scale* where *red* and *blue* indicate decreased and increased transcript levels, respectively with respect to the M82 reference cultivar (*white boxes*). *Black boxes* indicate not detected. *Asterisk* indicates statistically significant differences ($p < 0.05$) with respect to contents measured in fruits from the M82 reference cultivar

families, had increased level of *LYCβ* mRNA, thus confirming the regulatory role of this enzyme in carotenoid biosynthesis (Ronen et al. 2000).

The regulatory role proposed for some of the above pinpointed genes was reinforced by a correlation analysis. *VTE3(2)* and *HPPD* revealed to be positively correlated with tocopherol content. Accordingly, the tight link between the first MEP committed step, *DXS(1)*, and the tocopherol-core pathway was clearly evidenced by its correlation with *HPPD(1), VTE1*, *VTE2* and *VTE3(2)* (Fig. S3).

Discussion

Tocopherol biosynthetic pathway is ubiquitous and transcriptionally regulated by an intricate network resulting in constant VTE levels across leaf and fruit development

Tocopherol species were detected in young and fully expanded leaves and across fruit development in tomato. The higher tocopherol levels in leaves emphasize the hypothesis of its involvement in the protection of the photosynthetic apparatus in chloroplasts (Krieger-Liszkay and Trebst 2006), which whilst still occurring in green tomato fruits likely does so at much lower rates (Lytovchenko et al. 2011). The profiles presented here showed that α-tocopherol was the most abundant form as previously reported by Abushita et al. (1997) and Moco et al. (2007) and, additionally demonstrated that neither this form nor total tocopherol significantly varied across development. Unlike that observed in leaves, the composition of the minor tocopherol forms is timely regulated in fruits. β-tocopherol dramatically decreased from green to mature green stages (tenfold). Conversely, γ- and δ- species significantly increased upon mature green stage tenfold and fivefold, respectively (Table 1). These sequential changes in tocopherol composition are explained by the reduction observed in *VTE4* mRNA levels and the upregulation of *VTE3(1)* (Table S1). Furthermore, the increase in γ-tocopherol at the ripe stage might reflect its importance during seed development. In Arabidopsis, this form is predominant in mature seeds and its loss results in an increased oxidation of polyunsaturated fatty acids and reduced seed longevity (Sattler et al. 2004; Abbasi et al. 2007).

Variations in tocopherol composition and gene expression levels demonstrated that the three pathways involved in VTE biosynthesis are functionally and transcriptionally regulated in both leaves and fruits, in agreement with RNA-sequencing data recently published by The Tomato Genome Consortium (2012). The observation that most of the paralogous genes showed different, or even contrasting, mRNA accumulation patterns indicates that: *(i)* there is a lack of functional redundancy for the encoded enzymes, *(ii)* the advent of paralogous genes brought novel regulatory mechanisms to the pathway and *(iii)* paralogous genes might participate in different multienzymatic complexes, promoting metabolic channeling improving pathway efficiency as has already been shown in phenylpropanoid (Rasmussen and Dixon 1999; Vranová et al. 2012) and flavonoid (Winkel-Shirley 2001) biosyntheses. This hypothesis is also supported by our PCA and promoter sequences analysis results. In the former, organs and developmental stages are clearly separated. Interestingly, for green and mature green fruits, the variables displayed intermediate values between leaves and ripening fruits, reflecting the partial heterotrophy condition of the reproductive organ at these stages. The second approach revealed that the same set of transcriptional regulatory motifs was not shared by paralogous promoter sequences. A nice example of paralogous functional divergence is *GGPS*. Our data suggest that *GGPS(1)* is involved in supplying isoprenoid precursors for photosynthetic plastidial functions, as evidenced by their abundance and predominant mRNA accumulation in leaves. In turn, *GGPS(3)* and *GGPS(2)* seem to be responsible for the production of terpenoids in chromoplasts. Finally, the constant mRNA levels of *GGPS(4)* together with subcellular localization experiments (Almeida et al. unpublished data), leads us to propose its involvement in the synthesis of ubiquinol into the mitochondria (Table S1).

When the entire data-set (leaves and fruit samples) of gene mRNA profile was analyzed together with the tocopherol contents the resulting network displayed a major cluster with 18 highly interconnected genes (Fig. 3). Thirteen of them were found in the eigenvector 1 of the PCA explaining 43.9 % of data variance (Fig. 2) reenforcing their key roles in tocopherol metabolism. *VTE3(2)* emerged as a major player in tocopherol biosynthesis being the most interconnected gene in a central position of the network. Interestingly, even when VTE2 is the only tocopherol exclusive enzyme, our data suggested that its mRNA level is not limiting for VTE biosynthesis. While leaves contain twice tocopherol than fruits, *VTE2* did not show higher mRNA levels in photosynthetic organs. However, the constitutive expression of the apple fruit *VTE2* increased tocopherol levels in transgenic tomato leaves and fruits (Seo et al. 2011). This scenario suggests the existence of posttranscriptional regulatory mechanisms or the activity of other prenyltransferase as HST (Sadre et al. 2006; Tian et al. 2007). HST activity might contribute to tocopherol biosynthesis in an environment enriched for phytyl-diphosphate as leaves. This hypothesis is in line with the *HST* spatio-temporal transcriptional profile found

here. The *HST* mRNA levels were significantly higher in photosynthetic tissues than in ripe fruit. The maintenance of constant expression levels from mature green towards ripe might be indicative of the plastoquinone-dependent PDS activity for carotenoid biosynthesis (Norris et al. 1995; Phatthiyaa et al. 2007).

Across fruit development, the transcriptional regulation of VTE biosynthesis and the resultant content of tocopherol forms emerge as a complex intricate network that deeply depends on the changes in the intermediate fluxes throughout branching pathways. Tomato fruit is programmed to accumulate large amounts of many metabolites such as pigments, flavonoids and volatiles (Carrari and Fernie 2006). Indeed, our results evidenced that the transcription level of the MEP and post-chorismate pathway genes increases across ripening. Regarding the latter, this is reflected by the higher amounts of *CS* and *CM(1)* mRNA detected between breaker and ripe stages. Concomitantly, increased mRNA levels of *TYRA*, *TAT(1)* and *HPPD* strengthens the metabolic flux to homogentisate synthesis, suggesting the important role of these genes in tocopherol production. These findings are in agreement with previous reports for *TAT* and *HPPD*. In senescent Arabidopsis leaves, an increase in tocopherol content correlated with both the transcriptional level and enzymatic activity of TAT (Holländer-Czytko et al. 2005). Furthermore, tocopherols were substantially reduced in *tat* Arabidopsis mutants (Riewe et al. 2012). However, *HPPD* overexpression was not enough to strengthen the SK pathway flux towards tocopherol biosynthesis. Instead, bypassing the phenylalanine branching point by overexpressing a yeast prephenate dehydrogenase (*PDH*) together with *HPPD*, a tenfold increase in tocochromanol content was obtained, demonstrating that homogentisate flux is limiting for tocochromanol synthesis in leaves (Rippert et al. 2004). In the case of the MEP pathway, our qPCR array data suggest that the intense isoprenoid production at late ripening is determined by the high mRNA accumulation of *DXS(1), DXR*, *ISPE*, *HDR*, *IPI(1), GGPS(2)* and *GGPS(3)*. It is worth mentioning that, with the exception of ISPE, the product of all these genes were found in tomato chromoplast proteome (Barsan et al. 2010). Previous experimental evidences have shown the importance of *DXS* and, to a lower extent, of *DXR* and *HDR* transcripts in MEP-derived plastid isoprenoid accumulation (Lois et al. 2000; Paetzold et al. 2010; Carretero-Paulet et al. 2006; Botella-Pavía et al. 2004). In tomato, analyses of *DXS(1)*-overexpressing plants have demonstrated that this gene is undoubtedly a major controlling step in MEP pathway fluxes (Enfissi et al. 2005). Hence, in this context and in accordance with the coordinately mRNA accumulation of *VTE2* and *VTE3* observed, an increase in VTE content across fruit development would be expected. Nevertheless, total tocopherol remained constant. While induction of MEP pathway genes somehow guarantees GGP supply for carotenoid accumulation, the metabolite flux towards tocopherol synthesis is gradually reduced by the decrease in *GGDR* expression across ripening. The role of GGDR in determining VTE content has been evidenced by the fruit specific downregulation of *DET1* gene in transgenic tomato (Enfissi et al. 2010). These lines exhibited metabolic changes including increased levels of carotenoids and tocopherols though, the antioxidant contents did not correlate consistently with the transcriptional level of the tested genes. However, GGDR was remarkably upregulated in mature green stage correlating with the increment in VTE content observed. Ultimately, the limiting precursor for VTE production in tomato fruit is phytyl-diphosphate, which at late ripening could also be supplied from chlorophyll degradation-derived phytol. VTE5 catalyzes the conversion of the chlorophyll degradation-derived phytol in phytyl-phosphate, which is later phosphorylated, to be finally incorporated in tocopherol (Ischebeck et al. 2006; Valentin et al. 2006). In this sense, the contribution of chlorophyll degradation to tocopherol synthesis is strengthened by the constant levels of VTE and the high number of interconnection between chlorophylls, tocopherols, *GGDR, VTE5* and *CLH* observed in the network analysis. In addition, Schelbert et al. (2009) have described the chlorophyll dephytylation route catalyzed by pheophytinase that could also be involved in ripening process. Again, the absence of correlation between transcript levels and their putative enzymatic activities might suggest posttranscriptional and/or posttranslational controls. For instance, *DXS* is target of a posttranscriptional feedback regulatory mechanism, as suggested by the lack of correlation between protein and mRNA levels in response to different perturbations of MEP pathway flow (Guevara-García et al. 2005; Rodríguez-Villalón et al. 2009; Fraser et al. 2007).

As a proof-of-concept, 16 genotypes including wild species, commercial cultivars and Andean landrace genotypes were evaluated to test whether mRNA levels of the above pinpointed genes were indeed effecting tocopherol production. *HPPD* and *VTE3(2)* showed higher mRNA accumulation in ripe fruits from high-tocopherol-containing genotypes, re-enforcing the major role of these genes in VTE accumulation. Although endosperm plastids are structural and functional different from tomato chromoplast, constitutive expression of the Arabidopsis *HPPD* and *VTE3* in maize plants determined up to threefold increments of γ-tocopherol in kernels (Naqvi et al. 2010). However, due to the expressive carotenoids accumulation in tomato fruit, the phytyl-diphosphate precursor may be limiting and an enhanced input by DXS and/or GGDR is also needed. Most of the high-tocopherol-containing genotypes showed reduced carotenoid amounts, supporting

the idea that precursor competition is the main limiting feature for VTE biosynthesis.

The genotypes evaluated here comprise the wild species *S. pimpinellifolium* and *S. habrochaites*, four domesticated commercial cultivars and Andean landraces of the *S. lycopersicum* species. They have been collected based on variable morphological characters and across a wide geographic distribution with diverse climates and altitudes, which are criteria usually associated with genetic diversity (Marshall and Brown 1975, Witcombe and Gilani 1979). Moreover, Williams and St. Clair (1993) has reported that Andean landrace cultivars preserve larger genetic diversity than modern commercial varieties of tomato. The mentioned variability was evidenced by the differential expression profile observed. Thus, the results presented here demonstrate that coexpression analyses are suitable in the investigation of key regulatory steps in metabolic pathways and allow proposing candidate genes for further functional genomic studies (Fukushima et al. 2012).

Cis-regulatory motifs identification suggests that the transcriptional regulation of VTE core pathway genes is coregulated with specific steps of the precursor pathways

The fact that most of the 20 predicted conserved motifs in the promoter regions of the studied genes displayed high similarity to previously described plant *cis*-regulatory elements, their strong positional preference, and that they are overrepresented in the promoters of VTE pathway genes, suggest that these motifs are indeed functional *cis*-regulatory elements.

Neither the presence of shared motifs nor that of exclusive motifs ensures a coexpression profile. An example of this are the cases of *IPI(2)-CLH* and *VTE3(2)-TYRA(1)*. Both pairs of genes share the common exclusive motifs VTE14MEME6 and VTE14MEME7, respectively, and while the first pair shows a coordinated transcription profile, the second one does not. Moreover, the number of shared motifs seems not to be a key variable to determine coregulation. While *IPI(2)-CLH* shares only two motifs and the genes display a similar expression pattern, *VTE3(2)-TYRA(1)* shares five motifs but the genes do not show coordinated expression. Although most identified motifs were found in different repositories of known *cis*-regulatory elements with proven functions, these results should be taken with care as in most cases the functionality of these motifs depend on the genomic context in which they are inserted (Swanson et al. 2010).

Of particular note are the most highly ranked motifs, namely VTE14Av_28 (MNCP value = 14.05) and VTE14MEME5 (MNPC value = 13.0), showing similarity to described MYB transcription factor binding sites found in phenylpropanoid biosynthetic gene promoters from tobacco and *Antirrhinum majus* (Sablowski et al. 1994). These two motifs have also been found in regulatory regions of phenylalanine ammonia-lyase genes of parsley (Lois et al. 1989) and carrot (Takeda et al. 2002), which is a key step in the phenylpropanoid biosynthetic pathway (Fig. 4a, Table S3). Other evidence that these motifs may have a biological function is the conserved positional preference of VTE14Av_28 and VTE14MEME5 in the first 200 bp of the promoters when mapped on the VTE pathway genes (Table S3). These results allow us to suggest that MYB transcription factors might be main regulatory proteins of the analyzed pathway genes also in tomato.

Interestingly, the fact that among the five tomato specific motifs VTE12MEME6 and VTE15Av_12 had not been previously described in any species suggests these two as regulatory innovations in tomato. In addition, these elements are present in members of paralog groups, *GGPS(3)*, *CM(2)* and *SDH/DHQ(2),* in a specific manner. Moreover, VTE14Av_47 and 12MEME4 are exclusively found in the promoters of MEP gene [*HDR*, *HDS*, *GPPS* and *IPI(1)*] encoding enzymes, whose expression increases across fruit development. These motifs are recognized by ABA-responsive transcriptional factors (Shen and Ho 1995; Busk and Pages 1998; Ezcurra et al. 1999) in agreement with the well known increment of this hormone during this process.

The promoter analyses exposed the lack of exclusive *cis*-regulatory motifs for the VTE-core pathway genes. This finding is in agreement with the role of some of the *vte* genes beyond tocochromanol pathway: *VTE3, VTE1* and *VTE4* also participate in plastoquinol-9 and derived compounds synthesis (Zbierzak et al. 2009). Moreover, this result also reflects the tightly tocopherol biosynthesis dependence on precursors pathways. In this sense, we identified *cis*-regulatory elements shared by *VTE3* and *HPPD* genes, (pointed as major regulatory steps in VTE-core pathway) and with genes from the SK and/or MEP pathways (VTE12Av_46, VTE9Av_13, VTE14Av_42 and VTE12MS2). Given that changes in *cis*-regulatory activity are major sources of phenotypic divergence within and between species their identification and further functional characterization can help to resolve questions about genetic mechanisms of phenotypic evolution (Wittkopp and Kalay 2012).

Final considerations

Although MEP and SK are involved in the production of several different key compounds that dramatically change in abundance across fruit development and ripening, tocopherol level remains constant in tomato fruit. This intriguing issue seems to be related to fruit physiology. In

grape (*Vitis vinifera*), a non-climacteric fruit, tocopherol content declines gradually along its development (Horvath et al. 2006b). Mango (*Mangifera indica* L.), a climacteric fruit like tomato, exhibits an inverse pattern (Singh et al. 2011). The intense respiration and ethylene production along maturation that trigger changes in color, aroma, texture, and flavor (Carrari and Fernie 2006) in climacteric fruits are associated with an oxidative phenomenon which is considered as a functional modified form of senescence (Jiménez et al. 2002). As a result, during fruit ripening, a turnover of ROS is required to balance their levels between production and removal by the antioxidant systems. Within this oxidative environment, the maintenance or increase in tocopherol levels is clearly advantageous. In mango, it has been described that *HPPD* expression increases in concert with the increment in tocopherol and carotenoid levels across fruit ripening (Singh et al. 2011). This study provides evidences for the activation of the tocopherol biosynthetic pathway in fruits, which leads to a ripening-specific increase in VTE content. On the other hand, it is worth mentioning that high contents of tocopherol in later stages of ripening could result from an increase in ascorbate levels, which contribute to the efficient regeneration of tocopheroxyl radicals by the ascorbate–glutathione cycle (Kobayashi and DellaPenna 2008).

The evidences collected in this work point that metabolic engineering aiming the enhancement of tocopherol content in tomato fruit requires not only the manipulation of structural genes in VTE-core pathway, but also the understanding of precursor pathways bottlenecks ensuring intermediates influx. The results showed that the transcription level of the MEP and post-chorismate pathway genes increases across fruit development. However, carotenoids biosynthesis competes for intermediates and GGDR appears as a limiting step for the isoprenoid precursor availability. In this sense, the improvement of VTE content can be reached either by enhancing MEP entry point (i.e. *DXS*), increasing tocopherol-core pathway influx via *GGDR*, or by boosting the alternative source of phytyl-diphosphate via chlorophyll degradation. The link between ripening/chlorophyll degradation and tocopherol content rises as an unexplored metabolic hub for future VTE improvement. Later on, *HPPD* and *VTE3* mRNA levels strongly correlate with tocopherol content and composition in tomato fruits.

Materials and methods

Plant material

Tomato seeds from *Solanum lycopersicum* L. (cv M82) were obtained from the Tomato Genetic Resource Center (http://tgrc.ucdavis.edu). Tomato plants were grown in 20-l pots under greenhouse conditions: 16/8 h photoperiod, 24 ± 3 °C, 60 % humidity, and 300 ± 100 μmol m^{-2} s^{-1} incident photo-irradiance. Source (SrL) and sink (SnL) leaves were collected from eight-week-old plants. Fruits at green (G), mature green (MG), breaker (B) and ripe (R) stage were harvested 30, 45, 50 and 60 days after anthesis, respectively. All samples were obtained from six independent plants, immediately frozen into liquid N_2, and stored at −80 °C until use. Samples were pooled in three replicates for further analyses.

Seeds of landrace cultivars were obtained from the germplasm bank of the EEA-INTA-La Consulta (Argentina). Seedlings were grown until four true leaves in 150-ml pots and transplanted to soil under field-production conditions in the Campo Experimental del Instituto de Horticultura, Universidad Nacional de Cuyo, Mendoza, Argentina, 32°50′S, 68°52′W and 900 masl. The field experiment was conducted from October 2008 to March 2009 in a randomized design of three replicates with three plants each. The experiment was protected with an anti-hail mesh and crop irrigation was applied to keep soil available water content (AWC) constant. At ripe stage, two fruits per plant were harvested approximately 60–65 days after anthesis and immediately frozen in liquid N_2 and kept at −80 °C until use.

Tocopherol and pigment quantification by HPLC

Tocopherol was extracted and quantified exactly as described in Almeida et al. (2011). Lycopene, total carotene (α-, β- and γ-carotene) and chlorophylls were extracted and quantified exactly as described in Quadrana et al. (2011).

RNA extraction and cDNA synthesis

Total RNA was extracted from 50 mg of frozen leaves and 100 mg of frozen tomato fruit pericarps with TRIZOL reagent (Invitrogen) according to the manufacturer's instructions. After quantification by Nanodrop spectrophotometer and integrity check by agarose-gel electrophoresis, DNA traces were removed by treatment with amplification-grade DNAse I (Invitrogen) following the manufacturer's instructions. cDNA was synthesized from 1 μg of total RNA using random primers and the Super-Script III enzyme (Invitrogen) in a final volume of 20 μl. The suitability of each cDNA for PCR reaction and DNA contamination were checked using an intron-flanking pair of primers for the *vte1* gene (forward: GTACCACGTT GCGGG, reverse: GTTAGGTGCAACCTGAGACAA GTC). cDNA samples were 1/10 diluted to a final concentration of 5 ng reverse-transcribed RNA/μl and subsequently used for qPCR reactions.

Primer design, validation, qPCR condition and data analyses

Forty seven gene-specific pairs of primers (Table S5 according to the MIQE guidelines, Bustin et al. 2009) were designed based on tomato unigene sequences (http://solgenomic.net) using the PRIMER3 software (Rozen and Skaletsky 2000). To prevent amplification from traces of genomic DNA, depending on each gene structure, primer pairs spanning introns were selected based on exon prediction. Reactions were carried out in duplicate using 2X SYBR Green Master Mix reagent (Applied Biosystems) in a 20 µl final volume and a 7500 real-time PCR system (Applied Biosystems). The thermal conditions were 10 min at 95 °C, followed by 40 cycles of 15 s at 95 °C, 30 s at 55/60 °C (Table S5), and 30 s at 72 °C. The amplification of single products was confirmed by melting curve analysis and by agarose-gels electrophoresis. The optimal concentration of PCR primer pairs was determined in a 100–800 nM range based on the lowest Ct values and absence of primer dimer formation. PCR efficiency and Ct for each sample were calculated using algorithms incorporated into the LingReg software package (Ruijter et al. 2009). Primer efficiencies of the 51 genes ranged from 1.924 to 1.694 with values of 1.87 and 1.89 for mean and median, respectively (Table S5 and Fig. S4). Technical reproducibility assayed by linear regression revealed high confident qPCR array setting, as demonstrated by the R2 value of 0.963 (Fig. S5). Samples showing Ct values $\geq$34 were eliminated for subsequent analyses.

Selection of reference genes

Four reference genes were chosen based on Expósito-Rodríguez et al. (2008): *CAC*, *TIP41, EXPRESSED* and *EF-1α*. Gene stability was tested with NormFinder (Andersen et al. 2004), GeNorm (Vandesompele et al. 2002), and BestKeeper (Pfaffl et al. 2004) softwares. Since all three analyses indicated that the most stable genes were *expressed* and tip41 (Table S6), their mean was subsequently used for gene expression ratio calculations.

Gene expression analysis and statistical tests

Normalized gene expression was calculated by the $^{\Delta\Delta}$Ct method with the improvements proposed by Hellemans et al. (2007). This algorithm allows using several reference genes at the same time leading to a more accurate relative expression data according to the following equation:

$$R = \frac{E_{goi}^{\Delta Ct,goi}}{\sqrt[f]{\prod_0^f E_{ref_0}^{\Delta Ct,ref_0}}}$$

where R indicates the relative gene expression, E is the amplicon efficiency, ΔCt is the Ct difference between the control and the target samples, *goi* indicates the gene of interest, and *ref* the housekeeping genes. The median value of biological replicates was calculated from the mean of two technical replicates and normalized against the sample with the lowest relative expression in Table S1 or the M82 control value in Table S3. A permutation test, which lacks sample distribution assumptions (Pfaffl et al. 2002), was used to detect statistical ($p < 0.05$) differences in expression levels between organs, developmental stages and landrace cultivars using the algorithms incorporated to the fgStatistics software (http://sites.google.com/site/fgstatistics, Di Rienzo 2009, Córdoba, Argentina). Pearson correlation and PCA analyses were performed as described by Carrari et al. (2006) and Quadrana et al. (2011), respectively. Network construction and analyses were performed with expression and metabolite data using the WGCNA R package (Zhang and Horvath 2005). A signed network with threshold power (β) = 6 was performed according to Zhang and Horvath (2005) and Horvath (personal communication). The network was constructed with genes and metabolites presenting node connectivities $\geq$0.50 by using an edge-weighted force-directed layout incorporated to the Cytoscape software (Shannon et al. 2003). Coordinated variations between co-expressed genes and metabolites accumulation during fruit development were calculated as Euclidean distances by the omeSOM* software (version v2.27.15, available in http://sourcesinc.sourceforge.net/omesom/). For this analysis, data were normalized as previously described (Milone et al. 2010), and only genes and tocopherol isoforms presenting statistically significant variation along fruit ripening were included. A 5 × 5 map was selected to group coexpresssed genes showing either directed or inverted expression patterns. Results presented in Figure S2 group neighbor neurons with a Vn = 1. ANOVA followed by Tukey's tests ($p < 0.05$) were applied to compare the tocopherol and pigment contents between different tissues and landrace cultivars by using the InfoStat software.

In silico cis-regulatory element identification and evaluation

The IDs and genomic coordinates of 47 unique *S. lycopersicum* genes (Almeida et al. 2011) were retrieved from the ITAG2.3 genome annotation version (Bombarely et al. 2011) and the 750 bp upstream of the putative translation start codon were further analyzed. Highly similar sequences were searched using Purge (threshold 600) from the MEME Suite (Bailey et al. 2009), but no redundancy was

identified. Low-complexity regions and repeats were masked using TANTAN software with default parameters (Frith 2011). Three softwares using different identification and scoring algorithms were applied: MEME (Bailey and Elkan 1994), MotifSampler (Thijs et al. 2002), and Weeder (Pavesi and Pesole 2006). Motifs ranging from 8 to 14 bp for MEME and MotifSampler, and from 6 to 12 bp for Weeder were searched in both strands of the DNA sequences. All identified motifs were clustered, and redundant motifs were averaged using the script "motif_cluster" included in the program Gimmemotifs with default settings (van Heeringen and Veenstra 2011). To reduce the false positive discovery rate, we evaluated if each motif was significantly enriched in the promoter regions of the VTE genes, by using both the ROC-AUC and the MNCP parameters as calculated by the "motif_roc_metrics" script of the Gimmemotifs program. The comparison demonstrated that MNCP was more stringent for our set of data. Then, to determine the statistical significance of a given MNCP value, we generated 10,000 groups of 47 random *S. lycopersicum* promoters of the same length and calculated this parameter for all motifs. The fraction of random rank orders that gives MNCP values higher than those found with the real data were used as an estimate for the one-tailed *p* value for each motif (Clarke and Granek 2003). The significant overrepresented motifs detected were named as VTE (for vitamin E), a number indicating the consensus nucleotide length and letters standing abbreviations for MotifSampler (MS), MEME and Av for average in cases where redundant motifs were combined into a single motif. To assess the phylogenetic conservation of each motif, the motifs discovered were mapped on the promoters of the orthologous VTE genes (identified by reciprocal Blastn) from *Solanum pennellii* (Usadel and Fernie, unpublished data, sequences available on request) and *Solanum phureja* (The Potato Genome Sequencing Consortium 2011) using the script "pwmscan" as implemented by the program Gimmemotifs. Since binding sites of transcription factors often occur at some preferred distance from the transcription start site in promoter regions, we evaluated the statistical significance of the positional preference for each motif with the script "motif_localization_plots" from the program Gimmemotifs, which calculates a *p* value as a result of a Kolmogorov–Smirnov test, comparing each motif distribution to a uniform one. The similarity of the over-represented motifs with those present in AGRIS (Yilmaz et al. 2011), AthaMap (Bülow et al. 2009) and PLACE (Higo et al. 1999) databases was assessed with STAMP software using default parameters (Mahony and Benos 2007).

Acknowledgments L.Q. was recipient of a fellowship of Agencia Nacional de Promoción Científica y Tecnológica and Consejo Nacional de Investigaciones Científicas y Técnicas (Argentina). J.A. L.B. and F.G. were recipients of a fellowship of Fundação à Amparo da Pesquisa do Estado de São Paulo (Brazil). J.C.S. was recipient of a fellowship of Conselho Nacional de Desenvolvimento Científico e Tecnológico (Brazil). R.A. and F.C. are members of Consejo Nacional de Investigaciones Científicas y Técnicas (Argentina). This work was carried out in compliance with current laws governing genetic experimentation in Brazil and in Argentina. This work was partially supported with grants from Fundação à Amparo da Pesquisa do Estado de São Paulo, Conselho Nacional de Desenvolvimento Científico e Tecnológico and Universidade de São Paulo (Brazil); Max Planck Society (Germany); Instituto Nacional de Tecnologia Agropecuária, Consejo Nacional de Investigaciones Científicas y Técnicas and Agencia Nacional de Promoción Científica y Tecnológica (Argentina); and under the auspices of the European Solanaceae Integrated Project FOOD-CT-2006-016214.

References

Abbasi AR, Hajirezaei M, Hofius D, Sonnewald U, Voll LM (2007) Specific roles of α- and γ-tocopherol in abiotic stress responses of transgenic tobacco plants. Plant Physiol 143:720–738

Abushita AA, Hebshi EA, Daood HG, Biacs PA (1997) Determination of antioxidant vitamins in tomatoes. Food Chem 60:207–212

Alba R, Payton P, Fei Z, McQuinn R, Debbie P, Martin GB, Tanksley SD, Giovannoni JJ (2005) Transcriptome and selected metabolite analyses reveal multiple points of ethylene control during tomato fruit development. Plant Cell 17:2954–2965

Almeida J, Quadrana L, Asís R, Setta N, de Godoy F, Bermúdez L, Otaiza SN, Correa da Silva JV, Fernie AR, Carrari F, Rossi M (2011) Genetic dissection of vitamin E biosynthesis in tomato. J Exp Bot 62:3781–3798

Andersen CL, Jensen JL, Ørntoft TF (2004) Normalization of real-time quantitative reverse transcription-PCR data: a model-based variance estimation approach to identify genes suited for normalization, applied to bladder and colon cancer data sets. Cancer Res 64:5245–5250

Apel K, Hirt H (2004) Reactive oxygen species: metabolism, oxidative stress, and signal transduction. Annu Rev Plant Biol 55:373–399

Bailey TL, Elkan C (1994) Fitting a mixture model by expectation maximization to discover motifs in biopolymers. Proc Int Conf Intell Syst Mol Biol 2:28–36

Bailey TL, Bodén M, Buske FA, Frith M, Grant CE, Clementi L, Ren J, Li WW, Noble WS (2009) MEME suite: tools for motif discovery and searching. Nucleic Acids Res 37:W202–W208

Barsan C, Sanchez-Bel P, Rombaldi C, Egea I, Rossignol M, Kuntz M, Zouine M, Latché A, Bouzayen M, Pech JC (2010) Characteristics of the tomato chromoplast revealed by proteomic analysis. J Exp Bot 61:2413–2431

Bombarely A, Menda N, Tecle IY, Buels RM, Strickler S, Fischer-York T, Pujar A, Leto J, Gosselin J, Mueller LA (2011) The Sol Genomics Network (solgenomics.net): growing tomatoes using Perl. Nucleic Acids Res 39:1149–1155

Botella-Pavía P, Besumbes O, Phillips MA, Carretero-Paulet L, Boronat A, Rodriguez-Concepcion M (2004) Regulation of carotenoid biosynthesis in plants: evidence for a key role of hydroxymethylbutenyl diphosphate reductase in controlling the supply of plastidial isoprenoid precursors. Plant J 40:188–199

Bülow L, Engelmann S, Schindler M, Hehl R (2009) AthaMap, integrating transcriptional and post-transcriptional data. Nucleic Acids Res 37:D983–D986

Busk PK, Pages M (1998) Regulation of abscisic acid-induced transcription. Plant Mol Biol 37:425–435

Bustin SA, Benes V, Garson JA, Hellemans J, Huggett J, Kubista M, Mueller R, Nolan T, Pfaffl MW, Shipley GL, Vandesompele J, Wittwer CT (2009) The MIQE guidelines: minimum information for publication of quantitative real-time PCR experiments. Clin Chem 55:611–622

Carrari F, Fernie AR (2006) Metabolic regulation underlying tomato fruit development. J Exp Bot 57:1883–1897

Carrari F, Baxter C, Usadel B, Urbanczyk-Wochniak E, Zanor MI, Nunes-Nesi A, Nikiforova V, Centero D, Ratzka A, Pauly M, Sweetlove L, Fernie AR (2006) Integrated analysis of metabolite and transcript levels reveals the metabolic shifts that underlie tomato fruit development and highlight regulatory aspects of metabolic network behaviour. Plant Physiol 142:1380–1396

Carretero-Paulet L, Cairó A, Botella-Pavía P, Besumbes O, Campos N, Boronat A, Rodríguez-Concepción M (2006) Enhanced flux through the methylerythritol 4-phosphate pathway in Arabidopsis plants overexpressing deoxyxylulose 5-phosphate reductoisomerase. Plant Mol Biol 62:683–695

Clarke ND, Granek JA (2003) Rank order metrics for quantifying the association of sequence features with gene regulation. Bioinformatics 19:212–218

Córdoba E, Salmi M, León P (2009) Unravelling the regulatory mechanisms that modulate the MEP pathway in higher plants. J Exp Bot 60:2933–2943

Dal Cin V, Tiemana DM, Tohge T, McQuinn R, de Vos RCH, Osorio S, Schmelz EA, Taylor MG, Smits-Kroon MT, Schuurink RC, Haring MA, Giovannoni J, Fernie AR, Klee HJ (2011) Identification of genes in the phenylalanine metabolic pathway by ectopic expression of a MYB transcription factor in tomato fruit. Plant Cell 23:2738–2753

DellaPenna D, Mène-Saffrané L (2011) Vitamin E. In: Kader JC, Delseny M (eds) Advances in botanical research, vol 59. Academic Press, London, pp 179–227

Enfissi EMA, Fraser PD, Lois LM, Boronat A, Schuch W, Bramley PM (2005) Metabolic engineering of the mevalonate and non-mevalonate isopentenyl diphosphate-forming pathways for the production of health-promoting isoprenoids in tomato. Plant Biotech J 3:17–27

Enfissi EM, Barneche F, Ahmed I, Lichtlé C, Gerrish C, McQuinn RP, Giovannoni JJ, Lopez-Juez E, Bowler C, Bramley PM, Fraser PD (2010) Integrative transcript and metabolite analysis of nutritionally enhanced DE-ETIOLATED1 downregulated tomato fruit. Plant Cell 22:1190–1215

Expósito-Rodríguez M, Borges AA, Borges-Pérez A, Pérez JA (2008) Selection of internal control genes for quantitative real-time RT-PCR studies during tomato development process. BMC Plant Biol 8:131

Ezcurra I, Ellerström M, Wycliffe P, Stalberg K, Rask L (1999) Interaction between composite elements in the napA promoter: both the B-box ABA-responsive complex and the RY/G complex are necessary for seed-specific expression. Plant Mol Biol 40:699–709

Falk J, Munné-Bosch S (2010) Tocochromanol functions in plants: antioxidation and beyond. J Exp Bot 61:1549–1566

Fitzpatrick TB, Basset GJC, Borel P, Carrari F, DellaPenna D, Fraser PH, Hellmann H, Osorio S, Rothan C, Valpuesta V, Caris-Veyrat C, Fernie AR (2012) Vitamin deficiencies in humans: can plant science help? Plant Cell 24:395–414

Fraser PD, Enfissi EM, Halket JH, Truesdale MR, Yu DM, Gerrish C, Bramley PM (2007) Manipulation of phytoene levels in tomato fruit: effects on isoprenoids, plastids and intermediary metabolism. Plant Cell 19:3194–3211

Frith MC (2011) A new repeat-masking method enables specific detection of homologous sequences. Nucleic Acids Res 39:e23

Fukushima A, Nishizawa T, Hayakumo M, Hikosaka S, Saito K, Goto E, Kusano M (2012) Exploring tomato gene functions based on coexpression modules using graph clustering and differential coexpression approaches. Plant Physiol 158:1487–1502

Guevara-García A, San Roman C, Arroyo A, Cortes ME, De La Luz Gutierrez-Nava M, Leon P (2005) Characterization of the Arabidopsis clb6 mutant illustrates the importance of posttranscriptional regulation of the methyl-d-erythritol 4-phosphate pathway. Plant Cell 17:628–643

Hellemans J, Mortier G, De Paepe A, Speleman F, Vandesompele J (2007) qBase relative quantification framework and software for management and automated analysis of real-time quantitative PCR data. Genome Biol 8:R19

Higo K, Ugawa Y, Iwamoto M, Korenaga T (1999) Plant cis-acting regulatory DNA elements (PLACE) database: 1999. Nucleic Acids Res 27:297–300

Holländer-Czytko H, Grabowski J, Sandorf I, Weckermann K, Weiler EW (2005) Tocopherol content and activities of tyrosine aminotransferase and cystine lyase in Arabidopsis under stress conditions. J Plant Physiol 162:767–770

Horvath G, Wessjohann L, Bigirimana J, Jansen M, Guisez Y, Caubergs R, Horemans N (2006a) Differential distribution of tocopherols and tocotrienols in photosynthetic and non-photosynthetic tissues. Phytochemistry 67:1185–1195

Horvath G, Wessjohann L, Bigirimana J, Monica H, Jansen M, Guisez Y, Caubergs R, Horemans N (2006b) Accumulation of tocopherols and tocotrienols during seed development of grape (Vitis vinifera L. cv. Albert Lavallee). Plant Physiol Biochem 44:724–731

Ischebeck T, Zbierzak AM, Kanwischer M, Dormann P (2006) A salvage pathway for phytol metabolism in Arabidopsis. J Biol Chem 281:2470–2477

Jiménez A, Creissen G, Kular B, Firmin J, Robinson S, Verhoeyen M, Mullineaux P (2002) Changes in oxidative processes and components of the antioxidant system during tomato fruit ripening. Planta 214:751–758

Klee HJ (2010) Improving the flavor of fresh fruits: genomics, biochemistry, and biotechnology. New Phytol 187:44–56

Kobayashi N, DellaPenna D (2008) Tocopherol metabolism, oxidation and recycling under high light stress in Arabidopsis. Plant J 55:607–618

Krieger-Liszkay A, Trebst A (2006) Tocopherol is the scavenger of singlet oxygen produced by the triplet states of chlorophyll in the PSII reaction centre. J Exp Bot 57:1677–1684

Lois R, Dietrich A, Hahlbrock K, Schulz W (1989) A phenylalanine ammonia-lyase gene from parsley: structure, regulation and identification of elicitor and light responsive cis-acting elements. EMBO J 8:1641–1648

Lois LM, Rodríguez-Concepción M, Gallego F, Campos N, Boronat A (2000) Carotenoid biosynthesis during tomato fruit development: regulatory role of 1-deoxy-D-xylulose 5-phosphate synthase. Plant J 22:503–513

Loyola J, Verdugo I, González E, Casaretto JA, Ruiz-Lara S (2012) Plastidic isoprenoid biosynthesis in tomato: physiological and molecular analysis in genotypes resistant and sensitive to drought stress. Plant Biol (Stuttg) 14:149–156

Lytovchenko A, Eickmeier I, Pons C, Osorio S, Szecowka M, Lehmberg K, Arrivault S, Tohge T, Pineda B, Anton MT, Hedtke B, Lu Y, Fisahn J, Bock R, Stitt M, Grimm B, Granell A, Fernie AR (2011) Tomato fruit photosynthesis is seemingly unimportant in primary metabolism and ripening but plays a considerable role in seed development. Plant Physiol 157:1650–1663

Mahony S, Benos PV (2007) STAMP: a web tool for exploring DNA-binding motif similarities. Nucleic Acids Res 35:253–258

Marshall DR, Brown AHD (1975) Optimum sampling strategies in genetic conservation. In: Frankel OH, Hawkes JG (eds) Crop

genetic resources today and tomorrow. Cambridge University Press, Cambridge, pp 15–36

Meléndez-Martínez AJ, Fraser PD, Bramley PM (2010) Accumulation of health promoting phytochemicals in wild relatives of tomato and their contribution to in vitro antioxidant activity. Phytochemistry 71:1104–1114

Milone D, Stegmayer G, Kamenetzky L, Lopez M, Lee JM, Giovannoni JJ, Carrari F (2010) *omeSOM: a software for clustering and visualization of transcriptional and metabolite data mined from interspecific crosses of crop plants. BMC Bioinformatics 11:438–447

Moco S, Capanoglu E, Tikunov Y, Bino RJ, Boyacioglu D, Hall RD, Vervoort J, De Vos CH (2007) Tissue specialization at the metabolite level is perceived during the development of tomato fruit. J Exp Bot 58:4131–4146

Munné-Bosch S, Alegre L (2002) The function of tocopherols and tocotrienols in plants. Crit Rev Plant Sci 21:31–57

Naqvi S, Farré G, Zhu C, Sandmann G, Capell T, Christou P (2010) Simultaneous expression of Arabidopsis ρ-hydroxyphenylpyruvate dioxygenase and MPBQ methyltransferase in transgenic corn kernels triples the tocopherol content. Transgenic Res 20:177–181

Norris SR, Barrette TR, DellaPenna D (1995) Genetic dissection of carotenoid synthesis in Arabidopsis defines plastoquinone as an essential component of phytoene desaturation. Plant Cell 7:2139–2149

Paetzold H, Garms S, Bartram S, Wieczorek J, Uros-Gracia EM, Rodriguez-Concepción M, Boland W, Strack D, Hause B, Walter MH (2010) The isogene 1-deoxy-D-xylulose 5-phosphate synthase II controls isoprenoid profiles, precursor pathway allocation and density of tomato trichomes. Molecular Plant ssq032v1-ssq032

Pavesi G, Pesole G (2006) Using Weeder for the discovery of conserved transcription factor binding sites. Curr Protoc Bioinformatics Chapter 2: Unit 2.11

Pfaffl MW, Horgan GW, Dempfle L (2002) Relative expression software tool (REST) for group-wise comparison and statistical analysis of relative expression results in real-time PCR. Nucleic Acids Res 30:e36

Pfaffl MW, Tichopad A, Prgomet C, Neuvians TP (2004) Determination of stable housekeeping genes, differentially regulated target genes and sample integrity: BestKeeper–Excel-based tool using pair-wise correlations. Biotechnol Lett 26:509–515

Phatthiyaa A, Takahashib S, Chareonthiphakornc N, Koyamab T, Wititsuwannakuld D, Wititsuwannakul R (2007) Cloning and expression of the gene encoding solanesyl diphosphate synthase from Hevea brasiliensis. Plant Sci 4:824–831

Quadrana L, Rodriguez MC, Lopez M, Bermudez L, Nunes-Nesi A, Fernie AR, Descalzo A, Asis R, Rossi MM, Asurmendi S, Carrari F (2011) Coupling virus induced gene silencing to exogenous green fluorescence protein expression provides a highly efficient system for functional genomics, in Arabidopsis and across all stages of tomato fruit development. Plant Physiol 56:1278–1291

Rasmussen S, Dixon RA (1999) Transgene-mediated and elicitor-induced perturbation of metabolic channeling at the entry point into the phenylpropanoid pathway. Plant Cell 11:1537–1551

Riewe D, Koohi M, Lisec J, Pfeiffer M, Lippmann R, Schmeichel J, Willmitzer L, Altmann T (2012) A tyrosine aminotransferase involved in tocopherol synthesis in Arabidopsis. Plant J. doi: 10.1111/j.1365-313X.2012.05035.x

Rippert P, Scimemi C, Dubald M, Matringe M (2004) Engineering plant shikimate pathway for production of tocotrienol and improving herbicide resistance. Plant Physiol 134:92–100

Rodríguez-Villalón A, Gas E, Rodriguez-Concepcion M (2009) Phytoene synthase activity controls the biosynthesis of carotenoids and the supply of their metabolic precursors in dark-grown Arabidopsis seedlings. Plant J 60:424–435

Ronen G, Carmel-Goren L, Zamir D, Hirschberg J (2000) An alternative pathway to ß-carotene formation in plant chromoplasts discovered by map-based cloning of Beta and old-gold color mutations in tomato. Proc Natl Acad Sci USA 97:11102–11107

Rose JKC, Bashir S, Giovannoni JJ, Jahn MM, Saravanan RS (2004) Tackling the plant proteome: practical approaches, hurdles and experimental tools. Plant J 39:715–733

Rozen S, Skaletsky H (2000) Primer3 on the WWW for general users and for biologist programmers. Methods Mol Biol 132:365–386

Ruijter JM, Ramakers C, Hoogaars WM, Karlen Y, Bakker O, van den Hoff MJ, Moorman AF (2009) Amplification efficiency: linking baseline and bias in the analysis of quantitative PCR data. Nucleic Acids Res 37:e45

Sablowski RW, Moyano E, Culianez-Macia FA, Schuch W, Martin C, Bevan M (1994) A flower-specific Myb protein activates transcription of phenylpropanoid biosynthetic genes. EMBO J 13:128–137

Sadre R, Gruber J, Frentzen M (2006) Characterization of homogentisate prenyltransferases involved in plastoquinone-9 and tocochromanol biosynthesis. FEBS Lett 580:5357–5362

Sattler SE, Gilliland LU, Magallanes-Lundback M, Pollard M, DellaPenna D (2004) Vitamin E is essential for seed longevity and for preventing lipid peroxidation during germination. Plant Cell 16:1419–1432

Schelbert S, Aubry S, Burla B, Agne B, Kessler F, Krupinska K, Hörtensteiner S (2009) Pheophytin pheophorbide hydrolase (pheophytinase) is involved in chlorophyll breakdown during leaf senescence in Arabidopsis. Plant Cell 21:767–785

Seo YS, Kim SJ, Harn CH, Kim WT (2011) Ectopic expression of apple fruit homogentisate phytyltransferase gene (MdHPT1) increases tocopherol in transgenic tomato (Solanum lycopersicum cv. Micro-Tom) leaves and fruits. Phytochemistry 72: 321–329

Shannon P, Markiel A, Ozier O, Baliga NS, Wang JT, Ramage D, Amin N, Schwikowski B, Ideker T (2003) Cytoscape: a software environment for integrated models of biomolecular interaction networks. Genome Res 13:2498–2504

Shen Q, Ho TH (1995) Functional dissection of an abscisic acid(ABA)-inducible gene reveals two independent ABA-responsive complexes each containing a G-box and a novel cis-acting element. Plant Cell 7:295–307

Singh RK, Ali SA, Nath P, Sane VA (2011) Activation of ethylene-responsive p-hydroxyphenylpyruvate dioxygenase leads to increased tocopherol levels during ripening in mango. J Exp Bot 62:3375–3385

Swanson CI, Evans NC, Barolo S (2010) Structural rules and complex regulatory circuitry constrain expression of a notch- and EGFR-regulated eye enhancer. Dev Cell 18:359–370

Takahashi S, Badger MR (2011) Photoprotection in plants: a new light on photosystem II damage. Trends Plant Sci 16:53–60

Takeda J, It Y, Maeda K, Ozeki Y (2002) Assignment of UVB-responsive cis-element and protoplastization-(dilution-) and elicitor-responsive ones in the promoter region of a carrot phenylalanine ammonia-lyase Gene (gDcPAL1). Photochem Photobiol 76:232–238

Tharakaraman K, Mariño-Ramírez L, Sheetlin S, Landsman D, Spouge JL (2005) Alignments anchored on genomic landmarks can aid in the identification of regulatory elements. Bioinformatics 21(Suppl 1):i440–i448

The Potato Genome Sequencing Consortium (2011) Genome sequence and analysis of the tuber crop potato. Nature 475:189–197

The Tomato Genome Consortium (2012) The tomato genome sequence provides insights into fleshy fruit evolution. Nature 485:635–641

Thijs G, Moreau Y, De Smet F, Mathys J, Lescot M, Rombauts S, Rouze P, De Moor B, Marchal K (2002) INCLUSive: integrated clustering, upstream sequence retrieval and motif sampling. Bioinformatics 18:331–332

Tian L, DellaPenna D, Dixon RA (2007) The pds2 mutation is a lesion in the Arabidopsis homogentisate solanesyltransferase gene involved in plastoquinone biosynthesis. Planta 226: 1067–1073

Traber MG, Sies H (1996) Vitamin E in humans: demand and delivery. Annual Rev Nut 16:321–347

Tzin V, Malitsky S, Zvi MMB, Bedair M, Sumner L, Aharoni A, Galili G (2012) Expression of a bacterial feedback-insensitive 3-deoxy-d-arabino-heptulosonate 7-phosphate synthase of the shikimate pathway in Arabidopsis elucidates potential metabolic bottlenecks between primary and secondary metabolism. New Phytol 194:301–598

Valentin HE, Lincoln K, Moshiri F, Jensen PK, Qi Q, Venkatesh TV, Karunanandaa B, Baszis SR, Norris SR, Savidge B, Gruys KJ, Last RL (2006) The Arabidopsis vitamin E pathway gene5-1 mutant reveals a critical role for phytol kinase in seed tocopherol biosynthesis. Plant Cell 18:212–224

van Heeringen SJ, Veenstra GJ (2011) GimmeMotifs: a de novo motif prediction pipeline for ChIP-sequencing experiments. Bioinformatics 27:270–271

Vandesompele J, De Preter K, Pattyn F, Poppe B, Van Roy N, De Paepe A, Speleman F (2002) Accurate normalization of real-time quantitative RT-PCR data by geometric averaging of multiple internal control genes. Genome Biol 3. RESEARCH0034

Vranová E, Coman D, Gruissem W (2012) Structure and dynamics of the isoprenoid pathway network. Molecular Plant 5:318–333

Williams CE, St. Clair DA (1993) Phenetic relationships and levels of variability detected by restriction fragment length polymorphism and random amplified polymorphic DNA analysis of cultivated and wild accessions of *Lycopersicon esculentum*. Genome 36:619–630

Winkel-Shirley B (2001) Flavonoid biosynthesis. A colorful model for genetics, biochemistry, cell biology, and biotechnology. Plant Physiol 126:485–493

Witcombe JR, Gilani MM (1979) Variation in cereals from the Himalayas and the optimum strategy for sampling germplasm. J Appl Ecol 16:633–640

Wittkopp PJ, Kalay G (2012) Cis-regulatory elements: molecular mechanisms and evolutionary processes underlying divergence. Nat Rev Genet 13:59–69

Yelle S, Chetelat RT, Dorais M, Deverna JW, Bennett AB (1991) Sink metabolism in tomato fruit. IV. Genetic and biochemical analysis of sucrose accumulation. Plant Physiol 95:1026–1035

Yilmaz A, Mejia-Guerra MK, Kurz K, Liang X, Welch L, Grotewold E (2011) AGRIS: the Arabidopsis Gene Regulatory Information Server, an update. Nucleic Acids Res 39 (database issue)

Zbierzak AM, Kanwischer M, Wille C, Vidi PA, Giavalisco P, Lohmann A, Briesen I, Porfirova S, Bréhélin C, Kessler F, Dörmann P (2009) Intersection of the tocopherol and plastoquinol metabolic pathways at the plastoglobule. Biochem J 425:389–399

Zhang B, Horvath S (2005) A general framework for weighted gene co-expression network analysis. Stat Appl Genet Mol Biol 4. Article 17

CAPÍTULO II. ANÁLISE DO PERFIL TRANSCRICIONAL DOS GENES ASSOCIADOS À BIOSSÍNTESE DE VITAMINA E EM LINHAGENS INTROGREDIDAS (IL) QUE APRESENTAM AUMENTO NO CONTEÚDO DE TOCOFERÓIS

1. Introdução

O melhoramento tradicional ou a manipulação do metabolismo vegetal a fim de aumentar os níveis de compostos nutracêuticos, por exemplo carotenóides e vitamina E (tocoferol), é uma questão complexa e requer o entendimento sobre os diversos aspectos que controlam a biossíntese e o acúmulo desses compostos nos diferentes tecidos vegetais (Shumskaya & Wurtzel, 2013). Vias de biossíntese que possuem passos limitantes controlados por uma única enzima são raras e, em muitos casos, o controle do fluxo ao longo das rotas metabólicas é compartilhado por várias enzimas (Morandini, 2013). No caso da vitamina E (VTE), a via de biossíntese foi completamente elucidada e demanda um precursor isoprenóide e um derivado aromático, provenientes das vias do metil-eritritol-fosfato (MEP) e do chiquimato (SK), respectivamente. Na rota central, a adição da cadeia isoprênica fitil difosfato ao anel cromanol, a subsequente ciclização e a metilação da cabeça polar são catalisadas pelas enzimas codificadas pelos *loci VTE2, VTE1, VTE3* e *VTE4*, produzindo as quatro isoformas de tocoferóis (α-, β-, γ- e δ-tocoferol) de ocorrência natural (DellaPenna & Mène-Saffrané, 2011).

A exploração da variação natural do conteúdo de tocoferol em sementes de *Arabidopsis thaliana*, soja (*Glicine max*), colza (*Brassica napus*), girassol (*Helianthus annuus*) e em grãos de milho (*Zea mays*) permitiram identificar *loci* para caracteres quantitativos (QTL), incluindo alguns que contêm, dentro do seu intervalo, genes da via de biossíntese de tocoferol (Dwiyanti *et al.* 2011; Gilliland *et al.* 2006; Haddadi *et al.* 2012; Lipka *et al.*, 2013; Shutu *et al.* 2012; Wang *et al.* 2012). Em fruto, nosso grupo revelou a existência de QTL que afetam não só o conteúdo total, mas também a composição de tocoferóis em tomate (Almeida *et al.*, 2011). Para tanto, foram utilizadas linhagens introgredidas (ILs) nas quais fragmentos do genoma de *Solanum lycopersicum* (tomateiro cultivado) foram substituídos por correspondentes da espécie selvagem *Solanum pennellii*. Por meio da determinação do perfil de tocoferóis em ILs selecionadas com base na distribuição cromossômica dos genes envolvidos na biossíntese de VTE, 12 QTL foram mapeados nos cromossomos 6, 7, 8 e 9, alguns dos quais coincidem com QTL previamente descritos (Schauer *et al.*, 2006) (Figura 1). Entretanto, o conteúdo de VTE tem sido assinalado como um caráter metabólico de baixa herdabilidade, uma vez que, utilizando a mesma população de mapeamento - as ILs de *S. pennellii* - nem sempre o QTL é observado (Schauer *et al.*, 2008; Almeida *et al.*, 2011). Assim, a manipulação

do metabolismo com ênfase no melhoramento do conteúdo nutracêutico dos frutos depende da elucidação dos mecanismos moleculares que determinam esses QTL.

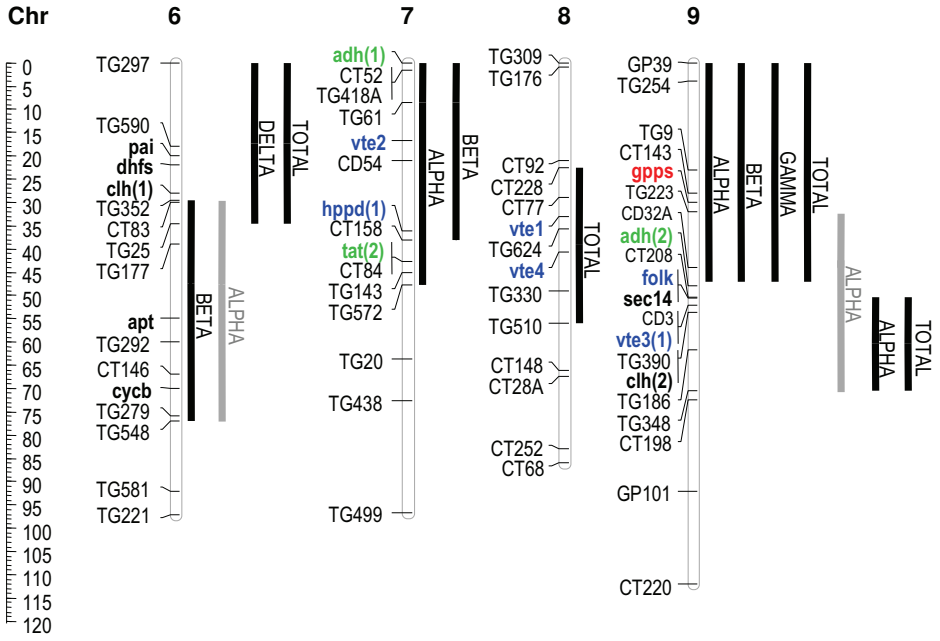

Figura 1. Mapeamento de QTL para VTE e seus respectivos genes candidatos. As barras pretas representam os QTL identificados por Almeida *et al.* (2011); as barras cinzas indicam os prévios QTL identificados por Schauer *et al.* (2006). Genes candidatos para cada QTL estão destacados em negrito. Os genes que codificam para as enzimas estão nomeados de acordo às seguintes abreviações: *FOSFORIBOSILANTRANILATO ISOMERASE* (*PAI*), *DIHIDROFOLATO SINTASE* (*DHFS*), *CLOROFILASE1* [*CLH(1)*], *ANTRANILATO FOSFORRIBOSILTRANSFERASE* (*APT*), *LICOPENO β CICLASE* (*CYCβ*), *AROGENATO DESIDROGENASE* [*ADH(1)*], *HOMOGENTISATO FITIL TRANSFERASE* (*VTE2*), 4-*HIDROXIFENILPIRUVATO DIOXIGENASE1* [*HPPD(1)*], *TIROSINA AMINOTRANSFERASE 2* [*TAT(2)*], *TOCOFEROL CICLASE* (*VTE1*), γ-*TOCOFEROL C-METIL TRANSFERASE* (*VTE4*), *GERANIL FOSFATO SINTASE* (*GPPS*), *AROGENATO DESIDROGENASE* [*ADH*(2)], *FARNESOL KINASE* (*FOLK*), *DIMETIL-FITILQUINOL METIL TRANSFERASE* [*VTE3(1)*], *CLOROFILASE2* [*CLH(2)*]. Em vermelho, genes pertencentes à via do MEP; em verde, genes envolvidos na rota do SK; em azul, genes da rota central da VTE; sem destaque, genes que pertencem a vias associadas ao metabolismo da VTE. Esta adaptação de Almeida *et al.* (2011) já inclui a atualização de nomenclatura feita considerando (i) a revisão da anotação gênica [*FOLK,* antigo *VTE5; GPPS,* antigo *GGPS(4)*]; (ii) a revisão da nomenclatura gênica dos genes: *PAI* ou *PRAI*; *DHFS* ou *FPGS*; *CYCβ* ou *LYCβ*; *TYRA* ou *ADH*. O parálogo *CLH(2)* posteriormente identificado com a finalização do genoma de *S. lycopersicum* também foi incluído no mapa.

A variação fenotípica quantitativa resulta, em parte, de perturbações genéticas multifatoriais das redes metabólicas e transcricionais, as quais são interconectadas e altamente dinâmicas (Mackay, 2014). Consequentemente, alterações nos níveis de expressão podem constituir fonte de diversidade fenotípica (Cubillos *et al.*, 2012). Buscando ampliar o entendimento sobre como ocorre a regulação da biossíntese de tocoferóis em tomateiro, nosso grupo desenvolveu um *array* de PCR quantitativa (qPCR) para VTE que permite a análise da expressão de uma coleção de genes codificantes para enzimas das vias biossintéticas de MEP, SK e central do tocoferol (Capítulo I, Quadrana *et al.*, 2013). A correlação entre os perfis transcricionais de folhas e frutos de *S. lycopersicum* e os conteúdos de pigmentos e de tocoferóis em diferentes estádios do desenvolvimento evidenciou pontos chaves na regulação das vias precursoras, além da rota central. Sobretudo, alguns desses pontos correspondem

a genes candidatos previamente identificados por Almeida *et al.* (2011), como por exemplo, *VTE3*, *VTE4*, *HPPD* e *TAT*.

Dessa maneira, se tais genes destacados como pontos chaves regulatórios da biossíntese de VTE, por meio das análises de correlação, são efetivamente centrais para regulação da via, é esperado que seus níveis de expressão acompanhem a variação do conteúdo tocoferol observada na diversidade natural de tomateiro. Tal hipótese foi posta à prova, por meio da avaliação de diferentes acessos de tomateiro, incluindo espécies silvestres, cultivares comerciais e variedades "crioulas" (*landraces*) que, por sua vez, apresentam fenótipos contrastantes para tocoferol e/ou carotenóides em frutos maduros. A realização do perfil transcricional de um subconjunto de genes potencialmente limitantes da biossíntese de tocoferóis em fruto maduro, revelou que a expressão de *VTE3* e *HPPD* está altamente correlacionada aos conteúdos de tococromanóis. Essas observações não só reforçam o papel regulatório dos genes propostos no acumúlo de VTE, mas, sobretudo, assinalam a relevância da regulação transcricional no conteúdo desse metabólito (Capítulo I, Quadrana *et al.*, 2013).

Com efeito, a disponibilidade do *array* de qPCR para VTE torna possível verificar prontamente se as variações no conteúdo de tocoferol, como aquelas apresentadas pelas ILs, resultam das diferenças qualitativas e/ou quantitativas na expressão de genes alvo. Embora sujeita ao efeito do ambiente, a modificação na quantidade dos transcritos pode ser consequência de alterações em sequências regulatórias (Druka *et al.*, 2010). Tais variações alélicas incluem polimorfismos associados às regiões alvejadas por micro RNAs (miRNA) ou àquelas relacionadas a marcas epigenéticas, determinando a ativação ou silenciamento do respectivo gene (Delker & Quint, 2011). Nessa perspectiva, a variação da abundância de mRNA em uma população de plantas pode ser tratada como um caráter herdável e, portanto, constituir um QTL de expressão (*e*QTL). Tem sido demonstrado de maneira convincente que *e*QTL contribuem para a alteração quantitativa de vários caracteres em plantas, dentre os quais compostos do metabolismo secundário em tomateiro (Delker & Quint, 2011; Alseekh *et al.*, 2015).

A conexão entre a variação fenotípica e *e*QTL é feita a partir da função gênica conhecida/predita e sua relação com o fenótipo observado. No caso dos caracteres metabólicos, a alta variabilidade fenotípica, aferida por técnicas de alta precisão, comparada aos níveis dos transcritos de genes envolvidos no metabolismo alvo pode gerar hipóteses robustas sobre a regulação do conteúdo do metabólito, as quais abrangem conceitos de fluxo metabólico e da regulação da expressão gênica (Wentzell *et al.*, 2007; Bolger *et al.*, 2014).

2. Objetivos específicos

Com intuito de associar eventuais *e*QTL aos QTL metabólicos para VTE previamente descritos por Almeida *et al.* (2011), e identificar possíveis efeitos epistáticos sobre os genes envolvidos nas vias de biossíntese de tocoferol, o presente trabalho propôs:

- Verificar a expressão dos alelos selvagens de *S. pennellii* correspondentes aos genes candidatos (Tabela 1) nas ILs que apresentam aumento no conteúdo de tocoferóis.
- Avaliar o impacto da presença do fragmento do genoma selvagem na expressão dos alelos domesticados (de *S. lycopersicum*) associados à rota biossíntética de VTE.

Tabela 1: Genes candidatos propostos analisados nesse estudo.

***Locus*[1]**	**Enzima**	**ID genômico[2]**	**Posição cromossomica[3]**	**Alelo Selvagem[4]**
CLH(1) *CLH*(2)	clorofilase	Solyc06g053980 Solyc09g065620	6 (32 cM) 9 (56.3 cM)	IL6-1/IL6-2 IL9-2/IL9-2-6
PRAI ou *PAI*	fosforibosilantranilato isomerase	Solyc06g051410	6 (24 cM)	IL6-1
FPGS ou *DHFS*	dihidrofolato sintase / folilpoliglutamato sintase	Solyc06g051900	6 (26 cM)	IL6-1
APT	antranilato fosforribosiltransferase	Solyc06g071550	6 (59 cM)	IL6-2
CYCβ	licopeno β ciclase	Solyc06g074240	6 (74 cM)	IL6-2
GPPS (antigo *GGPS(4)*)	geranil difosfato sintase (subunidade não-catalítica)	Solyc09g008920	9 (30 cM)	IL9-1
FOLK (antigo *VTE5*)	farnesol quinase	Solyc09g018510	9 (50.5 cM)	IL9-2
VTE3(1)	dimetilfitilquinol metil transferase	Solyc09g065730	9 (52 cM)	IL9-2/IL9-2-6
TYRA(2) ou *ADH*(2)	arogenato desidrogenase	Solyc09g011870	9 (48 cM)	IL9-2

[1] Para alguns genes a sigla utilizada por Almeida *et al.* (2011) foi atualizada.
[2] Identificação do *locus* no genoma de *S. lycopersicum* de acordo com Solanaceae Genomics Network (http://solgenomics.net).
[3] Cromossomo e posição no mapa genético Tomato-EXPEN 2000 V52 (http://solgenomics.net).
[4] Linhagem introgredida na qual se encontra o alelo selvagem de *S. pennellii*.

3. Material e métodos

3.1. Material vegetal

As sementes de tomate de *S. lycopersicum* L. (*cv*. M82) e das linhagens introgredidas (IL6-1, 6-2, 9-1, 9-2 e 9-2-6) de *S. pennellii* foram cedidas pelo *Tomato Genetic Resource Center* (http://tgrc.ucdavis.edu) e pelo Prof. Dani Zamir (The Hebrew University of Jerusalem, Israel). As plantas foram crescidas em casa de vegetação no IB-USP, sob condições naturais de temperatura e fotoperíodo, em potes de 15 L contendo terra vegetal e vermiculita (1:1; v/v), suplementadas com NPK 20:5:20 e Yoorin® (mistura de fósforo, cálcio, magnésio e micronutrientes silicatados). Folhas fonte (completamente expandidas) e pericarpo de frutos verde-maduros (40 dias depois da antese, dda) e frutos maduros (55 dias dda) foram coletados de plantas com aproximadamente 10 a 12 semanas de idade. Os tecidos foram imediatamente congelados em nitrogênio líquido e armazenados em freezer -80 ºC até posterior processamento. As amostras foram obtidas de cinco plantas independentes das quais foram feitos *pools* para obtenção de três réplicas biológicas utilizadas nos experimentos.

3.2. Análise da expressão gênica

3.2.1. Extração de RNA total e síntese de cDNA

Os tecidos congelados de folhas fonte, frutos verde-maduros e maduros foram processados em nitrogênio líquido e alíquotas de 150 mg de tecido triturado foram submetidas à extração de RNA total utilizando o reagente Trizol (Life Technologies), segundo o protocolo recomendado pelo fabricante. As amostras de RNA foram ressuspendidas em 20 µL de água DEPC 0,1 %. A quantidade, pureza e integridade do RNA total extraído foram estimadas por espectrofotômetro Nanodrop® (Thermo Scientific) e por eletroforese em gel de agarose 1 %. A concentração dos ácidos nucléicos foi estimada a partir da leitura da absorbância da amostra a 260 nm (A_{260nm}). O grau de pureza foi determinado por meio das análises das razões A_{260nm}/A_{280nm} e A_{260nm}/A_{230nm}, considerando amostras de alta qualidade com valores próximos a 1,8 e 2,0, respectivamente. Enquanto valores abaixo do esperado para A_{260nm}/A_{280nm} podem indicar a presença de contaminantes como proteínas, fenol e outros, para A_{260nm}/A_{230nm}, uma baixa razão pode indicar a presença de fenol, de resíduos de guanidina e de excesso de açúcares.

A remoção de potenciais traços contaminantes de DNA genômico foi feita a partir do tratamento de 2 µg de RNA total com DNAse I (Life Technologies). O RNA tratado foi reverso transcrito utilizando-se como iniciadores oligonucleotídeos randômicos (*random primers*) e o kit SuperScript® III Reverse Transcriptase (Life Technologies), de acordo com as recomendações do

fabricante. A ausência de contaminação de DNA genômico e eficiência da reação de transcriptase reversa foram avaliadas por meio de PCR, utilizando-se iniciadores do gene *PREFENATO AMINOTRANSFERASE* (RT-PAT-F e RT-PAT-R; Anexo I) os quais se anelam em diferentes éxons do gene. Dessa forma, o tamanho do fragmento amplificado a partir de DNA genômico corresponde a 943 pb e de cDNA a 150 pb. As reações de PCR foram conduzidas empregando-se tampão 1X, 200 nM de cada dNTPs, 200 nM de cada iniciador, 50 ng de cDNA e 1 U de enzima Taq polimerase (Life Technologies). As condições de amplificação utilizadas foram: denaturação inicial de 94 ºC por 10 min; seguida por 35 ciclos de 30 s a 94 ºC, 30 s a 60 ºC, 1 min a 72 ºC; uma extensão final a 72 ºC por 10 min. Os produtos de amplificação foram visualizados em gel de agarose 1,2 %. Por fim, as amostras de cDNA foram diluídas 10X, obtendo-se a concentração final de aproximadamente 5 ng de RNA reverso-transcrito/µL.

3.2.2. PCR quantitativa em tempo real (qPCR)

Para avaliar a expressão dos genes envolvidos na síntese de VTE em tomateiro, foram utilizados 48 pares de iniciadores específicos para os genes envolvidos nas vias do MEP (16), do SK (16), central do tocoferol (9), de rotas relacionadas (2), além dos três genes de referência descritos em Quadrana *et al.* (2013) (Anexo I). Além desses, foram incluídos no *array* de qPCR o gene *CLH*(2), posteriormente identificado no banco de dados da SGN (http://solgenomics.net), e *FOLK*. Com exceção dos genes *GGPS*, *GGDR*, *ADH, CYCβ*, todos os iniciadores utilizados abrangem junções éxon-éxon preditas, evitando a amplificação de DNA genômico (Anexo I).

As reações de qPCR foram conduzidas no equipamento 7500 Real Time PCR System (Life Technologies) em duplicata técnica. Cada 20 µL de reação incluiu a concentração otimizada de iniciadores e cDNA (Anexo I), além de 10 µL de 2X SYBR Green Master Mix (Life Technologies). As condições da reação foram 10 min a 95 ºC, seguida por 40 ciclos de 15 s a 95 ºC, 30 s a 55 ou 60 ºC (dependendo do iniciador, Anexo I) e 30 s a 72 ºC. Após a amplificação, a especificidade dos produtos foi avaliada por análise da curva de dissociação (*melting curve*). Foram utilizados controles negativos (NTC= *no template control*) sem a adição de cDNA. O Ct e a eficiência média da qPCR, baseada na fase exponencial de amplificação obtida a partir dos valores brutos de fluorescência, foram calculados utilizando-se o software LinReg (Ruijter *et al.* 2009).

Para a seleção dos genes referência, foi analisada a expressão de três genes - *CAC*, *TIP41, EXPRESSED* – conforme sugerido por Expósito-Rodríguez *et al.* (2008). A estabilidade de expressão de cada gene no conjunto amostral foi verificada por meio do software *GeNorm* (Vandesompele *et al.,* 2002).

A normalização da expressão gênica foi calculada a partir do método $^{\Delta\Delta}$Ct com as modificações propostas por Hellemans *et al.* (2007). Este algoritmo produz dados mais robustos de

expressão relativa pois permite incorporar mais de um gene de referência nas análises de acordo com a seguinte equação:

$$R = \frac{E_{goi}^{\Delta Ct, goi}}{\sqrt[f]{\prod_{0}^{f} E_{ref_0}^{\Delta Ct, ref_0}}}$$

onde *R* indica a expressão gênica relativa, *E* a eficiência média do amplicon, Δ*Ct* é diferença entre o controle e as amostras alvo, *goi* indica gene de interesse e *ref*, genes de referência. A mediana das replicatas biológicas foi obtida a partir da média aritmética das replicatas técnicas e expressa em relação ao controle M82. Um teste de permutação, que não assume modelo de distribuição (*p-value* é calculado randomicamente selecionando combinações das réplicas biológicas e técnicas, de acordo com o paradigma do teste de permutação), foi usado para detectar as diferenças estatísticas ($P<0.05$) entre os níveis de expressão dos respectivos genótipos por meio do algoritmo incorporado ao software fgStatistics (http://sites.google.com/site/fgstatistics, Di Rienzo, 2009, Córdoba, Argentina).

4. Resultados e discussão

Para realização dos perfis transcricionais, primeiramente foram selecionados o par de genes de referência para cálculo da expressão. Os valores de Ct obtidos para os genes *TIP41, CAC* e *EXPRESSED* foram convertidos em quantidades relativas de cDNA. Estes valores foram submetidos ao programa *GeNorm* (Vandesompele *et al.*, 2002) para obtenção do valor médio de estabilidade de expressão (*M*) (Tabela 2). Tendo em vista que genes com menor *M* possuem expressão mais estável entre amostras provenientes de diferentes tecidos, *CAC* e *EXPRESSED,* portanto, foram selecionados para o conjunto experimental analisado.

Tabela 2: Estabilidade de expressão dos genes de referência.

	TIP41	*CAC*	*EXPRESSED*
Valor médio de estabilidade de expressão (*M*)	0,125	0,115	0,102

A Figura 1 mostra um *heatmap* no qual estão sumarizadas as alterações nos níveis transcritos dos genes envolvidos na via biossintética de tocoferóis nas IL6-1, 6-2, 9-1, 9-2 e 9-2-6, que apresentam alteração no conteúdo de VTE (Schauer *et al.*, 2006; Almeida *et al.*, 2011). Os valores de expressão relativa para os 48 genes avaliados estão disponíveis na Tabela 3, 4 e 5. Embora os QTL identificados nas ILs correspondam a alterações metabólicas nos frutos, a expressão dos genes da via também foi analisada em folhas com objetivo de avaliar se a eventual mudança se restringe aos frutos ou estende-se à porção vegetativa.

De maneira geral, observou-se em folha o maior número de mudanças significativas na abundância dos transcritos. Além disso, a maioria das mudanças representa um aumento na expressão dos genes nas ILs em relação à M82 (Figura 1). As alterações nos níveis de RNAm em frutos verde-maduros e maduros identificadas somam evidências sobre a participação dos genes candidatos na determinação da base genética dos QTL para VTE. Os resultados serão apresentados e discutidos abaixo para cada IL.

4.1. Perfil transcricional das IL6-1 e 6-2

No cromossomo 6, foram descritos QTL que controlam o conteúdo de tocoferóis em tomate associados ao fragmento introgredido de *S. pennellii* da IL6-1, que apresenta aumento do conteúdo de δ- e tocoferol total, e da IL6-2, que possui aumento nos níveis de α- e β-tocoferol (Schauer *et al.*, 2006; Almeida *et al.*, 2011). A análise dessas regiões genômicas revelou cinco genes candidatos pertencentes a vias metabólicas relacionadas à biossíntese de tocoferóis. A IL6-1 possui os alelos

selvagens dos genes *PAI*, *DHFS* e *CLH*(1). Já o fragmento selvagem introgredido da IL6-2, além de *CLH(1),* possui também os *loci* correspondentes a *APT* e *CYCβ*. O produto protéico deste último, que atua na síntese de carotenóides, isoprenóides sintetizados a partir do precursor geranilgeranil difosfato, foi extensivamente caracterizado após sua clonagem posicional por Ronen *et al.* (2000).

Na IL6-1, o QTL para conteúdo total de tocoferóis poderia ser explicado por perturbações decorrentes tanto no fornecimento do anel cromanol quanto da cadeia isoprênica (Figura 1, Tabela 3, 4 e 5). Primeiramente, verificou-se altos níveis de RNAm para o alelo selvagem do gene *PAI* em frutos maduros e também em folhas. O produto deste gene participa da síntese de triptofano e, portanto, a presença do alelo selvagem poderia levar ao aumento no conteúdo deste aminoácido aromático na IL 6-1. Em *Arabidopsis*, a deleção de apenas um dos três genes que codificam para PAI (*pai1*) causa desenvolvimento anormal (He & Li, 2001), fato que evidencia sua importância na biossíntese do triptofano (Tzin & Galili, 2010), o precursor do ácido indol-acético. Também em *Arabidopsis*, sabe-se que o triptofano induz a atividade da corismato mutase (CM) (Eberhard *et al.*, 1996), enzima que catalisa a conversão de corismato em prefenato, o que poderia indiretamente aumentar o influxo da rota do SK em direção à VTE. Por sua vez, a expressão do alelo selvagem de *DHFS* está reduzida comparado ao controle M82, tanto em frutos quanto em folhas. DHFS participa da rota biossintética de folato, responsável pela conversão de dihidropteroato (DHP) em dihidrofolato (DHF). Segundo Mouillon *et al.* (2002), DHP têm efeito inibitório sobre a enzima DHPS responsável por sua síntese *in vitro*. Além disso, outro estudo *in vitro* apontou o efeito inibitório de DHP e DHF sobre a primeira enzima da síntese de folato, aminodeoxicorismato sintase (ADCS), que converte corismato em aminodeoxicorismato (ADC) (Sahr *et al.*, 2006). Nesse contexto, a redução da expressão de *DHFS* na IL poderia causar acúmulo do intermediário DHP que, por sua vez, promoveria uma redução no fluxo de carbono para essa via, segundo as evidências obtidas *in vitro.* Esse cenário seria favorável a uma maior disponibilidade de corismato direcionado para formação de tirosina e, posteriormente, maior influxo de precursor homogentisato para rota central de tocoferol.

Com relação a cadeia isoprênica fitil difosfato, a análise do perfil transcricional revelou que os níveis de transcritos *CLH(1)* estão alterados significativamente na IL6-1. Curiosamente, enquanto nas folhas ocorre uma redução nos níveis de RNAm, em frutos o dobro de transcritos é detectado. Esse aumento da expressão *CLH*(1) observado nos frutos resultaria em uma maior atividade defitiladora e, por conseguinte, um possível incremento na liberação do fitol a partir da degradação da clorofila que, convertido em fitil difosfato, seria incorporado na síntese de tocoferóis.

Em frutos da IL6-1, os genes que codificam enzimas das vias precursoras, quando alterados, tem a expressão induzida, exceto *DAHPS(2)*. É o caso de *ADH*(1), *CS(1), DHQS*, *TAT(1)* da rota do SK; de *DXS(1), DXR, CMS*, *ISPE, ISPF, HDR, HDS*, *IPI* e *GGPS*, da via do MEP; *HPPD*(1) e (2),

VTE3(1), da rota central do tocoferol. Essas alterações em conjunto poderiam contribuir para o cenário de maior disponibilidade do intermediário aromático corismato e da cadeia prenílica, promovendo um maior acúmulo de tocoferóis totais nos frutos maduros da IL6-1. Em folha, a modulação da expressão dos genes envolvidos nessas vias é também marcante. Particularmente, a robusta indução na expressão de *ADH(1),* observada tanto em folhas como em frutos, é notável nesta IL, sugerindo que a porção final da via do SK está induzida, embora, até o momento, nenhum QTL para chiquimato, fenilalanina, triptofano e tirosina tenha sido descrito nessa IL (Schauer *et al.*, 2006).

Para a IL6-2, entretanto, as mudanças no perfil transcricional ocorrem, mas não para os genes candidatos (Figura 1, Tabela 3, 4 e 5). Interessantemente, embora a região codificante do gene *CLH*(1) corresponda ao alelo de *S. pennellii* (Almeida *et al.*, 2011), essa linhagem não apresenta aumento da expressão desse gene em frutos como observado na IL6-1. Isto poderia ser explicado pela posição limítrofe do gene em relação aos fragmentos introgredidos de tal forma que a região promotora do gene *CLH*(1) corresponderia somente ao alelo selvagem na IL6-1. Por outro lado, a presença de outros fatores reguladores da expressão desse gene no fragmento introgredido da IL6-1 com efeito epistático também é uma explicação possível. Os genes candidatos *APT e* C*YCβ* apresentaram expressão similar ao controle. É importante mencionar que o alelo selvagem do *CYCβ* é mais expresso que o cultivado entre os estádios *breaker* e maduro do fruto (Ronen *et al.*, 2000), alguns pontos não avaliados neste estudo. Porém, a maior expressão do alelo selvagem pode ser detectada em folhas.

Semelhante ao descrito acima para frutos da IL6-1, as alterações no perfil transcricional da IL6-2 nos frutos verde-maduros promovem uma indução na expressão. Além disso, o impacto da introgressão sobre o restante da rota se evidencia tanto em fruto como também em folha, principalmente no aumento coordenado dos níveis dos transcritos dos genes do MEP (*IPI*, *ISPE*, *ISPF*, *GGPS* e *CMS*); da rota central da VTE [*HPPD*(1), *VTE1* e *VTE3*(1)] além de *FOLK* (Tabela 3, 4 e 5). Dessa forma, embora não seja possível associar a expressão dos genes candidatos ao QTL para VTE, é possível detectar a regulação transcricional a princípio favorável para o acúmulo desse metabólito na IL6-2.

4.2. Perfil transcricional das IL9-2 e 9-2-6

As ILs 9-2 e 9-2-6 apresentam aumento nos níveis de α-tocoferol e tocoferol total em frutos (Schauer *et al.*, 2006; Almeida *et al.*, 2011). Ambas ILs compartilham os alelos selvagens dos genes candidatos *VTE3*(1) e *CLH*(2), enquanto que a região introgredida da IL9-2 contém os genes *FOLK* (antigo *VTE5*), *ADH*(2) e *SEC14* (Almeida *et al.*, 2011); este último não foi avaliado no presente estudo.

A análise do perfil transcricional (Figura 1, Tabela 3, 4 e 5) revelou aumento nos níveis de RNAm dos genes *FOLK* e *ADH*(2) em frutos da IL9-2, fato que reforçaria o papel destes genes na determinação do QTL em questão. No caso de *CLH(2),* a diferença na expressão é dramática em folhas; o alelo de *S. pennellii* é 40 vezes mais expresso tanto na IL9-2 quanto na IL9-2-6 comparado a M82. Já em frutos verdes, enquanto não se detectam os transcritos desse gene no genótipo controle, em ambas ILs observa-se sua expressão, ainda que as quantidades de RNAm sejam pouco abundantes em termos absolutos. Esses resultados sugerem que *CLH(2)* teria pouca contribuição, se alguma, na atividade defitiladora da clorofila em frutos, assumindo-se que a síntese da cadeia isoprênica utilizada para produção de VTE ocorre *in loco*. Por outro lado, de maneira robusta, observa-se diferenças acentuadas na expressão do também candidato *VTE3*(1), cujo alelo selvagem apresenta níveis significativamente mais altos de mRNA que o cultivado, tanto em folha quanto em frutos.

Esses resultados motivaram nosso grupo a aprofundar no estudo das bases moleculares que determinam o $QTL_{9\text{-}2\text{-}6}$ (Almeida *et al.*, 2011), o qual, por sua vez, corresponde a um aumento de 50% no conteúdo de tocoferóis totais. O aumento da expressão da *VTE3*(1) em frutos foi igualmente detectado em linhagens recombinantes homozigotas e heterozigotas obtidas a partir do cruzamento entre *S. lycopersicum* (cv. M82) e IL9-2-6, fato que implica a dominância e a estabilidade do alelo selvagem através das gerações (F1 e F2) (Quadrana *et al.*, 2014; Anexo II). Além disso, o silenciamento transiente de *VTE3*(1) em frutos de tomate por VIGS reduziu os níveis de tocoferol, assinalando a importância desse gene para o conteúdo total e composição de VTE em frutos. A correlação positiva entre a presença do $QTL_{9\text{-}2\text{-}6}$ e os níveis de expressão de *VTE3*(1) sugere, portanto, que este *e*QTL determina o conteúdo de VTE na IL9-2-6. Experimentos adicionais revelaram que o *e*QTL da *VTE3*(1) é regulado epigeneticamente pela diferença no padrão de metilação entre o alelo de *S. pennellii* e *S. lycopersicum*. Tal diferença é atribuída à ocorrência de um elemento de transposição SINE: presente no promotor do alelo de *S. lycopersicum*, dependendo das condições de cultivo, sofre metilação e promove a redução na expressão de *VTE3*(1). Todavia, o alelo selvagem não possui o elemento SINE e, portanto, não é alvo de metilação no promotor, sem efeitos negativos na expressão (Quadrana *et al.*, 2014, Anexo II).

A diferença dos fragmentos introgredidos entre as IL9-2 e IL9-2-6 também reverbera em outros pontos da via de síntese de tocoferóis. A IL9-2 apresenta maior impacto no perfil transcricional do que a IL9-2-6. Por exemplo, é notável o acúmulo consistente de transcritos de *ISPE* nos três tecidos avaliados dessa IL. Embora ambas ILs apresentem maior expressão da rota central (*VTE1*, *VTE2*, *VTE4* e *VTE3*(1)) em folhas, o padrão encontrado para as vias componentes do MEP e SK é diferente entre os frutos IL9-2 e 9-2-6. Por outro lado, constatou-se em frutos dessas ILs uma redução consistente de *HST* codificante para enzima da via de síntese de plastoquinona, que compartilha com

a VTE o precursor cromanol homogentisato; tal observação sugere um favorecimento da produção de tocoferóis. Por fim, convém mencionar a maior expressão de *DHQ/SDH*(1) nos frutos da IL9-2, resultado coerente com a existência de um QTL reportado para o aumento da atividade enzimática da DHQ/SDH em frutos (Steinhauser *et al.*, 2011).

4.3. Perfil da IL9-1

Baseado no perfil metabólico da IL9-1, foram mapeados quatro QTL para VTE relacionados ao aumento de α-, β-, γ-tocoferol e total em frutos (Schauer *et al.*, 2006; Almeida *et al.*, 2011). Embora o gene *ADH*(2) também tenha sido predito dentro deste intervalo em Almeida *et al.* (2011), a clonagem posterior revelou que o alelo *ADH*(2) na IL9-1 corresponde ao de *S. lycopersicum*. Nesse caso, o gene candidato da IL seria *GPPS* [antigo GGPS(4)]. A atualização na anotação é baseada nos estudos recentes (Gutensohn *et al.*, 2013) que sugerem o *locus* Solyc09g008920 como codificante para a subunidade não catalítica da enzima heterodimérica GPPS. Com localização subcelular plastidial, GPPS estaria diretamente relacionada a síntese de monoterpenos que ocorre no citossol, por meio do redirecionamento do fluxo de isoprenóides no plastídeo para a produção do intermediário geranil difosfato, e subsequente exportação para o citossol. No entanto, a análise de expressão mostrou que a IL9-1 apresenta níveis semelhantes de transcrito *GPPS* comparado ao controle M82. Dessa maneira, não foram obtidos dados que permitam elaborar hipótese sobre a base molecular dos QTL para VTE descritos na IL9-1.

Com relação ao perfil transcricional, comparada às demais linhagens, a IL9-1 apresentou o menor número de alterações na abundância de mRNA em frutos. Notavelmente, no estádio verde-maduro, observa-se um aumento na expressão, principalmente, dos genes da via do SK [*CM*(1), *CS*(2), *DHQS*). Já no estádio maduro, a indução de *DXS*(1) e de *VTE3*(1) coincidem com o aumento de tocoferóis, ainda que haja redução na abundância de transcritos de *HPPD*(1) e *VTE4*.

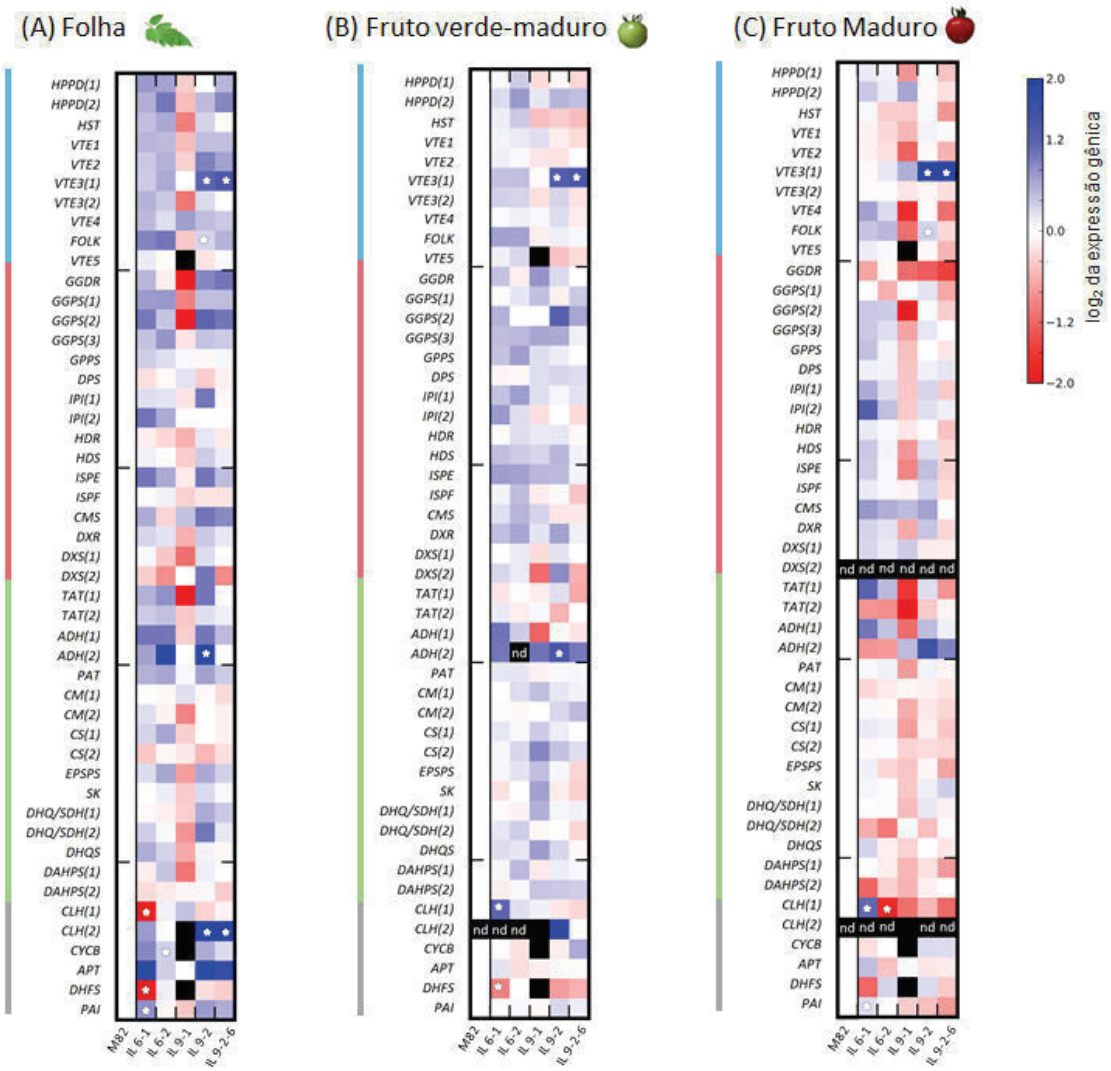

Figura 2. Perfil trancricional das IL6-1, 6-2, 9-1, 9-2 e 9-2-6. *Heat map* obtido a partir dos valores de $\log_2$ da razão de expressão entre a IL de *S. pennellii* e o parental controle M82 para folhas (A), frutos verde-maduros (B) e frutos maduros (C). Os genótipos estão representados por colunas; a primeira corresponde ao parental M82 e as demais às ILs. Os genes estão representados pelas linhas, organizados de acordo com a via bioquímica à qual pertencem (barra vertical colorida à esquerda): azul, rota central da VTE; cinza, rotas associadas à VTE; vermelho, via do MEP; verde, via do SK. Os genes que codificam para as enzimas estão nomeados de acordo às seguintes abreviações: 4-*HIDROXIFENILPIRUVATO DIOXIGENASE1* (*HPPD*), *TOCOFEROL CICLASE* (*VTE1*), *HOMOGENTISATO FITIL TRANSFERASE (VTE2), DIMETIL-FITILQUINOL METIL TRANSFERASE (VTE3), γ-TOCOFEROL C-METIL TRANSFERASE (VTE4), FITOL QUINASE (VTE5), FARNESOL QUINASE (FOLK), GERANILGERANIL REDUTASE (GGDR), GERANILGERANIL DIFOSFATO SINTASE (GGPS), GERANIL DIFOSFATO SINTASE (GPPS), DECAPRENIL FOSFATO SINTASE (DPS), ISOPENTENIL DIFOSFATO ISOMERASE (IPI), 4-HIDROXI-3-METILBUT-2-ENIL- DIFOSFATO SINTASE (HDS), 4-HIDROXI-3-METILBUT-2-ENIL- DIFOSFATO REDUTASE (HDR), 4-(CITIDINA 5'-DIFOSFO)-2-C-METIL-D-ERITRITOL QUINASE (ISPE), 2-C-METIL-D-ERITRITOL 2,4-CICLODIFOSFATO SINTASE (ISPF), 2-C-METIL-D-ERITRITOL 4-FOSFATO CITIDILILTRANSFERASE (CMS), 2-C-METIL-D- ERITRITOL 4-FOSFATO SINTASE (DXR), 1-DEOXI-D-XILULOSE-5-P SINTASE (DXS), TIROSINA AMINOTRANSFERASE (TAT), 3-DEOXI-D-ARABINO-HEPTULOSONATO-7-P SINTASE (DAHPS), 3-DEHIDROQUINATO SINTASE (DHQS), CHIQUIMATO DEHIDROGENASE(SDH)/3-DEHIDROQUINATO DEHIDRATSE (DHQ), CHIQUIMATO QUINASE (SK), 5-ENOLPIRUVILCHIQUIMATO-3-P SINTASE (EPSPS), CORISMATO SINTASE (CS), CORISMATO MUTASE (CM), PREFENATO AMINOTRANSFERASE (PAT), AROGENATO DEHIDROGENASE (ADH), CLOROFILASE (CLH), LICOPENO β CICLASE* (*CYCβ*), *ANTRANILATO FOSFORRIBOSILTRANSFERASE (APT), FOSFORIBOSILANTRANILATO ISOMERASE* (*PAI*), *DIHIDROFOLATO SINTASE* (*DHFS*). A intensidade do efeito está representada em escala de cores: azul indica aumento e vermelho indica decréscimo na abundância de transcritos. RNAm não detectado está indicado por 'nd'. Genótipos cuja expressão gênica não foi avaliada estão indicados apenas em preto. As diferenças significativas ($P < 0,05$), avaliadas por meio de teste de permutação, estão indicadas com *, apenas quando esta corresponde ao alelo selvagem de *S. pennellii.* As demais alterações significativas são mostradas na Tabela 3, 4 e 5.

Tabela 3. Valores de expressão relativa em folha.

Genes	M82	IL6-1	IL6-2	IL9-2	IL9-2-6	IL9-1
HPPD(1)	1.0 ± 0.39	1.68 ± 0.07	1.6 ± 0.24	1.38 ± 0.13	1.46 ± 0.29	0.77 ± 0.09
HPPD(2)	1.0 ± 0.37	1.51 ± 0.1	2.13 ± 0.43	1.41 ± 0.11	1.84 ± 0.46	0.7 ± 0.13
HST	1.0 ± 0.09	**1.38 ± 0.12**	**1.55 ± 0.33**	1.24 ± 0.11	0.97 ± 0.09	**0.51 ± 0.08**
VTE1	1.0 ± 0.16	**1.45 ± 0.03**	1.41 ± 0.18	**1.38 ± 0.06**	**1.37 ± 0.02**	0.71 ± 0.22
VTE2	1.0 ± 0.2	1.32 ± 0.16	1.46 ± 0.19	**1.9 ± 0.16**	**1.62 ± 0.09**	0.78 ± 0.09
VTE3(1)	1.0 ± 0.06	**1.3 ± 0.08**	**1.53 ± 0.24**	**2.28 ± 0.05**	**2.6 ± 0.06**	1.01 ± 0.15
VTE3(2)	1.0 ± 0.12	1.48 ± 0.13	1.32 ± 0.25	1.2 ± 0.15	1.27 ± 0.04	**0.49 ± 0.07**
VTE4	1.0 ± 0.08	**1.42 ± 0.06**	1.19 ± 0.13	**1.39 ± 0.12**	**1.32 ± 0.07**	1.64 ± 0.29
FOLK	1.0 ± 0.05	**1.86 ± 0.33**	**2.32 ± 0.41**	**1.24 ± 0.03**	**1.48 ± 0.1**	0.75 ± 0.18
VTE5	1.0 ± 0.08	1.13 ± 0.14	0.97 ± 0.23	0.86 ± 0.05	1.03 ± 0.12	NA
GGDR	1.0 ± 0.08	1.45 ± 0.14	0.9 ± 0.23	1.84 ± 0.05	1.7 ± 0.12	**0.19 ± 0.02**
GGPS(1)	1.0 ± 0.14	**1.66 ± 0.16**	**1.7 ± 0.7**	1.39 ± 0.36	1.38 ± 0.56	0.51 ± 0.11
GGPS(2)	1.0 ± 0.09	1.98 ± 0.76	1.33 ± 0.98	2.26 ± 1.04	**1.54 ± 0.1**	**0.22 ± 0.04**
GGPS(3)	1.0 ± 0.12	1.35 ± 0.07	**1.73 ± 0.19**	1.34 ± 0.05	1.29 ± 0.04	**0.86 ± 0.05**
GPPS	1.0 ± 0.05	**1.27 ± 0.04**	**1.18 ± 0.14**	0.96 ± 0.02	1.06 ± 0.03	1.04 ± 0.09
DPS	1.0 ± 0.05	0.85 ± 0.07	0.96 ± 0.08	0.77 ± 0.05	0.91 ± 0.06	1.16 ± 0.06
IPI(1)	1.0 ± 0.09	1.18 ± 0.08	**1.15 ± 0.14**	1.46 ± 0.2	0.96 ± 0.07	0.86 ± 0.03
IPI(2)	1.0 ± 0.1	**2.1 ± 0.32**	**1.54 ± 0.03**	1.02 ± 0.21	1.01 ± 0.06	0.97 ± 0.1
HDR	1.0 ± 0.12	0.9 ± 0.06	0.82 ± 0.04	1.13 ± 0.09	0.9 ± 0.04	**0.67 ± 0.02**
HDS	1.0 ± 0.21	1.09 ± 0.24	1.01 ± 0.89	1.31 ± 0.52	1.1 ± 0.28	0.78 ± 0.06
ISPE	1.0 ± 0.11	**1.85 ± 0.04**	**1.56 ± 0.12**	**1.47 ± 0.09**	1.39 ± 0.11	0.9 ± 0.09
ISPF	1.0 ± 0.09	1.02 ± 0.07	1.09 ± 0.08	0.86 ± 0.06	0.87 ± 0.09	0.78 ± 0.08
CMS	1.0 ± 0.11	**1.52 ± 0.03**	0.8 ± 0.3	**1.89 ± 0.19**	**1.8 ± 0.03**	1.37 ± 0.26
DXR	1.0 ± 0.25	1.23 ± 0.11	1.16 ± 0.07	1.32 ± 0.16	1.13 ± 0.09	0.67 ± 0.04
DXS(1)	1.0 ± 0.11	1.05 ± 0.09	0.75 ± 0.32	1.2 ± 0.29	0.95 ± 0.15	0.47 ± 0.19
DXS(2)	1.0 ± 0.21	0.78 ± 0.21	0.55 ± 0.18	2.49 ± 1.5	0.55 ± 0.22	0.93 ± 0.02
TAT(1)	1.0 ± 0.59	1.49 ± 0.12	1.76 ± 0.56	1.85 ± 0.41	1.29 ± 0.5	0.16 ± 0.02
TAT(2)	1.0 ± 0.14	1.3 ± 0.04	1.38 ± 0.11	1.18 ± 0.13	1.1 ± 0.36	0.75 ± 0.05
ADH(1)	1.0 ± 0.06	**2.18 ± 0.32**	**2.06 ± 0.16**	**1.89 ± 0.13**	1.41 ± 0.43	0.78 ± 0.37
ADH(2)	1.0 ± 0.05	1.6 ± 0.51	5.0 ± 1.88	**6.1 ± 1.1**	0.99 ± 0.49	0.99 ± 0.16
PAT	1.0 ± 0.07	**1.49 ± 0.07**	**1.58 ± 0.08**	**1.6 ± 0.12**	1.29 ± 0.19	1.05 ± 0.13
CM(1)	1.0 ± 0.08	0.99 ± 0.09	0.95 ± 0.07	0.98 ± 0.12	0.83 ± 0.07	1.17 ± 0.12
CM(2)	1.0 ± 0.01	**1.16 ± 0.08**	0.93 ± 0.22	0.99 ± 0.03	0.92 ± 0.1	0.52 ± 0.06
CS(1)	1.0 ± 0.03	**1.25 ± 0.13**	1.59 ± 0.29	0.99 ± 0.09	0.92 ± 0.1	**0.79 ± 0.1**
CS(2)	1.0 ± 0.14	0.75 ± 0.08	0.95 ± 0.1	0.69 ± 0.09	0.85 ± 0.13	0.88 ± 0.17
EPSPS	1.0 ± 0.13	1.2 ± 0.04	1.59 ± 0.26	1.54 ± 0.31	1.26 ± 0.32	0.61 ± 0.09
SK	1.0 ± 0.04	1.0 ± 0.04	1.1 ± 0.08	**1.2 ± 0.02**	1.05 ± 0.04	0.76 ± 0.07
DHQ/SDH(1)	1.0 ± 0.04	0.96 ± 0.08	0.93 ± 0.05	**1.54 ± 0.18**	**1.32 ± 0.07**	0.77 ± 0.05
DHQ/SDH(2)	1.0 ± 0.11	1.27 ± 0.25	1.03 ± 0.17	1.49 ± 0.29	1.14 ± 0.15	**0.57 ± 0.09**
DHQS	1.0 ± 0.17	**1.51 ± 0.15**	1.25 ± 0.06	1.07 ± 0.03	0.96 ± 0.11	**0.64 ± 0.04**
DAHPS(1)	1.0 ± 0.19	0.9 ± 0.22	1.33 ± 0.25	1.09 ± 0.3	1.13 ± 0.08	0.48 ± 0.08
DAHPS(2)	1.0 ± 0.07	0.83 ± 0.11	0.89 ± 0.31	1.04 ± 0.14	0.77 ± 0.14	0.94 ± 0.14
CLH(1)	1.0 ± 0.05	**0.32 ± 0.05**	1.07 ± 0.11	0.79 ± 0.16	0.93 ± 0.17	1.35 ± 0.7
CLH(2)	1.0 ± 0.04	1.68 ± 0.79	1.01 ± 0.63	**40.55 ± 4.97**	**48.21 ± 6.33**	NA
CYCB	1.0 ± 0.04	**1.85 ± 0.25**	1.26 ± 0.2	**1.53 ± 0.34**	**1.21 ± 0.04**	NA
APT	1.0 ± 0.84	3.25 ± 0.62	1.28 ± 1.09	**4.44 ± 0.33**	3.35 ± 0.36	**0.78 ± 0.19**
DHFS	1.0 ± 0.03	**0.34 ± 0.03**	1.08 ± 0.14	**0.83 ± 0.12**	**0.78 ± 0.05**	NA
PAI	1.0 ± 0.16	**1.77 ± 0.08**	0.95 ± 0.5	**1.68 ± 0.12**	**1.51 ± 0.25**	0.75 ± 0.53

As amostras de tecido foram obtidas de 5 plantas independentes que foram combinadas para obtenção de três réplicas biológicas. Os valores representam as medianas calculadas a partir das médias das duplicatas técnicas e relativizadas em relação ao parental controle M82. As diferenças estatísticas significativas ($P < 0,05$) estão indicadas em negrito de acordo com o teste de permutação (Pfaffl *et al.* 2002). NA: não avaliado; ND: avaliado, mas transcrito não detectado. Os genes estão nomeados de acordo com as abreviações da Figura 2.

Tabela 4. Valores de expressão relativa em fruto verde-maduro.

Genes	M82	IL6-1	IL6-2	IL9-2	IL9-2-6	IL9-1
HPPD(1)	1.0 ± 0.08	1.05 ± 0.12	1.29 ± 0.17	0.96 ± 0.1	**0.81 ± 0.02**	0.83 ± 0.03
HPPD(2)	1.0 ± 0.04	**1.21 ± 0.19**	1.67 ± 0.55	**1.45 ± 0.58**	1.38 ± 0.43	1.14 ± 0.8
HST	1.0 ± 0.07	1.11 ± 0.16	**1.31 ± 0.05**	**0.77 ± 0.08**	**0.71 ± 0.07**	0.72 ± 0.14
VTE1	1.0 ± 0.07	1.08 ± 0.13	**1.12 ± 0.07**	0.9 ± 0.02	**0.83 ± 0.07**	1.18 ± 0.18
VTE2	1.0 ± 0.06	1.09 ± 0.16	1.04 ± 0.15	**0.86 ± 0.06**	0.99 ± 0.26	0.88 ± 0.02
VTE3(1)	1.0 ± 0.13	**1.36 ± 0.08**	**1.38 ± 0.04**	**2.48 ± 0.16**	**2.66 ± 0.09**	0.98 ± 0.15
VTE3(2)	1.0 ± 0.12	1.26 ± 0.05	1.24 ± 0.01	1.23 ± 0.08	0.86 ± 0.08	0.85 ± 0.11
VTE4	1.0 ± 0.13	1.03 ± 0.02	1.1 ± 0.13	1.19 ± 0.2	0.9 ± 0.2	1.05 ± 0.22
FOLK	1.0 ± 0.07	**1.61 ± 0.17**	**1.6 ± 0.07**	1.1 ± 0.07	1.05 ± 0.1	0.9 ± 0.14
VTE5	1.0 ± 0.08	1.1 ± 0.19	1.22 ± 0.16	**0.73 ± 0.04**	**0.82 ± 0.08**	NA
GGDR	1.0 ± 0.08	1.36 ± 0.25	0.9 ± 0.12	**1.21 ± 0.01**	1.0 ± 0.07	1.72 ± 0.18
GGPS(1)	1.0 ± 0.04	1.02 ± 0.08	1.14 ± 0.06	0.92 ± 0.22	**1.32 ± 0.05**	1.37 ± 0.1
GGPS(2)	1.0 ± 0.46	1.48 ± 0.57	0.99 ± 0.28	2.42 ± 1.17	1.58 ± 0.35	1.01 ± 2.87
GGPS(3)	1.0 ± 0.12	1.4 ± 0.11	**1.43 ± 0.09**	**1.55 ± 0.23**	1.1 ± 0.16	**1.58 ± 1.03**
GPPS	1.0 ± 0.09	**1.37 ± 0.14**	**1.64 ± 0.19**	**1.1 ± 0.05**	1.02 ± 0.07	1.19 ± 0.21
DPS	1.0 ± 0.06	0.94 ± 0.03	0.97 ± 0.03	**1.23 ± 0.08**	**1.2 ± 0.05**	**1.19 ± 0.59**
IPI(1)	1.0 ± 0.04	**1.36 ± 0.18**	**1.66 ± 0.09**	1.06 ± 0.2	1.16 ± 0.05	1.18 ± 0.09
IPI(2)	1.0 ± 0.01	**1.68 ± 0.15**	1.18 ± 0.02	1.01 ± 0.03	0.82 ± 0.09	**0.84 ± 0.11**
HDR	1.0 ± 0.07	1.01 ± 0.1	1.19 ± 0.11	1.13 ± 0.23	0.95 ± 0.11	1.12 ± 0.18
HDS	1.0 ± 0.08	1.38 ± 0.25	1.3 ± 0.16	**1.45 ± 0.01**	1.09 ± 0.07	1.23 ± 0.14
ISPE	1.0 ± 0.04	**1.64 ± 0.2**	**1.62 ± 0.19**	**1.4 ± 0.24**	1.08 ± 0.21	1.44 ± 0.18
ISPF	1.0 ± 0.04	1.07 ± 0.29	**1.39 ± 0.2**	1.02 ± 0.07	0.74 ± 0.14	0.9 ± 0.08
CMS	1.0 ± 0.06	1.17 ± 0.23	**1.45 ± 0.35**	0.87 ± 0.07	0.88 ± 0.06	1.25 ± 0.41
DXR	1.0 ± 0.22	1.38 ± 0.17	1.58 ± 0.05	1.6 ± 0.26	1.1 ± 0.18	1.16 ± 0.08
DXS(1)	1.0 ± 0.03	0.98 ± 0.15	1.12 ± 0.17	1.16 ± 0.05	1 ± 0.04	0.83 ± 0.4
DXS(2)	1.0 ± 0.49	1.23 ± 0.3	1.11 ± 0.02	1.79 ± 0.26	0.67 ± 0.5	0.46 ± 0.21
TAT(1)	1.0 ± 0.19	0.87 ± 0.06	0.98 ± 0.37	1.17 ± 0.15	0.64 ± 0.17	0.91 ± 0.59
TAT(2)	1.0 ± 0.19	1.12 ± 0.24	0.9 ± 0.18	**0.69 ± 0.18**	0.99 ± 0.23	1.04 ± 0.38
ADH(1)	1.0 ± 0.16	**2.04 ± 0.33**	1.3 ± 0.35	0.95 ± 0.14	0.88 ± 0.43	0.44 ± 0.14
ADH(2)	1.0 ± 0.34	2.01 ± 1.15	ND	**2.65 ± 1.24**	1.96 ± 1.46	2.04 ± 0.94
PAT	1.0 ± 0.08	1.14 ± 0.05	1.14 ± 0.01	1.04 ± 0.06	1.06 ± 0.02	0.93 ± 0.34
CM(1)	1.0 ± 0.09	1.0 ± 0.13	1.19 ± 0.13	1.14 ± 0.08	1.08 ± 0.36	**1.38 ± 0.25**
CM(2)	1.0 ± 0.05	1.03 ± 0.04	0.97 ± 0.09	1.22 ± 0.07	**1.43 ± 0.16**	0.98 ± 0.18
CS(1)	1.0 ± 0.06	1.15 ± 0.04	1.05 ± 0.04	1.11 ± 0.06	0.98 ± 0.11	1.29 ± 0.31
CS(2)	1.0 ± 0.08	1.07 ± 0.04	1.23 ± 0.09	**1.36 ± 0.04**	1.18 ± 0.05	**1.85 ± 0.29**
EPSPS	1.0 ± 0.14	1.06 ± 0.02	1.16 ± 0.08	1.06 ± 0.08	0.8 ± 0.17	1.37 ± 0.36
SK	1.0 ± 0.05	0.85 ± 0.1	1.01 ± 0.1	0.9 ± 0.05	**0.78 ± 0.13**	1.61 ± 0.32
DHQ/SDH(1)	1.0 ± 0.02	0.97 ± 0.07	0.93 ± 0.05	1.06 ± 0	1.09 ± 0.04	1.48 ± 0.3
DHQ/SDH(2)	1.0 ± 0.28	1.14 ± 0.24	1.28 ± 0.22	1.0 ± 0.05	0.81 ± 0.27	0.96 ± 0.21
DHQS	1.0 ± 0.06	**1.19 ± 0.04**	1.15 ± 0.11	1.23 ± 0.08	0.97 ± 0.17	1.65 ± 0.19
DAHPS(1)	1.0 ± 0.11	1.06 ± 0.24	**1.42 ± 0.08**	1.11 ± 0.1	1.05 ± 0.08	0.89 ± 0.19
DAHPS(2)	1.0 ± 0.07	**0.9 ± 0.02**	1.05 ± 0.08	**1.32 ± 0.09**	**1.27 ± 0.07**	1.34 ± 0.14
CLH(1)	1.0 ± 0.12	**2.27 ± 0.17**	1.17 ± 0.18	0.88 ± 0.07	0.81 ± 0.24	1.09 ± 0.25
CLH(2)	ND	ND	ND	3.53 ± 5.78	1.0 ± 0.92	NA
CYCB	1.0 ± 0.1	0.98 ± 0.03	0.86 ± 0.16	0.91 ± 0.19	**1.55 ± 0.13**	NA
APT	1.0 ± 0.07	1.16 ± 0.15	0.84 ± 0.11	0.98 ± 0.03	1.02 ± 0.03	0.9 ± 0.07
DHFS	1.0 ± 0.07	**0.51 ± 0.06**	0.99 ± 0.1	**0.6 ± 0.15**	**0.67 ± 0.05**	NA
PAI	1.0 ± 0.06	1.02 ± 0.22	1.05 ± 0.07	1.22 ± 0.15	1.1 ± 0.03	0.95 ± 0.16

As amostras de tecido foram obtidas de 5 plantas independentes que foram combinadas para obtenção de três réplicas biológicas. Os valores representam as medianas calculadas a partir das médias das duplicatas técnicas e relativizadas em relação ao parental controle M82 (exceção *CLH*(2), cujo valor foi relativizado à IL9-2-6 pois no genótipo M82 não foi detectada a presença do RNAm). As diferenças estatísticas significativas ($P < 0,05$) estão indicadas em negrito de acordo com o teste de permutação (Pfaffl *et al.* 2002). NA: não avaliado; ND: avaliado, mas transcrito não detectado. Os genes estão nomeados de acordo com as abreviações da Figura 2.

Tabela 5. Valores de expressão relativa em fruto maduro.

Gene	M82	IL6-1	IL6-2	IL9-2	IL9-2-6	IL9-1
HPPD(1)	1.0 ± 0.02	**1.12 ± 0.01**	**1.09 ± 0.03**	1.04 ± 0.13	0.73 ± 0.17	**0.58 ± 0.02**
HPPD(2)	1.0 ± 0.1	1.32 ± 0.16	1.11 ± 0.05	0.96 ± 0.01	**0.85 ± 0.12**	1.58 ± 0.11
HST	1.0 ± 0.11	1.04 ± 0.06	**0.77 ± 0.07**	1.04 ± 0.47	**0.58 ± 0.02**	0.77 ± 0.18
VTE1	1.0 ± 0.11	0.93 ± 0.02	0.82 ± 0.04	1.07 ± 0.13	0.97 ± 0.17	0.69 ± 0.09
VTE2	1.0 ± 0.16	0.93 ± 0.18	0.85 ± 0.24	0.95 ± 0.12	0.68 ± 0.15	0.43 ± 0.02
VTE3(1)	1.0 ± 0.09	0.96 ± 0.08	1.13 ± 0.28	**5.41 ± 0.24**	**3.88 ± 0.17**	**1.5 ± 0.18**
VTE3(2)	1.0 ± 0.06	0.98 ± 0.03	1.03 ± 0.08	0.94 ± 0.19	0.83 ± 0.12	0.87 ± 0.09
VTE4	1.0 ± 0.35	1.62 ± 0.16	1.21 ± 0.21	0.97 ± 0.28	**0.47 ± 0.07**	**0.31 ± 0.03**
FOLK	1.0 ± 0.09	**1.33 ± 0.04**	1.44 ± 0.11	**1.25 ± 0.18**	0.82 ± 0.11	**0.47 ± 0.05**
VTE5	1.0 ± 0.17	1.11 ± 0.14	1.05 ± 0.07	0.96 ± 0.41	0.68 ± 0.22	NA
GGDR	1.0 ± 0.26	0.63 ± 0.14	0.96 ± 0.07	**0.42 ± 0.43**	0.35 ± 0.12	0.46 ± 0.04
GGPS(1)	1.0 ± 0.08	1.01 ± 0.07	**0.67 ± 0.08**	1.16 ± 0.14	0.63 ± 0.13	1.02 ± 0.2
GGPS(2)	1.0 ± 0.3	1.31 ± 0.08	1.29 ± 0.83	1.04 ± 0.24	0.77 ± 0.15	0.23 ± 0.02
GGPS(3)	1.0 ± 0.06	**1.32 ± 0.03**	1.19 ± 0.15	1.13 ± 0.07	1.02 ± 0.1	0.62 ± 0.11
GPPS	1.0 ± 0.06	**1.37 ± 0.08**	**1.08 ± 0.11**	1.01 ± 0.02	0.88 ± 0.04	0.72 ± 0.12
DPS	1.0 ± 0.06	1.09 ± 0.05	1.08 ± 0.04	1.09 ± 0.07	1.15 ± 0.04	0.74 ± 0.04
IPI(1)	1.0 ± 0.09	**1.54 ± 0.05**	1.19 ± 0.21	1.24 ± 0.12	0.76 ± 0.08	0.75 ± 0.08
IPI(2)	1.0 ± 0.44	2.46 ± 0.31	1.37 ± 0.25	1.18 ± 0.14	1.1 ± 0.19	**0.75 ± 0.12**
HDR	1.0 ± 0.02	**1.12 ± 0.03**	1.03 ± 0.08	1.02 ± 0.11	**0.72 ± 0.07**	0.88 ± 0.07
HDS	1.0 ± 0.13	**1.31 ± 0.37**	1.07 ± 0.24	**1.18 ± 0.06**	0.82 ± 0.29	0.58 ± 0.17
ISPE	1.0 ± 0.09	**1.28 ± 0.14**	1.04 ± 0.08	**1.37 ± 0.15**	0.78 ± 0.07	0.53 ± 0.08
ISPF	1.0 ± 0.12	1.12 ± 0.03	1.05 ± 0.03	1.25 ± 0.21	0.83 ± 0.06	0.93 ± 0.05
CMS	1.0 ± 0.07	**1.72 ± 0.05**	1.5 ± 0.23	**1.61 ± 0.04**	1.01 ± 0.28	1.41 ± 0.27
DXR	1.0 ± 0.05	**1.25 ± 0.02**	1.16 ± 0.23	**1.33 ± 0.11**	0.81 ± 0.17	0.64 ± 0.28
DXS(1)	1.0 ± 0.05	**1.22 ± 0.21**	1.12 ± 0.21	0.89 ± 0.19	0.9 ± 0.04	**1.3 ± 0.19**
DXS(2)	ND	ND	ND	ND	ND	ND
TAT(1)	1.0 ± 0.34	**2.33 ± 0.45**	1.43 ± 0.69	1.19 ± 0.47	0.57 ± 0.12	0.33 ± 0.14
TAT(2)	1.0 ± 0.48	0.57 ± 0.17	0.56 ± 0.44	0.76 ± 0.08	0.94 ± 0.19	0.22 ± 0.04
ADH(1)	1.0 ± 0.1	**2.02 ± 0.37**	1.35 ± 0.07	1.39 ± 0.31	1.09 ± 0.49	0.46 ± 0.38
ADH(2)	1.0 ± 0.25	0.57 ± 0.16	0.59 ± 0.07	2.97 ± 8.71	1.88 ± 0.58	1.4 ± 0.54
PAT	1.0 ± 0.06	1.04 ± 0.05	1.08 ± 0.08	**1.07 ± 0.01**	0.95 ± 0.07	0.59 ± 0.1
CM(1)	1.0 ± 0.06	0.82 ± 0.06	0.89 ± 0.19	0.92 ± 0.03	0.86 ± 0.15	0.94 ± 0.02
CM(2)	1.0 ± 0.07	1.05 ± 0.04	0.95 ± 0.05	0.89 ± 0.08	0.81 ± 0.16	0.65 ± 0.08
CS(1)	1.0 ± 0.04	**1.12 ± 0.05**	1.08 ± 0.01	0.91 ± 0.2	**0.75 ± 0.09**	0.61 ± 0.08
CS(2)	1.0 ± 0.09	0.97 ± 0.1	1.02 ± 0.07	0.83 ± 0.04	0.8 ± 0.11	0.79 ± 0.17
EPSPS	1.0 ± 0.06	1.09 ± 0.07	**0.81 ± 0.02**	0.94 ± 0.11	**0.62 ± 0.04**	0.74 ± 0.1
SK	1.0 ± 0.06	1.06 ± 0.04	1.02 ± 0.06	1.1 ± 0.07	1.28 ± 0.14	0.75 ± 0.1
DHQ/SDH(1)	1.0 ± 0.03	1.02 ± 0.03	1.03 ± 0.1	1.13 ± 0.04	0.92 ± 0.1	0.7 ± 0.14
DHQ/SDH(2)	1.0 ± 0.39	0.65 ± 0.04	**0.49 ± 0.09**	0.71 ± 0.1	1.02 ± 0.21	1.05 ± 0.13
DHQS	1.0 ± 0.09	1.24 ± 0.11	**0.91 ± 0.04**	1.02 ± 0.07	0.88 ± 0.14	0.79 ± 0.1
DAHPS(1)	1.0 ± 0.11	0.98 ± 0.07	0.9 ± 0.05	0.86 ± 0.04	0.59 ± 0.1	0.69 ± 0.11
DAHPS(2)	1.0 ± 0.11	**0.44 ± 0.05**	0.78 ± 0.12	0.91 ± 0.08	0.99 ± 0.09	0.68 ± 0.14
CLH(1)	1.0 ± 0.11	**2.21 ± 0.41**	**0.3 ± 0.16**	0.69 ± 0.16	**0.45 ± 0.02**	0.46 ± 0.13
CLH(2)	ND	ND	ND	ND	ND	NA
CYCB	1.0 ± 0.15	0.85 ± 0.19	0.99 ± 0.12	1.21 ± 0.2	1.2 ± 0.3	NA
APT	1.0 ± 0.08	1.38 ± 0.28	0.72 ± 0.12	0.87 ± 0.15	0.9 ± 0.05	1.02 ± 0.18
DHFS	1.0 ± 0.18	0.44 ± 0.25	1.25 ± 0.06	1.21 ± 0.22	0.76 ± 0.12	NA
PAI	1.0 ± 0.21	**1.19 ± 0.16**	0.97 ± 0.3	0.72 ± 0.37	0.59 ± 0.13	0.77 ± 0.12

As amostras de tecido foram obtidas de 5 plantas independentes que foram combinadas para obtenção de três réplicas biológicas. Os valores representam as medianas calculadas a partir das médias das duplicatas técnicas e relativizadas em relação ao parental controle M82. As diferenças estatísticas significativas ($P < 0,05$) estão indicadas em negrito de acordo com o teste de permutação (Pfaffl *et al.* 2002). NA: não avaliado; ND: avaliado, mas transcrito não detectado. Os genes estão nomeados de acordo com as abreviações da Figura 2.

5. Conclusão

Nesse estudo, a análise do perfil transcricional completo dos genes das rotas de biossíntese de tocoferol e vias associadas permitiu aprofundar o conhecimento e propor cenários possíveis para a determinação da base molecular de alguns QTL previamente identificados para VTE. Os resultados revelaram a existência de diferenças de expressão (*e*QTL) associados aos QTL de VTE: $QTL_{9\text{-}2}$ [*VTE3*(1), *FOLK* e *ADH*(2)], $QTL_{9\text{-}2\text{-}6}$ [*VTE3*(1)], $QTL_{6\text{-}1}$ [*CLH*(1), *PAI* e *DHFS*] e $QTL_{6\text{-}2}$ (*CYC*β). Em particular, o $QTL_{9\text{-}2\text{-}6}$ teve seu mecanismo genético elucidado pelo nosso grupo de pesquisa; nesse caso, o aumento de tocoferol é determinado por diferenças epigenéticas entre os alelos de *VTE3*(1) que afetam os níveis expressão desse gene. Além disso, a presença do fragmento genômico selvagem nas IL afetou a expressão dos genes da rota biossintética de VTE, evidenciando a ocorrência de efeitos epistáticos.

6. Referências bibliográficas

Almeida, J., Quadrana, L., Asis, R., Setta, N., de Godoy, F., Bermudez, L., Otaiza, S., *et al.* (2011) Genetic dissection of vitamin E biosynthesis in tomato. *Journal of Experimental Botany,* 62, 3781–3798.

Alseekh, S., Tohge, T., Wendenberg, R., Scossa, F., Omranian, N., Li, J., *et al*. (2015) Identification and Mode of Inheritance of Quantitative Trait Loci for Secondary Metabolite Abundance in Tomato. *The Plant Cell*, 27, 485-512.

Bolger, A., Scossa, F., Bolger, M. E., Lanz, C., Maumus, F., Tohge, T., *et al*. (2014) The genome of the stress-tolerant wild tomato species Solanum pennellii. *Nature Genetics*, 46, 1034–1038.

Delker, C., Quint, M. (2011) Expression level polymorphisms: Heritable traits shaping natural variation. *Trends in Plant Science*, 16, 481–488.

DellaPenna, D., Mène-Saffrané, L. (2011) Vitamin E. *Advances in Botanical Research*, 59, 179–227.

Di Rienzo, J. A. (2009) Statistical software for the analysis of experiments of functional genomics. RDNDA, Argentina. http://sites.google.com/site/fgStatistics/.

Dwiyanti, M. S., Yamada, T., Sato, M., Abe, J., Kitamura, K. (2011) Genetic variation of γ-tocopherol methyltransferase gene contributes to elevated α-tocopherol content in soybean seeds. *BioMed Central Plant Biology*, 11, 152.

Eberhard, J., Ehrler, T. T., Epple, P., Felix, G., Raesecke, H. R., Amrhein, N. (1996) Cytosolic and plastidic chorismate mutase isozymes from Arabidopsis thaliana: molecular characterization and enzymatic properties. *Plant Journal*, 10, 815-821.

Expósito-Rodriguez, M., Borges, A. A., Borges-Perez, A., Perez, J., Expósito-Rodríguez, M., Borges-Pérez, A., *et al*. (2008) Selection of internal control genes for quantitative real-time RT-PCR studies during tomato development process. *BMC Plant Biology*, 8, 131.

Gilliland, L. U., Magallanes-Lundback, M., Hemming, C., Supplee, A., Koornneef, M., Bentsink, L., *et al*. (2006) Genetic basis for natural variation in seed vitamin E levels in Arabidopsis thaliana. *Proceedings of the National Academy of Sciences of United States of America*, 103, 18834–18841.

Gutensohn, M., Orlova, I., Nguyen, T. T. H., Davidovich-Rikanati, R., Ferruzzi, M. G., Sitrit, Y., *et al*. (2013) Cytosolic monoterpene biosynthesis is supported by plastid-generated geranyl diphosphate substrate in transgenic tomato fruits. *Plant Journal*, 75, 351–363.

Haddadi, P., Ebrahimi, A., Langlade, N. B., Yazdi-samadi, B., Berger, M., Calmon, A., *et al*. (2012) Genetic dissection of tocopherol and phytosterol in recombinant inbred lines of sunflower through quantitative trait locus analysis and the candidate gene approach. *Molecular Breeding*, 29, 717–729.

He, Y., Li, J. (2001) Differential expression of triplicate phosphoribo sylanthranilate isomerase isogenes in the tryptophan biosynthetic pathway of Arabidopsis thaliana (L.). Heynh. *Planta*, 212, 641-647.

Hellemans, J., Mortier, G., De Paepe, A., Speleman, F., Vandesompele, J. (2007) qBase relative quantification framework and software for management and automated analysis of real-time quantitative PCR data. *Genome Biology*, 8, 19.

Lipka, A. E., Gore, M. A., Lundback, M. M., Mesberg, A., Lin, H., Tiede, T., *et al*. (2013) Genome-wide association study and pathway-level analysis of tocochromanol levels in maize grain. *G3: Genes | Genomes | Genetics*, 3, 1287–1299.

Mackay, T. F. (2014) Epistasis and quantitative traits: using model organisms to study gene-gene interactions. *Nature Reviews Genetics*, 15, 22-33.

Morandini, P. (2013) Control limits for accumulation of plant metabolites: brute force is no substitute for understanding. *Plant Biotechnology Journal*, 11, 253–67.

Mouillon, J. M., Ravanel, S., Douce, R., Rébeillé, F. (2002) Folatesynthesis in higher-plant mitochondria: coupling between thedihydropterin pyrophosphokinase and the dihydropteroate synthase activities. *Biochemical Journal*, 363, 313–319.

Quadrana, L., Almeida, J., Asís, R., Duffy, T., Dominguez, P. G., Bermúdez, L., *et al*. (2014) Natural occurring epialleles determine vitamin E accumulation in tomato fruits. *Nature Communications*, 5, 3027.

Quadrana, L., Almeida, J., Otaiza, S. N., Duffy, T., Corrêa da Silva, J. V., de Godoy, F., *et al*. (2013) Transcriptional regulation of tocopherol biosynthesis in tomato. *Plant Molecular Biology*, 81, 309–325.

Ronen, G., Carmel-goren, L., Zamir, D., Hirschberg, J. (2000) An alternative pathway to beta-carotene formation in plant chromoplasts discovered by map-based cloning of Beta and old-gold color mutations in tomato. *Proceedings of the National Academy of Sciences of the United States of America*, 97, 11102-11107.

Ruijter, J. M., Ramakers, C., Hoogaars, W. M., Karlen, Y., Bakker, O., van den Hoff, M. J., *et al*. (2009) Amplification efficiency: linking baseline and bias in the analysis of quantitative PCR data. *Nucleic acids research*, 37, 45.

Sahr, T., Ravanel, S., Basset, G., Nichols, B. P., Hanson, A. D., Rébeillé, F. (2006) Folate synthesis in plants: purification, kinetic properties, and inhibition of aminodeoxychorismate synthase. *Biochemical Journal*, 396, 157–162.

Schauer, N., Semel, Y., Roessner, U., Gur, A., Balbo, I., Carrari, F., *et al*. (2006) Comprehensive metabolic profiling and phenotyping of interspecific introgression lines for tomato improvement. *Nature Biotechnology*, 24, 447–54.

Shumskaya, M., Wurtzel, E. T. (2013) The carotenoid biosynthetic pathway: Thinking in all dimensions. *Plant Science*, 208, 58–63.

Shutu, X., Dalong, Z., Ye, C., Yi, Z., Shah, T., Ali, F., *et al*. (2012) Dissecting tocopherols content in maize (*Zea mays* L.), using two segregating populations and high-density single nucleotide polymorphism markers. *BMC Plant Biology*, 12, 201.

Steinhauser, M. C., Steinhauser, D., Gibon, Y., Bolger, M., Arrivault, S., Usadel, B., *et al*. (2011) Identification of enzyme activity quantitative trait loci in a *Solanum lycopersicum* x *Solanum pennellii* introgression line population. *Plant Physiology*, 157, 998–1014.

Tzin, V., Galili, G. (2010) New insights into the shikimate and aromatic amino acids biosynthesis pathways in plants. *Molecular Plant*, 3, 956–972.

Wang, X., Zhang, C., Li, L., Fritsche, S., Endrigkeit, J., Zhang, W., *et al*. (2012) Unraveling the Genetic Basis of Seed Tocopherol Content and Composition in Rapeseed (*Brassica napus* L.). *Plos One*, 7, 8–14.

Wentzell, A. M., Rowe, H. C., Hansen, B. G., Ticconi, C., Halkier, B. A., Kliebenstein, D. J. (2007) Linking metabolic QTLs with network and cis-eQTLs controlling biosynthetic pathways. *Plos Genetics*, 3, 1687–1701.

CAPÍTULO III. ESTUDO DO EFEITO DOS GENES *CLOROFILASE1, FARNESOL QUINASE* E *FITOL QUINASE* NA BIOSSÍNTESE DE TOCOFERÓIS EM FRUTOS DE TOMATE VIA SILENCIAMENTO GÊNICO POR INDUZIDO VÍRUS

1. Introdução

O estudo do perfil transcricional da via de biossíntese de tocoferol ao longo do desenvolvimento de folhas e frutos sugeriu que a disponibilidade do precursor fitil-difosfato é uma das restrições metabólicas para produção desse antioxidante em tomateiro (Capítulo I, Quadrana *et al.*, 2013). Tal hipótese é baseada na estreita correlação entre a abundância de transcritos de genes associados ao controle da entrada e saída dos precursores da via do MEP, *DXS* e *GGDR,* e o conteúdo de VTE. Além disso, esse mesmo trabalho revelou a relação entre o metabolismo de VTE e de clorofila, já que os níveis dos transcritos de *VTE5* e *CLH* correlacionaram com os níveis desses metabólitos. Assim, esses resultados sugerem que *VTE5* e *CLH* colaboram com o fornecimento da cadeia prenílica para síntese de tocoferóis em folha e fruto, sendo necessário um estudo funcional detalhado que avalie o seu envolvimento na biossíntese desses compostos nutracêuticos em tomateiro.

Tanto a geração e caracterização de linhagens mutantes quanto a supressão da expressão gênica via silenciamento constituem abordagens bastante úteis para o entendimento da função gênica (Senthil-Kumar & Mysore, 2014). Essa última pode ser induzida pelo mecanismo de RNA de interferência (RNAi), desencadeado por um RNA fita-dupla (dsRNA), que resulta na degradação específica de mRNAs homólogos ou inibição da tradução (silenciamento gênico pós-transcricional, PTGS) ou ainda na inativação do promotor por metilação (silenciamento gênico transcricional, TGS) (Baulcombe, 2004; Brodersen & Voinet, 2006; Zhao *et al.*, 2014). O silenciamento gênico em plantas ocorre naturalmente por meio de múltiplas vias distintas com funções reconhecidas no combate a vírus, no controle de elementos de transposição e na regulação do desenvolvimento (Pikaard & Scheid, 2014). Desde a descoberta inicial do RNAi em plantas, rapidamente percebeu-se que este mecanismo poderia ser explorado experimentalmente para reduzir a expressão gênica utilizando técnicas de transgenia (Mansoor *et al.*, 2006). Tal fato fez com que o silenciamento gênico mediado por RNAi emergisse como estratégia eficaz e poderosa a qual vêm sendo amplamente empregada em organismos vegetais.

Dentre as diversas técnicas de silenciamento, uma baseia-se na introdução no tecido vegetal de vetores virais recombinantes carregando a sequência parcial do (trans)gene do hospedeiro que se deseja silenciar (Liu *et al.*, 2002). Esse sistema é denominado de Silenciamento Gênico Induzido por Vírus (*Virus Induced Gene Silencing*, VIGS) e constitui uma abordagem interessante para iniciar o estudo funcional de genes principalmente pela rapidez comparado à obtenção de plantas transgênicas

estáveis e pela possibilidade de verificação do silenciamento restrito a um tecido alvo (Figura 1) (Fu *et al.*, 2005; Orzaez *et al.*, 2006). No entanto, em virtude da extensão heterogênea do silenciamento dependente do sucesso da transformação, é fundamental a presença de um marcador visual que permita monitorar e identificar as regiões silenciadas nos tecidos infectados (Orzaez *et al.* 2009; Quadrana *et al.*, 2011).

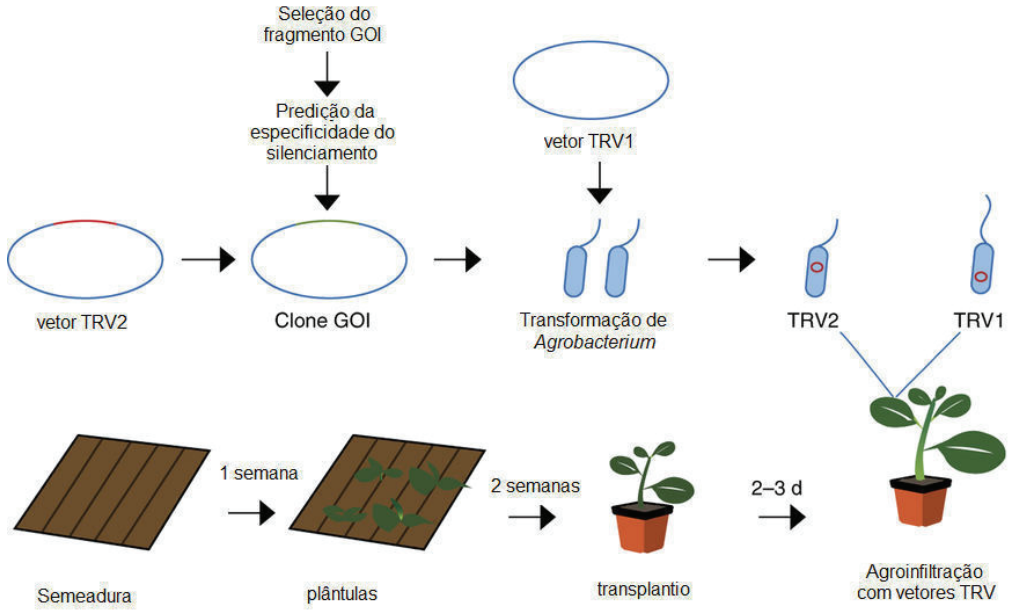

Figura 1: Visão geral do protocolo de VIGS em plantas. O gene de interesse (GOI) é clonado no vetor TRV2. A seleção do fragmento gênico apropriado é fundamental para induzir o silenciamento e garantir a especificidade do alvo. O vetor TRV1 possui as funções que permitem a propagação do vírus. Transformação de *Agrobacterium* com os vetores TRV e agroinfiltração em plântulas (no exemplo, tabaco) com cerca de 3 semanas. As plantas silenciadas podem já podem ser utilizadas a partir de três semanas após infiltração (Adaptado de Senthil-Kumar & Mysore, 2014).

Em tomateiro, foi estabelecido um sistema para VIGS que se baseia no vetor viral TRV (*Tobacco Rattle Virus*) e utiliza como gene repórter *PROTEÍNA FLUORESCENTE VERDE* (*GREEN FLUORESCENT PROTEIN*, *GFP)* (Quadrana *et al.,* 2011). O cosilenciamento é induzido pela expressão transiente de um fragmento de *GFP* fusionado a um fragmento do gene alvo em plantas transgênicas que expressam constitutivamente a proteína GFP. O vetor é introduzido por meio da transformação mediada por *Agrobacterium tumefaciens* no pedúnculo floral. A região do fruto silenciada é identificada pela ausência de fluorescência sob luz U.V., viabilizando sua dissecção para posterior caracterização metabólica (Quadrana *et al.*, 2011). Este sistema foi escolhido como abordagem inicial para avaliar o impacto do silenciamento dos genes envolvidos no metabolismo do fitol, *VTE5-like* e *CLH(1),* no conteúdo de tocoferol em frutos de tomateiro.

2. Objetivos específicos

Avaliar o impacto do silenciamento gênico de *VTE5, FOLK e CLH(1)* em tomateiro pela técnica de silenciamento gênico induzido por vírus.

3. Material e métodos

3.1. Material vegetal

A clonagem das sequências foi feita a partir de cDNA de *S. lycopersicum* (*cv*. M82). Para indução do VIGS, foram utilizadas plantas de *S. lycopersicum* (*cv*. Moneymaker) selvagens e transgênicas que expressam constitutivamente GFP (Quadrana *et al.*, 2011).

As plantas foram crescidas em casa de vegetação em vasos plásticos (15 L) com mistura de terra vegetal e vermiculita (1:1, v/v), suplementado com NPK 20:5:20 (8 g/L) e Yoorin® (1 g/L), sob condições naturais de temperatura e fotoperíodo.

Para o silenciamento de frutos, as seis primeiras inflorescências de cinco plantas foram agroinfiltradas para cada tratamento (construção de interesse). Pericarpo de frutos verde-maduros (cuja placenta estava totalmente translúcida gelatinosa) e maduro (seis dias após o aparecimento dos primeiros sinais de acúmulo de carotenóides) foram coletados, os quais correspondem a aproximadamente 40 e 55 dias após antese. Após a confirmação do silenciamento, as amostras de frutos foram utilizadas para elaboração de *pools,* obtendo-se três a cinco réplicas biológicas. Dessa maneira, ao final, cada réplica biológica conteve material vegetal proveniente de ao menos uma planta independente.

Para o experimento independente de VIGS em folhas, 10 plântulas de 16 dias pós-germinação foram agroinfiltradas para cada tratamento (construção de interesse). Fragmentos de folhas fonte silenciadas foram coletadas 30 dias após a infiltração. Nesse caso, o material vegetal proveniente de cada indivíduo independente constituiu uma réplica biológica.

Todos os tecidos vegetais coletados, foram congelados imediatamente em nitrogênio líquido e armazenados a -80ºC até posterior processamento.

3.2. Cepas bacterianas e vetores

3.2.1. *Escherichia coli*

As células de *E. coli* das cepas *DH10B* e *DB3.1* foram utilizadas para fins de clonagem. As culturas foram crescidas em meio LB (Luria-Bertani) a 37 °C e, nos casos de cultivo líquido, sob a agitação de 200 rpm. Após a transformação das cepas com vetor plasmidial, o antibiótico de seleção correspondente foi adicionado ao meio de cultivo (Tabela 1).

O preparo de células *E. coli* competentes foi realizado segundo descrito por Hanahan (1983) com modificações. A partir de uma colônia isolada de *E. coli,* foi feito um pré-inóculo com 2 mL de meio SOB (Sambrook *et al.*, 1989) e mantido por 18 h a 37 °C sob agitação constante de 200 rpm. O

pré-inoculo foi transferido para 50 mL de meio LB e incubado a 37 °C sob agitação constante até atingir um valor entre 0,5 a 0,6 de absorbância a 600 nm. Em seguida, adicionou-se 0,5 mL de $MgCl_2$ 2 M e a cultura foi resfriada em gelo por 15 min. Seguiu-se uma centrifugação suave a 3000 rpm por 20 min a 4 °C. O sobrenadante foi descartado, o precipitado ressuspendido em 15 mL de solução RFI e mantido em gelo por 10 min. Repetiu-se a centrifugação a 3000 rpm por 20 min a 4 °C, sendo novamente o sobrenadante descartado. O precipitado de células foi ressuspendido delicadamente em 2 mL da solução RFII. Alíquotas de 50 μL foram feitas, congeladas em nitrogênio líquido e armazenadas em freezer a -80°C. Todas as manipulações de células foram realizadas em fluxo laminar, sob condições de assepsia.

Solução RFI: Acetato de potássio pH 6,9 (30 mM), cloreto de manganês (50 mM), cloreto de potássio (100 mM), cloreto de cálcio (10 mM) e glicerol (15 %). Esterilizada em autoclave por 15 min a 120 °C.

Solução RFII: MOPS pH 7,0 (10 mM), cloreto de cálcio (75 mM), cloreto de potássio (10 mM) e glicerol (15 %). Esterilizada em autoclave por 15 min a 120°C.

3.2.2. *Agrobacterium tumefaciens*

Para transformação de folhas e flores de tomateiro, células de *A. tumefaciens* da cepa GV3101 foram utilizadas as quais possuem resistência cromossômica à rifampicina (25 mg/L) e à gentamicina (50 mg/L) no plasmídeo Ti. As bactérias foram cultivadas em meio LB a 28 ºC e, nos casos de cultivo líquido, mantidas sob agitação de 170 rpm.

A obtenção de células competentes foi realizada segundo descrito por Brasileiro *et al.* (1998). A partir de uma colônia isolada de *A. tumefaciens,* foi feito um pré-inóculo com 3 mL de meio LB durante 24 h a 28 °C sob agitação de 170 rpm constante. Após esse período, 1 mL do pré-inoculo foi transferido para 50 mL de meio LB e mantido a 28 °C sob agitação constante por cerca de 14 h, até atingir um valor entre 0,6 a 1,0 de absorbância a 600 nm. Em seguida, a cultura foi resfriada em gelo por 15 min. Seguiu-se uma centrifugação suave a 2000 *g* por 15 min a 4 °C. O sobrenadante foi descartado e o precipitado de células ressuspendido em 1 mL de solução $CaCl_2$ 20 mM e glicerol 10 %. Alíquotas de 100 μL foram imediatamente congeladas em nitrogênio líquido e armazenadas em freezer a -80 °C.

3.2.3. Plasmídeos

Os vetores utilizados para as diferentes clonagens estão listados na Tabela 1.

Tabela 1. Vetores utilizados para estudos funcionais

Vetor	Tipo	Resistência[1]	Características	Referência
pCR2.1-TOPO®	vetor intermediário para clonagem	canamicina (50 µg/mL) ampicilina (50 µg/mL)	Vetor linearizado com resíduo 3' de timidina (T), que permite a inserção direta de fragmentos amplificados por Taq polymerase com resíduos 3' de adenosina (A). Possui sítios EcoRI que flanqueiam o fragmento clonado.	Life Technologies
pTOPO-*GFP*380	vetor intermediário clone *GFP*	canamicina (50 µg/mL) ampicilina (50 µg/mL)	Vetor pCR2.1-TOPO com o fragmento de 380 pb do gene *GFP*.	Quadrana *et al.* (2011)
pCR8/GW/ TOPO	vetor de entrada *gateway*	espectinomicina (100 µg/mL)	Vetor linearizado, com resíduo 3' de T, que permite a inserção direta de fragmentos amplificados por Taq polymerase com resíduos 3' de A. Possui os sítios *attL1* e *attL2* para recombinação sítio-específica com um vetor destino no sistema Gateway®; sítios EcoRI flanqueiam o fragmento clonado.	Life Technologies
pTRV2GW	vetor binário destino *gateway*	canamicina (50 µg/mL)	Possui duas cópias do promotor CaMV 35S, o gene que codifica para proteína do capsídeo (CP), sítios *attR1* e *attR2* para recombinação sítio-específica no sistema Gateway® do fragmento GOI e terminador da nopalina sintase (NOSt); a seleção negativa é feita pelo gene ccdB e com o antibiótico cloranfenicol (25 µg/mL).	Quadrana *et al.* (2011)
pTRV1	vetor binário para co-infiltração	canamicina (50 µg/mL)	Possui duas cópias do promotor CaMV 35S, genes que codificam para: duas replicases (Rd/Rp), proteína de movimento (MP); proteína rica em cisteína 16K e terminador da nopalina sintase (NOSt).	Quadrana *et al.* (2011)

[1] Resistência em células procarióticas.

3.3. Extração de RNA total e síntese de cDNA

A extração de RNA foi realizada como descrito no item 3.2.1 (Capítulo II). Uma alíquota de 1 µg de RNA total foi submetida a tratamento com DNAse I (Life Technologies). Na sequência, o RNA tratado foi convertido a cDNA utilizando como iniciadores uma combinação de oligoDT e *random primers* e o kit SuperScript® III Reverse Transcriptase (Life Technologies), segundo recomendações do fabricante. A ausência de contaminação de DNA genômico e eficiência da reação de transcriptase reversa foram avaliadas por meio de PCR, utilizando-se os iniciadores ActinaUp e ActinaLow (Anexo III), os quais flanqueiam íntrons. As reações de PCR foram conduzidas empregando-se tampão 1X, 1,5 mM de $MgCl_2$, 200 µM de cada dNTPs, 200 nM de cada iniciador, 50 ng de cDNA e 2U de Taq DNA polimerase (Life Technologies). As condições de amplificação

utilizadas foram: 94 ºC por 3 min, em seguida 35 ciclos de 30 s a 94 ºC, 30s a 50 ºC, 1 min a 72 ºC; e uma extensão final de 10 min a 72 ºC. Como controle positivo, foi utilizado 50 ng de DNA genômico. Dessa forma, o tamanho do fragmento amplificado do gene de actina a partir de DNA genômico corresponderia a 812 pb e de cDNA a 521 pb. Os produtos de amplificação foram visualizados em gel de agarose 1 %.

3.4. Construção dos vetores de VIGS

3.4.1. Clonagem do fragmento do gene de interesse (*GOI*) para VIGS

Para amplificação dos fragmentos de interesse foram utilizados 100 ng de cDNA, tampão 1X, 200 µM de cada dNTP, 200 nM de cada iniciador (Anexo III), 1,5 mM de $MgCl_2$ e 2 U de enzima Taq polimerase (Life Technologies). As condições de amplificação empregadas foram: 94 ºC por 3 min; seguida por 35 ciclos de 94 ºC por 15 s, temperatura de anelamento por 30 s (Anexo III), 72 ºC por 30 s; e uma extensão final a 72 ºC por 10 min. Os produtos de PCR foram verificados em gel de agarose 1,2% e, na sequência, purificados diretamente da reação de PCR com o kit *GFX® PCR DNA and Gel Band Purification* (Amersham Biosciences) seguindo as instruções do fabricante. Uma vez purificados, os produtos de PCR foram quantificados utilizando marcador de massa de concentração conhecida (*High DNA Mass Ladder*, Life Technologies) por meio de eletroforese em gel de agarose 0,8 %. Em seguida, os fragmentos GOI foram clonados no vetor pCR2.1-TOPO®, utilizado o kit TOPO®TA Cloning® (Life Technologies) nas seguintes condições: 30 ng do produto de PCR purificado, 1 µL de solução salina, 1 µL de vetor e água ultrapura até um volume final de 6 µL. A reação foi mantida por 30 minutos à temperatura ambiente.

A transformação das células *E. coli* DH10B foi feita adicionando-se 2 µL do produto de ligação a uma alíquota de células competentes. Após incubação de 30 minutos no gelo, as células foram submetidas ao choque térmico (42 ºC por 45 s, seguidos de 2 min em gelo). Na sequência, foram adicionados 500 µL de meio SOC à mistura para a etapa de recuperação, a qual foi mantida por 40 min sob agitação constante 200 rpm. Posteriormente, 200 µL de cada cultivo foram plaqueados em meio LB sólido suplementado com antibiótico adequado (Tabela 1) para seleção das colônias transformantes. As placas permaneceram em estufa a 37 ºC por 18 h. As colônias isoladas foram transferidas para 2 mL de meio LB líquido suplementado com antibiótico adequado, mantidas por 16 h a 37º C sob agitação constante. A mini-preparação do DNA plasmidial de pTOPO-*VIGS-FOLK,* pTOPO-*VIGS-VTE5* e pTOPO-*VIGS-CLH(1)* foi feita a partir dos cultivos saturados, utilizando-se o kit *Qiagen Miniprep* (Qiagen) segundo protocolo sugerido pelo fabricante, e os plasmídeos isolados quantificados por Nanodrop® (Thermo Scientific). A integridade do DNA purificado foi verificada por eletroforese em gel de agarose 0,8 %. Para confirmação da identidade do fragmento, foi feito o

sequenciamento dos vetores utilizando-se os iniciadores M13F e M13R (Anexo III), e o kit *BigDye® Terminator v3.1 Cycle Sequencing* (Life Technologies).

3.4.2. Clonagem do fragmento *GFP-GOI*

Dois microgramas dos vetores pTOPO-*GFP380,* pTOPO-VIGS-*FOLK,* pTOPO-VIGS-*VTE5,* pTOPO-VIGS-*CLH(1)* foram digeridos com enzima EcoRI (New England Biolabs). Os produtos da digestão foram separados por gel agarose 1,0%. A banda correspondente ao fragmento clonado foi isolada do gel e submetida à purificação com o kit *GFX® PCR DNA and Gel Band Purification* (Amersham Biosciences). Os fragmentos de restrição *GOI* e *GFP* purificados foram ligados utilizando a enzima T4 ligase (Life Technologies) nas seguintes condições: 30 ng do fragmento *GOI*, 30 ng do fragmento *GFP*, tampão de reação ligase 1X, 0,5 U da enzima, água ultrapura até atingir volume final de 20 µL. A reação foi mantida à temperatura ambiente por 3 h. Posteriormente, 2 µL do produto da ligação foi utilizado como molde para amplificação por PCR cujas condições foram: tampão 1X, 1,5 mM de $MgCl_2$, 200 µM de cada dNTP, 200 nM do iniciador GFP-F e GOI-R (Anexo III), e 2 U de enzima Taq polimerase (Life Technologies). As condições de amplificação empregadas foram: 94 ºC por 3 min; 35 ciclos de 94 ºC por 15 s, temperatura de anelamento por 1 min (Anexo III), 72 ºC por 30 s; e uma extensão final a 72 ºC por 10 min. Os produtos de PCR foram verificados em gel de agarose 1,2 % e, na sequência, purificados com o kit *GFX® PCR DNA and Gel Band Purification* (Amersham Biosciences). Em seguida, os fragmentos *GFP-GOI* foram clonados no vetor de entrada pCR8/GW/TOPO® (Tabela 1), utilizando-se o kit pCR®8/GW/TOPO® TA Cloning Kit (Life Technologies) conforme procedimento descrito no item 3.4.1. A transformação das células competentes de *E. coli* DH10B e o isolamento dos clones pCR8GWTOPO*GFP-FOLK,* pCR8GWTOPO*GFP-VTE5 e* pCR8GWTOPO*GFP-CLH(1)* foram feitas conforme descrito no item 3.4.1. A identidade do fragmento clonado foi confirmada por sequenciamento, utilizando-se os iniciadores M13F e M13R (Anexo III).

3.4.3. Obtenção da construção pTRV2*GFP-GOI*

O vetor de entrada pCR8GWTOPO*GFP-GOI* foi recombinado com o vetor destino pTRV2GW (Tabela 1), utilizando-se a enzima LR clonase II (Life Technologies), de acordo com protocolo sugerido pelo fabricante. A transformação das células competentes de *E. coli* DH10B e isolamento do DNA plasmidial foram realizadas conforme descrito 3.4.1. Os clones obtidos, pTRV2*GFP-FOLK,* pTRV2*GFP-VTE5* e pTRV2*GFP-CLH(1)* tiveram sua identidade confirmada por sequenciamento, utilizando-se os iniciadores TRVF e TRVR (Anexo III).

3.4.4. Transformação de *A. tumefaciens* e seleção de clones pTRV2*GFP-GOI*

Após confirmação da identidade, 1 µg de pTRV2*GFP-GOI* foi utilizada para transformar células de *A. tumefaciens* GV3101 competentes segundo protocolo descrito por Brasileiro *et al.* (1998). Após incubação por 30 min em gelo, as células foram submetidas ao choque térmico (2 min em nitrogênio líquido, seguidos de 5 min a 37 ºC). Na sequência, foram adicionados 1 mL de meio LB para a etapa de recuperação, e a mistura mantida por 2 h sob agitação constante a 200 rpm. Posteriormente, 100 µL de cada cultivo foram plaqueados em meio LB-ágar suplementado com antibiótico adequado (Tabela 1) para seleção das colônias transformantes. As placas permaneceram em estufa a 28 ºC por 48 h. A triagem das colônias positivas foi feita por PCR de colônia, utilizando-se o par de iniciadores GFP-F e GOI-R (Anexo III) para cada fragmento. As condições da reação foram: 1X tampão, 1,5 mM de $MgCl_2$, 200 µM de cada dNTPs, 200 nM de cada iniciador e 2 U de Taq DNA polimerase (Life Technologies). As condições de amplificação utilizadas foram 94ºC por 10 min, seguido de 35 ciclos de 30s a 94 ºC, 30 s a temperatura de anelamento específica, 2 min a 72 ºC; e uma extensão final de 10 min a 72 ºC. Os produtos de PCR foram visualizados em gel de agarose 0,8 %.

3.4.5. Agroinfiltração de botões florais e de folhas com TRV

Uma colônia recombinante de *A. tumefaciens* GV3101 para pTRV2*GFP-GOI,* pTRV2*GFP* e pTRV1 foi transferida para um pré-inóculo de 3 mL de meio LB contendo antibióticos apropriados. O cultivo foi mantido sob agitação constante de 170 rpm, 28 ºC por 24 h. Posteriormente, transferiu-se 1 mL do pré-inóculo para um inóculo de 50 mL de LB com os mesmos antibióticos; este foi incubado por cerca de 14 h até atingir OD_{600} entre 0,6 a 1,0. A cultura foi então submetida à centrifugação a 4500 rpm por 15 min a 4°C. O pellet foi ressuspendido em meio MES líquido contendo acetoseringona (150 µM) até atingir a OD_{600} 1 e então mantido por 4h no escuro.

Imediatamente antes da inoculação, se mesclou quantidades equivalentes das suspensões de células de *Agrobacterium* contendo a construção pTRV2*GFP-GOI* e pTRV1 ou pTRV2*GFP* e pTRV1. As misturas foram injetadas com auxílio de uma seringa no caule de plântulas ou nos pedúnculos florais de plantas transgênicas GFP de *S. lycopersicum* (*cv*. Moneymaker) de acordo com Quadrana *et al.* (2011). Foram coletados frutos agroinfiltrados em estádio verde-maduro e maduro. No caso das folhas, selecionou-se a primeira ou segunda folha completamente expandida de acordo com maior sinal de silenciamento. As regiões silenciadas foram identificadas a partir da ausência de fluorescência do tecido sob luz U.V., seccionadas e congeladas para posterior análise.

3.5. Análise da expressão gênica

A confirmação do silenciamento do gene alvo [*CLH*(1), *FOLK* e *VTE5*] nas amostras agroinfiltradas com os respectivos vetores foi feita de acordo com o item 3.2.2 (Capítulo II). Nas amostras de frutos positivas para o silenciamento, foram ainda avaliados os níveis de expressão dos genes envolvidos no metabolismo do fitol [*GGDR, CLH(4), CHLG, PAO* e *PPH*] e na síntese de tocoferol [*HPPD(2), VTE1, VTE2, VTE3 e VTE4*]. Para o cálculo da expressão gênica normalizada, utilizou-se os genes *CAC* e *EXPRESSED*.

3.6. Quantificação do conteúdo de tocoferóis por cromatografia líquida de alta eficiência (HPLC)

3.6.1. Preparação dos extratos

Para extração de tocoferóis, foi utilizado o protocolo descrito por Almeida *et al.* (2011). Frutos de tomate foram triturados a pó fino em nitrogênio líquido e 500 mg do material foi extraído com 1,5 mL de metanol. Após agitação em vortex por 1 min, 1,5 mL de clorofórmio foi adicionado e a mistura obtida sonicada em gelo por 5 min. Na sequência, foram adicionados 2,5 mL de solução TrisNaCl (Tris 50 mM pH 7,5/NaCl 1M), realizada agitação da mistura em vortex e sonicação, seguida de centrifugação a 3000 rpm por 5 min a 4 ºC. A fase clorofórmica foi então recuperada e o pellet submetido a nova reextração com 2 mL de clorofórmio. Os dois extratos obtidos foram reunidos em um só tubo e o volume final ajustado a 4 mL com clorofórmio. Uma alíquota de 3 mL do extrato foi seca em nitrogênio gasoso antes da injeção, ressuspendida em 0,2 mL de solução de fase móvel e posteriormente filtradas em papel filtro.

3.6.2. Determinação por HPLC

O conteúdo de tocoferol foi determinado por HPLC (Hewlett-Packard serie 1100) acoplado a detector de fluorescência (Agilent Technologies, série 1200). A separação cromatográfica foi realizada em coluna de fase normal LiChrospher® 100 DIOL (5 µm) LiChroCART® 250-4 (Agilent Technologies), operada em temperatura ambiente usando um sistema de solvente isocrático de 95:5 heptano/éter metil terc-butílico em fluxo de 1,6 mL/min. Os compostos eluídos foram detectados por fluorescência com excitação a 296 nm e emissão a 340 nm. As espécies de tocoferol foram identificadas e quantificadas por meio da comparação do tempo de retenção e das áreas dos picos de padrões adquiridos comercialmente (Merck).

3.7. Quantificação de clorofila

A quantificação de clorofila foi realizada a partir de 100 mg material triturado congelado fresco de acordo com Porra *et al.* (1989). Utilizou-se 1 mL de acetona 80% para maceração das amostras seguida de incubação por 1h à 4ºC no escuro. A mistura foi centrifugada a 13000 rpm por 5 min e o sobrenadante obtido foi utilizado para leitura em espectrofotômetro. O cálculo da concentração de clorofila foi feito baseado nas seguintes equações:

Clorofila a= 12,25 * Abs 663 – 2,55 * Abs 646

Clorofila b= 20,31 * Abs 646 – 4,91 * Abs 663

4. Resultados

Fragmentos parciais de *CLH(1)*, *FOLK* e *VTE5* foram clonados no vetor TRV2*GFP* (Figura 2). Diante da ausência de detecção dos transcritos *CLH*(2) em frutos de tomateiro de diferentes cultivares (Capítulo II; Lira *et al.*, 2014), esse gene não foi incluído no experimento de VIGS. Inflorescências de plantas transgênicas GFP de tomateiro (*cv*. Moneymaker) foram infiltradas com células de *Agrobacterium* contendo TRV2*GFP-GOI* e TRV1 (Figura 2). O controle experimental foi produzido a partir da infiltração com TRV2*GFP* e TRV1. Todas as plantas transgênicas GFP agroinfectadas, tanto controle quanto tratamento, cresceram sem apresentar diferenças significativas na porção vegetativa. Com relação aos frutos, foi possível notar maior frequência de frutos de menor tamanho e partenocárpicos entre os tratamentos.

Os frutos nos estádios verde-maduro e maduro foram submetidos à triagem sob luz U.V. para detecção da fluorescência da proteína GFP. A ausência de fluorescência era um primeiro indício de cosilenciamento de *GFP* e de *GOI* (Figura 2). A confirmação do silenciamento dos genes alvos *CLH(1)*, *FOLK* e *VTE5* foi feita por qPCR (Figura 3). Foi possível observar redução nos níveis de mRNA entre 50% a 80% em relação ao controle TRV2*GFP*. Enquanto os frutos de TRV2*GFP-FOLK* atingiram as maiores eficiências no silenciamento, frutos verde-maduros de TRV2*GFP-CLH(1)* mantiveram em média 50% dos trancritos de *CLH(1)*.

O efeito do silenciamento de cada *GOI* no metabolismo de VTE foi avaliado pela determinação do perfil de tocoferóis por HPLC (Figura 4). Em geral, os frutos dos tratamentos apresentaram conteúdo de tocoferóis semelhantes ao controle. No estádio de verde-maduro, não houve diferenças significativas detectadas. No entanto, alterações no conteúdo de tocoferóis foram observadas nos frutos maduros. Frutos TRV2*GFP-FOLK* apresentaram redução de cerca de 20% no conteúdo de α-tocoferol e total, além de uma redução significativa de 10% em β-tocoferol. Já os frutos de TRV2*GFP-VTE5* apresentaram apenas uma queda de 40% na isoforma δ, que contribui com uma pequena fração para o conteúdo total de tocoferóis em fruto.

Em seguida, o conteúdo de clorofila total foi avaliado espectrofotometricamente no estádio verde-maduro (Figura 5). Os frutos silenciados dos tratamentos mantiveram o conteúdo de clorofila semelhante ao controle.

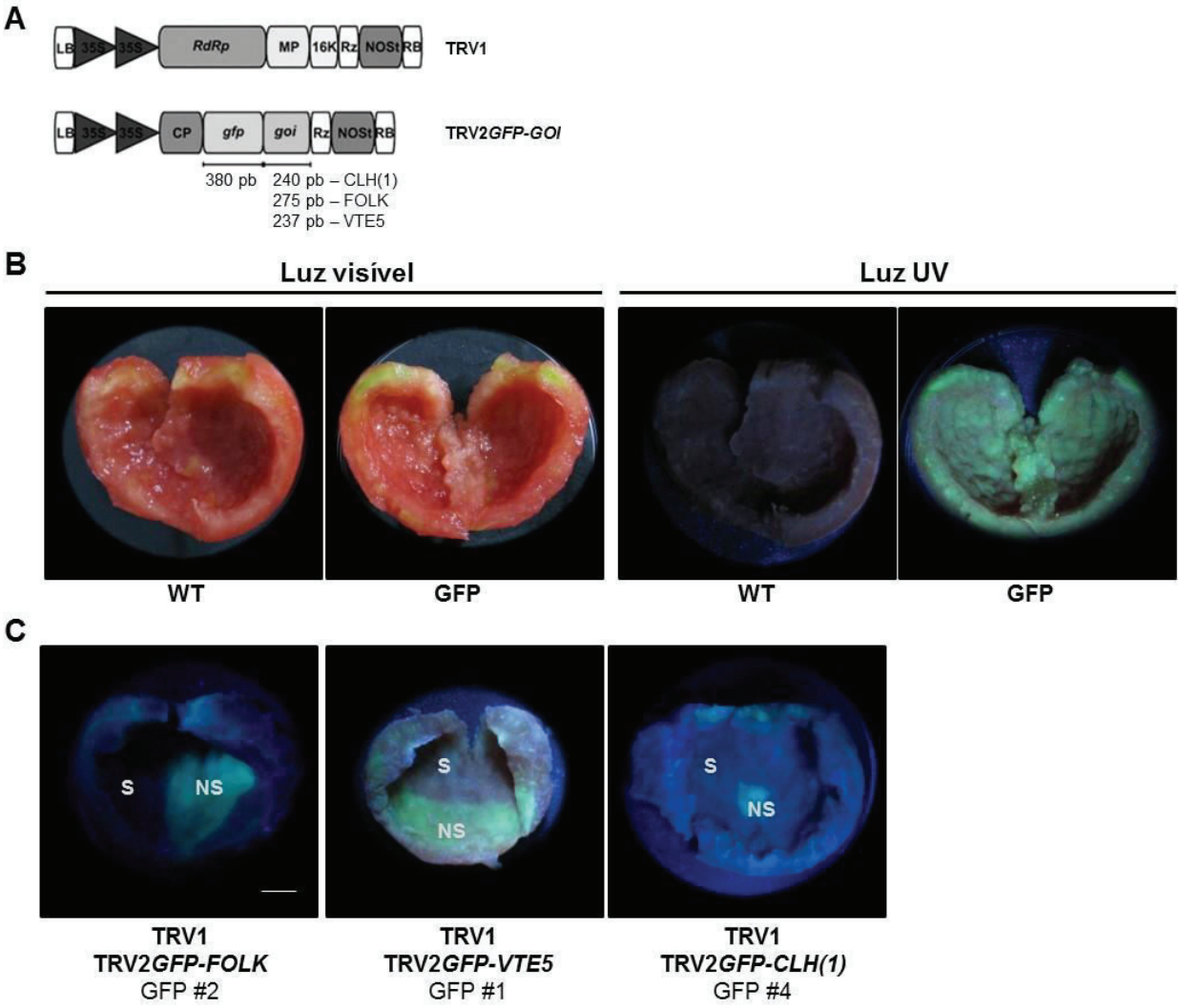

Figura 2: Silenciamento do gene *GFP* em frutos transgênicos de tomate. (A) Esquema dos vetores TRV1, TRV2*GFP-GOI* utilizados no experimento. O tamanho do fragmento de cada gene assim como do *GFP* está indicado. LB: borda esquerda do T-DNA; RB: borda direita do T-DNA; 35S: promotor CaMV *35S* (2x); Rd/Rp: replicase; MP: proteína de movimento; CP: proteína do capsídeo; NOSt: terminador da nopalina sintase; 16K: proteína de função desconhecida; pb: pares de bases. (B) Secção transversal do pericarpo de fruto maduro selvagem (WT) e transgênico (GFP) em luz visível, sem diferenças fenotípicas, e sob luz U.V., na qual é possível detectar a fluorescência da proteína GFP. (C) Pericarpo de fruto maduro de plantas transgênicas GFP cujas inflorescências foram agroinfiltradas com TRV1 e TRV2*GFP-GOI.* NS indica regiões do fruto onde não houve silenciamento do gene *GFP*, enquanto S corresponde às regiões silenciadas. Barra = 1 cm.

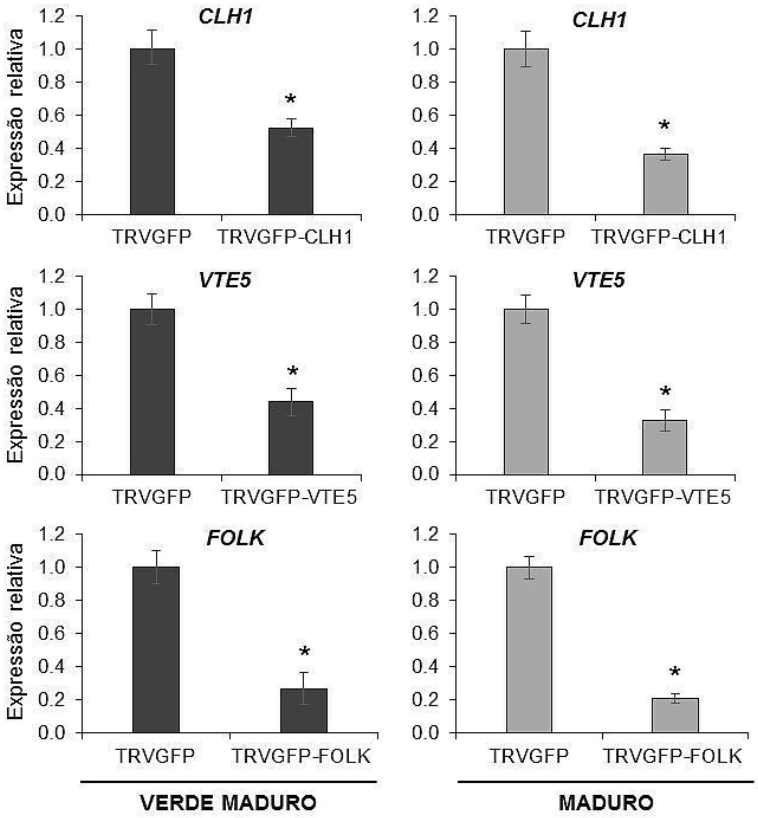

Figura 3: Silenciamento do *GOI* nos frutos transgênicos GFP. Expressão relativa de *CLH*(1), *FOLK* e *VTE5* em pericarpos de frutos agroinfectados com TRV1/TRV2*GFP* (TRVGFP, controle) e com TRV1/TRV2*GFP-CLH(1)* [TRVGFP-CLH(1)]; TRV1/TRV2*GFP-FOLK* (TRVGFP-FOLK); TRV1/TRV2*GFP-VTE5* (TRVGFP-VTE5). Os gráficos indicam a média da expressão relativa das réplicas biológicas (n ≥ 4, provenientes de 3 plantas independentes ± erro padrão). Asteriscos apontam as diferenças estatisticamente significativas (Teste de permutação, P < 0,05).

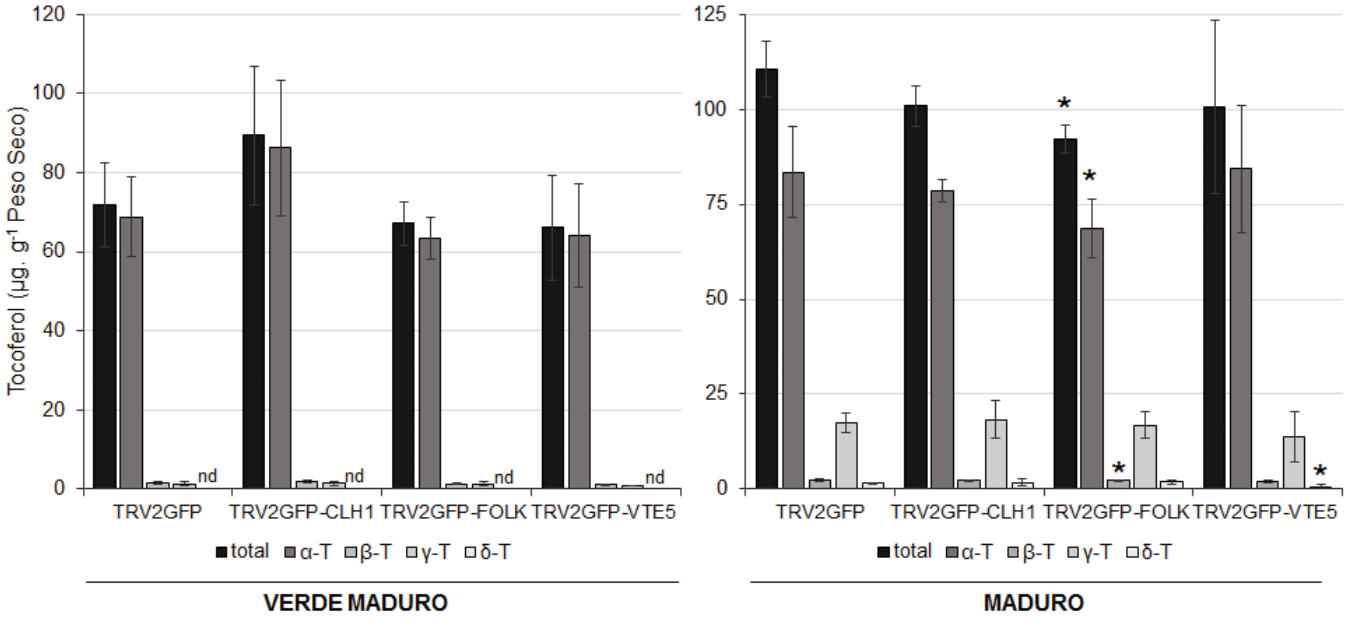

Figura 4: Efeito do silenciamento por VIGS de *CLH(1)*, *FOLK* e *VTE5* no conteúdo de tocoferol em frutos. α-, β-, γ-, δ-tocoferol e total em frutos verde-maduros e maduros. Os dados representam a média do conteúdo de tocoferol em diferentes réplicas biológicas (n ≥ 4) provenientes de 3 plantas independentes ± desvio padrão. Asteriscos apontam diferenças estatisticamente significativas em relação ao controle TRVGFP. (*t*-teste, P < 0,05).

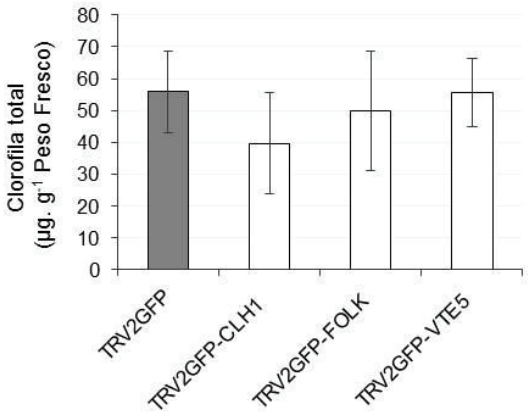

Figura 5: Efeito do silenciamento por VIGS de *CLH(1)*, *FOLK* e *VTE5* no conteúdo de clorofila. Os dados representam a média do conteúdo de clorofila total em frutos verde-maduros de diferentes réplicas biológicas (n ≥ 4) provenientes de 3 plantas independentes ± desvio padrão. Asteriscos apontam diferenças estatisticamente significativas em relação ao controle TRVGFP (*t*-teste, P < 0,05).

Finalmente, verificou-se o perfil transcricional dos genes envolvidos no metabolismo do fitol [*GGDR, CLH(4), CHLG, PAO* e *PPH*] e na síntese de tocoferol [*HPPD(2), VTE1, VTE2, VTE3 e VTE4*] (Figura 6). Frutos de ambos os estádios de TRV2*GFP-CLH(1)* apresentaram diversas alterações nos níveis dos transcritos avaliados. Em frutos verde-maduros, houve redução na expressão de *GGDR* e de *CHLG* em comparação ao controle TRV*GFP*, fato que pode indicar uma regulação para a redução da síntese de clorofila. Além disso, a redução na expressão de *VTE5* nesse estádio também sugere alteração na reciclagem do fitol. A regulação transcricional da rota central também foi afetada com redução na expressão de *VTE1*, *VTE2*, *VTE3(1)*. Já em frutos maduros, o aumento nos transcritos de *PAO* e *VTE5*, sugerem uma maior indução da degradação da clorofila e reciclagem do fitol. No entanto, nem o silenciamento da *CLH(1)* nem as alterações nos níveis de mRNA decorrentes impactaram o conteúdo de tocoferol nos frutos. O silenciamento de *FOLK* causou também redução da expressão de *VTE5* em frutos verde-maduros, que não é produto de cosilenciamento, uma vez que em frutos maduros a expressão de *VTE5* é similar ao controle. A redução no conteúdo de tocoferóis desses frutos é acompanhada por uma redução na expressão dos genes relacionados à rota central, que inclui *HPPD(2)*, *VTE1*, *VTE2*, *VTE3(1)*. Por último, o silenciamento de *VTE5* em frutos TRV2*GFP-VTE5* produziu alterações pontuais na expressão gênica apenas em frutos maduros, reduzindo o nível dos transcritos *VTE3(1)* e *VTE1;* a redução deste último pode estar de alguma forma relacionada com o menor conteúdo de δ-tocoferol observado.

Embora os ortólogos dos três genes alvo desse estudo tenham sido funcionalmente caracterizados em *A. thaliana*, apenas para *AtVTE5* foi demonstrado que a sua deficiência resulta na redução do conteúdo de tocoferóis em sementes e levemente em folhas (Valentin *et al.*, 2006). Desta forma, perante a ausência de efeito do silenciamento de *VTE5* no conteúdo de VTE em frutos de tomateiro, alguns questionamentos foram levantados: (i) eventual inviabilidade do método de VIGS para o estudo do metabolismo de fitol em tomateiro; (ii) o conteúdo de VTE nos frutos depende do metabolismo de tocoferol em outros órgãos. Para tentar esclarecer esses pontos, foi realizado um

experimento VIGS semelhante, mas desta vez silenciando *VTE5* em folhas. Para isso, plântulas transgênicas GFP foram infiltradas com *Agrobacterium* contendo TRV2*GFP-VTE5* e TRV1. Nesse caso, as folhas apresentaram 60 % de silenciamento de *VTE5* porém houve redução de aproximadamente 40 % no conteúdo de tocoferol total (Figura 7).

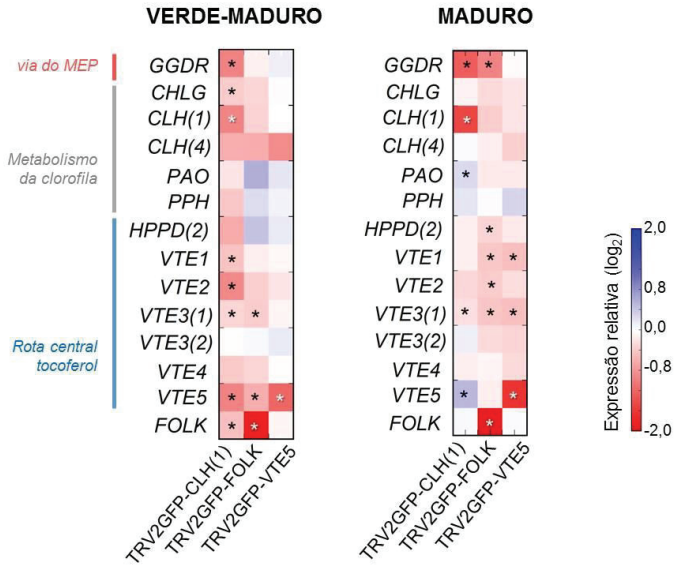

Figura 6: Perfil trancricional de frutos de tomate silenciados para *CLH(1)*, *FOLK* e *VTE5* por VIGS. *Heat map* obtido a partir dos valores de $\log_2$ da expressão relativa entre o respectivo controle (TRV*GFP*) de cada tecido e seus tratamentos nos estádios de fruto verde-maduro e maduro. Os genótipos estão representados por colunas. Os genes estão organizados de acordo com sua via metabólica (barra vertical colorida à esquerda). A expressão relativa foi obtida a partir da média das réplicas biológicas ($n \geq 4$). As diferenças significativas ($P < 0,05$), avaliadas por meio de teste de permutação, estão indicadas com *; em branco, os genes alvo do silenciamento; em preto, os demais genes.

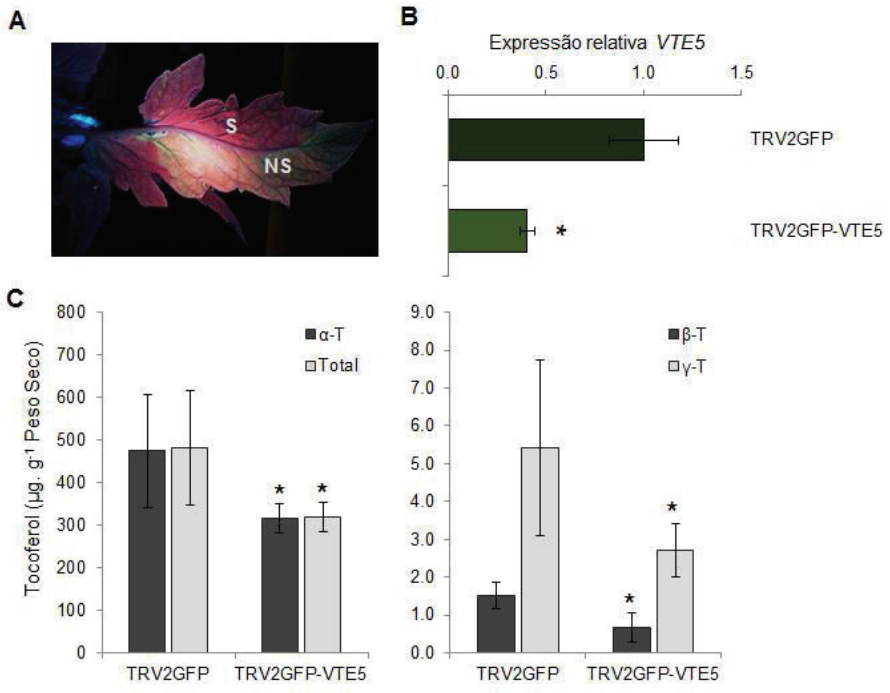

Figura 7: Silenciamento de *VTE5* em folhas transgênicas GFP agroinfiltradas com TRV2*GFP-VTE5* e efeito no conteúdo de tocoferol. (A) Folha fonte de plantas transgênicas GFP agroinfiltradas com TRV1 e TRV2*GFP-VTE5*. NS indica regiões onde não houve silenciamento do gene *GFP*, enquanto S sinaliza às regiões silenciadas. (B) Média da expressão relativa das réplicas biológicas (n = 5) ± erro padrão. Asteriscos apontam as diferenças estatisticamente significativas em relação ao controle TRVGFP (Teste de permutação; $P < 0,05$). (C) Média do conteúdo de tocoferol das réplicas biológicas (n = 5) ± desvio padrão. Asteriscos apontam diferenças estatisticamente significativas em relação ao controle TRV2*GFP*. (*t*-teste, $P < 0,05$).

5. Discussão

O método de VIGS estabeleceu-se como uma abordagem rápida para supressão da atividade gênica e avaliação dos fenótipos resultantes (Fu *et al.*, 2005; Ramegowda *et al.*, 2014). A principal vantagem desse método é prescindir de transformantes estáveis e, dessa forma, em um período relativamente curto, comparam-se os fenótipos de linhagens silenciadas para determinado gene. No entanto, uma das restrições da técnica é a falta de silenciamento uniforme nos tecidos vegetais, sendo imprescindível a utilização de um marcador visual que viabilize de modo fácil e eficiente a seleção das regiões alvejadas pelo mecanismo de RNAi. Utilizando o sistema de VIGS acoplado a expressão constitutiva do gene repórter *GFP* desenvolvido por Quadrana *et al.* (2011) em tomateiro, avaliou-se o efeito do silenciamento de genes putativos relacionados à degradação de clorofila e metabolismo do fitol, *CLH*(1), *FOLK e VTE5* em frutos de tomate.

Os resultados mostraram que apenas os frutos maduros de TRV2GFP-*FOLK* apresentaram redução significativa (20 %) no conteúdo de tocoferol total. Tais frutos, coincidentemente, apresentaram também maior eficiência no silenciamento dentre os três genes avaliados, acompanhado de uma redução coordenada dos genes da rota central de tocoferol [*HPPD*(2), *VTE1*, *VTE2* e *VTE3*(1)]. Ainda que para FOLK de *A. thaliana* tenha sido demonstrada atividade de farnesol kinase (Fitzpatrick *et al.*, 2011), os dados obtidos neste trabalho sugerem que a proteína homóloga de *S. lycopersicum* impacta o metabolismo de VTE.

É interessante pontuar que nenhum dos tratamentos produziu efeito no acúmulo de clorofila, mesmo os frutos infiltrados com TRV2*GFP-CLH(1)*. Esse resultado reforça a hipótese que *CLH(1)* não desempenha papel central na defitilação da clorofila durante o amadurecimento em frutos de tomate (Guyer *et al.*, 2014; Lira *et al.*, 2014). No entanto, análises subsequentes da expressão dos genes envolvidos na via de biossíntese de tocoferóis e no metabolismo da clorofila revelaram um perfil bastante interessante. TRV2*GFP-CLH*(1) apresenta uma redução substancial no perfil transcricional dos genes relacionados à síntese de clorofila no estádio verde maduro, *GGDR* e *CLHG*, seguida por um aumento da expressão do gene relacionado à degradação desse pigmento *PAO* além de *VTE5* nos frutos maduros, observações que sugerem uma resposta de ajuste metabólico da via da clorofila neste tratamento.

Curiosamente, embora mutantes *vte5* de *Arabidopsis* apresentem claro impacto no conteúdo de VTE em sementes (Valentin *et al.*, 2006), os frutos de tomate silenciados para *VTE5* mostraram níveis similares de tocoferóis ao controle TRV2*GFP*. O perfil de expressão não expôs nenhuma regulação transcricional compensatória. Mesmo que uma possível ausência do envolvimento de VTE5 na determinação do conteúdo de VTE em frutos não possa ser descartada, tal cenário diverge

da hipótese proposta a partir do perfil transcricional realizado ao longo do desenvolvimento do tomateiro (Capítulo I). Embora a abordagem de VIGS seja bastante interessante, como toda técnica apresenta limitações, as quais vão além da heterogeneidade do silenciamento nos tecidos vegetais. Os vetores que deflagram o mecanismo sequência-específica de RNAi têm como arcabouço esqueletos virais modificados. Dessa forma, interferências mínimas de sintomas virais não podem ser completamente excluídas na interpretação dos dados dependendo da via alvo do estudo, ainda que um vetor viral adequado seja utilizado (Senthil-Kumar & Mysore, 2011; Ramegowda *et al.*, 2014) e os controles experimentais apropriados sejam empregados. Notavelmente, o vetor TRV é reconhecido por seus sintomas de infecção pouco óbvios (Ratcliff *et al.*, 2001). Além disso, embora a viabilidade do sistema de VIGS tenha sido demonstrada para o estudo do metabolismo de VTE em tomateiro (Quadrana *et al.*; 2011; 2014) de alguma forma a conexão entre degradação de clorofila e síntese de tocoferóis poderia estar prejudicada nesse sistema. Nesse contexto, realizou-se o experimento de VIGS de *VTE5* em folhas de tomateiro. Ainda que a efetividade do silenciamento em folha tenha sido similar a fruto verde-maduro, reduzindo em 60 % os níveis de mRNA, o conteúdo de tocoferol diminuiu cerca de 40 % em relação ao controle TRV2*GFP* em folhas. Diante desses resultados, algumas hipóteses podem ser formuladas. Primeiramente, a expressão residual de *SlVTE5* proporciona atividade fitol quinase suficiente para sustentar a fosforilação do fitol direcionado para síntese de tocoferóis em fruto. Além disso, efeitos compensatórios não identificados no fruto podem ser responsáveis pela manutenção da cadeia prenílica para VTE (mecanismos pós-transcricionais). Outro cenário possível, seria a possibilidade de transporte do intermediário fitol entre os tecidos não silenciados para os silenciados; essa alternativa implica o transporte desse composto de natureza lipofílica a longa distância, mecanismo ainda pouco conhecido em plantas. Em definitivo, a diferença dos resultados obtidos a partir dos experimentos de VIGS em folhas e frutos é bastante intrigante.

Dessa maneira, futuras investigações são necessárias buscando aprofundar a caracterização funcional não só de *VTE5*, como também para *FOLK* e *CLH(1)* a fim de delinear um cenário mais infomativo sobre o papel desses genes no metabolismo de VTE e na fisiologia de tomateiro.

6. Conclusão

Buscando entender a interrelação entre degradação da clorofila e biossíntese de VTE em frutos, o presente estudo realizou uma primeira caracterização funcional dos genes envolvidos na reciclagem do fitol da clorofila, *CLH(1)* e *VTE5*, assim como de *FOLK*, putativo parálogo de *VTE5*, utilizando a abordagem de VIGS. Em frutos, apenas o silenciamento de FOLK produziu redução no conteúdo de tocoferóis totais em fruto maduro. No entanto, o silenciamento de *VTE5* em folha resultou na redução do conteúdo de tocoferol nesse órgão. Tais resultados motivaram a realização de experimentos adicionais (Capítulos V e VI) para esclarecer qual o impacto desses genes no metabolismo de VTE.

7. Referências Bibliográficas

Almeida, J., Quadrana, L., Asis, R., Setta, N., de Godoy, F., Bermudez, L., Otaiza, S., *et al.* (2011) Genetic dissection of vitamin E biosynthesis in tomato. *Journal of Experimental Botany,* 62, 3781–3798.

Baulcombe, D. (2004) RNA silencing in plants. *Nature*, 431, 356–363.

Brasileiro, A. C. M., Carneiro, V. T. C. (1998) Manual de transformação de genética de plantas. *EMBRAPA*, 99-107.

Brodersen, P., Voinnet, O. (2006) The diversity of RNA silencing pathways in plants. *Trends in Genetics*, 22, 268–80.

Fitzpatrick, A. H., Bhandari, J., Crowell, D. N. (2011) Farnesol kinase is involved in farnesol metabolism, ABA signaling and flower development in Arabidopsis. *The Plant Journal*, 66, 1078–88.

Fu, D. Q., Zhu, B.Z., Zhu, H. L., Jiang, W. B., Luo, Y. B. (2005) Virus-induced gene silencing in tomato fruit. *Plant Journal*, 43, 299-308.

Guyer, L., Hofstetter, S., Christ, B., Lira, B. S., Rossi, M., Hortensteiner, S. (2014) Different mechanisms are responsible for chlorophyll dephytylation during fruit ripening and leaf senescence in tomato. *Plant Physiology*, 166, 44-56.

Lira, B. S., de Setta, N., Rosado, D., Almeida, J., Freschi, L., Rossi, M. (2014) Plant degreening: evolution and expression of tomato (*Solanum lycopersicum*) dephytylation enzymes. *Gene*, 546, 359-366.

Liu, Y., Schiff, M., Dinesh-Kumar, S. P. (2002) Virus-induced gene silencing in tomato. *Plant Journal*, 31, 777–786.

Mansoor, S., Amin, I., Hussain, M., Zafar, Y., Briddon, R. W. (2006) Engineering novel traits in plants through RNA interference. *Trends in Plant Science*, 11, 559–565.

Orzaez, D., Mirabel, S., Wieland, W. H., Granell, A. (2006) Agroinjection of tomato fruits. A tool for rapid functional analysis of transgenes directly in fruit. *Plant Physiology*, 140, 3-11.

Orzaez, D., Medina, A., Torre, S., Moreno, J. P. F., Rambla, J. L., del-Carmen, A. F., *et al*. (2009) A visual reporter system for virus-induced gene silencing in tomato fruit based on anthocyanin accumulation. *Plant Physiology*, 150, 1122-34.

Pikaard, C., Scheid, O. M. (2013) Epigenetic regulation in plants. *Cold Spring Harbor Perspectives in Biology*, 1, a019315.

Quadrana, L., Rodriguez, M. C., Lopez, M., Bermudez, L. M., Nesi, A. N., Fernie, A. R., *et al*. (2011) Coupling virus induced gene silencing to exogenous green fluorescence protein expression provides a highly efficient system for functional genomics, in Arabidopsis and across all stages of tomato fruit development. *Plant Physiology*, 56, 1278–1291.

Quadrana, L., Almeida, J., Asis, R., Otaiza, S., Duffy, T., Silva, J. V., *et al*. (2013) Transcriptional regulation of vitamin E biosynthesis in tomato. *Plant Molecular Biology*, 81, 309-325.

Ramegowda, V., Mysore, K. S., Kumar, M. S. (2014) Virus-induced gene silencing is a versatile tool for unraveling the functional relevance of multiple abiotic-stress-responsive genes in crop plants. *Frontiers in Plant Science*, 5, 1–12.

Ratcliff, F., Hernandez, A. M., Baulcombe, D. C. (2001) Technical Advance: Tobacco rattle virus as a vector for analysis of gene function by silencing. *The Plant Journal*, 25, 237–245.

Sambrook, J., Fritsch, T., Maniatis, T. (1989) Molecular cloning: A laboratory manual. *Cold Spring Harbor Laboratory Press*, 1, 7-58.

Senthil-Kumar, M., Mysore, K. S. (2011) New dimensions for VIGS in plant functional genomics. *Trends in Plant Science*, 16, 656–665.

Senthil-Kumar, M., Mysore, K. S. (2014) Tobacco rattle virus-based virus-induced gene silencing in Nicotiana benthamiana. *Nature Protocols*, 9, 1549–62.

Zhao, M., San Leõn, D., Delgadillo, M. O., García, J. A., Mateo, C. S. (2014) Virus-induced gene silencing in transgenic plants: Transgene silencing and reactivation associate with two patterns of transgene body methylation. *Plant Journal*, 79, 440–452.

CAPÍTULO IV. AVALIAÇÃO DO CONTEÚDO DE TOCOFERÓIS EM MUTANTES DE TOMATEIRO DEFICIENTES NO AMADURECIMENTO DE FRUTO, NA SENESCÊNCIA E NA PERCEPÇÃO DE ÁCIDO JASMÔNICO

Os Resultados, Material e Métodos e Discussão deste capítulo são apresentados na forma de artigo publicado no periódico *Phytochemistry*. O material suplementar corresponde ao Anexo IV.

Almeida, J., Asís, R., Molineri, V. N., Sestari, I., Lira, B. S., Carrari, F., Peres, L. E. P., Rossi, M. (2015). Fruits from ripening impaired, chlorophyll degraded and jasmonate insensitive tomato mutants have altered tocopherol content and composition. *Phytochemistry*, *111*, 72–83.

Resumo

Os isoprenóides são compostos precursores das vias de biossíntese de clorofilas, carotenóides e tocoferóis, consequentemente, o estudo do seu metabolismo é de fundamental importância para o entendimento do *crosstalk* regulatório que contribui para qualidade nutricional dos frutos de tomate. Por meio de uma análise integrada do perfil metabólico e de expressão gênica, o metabolismo de isoprenóides foi dissecado em mutantes de tomateiro deficientes no amadurecimento do fruto (*ripening inhibitor* e *non-ripening*), com alteração no padrão de senescência (*lutescent1* and *green flesh*) e insensíveis ao ácido jasmônico (*jasmonic acid insensitive 1-1*), todos no fundo genético de Micro-Tom. Os resultados evidenciaram que quanto mais à montante a localização do gene mutado no contexto regulatório, mais vastos são os efeitos sobre o perfil transcricional dos genes relacionados ao metabolismo de isoprenóides. Embora as mutações analisadas provoquem efeitos distintos no metabolismo de clorofila, de carotenóides e de tocoferóis, um ajuste metabólico tornou-se evidente de maneira que a capacidade antioxidante total permaneceu constante. Os perfis transcricionais obtidos a partir dos frutos de mutantes deficientes no amadurecimento e na senescência sugerem que a manutenção da síntese *de novo* de fitil-difosfato pode compensar, nos estádios finais do desenvolvimento, a falta do fitol proveniente da degradação de clorofila para produção de tocoferóis. De maneira interessante, um impedimento na percepção do jasmonato levou a um aumento do conteúdo total de tocoferóis nos frutos maduros acompanhado pelo aumento na sua capacidade antioxidante, destacando a contribuição dos tocoferóis para esse caráter de importância nutricional.

Phytochemistry xxx (2014) xxx–xxx

Contents lists available at ScienceDirect

Phytochemistry

journal homepage: www.elsevier.com/locate/phytochem

Fruits from ripening impaired, chlorophyll degraded and jasmonate insensitive tomato mutants have altered tocopherol content and composition

Juliana Almeida [a], Ramón Asís [b], Virginia Noel Molineri [b], Ivan Sestari [c], Bruno Silvestre Lira [a], Fernando Carrari [d], Lázaro Eustáquio Pereira Peres [e], Magdalena Rossi [a,*]

[a] Departamento de Botânica, Instituto de Biociências, Universidade de São Paulo, São Paulo, SP, Brazil
[b] CIBICI, Facultad de Ciencias Químicas, Universidad Nacional de Córdoba, Córdoba, Argentina
[c] Universidade Federal de Santa Catarina, Campus Curitibanos, Curitibanos, SC, Brazil
[d] Instituto de Biotecnología, Instituto Nacional de Tecnología Agropecuaria and Consejo Nacional de Investigaciones Científicas y Técnicas, Hurlingham, Buenos Aires, Argentina
[e] Departamento de Ciências Biológicas, Escola Superior de Agricultura "Luiz de Queiroz", Universidade de São Paulo, Piracicaba, SP, Brazil

ARTICLE INFO

Article history:
Received 2 August 2014
Received in revised form 20 October 2014
Available online xxxx

Keywords:
Tomato mutants
Solanum lycopersicum
Solanaceae
Atocopherol
Carotenoids
Chlorophyll
Jasmonic acid
Ripening
Antioxidant capacity

ABSTRACT

Since isoprenoids are precursors in chlorophyll, carotenoid and tocopherol pathways, the study of their metabolism is of fundamental importance in understanding the regulatory cross-talk that contributes to the nutritional quality of tomato fruits. By means of an integrated analysis of metabolite and gene expression profiles, isoprenoid metabolism was dissected in ripening-impaired (*ripening inhibitor* and *non-ripening*), senescence-related (*lutescent1* and *green flesh*) and jasmonate insensitive (*jasmonic acid insensitive 1-1*) tomato mutants, all in the Micro-Tom genetic background. It was found that the more upstream the location of the mutated gene, the more extensive the effect on the transcriptional profiles of the isoprenoid-related genes. Although there was a distinct effect in the analyzed mutations on chlorophyll, carotenoid and tocopherol metabolism, a metabolic adjustment was apparent such the antioxidant capacity mostly remained constant. Transcriptional profiles from fruits of ripening and senescence-related tomato mutants suggested that maintenance of the *de novo* phytyl diphosphate synthesis might, in later ripening stages, compensate for the lack of chlorophyll-derived phytol used in tocopherol production. Interestingly, an impairment in jasmonate perception led to higher total tocopherol levels in ripe fruits, accompanied by an increase in antioxidant capacity, highlighting the contribution of tocopherols to this nutritionally important trait.

© 2014 Elsevier Ltd. All rights reserved.

1. Introduction

Fruit ripening involves a series of coordinated biochemical and physiological processes resulting in organoleptic changes in texture, aroma and color (Seymour et al., 1993). One of the most important and visible changes in tomato (*Solanum lycopersicum* L.), a climacteric fruit, involves de-greening and accumulation of carotenoids; a phenomenon that is associated with a chloroplast-to-chromoplast transition (Egea et al., 2011). Tomato is one of the most consumed fruits worldwide and is a major source of many dietary nutrients, such as minerals, antioxidants and vitamins; all of which contribute to the prevention of chronic diseases (Seybold et al., 2004; Perez-Fons et al., 2014). In particular tocopherols, which belong to the vitamin E (VTE) family, are potent lipid soluble antioxidant molecules that reduce free-radical damage to membrane lipids by scavenging peroxyl radicals (Brigelius-Flohé et al., 2002; Niki and Traber, 2012). Tocopherols can also act as scavengers of singlet oxygen ($^1O_2$) and, in plants, this function is related to protection of the photosynthetic apparatus from oxygen toxicity (Trebst, 2003; Krieger-Liszkay and Trebst, 2006).

Tocopherols are isoprenoid-derived compounds that are synthesized from the condensation of a chromanol ring and a prenyl side-chain from the shikimate (SK) and 2-C-methyl-D-erythritol 4-phosphate (MEP) pathways, respectively (Dellapenna and

* Corresponding author at: Departamento de Botânica, Instituto de Biociências, Universidade de São Paulo, Rua do Matão, 277, 05508-900 São Paulo, Brasil. Tel.: +55 11 3091 7556; fax: +55 11 3091 7547.
E-mail addresses: juliana.almeida.silva@usp.br (J. Almeida), rasis@fcq.unc.edu.ar (R. Asís), vicky_412@hotmail.com (V.N. Molineri), ivan.sestari@ufsc.br (I. Sestari), bslira.bsl@gmail.com (B.S. Lira), carrari.fernando@inta.gob.ar (F. Carrari), lazaro.peres@usp.br (L.E.P. Peres), mmrossi@usp.br (M. Rossi).

http://dx.doi.org/10.1016/j.phytochem.2014.11.007
0031-9422/© 2014 Elsevier Ltd. All rights reserved.

Pogson, 2006). The MEP pathway also provides precursors for other plastid isoprenoids, such as chlorophylls (Chls) and carotenoids, the latter of which can be divided into two classes based on their chemical structures: linear or cyclized hydrocarbons, termed carotenes, and xanthophylls that are oxygenated derivatives of carotenes. The xanthophylls lutein, violaxanthin and neoxanthin are components of the light harvesting complex (LHC) and act both as antenna pigments and as protective molecules, by reducing the production of reactive oxygen species (ROS). β-Carotene is a component of the photosynthetic reaction center (Dall'Osto et al., 2006) and during tomato fruit ripening, it accumulates together with the primary ripening-related pigment lycopene (Bramley, 2002).

A recent study focusing on the transcriptional regulation of tocopherol biosynthesis in tomato (cv. M82) (Quadrana et al., 2013) showed that expression of genes encoding enzymes of the tocopherol-core, MEP and SK pathways are controlled both temporally and spatially, and that the supply of the prenyl donor, phytyl diphosphate, appears to be a limiting step in VTE accumulation at later fruit stages. In *Arabidopsis thaliana*, it has been shown that phytyl diphosphate for tocopherol biosynthesis can also originate from the activity of phytol kinase (VTE5), which functions in phytol recycling after Chl degradation (Ischebeck et al., 2006; Valentin et al., 2006). The strong correlation between the expression of *VTE5* and the VTE biosynthetic genes, and the content of Chls and VTE in tomato leaves and fruits supports the contribution of phytol recycling enzymes to tocopherol biosynthesis in this species as well (Quadrana et al., 2013).

This metabolic cross-talk suggests that changes in carotenoid biosynthesis and Chl metabolism might affect tocopherol content, but a better understanding of the accumulation of these metabolites depends on deciphering the complexity of the isoprenoid metabolic network and its branching (Vranová et al., 2012). To this end, senescence and ripening-related tomato mutants represent potentially excellent models, since they provide a means to study metabolic fluxes between these pathways (Table 1). *Non-ripening* (*nor*) and *ripening inhibitor* (*rin*) are tomato mutants with impaired fruit ripening, which fail to undergo typical ripening-related *de novo* carotenoid biosynthesis and Chl degradation (Giovannoni, 2004). Another mutant, *green flesh* (*gf*) is deficient in the STAY-GREEN1 (SGR1) protein involved in destabilization of the Chl-apoprotein complexes and recruitment of the Chl catabolic enzymes, which are a prerequisite for Chl catabolism; thus the fruit retains Chls even at the ripe stage (Barry et al., 2008; Park et al., 2007; Hörtensteiner, 2009). In contrast, the *lutescent* (*l*) mutant displays premature leaf senescence and its fruits lack Chl (Barry et al., 2012).

The ethylene and cytokinin signaling pathways are well-defined and mediate senescence and de-greening, while other hormones, such as jasmonic acid (JA), have also been demonstrated to affect these processes (Lim et al., 2007). Altered patterns of senescence and de-greening have been reported in JA-insensitive or JA-defi-

Table 1
Solanum lycopersicum L. (cv. Micro-Tom) genotypes used in this study.

Genotype	Mature green fruit	Ripe fruit	Mutant gene function/phenotype	Tomato *locus*[a]	Reference
Micro-Tom (MT) *dwarf* (*d*) and *self-pruning* (*sp*) (control genotype)			*D* is a brassinosteroid biosynthesis enzyme encoding gene. The mutant allele reduces all organ sizes, except the fruits. *SP* regulates vegetative to reproductive switching of sympodial meristems. The mutant shows a determinate growth habit	Solyc02g089160 Solyc06g074350	Meissner et al. (1997), Martí et al. (2006), Bishop et al. (1999)
MT-*non ripening* (MT-*nor*)			*NOR* is a NAC transcription factor. Mutant fruits do not ripe due to an alteration of the program that triggers climacteric ethylene biosynthesis	Solyc10g006880	Giovannoni et al. (1995)
MT-*ripening inhibitor* (MT-*rin*)			*RIN* is a MADS-box transcription factor. Mutants show an altered fruit ripening program, which fails to trigger climacteric respiration and ripening related ethylene biosynthesis	Solyc05g012020	Vrebalov et al. (2002)
MT-*green flesh* (MT-*gf*)			*gf* plants harbor a mutant allele of the STAY-GREEN1 protein encoding gene. The plants are deficient in chlorophyll degradation and present brownish fruits with green seed placental tissues	Solyc08g080090	Barry et al. (2008)
MT-*lutescent 1* (MT-*l*)			*L* is *locus* with unknown function. Mutant plants present non-pigmented ovaries and yellowish leaves	?	Jen (1974)
MT-*jasmonic acid insensitive 1-1* (MT-*jai*)			*JAI* is an F-box protein. Mutant plants are insensitive to JA and show delayed senescence of petals and styles, as well as glabrous ovaries	Solyc05g052620	Li et al. (2004)

[a] Sol Genomics Network (http://solgenomics.net/).

cient mutants, as well as following exogenous JA applications (Lim et al., 2007; Seltmann et al., 2010). JA treatment has been reported to promote climacteric fruit ripening by increasing ethylene production, accelerating Chl degradation and β-carotene biosynthesis (Fan et al., 1998). Moreover, the tomato JA-deficient mutants *spr2* and *def1* are impaired in lycopene accumulation and show reduced expression levels of lycopene biosynthetic genes (Liu et al., 2012). Although it has been proposed that JA might function independently of ethylene to promote ripening in tomato fruits, the underlying mechanism is still poorly understood (Liu et al., 2012). The tomato *jasmonic acid insensitive 1-1* (*jai*) mutant is, however, defective in the receptor component of the JA signal transduction pathway and fails to produce defense related compounds (Li et al., 2004), and although this mutant does not have an obvious senescence-related phenotype in vegetative tissues, it has delayed petal senescence and produces fruit lacking mature seeds (Li et al., 2004). Whether *JAI* also affects fruit ripening and ripening-related metabolic pathways remain to be determined.

Few studies have provided comprehensive insights into the regulation of the metabolic network that distribute common precursors towards isoprenoid compounds throughout fruit ripening. Described herein is an evaluation of how the impairment of different aspects of fruit development and ripening influence the metabolism of Chls, carotenoids and tocopherol and, consequently, fruit antioxidant capacity, by taking advantage of a collection of near isogenic tomato mutants.

2. Results and discussion

2.1. Transcriptional regulation of isoprenoid metabolism controls the pigment and antioxidant content of tomato fruits

During the transition from chloroplasts to chromoplasts in ripening tomato fruits, chlorophyll breakdown, carotenoid accumulation and tocopherol biosynthesis are tightly regulated, and the cross-talk between these isoprenoid branching pathways contributes to fruit nutritional quality (Vranová et al., 2012; Seymour et al., 2013a). In this current study, these metabolic interactions (Fig. 1) were explored by combining biochemical and gene expression analyses of ripening impaired, senescence-related and jasmonate insensitive tomato mutants (Table 1). The content of tocopherols, carotenoids and Chl were quantified in mature green (MG) and ripe (R) fruits from the MT-*rin*, MT-*nor*, MT-*gf*, MT-*l* and MT-*jai* mutants, as well as in the corresponding MT control (Fig. 2 and Table 2), using high-performance liquid chromatography (HPLC). Additionally, the expression patterns of twenty-five genes involved in the MEP (*DXS(1)*, *ISPE* and *GGDR*), post-chorismate SK (*ADH(1)*, *ADH(2)*, *TAT(1)*, *TAT(2)*, *HPPD(1)*, *HPPD(2)*) tocopherol-core (*VTE1*, *VTE2*, *VTE3(1)*, *VTE3(2)* and *VTE4*), carotenoid biosynthetic (*PDS*, *PSY(1)*, *PSY(2)*, *LCYβ*, *CYCβ*), Chl metabolism (*CHLG*, *CLH(1)*, *CLH(4)*, *PPH*, *PAO*) and phytol recycling (*VTE5*) pathways were assessed by qPCR (Figs. 1 and 3, Table S1 and Table S2).

Fruits from all the mutant and MT-wild type genotypes showed marked changes in levels of the analyzed isoprenoid-derived compounds during ripening (Fig. 2 and Table 2), with MT-*jai* showing the greatest number of metabolic changes, at both the MG and R stages, compared to the control. The MT-*rin* mutant showed the most highly altered gene expression profile, with significant differences in mRNA accumulation for all twenty-five analyzed genes in at least one of the tested ripening stages. In comparison, twenty and sixteen genes were differentially expressed in the fruits of the MT-*nor* and MT-*gf* mutant, respectively. Finally, the least altered expression profiles were seen in the MT-*l* and MT-*jai* mutants, for which only eight genes showed differential patterns of mRNA accumulation (Fig. 1 and Table S1). Thus, the more upstream the role of the mutated gene, in a regulatory context, the greater the impact on the transcriptional profile of the isoprenoid-biosynthesis related genes. This was especially evident when comparing the MT-*rin* and MT-*gf* genotypes, since while the former harbors a deletion in a ripening master transcription factor and shows a dramatically affected expression pattern in all the analyzed genes, the *gf* mutation affects a protein that regulates Chl degradation and, consequently, most of the genes with altered expression profiles are those associated with Chl metabolism (four out of six) and the VTE biosynthetic (four out of five) pathway (Fig. 1 and Table S1).

In order to evaluate the biochemical and gene expression profiles in an integrated manner, principal component analyses (PCA) were performed (Fig. 4). When the whole data set was analyzed, samples grouped by ripening stages. Samples from R fruits were scattered along PC1, while MG fruits were dispersed along the second component, suggesting that the metabolite and transcript profiles are more variable at the R than at the MG stage (Fig. 4A). When the same analysis was applied to data from the two stages separately, the first two dimensions explained approximately 53% of the variance for both the MG and R stages. At the MG stage, four groups were distinguished: MT-*l*, MT-*jai*, MT control and a cluster encompassing samples from the MT-*nor*, MT-*rin* and MT-*gf* mutants (Fig. 4B). However, at the R stage, all analyzed genotypes separated from each other by the first two PCA dimensions (Fig. 4C). It is notable that both metabolites and genes were found amongst the top eigenvectors, indicating that both types of variables contributed equally to sample separation. Moreover, when PCA were carried out exclusively with metabolites or gene expression profile data, samples were poorly separated (data not shown).

In the MT control genotype, the increased expression of the key enzyme encoding gene *DXS(1)* (Lois et al., 2000) and *PSY(1)* (Fraser et al., 2007), together with the transcriptional downregulation of *GGDR*, provides more isoprenoid intermediates for carotenoid biosynthesis (Fig. 3 and Table S1). Notwithstanding the transcriptional reduction of the phytol biosynthetic enzyme, tocopherol contents remained constant, suggesting the compensation via Chl breakdown, as proposed by Quadrana et al. (2013).

2.2. The MT-nor and MT-rin mutants

A number of transcription factors required for the initiation and promotion of tomato fruit ripening have been identified; however, the molecular mechanisms by which they interact are still largely unknown (Seymour et al., 2013b). *RIN* and *NOR* regulate the expression of genes involved in various aspects of fruit ripening, including carotenoid biosynthesis (Giovannoni et al., 1995; Vrebalov et al., 2002; Osorio et al., 2011; Martel et al., 2011; Fujisawa et al., 2013). The data herein show that R fruits from the MT-*rin* and MT-*nor* mutants had reduced levels of lycopene and higher levels of the photosynthetic xanthophyll neoxanthin than the control fruits (Table 2 and Fig. 5). Interestingly, these mutants were not deficient in β-carotene, and MT-*nor* actually accumulated more of this compound than the control at the R stage.

Publicly available chromatin immune precipitation (ChIP) assay data coupled with qPCR and/or large-scale gene expression analyses allowed retrieval of a catalog of genes that are directly or indirectly regulated by RIN (Martel et al., 2011; Fujisawa et al., 2011, 2012, 2013). The *DXS*, *ISPE* and geranylgeranyl diphosphate synthase (*GGPS*(2)) genes involved in the MEP pathway are all positively regulated in a RIN-dependent manner (Fujisawa et al., 2012, 2013). RIN also directly interacts with the promoter region of the *PSY(1)* gene, which constitutes the rate-limiting step of carotenoid biosynthesis (Fraser et al., 2007), favoring its transcrip-

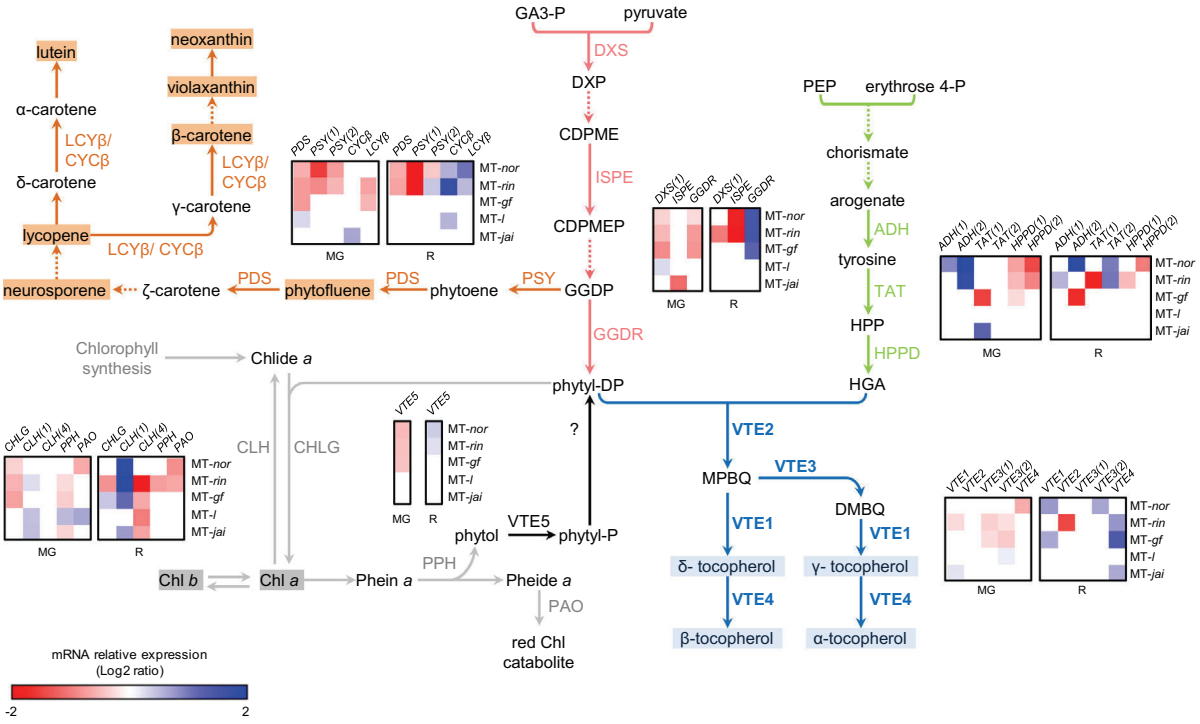

Fig. 1. Schematic view of the crosstalk between tocopherol, carotenoid and chlorophyll metabolism. The methyl erythritol phosphate, shikimate, tocopherol biosynthetic, carotenoid biosynthetic, chlorophyll metabolic and phytol recycling pathways are indicated in red, green, blue, orange, grey and black, respectively. The indicated enzyme encoding genes are those for which expression profiles were assayed. The genes are named according to the following abbreviations: 1-deoxy-D-xylulose-5-P synthase (*DXS*); 4-(cytidine 5′-diphospho)-2-C-methyl-D-erythritol kinase (*ISPE*); geranylgeranyl reductase (*GGDR*); arogenate dehydrogenase (*ADH*); tyrosine aminotransferase (*TAT*); 4-hydroxyphenylpyruvate dioxygenase (*HPPD*); homogentisate phytyl transferase (*VTE2*); 2,3-dimethyl-5-phytylquinol methyltransferase (*VTE3*); tocopherol cyclase (*VTE1*); γ-tocopherol C-methyl transferase (*VTE4*); phytoene synthase (*PSY*); phytoene desaturase (*PDS*); chloroplast-specific β-lycopene cyclase (*LCYβ*); chromoplast-specific β-lycopene cyclase (*CYCβ*); chlorophyll synthase (*CHLG*); chlorophyllase (*CLH*); pheophytinase (*PPH*); pheophorbide *a* oxygenase (*PAO*) and; phytol kinase (*VTE5*). Abbreviated intermediate metabolites are: glyceraldehyde 3-phosphate (GA3-P); 1-deoxy-D-xylulose-5-P (DXP); 4-(cytidine 5′-diphospho)-2-C-methyl-D-erythritol (CDPME); 2-phospho-4-(cytidine 5′-diphospho)-2-C-methyl-D-erythritol (CDPMEP); geranylgeranyl-2P (GG-2P); phosphoenolpyruvate (PEP); hydroxyphenylpyruvate (HPP); homogentisate (HGA); chlorophyllide *a* (Chlide *a*); chlorophyll *a* (Chl *a*); chlorophyll *b* (Chl *b*); pheophytin (Phein *a*); pheophorbide *a* (Pheide *a*); 2-methyl-6-geranylgeranylbenzoquinol (MPBQ) and; 2,3-dimethyl-6-geranylgeranylbenzoquinol (DMBQ). Highlighted metabolites were quantified. Gene expression profiles of each enzyme-encoding gene were measured by qPCR in samples of pericarp from mature green (MG) and ripe (R) tomato fruits ($n \geqslant 3$). Expression data are represented as $\log_2$ fold changes compared to the corresponding development stage of the Micro-Tom control by a color scale, where red and blue indicate statistically significant decreasing and increasing transcript levels ($p < 0.05$), respectively. (For interpretation of the references to colour in this figure legend, the reader is referred to the web version of this article.)

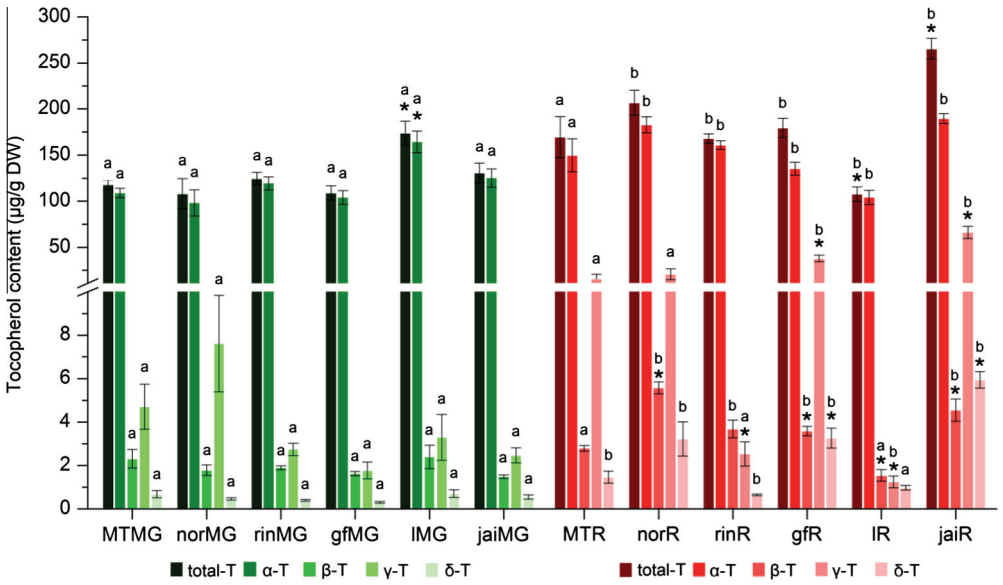

Fig. 2. Tocopherol content of the pericarp of fruits at the mature green (MG) and ripe (R) stages. Different letters indicate significant differences between both stages of the same genotype ($p < 0.05$). Asterisks denote significant differences compared to the corresponding stage of the Micro-Tom wild type control genotype ($p < 0.05$).

Table 2
Chlorophyll and carotenoid content of the pericarp of fruits at mature green (MG) and ripe (R) stages.

Genotype	Chlorophyll *a*	Chlorophyll *b*	Neoxanthin	Violaxanthin	Lutein	β-Carotene	Phytofluene	Neurosporene	Lycopene
Mature green									
MTMG	1.00 ± 0.06 *a*	1.00 ± 0.08 *a*	1.00 ± 0.07	1.00 ± 0.10	1.00 ± 0.11 *a*	1.00 ± 0.17 *a*	nd	nd	nd
MT-*nor*MG	0.95 ± 0.12 *a*	0.57 ± 0.08 *a*	1.08 ± 0.21 *a*	0.85 ± 0.11	0.92 ± 0.12 *a*	0.95 ± 0.13 *a*	nd	nd	nd
MT-*rin*MG	1.09 ± 0.09 *a*	1.09 ± 0.06 *a*	1.02 ± 0.05 *a*	1.09 ± 0.15	1.04 ± 0.06 *a*	1.14 ± 0.06 *a*	nd	nd	nd
MT-*gf*MG	1.27 ± 0.10 *a*	1.32 ± 0.12 *a*	1.46 ± 0.05*a*	1.23 ± 0.13	1.16 ± 0.07 *a*	1.25 ± 0.16 *a*	nd	nd	nd
MT-*l*MG	nd	nd	nd	nd	0.41 ± 0.02*a*	0.27 ± 0.03*a*	nd	nd	0.01 ± 0.00 *a*
MT-*jai*MG	1.65 ± 0.16*a*	1.53 ± 0.15*a*	1.77 ± 0.21*	2.97 ± 0.36*a*	1.33 ± 0.03 *a*	1.62 ± 0.04*a*	nd	nd	nd
Ripe									
MTR	0.02 ± 0.01 *b*	0.04 ± 0.00 *b*	nd	nd	0.80 ± 0.08 *a*	1.57 ± 0.15 *b*	1.00 ± 0.16	1.00 ± 0.03	1.00 ± 0.09
MT-*nor*R	0.34 ± 0.03*b*	0.25 ± 0.03*b*	0.43 ± 0.01*b*	nd	0.98 ± 0.12 *a*	2.71 ± 0.23*b*	nd	0.24 ± 0.01*	0.01 ± 0.00*
MT-*rin*R	0.38 ± 0.05*b*	0.36 ± 0.02*b*	0.48 ± 0.05*b*	nd	0.72 ± 0.05 *b*	1.32 ± 0.03 *a*	nd	0.21 ± 0.00*	nd
MT-*gf*R	0.45 ± 0.03*b*	0.56 ± 0.01*b*	0.84 ± 0.03*b*	nd	0.89 ± 0.04 *b*	1.62 ± 0.13 *a*	0.52 ± 0.12	0.90 ± 0.15	0.93 ± 0.24
MT-*l*R	nd	nd	nd	nd	0.89 ± 0.10 *b*	2.19 ± 0.36 *b*	1.04 ± 0.17	1.39 ± 0.24	1.67 ± 0.28 *b*
MT-*jai*R	0.11 ± 0.03*b*	0.22 ± 0.07*b*	nd	1.49 ± 0.35*b*	1.23 ± 0.05*a*	3.09 ± 0.39*b*	1.40 ± 0.21	1.07 ± 0.37	0.98 ± 0.11

Pigment levels in mature green (MG) and ripe (R) fruits. Data were normalized against MT-MG or MT-R. Asterisks denote significant differences from the corresponding stage of the MT wild type control genotype ($p < 0.05$). Different letters indicate significant differences between the stages of the same genotype ($p < 0.05$). nd indicates metabolite not detected.

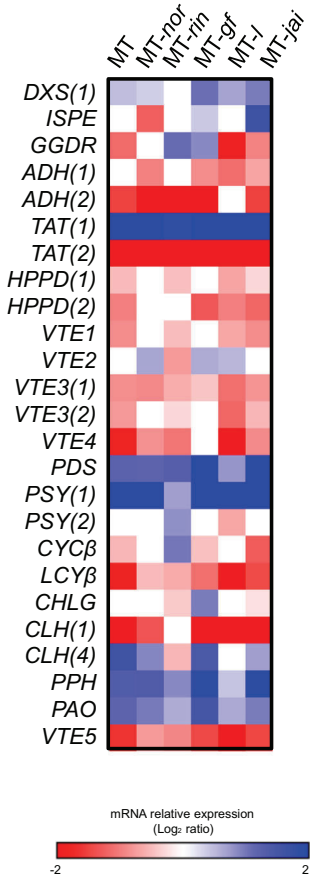

Fig. 3. Expression ratio between ripe (R) and mature green (MG) fruits within genotypes. The $\log_2$ of the expression ratios is indicated by a color scale where red and blue indicate statistically significant decreases and increases of transcript abundance ($p < 0.05$), respectively.

tion (Martel et al., 2011). Moreover, *NOR* expression is directly induced by RIN (Fujisawa et al., 2013), explaining the highly similar metabolic and gene expression profiles observed in MT-*rin* and MT-*nor*.

Here, lycopene deficiency in both mutants correlates with the reduced expression of *PSY(1)*, supporting previously reported observations (Kitagawa et al., 2005; Osorio et al., 2011; Martel et al., 2011). *PSY(1)* is the most highly expressed (The Tomato Genome Consortium, 2012) and functional studies demonstrated that this paralog has an essential role in carotenogenesis during tomato ripening (Fantini et al., 2013). Ripening mutants also showed significant decreased *PDS* mRNA levels (Fig. 5), as previously reported (Martel et al., 2011). Besides inhibition of the metabolic flux towards carotenoids, the lack of lycopene accumulation in R fruits of MT-*rin* and MT-*nor* is likely a consequence of *LCYβ* and *CYCβ* repression failure, resulting in higher amounts of the final product of the pathway, neoxanthin (Fig. 5). The low carotenoid content of R fruits of these two mutants could potentially result in more GGDP precursor being available for tocopherol biosynthesis. However, the downregulation of MEP pathway genes, *DXS* and *ISPE* (Fig. 1), could account for the maintenance of total tocopherol content in the ripening mutant fruits (Fig. 5). This result also supports the role for RIN as a transcriptional regulator of *DXS* and *ISPE* (Fujisawa et al., 2012, 2013). In addition, R fruits of the mutant genotypes showed higher levels of *GGDR* mRNA than the control (Fig. 5). As with *PDS*, for which the ChIP assays failed to detect an effect of RIN on expression (Martel et al., 2011), *GGDR* and the aforementioned *LCYβ* and *CYCβ* promoters contain putative CArG cis-elements, which are predicted RIN-binding motifs (Quadrana et al., 2013). Thus, these data suggest that NOR and RIN could be involved directly or indirectly in the down-regulation of *GGDR*, as well as the carotenoid genes *LCYβ* and *CYCβ*, at the onset of ripening (Fig. 1).

Regarding the SK pathway, in the MT control genotype, the transcriptional profile of *TAT(1)*, *TAT(2)*, *ADH(1)*, *ADH(2)*, *HPPD(1)* and *HPPD(2)* genes showed the same temporal fluctuation along ripening and similar relative expression within paralogs as that described for the Heinz cultivar (The Tomato Genome Consortium, 2012) (data not shown). However, in MT-*nor* and MT-*rin* mutants, these paralogs displayed a distinct pattern of alterations compared to the controls that apparently do not impact on homogentisate availability for tocopherol biosynthesis, suggesting a certain level of functional redundancy between paralogs (Fig. 5).

Both mutants are known to be deficient in Chl degradation and accordingly, it was observed that their R stage fruits retained approximately 30% of the total Chl *a* and *b* present at the MG stage (Table 2). Fruit de-greening is dependent on the activity of the Chl breakdown complex, which is regulated by the SGR protein, a key control point of Chl catabolism (Barry et al., 2008; Hu et al., 2011; Thomas and Ougham, 2014; Lira et al., 2014). The Chl degradation complex aggregates all the enzymes that catalyze the stepwise degradation of Chl to a primary fluorescent Chl catabolite,

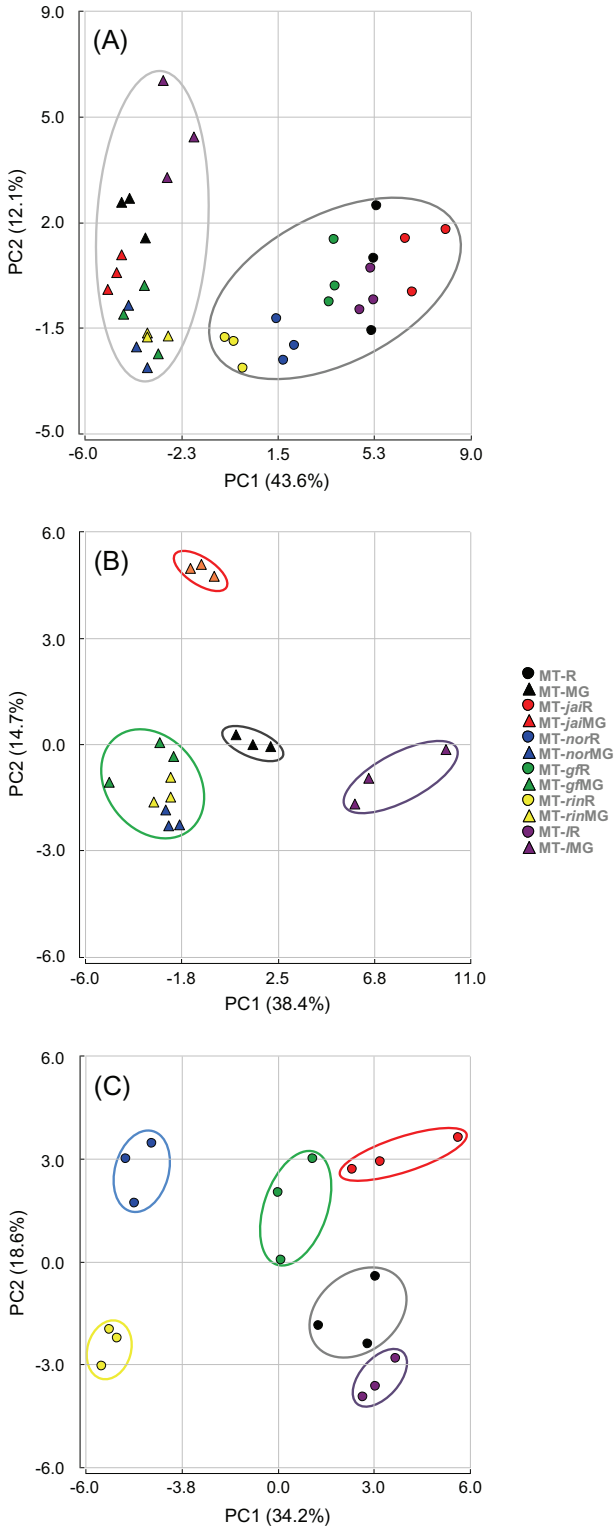

Fig. 4. Principal component analysis (PCA) of metabolic and gene expression profiles in the pericarp of tomato fruits. Metabolic and gene expression profiles of both mature green (MG) and ripe (R) (A); MG only (B); or R only (C) fruits subjected to PCA analysis.

including PPH and PAO (Sakuraba et al., 2012). *SGR1* is another direct target of RIN in tomato and its expression level is much higher in wild type than in the *rin* mutant throughout fruit development (Hu et al., 2011; Fujisawa et al., 2013), which might account in part for the Chl retention in R fruits of the MT-*nor* and MT-*rin* mutants (Fig. 5). Furthermore, these fruits also showed an apparent reduction in activity of the PAO-pathway, as indicated by a down-regulation of *PAO* and *PPH* expression (Fig. 5). Since MT-*gf*, an *sgr1* mutant, did not display the same patterns, it seems that NOR and RIN are directly or indirectly responsible for *PAO* and *PPH* expression reduction rather than being a consequence of SGR deficiency. Although *GGDR* is not down-regulated in MG or R fruits of the MT-*nor* and MT-*rin* mutants (Fig. 3), and *de novo* phytyl diphosphate biosynthesis might therefore not be repressed, the reduced levels of *CHLG* mRNA suggests that Chl biosynthesis is less active in the mutant fruits than in those of the control (Fig. 5). Furthermore, the maintenance of *CLH(1)* mRNA levels observed during MT-*nor* and MT-*rin* fruit development correlates with the Chl content as observed by Lira et al. (2014). Finally, *CLH(4)* has also been reported as a target of RIN (Fujisawa et al., 2012), and, in support of this, its expression was reduced in R fruits of the MT-*rin* mutant (Fig. 5).

In the context of tocopherol biosynthesis, the control fruits showed decreasing levels of *VTE3*, *VTE1* and *VTE4* expression throughout ripening, while *VTE2* remained constant (Fig. 3 and Table S2), which is in agreement with data previously reported by Quadrana et al. (2013). In contrast, MT-*rin* and MT-*nor* mutant fruits exhibited differing expression profiles for the tocopherol-core pathway genes (Figs. 1 and 3 and Table S1). For example, MT-*rin* R fruits showed a substantial repression of *VTE2* expression and a noticeable reduction of γ-tocopherol content compared to the control (Fig. 5), suggesting that NOR and RIN differentially modulate VTE biosynthesis. It was also noted that although levels of the Chl-derived phytol were lower in these ripening mutants, the maintenance of high expression levels of *GGDR* appear to be sufficient to the supply the prenyl side-chain for tocopherol production at the R stage (Fig. 5).

The findings here are consistent with previously published data concerning the signaling pathways regulated by RIN (Martel et al., 2011; Fujisawa et al., 2011, 2012, 2013). Furthermore, new evidence is provided regarding steps in the isoprenoid metabolism regulated by RIN and NOR in tomato fruits, as well as data promoting a better understanding of the differences observed in the metabolite profiles of the MT-*rin* and MT-*nor* mutant fruits.

2.3. The MT-*gf* mutant

The tomato *gf* mutant carries an amino acid substitution in an invariant residue of the ortholog of the Arabidopsis SGR protein (Barry et al., 2008). Since *gf* is not a knockout mutant, the activity of the Chl catabolic enzymes is not completely impaired in the mutant, and so the fruits retain detectable levels of Chl *a* and Chl *b* at the R stage (Table 2). The abnormal de-greening process correlates with multiple changes in the expression patterns of genes encoding enzymes involved in Chl and carotenoid metabolism, as well as in the MEP-, SK-, and tocopherol-core pathways. Interestingly, these results showed an effect of the *gf* mutation earlier than the onset of fruit ripening, as previously reported by Cheung et al. (1993). At the MG stage, the presence of the mutant allele resulted in the down-regulation of *DXS*, *GGDR*, *CHLG*, *PPH*, *VTE5*, *PDS*, *LCYβ*, *VTE3*, *TAT(1)* and *HPPD* transcripts (Fig. 5). Ripe fruits from the MT-*gf* mutant showed higher levels of *CLH(1)* mRNA compared to the control. This data correlates well with observations reported by Akhtar et al. (1999), that an accumulation of chlorophyllide *a* and *b* in R fruits from the *gf* mutant occurs following an increase in CLH activity. Interestingly, the increased levels of *GGDR* and *CHLG* mRNAs suggest that Chl biosynthesis remained active during late ripening in MT-*gf* mutant fruit (Fig. 5). It has been reported that Chl retention in *gf* is associated with the maintenance of chloroplast structure and photosynthesis related proteins, including the light-harvesting Chl *a*/*b*-binding proteins of photosystem II

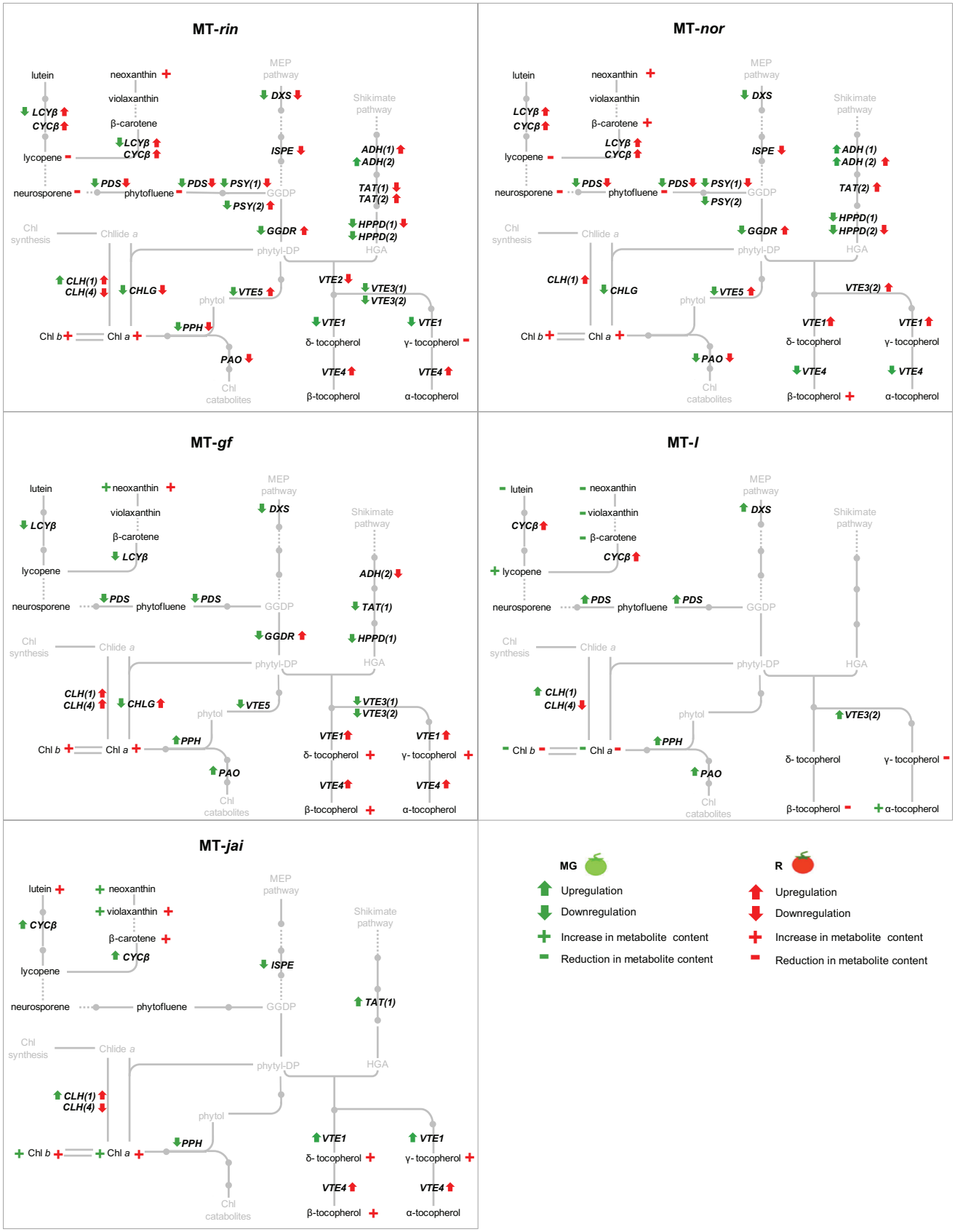

Fig. 5. Integrated view of the observed changes in chlorophyll, tocopherol and carotenoid content and gene transcriptional profiles for each tomato mutant compared with the corresponding stage of the Micro-Tom control. Gene expression (Table S1) and metabolite content changes (Fig. 2 and Table 2) are indicated by arrows and + or − signals, respectively. Mature green (MG) and ripe (R) stages are indicated by green and red colors, respectively.

and the small subunits of ribulose bisphosphate carboxylase/oxygenase, as well as their mRNAs (Cheung et al., 1993; Akhtar et al., 1999). It can, therefore, be inferred from these results that the Chl biosynthesis machinery is still functional in R stage fruits. Changes in transcriptional regulation of Chl biosynthetic genes were previously reported in the *Arabidopsis phytochrome A* mutant (Brouwer et al., 2014). Induced leaf yellowing in this mutant correlates to the repression of Chl biosynthesis associated genes rather than to an increase of its catabolism. Moreover, the maintenance of chloroplast structure is further evidence for the GGDR activity, since this enzyme is functional as long as it is anchored to membrane by light-harvesting-like protein LIL3 as previously reported (Tanaka et al., 2010; Takahashi et al., 2014).

The MT-*gf* mutant showed several alterations in tocopherol metabolism (Fig. 5). Despite the impairment in Chl catabolism, transcript levels of *VTE1* and *VTE4* increased at the R stage, a change is proposed to allow maintenance of total tocopherol contents equivalent to levels observed in the control fruit (Fig. 2). From MG to R, while fruits of the control genotype exhibited constant expression levels of *VTE2* and reduced levels of *VTE3(1)* and *(2)*, the corresponding MT-*gf* fruits showed an increase in *VTE2* and stable *VTE3(2)* mRNA levels, which suggests a corresponding increase in tocopherol biosynthesis (Fig. 3). Indeed, higher levels of β-, γ- and δ-tocopherol were detected in R MT-*gf* fruits compared to the control (Fig. 5). The perturbations in Chl and tocopherol accumulation do not seem to affect GGDP availability for carotenoid biosynthesis, since the carotenoid profile of the MT-*gf* mutant fruit resembles that of control fruits with the exception of neoxanthin (Table 2). The stronger up-regulation of *DXS(1)* and *PDS* expression from MG to R (Fig. 3 and Table S2) in this genotype may account in part for the maintenance of carbon precursors for the carotenoid pathway.

Recently, SGR1 has been shown to regulate lycopene and β-carotene biosynthesis in tomato fruits by direct interaction with PSY(1), thereby inhibiting its activity (Luo et al., 2013). Tomato *SGR1*-silenced lines showed *PSY(1)* mRNA accumulation and plastid conversion at the early stages of fruit ripening, resulting in increased lycopene and β-carotene contents in R fruits (Luo et al., 2013). In contrast, the *gf* mutation has no apparent effect on lycopene and β-carotene levels (Table 2), which is consistent with the study of Akhtar et al. (1999). One possible explanation for this apparent controversy is that the point mutation does not compromise the interaction with PSY. In addition, the accumulation of neoxanthin observed in these fruits (Fig. 5) might indicate that the Chl degradation deficiency partially impairs the disassembly of the photosynthetic apparatus. In agreement with this idea, it has been proposed that in the *sgr* mutant, Chl retention within the LHC shields its photosensitivity property; however the mechanism of energy dissipation under these conditions remains to be elucidated (Cheung et al., 1993; Sakuraba et al., 2012).

2.4. The MT-*l* mutant

The MT-*l* mutant contains a mutation in an unknown locus, resulting in premature leaf yellowing and albino fruits; however, Chl biosynthesis is not impaired in this genotype since at early stages of development the plant displays normal Chl production (Barry et al., 2012). The albino phenotype of the fruits is, however, consistent with the absence of Chls (Table 2).

The up-regulation of PAO-dependent Chl breakdown correlates with increased *PAO* and *PPH* mRNA levels (Fig. 1 and Table S1), suggesting that the lack of Chl in MG fruits is the result of accelerated degradation, rather than a reduction in biosynthesis. In addition to the lack of Chls, MG fruits from the MT-*l* mutant were also shown to have lower levels of violaxanthin and neoxanthin (Fig. 5), further implicating an impairment in the photosynthetic machinery.

Intriguingly, although *LCYβ* and *CYCβ* mRNA levels were comparable to those of the controls (Fig. 5), MG fruits from the MT-*l* mutants had detectable levels of lycopene, reduced β-carotene and lutein content and a lack of the xanthophylls neoxanthin and violaxanthin (Table 2). The observed increase in lycopene is in agreement with results previously reported by Jen (1974). The altered carotenoid profile exhibited by MT-*l* could be the consequence of another important regulatory mechanism involved in carotenoid accumulation, which relates to changes in storage and sequestration of carotenoids within various plastid structures (Cazzonelli and Pogson, 2011; Nogueira et al., 2013). Analysis of the chloroplasts from cotyledons of the *l* mutant have shown them to be impaired in thylakoid membrane development (Barry et al., 2012), and it may be that an equivalent alteration in fruit chloroplast structure of MT-*l* affects carotenoid accumulation. This chemotype, together with higher level of *DXS* mRNA, suggests increased metabolic flux towards tocopherol at the MG stage, which correlates with the observed increase in α- and total tocopherol levels compared to the control (Fig. 2).

At the R stage, transcriptional profile of the MEP pathway genes and carotenoid content of the MT-*l* fruits showed similar levels to control fruits. However, the dramatic phenotype of this Chl-deficient mutant was associated with a reduction in tocopherol levels at the R stage (Fig. 5). The absence of phytol derived from Chl breakdown is likely the cause of the observed reduction in β- and γ-tocopherol, which together resulted in a 35% decrease in total tocopherol content (Fig. 2). Although the ripening-impaired mutants (*nor* and *rin*) and the Chl retainer *gf* showed a reduction in the availability of Chl-derived phytol (Fig. 5), it can be proposed that the maintenance of high *GGDR* mRNA levels at the R stage in these mutants ensures sufficient levels of prenyl chain to maintain constant tocopherol levels. This compensatory mechanism might explain why seeds of *A. thaliana sgr* mutants show only a modest tocopherol reduction compared to wild type (Zhang et al., 2014). In contrast, in the MT-*l* mutant, besides the complete depletion of Chl-derived phytol, the *GGDR* expression showed a similar reduction to the control, further highlighting the importance of phytol derived from Chl degradation for tocopherol production during tomato fruit ripening (Quadrana et al., 2013).

2.5. The MT-*jai* mutant

The MT-*jai* mutant harbors a loss of function allele in the *CORONATINE-INSENSITIVE1* (*COI1*) *locus*, which encodes an F-box protein from the Skp/Cullin/F-box complex (SCF^{COI1}); a key component of the JA signaling pathway (Li et al., 2004). Upon perception of JA, COI1 promotes the degradation of the JAZ repressor (jasmonate ZIM-domain), thereby releasing transcription factors that will in turn activate JA-mediated responses (Wasternack and Hause, 2013). Although the role of JA in the regulation of plant fertility, secondary metabolism, and defense responses (Wasternack and Hause, 2013), including stress-induced leaf senescence (Kariola et al., 2005; Lira et al., 2014), has been widely reported, its role in fruit ripening remains poorly described (Fan et al., 1998).

During tomato fruit development, immediately prior to the MG jelly placenta stage, the endogenous concentration of JA peaks, causing an increase in ethylene production and accelerating chlorophyll degradation and carotenoid synthesis (Fan et al., 1998). In addition, it was shown that the JA-deficient mutants *spr2* and *def1* produce less ethylene at the breaker stage, accumulate less lycopene, and show a down-regulation of *DXS(1)*, *PSY* and *PDS* expression, while JA-overproducing transgenic plants show the opposite pattern (Liu et al., 2012). The JA and ethylene signaling pathways share a point of convergence, since JAZ also represses the EIN3/EIL1 protein, which is a positive regulator of ethylene responses, in a SCF^{COI1}-dependent manner (Zhu et al., 2011; Li

et al., 2013). N*EVER RIPE* (*nr*), an ethylene-insensitive mutant, shows a significant delay in fruit ripening does not reach the red ripe stage and exhibits very low levels of lycopene (Wilkinson et al., 1995; Osorio et al., 2011). However, the exogenous application of JA to *nr* partially rescues this phenotype, promoting the expression of lycopene biosynthetic genes and lycopene accumulation. These results indicate that even though JA and ethylene have a synergistic effect on tomato fruit ripening, JA signal transduction is not ethylene-dependent.

It was observed in this study that MT-*jai* fruits accumulated higher levels of Chl *a* and *b* at both ripening stages compared to the control (Table 2), and showed an increase in *CLH(1)* transcript abundance (Fig. 1). This observation is congruent with a role for *CLH(1)* in Chl recycling (Lira et al., 2014), although additional data are required to confirm this hypothesis. Interestingly, fruits from the JA insensitive mutant showed higher levels of β-carotene, violaxanthin and neoxanthin at the MG stage, and β-carotene, violaxanthin and lutein at the R stage than the controls (Fig. 5), which can be proposed to be a consequence of the higher accumulation of the fruit-specific *CYCβ* mRNA at the MG stage (Fig. 5). Moreover, in the transition from MG to R stages, the expected increase in *DXS*, *ISPE*, *PSY(1)* and *PDS* expression was stronger than in the control, which likely further contributed to the increased carotenoid content in R fruits (Fig. 3 and Table S2). Although these results may seem contradictory to those obtained for the *spr2* and *def1* mutants, they may in fact suggest the existence of a new variable in the complex regulatory network that controls fruit ripening. The absence of the JA peak before the MG stage in the *spr2* and *def1* mutants compromises ethylene production at the breaker stage, when the fruits exhibit the first visible trace of carotenoid accumulation. However, MT-*jai* is not defective in JA biosynthesis and the metabolic differences are primarily the results of the impairment of COI-dependent JA perception. In conclusion, the data herein suggest a COI-independent JA signaling pathway in tomato fruits, as previously proposed for *A. thaliana* (Caño-Delgado et al., 2003; Mueller and Berger, 2009).

Tocopherol levels also showed an increase in R fruits of MT-*jai* (Fig. 2), which are proposed to reflect, at least in part, the observed increases in *VTE1* and *TAT*(1) transcript levels at the MG and, *VTE4* at the R stage (Fig. 5). It has been demonstrated that fruit pericarp is an important source of carbon assimilate for determining seed metabolic profile (Lytovchenko et al., 2011). Chlorophyll degradation-derived phytol serves as an intermediate in tocopherol synthesis for seed VTE accumulation (Valentin et al., 2006). Since tocopherols are abundant in tomato seeds (Ellen et al., 2010) and, indeed, homozygous MT-*jai* fruits are seedless, the lack of seeds might contribute to the increased levels of tocopherols observed in the pericarp of these fruits (Fig. 5). The increase in β-carotene, violaxanthin and lutein (Table 2), together with increased VTE content suggest that the R fruits of the MT-*jai1* mutant have greater nutritional value and the highest antioxidant capacity of the tested genotypes (see below).

2.6. Analysis of antioxidant capacity

Profiling of pigment composition (Table 2) showed that the Chl and carotenoid contents of the mutant fruits were substantially different from those of the control. The Trolox equivalent antioxidant capacity (TEAC) showed little difference between the two ripening stages (Table 3) and the only genotypes with an increase in antioxidant capacity during ripening were the MT-*nor* and MT-*jai* mutants, and these two genotypes also showed an increase in β-carotene and total tocopherol levels. In contrast, MT-*l* fruits, which accumulated carotenes to the same degree as control fruits, but displayed a reduction in total-tocopherol, did not show a difference in antioxidant capacity between the MG and R stages. MT-*jai* was the only mutant with a higher total tocopherol content than the control at the R stage accompanied by an increase in antioxidant capacity, suggesting a major contribution of VTE to total antioxidant capacity in tomato fruits. Notably, R fruits from the MT-*jai* mutant also contained higher amounts of violaxanthin and lutein. Lutein has been reported to undergo the slowest degradation of the carotenoids in olive fruits and the radical species resulting from the molecular structure of lutein exhibit less propagation than those from β-carotene (Roca and Mínguez-Mosquera, 2001). It, therefore, cannot be disregarded that the potential effect of the increased lutein content is on the higher TEAC observed in MT-*jai* fruits. Underlining the influence of tocopherol on the antioxidant capacity of MT-*jai* fruits, previous studies have shown that the peroxyl radical scavenging capacity of β-carotene and lycopene is about one-tenth that of α-tocopherol, and the efficacy of lipid peroxidation inhibition is considerably smaller (Takashima et al., 2012). Moreover, the chemical species formed from carotenoids when they scavenge radicals are not stable, and may undergo several secondary reactions, thereby compromising the effects and efficacy of carotenoids as antioxidants (Takashima et al., 2012). The interactions between antioxidant compounds are complex and differences in the nature, concentrations and ratios in which they are present, are all important variables in defining antioxidant capacity (Gawlik-Dziki, 2012). A previous study of antioxidant capacity of lipophilic extracts obtained from different tomato varieties showed that tocopherol and β-carotene/lycopene act in a synergistic manner positively affecting antioxidant properties (Zanfini et al., 2010).

Table 3
Trolox equivalent antioxidant capacity (TEAC) in mature green (MG) and ripe (R) fruits.

Genotype	TEAC[a] Mean ± SE
MTMG	456.16 ± 39.27 *a*
MTR	641.62 ± 82.6 *a*
MT-*nor*MG	333.47 ± 16.2 *a*
MT-*nor*R	573.96 ± 83.67 *b*
MT-*rin*MG	403.32 ± 41.33 *a*
MT-*rin*R	534.59 ± 21.34 *a*
MT-*gf*MG	514.22 ± 87.38 *a*
MT-*gf*R	679.92 ± 24.25 *a*
MT-*l*MG	442.8 ± 49.66 *a*
MT-*l*R	525.97 ± 98.27 *a*
MT-*jai*MG	495.79 ± 35.88 *a*
MT-*jai*R	1,001.24 ± 152.96*b

Different letters indicate significant differences between stages of the same genotype ($p < 0.05$). Asterisks denote significant differences from the corresponding stage of the MT control genotype ($p < 0.05$).
[a] μmol of trolox equivalent/g of dry weight.

3. Concluding remarks

In this study, the metabolic network that links isoprenoid biosynthesis and recycling during ripening were explored in ripening impaired, senescence related and jasmonate insensitive tomato mutants. Although these pathways have been characterized in detail separately, few studies have addressed the potential cross-talk between isoprenoid derived pathways in a comprehensive manner.

The integrated analyses presented here revealed a remarkable plasticity of the interconnected Chl, carotenoid and tocopherol metabolic pathways, which is in part explained by the transcriptional regulation of the enzyme encoding genes from the corresponding pathways. This conclusion is supported by the fact that neither metabolites nor mRNA quantification alone discriminated between the mutant genotypes when non-parametric analyses

were applied (Fig. 4). The impact of transcriptional regulation on metabolite contents was proven by a weighted network analysis including mRNA, metabolites and TEAC quantification data (Fig. S1). The most striking difference in the topology of the constructed networks is that in all mutant genotypes, tocopherols appear highly connected with the other components, but this is not the case with the control genotype. This suggests that tocopherol composition is modified in the mutants diverting the isoprenoid metabolism, thereby keeping the antioxidant capacity constant. Network analyses also showed that in genotypes where Chl degradation is impaired, *GGDR* is connected with the tocopherol cluster but not the Chl cluster, supporting a putative role for this enzyme in supplying the prenyl side-chain for VTE biosynthesis, as discussed above. The analyses presented here indicate that transcription is a main regulatory mechanism of the isoprenoid metabolism; however, it is noted here that post-transcriptional and epigenetic regulation might also account for the complexity of this regulatory network (Martinis et al., 2013; Quadrana et al., 2014).

The biochemical analyses and gene expression profiles obtained from mutant-based resources contribute to a more detailed understanding of isoprenoid metabolism than was made possible by previously published data related to the RIN and NOR signal transduction pathways (Osorio et al., 2011; Martel et al., 2011; Fujisawa et al., 2013). Furthermore, this study provides insights into the effect of the *gf*, *l* and *jai* mutations on the regulatory networks that determine the composition of nutritionally important metabolites in tomato fruits. As a consequence of its wide distribution and high levels of global consumption, tomato is an important component of the human diet. The data presented here demonstrate that tocopherols make an important contribution to the antioxidant capacity of the tomato fruits, and suggest targets for future manipulation of their nutritional.

4. Experimental

4.1. Plant material

Seeds of *Solanum lycopersicum* L. (cv. Micro-Tom) (MT), and the mutants *lutescent 1* (*l*) (Barry et al., 2012), *green flesh* (*gf*) (Barry et al., 2008), *rin* (Vrebalov et al., 2002) and *nor* (Casals et al., 2012) in the MT background were produced in the Laboratory of Hormonal Control of Plant Development (www.esalq.usp.br/tomato). The mutations were introgressed by six successive backcrosses to the MT cultivar as the recurrent parent (BC6 generation), resulting in plants where at least 99% of the genome corresponds to MT. The *jai1-1* mutant (*jai*) in the MT background was kindly provided by Dr. Gregg Howe from Michigan State University. Due to the female sterility of *jai*, 1:1 segregating homozygous plants, which resulted from crosses between heterozygous MT-*jai* and homozygous *jai* (pollen donor), were screened in a methyl jasmonate (MeJA)-containing medium (Li et al., 2004; Campos et al., 2009). A brief description of all genotypes is presented in Table 1. Other than MT-*jai*, all the analyzed plants were homozygous for the mutations. The plants were grown in 8 l rectangular plastic pots containing a 1:1 mixture of commercial substrate (Plantmax HT, Eucatex, São Paulo, Brazil) and expanded vermiculite, supplemented with 1 g l^{-1} of NPK 10:10:10 and 4 g l^{-1} of dolomite limestone ($MgCO_3 + CaCO_3$). Plants were grown in a greenhouse under automatic irrigation (four times a day) in an average mean temperature of 25 °C; 11.5 h/13 h (winter/summer) photoperiod and 250–350 μmol m^{-2} s^{-1} of incident photo-irradiance. Fruit pericarp material (without placenta and locule walls) from the mature green (MG, jelly placenta), and ripe (R, placenta without Chl) stages was harvested. The MG stage was reached at approximately 35 days after anthesis (daa) for the MT, MT-*l*, MT-*gf*, MT-*jai* and MT-*rin* genotypes; and 38 daa for the MT-*nor* genotype. The R stage pericarp samples were collected at 45 daa for the MT, MT-*l*, MT-*gf* and MT-*jai* genotypes, 50 daa for the MT-*rin* mutant and at 54 daa for the MT-*nor* mutant. All samples were frozen in liq. N_2, homogenized and stored at −80 °C until further use. Samples were named with the mutant name followed by the ripening stage: MTMG, MTR, MT-*nor*MG, MT-*nor*R, MT-*rin*MG, MT-*rin*R, MT-*gf*MG, MT-*gf*R, MT-*l*MG, MT-*l*R, MT-*jai*MG and MT-*jai*R (Table 1).

4.2. Tocopherol and pigment quantification by HPLC

Tocopherols and pigments were extracted as described in Almeida et al. (2011) and the samples adjusted to a final volume (4 ml). For tocopherol analysis, aliquots (3 ml) were dried under N_2 and dissolved in a mobile phase (200 μl) composed of hexane/tert-butyl methyl ether (90:10). Chromatography was carried out on a Hewlett–Packard series 1100 HPLC system coupled with a fluorescence detector (Agilent Technologies series 1200) on a normal-phase column (LiChrosphere® 100 Diol Si (250 mm × 4.0 mm, 5 μm; Agilent Technologies, Germany) at room temperature, with the mobile phase running isocratically at 1 ml min^{-1}. Eluted compounds were detected by excitation at 295 nm and quantifying their fluorescence at 330 nm.

For pigment analysis, aliquots (500 μl) of extract were dried under N_2 and dissolved in MeOH: EtOAC (500 μl, 50:50, v/v). Chromatography was performed with an Agilent 1200 Series HPLC system coupled with a Diode Array Detector on a reversed phase column (Zorbax Eclipse Plus C18 (150 mm × 4.6 mm, 5 μm; Agilent Technologies, USA) at room temperature using a 0.6 ml min^{-1} flow rate. The elution was performed with a linear gradient of 100% solvent A (CH_3CN/MeOH/Tris buffer [0.1 M, pH 8] in a 72:8:3 ratio) to 100% solvent B (MeOH/EtOAC in a 68:32 ratio) from 0 to 25 min, followed by 10 min with 100% solvent B. For column equilibration, the mobile phase was returned to 100% solvent A and maintained for 5 min. Throughout the chromatography run, the eluate was monitored continuously from 200 to 800 nm. Lutein, β-carotene, and lycopene were quantified at 440 nm by comparison with an external standard (Sigma–Aldrich Chemical Co., USA). Phytofluene, Chl *a* and Chl *b* were quantified based on their absorption coefficient: ε1% (348 nm) = 1577, ε(431 nm) = 95.99 cm^{-1} mM^{-1} and ε(430 nm) = 57.43 cm^{-1} mM^{-1}, respectively. These compounds were expressed as μg g^{-1} of dry weight. Neurosporene, violaxanthin, neoxanthin and pheophytin were identified and quantified at 440 nm and expressed as area (mAU*seg) per g of fruit dry weight.

4.3. Trolox equivalent antioxidant capacity (TEAC)

The antioxidant capacity of the tocopherol and pigment extracts was assayed as previously described (Re et al., 1999), with minor modifications. The pre-formed radical monocation of 2,2′-azinobis-(3-ethylbenzothiazoline-6-sulfonic acid) ($ABTS^{\cdot+}$) was produced by oxidation of 7 mM ABTS with potassium persulphate (2.45 mM final concentration) dissolved in H_2O. The mixture was placed in the dark at room temperature for 12–16 h before use, and the $ABTS^{\cdot+}$ solution was diluted with EtOH and equilibrated at 30 °C to an absorbance of 0.70 ± 0.02 at 734 nm. Aliquots of 25 μL extract or Trolox standard was mixed with 1 ml of diluted $ABTS^{\cdot+}$ solution, vortexed for 10 s, and the absorbance measured at 734 nm after 4 min at 30 °C. Values were obtained by interpolating the absorbance on a calibration curve using Trolox (0.03–0.50 mM) and were expressed as μmol of Trolox equivalent per g of dry weight. All samples were analyzed in triplicate.

4.4. Quantitative polymerase chain reaction (qPCR)

RNA extraction and qPCR reactions were performed as described by Quadrana et al. (2013). Annotated gene function and primer sequences are described in Table S3. All reactions were performed using two technical replicates and at least three biological replicates. mRNA levels were quantified using a 7500 Real-Time PCR system (Applied Biosystems) and SYBR Green Master Mix (Applied Biosystems). Data were analyzed using the LinRegPCR software package (Ruijter et al., 2009) to obtain Ct values and to calculate primer efficiency. Expression values were normalized to the mean of two constitutively expressed genes, *CAC* and *EXPRESSED* (Quadrana et al., 2013). A permutation test lacking sample distribution assumptions (Pfaffl et al., 2002) was applied to detect statistical differences ($p < 0.05$) in expression levels between mutants and the control using the algorithms in the fgStatistics software package (Di Rienzo, 2009).

4.5. Data analysis and statistics

Data obtained from tocopherol, pigment and antioxidant capacity measurements were analyzed using the InfoStat software package (Di Rienzo et al., 2011). When a data set showed homoscedasticity, an ANOVA test followed by a Tukey test ($p < 0.05$) was used to compare genotypes and fruit developmental stages. In the absence of homoscedasticity, a non-parametric ANOVA test was performed by applying the Kruskal–Wallis test ($p < 0.05$). All values represent the mean of at least four biological replicates.

PCA analyses were performed using the InfoStat software package and heatmaps were produced using GENE-E (http://www.broadinstitute.org/cancer/software/GENE-E/). Network construction and analyses was performed with expression and metabolite data using the WGCNA R software package (Zhang and Horvath, 2005). A signed network with threshold power (b) = 6 was produced according to Zhang and Horvath (2005) and Horvath (personal communication). The network was constructed with genes and metabolites presenting node connectivities $\geqslant 0.65$ by using an edge-weighted force-directed layout incorporated in the Cytoscape software package (Shannon et al., 2003).

Acknowledgements

JA and BSL were recipients of a FAPESP fellowship. MR and LEPP were funded by a fellowship from CNPq. This work was partially supported by grants from FAPESP (Brazil), CNPq (Brazil) and USP (Brazil). The authors wish to thank Dr. Gregg A. Howe (Michigan State University) for supplying the *jai* mutant in the MT background and Dr. Roger Chetelat (Tomato Genetics Resource Center, Davis, USA) who provided the *l*, *nor*, *rin* and *gf* mutants in different backgrounds. We thank PlantScribe (www.plantscribe.com) for carefully editing this manuscript.

Appendix A. Supplementary data

Supplementary data associated with this article can be found, in the online version, at http://dx.doi.org/10.1016/j.phytochem.2014.11.007.

References

Akhtar, M.S., Goldschmidt, E.E., John, I., Rodoni, S., Matile, P., Grierson, D., 1999. Altered patterns of senescence and ripening in gf, a stay-green mutant of tomato (*Lycopersicon esculentum* Mill.). J. Exp. Bot. 50, 1115–1122.

Almeida, J., Quadrana, L., Asís, R., Setta, N., De Godoy, F., Bermúdez, L., Otaiza, S.N., Corrêa da Silva, J.V., Fernie, A.R., Carrari, F., Rossi, M., 2011. Genetic dissection of vitamin E biosynthesis in tomato. J. Exp. Bot. 62, 3781–3798.

Barry, C.S., Aldridge, G.M., Herzog, G., Ma, Q., McQuinn, R.P., Hirschberg, J., Giovannoni, J.J., 2012. Altered chloroplast development and delayed fruit ripening caused by mutations in a zinc metalloprotease at the *lutescent2* locus of tomato. Plant Physiol. 159, 1086–1098.

Barry, C.S., McQuinn, R.P., Chung, M.Y., Besuden, A., Giovannoni, J.J., 2008. Amino acid substitutions in homologs of the STAY-GREEN protein are responsible for the *green-flesh* and *chlorophyll retainer* mutations of tomato and pepper. Plant Physiol. 147, 179–187.

Bishop, G.J., Nomura, T., Yokota, T., Harrison, K., Noguchi, T., Fujioka, S., Takatsuto, S., Jones, J.D.G., Kamiya, Y., 1999. The tomato DWARF enzyme catalyses C-6 oxidation in brassinosteroid biosynthesis. Proc. Natl. Acad. Sci. U.S.A. 96, 1761–1766.

Bramley, P.M., 2002. Regulation of carotenoid formation during tomato fruit ripening and development. J. Exp. Bot. 53, 2107–2113.

Brigelius-Flohé, R., Kelly, F.J., Salonen, J.T., Neuzil, J., Zingg, J.M., Azzi, A., 2002. The European perspective on vitamin E: current knowledge and future research. Am. J. Clin. Nutr. 76, 703–716.

Brouwer, B., Gardestrom, P., Keech, O., 2014. In response to partial plant shading, the lack of phytochrome A does not directly induce leaf senescence but alters the fine-tuning of chlorophyll biosynthesis. J. Exp. Bot.. http://dx.doi.org/10.1093/jxb/eru060.

Campos, M.L., Almeida, M., Rossi, M.L., Martinelli, A.P., Junior, C.G.L., Figueira, A., Rampelotti-Ferreira, F.T., Vendramim, J.T., Benedito, V.A., Peres, L.E.P., 2009. Brassinosteroids interact negatively with jasmonates in the formation of anti-herbivory traits in tomato. J. Exp. Bot. 60, 4347–4361.

Caño-Delgado, A., Penfield, S., Smith, C., Catley, M., Bevam, M., 2003. Reduced cellulose synthesis invokes lignification and defense responses in *Arabidopsis thaliana*. Plant J. 34, 351–362.

Casals, J., Pascual, L., Canizares, J., Cebolla-Cornejo, J., Casanas, F., Nuez, F., 2012. Genetic basis of long shelf life and variability into Penjar tomato. Genet. Resour. Crop Evol. 59, 219–229.

Cazzonelli, C.I., Pogson, B.J., 2011. Source to sink: regulation of carotenoid biosynthesis in plants. Trends Plant Sci. 15, 266–274.

Cheung, A.Y., McNellis, T., Piekos, B., 1993. Maintenance of chloroplast components during chromoplast differentiation in the tomato mutant *green flesh*. Plant Physiol. 101, 1223–1229.

Dall'Osto, L., Lico, C., Alric, J., Giuliano, G., Havaux, M., Bassi, R., 2006. Lutein is needed for efficient chlorophyll triplet quenching in the major LHCII antenna complex of higher plants and effective photoprotection in vivo under strong light. BMC Plant Biol. 6, 32.

DellaPenna, D., Pogson, B.J., 2006. Vitamin synthesis in plants: tocopherols and carotenoids. Annu. Rev. Plant Biol. 57, 711–738.

Di Rienzo, J.A., Casanoves, F., Balzarini, M.G., Gonzalez, L., Tablada, M., Robledo, C.W., 2011. InfoStat Versión 2011. FCA, Universidad Nacional de Córdoba, Argentina, <http://www.infostat.com.ar/>.

Di Rienzo, J.A., 2009. Statistical Software for the Analysis of Experiments of Functional Genomics. RDNDA, Argentina, <http://sites.google.com/site/fgStatistics/>.

Egea, I., Bian, W., Barsan, C., Jauneau, A., Pech, J.C., Latché, A., Li, Z.G., Chervin, C., 2011. Chloroplast to chromoplast transit ion in tomato fruit: spectral confocal microscopy analyses of carotenoids and chlorophylls in isolated plastids and time-lapse recording on intact live tissue. Ann. Bot. (Lond.) 108, 291–297.

Ellen, F.J., Moser, J.K., Kenar, J.A., Taylor, S.L., 2010. Extraction and analysis of tomato seed oil. J. Am. Oil Chem. Soc. 87, 755–762.

Fan, X., Mattheis, J.P., Fellman, J.K., 1998. A role for jasmonates in climacteric fruit ripening. Planta 204, 444–449.

Fantini, E., Falcone, G., Frusciante, S., Giliberto, L., Giuliano, G., 2013. Dissection of tomato lycopene biosynthesis through virus-induced gene silencing. Plant Physiol. 163, 986–998.

Fraser, P.D., Enfissi, E.M., Halket, J.M., Truesdale, M.R., Yu, D., Gerrish, C., Bramley, P.M., 2007. Manipulation of phytoene levels in tomato fruit: effects on isoprenoids, plastids, and intermediary metabolism. Plant Cell 19, 3194–3211.

Fujisawa, M., Nakano, T., Ito, Y., 2011. Identification of potential target genes for the tomato fruit-ripening regulator *RIN* by chromatin immunoprecipitation. BMC Plant Biol. 11, 26.

Fujisawa, M., Nakano, T., Shima, Y., Ito, Y., 2013. A large-scale identification of direct targets of the tomato MADS box transcription factor *RIPENING INHIBITOR* reveals the regulation of fruit ripening. Plant Cell 25, 371–386.

Fujisawa, M., Shima, Y., Higuchi, N., Nakano, T., Koyama, Y., Kasumi, T., Ito, Y., 2012. Direct targets of the tomato-ripening regulator RIN identified by transcriptome and chromatin immunoprecipitation analyses. Planta 235, 1107–1122.

Gawlik-Dziki, U., 2012. Changes in the antioxidant activities of vegetables as a consequence of interactions between active compounds. J. Funct. Foods 4, 872–882.

Giovannoni, J., Noensie, E.N., Ruezinsky, D.M., Lu, X., Tracy, S.L., Ganal, M.W., Martin, G.B., Pillen, K., Alpert, K., Tanksley, S.D., 1995. Molecular genetic analysis of the ripening-inhibitor and non-ripening loci of tomato: a first step in genetic map-based cloning of fruit ripening genes. Mol. Gen. Genet. 248, 195–206.

Giovannoni, J.J., 2004. Genetic regulation of fruit development and ripening. Plant Cell 16, S170–180.

Hörtensteiner, S., 2009. Stay-green regulates chlorophyll and chlorophyll-binding protein degradation during senescence. Trends Plant Sci. 14, 155–162.

Hu, Z.L., Deng, L., Yan, B., Pan, Y., Luo, M., Chen, X.Q., Hu, T.Z., Chen, G.P., 2011. Silencing of the *LeSGR1* gene in tomato inhibits chlorophyll degradation and exhibits a stay-green phenotype. Biol. Plant. 55, 27–34.
Ischebeck, T., Zbierzak, A.M., Kanwischer, M., Dörmann, P., 2006. A salvage pathway for phytol metabolism in Arabidopsis. J. Biol. Chem. 281, 2470–2477.
Jen, J.J., 1974. Carotenoids of yellow and red lutescent tomatoes. J. Agric. Food Chem. 22, 908–910.
Kariola, T., Brader, G., Li, J., 2005. Chlorophyllase 1, a damage control enzyme, affects the balance between defense pathways in plants. Plant Cell 17, 282–294.
Kitagawa, M., Ito, H., Shiina, T., Nakamura, N., Inakuma, T., Kasumi, T., Ishiguro, Y., Yabe, K., Ito, Y., 2005. Characterization of tomato fruit ripening and analysis of gene expression in F1 hybrids of the ripening inhibitor (rin) mutant. Physiol. Planta 123, 331–338.
Krieger-Liszkay, A., Trebst, A., 2006. Tocopherol is the scavenger of singlet oxygen produced by the triplet states of chlorophyll in the PSII reaction centre. J. Exp. Bot. 57, 1677–1684.
Li, L., Zhao, Y., McCaig, B.C., Wingerd, B.A., Wang, J., Whalon, M.E., Pichersky, E., Howe, G.A., 2004. The tomato homolog of CORONATINE-INSENSITIVE1 is required for the maternal control of seed maturation, jasmonate-signaled defense responses, and glandular trichome development. Plant Cell 16, 126–143.
Li, Z., Peng, J., Wen, X., Guo, H., 2013. Ethylene-insensitive3 is a senescence-associated gene that accelerates age-dependent leaf senescence by directly repressing miR164 transcription in Arabidopsis. Plant Cell 25, 3311–3328.
Lim, P.O., Kim, H.J., Nam, H.G., 2007. Leaf senescence. Annu. Rev. Plant Biol. 58, 115–136.
Lira, B., de Setta, N., Rosado, D., Almeida, J., Freschi, L., Rossi, M., 2014. Plant degreening: evolution and expression of tomato (*Solanum lycopersicum*) dephytylation enzymes. Gene, <http://dx.doi.org/10.1016/j.gene.2014.05.051/>.
Lois, L.M., Rodríguez-Concepción, M., Gallego, F., Campos, N., Boronat, A., 2000. Carotenoid biosynthesis during tomato fruit development: regulatory role of 1-deoxy-D-xylulose 5-phosphate synthase. Plant J. 22, 503–513.
Lytovchenko, A., Eickmeier, I., Pons, C., Osorio, S., Szecowka, M., Lehmberg, K., Stephanie Arrivault, S., Takayuki, T., Pineda, B., Anton, M.T., Hedtke, B., Lu, Y., Fisahn, J., Bock, R., Stitt, M., Grimm, B., Granell, A., Fernie, A.F., 2011. Tomato fruit photosynthesis is seemingly unimportant in primary metabolism and ripening but plays considerable role in seed development. Plant Physiol. 157, 1650–1663.
Liu, L., Wei, J., Zhang, M., Zhang, L., Li, C., Wang, Q., 2012. Ethylene independent induction of lycopene biosynthesis in tomato fruits by jasmonates. J. Exp. Bot. 63, 5751–5761.
Luo, Z., Zhang, J., Li, J., Yang, C., Wang, T., Ouyang, B., Li, H., Giovannoni, J., Ye, Z., 2013. A STAY-GREEN protein SlSGR1 regulates lycopene and β-carotene accumulation by interacting directly with SlPSY1 during ripening processes in tomato. New Phytol. 198, 442–452.
Martel, C., Vrebalov, J., Tafelmeyer, P., Giovannoni, J., 2011. The tomato MADS-box transcription factor ripening inhibitor interacts with promoters involved in numerous ripening processes in a colorless nonripening-dependent manner. Plant Physiol. 157, 1568–1579.
Martí, E., Gisbert, C., Bishop, G.J., Dixon, M.S., Garcia-Martinez, J.L., 2006. Genetic and physiological characterization of tomato cv. Micro-Tom. J. Exp. Bot. 57, 2037–2047.
Martinis, J., Glauser, G., Valimareanu, S., Kessler, F., 2013. A chloroplast ABC1-like kinase regulates vitamin E metabolism in *Arabidopsis thaliana*. Plant Physiol. 162, 652–662.
Meissner, R., Jacobson, Y., Melamed, S., Levyatuv, S., Shalev, G., Ashri, A., Elkind, Y., Levy, A., 1997. A new model system for tomato genetics. Plant J. 12, 1465–1472.
Mueller, M.J., Berger, S., 2009. Reactive electrophilic oxylipins: pattern recognition and signalling. Phytochemistry 70, 1511–1521.
Niki, E., Traber, M.G., 2012. History of vitamin E. Ann. Nutr. Metab. 61, 207–212.
Nogueira, M., Mora, L., Enfissi, E.M.A., Bramley, P.M., Fraser, P.D., 2013. Subchromoplast sequestration of carotenoids affects regulatory mechanisms in tomato lines expressing different carotenoid gene combinations. Plant Cell 25, 4560–4579.
Osorio, S., Alba, R., Damasceno, C.M.B., Lopez-Casado, G., Lohse, M., Zanor, M.I., Tohge, T., Usadel, B., Rose, J.K.C., Fei, Z., Giovannoni, J.J., Fernie, A.R., 2011. Systems biology of tomato fruit development: combined transcript, protein, and metabolite analysis of tomato transcription factor (nor, rin) and ethylene receptor (nr) mutants reveals novel regulatory interactions. Plant Physiol. 157, 405–425.
Park, S.Y., Yu, J.W., Park, J.S., Li, J., Yoo, S.C., Lee, N.Y., Lee, S.K., Jeong, S.W., Seo, H.S., Koh, H.J., Jeon, J.S., Park, Y.I., Paek, N.C., 2007. The senescence-induced staygreen protein regulates chlorophyll degradation. Plant Cell 19, 1649–1664.
Perez-Fons, L., Wells, T., Corol, D.I., Ward, J.L., Gerrish, C., Beale, M.H., Seymour, G.B., Bramley, P.M., Fraser, P.D., 2014. A genome-wide metabolomic resource for tomato fruit from *Solanum pennellii*. Sci. Rep. 4, 1–8.
Pfaffl, M.W., Horgan, G.W., Dempfle, L., 2002. Relative expression software tool (REST) for group-wise comparison and statistical analysis of relative expression results in real-time PCR. Nucleic Acids Res. 30, e36.
Quadrana, L., Almeida, J., Otaiza, S.N., Duffy, T., Corrêa da Silva, J.V., de Godoy, F., Asís, R., Bermúdez, L., Fernie, A.R., Carrari, F., Rossi, M., 2013. Transcriptional regulation of tocopherol biosynthesis in tomato. Plant Mol. Biol. 81, 309–325.
Quadrana, L., Almeida, J., Asís, R., Duffy, T., Dominguez, P.G., Bermúdez, L., Conti, G., da Silva, J.V.C., Colot, V., Asurmendi, S., Fernie, A.R., Rossi, M., Carrari, F., 2014. Natural occurring epialleles determine vitamin E accumulation in tomato fruits. Nat. Commun.. http://dx.doi.org/10.1038/ncomms5027.
Re, R., Pellegrini, N., Proteggente, A., Pannala, A., Yang, A., Rice-Evans, C., 1999. Antioxidant activity applying an improved ABTS radical cation decolorization assay. Free Radical Biol. Med. 26, 1231–1237.
Roca, M., Mínguez-Mosquera, M.I., 2001. Changes in chloroplast pigments of olive varieties during fruit ripening. J. Agric. Food Chem. 49, 832–839.
Ruijter, J.M., Ramakers, C., Hoogaars, W.M., Karlen, Y., Bakker, O., van den Hoff, M.J., Moorman, A.F.M., 2009. Amplification efficiency: linking baseline and bias in the analysis of quantitative PCR data. Nucleic Acids Res. 37, e45.
Sakuraba, Y., Schelbert, S., Park, S.Y., Han, S.H., Lee, B.D., Andrès, C.B., Kessler, F., Hörtensteiner, S., Paek, N.C., 2012. STAY-GREEN and chlorophyll catabolic enzymes interact at light-harvesting complex II for chlorophyll detoxification during leaf senescence in Arabidopsis. Plant Cell 24, 507–518.
Seltmann, M.A., Stingl, N.E., Lautenschlaeger, J.K., Krischke, M., Mueller, M.J., Berger, S., 2010. Differential impact of lipoxygenase2 and jasmonates on natural and stress-induced senescence in *Arabidopsis thaliana*. Plant Physiol. 152, 1940–1950.
Seybold, C., Fröhlich, K., Bitsch, R., Otto, K., Böhm, V., 2004. Changes in contents of carotenoids and vitamin E during tomato processing. J. Agric. Food Chem. 52, 7005–7010.
Seymour, G., Taylor, J., Tucker, G. (Eds.), 1993. Biochemistry of fruit ripening. Chapman and Hall, London, 442 pp.
Seymour, G.B., Chapman, N.H., Chew, B.L., Rose, J.K., 2013a. Regulation of ripening and opportunities for control in tomato and other fruits. Plant Biotech. J. 11, 269–278.
Seymour, G.B., Østergaard, L., Chapman, N.H., Knapp, S., Martin, C., 2013b. Fruit development and ripening. Annu. Rev. Plant Biol. 64, 219–241.
Shannon, P., Markiel, A., Ozier, O., Baliga, N.S., Wang, J.T., Ramage, D., Amin, N., Schwikowski, B., Ideker, T., 2003. Cytoscape: a software environment for integrated models of biomolecular interaction networks. Genome Res. 13, 2498–2504.
Takahashi, K., Takabayashi, A., Tanaka, A., Tanaka, R., 2014. Functional analysis of light-harvesting-like protein 3 (LIL3) and its light-harvesting chlorophyll-binding motif in Arabidopsis. J. Biol. Chem. 289, 987–999.
Takashima, M., Shichiri, M., Hagihara, Y., Yoshida, Y., Niki, E., 2012. Capacity of peroxyl radical scavenging and inhibition of lipid peroxidation by β-carotene, lycopene, and commercial tomato juice. Food Funct. 3, 1153–1160.
Tanaka, R., Rothbart, M., Oka, S., Takabayashi, A., Takahashi, K., Shibata, M., Myouga, F., Motohashi, R., Shinozaki, K., Grimm, B., Tanaka, A., 2010. LIL3, a light-harvesting-like protein, plays an essential role in chlorophyll and tocopherol biosynthesis. Proc. Natl. Acad. Sci. U.S.A. 107, 16721–16725.
The Tomato Genome Consortium, 2012. The tomato genome sequence provides insights into fleshy fruit evolution. Nature 485, 635–641.
Thomas, H., Ougham, H., 2014. The stay-green trait. J. Exp. Bot.. http://dx.doi.org/10.1093/jxb/eru037.
Trebst, A., 2003. Function of β-carotene and tocopherol in photosystem II. Z. Naturforsch. C. 58, 609–620.
Valentin, H.E., Lincoln, K., Moshiri, F., Jensen, P.K., Qi, Q., Venkatesh, T.V., Karunanandaa, B., Baszis, S.R., Norris, S.R., Savidge, B., Gruys, K.J., Last, R.L., 2006. The Arabidopsis vitamin E pathway gene5-1 mutant reveals a critical role for phytol kinase in seed tocopherol biosynthesis. Plant Cell 18, 212–224.
Vranová, E., Coman, D., Gruissem, W., 2012. Structure and dynamics of the isoprenoid pathway network. Mol. Plant 5, 318–333.
Vrebalov, J., Ruezinsky, D., Padmanabhan, V., White, R., Medrano, D., Drake, R., Schuch, W., Giovannoni, J.J., 2002. A MADS-box gene necessary for fruit ripening at the tomato ripening-inhibitor (*RIN*) locus. Science 296, 343–346.
Wasternack, C., Hause, B., 2013. Jasmonates: biosynthesis, perception, signal transduction and action in plant stress response, growth and development. An update to the 2007 review in Annals of Botany. Ann. Bot. 111, 1021–1058.
Wilkinson, J.Q., Lanahan, M.B., Yen, H.C., Giovannoni, J.J., Klee, H.J., 1995. An ethylene-inducible component of signal transduction encoded by never-ripe. Science 270, 1807–1809.
Zanfini, A., Corbini, G., Rosa, C.L., Dreassi, E., 2010. Antioxidant activity of tomato lipophilic extracts and interactions between carotenoids and α-tocopherols in synthetic mixtures. LWT Food Sci. Technol. 43, 67–72.
Zhang, B., Horvath, S., 2005. A general framework for weighted gene co-expression network analysis. Stat. Appl. Genet. Mol. Biol. 4 (Article17).
Zhang, W., Liu, T., Ren, G., Hörtensteiner, S., Zhou, Y., Cahoon, E.B., Zhang, C., 2014. Chlorophyll degradation: the tocopherol biosynthesis related phytol hydrolase in Arabidopsis seeds is still missing. Plant Physiol.. http://dx.doi.org/10.1104/pp.114.243709.
Zhu, Z., An, F., Feng, Y., Li, P., Xue, L., A, M., Jiang, Z., Kim, J.M., To, T.K., Li, W., Zhang, X., Yu, Q., Dong, Z., Chen, W.Q., Seki, M., Zhou, J.M., Guo, H., 2011. Derepression of ethylene-stabilized transcription factors (EIN3/EIL1) mediates jasmonate and ethylene signaling synergy in Arabidopsis. Proc. Natl. Acad. Sci. U.S.A. 108, 12539–12544.

CAPÍTULO V. CARACTERIZAÇÃO FUNCIONAL DO GENE *CLOROFILASE1* EM TOMATEIRO

1. Introdução

A clorofila (Chl), pigmento essencial para a fotossíntese, é uma das biomoléculas mais abundantes na Terra (Hörtensteiner, 2009). Sua complexa estrutura é composta por um macrociclo tetrapirrólico, contendo magnésio, ligado a uma cauda prenílica (Tanaka & Tanaka, 2007). Esta cadeia lateral lipofílica derivada dos isoprenóides, o fitil difosfato, permite não só a correta associação entre as proteínas e os pigmentos fotossintéticos formando complexos estáveis, mas também uma melhor coordenação das moléculas de clorofila nesses complexos; tal fato resulta na eficiente utilização da energia luminosa e diminui, assim, o estresse oxidativo (Keller *et al.*, 1998; Shpilyov *et al.*, 2013).

A síntese *de novo* do fitil difosfato para biogênese de clorofila ocorre pela via plastidial do metil-eritritol fosfato (MEP). No passo final da biossíntese, o precursor é então esterificado ao intermediário clorofilídeo produzido pela via do tetrapirrol, produzindo clorofila *a* (Kim et al; 2013). Em contraste, durante a degradação da clorofila, a remoção da cadeia lateral é um dos eventos iniciais.

A quebra da clorofila é um processo complexo, finamente regulado, com múltiplas etapas, que ocorre não apenas durante a senescência e o amadurecimento de frutos, mas também no estado estacionário (*steady-state*), durante o pós-colheita e em resposta a estresses bióticos e abióticos (Hörtensteiner, 2013). A sequência de eventos, ainda não completamente elucidada, envolve a ação de diversas enzimas do catabolismo de clorofila, uma substância quelante de metal (MCS) de identidade molecular desconhecida, além de mecanismos de transporte para transferir os produtos de degradação do cloroplasto ao vacúolo central (Balazadeh, 2014). Com relação à defitilação, até recentemente, a atividade era atribuída somente à enzima CLOROFILASE (CLH; Figura 1) (Takamyia *et al.*, 2000; Schelbert *et al.*, 2009). Entretanto, a caracterização funcional das proteínas de *Arabidopsis thaliana*, AtCLH1 e AtCLH2, demonstrou que nenhuma das isoformas é direcionada ao plastídeo, além destas não contribuírem para a perda de clorofila durante a senescência foliar evidenciado pelo fenótipo do duplo mutante, *chl1-chl2* (Schenk *et al.*, 2007; Hu *et al.*, 2015). CLH também não participa do complexo enzimático de degradação da clorofila recrutado pela proteína STAY-GREEN (SGR), do qual fazem parte todas as enzimas caracterizadas envolvidas na conversão da clorofila até o catabólito fluorescente primário (pFCC) (Sakuraba *et al.*, 2012). Em contraposição a esses achados, os estudos com *Citrus* ssp sugerem que CsCLH atua como enzima limitante no catabolismo de clorofila dentro do cloroplasto de flavedo, durante o desverdecimento induzido por etileno, e seu controle ocorre de maneira pós-traducional (Harpaz-Saad *et al.*, 2007; Azoulay Shemer

et al., 2008). Em brócolis (*Brassica oleracea*), BoCLH1 aparentemente contribui para a quebra da clorofila que ocorre durante o pós-colheita em inflorescências (Chen *et al.*, 2008).

A identificação de uma esterase plastidial, denominada FEOFITINASE (PPH; Schelbert *et al.*, 2009) que especificamente defitila feofitina, preencheu, em parte, a lacuna do conhecimento sobre esse processo ao menos durante a senescência foliar em *Arabidopsis* (Figura 1). Recentemente, foi também demonstrado que a PPH é responsável pela defitilação da Chl durante a senescência foliar em tomateiro (Guyer *et al.*, 2014). Muito embora, para o amadurecimento de frutos, a remoção da cadeia lateral ainda não foi esclarecida; os tomates deficientes em PPH apresentam um acúmulo transiente de feofitina, mas ao final são capazes de degradar o pigmento como frutos selvagens (Guyer *et al.*, 2014). Aprofundando-se nessa questão, Zhang *et al.* (2014) mostrou em sementes de *Arabidopsis* que nem as mutantes *pph* nem os triplos *pph,clh1,clh2* apresentam fenótipo de retenção de clorofila, diferentemente dos mutantes para SGR. Tais observações sugerem o envolvimento de outras hidrolases de fitol durante a perda de clorofila no amadurecimento de frutos e de sementes (Guyer *et al.*, 2014; Zhang *et al.*, 2014).

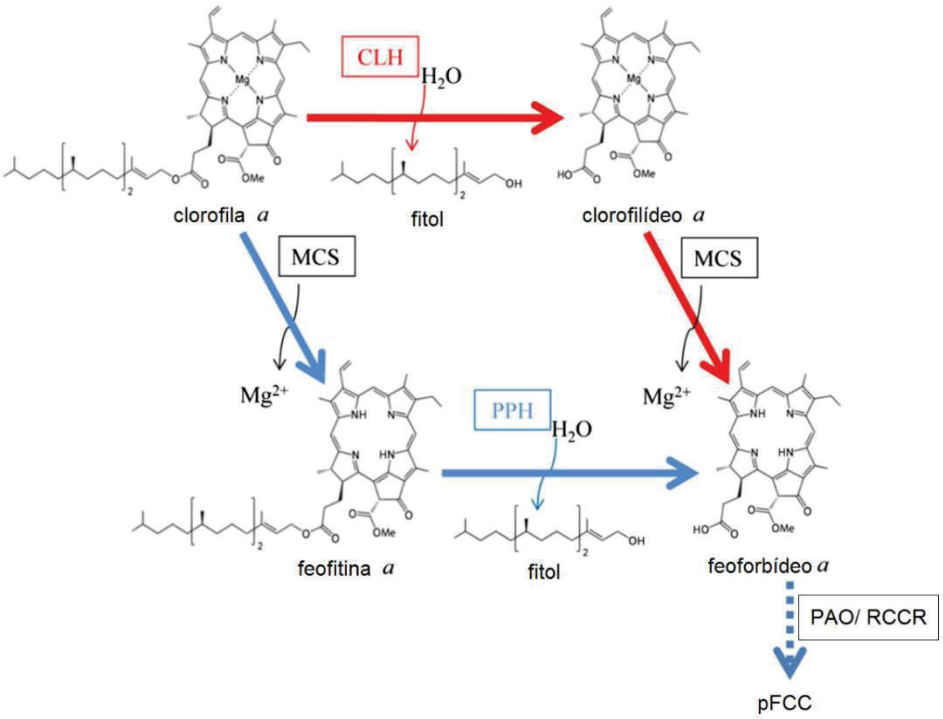

Figura 1: Etapas iniciais da via PAO (FEOFORBÍDEO *a* OXIGENASE) de degradação de clorofila. As setas em vermelho representam a sequência de reações envolvidas na defitilação a partir da CLH; as setas azuis representam aquelas relacionadas à PPH até a formação de pFCC. Este será transportado ao vacúolo onde ocorre a conversão para os produtos finais da degradação de clorofila. Adaptado de Hu *et al.* (2015). RCCR: redutase do catabólito da clorofila vermelho (*red chlorophyll catabolite*).

O fitil difosfato é também precursor prenílico obrigatório da síntese de tocoferol; este é direcionado para a rota central da vitamina E (VTE) via condensação com o homogentisato derivado da via do chiquimato (DellaPenna & Pogson, 2006). Alternativamente à síntese *de novo* a partir da redução do geranilgeranil difosfato pela enzima geranilgeranil difosfato reductase (GGDR), foi demonstrado que o fitil difosfato utilizado para a produção de tocoferóis também pode ser produzido a partir da ativação do fitol liberado durante degradação da clorofila (Valentin *et al.*, 2006; Ischebeck *et al.*, 2006). Essa via de reciclagem do fitol requer a atividade de duas quinases, das quais o *locus* codificante apenas para uma delas, fitol quinase (*VTE5*), foi clonado até o momento (Valentin *et al.*, 2006).

Dada a complexidade associada ao metabolismo do fitol advindo da degradação da clorofila, é razoável propor que as atividades das enzimas defitiladoras possam ser limitantes para a biossíntese do tocoferol. Os resultados anteriores obtidos neste trabalho (Capítulo I; Quadrana *et al.*, 2013) mostram que os níveis dos transcritos de *GGDR*, *VTE5* e *CLH* correlacionam com o conteúdo de tocoferol em folhas e frutos de tomateiro. Particularmente, o silenciamento de *CLH(1)* por VIGS não afetou o conteúdo nem de tocoferol nem de clorofila (Capítulo III). Sendo assim, um estudo funcional aprofundado se faz necessário em tomateiro para avaliar se a atividade defitiladora da CLH(1) estaria relacionada à degradação de clorofila e/ou à biossíntese de VTE o organismo vegetal como um todo.

2. Objetivos específicos

Com intuito de somar evidências sobre a função fisiológica de *CLH(1)* em *S. lycopersicum*, o presente trabalho propôs:

- Verificar a localização subcelular da proteína CLH(1).
- Caracterizar fenotipicamente tomateiros deficientes em CLH(1).

3. Material e métodos

3.1. Material vegetal

Para o estudo da localização subcelular, o alelo de *Solanum pennellii* de *CLH(1)* foi clonado a partir de cDNA proveniente da IL6-2. A agroinfiltração foi conduzida em *Nicotiana benthamiana* com aproximadamente quatro semanas de idade.

Para o silenciamento gênico por RNAi, plantas de *S. lycopersicum* (*cv*. Micro-Tom) foram utilizadas para transformação genética estável no laboratório de Controle Hormonal e Desenvolvimento Vegetal do prof. Lázaro Peres (ESALQ-USP). Os indivíduos das progênies segregantes T1 e T2 das linhagens transgênicas RNAi foram submetidos à seleção inicial com antibiótico através da aplicação por *spray* de canamicina (400 mg/L) em plântulas de 14 dias (após semeadura) durante três dias consecutivos (Pino *et al.*, 2010).

As plantas de Micro-Tom e tabaco foram crescidas em casa de vegetação em vasos plásticos (0.35 L) contendo terra vegetal e vermiculita expandida (1:1, v/v), suplementado com NPK 10:10:10 (8 g/L), Yoorin® (1 g/L) e dolomita ($MgCO_3$+$CaCO_3$; 4g/L), sob condições naturais de temperatura e iluminação.

Tecidos vegetais foram coletados entre o período de 12h às 14 h, congelados imediatamente em nitrogênio líquido e armazenados a -80 ºC. A primeira folha completamente expandida e tecido de pericarpo de frutos coletados a aproximadamente 35, 38, 40 e 43 dias após a antese, os quais correspondem aos estádios de verde-maduro (*mature green*, MG), 1 dia após pintando (*breaker*+1; B+1), 3 dias após pintando (*breaker*+3; B+3) e maduro foram utilizados para caracterização fenotípica das linhagens transgênicas. O material vegetal destinado à quantificação de açúcares totais, pigmentos e prenilipídeos foi liofilizado até a secagem completa antes da extração.

3.2. Cepas bacterianas e vetores

3.2.1. *Escherichia coli*

As linhagens de E. coli utilizadas para fins de clonagem foram *DH10B* e *DB3.1*. Os procedimentos de cultivo estão descritos no item 3.2.1 (Capítulo III).

3.2.2. *Agrobacterium tumefaciens*

A. tumefaciens cepa GV3101 foi utilizada para foi utilizada para o experimento de expressão transitória em células de tabaco. A cepa EHA105, que possui resistência cromossômica à rifampicina

(50 mg/L), foi utilizada para transformação estável de Micro-Tom. Os procedimentos de cultivo foram os mesmos descritos no item 3.2.2 (Capítulo III).

3.2.3. Plasmídeos

Os vetores utilizados para as diferentes clonagens estão listados na Tabela 1.

Tabela 1. Vetores utilizados para estudos funcionais

Vetores	Tipo	Resistência[1]	Características	Origem
pENTR/ D-TOPO	vetor de entrada *gateway*	canamicina (50 µg/mL)	Vetor linearizado com sítio de clonagem direcional para produtos de PCR de "ponta cega". Possui os sítios *attL1* e *attL2* para recombinação sítio-específica do clone de entrada com um vetor destino no sistema *Gateway*®.	Life Technologies
pK7FWG2	vetor de destino *gateway* para localização subcelular	espectinomicina (100 µg/mL) estreptomicina (300 µg/mL)	Possui um promotor *35s*; sítios *attR1* e *attR2*, para recombinação sítio-específica no sistema *Gateway*® para fusão da porção C-terminal da proteína de interesse a GFP; terminador *35s*; a seleção negativa é feita pelo gene ccdB.	Karimi *et al.* (2002)
pK7GWIWG2 (I)	vetor de destino *gateway* para RNAi	espectinomicina (100 µg/mL) estreptomicina (300 µg/mL)	Possui promotor CaMV 35s; possui duas cópias do ccdB flanqueadas pelos sítios *attR1* e *attR2* e separadas por uma sequência de intron que viabiliza a inserção do fragmento gênico na orientação senso e antisenso; terminador 35s. Essa configuração permite, após a transcrição, a formação de um RNA em forma de grampo. O gene *NPT*, marcador do T-DNA, confere resistência à canamicina (50 µg/mL) em plantas.	Karimi *et al.* (2002)

[1] Resistência em células procarióticas.

3.3. Extração de RNA total e síntese de cDNA

A extração de RNA total e síntese de cDNA foi realizada como descrito no item 3.3 (Capítulo III).

3.4. Obtenção da construção para estudo da localização subcelular da proteína SlCLH(1)

A amplificação do fragmento completo de cDNA, com exceção do códon de parada, foi feita por PCR utilizando a polimerase de DNA Taq Platinum *pfx* (Life Technologies). Foram utilizados 100 ng de cDNA, tampão 1X, 0.3 mM de cada dNTP, 300 nM de cada iniciador (Anexo III), 1 mM de Mg_2SO_4, e 2 U de enzima. As condições de amplificação empregadas foram: denaturação inicial de 94 ºC por 3 min; 35 ciclos de 94 ºC por 15 s, temperatura de anelamento por 30 s (Tabela 5), 68 ºC por 3 min para extensão; e uma extensão final a 68 ºC por 10 min. O fragmento amplificado com tamanho esperado foi purificado diretamente da reação de PCR com o kit *GFX® PCR DNA and Gel*

Band Purification (Amersham Biosciences) seguindo as instruções do fabricante. Uma vez purificado, o produto de PCR foi quantificado utilizando marcador de massa de concentração conhecida (High DNA Mass Ladder, Life Technologies) por meio de eletroforese em gel de agarose 0,8 %. Para clonagem no vetor de entrada, o produto purificado foi clonado no vetor de entrada pENTR/D-TOPO® (Life Technologies) nas seguintes condições: 50 ng do produto de PCR purificado, 1 µL de solução salina, 1 µL de vetor e água ultrapura até volume final de 6 µL. A reação foi mantida por 30 minutos à temperatura ambiente. A transformação das células competentes de *E. coli* DH10B, minipreparação plasmidial e confirmação do fragmento foram feitas segundo descrito no item 3.4.1 (Capítulo III). Posteriormente, o vetor de entrada foi recombinado com o vetor destino pK7FWG2 (Tabela 4), utilizando-se a enzima LR clonase II (Life Technologies), de modo que o fragmento completo do gene de interesse fosse fusionado *in frame* com a proteína GFP. A transformação das células competentes de *E. coli* DH10B e extração do DNA plasmidial, foi realizada conforme descrito no item 3.4.1 (Capítulo III). O clone obtido pK7FWG2*SpCLH(1)* foi analisado por restrição com endonuclease EcoRI e confirmado por sequenciamento, utilizando-se os iniciadores 35SRight e Egfp. Após confirmação da identidade, 1 µg de cada construção foi utilizado para transformar células competentes de *A. tumefaciens* GV3101 segundo descrito no item 3.4.4 (Capítulo III).

3.5. Transformação transiente de folhas de *Nicotiana benthamiana* por agroinfiltração

Uma colônia de *A. tumefaciens* GV3101 contendo o plasmídeo pK7FWG2*SpCLH(1)* foi transferida para um pré-inóculo de 3 mL de meio LB contendo antibióticos apropriados. O cultivo foi deixado sob agitação constante de 170 rpm, 28 ºC por 24 h. Posteriormente, 1 mL do pré-inóculo foi transferido para um inóculo de 50 mL de LB com os mesmos antibióticos; este foi incubado por cerca de 14 h até atingir OD_{600} entre 0,6 a 1,0. A cultura foi então submetida à centrifugação a 4500 rpm por 15 min a 4 °C. O precipitado de células foi ressuspendido em meio MES líquido com 150 µM de acetoseringona até atingir a OD_{600} entre 0,5 e 0,6. Uma seringa sem agulha foi utilizada para infiltrar 1 mL da suspensão na região abaxial das folhas de *N. benthamiana*. Para controle experimental de direcionamento subcelular, plantas de tabaco foram infiltradas com *A. tumefaciens* contendo vetor: (i) pBIN-35S-gfp (Quadrana *et al.*, 2011), que possui o gene Egfp fusionado a um peptídeo sinal para retículo endoplasmático sob o controle do promotor 35S; (ii) pK7FWG2-SlHPPD(2)Lyc, que possui o fragmento completo do cDNA do gene *HIDROXIFENILPIRUVATO DIOXIGENASE* de *S. lycopersicum* [SlHPPD(2)] fusionado ao GFP (de Godoy *et al.*, 2013), cuja localização é citossólica. Após 48 h, os fragmentos foliares foram examinados em microscópio laser confocal Zeiss LSM 400.

A excitação do GFP foi feita a 488 nm e a observação da emissão a 530 nm, enquanto a clorofila foi excitada a 543 nm e a emissão da sua fluorescência detectada acima de 590 nm.

3.6. Construção dos vetores para silenciamento gênico por RNAi

A amplificação dos fragmentos de cDNA foi feita por PCR, utilizando os iniciadores descritos no Anexo III e a polimerase de DNA Taq Platinum *pfx* (Life Technologies), seguida de purificação. O produto de PCR purificado foi então clonado no vetor de entrada pENTR/D-TOPO® (Life Technologies) segundo procedimento descrito acima no item 3.4. Posteriormente, o vetor de entrada foi recombinado com o vetor binário pK7GWIWG2 (Tabela 1), utilizando-se a enzima LR clonase II (Life Technologies). O clone obtido pK7GWIWG2*SlCLH(1)* foi analisado por restrição com endonuclease EcoRI e confirmado por sequenciamento, utilizando-se os iniciadores 35S-Right e 35S-Left (Anexo III). Após confirmação da identidade, 1 µg da construção foi utilizado para transformar células competentes de *A. tumefaciens* EHA105 segundo protocolo 3.4.4 (Capítulo III).

3.7. Transformação genética estável

A obtenção de linhagens transgênicas RNAi estáveis de *S. lycopersicum* (*cv*. Micro-Tom) foi feita via transformação genética com *A. tumefaciens* segundo o protocolo descrito por Pino *et al.* (2010). Para esterilização das sementes de Micro-Tom, utilizou-se solução 30% de hipoclorito comercial (2,7 % hipoclorito de sódio, v/v) com agitação por 15 min em vórtex. Em seguida, as sementes foram lavadas com água destilada estéril. As sementes esterilizadas foram inoculadas em meio MS (Murashige & Skoog) ½ X sólido e mantidas por 4 dias a 25 ºC no escuro. Após esse período, as plântulas foram transferidas para fotoperíodo de 16h (c.a. 45 µmol PAR m^{-2} s^{-1}) e foram mantidas por mais 4 dias. Explantes cotiledonares de plântulas de 8 dias (após a semeadura) foram isolados, retirando-se as extermidades. Os explantes foram dispostos em placa de Petri contendo Meio Indutor de Raiz com 100 µM de acetoseringona, com a face abaxial voltada para o meio. Na sequência, cerca de 200 µL da suspensão de *A. tumefaciens* contendo a construção de interesse foram aplicadas sobre cada explante e mantidos a temperatura ambiente por 10 min. Após esse período, retirou-se o excesso de suspensão com papel filtro estéril. As placas foram incubadas por 2 dias a 28ºC na ausência de luz. Em seguida, os explantes foram transferidos para Meio Indutor de Parte Aérea com 100 mg/L de kanamicina para seleção transformantes e 25 mg/L Meropenem para eliminação do crescimento de células de *A. tumefaciens*. Os explantes foram mantidos em 16h de fotoperíodo a 25ºC por três semanas. Após o crescimento da parte aérea, os brotos bem desenvolvidos foram excisados e transferidos para meio MS com 100 mg/L de kanamicina e 25 mg/L Meropenem

até o enraizamento. As plantas regeneradas com raízes foram então transferidas para casa de vegetação e aclimatadas.

Meio MS sólido para transformação - sais MS com vitaminas B5; 30 g/L sacarose e 6 g/L ágar - pH do meio ajustado para 5,8 antes de autoclavar com KOH.
Meio Indutor de Raiz (RIM) – sais MS; vitaminas B5; 30 g/L sacarose; 6 g/L ágar; 0.4 µM de ANA (ácido α-naftalenoacético, auxina).
Meio Indutor de Parte Aérea (SIM) - sais MS; vitaminas B5; 30 g/L sacarose; 6 g/L ágar; 5 µM de BAP (6-benzilaminopurina, citocinina).

3.8. Verificação da presença do transgene

A confirmação da presença do transgene nas plantas regenerantes foi feita por PCR a partir de DNA genômico de folha extraído com *DNeasy Plant Mini Kit* (Qiagen) conforme orientações do fabricante. Na reação de PCR, foram utilizados 50 ng de DNA como molde e 200 nM dos iniciadores 35S-Right e RNAiCLH(1)-R (Anexo III), seguindo as condições descritas no item 3.4.1 (Capítulo III). Os produtos de PCR, cujo tamanho esperado corresponde a 304 pb, foram então verficados em gel de agarose 1 %.

3.9. Análise de expressão gênica nas linhagens RNAi transgênicas

Após confirmação da presença do transgene, as linhagens transgênicas RNAi obtidas por eventos de transformação independente foram testadas quanto ao nível de silenciamento. A primeira folha totalmente expandida e frutos verde-maduros e maduro foram utilizados para confirmação do silenciamento por qPCR segundo os procedimentos descritos no item 3.2.2 (Capítulo II).

O perfil transcricional de genes envolvidos na via do MEP [*DXS(1); GGPS(2)* e *GGDR*], na via do chiquimato [*HPPD(1)* e *HPPD(2)*], metabolismo da clorofila [*CHLG, CLH(2), CLH(4), SGR1, PAO* e *PPH*], reciclagem do fitol (*VTE5*), rota central do tocoferol [*VTE1, VTE2, VTE3* e *VTE4*], carotenóides [*PSY*(1) e *PSY*(2)] e plastoquinonas (*SPS* e *HST*) foi avaliado em folhas, frutos verde-maduros e maduros das linhagens transgênicas. Para normalização do cálculo da expressão gênica, utilizou-se os genes *CAC* e *EXPRESSED*. Os iniciadores utilizados estão descritos no Anexo I.

3.10. Caracterização fenotípica das linhagens *SlCLH(1)*-RNAi transgênicas

3.10.1. Quantificação de prenilipídeos por cromatografia líquida de ultra eficiência acoplada à espectrometria de massas

O perfil de prenilipídeos de folha e fruto foi feito segundo Martinis *et al.* (2013) com alterações. Ressuspendeu-se 15 mg de tecido liofilizado em 0,5 mL de tetrahidrofurano:metanol:água (42,5:42,5:15, v/v). A mistura foi homogenizada usando *glass beads* (1 mm de diâmetro) durante três 3 min a 30 Hz em *tissue lyser* (Qiagen). Em seguida, foram realizadas duas etapas de centrifugação (3 min, 14,000 rpm a 4°C, cada). Os sobrenadantes foram transferidos para *vials* de HPLC e, na sequência, analisados por Cromatrografia Líquida de Ultra Eficiência Acoplada à Espectrometria de Massa com Ionização Química à Pressão Atmosférica e Analisador Quadrupolo em Tempo de Voo (UHPLC-APCI-QTOF MS). Os prenilipídeos foram separados em coluna Acquity BEH C18 (50 × 2,1 mm; 1,7 μm) sob as seguintes condições: Solvente A = água; Solvente B = metanol; 80-100% B por 3 min, 100% B em 2 min, reequilibração a 90% B por 0,5 min. O fluxo foi de 800 μL/min e o volume de injeção corresponde a 2,5 μL. α-tocoferol, γ-tocoferol, δ-tocoferol, PQ-9 e PC-8 foram quantificados baseados em curvas de calibração construídas a partir de padrões.

3.10.2. Clorofila e carotenóides

Clorofila e catabólitos verdes foram extraídos de 10 mg de tecido liofilizado durante 17 h a -20ºC em acetona com 10% (v/v) 0.2 M Tris-HCl, pH 8.0, resfriada a –20 °C na proporção de 5 mL por grama de massa fresca inicial. Após duas centrifugações (2 min, 16000*g* a 4°C cada), os sobrenadantes foram analisados por HPLC segundo Langmeier *et al.*, (1993). A cromatografia foi desenvolvida em coluna de fase reversa (ODS C18 Hypersil 5μM) com sistema de solventes: A = 1M de acetato de amônio:metanol 1:4 (v/v); B = acetona/metanol 1:4 (v/v). O programa inicia com um gradiente linear de A para B por 15 min, seguido de fluxo isocrático de B por 10 min e retorno ao solvente A por 2 min. Clorofila *a*, clorofila *b*, feofitina *a* foram identificados pelo espectro de absorção a 665 nm. A quantificação dos compostos foi feita com curvas de calibração construídas da partir de padrões externos (Schelbert *et al.*, 2009).

Para quantificação dos carotenóides, foi realizada a mesma extração orgânica descrita no item 3.6.1 (Capítulo III). Uma alíquota de 400 μL do extrato orgânico foi seca sob nitrogênio gasoso e o resíduo ressuspendido em 150 μL de metanol:acetato de etila (50:50, v/v). A cromatografia foi realizada em HPLC (Agilent 1200 Series) acoplado a Detector de Arranjo de Diodos utilizando uma coluna de fase reversa [Zorbax Eclipse Plus C18 (150 mm × 4,6 mm, 5 μm), Agilent Technologies] em temperatura ambiente com fluxo de 0.6 mL/min. A eluição foi feita com gradiente linear de A =

acetonitrila:metanol:Tris buffer 0.1M pH 8 [72:8:3, v/v/v) para o solvente B= metanol:acetato de etila 68:32 (v/v) por 25 min, seguidos de 10 min em solvente B. Para reequilíbrio da coluna, a fase móvel retornou para solvente A e foi mantida durante 5 min. Os carotenóides foram identificados a 440 nm de acordo com (i) a ordem de eluição, (ii) o espectro de absorção (Gupta *et al.*, 2015) e (iii) a comigração com padrões autênticos disponíveis (all-trans-licopeno, all-trans-β-caroteno, luteína, violaxantina, neoxantina, zeaxantina).

3.10.3. Quantificação de açúcares solúveis e amido

A quantificação de açúcares solúveis foi feita de acordo com De Souza *et al.* (2013). Dez miligramas de tecido liofilizado de folha e fruto foram submetidos à extração com 1,5 mL de etanol 80 % a 80 ºC por 20 min. Em seguida, centrifugou-se a mistura por 5 min a 14000 rpm e o coletou-se o sobrenadante. O pellet foi então submetido a quatro extrações subsequentes com etanol 80 %. O volume total de sobrenadantes (7,5 mL) foi seco sob vácuo e ressuspenso em 1 mL de água ultrapura. Para remover os pigmentos, foi feita uma extração com 0.5 mL de clorofórmio. A identificação e quantificação dos açúcares solúveis foi realizada por Cromatografia de Troca Iônica de Alta Eficiência (HPAEC/PAD), utilizando uma coluna CarboPac PA1 eluída em fluxo isocrático de 150 mM NaOH de 1 mL/min. Glicose, frutose e sacarose foram quantificados com base em curva de padrão externo construída a partir de soluções com padrões de alta pureza entre 50 a 200 µM.

A quantificação de amido foi realizada segundo o protocolo descrito por Amaral *et al.* (2007). O precipitado resultante da sequência de extrações com etanol 80 % secou durante 16h em estufa a 60ºC. O precipitado seco foi incubado com 0,5 mL de enzima α-amilase de *Bacillus licheniformis* (120 U/mL, MEGAZYME) e mistura mantida a 75 ºC durante 30 min. Após esse período, repetiu-se o procedimento uma vez mais. A mistura foi então resfriada até 50 ºC e, na sequência, foram adicionados 0,5 mL da enzima amiloglucosidase de *Aspergillus niger* (30 U/mL, MEGAZYME) e a preparação mantida a 50 ºC por 30 min. O procedimento foi repetido uma vez mais, totalizando volume final de 2 mL por amostra. A reação foi interrompida com 100 µL de ácido perclórico 0,8 M. Após centrifugação a 10000 x *g* por 2 min, alíquotas de 20 µL para folha e 50 µL para frutos foram incubadas com glicose oxidase/peroxidase e D-4-aminoantipirina (GOD/POD) (Labtest®, Brasil) a 30ºC por 15 min em microplaca de ELISA. A absorbância do produto da reação quinoneimina, o qual é diretamente proporcional a concentração de glicose, foi detectada a 490 nm via espectrofotômetro. A concentração de amido em µg de glicose equivalente foi determinada a partir de curva padrão externo, utilizando solução do padrão glicose (Sigma) entre 2.5 a 12.5 µg/mL.

3.10.4. Parâmetros de fluorescência e trocas gasosas

A avaliação de trocas gasosas e fluorescência da clorofila foram realizadas em plantas T2 de 5 semanas de idade utilizando o sistema portátil Licor-6400 (LI-COR 6400XT; LI-COR), que consiste em um sistema aberto para trocas gasosas contendo um analisador de gases por infravermelho (IRGA) e uma câmara fluorimétrica acoplada (Modelo 6400–40, Li-Cor). As medidas foram realizadas no folíolo terminal da primeira folha totalmente expandida de plantas em estado vegetativo, no período das 10 h às 14 h. A referência de CO_2 de 400 ppm e temperatura foliar de 25 °C foram mantidas ao longo do experimento. A umidade relativa foi controlada externamente (40-60 %). Foram realizadas curvas de resposta da taxa de assimilação de carbono (*A*) à luz, variando o fluxo de fótons fotossinteticamente ativos (FFFA) de 600, 400, 200, 100, 75, 50, 25 a 0 em cinco plantas por tratamento. A condutância estomática foliar (g_s), respiração no escuro (*Rd*) e parâmetros de fluorescência foram avaliados sob FFFA de 600 µmol m^{-2} s^{-1}. Os parâmetros de fluorescência foram calculados de acordo com Genty *et al.* (1989), conforme descrito a seguir. A máxima eficiência quântica fotoquímica sob luz (Fv'/Fm') foi determinada pela equação (I):

$$Fv'/Fm' = (Fm'-Fo')/Fm'$$

Onde: Fm' é a fluorescência máxima da folha adaptada à luz e Fo' é a fluorescência mínima da folha adaptada à luz. A estimativa da eficiência quântica fotoquímica operante no fotossistema II (Φ_{PSII}), foi calculada pela seguinte equação:

$$\Phi_{PSII} = (Fm' - Fs)/Fm'$$

Onde: Fs é a fluorescência da clorofila produzida em estado estacionário.

A razão que estima a fração de eficiência máxima utilizada pelo fotossistema II, *quenching* fotoquímico (qP) é calculada pela equação:

$$qP = (Fm'-Fs)/(Fm'-Fo')$$

O cálculo da taxa de transporte de elétrons (J_{PSII}) foi feito segundo a equação:

$$J_{PSII} = [(Fm'-F')/Fm']*FFFA*\alpha_{leaf}*f$$

Onde: a diferença entre os valores de Fm' e F' imediatamente após a aplicação do pulso de luz saturante; α_{leaf}, a absorbância da folha (a qual se assume 0.85), e *f* é a fração de elétrons utilizados pelo fotossistema II, o qual se assume ser 0,5 para plantas do tipo C3.

4. Resultados

4.1. Verificação da localização subcelular

Com intuito de melhor entender a função biológica de CLH(1), primeiramente, analisou-se a localização subcelular da proteína. A proteína de fusão CLH(1)-GFP foi expressa transientemente sob o controle do promotor 35S do vírus do mosaico da couve-flor (CaMV) em células do mesofilo foliar de tabaco. As análises das imagens de microscopia confocal mostram que CLH(1) acumula-se fora dos cloroplastos da célula, porém seu padrão da distribuição não acompanha exatamente o correspondente para proteínas citossólicas, como por exemplo a HPPD(2). O acúmulo da proteína de fusão indica localização vesicular com aspecto semelhante ao apresentado pelo controle de retículo endoplasmático (Figura 2). Esses resultados estão de acordo com os obtidos recentemente em protoplastos de *Arabidopsis* (Schenk *et al.*, 2007; Hu *et al.*, 2015).

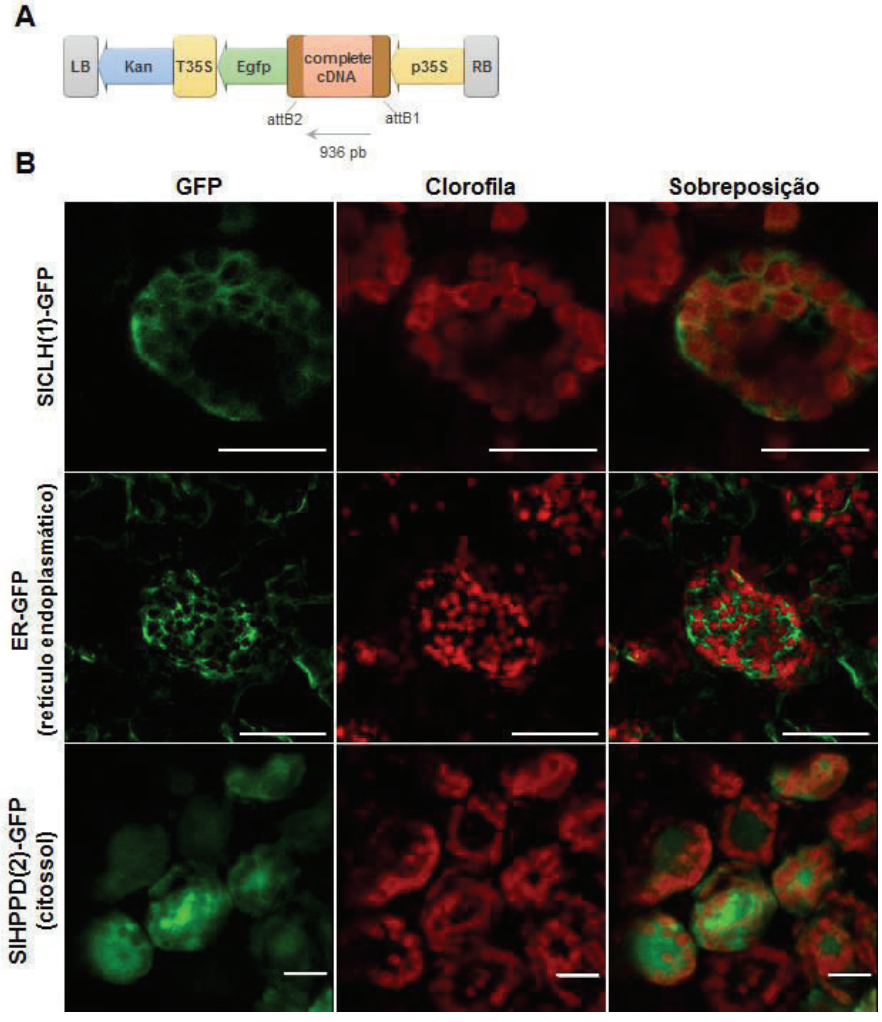

Figura 2: Localização subcelular CLH(1) de *S. lycopersicum*. (A) Esquema da construção pK7FWG2*SpCLH(1)*. LB: borda esquerda; Kan: gene de resistência a canamicina; T*35S:* terminador *35S* do CaMV; Egfp: *green fluorescent protein*; complete cDNA: sequência do gene CLH(1); *p35S*: promotor *35S* do CaMV; RB: borda direita. (B) Direcionamento da proteína SlCLH(1)-GFP para retículo endoplasmático de células de mesófilo foliar de *N. benthamiana.* ER-GFP: controle GFP com peptídeo sinal de direcionamento para retículo endoplasmático. SlHPPD(2)-GFP: proteína de fusão de localização citossólica utilizada como referência. As imagens de microscopia confocal mostram a fluorescência detectada de GFP, a auto-fluorescência da clorofila (clorofila) e a sobreposição das imagens anteriores. Barra = 20 µm.

4.2. Obtenção de linhagens transgênicas estáveis silenciadas para *CLH(1)*

Para investigar o envolvimento de CLH(1) na etapa inicial da degradação de clorofila e sua possível relação com a produção da cadeia lateral para VTE, foram geradas plantas transgênicas estáveis de *S. lycopersicum* (*cv*. Micro-Tom) silenciadas para *CLH(1)* por RNA de interferência [*SlCLH(1)*-RNAi]. Para tanto, foi obtida a construção pK7GWIWG2*SlCLH(1)* contendo um fragmento de 168 pb, sentido senso e antissenso, localizado no primeiro éxon do gene (Figura 3A). A especificidade do silenciamento para o gene de interesse foi avaliada por meio de buscas baseada em BLAST no banco dados da *Solanaceae Genomics Network* (http://solgenomics.net/). Após a transformação genética por *A. tumefaciens*, foram obtidas 10 linhagens independentes aclimatadas em casa de vegetação (Figura 3B). A verificação do silenciamento nos transformantes foi feita por qPCR (Figura 3C). Após desenvolver frutos maduros, sementes das plantas silenciadas #8, #12 e #14 foram coletadas para análises fenotípicas da geração T1.

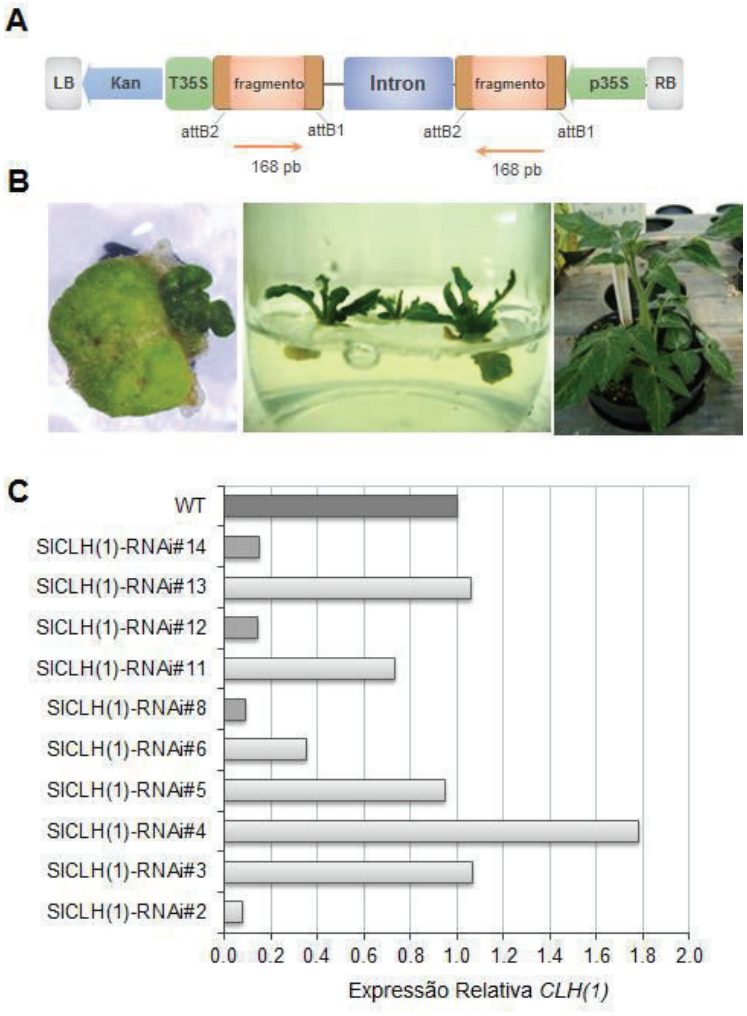

Figura 3: Obtenção de linhagens transgênicas *SlCLH(1)*-RNAi. (A) Esquema da construção pK7GWIWG2*SlCLH(1)* utilizada para obtenção das plantas transgênicas de *S. lycopersicum* (*cv*. Micro-Tom). LB: borda esquerda; Kan: gene de resistência a canamicina; T35S: terminador 35S do CaMV; 168 pb: fragmento da sequência codificante do gene *CLH(1)*; P35S: promotor 35S do CaMV; RB: borda direita; attB: sítios de recombinação no vetor de expressão. (B) Aspecto da regeneração *in vitro* dos explantes cotiledonares. Explantes foram pré-incubados com *Agrobacterium* contendo o vetor pK7GWIWG2*SlCLH(1)*. Após a regeneração em presença de canamicina, ápices caulinares bem desenvolvidos foram transferidos para meio MS com canamicina para enraizamento. Em seguida, as plantas T0 foram aclimatadas em casa de vegetação (da esquerda para direita). (C) Níveis de mRNA de *CLH1* em folhas de plantas transgênicas T0. As barras representam a média de três replicatas técnicas. Os valores de expressão foram normalizados com *EXPRESSED* e apresentados como abundância relativa de transcritos comparados ao controle (WT). Barras cinza escuro indicam as linhagens selecionadas para análise em T1.

4.3. Caracterização fenotípica de plantas de tomateiro silenciadas para *CLH(1)*

A seleção de plântulas transgênicas T1 pela pulverização com canamicina resultou em indivíduos resistentes *SlCLH(1)*-RNAi, os quais apresentaram folhas verdes após o tratamento com agente seletor. Dentre as linhagens avaliadas, apenas a progênie T1 de *SlCLH(1)*-RNAi#12 (seis plantas) se apresentou uniformemente resistente à canamicina. A falta de segregação do transgene pode ser indicativa da presença de mais de uma cópia, embora o número de plantas avaliadas tenha sido muito reduzido. Nas plantas resistentes à canamicina, a presença do transgene foi confirmada pela amplificação da sequência de T-DNA a partir do DNA genômico (Figura 4A). Em seguida, o nível de silenciamento foi verificado em folhas fonte, frutos verde-maduros e maduros qPCR. As três linhagens selecionadas apresentaram apenas 20 % da expressão de *CLH(1)* em relação às plantas selvagens Micro-Tom (*wild-type*, WT) (Figura 4B).

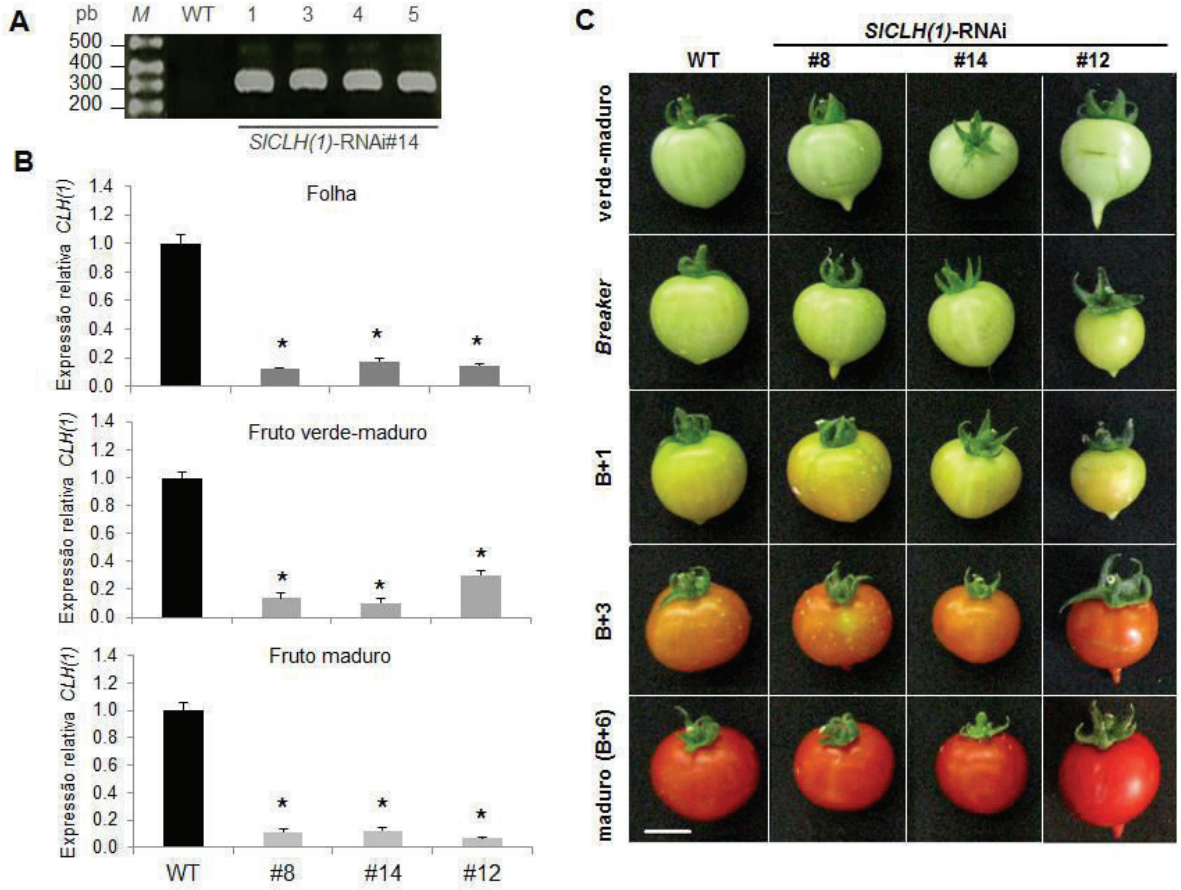

Figura 4: Silenciamento de *CLH(1)* nas linhagens transgênicas e fenótipo dos frutos durante o amadurecimento. (A) Análise por eletroforese para confirmação da presença do transgene em plantas da progênie T1. Exemplo dos produtos de amplificação obtidos a partir do DNA gênomico cujo tamanho correspondem a 304 pares de bases (pb). *M*: marcador de tamanho molecular (*1kb Plus DNA ladder – Life Technologies*). (B) Expressão relativa *CLH(1)* em folhas, frutos verde-maduros e maduros. Os gráficos indicam a média da expressão relativa das réplicas biológicas (n = 5) ± erro padrão. Asteriscos apontam as diferenças estatisticamente significativas (Teste de permutação, $P < 0,05$). (C) Fenótipo de fruto no estádio de verde-maduro, de *breaker*, 1 dia após *breaker* (B+1), 3 dias após *breaker* (B+1) e maduro (corresponde a 6 dias após o *breaker,* B+6). Barra = 1 cm.

Plantas de *SlCLH(1)*-RNAi#8 e *SlCLH(1)*-RNAi#14 não apresentaram nenhuma alteração fenotípica evidente comparadas às plantas selvagens, incluindo o processo de amadurecimento dos frutos (Figura 4C). No entanto, na linhagem #12, foi possível observar mudanças fenotípicas associadas (i) à lâmina foliar, maiores e mais verdes em relação às selvagens, promovendo um aumento na porção vegetativa; (ii) à redução no número de inflorescências e consequentemente no número de frutos; (iii) ao desenvolvimento do fruto, promovendo atraso na formação e posterior amadurecimento, além de redução massiva na quantidade de sementes. O aparecimento de plantas com fenótipo anormal é um fenômeno frequentemente observado em plantas transgênicas. Tais anormalidades são predominantemente atribuídas à ocorrência de variação somaclonal (por exemplo, poliploidização) na fase de regeneração dos transformantes durante a cultura de tecidos (Davidson *et al.*, 2002; Sigareva *et al.*, 2004) ou a eventuais mutações consequência da inserção do transgene. Embora o fenótipo de *SlCLH(1)*-RNAi#12 possa sobretudo ser consequência da variação somaclonal, esta linhagem ainda sim foi considerada para caracterização fenotípica das plantas silenciadas.

4.3.1. Quantificação de clorofila e catabólitos verdes

Para avaliar se o silenciamento de *CLH(1)* promove alteração na via degradação de clorofila em tomateiro, o conteúdo de clorofila e de seus catabólitos verdes (clorofilide, feofitina *a* e feoforbide) foi determinado por HPLC em folhas e em frutos em diferentes estádios no amadurecimento (verde-maduro, *breaker*+1 e *breaker*+3) (Figura 5). Convém mencionar que as folhas maduras das plantas transgênicas da linhagem #8 e #14 não apresentaram visualmente diferenças na coloração, além do processo de senescência ocorrer aparentemente sem diferenças nas plantas transgênicas comparado às selvagens. Em relação aos catabólitos verdes, o perfil de HPLC mostrou que feofitina *a* (Phein *a*) foi o único composto detectado nas análises realizadas. Esta observação está de acordo com os dados previamente reportados para tomateiro (Guyer *et al.*, 2014). Não houve diferenças significativas nos conteúdos de clorofila *a*, clorofila *b* e Phein *a* entre transgênicas e controle em ambos os órgãos avaliados. A exceção foram os frutos da linhagem #12, cujo acúmulo de clorofila e os níveis reduzidos de Phein *a* confirmam o atraso no desenvolvimento do fruto previamente mencionado. Estes resultados sugerem que o silenciamento de *CLH(1)* não altera significativamente o acúmulo de clorofila e Phein *a* em tomateiro.

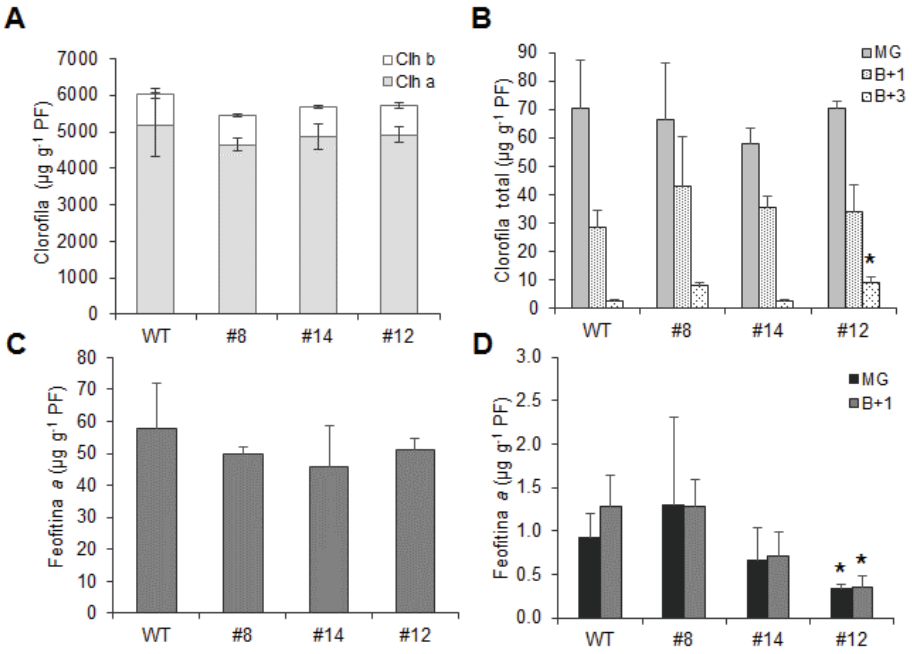

Figura 5: Conteúdo de clorofila e feofitina *a* nas linhagens transgênicas silenciadas para *CLH(1)*. Quantificação de clorofila e feofitina *a* em folhas (A, C) e frutos (B, D) no estádio de verde-maduro (MG), 1 dia após *breaker* (B+1) e 3 dias após *breaker* (B+3). Os valores correspondem a média (n = 5) de cada genótipo. As barras correspondem ao desvio padrão. Diferenças estatísticas significativas estão indicadas com asteriscos (ANOVA/ teste de Dunnett, $P < 0,05$) em comparação ao controle (WT). PF, peso fresco.

4.3.2. Conteúdo de tocoferol

Para examinar a possibilidade de CLH(1) fornecer fitol para a síntese de tocoferol, o conteúdo de VTE foi determinado por HPLC. Os resultados mostram que o silenciamento de *SlCLH*(1) não afeta a quantidade de tocoferol nem em folhas nem em frutos (Figura 6).

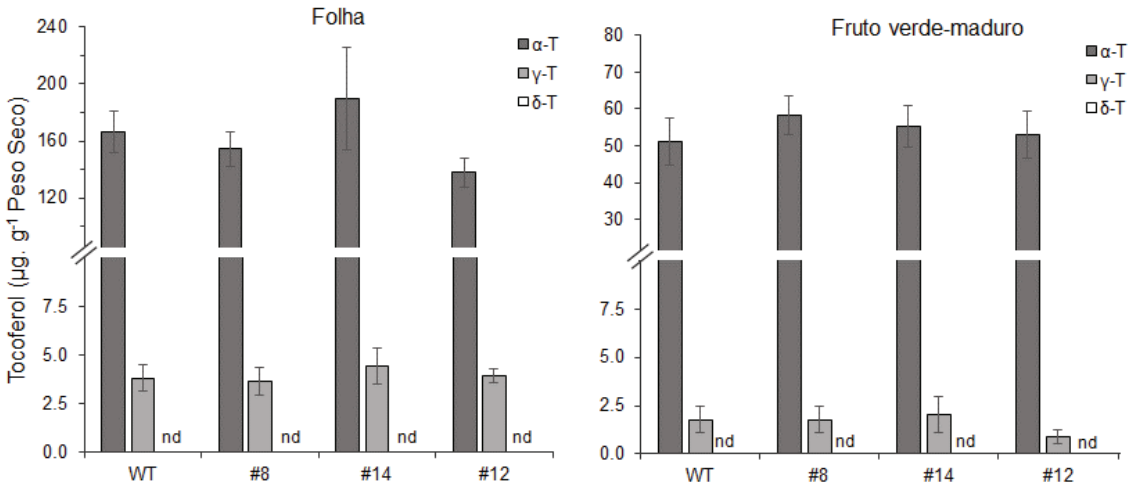

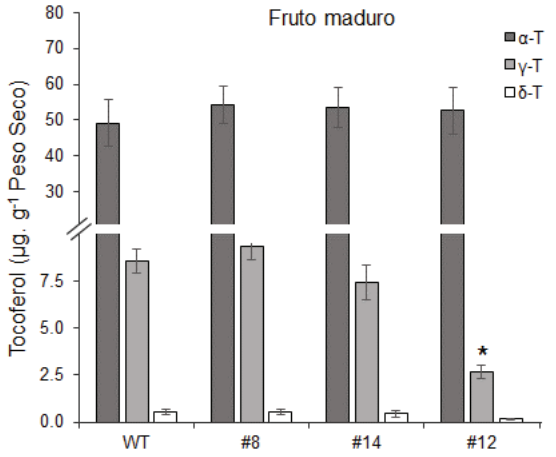

Figura 6: Conteúdo de tocoferóis nas linhagens transgênicas silenciadas para *CLH(1)*. Os valores correspondem a média (n = 5) de cada genótipo. As barras correspondem ao desvio padrão. Diferenças estatísticas significativas estão indicadas na figura com asteriscos (ANOVA/ teste de Dunnett, P < 0,05) em comparação ao controle (WT).

4.3.3. Perfil de prenilipídeos

Embora as linhagens transgênicas de *SlCLH(1)*-RNAi não apresentem diferenças no conteúdo de VTE e clorofila, buscou-se avaliar o impacto da deficiência de CLH(1) no metabolismo dos demais prenilipídeos derivados da via dos isoprenóides plastidiais, os quais incluem prenilquinonas (plastoquinona-9, PQ-9), outros tococromanóis (plastocromanol, PC-8) e carotenóides. Os prenilipídeos de folhas e frutos foram quantificados por UHPLC-APCI-QTOFMS (tococromanóis e prenilquinonas) e HPLC (carotenóides) e estão sumarizados na Tabela 2. Em folhas, o perfil se mostrou similar entre as linhagens transgênicas *SlCLH(1)*-RNAi e as plantas selvagens. Já em frutos, não foi observado uma tendência clara entre as linhagens #8 e # 14; para a linhagem #12 era esperado perfil distinto em virtude das alterações fenotípicas previamente mencionadas. Enquanto frutos verde-maduros e maduros de *SlCLH(1)*-RNAi#8 exibem um aumento de pelo menos 50% nos níveis de PQ-9, de PC-8 e de seus respectivos produtos de oxidação PQ-OH e PC-OH, além da prenilquinona mitocondrial ubiquinona-10, frutos de *SlCLH(1)*-RNAi#14 apresentam níveis iguais ao controle (Tabela 2).

4.3.4. Parâmetros fotossintéticos e determinação dos carboidratos foliares

Para avaliar o possível efeito do silenciamento do gene *CLH(1)* na atividade fotossintética verificou-se as trocas gasosas a diferentes densidades de fluxo de fótons bem como os parâmetros de fluorescência da clorofila nas plantas transgênicas e controle. Não foram registradas alterações significativas na taxa de assimilação de CO_2 para as linhagens *SlCLH(1)*-RNAi, excetuando a linhagem #12, ainda que em média os valores sejam superiores para #8 e #14 (Figura 7; Tabela 3). A respeito dos parâmetros de fluorescência de clorofila, é possível observar um aumento na eficiência quântica máxima do PSII adaptado à luz (F_v'/F_m'), indicando potencialmente uma melhor conservação dessa estrutura (Tabela 3).

Tabela 2: Alterações no perfil de prenilipídeos de linhagens transgênicas *SlCLH(1)*-RNAi.

Prenilipídeos (quantidade relativa)	WT	*SlCLH(1)*-RNAi #8	*SlCLH(1)*-RNAi #14	*SlCLH(1)*-RNAi #12
Folha				
α-TQ	1.00 ± 0.18	1.11 ± 0.29	0.85 ± 0.57	0.66 ± 0.13
PQ-9	1.00 ± 0.18	0.85 ± 0.22	0.94 ± 0.20	0.77 ± 0.12
PQ-H_2	1.00 ± 0.66	1.66 ± 0.30	1.43 ± 0.34	0.99 ± 0.20
PQ-OH	1.00 ± 0.20	0.95 ± 0.17	0.95 ± 0.25	0.66 ± 0.11
PC-OH	1.00 ± 0.21	0.87 ± 0.14	1.05 ± 0.31	**0.60 ± 0.16**
PC-8	1.00 ± 0.30	0.93 ± 0.22	1.13 ± 0.39	0.81 ± 0.20
UQ-10	1.00 ± 0.24	0.76 ± 0.15	0.85 ± 0.11	0.96 ± 0.10
filoquinona	1.00 ± 0.16	0.88 ± 0.13	1.09 ± 0.20	0.98 ± 0.14
β-caroteno	1.00 ± 0.07	0.91 ± 0.07	1.02 ± 0.15	0.96 ± 0.10
luteina	1.00 ± 0.07	0.97 ± 0.09	1.06 ± 0.09	1.06 ± 0.04
violaxantina/neoxantina	1.00 ± 0.06	1.01 ± 0.06	1.09 ± 0.11	1.08 ± 0.09
Fruto verde-maduro				
α-TQ	1.00 ± 0.15	1.53 ± 0.30	1.43 ± 0.36	0.93 ± 0.62
PQ-9	1.00 ± 0.15	**2.23 ± 0.60**	1.00 ± 0.16	1.25 ± 0.73
PQ-H_2	1.00 ± 0.30	1.57 ± 0.65	0.92 ± 0.16	1.34 ± 0.81
PQ-OH	1.00 ± 0.26	**2.29 ± 0.63**	1.12 ± 0.43	1.30 ± 0.77
PC-OH	1.00 ± 0.42	1.28 ± 0.41	0.77 ± 0.25	0.43 ± 0.28
PC-8	1.00 ± 0.15	**1.57 ± 0.19**	0.98 ± 0.10	**1.20 ± 0.76**
UQ-10	1.00 ± 0.13	**1.58 ± 0.43**	1.13 ± 0.17	**1.67 ± 0.94**
filoquinona	1.00 ± 0.27	1.35 ± 0.40	0.94 ± 0.22	1.07 ± 0.62
β-caroteno	1.00 ± 0.26	1.13 ± 0.26	0.87 ± 0.21	0.93 ± 0.07
luteina	1.00 ± 0.22	1.18 ± 0.17	1.00 ± 0.16	0.76 ± 0.43
violaxantina/neoxantina	1.00 ± 0.23	1.20 ± 0.26	0.97 ± 0.14	1.07 ± 0.62
Fruto maduro				
α-TQ	1.00 ± 0.25	1.22 ± 0.25	0.95 ± 0.26	1.11 ± 0.04
PQ-9	1.00 ± 0.17	**2.71 ± 0.78**	0.91 ± 0.03	0.83 ± 0.04
PQ-H_2	1.00 ± 0.29	1.95 ± 0.82	1.13 ± 0.15	1.21 ± 0.31
PQ-OH	1.00 ± 0.27	0.99 ± 0.48	0.83 ± 0.39	1.05 ± 0.20
PC-OH	1.00 ± 0.07	**2.71 ± 1.25**	1.57 ± 0.63	1.59 ± 0.72
PC-8	1.00 ± 0.15	**1.83 ± 0.20**	0.95 ± 0.12	1.25 ± 0.04
UQ-10	1.00 ± 0.14	**2.44 ± 0.16**	0.91 ± 0.11	1.09 ± 0.13
filoquinona	1.00 ± 0.18	1.26 ± 0.23	0.90 ± 0.11	1.04 ± 0.12
luteina	1.00 ± 0.13	1.33 ± 0.44	1.06 ± 0.23	1.02 ± 0.13
neurosporeno	1.00 ± 0.22	0.96 ± 0.35	0.81 ± 0.29	**0.44 ± 0.09**
ζ-caroteno	1.00 ± 0.20	1.16 ± 0.56	0.71 ± 0.23	**0.27 ± 0.15**
β-caroteno	1.00 ± 0.06	1.12 ± 0.33	0.88 ± 0.14	0.85 ± 0.12
licopeno	1.00 ± 0.06	1.00 ± 0.15	0.86 ± 0.08	**0.64 ± 0.13**

Os dados foram normalizados com respeito ao peso das amostras e expressos em relação ao controle (WT) em cada tecido. Valores são médias ± desvio padrão (n=5). Termos em negrito indicam diferenças estatísticas entre as linhagens transgênicas e o controle (ANOVA/ Teste de Dunnett; $P < 0,05$). α-tocoferoxil (α-TQ), plastoquinona-9 (PQ-9), plastoquinol-9 (PQ-H_2), hidroxi-plastoquinona (PQ-OH), plastocromanol-8 (PC-8), hidroxi-plastocromanol (PC-OH), ubiquinona-10 (UQ-10).

A determinação do conteúdo de açúcares solúveis e amido em folhas das plantas transgênicas de 5 semanas de idade não revelou um cenário claro para o metabolismo de carboidratos (Figura 8). Assim como ocorreu no perfil de lipídeos, novamente, os resultados das linhagens #8 e #14 não coincidiram; enquanto folhas de *SlCLH(1)*-RNAi#8 apresentaram redução no conteúdo de sacarose

e substancial aumento nos níveis de amido comparados ao controle, folhas de *SlCLH(1)*-RNAi#14 não mostraram alteração na quantificação de açúcares solúveis e amido. Esses resultados sugerem que as alterações específicas observadas para linhagem #8 estão provavelmente associadas ao evento de transformação e não seriam portanto consequências do silenciamento de *CLH(1).*

Tabela 3: Parâmetros fotossintéticos das linhagens *SlCLH(1)*-RNAi.

	Assimilação [a] (μmol CO_2 m^{-2} s^{-1})	g_s (μmol $m^{-2}.s^{-1}$)	R_d (μmol $m^{-2}.s^{-1}$)	F_v'/F_m'	Φ_{PSII}	*qP*	J_{PSII}	Transpiração (mmol H_2O $m^{-2}.s^{-1}$)
WT	6.1 ± 0.46	0.05 ± 0.02	1.97 ± 0.55	0.58 ± 0.03	0.88 ± 0.24	0.75 ± 0.04	114.8 ± 9.2	1.97 ± 0.27
#8	8.26 ± 2.15	0.06 ± 0.04	1.94 ± 0.48	0.61 ± 0.04	0.76 ± 0.31	0.73 ± 0.04	116.9 ± 14.5	1.94 ± 0.46
#14	8.42 ± 2.22	0.06 ± 0.03	2.56 ± 0.8	**0.63 ± 0.02**	0.68 ± 0.28	0.78 ± 0.04	126.9 ± 10.1	2.56 ± 0.4
#12	**8.62 ± 1.61**	0.07 ± 0.03	2.33 ± 0.91	**0.63 ± 0.02**	0.68 ± 0.28	0.78 ± 0.03	126.2 ± 10.1	2.33 ± 0.34

[a] Resposta de assimilação obtida à densidade do fluxo de fótons de 600 μmol m^{-2} s^{-1}.
g_s, condutância estomática foliar; R_d, Respiração diurna; F_v'/F_m', eficiência quântica máxima do PSII adaptado à luz; Φ_{PSII}, eficiência operante no PSII; *qP*, quenching fotoquímico; J_{PSII}, taxa de transporte de elétrons. Os termos em negrito indicam diferenças estatísticas com relação às plantas controle (WT) (Teste t, $P < 0,05$).

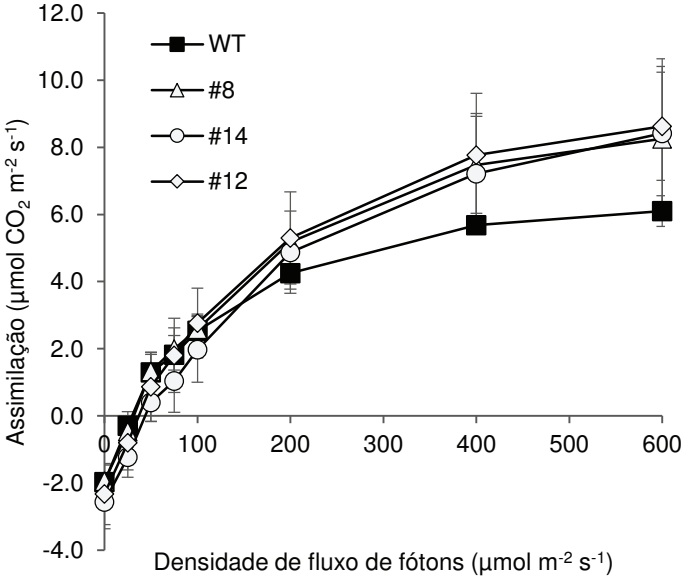

Figura 7: Curva de assimilação nas linhagens transgênicas silenciadas para *CLH(1)*. Resposta de assimilação de carbono obtida a diferentes densidades de fluxo de fótons.

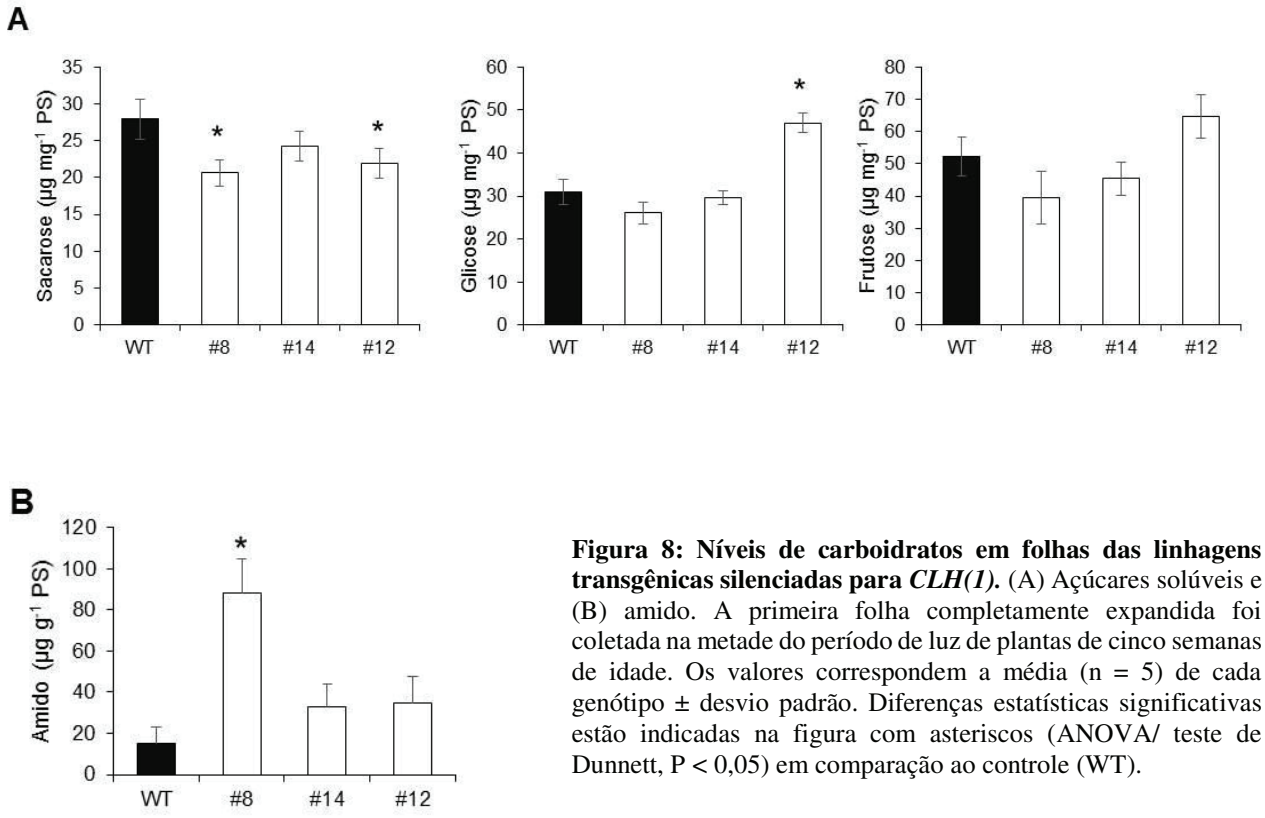

Figura 8: Níveis de carboidratos em folhas das linhagens transgênicas silenciadas para *CLH(1)*. (A) Açúcares solúveis e (B) amido. A primeira folha completamente expandida foi coletada na metade do período de luz de plantas de cinco semanas de idade. Os valores correspondem a média (n = 5) de cada genótipo ± desvio padrão. Diferenças estatísticas significativas estão indicadas na figura com asteriscos (ANOVA/ teste de Dunnett, P < 0,05) em comparação ao controle (WT).

4.3.5. Perfil de expressão

A expressão dos genes envolvidos na via do MEP [*DXS(1); GGPS(2)*; *GGDR*], na via do chiquimato [*HPPD(1)*; *HPPD(2)*], na síntese (*CHLG*) e degradação da clorofila [*CLH(2), CLH(4), SGR1, PAO* e *PPH*], reciclagem do fitol (*VTE5*), rota central do tocoferol [*VTE1, VTE2, VTE3* e *VTE4*], carotenóides [*PSY*(1), *PSY*(2)] e plastoquinonas (*SPS* e *HST*) foram avaliados em folhas, frutos verde-maduros e maduros das linhagens *SlCLH(1)*-RNAi (Tabela 4). O foco da análise recaiu sobre as alterações na expressão gênica coincidentes nas linhagens #8 e #14. De acordo com esse critério, observa-se que folhas transgênicas possuem redução na expressão de *SGR1* e *VTE3(1)*. Este último, por sua vez, é o único gene que apresentou padrão de expressão alterado nos frutos das plantas deficientes em *CLH(1)*; os níveis de transcritos estão reduzidos tanto no estádio verde-maduro quanto maduro.

Tabela 4: Alteração na expressão dos genes que codificam enzimas relacionadas ao metabolismo de isoprenóides nas linhagens *SlCLH(1)*-RNAi.

	Folha				Fruto verde-maduro				Fruto maduro			
Genes	MT	#8	#14	#12	MT	#8	#14	#12	MT	#8	#14	#12
DXS(1)	1.0 ± 0.06	**1.38 ± 0.09**	0.94 ± 0.09	**1.23 ± 0.02**	1.0 ± 0.09	0.87 ± 0.13	0.82 ± 0.19	1.0 ± 0.08	1.0 ± 0.13	0.95 ± 0.12	0.84 ± 0.15	1.10 ± 0.24
GGPS(2)	1.0 ± 0.14	**1.6 ± 0.1**	1.12 ± 0.26	1.11 ± 0.14	1.0 ± 0.08	0.81 ± 0.23	**1.45 ± 0.13**	**1.52 ± 0.11**	1.0 ± 0.09	0.68 ± 0.06	**0.93 ± 0.07**	0.74 ± 0.3
GGDR	1.0 ± 0.07	**1.4 ± 0.07**	0.87 ± 0.16	1.16 ± 0.1	1.0 ± 0.17	0.8 ± 0.11	0.72 ± 0.12	1.36 ± 0.22	1.0 ± 0.27	0.61 ± 0.1	0.58 ± 0.13	0.82 ± 0.19
HST	1.0 ± 0.01	**1.5 ± 0.05**	1.18 ± 0.23	**1.55 ± 0.05**	1.0 ± 0.09	1.03 ± 0.06	0.81 ± 0.09	1.15 ± 0.07	1.0 ± 0.22	0.98 ± 0.17	0.54 ± 0.2	**1.97 ± 0.69**
HPPD(1)	1.0 ± 0.08	1.04 ± 0.01	1.11 ± 0.07	1.01 ± 0.03	1.0 ± 0.03	**1.5 ± 0.09**	0.90 ± 0.14	**1.16 ± 0.05**	1.0 ± 0.1	0.98 ± 0.12	0.76 ± 0.19	1.46 ± 0.38
HPPD(2)	1.0 ± 0.14	1.04 ± 0.07	**1.69 ± 0.06**	0.96 ± 0.05	1.0 ± 0.06	**2.03 ± 0.3**	1.03 ± 0.03	0.99 ± 0.06	1.0 ± 0.11	**1.33 ± 0.12**	1.25 ± 0.28	1.48 ± 0.33
VTE1	1.0 ± 0.06	**1.23 ± 0.01**	0.94 ± 0.14	1.09 ± 0.09	1.0 ± 0.1	0.8 ± 0.04	**0.77 ± 0.07**	**1.25 ± 0.14**	1.0 ± 0.19	0.94 ± 0.04	0.7 ± 0.14	1.42 ± 0.26
VTE2	1.0 ± 0.02	**1.2 ± 0.05**	1.03 ± 0.08	**1.14 ± 0.07**	1.0 ± 0.02	**0.75 ± 0.03**	1.08 ± 0.17	1.0 ± 0.11	1.0 ± 0.2	0.98 ± 0.07	0.91 ± 0.18	0.69 ± 0.17
VTE3(1)	1.0 ± 0.02	**0.59 ± 0.01**	**0.64 ± 0.03**	**0.66 ± 0.03**	1.0 ± 0.07	**0.7 ± 0.03**	**0.55 ± 0.09**	**0.72 ± 0.03**	1.0 ± 0.11	**0.62 ± 0.04**	**0.55 ± 0.12**	0.85 ± 0.26
VTE3(2)	1.0 ± 0.03	1.02 ± 0.01	0.95 ± 0.08	1.04 ± 0.01	1.0 ± 0.04	**0.85 ± 0.04**	0.80 ± 0.10	0.96 ± 0.06	1.0 ± 0.15	0.93 ± 0.12	0.82 ± 0.2	1.16 ± 0.27
VTE4	1.0 ± 0.09	1.1 ± 0.05	0.95 ± 0.1	1.07 ± 0.1	1.0 ± 0.1	**0.75 ± 0.05**	0.91 ± 0.15	0.88 ± 0.03	1.0 ± 0.1	0.91 ± 0.13	**0.61 ± 0.13**	**2.29 ± 0.52**
VTE5	1.0 ± 0.07	**0.86 ± 0.03**	0.87 ± 0.08	**0.85 ± 0.04**	1.0 ± 0.07	1.01 ± 0.08	**0.76 ± 0.04**	**1.52 ± 0.04**	1.0 ± 0.04	0.89 ± 0.14	0.84 ± 0.19	1.05 ± 0.3
PSY(1)	1.0 ± 0.1	1.18 ± 0.08	0.89 ± 0.17	**0.75 ± 0.04**	1.0 ± 0.12	1.04 ± 0.36	2.35 ± 0.95	**0.55 ± 0.07**	1.0 ± 0.06	0.87 ± 0.07	0.86 ± 0.16	1.19 ± 0.19
PSY(2)	1.0 ± 0.03	0.93 ± 0.04	0.86 ± 0.09	**0.87 ± 0.04**	1.0 ± 0.04	0.86 ± 0.09	**0.61 ± 0.17**	1.03 ± 0.11	1.0 ± 0.07	1.03 ± 0.01	**0.54 ± 0.11**	**0.78 ± 0.06**
SGR1	1.0 ± 0.26	**0.5 ± 0.12**	**0.57 ± 0.14**	**0.46 ± 0.16**	1.0 ± 0.29	1.1 ± 0.28	1.48 ± 0.41	0.87 ± 0.15	1.0 ± 0.05	0.91 ± 0.07	0.78 ± 0.2	1.27 ± 0.32
CHLG	1.0 ± 0.01	1.05 ± 0.06	0.93 ± 0.09	0.96 ± 0.05	1.0 ± 0.02	0.96 ± 0.02	0.83 ± 0.06	1.0 ± 0.07	1.0 ± 0.12	0.89 ± 0.09	0.72 ± 0.14	1.37 ± 0.37
PAO	1.0 ± 0.04	**0.81 ± 0.01**	**1.09 ± 0.03**	**0.88 ± 0.06**	1.0 ± 0.12	0.99 ± 0.16	**1.30 ± 0.14**	**1.48 ± 0.05**	1.0 ± 0.01	0.99 ± 0.09	0.79 ± 0.09	**0.88 ± 0.07**
PPH	1.0 ± 0.06	**0.81 ± 0.02**	1.02 ± 0.02	**0.69 ± 0.02**	1.0 ± 0.05	**0.78 ± 0.08**	0.91 ± 0.28	**1.19 ± 0.04**	1.0 ± 0.17	1.27 ± 0.19	0.76 ± 0.25	1.58 ± 0.63
CLH(1)	1.0 ± 0.06	**0.13 ± 0.01**	**0.18 ± 0.02**	**0.15 ± 0.01**	1.0 ± 0.04	**0.14 ± 0.03**	**0.1 ± 0.03**	**0.3 ± 0.04**	1.0 ± 0.05	**0.11 ± 0.02**	**0.12 ± 0.02**	**0.06 ± 0.01**
CLH(2)	1.0 ± 0.2	0.92 ± 0.07	**0.66 ± 0.06**	1.12 ± 0.06	nd	nd	nd	nd	nd	nd	nd	nd
CLH(4)	1.0 ± 0.2	1.0 ± 0.11	0.68 ± 0.07	**1.72 ± 0.29**	1.0 ± 0.12	1.92 ± 0.97	1.54 ± 0.38	**9.8 ± 4.67**	1.0 ± 0.17	0.71 ± 0.26	0.65 ± 0.18	0.61 ± 0.24
SPS	1.0 ± 0.12	0.87 ± 0.08	0.96 ± 0.05	**0.61 ± 0.06**	1.0 ± 0.1	**0.62 ± 0.06**	0.72 ± 0.25	**1.24 ± 0.06**	1.0 ± 0.11	1.18 ± 0.18	0.77 ± 0.19	1.13 ± 0.13

Os dados representam médias de pelo menos três replicatas biológicas e correspondem aos valores da razão da expressão em relação ao controle (WT) no respectivo órgão. Termos em negrito indicam as diferenças estatisticamente significativas (Teste de permutação, $P < 0,05$). Nd, não detectado.

5. Discussão

Neste estudo foi realizada a caracterização funcional do gene *CLH(1)* de *S. lycopersicum*. Por muito tempo, a enzima CLH foi considerada a única responsável pela remoção da cadeia lateral do fitol da clorofila durante a etapa inicial da degradação do pigmento (Schelbert *et al.*, 2009). No entanto, desde a caracterização de mutantes de *Arabidopsis* deficientes em CLH, os quais apresentam efeitos sutis na perda de clorofila na senescência foliar (Schenk *et al.*, 2006), e a identificação de outra enzima defitiladora, a feofitinase, comprometida nesse processo (PPH, Schelbert *et al.*, 2009), várias questões têm sido levantadas acerca da função das CLHs em plantas. Embora sua atividade defitiladora de clorofila seja bem estabelecida *in vitro, in planta* a principal controvérsia reside na separação espacial entre enzima e seu substrato, a clorofila (Hu *et al.*, 2015). Nossos dados de localização subcelular mostram que a proteína de fusão CLH(1)-GFP também não é direcionada ao cloroplasto. Além disso, o padrão de distribuição da fluorescência sugere a localização da proteína em outros compartimentos celulares, como por exemplo, retículo endoplasmático. Recentemente, Hu *et al.* (2015) demonstraram que as proteínas CLH de *Arabidopsis* estão localizadas no retículo endoplasmático e no tonoplasto. Embora os resultados aqui apresentados aparentemente coincidam com os de *Arabidopsis*, estes contrastam com aqueles reportados para outras espécies. O peptídeo sinal de *Ginkgo biloba* fusionado ao GFP é direcionado ao plastídeo de protoplastos de *Arabidopsis* (Okazawa *et al.*, 2006). Já o estudo do direcionamento da CLH de *Citrus* (CsCLH) revelou, por imunodetecção, sua localização plastidial em flavedo (casca do fruto); posteriormente, foi demonstrado que a CsCLH está sujeita a regulação pós-traducional por meio da clivagem da porção N- e C-terminal (Azoulay Shemer *et al.*, 2008; 2011). A causa dos conflitos na localização subcelular de CLH é desafiadora e investigações adicionais são necessárias para esclarecer essa questão. Por um lado, os resultados obtidos em *Citrus* podem refletir uma particularidade que ocorre em flavedo. De fato, nossos resultados sugerem que CLH(1) de *S. lycopersicum* não é direcionada ao cloroplasto, ainda que não se possa excluir completamente que SlCLH(1) seja alvo de processamento pós-traducional, assim como demonstrado para CsCLH. No entanto, vale ressaltar que tal modificação pós-traducional em *Citrus* ocorre dentro do plastídeo e modula apenas a atividade da enzima, sem efeito no direcionamento subcelular (Azoulay-Shemer *et al.*, 2011).

Apesar de CLH não contribuir para a degradação da clorofila durante a senescência foliar, a presença marcante dessa proteína em tecidos fotossinteticamente ativos sugere um papel na homeostase da clorofila (Lira *et al.*, 2014). Nesse caso, como parte do aparato fotossintético, a clorofila está em constante *turnover* (reciclagem) resultado da degradação/reposição da proteína D1 do centro de reação, que é passível aos danos oxidativos, localizada no fotossistema II (Lin *et al.*,

2014). Esse processo implica a constante de- e re-esterificação da clorofila (Lin *et al.*, 2014), sendo que o fitol liberado, após fosforilações sequenciais, poderia ser utilizado na síntese de tocoferol (Valentin *et al.*, 2006; Ischebeck *et al.*, 2006). Nossos resultados anteriores mostraram que, embora não seja determinante para o QTL de VTE analisado, a expressão de *CLH(1)* está induzida nos frutos das IL6-1 com alto conteúdo de tocoferol (Capítulo II), mesmo que o silenciamento de *CLH(1)* por VIGS em fruto não tenha alterado esses compostos (Capítulo III).

Nesse sentido, buscando aprofundar o entendimento do processo de defitilação de clorofila e sua relação com a síntese de tocoferóis, linhagens transgênicas estáveis de tomateiro silenciadas para *CLH(1)* foram obtidas. Os resultados demonstraram que tomateiros com níveis reduzidos de transcritos de *CLH(1)* não apresentam alteração no conteúdo de clorofila e dos catabólitos verdes e nem de tocoferóis, tanto em folhas como em frutos. Esses dados concordam com os reportados para sementes de *Arabidopsis* por Zhang *et al.* (2014). Os autores analisaram mutantes para as duas *CLHs* e a *PPH,* assim como a combinação destas em triplos mutantes, concluindo que essas enzimas não contribuem para liberação do fitol incorporado na síntese de tocoferol nas sementes. Já a sobrexpressão da *PPH* resultou em discreto aumento dos níveis desse antioxidante. Desta forma, o trabalho sugere a existência de defitilases ainda desconhecidas (Zhang *et al.*, 2014).

Embora os resultados obtidos para tocoferol e clorofila coincidam entre as linhagens *SlCLH(1)-RNAi*, a detalhada caracterização fenotípica mostrou que os transformantes analisados apresentam modificações que podem estar associadas aos eventos transgenia específicos para cada linhagem. Aparentemente, as alterações fenotípicas observadas para *SlCLH(1)*-RNAi#12 podem ser decorrentes de efeito de variação somaclonal como ploidização. Além disso, as discrepâncias observadas entre perfis metabólico das linhagens #8 e #14 dificultam a avaliação de possíveis consequências do silenciamento de *CLH(1)* na fisiologia de tomateiro. Contudo, dentre as alterações compartilhadas pelas três linhagens, destaca-se a tendência de aumento na taxa fotossintética acompanhada pela tendência na redução de sacarose. Coincidentemente, folhas das plantas transgênicas no mesmo estádio de desenvolvimento também apresentam redução na expressão de *SGR1* e na *PPH*, sugerindo uma correlação entre essas observações.

É importante assinalar que o silenciamento *CLH(1)* não produziu efeitos consistentes na expressão dos demais parálogos avaliados e, portanto, pode ser considerado específico. Diante da redundância dessa família gênica, uma das alternativas para futuros estudos seria a obtenção de plantas deficientes para os quatro genes parálogos de *CLH*.

6. Conclusão

Os resultados apresentados permitem concluir que a CLH(1) de *S. lycopersicum* apresenta localização extraplastidial com padrão semelhante ao de proteínas de retículo endoplasmático. Além disso, o silenciamento do gene não resultou em alterações no conteúdo de tocoferol nem de clorofilas e dos catabólitos verdes. Tais observações sugerem que CLH(1) não contribui para defitilação da clorofila que ocorre tanto no *turnover* regular da folha quanto no amadurecimento de frutos e, portanto, não está envolvida no aporte de fitol para a síntese de VTE. Dessa forma, a atividade das demais defitilases conhecidas (*i.e.* PPH) ou ainda hidrolases não caracterizadas poderiam suprir essa função.

7. Referências Bibliográficas

Almeida, J., Quadrana, L., Asis, R., Setta, N., de Godoy, F., Bermudez, L., Otaiza, S., *et al.* (2011) Genetic dissection of vitamin E biosynthesis in tomato. *Journal of Experimental Botany,* 62, 3781–3798.

Azoulay-Shemer, T., Harpaz-Saad, S., Belausov, E., Lovat, N., Krokhin, O., Spicer, V., Standing, K.G., *et al.* (2008). Citrus chlorophyllase dynamics at ethylene-induced fruit color-break; a study of chlorophyllase expression, post-translational processing kinetics and in-situ intracellular localization. *Plant Physiology,* 148, 108–118.

Azoulay-Shemer, T., Harpaz-Saad, S., Cohen-Peer, R., Mett, A., Spicer, V., Lovat, N., Krokhin, O., *et al.* (2011) Dual N- and C-terminal processing of citrus chlorophyllase precursor within the plastid membranes leads to the mature enzyme. *Plant & Cell Physiology*, 52, 70–83.

Balazadeh, S. (2014) Stay-Green Not Always Stays Green. *Molecular Plant*, 7, 1264–1266.

Chen, L. F. O., Lin, C. H., Kelkar, S. M., Chang, Y. M., Shaw, J. F. (2008) Transgenic broccoli (*Brassica oleracea var. italica*) with antisense chlorophyllase (BoCLH1) delays postharvest yellowing. *Plant Science,* 174, 25–31.

Davidson, M. M., Jacobs, J. M. E., Reader, J. K., Butler, R. C., Wratten, S. D., Conner, A. J. (2002) Development and Evaluation of Potatoes Transgenic for a *cry* 1Ac9 Gene Conferring Resistance to Potato Tuber Moth. *Journal of the American Society for Horticultural Science*, 127, 590–596.

DellaPenna, D., Pogson, B. J. (2006). Vitamin synthesis in plants: tocopherols and carotenoids. *Annual Review of Plant Biology*, 57, 711–738.

Guyer, L., Schelbert Hofstetter, S., Christ, B., Lira, B. S., Rossi, M., Hörtensteiner, S. (2014) Different mechanisms are responsible for chlorophyll dephytylation during fruit ripening and leaf senescence in tomato. *Plant Physiology,* 166, 44-56.

Harpaz-Saad, S., Azoulay, T., Arazi, T., Ben-Yaakov, E., Mett, A., Shiboleth, Y. M., Hörtensteiner, S., *et al.* (2007) Chlorophyllase is a rate-limiting enzyme in chlorophyll catabolism and is posttranslationally regulated. *The Plant Cell*, 19, 1007–1022.

Hörtensteiner, S. (2009) Stay-green regulates chlorophyll and chlorophyll binding protein degradation during senescence. *Trends Plant Science,* 14, 155–162.

Hörtensteiner, S. (2013) Update on the biochemistry of chlorophyll breakdown. *Plant Molecular Biology*, 82, 505–517.

Hu, X., Makita, S., Schelbert, S., Sano, S., Ochiai, M., Tsuchiya, T., Hasegawa, S.F., *et al.* (2015) Re-examination of chlorophyllase function implies its involvement in defense against chewing herbivores. *Plant Physiology*, 167, 660-670.

Ischebeck, T., Zbierzak, A. M., Kanwischer, M., Dörmann, P. (2006) A salvage pathway for phytol metabolism in *Arabidopsis*. *The Journal of Biological Chemistry,* 281, 2470–2477.

Keller, Y., Bouvier, F., d'Harlingue, A., Camara, B. (1998) Metabolic compartmentation of plastid prenyllipid biosynthesis - evidence for the involvement of a multifunctional geranylgeranyl reductase. *European Journal of Biochemistry / FEBS*, 251, 413–417.

Kim, S., Schlicke, H., Van Ree, K., Karvonen, K., Subramaniam, A., Richter, A., Grimm B, Braam, J. (2013) Arabidopsis chlorophyll biosynthesis: an essential balance between the methylerythritol phosphate and tetrapyrrole pathways. *The Plant Cell*, 25, 4984–4993.

Lin, Y.-P., Lee, T., Tanaka, A., Charng, Y. (2014) Analysis of an Arabidopsis heat-sensitive mutant reveals that chlorophyll synthase is involved in reutilization of chlorophyllide during chlorophyll turnover. *The Plant Journal,* 80, 14–26.

Lira, B. S., de Setta, N., Rosado, D., Almeida, J., Freschi, L., Rossi, M. (2014) Plant degreening: evolution and expression of tomato (*Solanum lycopersicum*) dephytylation enzymes. *Gene*, 546, 359-366.

Okazawa, A., Tang, L., Itoh, Y., Fukusaki, E. (2006) Characterization and Subcellular Localization of Chlorophyllase from Ginkgo biloba. *Z Naturforsch C.* 61, 111-117.

Pino, L. E., Lombardi-Crestana, S., Azevedo, M. S., Scotton, D. C., Borgo, L., Quecini, V., Figueira, A., Peres, L. E. (2010) The Rg1 allele as a valuable tool for genetic transformation of the tomato "Micro-Tom" model system. *Plant Methods*, 6, 23.

Quadrana, L., Rodriguez, M. C., López, M., Bermúdez, L., Nunes-Nesi, A., Fernie, A. R., Descalzo, A., *et al*. (2011) Coupling virus-induced gene silencing to exogenous green fluorescence protein expression provides a highly efficient system for functional genomics in Arabidopsis and across all stages of tomato fruit development. *Plant Physiology*, 156, 1278–1291.

Quadrana, L., Almeida, J., Otaiza, S. N., Duffy, T., Corrêa da Silva, J. V, de Godoy, F., Asis, R., *et al.* (2013). Transcriptional regulation of tocopherol biosynthesis in tomato. *Plant Molecular Biology*, 81, 309–325.

Sakuraba, Y., Schelbert, S., Park, S.-Y., Han, S.-H., Lee, B.-D., Andrès, C. B., Kessler F, *et al*. (2012). STAY-GREEN and chlorophyll catabolic enzymes interact at light-harvesting complex II for chlorophyll detoxification during leaf senescence in Arabidopsis. *The Plant Cell,* 24, 507–518.

Schelbert, S., Aubry, S., Burla, B., Agne, B., Kessler, F., Krupinska, K., Hörtensteiner, S. (2009) Pheophytin pheophorbide hydrolase (pheophytinase) is involved in chlorophyll breakdown during leaf senescence in Arabidopsis. *The Plant Cell*, 21, 767–785.

Schenk, N., Schelbert, S., Kanwischer, M., Goldschmidt, E. E., Dörmann, P., Hörtensteiner, S. (2007) The chlorophyllases AtCLH1 and AtCLH2 are not essential for senescence-related chlorophyll breakdown in Arabidopsis thaliana. *FEBS Letters*, 581, 5517–25.

Shpilyov, A. V, Zinchenko, V. V, Grimm, B., Lokstein, H. (2012) Chlorophyll a phytylation is required for the stability of photosystems I and II in the cyanobacterium *Synechocystis sp*. PCC 6803. *The Plant Journal*, 73, 336–346.

Sigareva, M., Spivey, R., Willits, M. G., Kramer, C. M., Chang, Y. F. (2004) An efficient mannose selection protocol for tomato that has no adverse effect on the ploidy level of transgenic plants. *Plant Cell Reports*, 23, 236–245.

Takamiya, K. I., Tsuchiya, T., Ohta, H. (2000) Degradation pathway(s) of chlorophyll: what has gene cloning revealed? *Trends in Plant Science,* 5, 426–43.

Tanaka, A., Tanaka, R. (2006) Chlorophyll metabolism. *Current Opinion in Plant Biology,* 9, 248–255.

Valentin, H. E., Lincoln, K., Moshiri, F., Jensen, P. K., Qi, Q., Venkatesh, T.V., *et al.* (2006) The Arabidopsis vitamin E pathway gene5-1 mutant reveals a critical role for phytol kinase in seed tocopherol biosynthesis. *The Plant Cell,* 18, 212–224.

Zhang, W., Liu, T., Ren, G., Hörtensteiner, S., Zhou, Y., Cahoon, E. B., Zhang, C. (2014) Chlorophyll Degradation: The Tocopherol Biosynthesis-Related Phytol Hydrolase in Arabidopsis Seeds Is Still Missing. *Plant Physiology*, 166, 70–79.

CAPÍTULO VI. CARACTERIZAÇÃO FUNCIONAL DO GENE *FITOL QUINASE* EM TOMATEIRO

Os Resultados, Material e Métodos e Discussão deste capítulo são apresentados na forma de artigo submetido ao periódico *Plant Physiology*.

Almeida, J., Azevedo, M. S., Spicher L., Glauser, G., vom Dorp, K., Guyer, L., Carranza, A. V., Asis, R., de Souza, A. P., Buckeridge, M., Demarco, D., Bres, C., Rothan, C., Peres, L. E. P., Hörtensteiner, S., Kessler, F., Dörmann, P., Carrari, F., Rossi, M. *Tocopherol content is highly dependent on PHYTOL KINASE in tomato* (submetido).

Resumo

Tocoferol, composto com atividade de vitamina E, é um componente do sistema antioxidante plastidial conservado em organismos fotossintetizantes. A síntese de tocoferol envolve a condensação de um grupo de cabeça aromática com uma cadeia lateral prenil isoprênica. Este último, o fitil difosfato, pode ser originado a partir da síntese *de novo*, pela via do 2-C-metil-D-eritritol 4-fosfato, ou pela reciclagem da cauda fitol da clorofila, que depende da atividade de fitol quinase (VTE5). Como as plantas coordenam o metabolismo de isoprenóides para suprir a biossíntese de tocoferóis em diferentes contextos plastidiais ainda não é bem esclarecido. No presente trabalho, nós caracterizamos plantas de *Solanum lycopersicum* deficientes na expressão de dois genes homólogos a *VTE5* identificados por análises filogenéticas, denominados *SlVTE5* e *SlFOLK*. Nossos dados mostram que enquanto *SlFOLK* não afeta o conteúdo de tocoferol, a produção deste metabólito é mais de 80% dependente de *SlVTE5* em tomate, tanto em folhas como em frutos. A deficiência de VTE5 impacta dramaticamente o metabolismo de lipídeos, incluindo prenilquinonas, carotenóides e ésteres de fitol de ácidos graxos, contudo, os resultados diferem de maneira impressiva entre folhas e frutos. Além disso, plantas deficientes em VTE5 apresentam acúmulo de amido nas folhas e taxas reduzidas de assimilação de CO_2. Em conjunto, nossos dados fornecem valiosas informações sobre a distinta regulação do metabolismo de isoprenóides em folhas e frutos, expondo uma complexa intercomunição entre o metabolismo de carbono e lipídeos, que resulta no bloqueio do transporte de carbono nas plantas deficientes para VTE5.

Tocopherol content is highly dependent on *PHYTOL KINASE* in tomato

Juliana Almeida[1], Mariana da Silva Azevedo[2], Livia Spicher[3], Gaétan Glauser[4], Katharina vom Dorp[5], Luzia Guyer[6], Andrea del Valle Carranza[7], Ramón Asis[7], Amanda Pereira de Souza[1], Marcos Buckeridge[1], Diego Demarco[1], Cécile Bres[8], Christophe Rothan[8], Lázaro Eustáquio Pereira Peres[2], Stefan Hörtensteiner[6], Félix Kessler[3], Peter Dörmann[5], Fernando Carrari[9], Magdalena Rossi[1].

1 Departamento de Botânica, Instituto de Biociências, Universidade de São Paulo, Rua do Matão, 277, 05508-900, São Paulo, Brazil.
2 Departamento de Ciências Biológicas, Escola Superior de Agricultura "Luiz de Queiroz", Universidade de São Paulo, Av. Pádua Dias, 11, CP 09, 13418-900, Piracicaba, Brazil.
3 Laboratory of Plant Physiology, University of Neuchâtel, 2000, Neuchâtel, Switzerland.
4 Neuchâtel Platform of Analytical Chemistry, University of Neuchâtel, 2000 Neuchâtel, Switzerland.
5 Institute of Molecular Physiology and Biotechnology of Plants, University of Bonn, 53115 Bonn, Germany.
6 Institute of Plant Biology, University of Zurich, Zollikerstrasse 107, CH-8008 Zurich, Switzerland.
7 CIBICI, Facultad de Ciencias Químicas, Universidad Nacional de Córdoba, CC 5000, Córdoba, Argentina.
8 INRA and Université de Bordeaux, UMR 1332 Biologie du Fruit et Pathologie, F-33140 Villenave d'Ornon, France
9 Instituto de Biotecnología, Instituto Nacional de Tecnología Agropecuaria and Consejo Nacional de Investigaciones Científicas y Técnicas, PO Box 25, B1712WAA, Castelar, Argentina.
* Corresponding Author.

Summary: Downregulation of *PHYTOL KINASE* dramatically reduces tocopherol content, and also alters lipid metabolism, which ultimately affect carbon partitioning in tomato plants.

ABSTRACT

Tocopherol, a vitamin E compound, is a conserved constituent of the plastidial antioxidant network in photosynthetic organisms. The synthesis of tocopherol involves the condensation of an aromatic head group with an isoprenoid prenyl side chain. The latter, phytyl diphosphate, can be derived from the *de novo* biosynthesis, *via* 2-C-methyl-D-erythritol 4-phosphate pathway, or from chlorophyll phytol tail recycling, which depends on phytol kinase (VTE5) activity. How plants coordinate the isoprenoid lipid metabolism for supplying tocopherol biosynthesis in different plastid contexts is not well understood. Here we characterized *Solanum lycopersicum* plants impaired in the expression of two *VTE5*-like genes identified by phylogenetic analyses, named *SlVTE5* and *SlFOLK*. Our data show that while *SlFOLK* does not affect tocopherol content, the production of this metabolite is over to 80% dependent on *SlVTE5* in tomato, both in leaves and fruits. VTE5 deficiency greatly impacted lipid metabolism, including prenylquinones, carotenoids and fatty acid phytyl esters, however, the outcomes impressively differ within fruit and leaves. Additionally, VTE5-deficient plants displayed starch accumulation in leaves and lower CO_2 assimilation rates. Taken together, our results provide valuable insights into the distinct regulation of isoprenoid metabolism in leaves and fruits unraveling an intriguingly cross-talk between lipid and carbon metabolisms, which results in carbohydrate export blockage in the *VTE5*-impaired plants.

INTRODUCTION

Tocopherols are potent lipid-soluble antioxidants and together with tocotrienols comprise the vitamin E (VTE) family of compounds, which are synthesized only by photosynthetic organisms (Kamal-Eldin and Appelqvist, 1996; DellaPenna and Pogson, 2006). Since plants are the major source of VTE required for human nutrition, understanding of the mechanisms underlying its synthesis and accumulation in crop species is of great interest (Grusak and DellaPenna, 1999; Fitzpatrick et al., 2012). The antioxidant function of tocopherols relies on their ability to scavenge peroxyl radicals, limiting lipid oxidation of polyunsaturated fatty acids (PUFAs) (Serbinova et al., 1991; Traber and Atkinson, 2008), and also singlet oxygen ($^1O_2$) (Kaiser et al., 1990; Di Mascio et al., 1990; Fukuzawa et al., 1997). In plants, light-driven photosynthetic processes are the main contributors to reactive oxygen species (ROS) production in chloroplasts owing to electron-transport chains and photosensitizing molecules such as chlorophyll (Chl) (Edreva, 2005; Demmig-Adams et. al, 2014). The delicate equilibrium between ROS production and their detoxification in chloroplast, which determines damage, protection or signaling response, is controlled by a diversified ROS-scavenging system, including non-enzymatic antioxidant mechanisms (Edreva, 2005; Foyer and Noctor, 2005). Tocopherols, as part of the photoprotective machinery, are particularly involved in controlling the level of $^1O_2$ in photosystem II (PSII), and the extent of lipid peroxidation in thylakoid membranes specially under stress conditions (Triantaphylidès and Havaux, 2009; Rastogi et al., 2014; Miret and Munné-Bosch, 2015). Besides, non-photoprotective roles of tocopherol have also been demonstrated *in planta*, which include well-established function in seed longevity, seedling germination (Sattler et al., 2004; Mène-Saffrané et al., 2010) and photoassimilate export (Maeda et al., 2006; 2008; Asensi-Fabado et al., 2014); although for this latter the precise underlying mechanism remains elusive (Maeda et al., 2014).

Accumulation of tocopherol in plant tissues is a tightly controlled process and several studies determined that tocopherol levels change significantly during plant growth and development, as well as in response to environmental stimuli including high light, low temperature, salt and osmotic stress (Munné-Bosch, 2005; Maeda et al., 2006; Abbasi et al., 2007; Loyola et al., 2012; Quadrana et al., 2013; Eugeni-Piller et al., 2014). Additionally, transgenic approaches have demonstrated that VTE content correlates with the expression of the biosynthesis- and recycling-related genes (reviewed by DellaPenna and Mène-Saffrané, 2011). Tocopherol synthesis occurs in plastids and requires two precursors, a prenyl side chain and a tyrosine catabolite-derived chromanol head group. The prenyl moiety phytyl diphosphate and homogentisate derived from the plastidial 2-C-methyl-D-erythritol 4-phosphate (MEP) and the shikimate pathway, respectively, are condensed by homogentisate phytyl transferase (VTE2), the only enzyme unique for tocopherol synthesis. From this precursor, the four

naturally occurring tocopherol forms (α-, β-, γ- and δ-tocopherol), which vary in the methylation pattern of the chromanol group, are synthesized *via* the action of dimethyl-phytylquinol methyl transferase (VTE3), tocopherol cyclase (VTE1) and tocopherol γ-methyl transferase (VTE4). These enzymes are also responsible for the synthesis of the other tocochromanols compounds, which not only include tocotrienols but also plastochromanol (PC-8), a product of plastoquinone (PQ-9) cyclization (Zbierzak et al., 2010).

In addition to the *de novo* synthesis, the phytyl diphosphate precursor may also originate from Chl turnover or degradation. After the hydrolysis from Chl by the action of dephytylases like pheophytinase (PPH), phytol is sequentially phosphorylated by two enzymes, phytol kinase (VTE5) and phytyl-phosphate kinase (Ischebeck et al., 2006; Valentin et al., 2006). While the *locus* responsible for the latter activity remains unknown, VTE5 has been characterized in *Arabidopsis thaliana* where its mutant allele, *vte5*, causes a substantial reduction of the tocopherol content in seeds and to a lesser extent in leaves (Valentin et al., 2006). Furthermore, based on sequence similarity, a *locus* encoding a putative VTE5 paralog was identified in *A. thaliana*, which further was characterized as a farnesol kinase (FOLK) (Fitzpatrick et al., 2011). However, its involvement in tocopherol biosynthesis was not addressed. So far, VTE5 has only been characterized in Arabidopsis and its contribution to tocopherol content is largely unknown in other species and organs, such as in fleshy fruits. Therefore, the impact of VTE5 deficiency on plant metabolism remains unexplored. *Solanum lycopersicum* is an interesting model species for studying tocopherol metabolism. Besides being an important food crop worldwide, tomato fruits are a significant source of VTE for human diet (Chun et al., 2006). Moreover, the fruit ripening process, which encompasses the conversion of chloroplasts into chromoplasts, couples Chl degradation and an active MEP pathway (Seymour et al., 2013), both sources of the prenyl precursor for tocopherol biosynthesis (Almeida et al., 2015). A previous study on the regulation of tocopherol biosynthesis in this species demonstrated a strong correlation between *VTE5* mRNA levels and the contents of Chl and tocopherol in tomato leaves and fruits, suggesting the contribution of phytol recycling to tocopherol biosynthesis (Quadrana et al., 2013). Moreover, expression analysis of senescence-related tomato mutants suggested that maintenance of the *de novo* phytyl diphosphate synthesis might, at later ripening stages, compensate for the lack of Chl-derived phytol used in tocopherol production of fruits (Almeida et al., 2015).

To better understand the extent of the contribution of the VTE5-dependent phytol salvage pathway to VTE biosynthesis in organs with distinct plastidial functions, we functionally characterized *VTE5*-like genes in tomato. Tocopherol content was dramatically compromised both in leaves and fruits of *SlVTE5*-knockdown plants. By contrast, analyzes of *folk* mutant genotype ruled out that *SlFOLK* is a major contributor to phytol kinase activity required for tocopherol biosynthesis.

Additionally, VTE5 deficiency differentially impacts phytyl ester and prenyllipid metabolism in fruits and leaves, and also affects photosynthesis and sugar partitioning.

RESULTS

VTE5 and FOLK proteins belong to sister clades and are targeted to chloroplasts

By using the *A. thaliana* VTE5 protein sequence (At5g04490; Valentin et al., 2006) as query, a survey for homologous sequences in the *S. lycopersicum* genome was performed in the Solanaceae Genomics Network (http://solgenomics.net/). Two *loci* were identified; Solyc03g071720 and Solyc09g018510. In order to establish the orthology relationships, a phylogenetic analysis was performed with VTE5 homologous protein sequences of 14 flowering species with completely sequenced genomes. The tree revealed two clades whose topology coincided with the established phylogenetic relationships between the analyzed species. One clade contains the *A. thaliana* VTE5 protein sequence (Valentin et al., 2006) that clustered together with Solyc03g071720. The other clade groups At5g58560, an earlier proposed VTE5 paralog that was further identified as a farnesol kinase (FOLK; Fitzpatrick et al., 2011), together with Solyc09g018510 (Fig. 1A). This analysis displayed VTE5 and FOLK proteins as sister clades, and the respective genes were named *SlVTE5* and *SlFOLK*. Both genes showed similar expression patterns with highest mRNA levels found in green tomato tissues (Supplemental Fig. S1). Confocal laser scanning microscopy of the SlVTE5-GFP and SlFOLK-GFP fusion proteins transiently expressed in *Nicotiana benthamiana* leaves showed that their fluorescence signals due to GREEN FLUORESCENT PROTEIN (GFP) co-localized with the autofluorescence of Chl, indicating that the encoded proteins were targeted to plastids (Fig. 1B). This result is in accordance with the putative function of SlVTE5. However, in the case of SlFOLK, chloroplast targeting is quite controversial according to previous reports of subcellular localization of FOLK activity. The phosphorylation of farnesol has been described occurring associated with isolated membranes from *Arabidopsis* seedling (Fitzpatrick et al. (2011) and with microsomal fractions obtained from tobacco culture cells (Thai et al., 1999).

Tomato VTE contents are highly dependent on SlVTE5 but not on SlFOLK

In order to gain further experimental evidence regarding SlVTE5 function in the VTE biosynthesis, plants with reduced VTE5 expression levels were generated by RNAi expression. Among ten independent primary *SlVTE5*-RNAi transformants, three lines with a significant reduction in *VTE5* mRNA levels were selected for further analyses; *SlVTE5*-RNAi#1, *SlVTE5*-RNAi#7 and *SlVTE5*-RNAi#11 (Supplemental Fig. S2A). *SlVTE5*-knockdown lines showed no evident morphological alterations under normal growth conditions. Moreover, the pattern of fruit degreening was apparently unaltered in these silenced lines (Supplemental Fig. S2B).

High performance liquid chromatography (HPLC) analyses showed that *SlVTE5* knockdown resulted in a dramatic reduction (80-90%) of total tocopherol contents both in leaves and in fruits

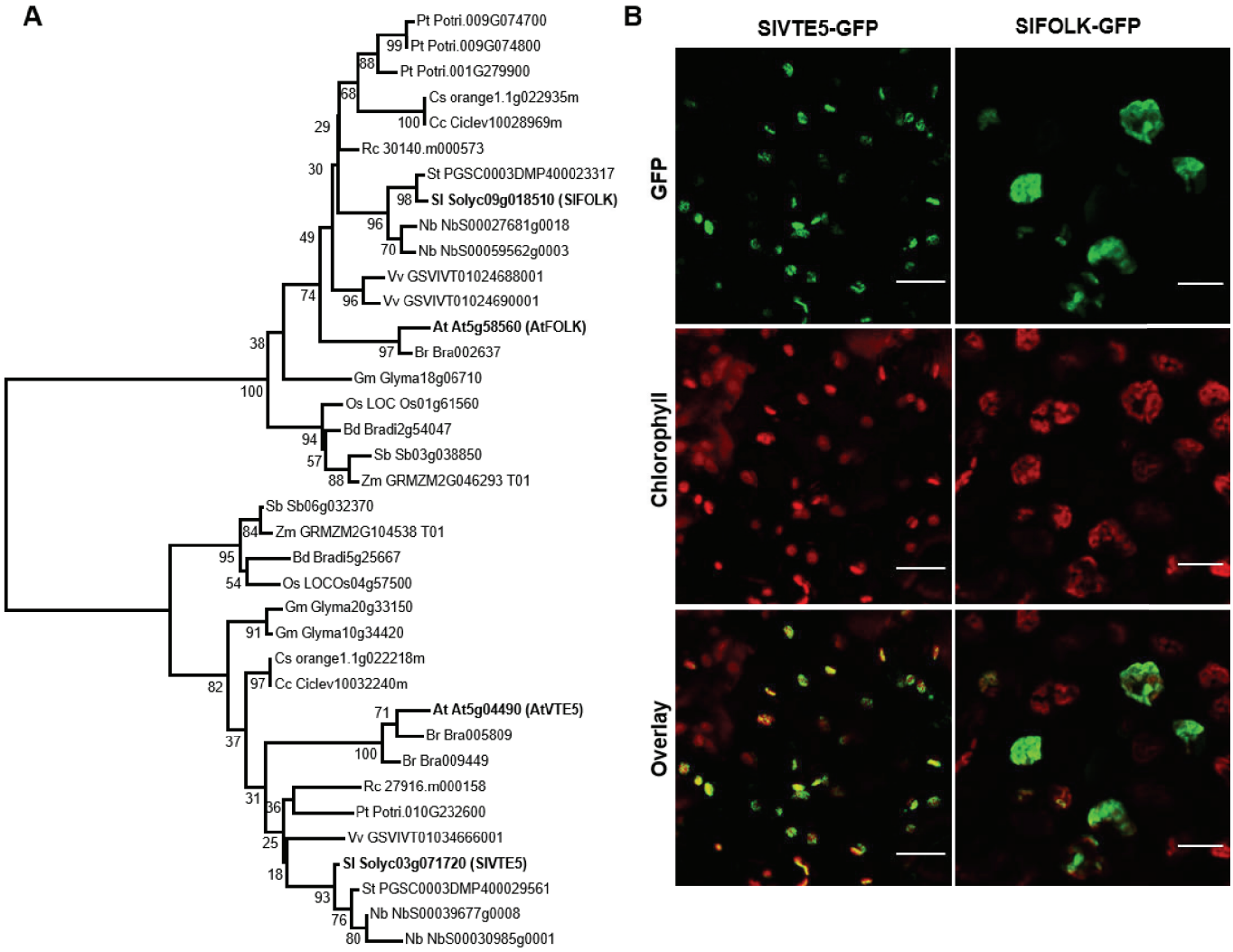

Figure 1. Phylogenetic analysis and subcellular localization of VTE5 and FOLK proteins. (A) Neighbor-joining phylogeny of VTE5 and FOLK homologs in flowering plants, which were identified by Blastp searches using AtVTE5 as the query against the Phytozome database (http://www.phytozome.net). Br, *Brassica rapa;* Bd, *Brachypodium distachyon*; Cc, *Citrus clementina*; Cs, *Citrus sinensis*; Pt, *Populus trichocarpa;* Nb, *Nicotiana benthamiana*; St, *Solanum tuberosum;* Sb, *Sorghum bicolor;* Zm, *Zea mays;* Os, *Oryza sativa;* Vv, *Vitis vinifera;* Rc, *Ricinus communis.* Gene numbers following names are based on those listed at Phytozome, with the exception of Arabidopsis ID. (B) Transient expression of SlVTE5-GFP and SlFOLK-GFP fusion proteins in foliar tobacco epidermal and mesophyll cells, respectively, indicate chloroplast targeting by confocal microscopy. Scale bars correspond to 10 μm and 20 μm for SlVTE5-GFP and SlFOLK-GFP images, respectively.

(Fig. 2A). Relative tocopherol composition remained unaltered in both organs as all four forms were reduced proportionally as compared to the total content in transgenic lines (Supplemental Table S1). Notably, we detected only traces of tocotrienols in *SlVTE5*-RNAi lines (data not shown). These results ruled out the possibility that depletion of tocopherols could be compensated by tocotrienol production in these plants.

The VTE5 deficiency in transgenic lines would be expected to increase free phytol content (Valentin et al., 2006). We therefore assayed the amount of this metabolite in leaves and fruits by gas chromatography coupled to mass spectrometry (GC-MS). While in mature leaves and ripe fruits of wild-type tomato plants free phytol amount ranged from 100 to 190 nmol g^{-1} of dry weight, in the

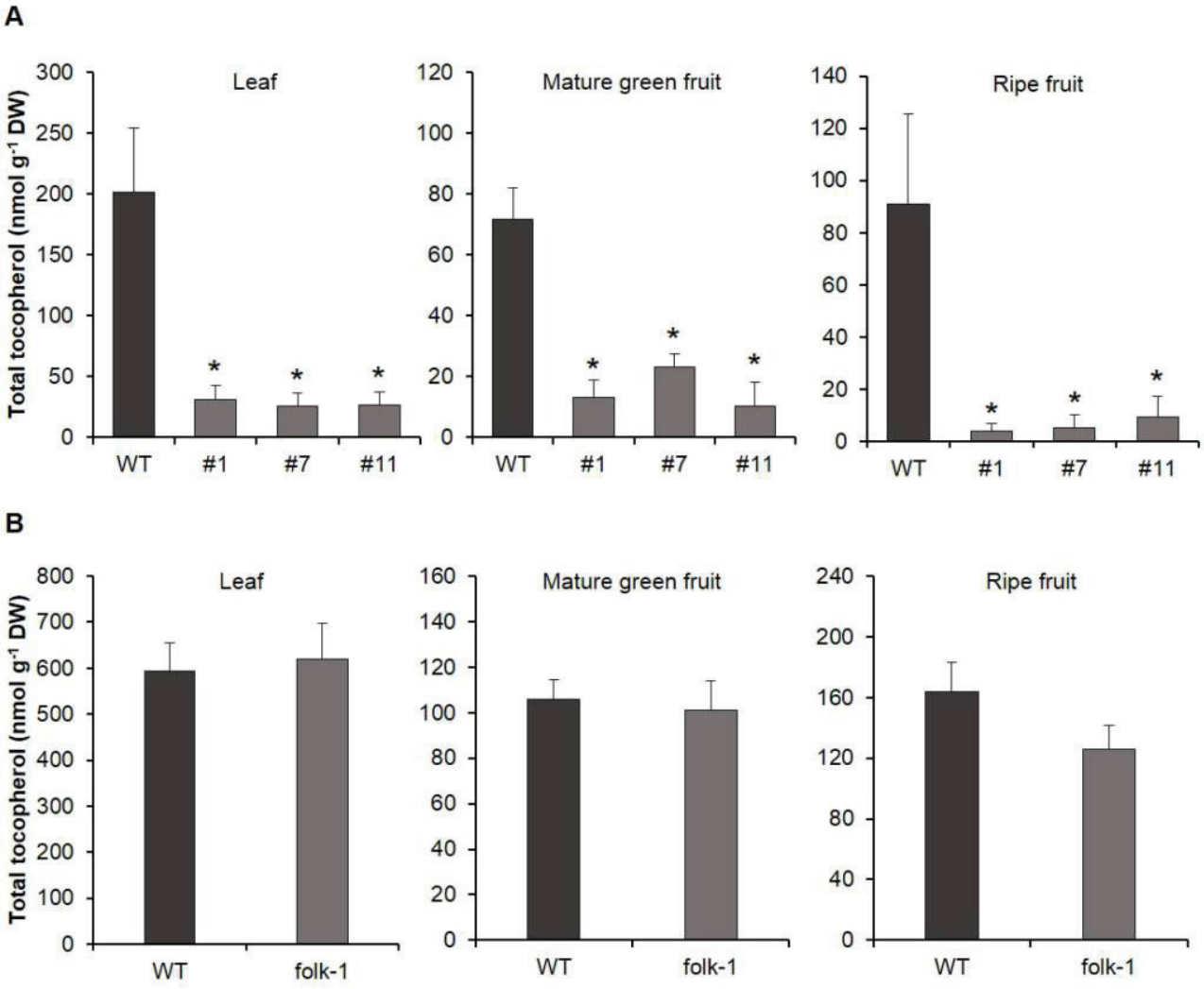

Figure 2. Total tocopherol content in *SlVTE5*-knockdown lines and *folk-1* mutant. Total tocopherol was measured in leaves, mature green and ripe fruits of *SlVTE5*-RNAi lines (A) and *folk-1* mutant (B). Data represent the mean ± SD of five biological replicates. Asterisk denotes significant differences between the wild-type (WT) and the transgenic lines (ANOVA/Dunnett's test, $P < 0.05$). DW, dry weight.

counterparts from *SlVTE5*-RNAi lines this prenyl alcohol accumulated four to five times more (Fig. 3). Interestingly, the molar amount of free phytol that accumulated in leaves was in the same order of magnitude as the reduction in total tocopherol contents, in contrast, the increase in free phytol was 10 times higher than the decrease in VTE in ripe fruits (Supplemental Table S2).

Due to sequence similarity between the tomato chloroplast-targeted phosphatidate cytidylyltransferases proteins SlVTE5 and SlFOLK, and the lack of a complete functional characterization of the latter, the putative impact of SlFOLK on tocopherol metabolism was also explored. In this case, a Targeting Induced Local Lesions IN Genomes (TILLING)-based molecular screening was applied to identify a loss-of-function mutation in the *SlFOLK* using a tomato (*S. lycopersicum,* cv. Micro-Tom) mutant collection generated by ethyl methanesulfonate (EMS) (Just et al., 2013). Among the identified mutants, one, named *folk-1*, displayed a G to A mutation disrupting the 3' splicing site of intron 4. Sequence analyses of *folk-1* cDNA from homozygous mutant plants revealed that this lesion led to the use of a cryptic 3′ splicing site in intron 4, resulting in a mRNA

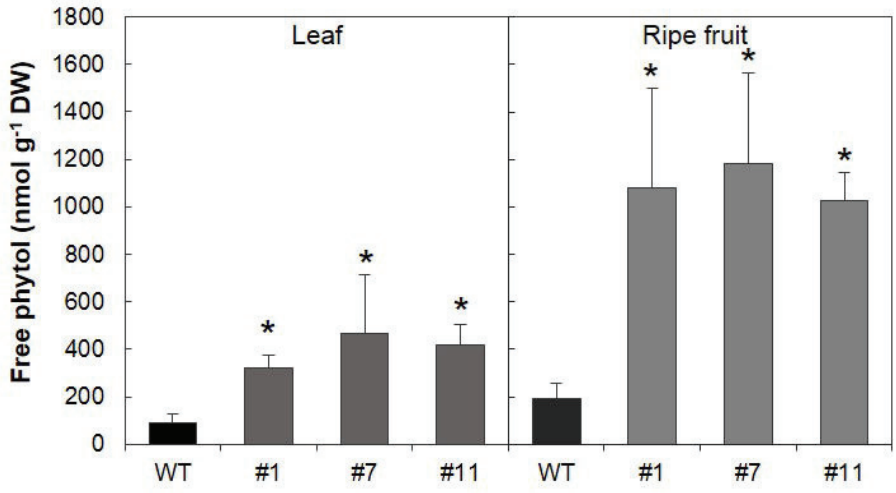

Figure 3. Free phytol content in leaves and ripe fruits of the *SlVTE5*-knockdown tomato plants. Data represent the mean ± SD of at least three biological replicates. Asterisk denotes significant differences between the wild-type (WT) and the transgenic lines (ANOVA/Dunnett's test, $P < 0.05$). DW, dry weight.

that lacks exon 4 and contains a fragment of intron 4 (Supplemental Fig. S3A). This aberrantly spliced transcript thereby contains a premature stop codon that presumably leads to a truncated protein (Supplemental Fig. S3B). Alternative transcripts that carry premature termination codons are often subjected to nonsense-mediated decay, a regulatory RNA degradation pathway (Kim et al., 2009). In this sense, expression analysis by qPCR showed that the amount of the aberrant mRNA in *folk-1* corresponded to only 10% of the fully spliced transcript found in wild-type plants (Supplemental Fig. S3C). VTE levels in these mutants were much the same as in wild-type plants, suggesting a small, if any, contribution of *SlFOLK* to tocopherol biosynthesis both in leaves and in fruits of *S. lycopersicum* (Fig. 2B). Having demonstrated the major role of VTE5 in tomato tocopherol metabolism, we further performed a comprehensive phenotypic characterization of *SlVTE5*-silenced plants.

Downregulation of SlVTE5 boosted phytyl ester synthesis in leaves

Free phytol can be esterified directly with fatty acids derived from activated acyl groups. Fatty acid phytyl esters (FAPEs) increase during stress-associated Chl degradation (*i.e.* nitrogen deprivation) and senescence (Ischebeck et al., 2006; Gaude et al., 2007; Lippold et al., 2012). To address the question whether the increased phytol levels might affect FAPE contents in the *SlVTE5*-downregulated plants, the levels of these compounds were measured by direct infusion quadrupole-time-of-flight tandem mass spectrometry (Q-TOF MS/MS). Notably, *SlVTE5* silencing resulted in a dramatic increase of FAPE content up to 10-fold in leaves. In contrast, fruits from *SlVTE5*-RNAi transgenic plants exhibited levels of FAPE identical to those of wild-type plants (Fig. 4).

Besides the total amount, *SlVTE5*-knockdown highly affected FAPE composition in leaves (Fig. 5A). With the exception of palmitic (16:0) and linolenic (18:3) acids, the profile analysis showed that the contribution of the different acyl chains was not proportional to the increment in

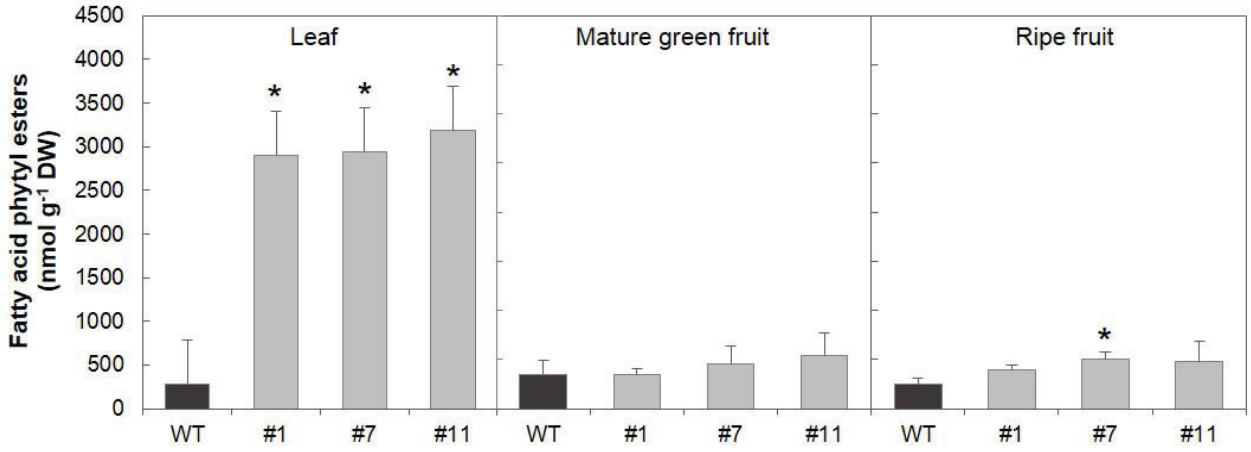

Figure 4. Total fatty acid phytyl ester (FAPE) content in *SlVTE5*-knockdown tomato plants. Data represent the mean ± SD of at least three biological replicates. Asterisk denotes significant differences between the wild-type (WT) and the transgenic lines (ANOVA/Dunnett's test, $P < 0.05$). DW, dry weight.

total FAPE content observed in VTE5-deficient plants. Particularly, FAPEs containing oleic acid (18:1), hexadecatrienoic acid (16:3), and medium-chain fatty acids (10:0, 12:0, 14:0) showed a reduction in their relative content, while FAPEs containing stearic acid (18:0) and linoleic acid (18:2) became the predominant forms, increasing at least two-fold compared to wild-type. In agreement with the finding that FAPE total content in transgenic fruits were similar to those in wild-type (Fig. 4), the FAPE compositions at mature green and ripe stages remained almost unchanged (Fig. 5B and 5C).

Chlorophyll content is not affected in SlVTE5-knockdown lines

To examine whether *SlVTE5*-silencing affects Chl metabolism, we determined Chl *a*, Chl *b* and pheophytin *a* (Phein *a*) levels in leaves and fruits at three different ripening stages by HPLC. The contents of these compounds were largely unaltered in both tested organs, suggesting that accumulation of phytol did not significantly affect Chl and Phein *a* levels in tomato (Fig. 6).

SlVTE5 silencing alters prenyllipid metabolism in fruits

Besides tocopherols, the plastidial antioxidant network includes a variety of prenyllipids derived from the MEP isoprenoid pathway with strong antioxidant properties, such as carotenoids, prenylquinones (plastoquinone-9, PQ-9) and other tocochromanols (e.g. plastochromanol-8, PC-8) (Nowicka et al., 2013). To investigate whether tocopherol deficiency in *SlVTE5*-silenced lines is compensated by any other non-enzymatic antioxidant mechanism, we performed a comprehensive profiling of prenyllipids (Table I). Prenylquinone and tocochromanol contents were determined from a lipidomic profile obtained by reverse-phase ultra-high pressure liquid chromatography coupled to quadrupole-time-of-flight mass spectrometry (UHPLC-QTOF MS) method. In leaves and ripe fruits of the transgenic plants, depletion of tocopherol was accompanied by a decrease of α-

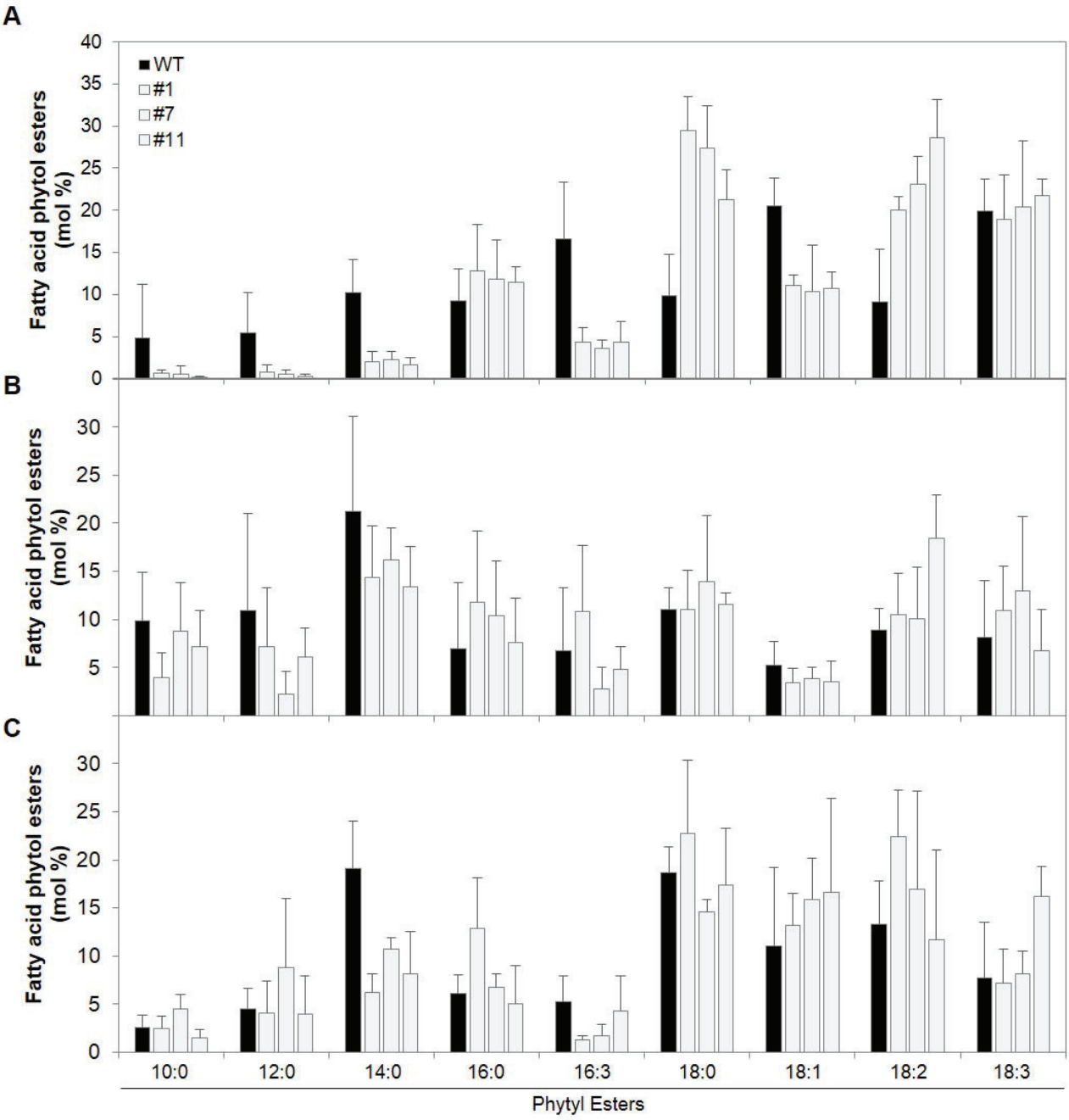

Figure 5. Molecular species composition of fatty acid phytyl esters (FAPEs) in *SlVTE5*-knockdown tomato plants. FAPEs were measured in leaves (A), mature green (B) and ripe fruits (C). Data represent the mean ± SD of at least three biological replicates.

tocopherolquinone, an oxidized intermediate of the tocopherol redox cycle (Table I); yet the level of this metabolite remained unchanged in mature green fruits. Remarkably, the levels of photosynthetic electron carrier phylloquinone (vitamin K) (Lohmann et al., 2006), another product of phytyl diphosphate-dependent biosynthesis, did not change between *SlVTE5*-knockdown lines and wild-type control.

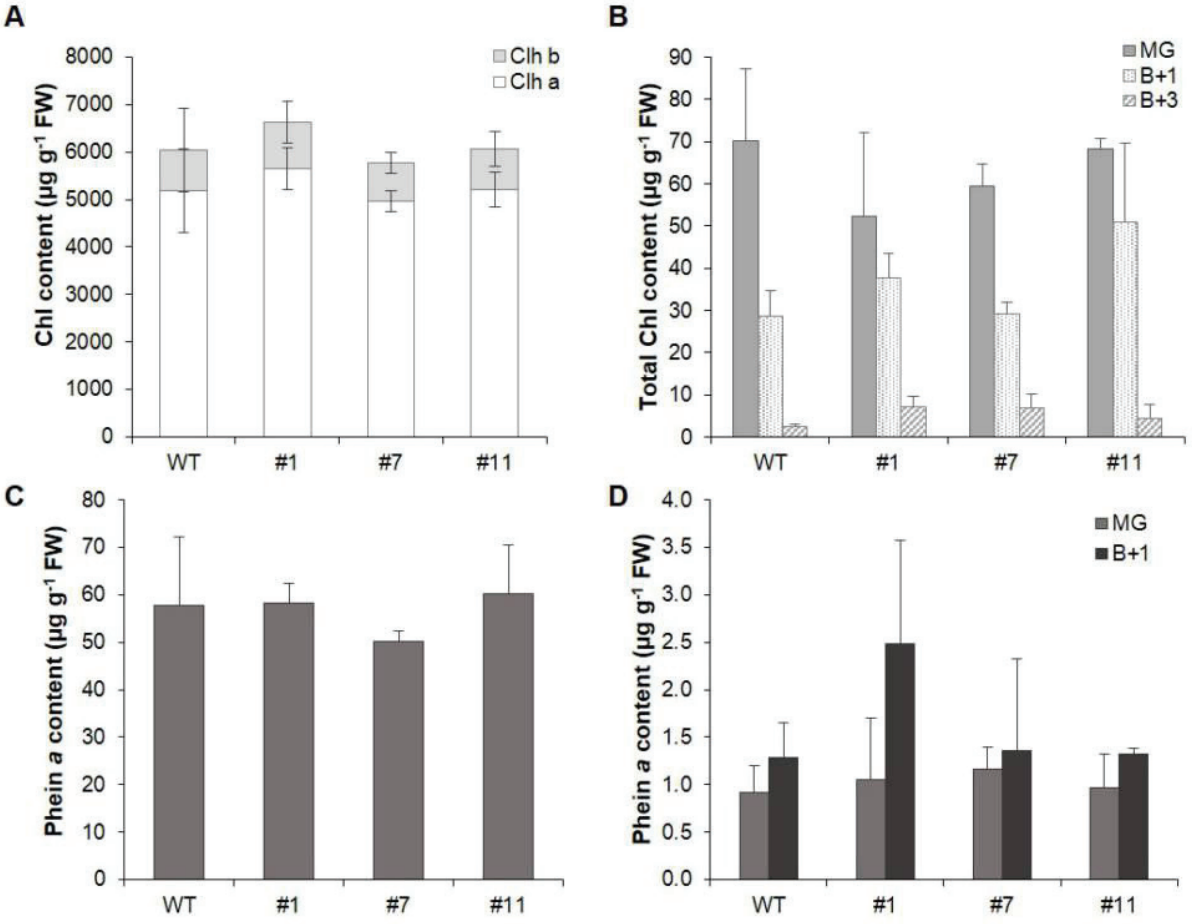

Figure 6. Chlorophyll (Chl) and pheophytin *a* (Phein *a*) content in *SlVTE5*-knockdown tomato plants. Quantification of Chl and Phein *a* in leaves (A, C) and in fruits (B, D) at mature green (MG), breaker+1 (B+1) and breaker+3 (B+3) stage. Data represent the mean ± SD of at least three biological replicates. No significant differences were observed (ANOVA/Dunnett's test, $P > 0.05$). FW, fresh weight.

The presence of the reduced and oxidized forms of PQ-9 in tomato plants has already been reported (Jones et al., 2013) and our data showed that PC-8 is also found in *S. lycopersicum*, both in leaves and fruits (Supplemental Fig S4). As described for other species (Kruk et al., 2014), in wild-type tomato, PC-8 was less abundant than tocopherols in leaves; while the amount of these tocochromanols were similar in tomato fruits (Fig. 2 and Supplemental Fig S4).

The comparison of prenyllipid profiles between wild-type and *SlVTE5*-knockdown leaves revealed that PQ-9 forms (PQ-9, PQH_2-9 and PQ-OH) remained unchanged. By contrast, a reduction to 50% of PC-8 content was observed in *SlVTE5* transgenic RNAi lines, which was accompanied by lower levels of its oxidation product, PC-OH (Table I). In sharp contrast, the prenylquinone pool of fruits from the *SlVTE5*-RNAi lines was significantly increased. PQ-9 levels were more than two-fold higher in the silenced lines, although the reduced form PQH_2-9 remained unchanged. Intriguingly, the levels of the mitochondrial prenylquinone UQ-10 were also about two-fold increased in *SlVTE5*-RNAi fruits. In addition, PC-8 accumulated up to two-fold in both mature green and ripe fruits of the

transgenic lines (Table I). These results suggest that the pools of PQ-9 and PC-8 contributes to fulfilling antioxidant function in the transgenic fruits.

Carotenoid contents, measured by HPLC in leaves and mature green fruits, remained largely unaltered in the transgenic lines (Table I). Although no differences in visual appearance were identified (Supplemental Fig S2), at the ripe stage, silenced fruits exhibited 30% less lycopene than the wild-type plants. Moreover, lycopene precursors (phytoene, phytofluene and ζ-carotene) were also reduced. This observation suggests a perturbation in the carbon flux towards carotenoid synthesis in the *SlVTE5*-RNAi fruits.

Tocopherol deficiency affects antioxidant capacity

Differences in the total antioxidant capacity between *SlVTE5*-RNAi and wild-type tomato plants were evaluated in non-polar extracts by the Trolox equivalent antioxidant capacity (TEAC) assay, which measures 2,2′-azino-bis (3-ethylbenzo-thiazoline)-6-sulfonic acid (ABTS) radical-scavenging capacity. The TEAC assay showed a reduction in leaves and fruits of the *SlVTE5*-knockdown lines, in a statistically significant way in line #1 (in leaves), in line #7 at the mature green stage and in lines #1 and #11 at the ripe stage (Fig. 7). These results emphasize the role of tocopherol in antioxidant protection since the increase in prenyllipid contents exhibited in the fruits of the transgenic lines did not compensate the TEAC values up to those observed in wild-type plants. However, VTE deficiency in leaves has a milder effect on the antioxidant capacity though no obvious compensatory effect was identified among the measured compounds.

VTE5 deficiency affects the expression of VTE metabolism-related genes

The biochemical profile described above showed that *SlVTE5* silencing results in an adjustment in prenyllipid and FAPE metabolism. In order to understand whether these changes could be associated with differential gene expression regulation, mRNA levels of genes encoding proteins involved in MEP, shikimate, tocochromanol, carotenoid and Chl metabolism (Quadrana et al, 2013; Lira et al, 2014; Almeida et al., 2015), as well as in prenylquinone and FAPE synthesis were measured by real time quantitative PCR (qPCR) (Fig. 8A). Genes that showed significantly different mRNA levels in at least two transgenic *SlVTE5 RNAi* lines and, when applicable, the third followed the same trend are shown in Fig. 8. The complete set of data is shown in Supplemental Table S3.

Genes of tocochromanol biosynthesis did not exhibit a consistent expression tendency in leaves of *SlVTE5*-knockdown lines. In fruit, the elevated expression of *HPPD(1)* and *HPPD(2)* is in agreement with the increased prenylquinone content in silenced plants. Moreover, in ripe fruit of the transformants, increase in *VTE3(1)* expression also coincided with the higher content of PC-8 and PQ-9. Intriguingly, the expression of the gene encoding the SOLANESYL-DIPHOSPHATE

SYNTHASE (SPS), which catalyzes the formation of the PQ-9 or PC-8 side chain, was decreased in mature green fruits, suggesting a negative feedback regulatory mechanism.

In leaves, an apparent reduction in the Chl degradation pathway was observed in *SlVTE5*-RNAi, as indicated by a downregulation of *STAY-GREEN1* (*SGR1*) and *PHEOPHORBIDE A OXYGENASE* (PAO) expression. Although Chl contents remained invariant, the observed

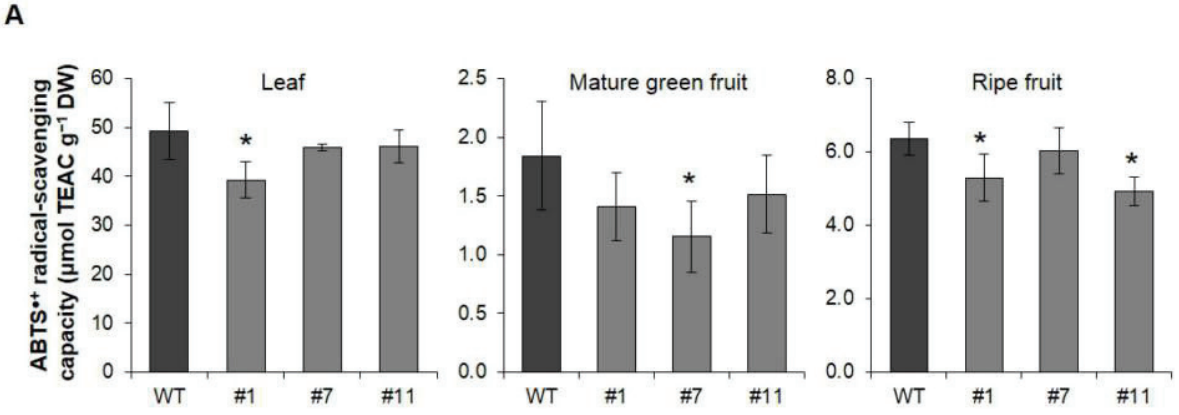

Figure 7. Trolox equivalent antioxidant capacity (TEAC) in leaves and fruits of *SlVTE5*-knockdown tomato plants. Data represent the mean ± SD of five biological replicates. Measurements are from three technical replicates. Asterisk denotes significant differences between the wild-type (WT) and the transgenic lines (ANOVA/Dunnett's test, $P < 0.05$). DW, dry weight.

transcriptional down-regulation may reflect a response to phytol accumulation. This scenario contrasts with that observed in fruits where *SGR1* was up-regulated in transgenic plants compared to wild-type. Additionally, ripe fruit of transgenic lines showed higher mRNA levels of *PHEOPHYTINASE* (*PPH*).

Regarding carotenoid biosynthesis, only certain genes showed significant changes in their mRNA levels in leaves and mature green fruits of the transformants, although the biochemical profiles of these compounds remained unaltered when compared to wild-type. By contrast, in ripe fruits, the increased levels of *CHROMOPLAST-SPECIFIC β-LYCOPENE CYCLASE* (*CYC-β*) transcripts could account for the reduction in lycopene and its immediate precursors verified in the transgenic lines.

Finally, the *PALE YELLOW PETAL 1* (*PYP1*) gene, the ortholog of the *A. thaliana PHYTYL ESTER SYNTHASE1* (*PES1*) (Ariizumi et al., 2014), showed increased levels of transcripts in the leaves of the *SlVTE5*-knockdown lines, in agreement with the higher FAPE contents observed in these organs.

Measurements of carbohydrate metabolism, photosynthesis and yield parameters suggest carbon export impairment in VTE5 deficient plants

To evaluate whether tocopherol deficiency affects carbon fixation and partitioning, starch and soluble sugar content, photosynthetic performance and yield parameters were assessed. Leaves of 5-week-old silenced plants showed up to 4.5-fold increase in starch content accompanied by a 20%

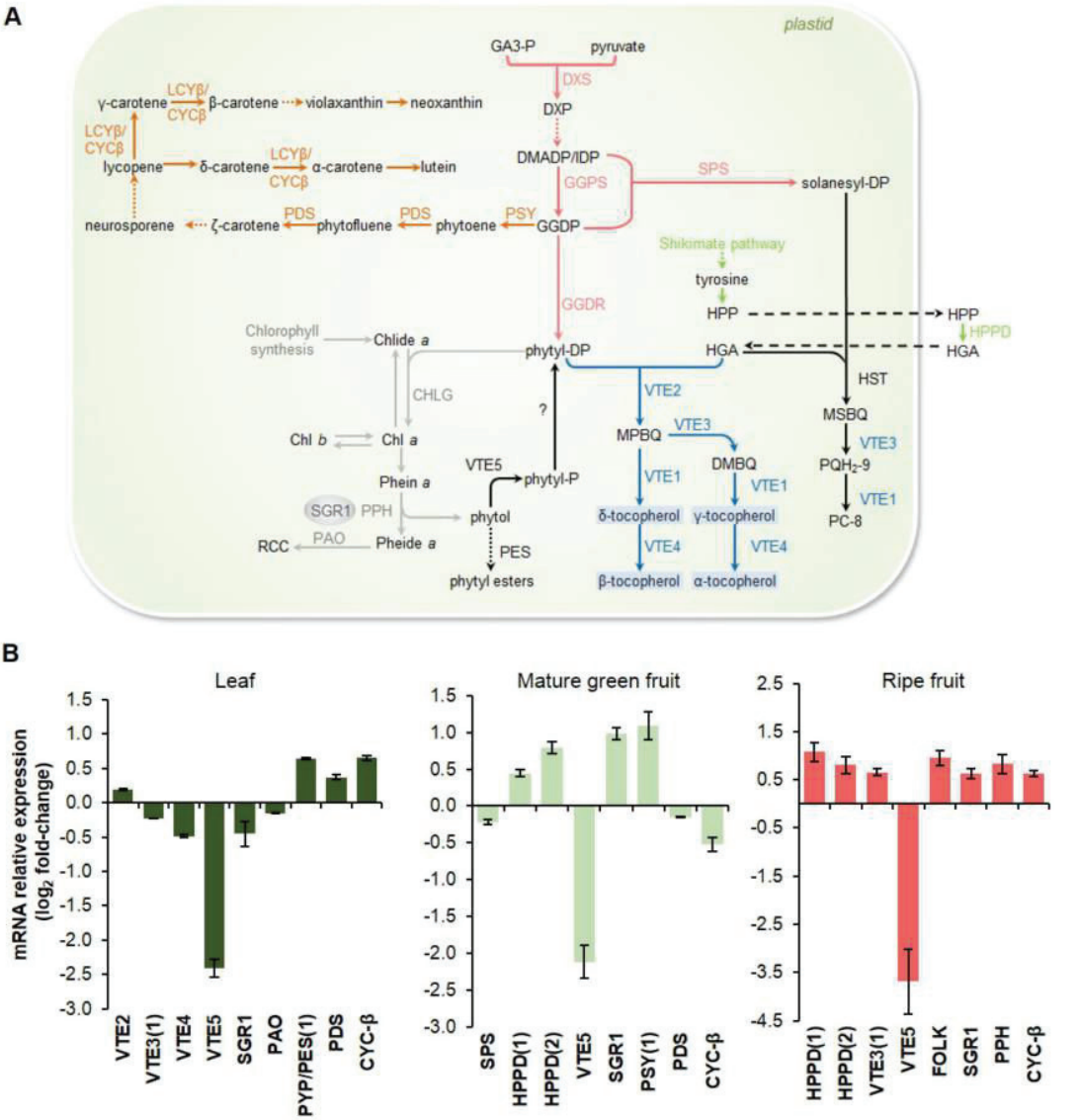

Figure 8. Changes in gene expression levels of some key isoprenoid-metabolism related genes resulting from *SlVTE5* downregulation in both leaves and fruits. (A) Steps in the pathways of which transcripts of genes encoding enzymes were measured are indicated by gene abbreviations. The genes are the following: 1-deoxy-D-xylulose-5-P synthase (DXS); geranylgeranyl diphosphate reductase (GGDR); 4-hydroxyphenylpyruvate dioxygenase (HPPD); homogentisate phytyl transferase (VTE2); 2,3-dimethyl-5-phytylquinol methyltransferase (VTE3); tocopherol cyclase (VTE1); γ-tocopherol-C-methyl transferase (VTE4); phytoene synthase (PSY); phytoene desaturase (PDS); chloroplast-specific β-lycopene cyclase (LCYβ); chromoplast-specific β-lycopene cyclase (CYCβ); chlorophyll synthase (CHLG); staygreen 1 (SGR1); pheophytinase (PPH); pheophorbide a oxygenase (PAO); phytol kinase (VTE5); farnesol kinase (FOLK); homogentisate solanesyl transferase (HST); solanesyl-diphosphate synthase (SPS). Abbreviated intermediate metabolites are: glyceraldehyde 3-phosphate (GA3-P); 1-deoxy-D-xylulose-5-P (DXP); isopentenyl diphosphate (IDP); dimethylallyl diphosphate (DMADP); geranylgeranyl-diphosphate (GGDP); hydroxyphenylpyruvate (HPP); homogentisate (HGA); chlorophyllide a (Chlide a); chlorophyll a (Chl a); chlorophyll b (Chl b); pheophytin a (Phein a); pheophorbide a (Pheide a); red chlorophyll catabolite (RCC); 2-methyl-6-geranylgeranylbenzoquinol (MPBQ); 2,3-dimethyl-6-geranylgeranylbenzoquinol (DMBQ); 2-methyl-6-solanyl-1,4-benzoquinol (MSBQ); plastoquinol-9 (PQH_2-9); plastochromanol-8 (PC-8). (B) Expression data are means ± SEM of three biological replicates of $\log_2$-fold changes compared to the corresponding organ of the wild-type control. Only genes that showed significantly different mRNA levels in *SlVTE5*-knockdown lines are shown (permutation test, $P < 0.05$). For simplicity, solely data from *SlVTE5*-RNAi#7 were represented. The complete data set is available in Supplemental Table S3.

decrease in sucrose levels compared to wild-type control (Fig. 9). Concomitantly, the carbon assimilation rates were reduced in *SlVTE5*-knockdown plants, while the photochemical parameters displayed moderate reductions in maximum photosystem II (PSII) quantum efficiency (F_v'/F_m') and

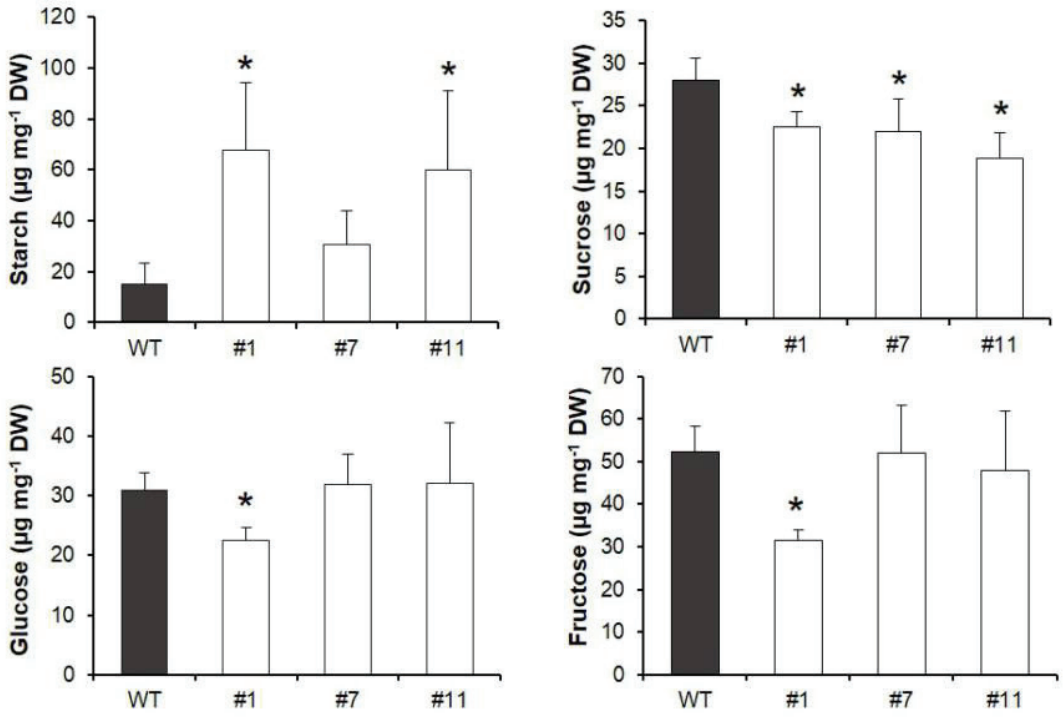

Figure 9. Starch and soluble sugars levels in source leaves in *SlVTE5*-knockdown tomato plants. First-fully expanded leaves were harvested from 5-week-old plants at the middle of the light cycle. Starch is given in µg glucose equivalents. Data are means ± SD of five biological replicates. Asterisk denotes significant differences between the wild-type (WT) and the transgenic lines (ANOVA/Dunnett's test, $P < 0.05$). DW, dry weight.

efficiency of PSII activity (Φ_{PSII}) (Fig. 10). The chloroplast ultrastructure was mostly preserved in transgenic lines (Supplemental Fig. S5).

In agreement with carotenoid profiling and gene expression pattern, transgenic plants displayed a delay in fruit development and ripening as indicated by the frequency of red and green fruits, as well as, the red fruit yield compared to control genotype at harvest time (Table II). Moreover, they displayed a yield penalty evidenced by a modest reduction in the harvest index. These results suggest that efficiency in photosynthate partitioning is compromised by the VTE deficiency.

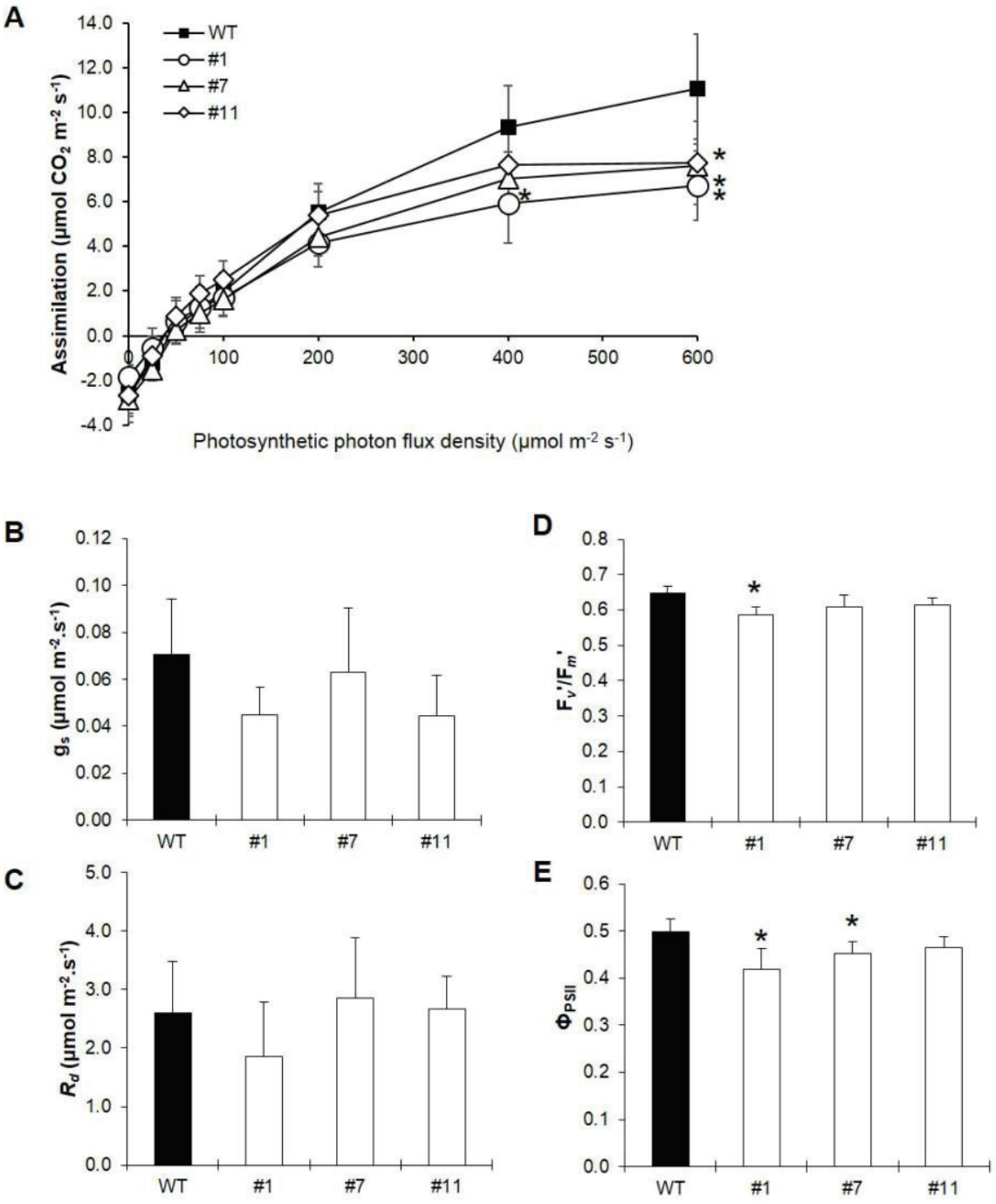

Figure 10. Gas-exchange and PSII efficiency parameters in *SlVTE5*-knockdown tomato plants. The response of carbon assimilation (A) to light intensity (A); leaf stomatal conductance (g_s) (B); leaf dark respiration (R_d) (C); light-adapted PSII maximum quantum efficiency (F'_v/F'_m) (D) and PSII operating efficiency (Φ_{PSII}) (E). Data correspond to measurements in the first fully expanded leaf of 5-week-old plants and represent the means ± SD of 5 biological replicates. Asterisk denotes significant differences between the wild-type (WT) and the transgenic lines (ANOVA/Dunnett's test, $P < 0.05$).

DISCUSSION

Several reports have dissected tocopherol biosynthesis, identified QTLs that determine VTE accumulation and characterized regulatory mechanisms that control the VTE biosynthetic pathway (DellaPenna and Mène-Saffrané, 2011; Almeida et al, 2011; Quadrana et al., 2013; Martinis et al., 2013, 2014; Quadrana et al., 2014; C. Zhang et al., 2013; W. Zhang et al., 2014). One well-defined metabolic constraint is the availability of phytyl diphosphate precursor for tocopherol biosynthesis, which can be derived from *de novo* biosynthesis *via* MEP pathway and from Chl phytyl tail recycling (Ischebeck et al., 2006; Zhang et al., 2013; Quadrana et al., 2013). It is known that the phytol hydrolysis of Chl is the primary source of prenyl chain for tocopherol biosynthesis in *A. thaliana* seeds (Valentin et al., 2006). However, functional analysis of the phytol salvage pathway has been limited to this species. In this study, we took advantage of the Chl degradation coupled with an active MEP pathway during tomato fruit ripening to further understand the cross-talk between both pools of phytyl diphosphate. Moreover, the comprehensive metabolite profiling performed in tomato *SlVTE5*-silenced plants allowed to gain insights into the interactions between phytol recycling and lipid and carbon metabolisms, exposing distinct metabolic adjustment in leaves and fruits. Even with an active phytyl diphosphate *de novo* synthesis, the *SlVTE5*-knockdown tomato plants showed 80% and 85% reduction in VTE content in leaves and fruits, respectively, when compared with the wild-type genotype. These data demonstrated that in tomato VTE biosynthesis is mostly dependent on the salvage pathway for phytyl diphosphate synthesis in both source and sink organs. Furthermore, these findings suggest that *SlVTE5* is the main – if not sole – contributor to VTE5 activity. The analysis of the tomato *folk-1* mutant suggested that *SlFOLK* is not involved in reactivation of free phytol. Moreover, the chloroplast targeting of SlFOLK-GFP apparently contrasts with its putative role as farnesol kinase. Farnesol is the product of the salvage pathway for farnesyl diphosphate isoprenoid intermediate (Hermmerlin et al., 2012). Feeding experiments using tobacco cells demonstrated that farnesol is readily taken up by plant cells and incorporate into sterols, proteins and UQ-10, all non-chloroplastic isoprenoids derivatives (Thai et al., 1999; Hemmerlin and Bach, 2000). FOLK activity was found associated with microsomal fractions obtained from tobacco culture cells (Thai et al., 1999) and isolated membranes from Arabidopsis seedlings (Fitzpatrick et al., 2011). In this context, future work will be necessary to unveil the role of *SlFOLK* in plant lipid metabolism.

In agreement with the downregulation of *SlVTE5* expression, free phytol, the substrate of the phytol kinase reaction, accumulates in leaves of the transgenic lines. Interestingly, the amount of free phytol accumulating corresponds to the decrease in tocopherol content, suggesting that a large proportion of phytol-diphosphate derived from the phytol phosphorylation pathway is used for tocopherol biosynthesis in tomato. Furthermore, FAPEs are strongly increased in the *SlVTE5*-RNAi lines mature leaves. These results raise an intriguing issue concerning the origin of the phytol that sustains FAPE synthesis in *SlVTE5*-knockdown lines. FAPEs are plastogobule compounds that

represent a class of stress-induced lipids in higher plants and it has been proposed that they are transient sinks for the deposition of fatty acids and phytol (Gaude et al., 2007). It was demonstrated that the phytol moiety of FAPEs is mostly derived from Chl degradation (Lippold et al., 2012). While the amount of Chl in the transgenic lines remained unchanged, it is possible that Chl turnover is increased. This might indicate that phytol for FAPE synthesis could be derived from Chl turnover in *SlVTE5*-RNAi lines. Alternatively, the origin of FAPE-associated phytol might be explained by the impairment in catabolism, which in plants involves the production of phytenoyl-CoA in chloroplasts that is further degraded by α-oxidation in peroxisomes and mitochondria similar to that described in animals (Araújo et al., 2011). It is worth to mention that phylloquinone levels, another phytyl diphosphate chain–containing molecule, remained similar to control both in leaves and fruits, indicating that SlVTE5-dependent salvage pathway does not affect vitamin K synthesis in tomato. This result coincides with the previous observation of feeding experiments of Arabidopsis seedlings with radiolabelled phytol (Ischebeck et al., 2006).

Tocopherol deficiency not only impacts lipid profile but also carbon metabolism and the whole plant physiology. *SlVTE5*-knockdown tomato plants showed higher starch accumulation in mature leaves that correlated with a lower CO_2 assimilation rate, suggesting a carbohydrate-mediated feedback inhibition rather than a direct impact of tocopherol deficiency on photosynthetic capacity (Adams et al., 2013; Asensi-Fabado et al., 2014). Besides, the reduction of the photochemical parameters in VTE5-deficient plants is indicative of a mild impairment at PSII. These photosynthetic and carbon flux alterations were accompanied by a subtle reduction of the number of harvestable fruits and harvest index under normal growth conditions, suggesting a blockage of sugar export from leaves towards sink organs in *SlVTE5*-knockdown tomato plants. A similar phenotype has been described in potato *VTE1*-RNAi lines (Hofius et al., 2004; Asensi-Fabado et al., 2014) and *vte2 A. thaliana* during low-temperature adaptation (Maeda et al., 2006; 2008). Regarding the molecular mechanism, Song et al. (2010) provided robust genetic evidence that alterations in extra-plastidic lipid metabolism are upstream of the defect in photoassimilate export in VTE deficient plants, which is mediated by fatty acid desaturases (FADs). Particularly, it was reported that VTE depletion led to increase linoleic acid (18:2) content and reduced level of linolenic acid (18:3). Consistent with this, one of the acyl groups that mostly contribute to the total FAPEs increase in the chloroplasts of the *SlVTE5*-silenced tomato lines was 18:2. In addition, our lipidomic data revealed that the plastidal digalactosyldiacylglycerol (DGDG), which mainly consist of pairs including 18:3 species, were reduced in leaves of *SlVTE5*-RNAi compared to wild-type (Supplemental Table S4), resembling the lipid alterations previously reported (Maeda et al., 2006; 2008). It has been proposed that changes in membrane lipid composition as a result of tocopherol deficiency might affect the properties of the secretory membrane systems (Maeda et al., 2008; 2014). Recently, the sugar export blockage

phenotype observed in VTE deficient plants was found to be independent of callose deposition in phloem parenchyma cells (Asensi-Fabado et al., 2014; Maeda et al., 2014), raising a question regarding the underlying mechanism. Since tomato has been described as an apoplastic phloem loader (Muller et al., 2014), we could speculate that the alteration of endomembrane vesicle formation affects the sucrose efflux mediated by SWEET proteins, which have been described as key players for phloem transport (Chen et al., 2012). Alternatively, the carbon export impairment observed in *SlVTE5*-knockdown tomato plant could be the result of the cross-talk between lipid and sugar metabolism by a yet unknown process probably involving sugar sensing proteins as proposed by Asensi-Fabado et al. (2014).

VTE5 deficiency triggered different metabolic responses in fruits compared to those described for leaves, probably reflecting the intrinsic physiological differences between organs and their corresponding plastids. Firstly, fruits of *SlVTE5*-silenced plants accumulated predominantly phytol in the free form rather than channeled into FAPEs synthesis. Secondly, the observation that non-tocopherol prenylquinone pool, including PQ-9 and PC-8, are increased in fruits of *SlVTE5*-silenced plants suggests that a regulatory compensation mechanism between the tocopherol and prenylquinone pathways exists in this organ. The ability of plastoquinol (PQH_2-9), ubiquinol (UQH_2-10), the reduced forms of PQ-9 and UQ-10, respectively, and PC-8 to scavenge ROS and inhibit lipid peroxidation have been demonstrated before (Kruk and Trebst, 2008; Nowicka et al., 2013; Rastogi et al., 2014). Moreover, PQ-9 and PC-8 have already been associated with inhibition of lipid peroxidation and $^1O_2$ scavenging in VTE deficient *A. thaliana vte2* mutants (Mène-Saffrané et al., 2010). Likewise, in tomato leaves, the reduction of PQ-9 content by virus-induced gene silencing approach resulted in increased tocopherol and UQ-10 levels (Jones et al., 2013). It is worth mentioning that even with the compensatory effect of prenylquinones and PC-8, the TEAC was reduced in mature green and ripe fruits of the *SlVTE5*-silenced lines, highlighting the role of tocopherol in determining antioxidant capacity (Almeida et al., 2015). Finally, *SlVTE5*-RNAi ripe fruits exhibited perturbations in carotenoid pathway. The reduced amount of lycopene and its biosynthetic precursors can be explained by the higher transcripts levels of *SGR1* found at mature green and ripe stages. Besides having an important role in the regulation of plant Chl degradation and senescence (Hortensteiner, 2009), SGR1 also regulates lycopene and β-carotene biosynthesis by direct interaction with PSY(1), thereby inhibiting its activity (Luo et al., 2013). Simultaneously, the failure of coordinate transcriptional repression of the *CYC-β* in *SlVTE5*-knockdown ripe fruits could also account for the reduced abundance of acyclic carotenoids. The amounts of β-carotene and lutein in transgenic fruits were similar to those in wild-type at the expense of the preceding carotenoids. Additionally, it has been demonstrated that the level of *PPH* transcripts decreases during tomato fruit ripening (Lira et al., 2014); however, *SlVTE5*-silenced ripe fruits displayed higher levels of *PPH*

transcripts than control genotype. Thus, the comprehensive analysis of the biochemical and transcriptional data together with the results of the yield experiment indicates that the B+6 profiled transgenic fruits are indeed less ripe than wild type ones. The reduction in carbohydrate export described above might be in part responsible for the delay in fruit development and ripening resulting in a reduced proportion of mature fruits at harvest time in *SlVTE5*-knockdown plants.

CONCLUSIONS

The results presented here clearly show that in tomato VTE biosynthesis is largely dependent on the salvage pathway for phytyl diphosphate synthesis rather than the *de novo* synthesis of phytyl diphosphate from the MEP pathway in both leaves and fruits. VTE5 deficiency affected lipid metabolism evidenced by the abundance and composition of FAPEs in leaves and prenyllipids in fruits. Together, these results exposed the complexities of the metabolic regulation that emerge from isoprenoid pathway network, which involves a tight control between precursor supply and utilization highly dependent on the plastid type. Moreover, our data highlighted the cross-talk between lipid and carbon metabolism mediated by tocopherol that resulted in the impairment of carbon export in *SlVTE5*-knockdown tomato plants that compromise fruit development and ripening.

MATERIALS AND METHODS

Plant material, growth conditions and sampling

Seeds of tomato (*Solanum lycopersicum* L., cv. Micro-Tom) were obtained from the Laboratory of Hormonal Control of Plant Development (www.esalq.usp.br/tomato). The *farnesol kinase-1* (*folk-1*) tomato mutant was isolated from a mutagenized EMS Micro-Tom collection from INRA, France, as previously described (Just et al., 2013). *Nicotiana benthamiana* seeds were obtained from INTA, Argentina. Tomato and tobacco plants were grown in a greenhouse under automatic irrigation (four times a day) at an average mean temperature of 25°C, 11.5 h/13 h (winter/summer) photoperiod and 250-350 μmol m^{-2} s^{-1} of incident photo-irradiance. Source (the first fully expanded leaf) and sink (first apical leaf not fully expanded) leaves were sampled. Fruits at mature green, breaker+1 (B+1), breaker+3 (B+3) and ripe (B+6) stages were harvested approximately at 35, 38, 40 and 43 days after anthesis, respectively. All samples were frozen in liquid N_2, homogenized and stored at -80 °C. Leaves and pericarp tissue powder destined for pigment, prenyllipid and sugar determination were lyophilized until completely dry before extraction. For yield evaluation, an independent experiment was performed. Destructively harvest took place at a point where the largest possible number of

fruits were ripe without visible overripening (15-week-old) (Vicente et al., 2015). At harvest time, aerial biomass was weighted and all the fruits were counted and weighted.

Phylogenetic Analysis

For phylogenetic analysis, Blastp searches were performed using the protein sequences of *A. thaliana* VTE5 (At5g04490) and FOLK (At5g58560) as queries against the tomato genome (http://solgenomics.net). Putative VTE5 and FOLK sequences from other plant species were similarly identified by Blastp from the genomes of *Brassica rapa*, *Brachypodium distachyon*, *Citrus clementina*, *Citrus sinensis*, *Populus trichocarpa, Solanum tuberosum, Sorghum bicolor, Zea mays, Oryza sativa, Vitis vinifera, Ricinus communis* found in the Phytozome database (http://www.phytozome.net/ database). *Nicotiana benthamiana* sequences were also obtained from the Sol Genomics Network database (http://solgenomics.net). The sequences were aligned using the MUSCLE package available in the MEGA 5.0 software with default parameters (Tamura et al., 2007), and Neighbor-Joining phylogeny with 5000 bootstrap replications were created with the distances calculated according to the best model pointed by MEGA 5.0.

Subcellular localization assay

For subcellular localization experiments, full-length complementary DNA (cDNA) minus stop codon of predicted protein-coding *SlVTE5* (Solyc03g071720, 951 bp) and *SlFOLK* (Solyc09g018510, 861 bp) were amplified by PCR using Taq Platinum Pfx DNA polymerase (Life Technologies) with following primers pairs: FUS-VTE5-F and FUS-VTE5-R; FUS-FOLK-F and FUS-FOLK-R (Supplemental Table S5). Amplification products were cloned separately into a pENTR/d-TOPO vector (Life Technologies) and then, the expression cassettes were transferred to the binary vector pK7FWG2 (Karimi et al., 2002) by recombination using LR clonase (Life Technologies) resulting in C-terminal GFP fusion protein (pK7FWG2-*SlVTE5* and pK7FWG2-*SlFOLK*). The constructs were transferred into *A. tumefaciens* strain GV3101. Transient expression in *N. benthamiana* cells and imaging by confocal laser scanning microscopy were performed as described by de Godoy et al. (2013).

Generation of SlVTE5-knockdown lines

Transgenic plants expressing a *SlVTE5*-specific intron-spliced hairpin sequence under the control of the cauliflower mosaic virus 35S promoter were obtained for RNA interference (RNAi)-mediated silencing of Solyc03g071720 *locus*. A 237 bp fragment of *SlVTE5* was amplified by PCR using the primers RNAi-VTE5-F and RNAi-VTE5-R listed in Supplemental Table S5 and Taq DNA polymerase (Life Technologies). PCR products were cloned into pENTR/d-TOPO vector (Life

Technologies) via directional cloning, and then recombined into the binary vector pK7GWIWG2 (Karimi et al., 2002), using LR clonase (Life Technologies) to generate a hairpin construct (pK7GWIWG2(I)-*SlVTE5*). After sequence verification by restriction digest analysis and sequencing, the plasmid was transferred to *Agrobacterium tumefaciens* strain EHA105. Agrobacterium-mediated transformation of *S. lycopersicum* (cv. Micro-Tom) cotyledon explants was performed according to Pino et al. (2010). Primary transformants (T0) that rooted on 100 mg L^{-1} kanamycin were transferred to compost and grown in the greenhouse as described above.

For T1 and T2 segregation progenies, transgenic lines were subjected to initial antibiotic selection performed in the greenhouse by spraying 400 mg L^{-1} kanamycin on 14-day-old seedlings for three consecutive days (Pino et al., 2010). The presence of the transgene in T0, T1 and T2 kanamycin-resistant plants was detected by PCR in genomic DNA using a 35S promoter primer (35S-right, 5'-CCCACTATCCTTCGCAAG-3') and the RNAi-VTE5-R primer.

Identification of the folk-1 tomato mutant by TILLING

Mutations in *SlFOLK* were identified by screening a highly EMS-mutagenized *S. lycopersicum* (cv. Micro-Tom) population (Just et al., 2013). The screened genomic region included gene fragment predicted by CODDLE (Codons Optimised to Discover Deleterious Lesions) program (Till et al., 2003) to result in most likely deleterious effects on proteins. The TILLING protocol was performed essentially as previously described (Okabe et al. 2011). Amplicons were obtained by nested-PCR using unlabeled external primers and internal primers 5'labelled with IRDye 700 and IRDye 800 dye described in Supplemental Table S5. Induced point mutations were identified by means of the mismatch-specific endonuclease ENDO 1. Digested and labelled DNA fragments were separated on a LI-COR DNA analyser (LI-COR, USA) using denaturing polyacrylamide gels.

The distribution of the mutation and prediction analysis of its relevance was achieved by using PARSESNP (Project Aligned Related Sequences and Evaluate SNPs) software (Taylor and Greene, 2003) and SIFT (Sorting Intolerant from Tolerant) software (Ng and Henikoff, 2003; http://sift.jcvi.org/).

qPCR analysis

RNA extraction, cDNA synthesis, primer design and qPCR assays were performed as described by Quadrana et al. (2013). Primer sequences used are detailed in Supplemental Table S5. qPCR reactions were carried out in a 7500 real-time PCR system (Applied Biosystems) using 2X SYBR Green Master Mix reagent (Life Technologies) in a 20 µl final volume. Absolute fluorescence data were analyzed using the LinRegPCR software package (Ruijter et al., 2009) in order to obtain quantification cycle (Cq) values and to calculate PCR efficiency. Expression values were normalized

against the geometric mean of two reference genes, *CAC* and *EXPRESSED,* according to Quadrana et al. (2013). A permutation test lacking sample distribution assumptions (Pfaffl et al., 2002) was applied to detect statistical differences ($P < 0.05$) in expression ratios using the algorithms in the fgStatistics software package (Di Rienzo, 2009).

Leaf gas exchange and fluorescence measurements

Gas exchange and chlorophyll fluorescence parameters were evaluated in five-week-old plants using a portable open gas-exchange system incorporating infra-red CO_2 and water vapor analyzers (LI-6400XT system; LI-COR) equipped with an integrated modulated chlorophyll fluorometer (LI-6400-40; LI-COR). Reference [CO_2] was held at 400 µmol mol^{-1} and temperature at 25˚C for all measurements. Air humidity inside the leaf chamber was controlled to the externally measured greenhouse relative humidity (50-60%). Carbon assimilation rate (A), leaf stomatal conductance (g_s), leaf dark respiration (R_d) and fluorescence parameters were measured at 600 µmol PPFD m^{-2} s^{-1} in the first fully expanded leaf between 10 am and 2 pm. The parameters derived from chlorophyll fluorescence, including light-adapted PSII maximum quantum efficiency (F'_v/F'_m), proportion of open PSII centers (photochemical quenching, qP), PSII operating efficiency (Φ_{PSII}), were calculated according to Genty et al. (1989).

Tocopherol, free phytol and fatty acid phytyl ester quantification

Tocopherol measurements were performed as previously described (Yang et al., 2011). For determination of free phytol, total lipid was extracted from lyophilized tissues, silylated and then quantified according to Lippold et al. (2012). Fatty acid phytyl esters were measured by direct infusion nanospray quadrupole-time-of-flight tandem mass spectrometry (Q-TOF-MS/MS; Agilent 6530 Accurate Mass Q-TOF) using methanol:chloroform:300 mM ammonium acetate [665:300:35 (v/v/v); Welti et al., 2002] as the solvent system. Fatty acid phytyl esters were detected in the positive ion mode by neutral loss scanning for m/z 278.2974, a fragment characteristic for the phytol moiety.

Chlorophyll and chlorophyll catabolites

Chlorophyll and green catabolites (chlorophyllide, pheophorbide, pheophytin) were extracted from 10 mg of lyophilized tissue during 17h at -20°C in 90% (v/v) acetone, 10% (v/v) 0.2 M Tris-HCl, pH 8.0, precooled to –20°C (5 mL g^{-1} initial fresh weight). After twice centrifugation (2 min, 16,000g, 4°C), supernatants were analyzed by HPLC as described (Langmeier et al., 1993). Chromatography was developed in a reverse phase HPLC column (ODS C18 Hypersil 5µM) with the solvent system consisteing of A [1M ammonium acetate:methanol, 1:4 (v/v)] and B [acetone:methanol, 1:4 (v/v)].

The program started with a linear gradient from A to B (15 min), continued with an isocratic run with B (10 min) and returned to A (2 min). Pigments were identified by their absorption spectra at 665 nm. For quantification, peak areas were analyzed and referred to calibration curves built from known quantities of standard pigments (Schelbert et al., 2009).

Prenyllipid analyses

Tocochromanols and prenylquinones were analysed by ultra-high pressure liquid chromatography coupled with atmospheric pressure chemical ionization-quadrupole time-of-flight mass spectrometry (UHPLC-APCI-QTOF-MS) as described in Martinis et al. (2013) with the following modifications. Briefly, 15 mg of lyophilized leaf and fruit tissue were exactly weighed and resuspended in 500 µL of tetrahydrofurane:methanol:water 42,5:42,5:15 (v/v/v). The mixture was homogenized using glass beads (1 mm of diameter) for 3 min at 30 Hz in a tissue lyser. After two rounds of centrifugation (3 min, 14,000*g* and 4°C), supernatants were transferred to HPLC vials. Prenyllipids were separated on a reverse-phase Acquity BEH C18 column (50 × 2.1 mm, 1.7 µm) under the following conditions: solvent A = water; solvent B = methanol; 80-100% B in 3 min, 100% B for 2 min, re-equilibration at 90% B for 0.5 min. The flow rate was 0.8 mL/min, and the injection volume was 2.5 µL. α-tocopherol, γ-tocopherol, δ-tocopherol, PQ-9 and PC-8 were quantified based on calibration curves obtained from standard compounds. Data were processed using MassLynx version 4.1 (Waters).

Carotenoids were extracted and detected as described in Almeida et al. (2011). Briefly, 400 µL of non-polar extracts were dried under N_2 and the residues resuspended in 150 µL methanol:ethyl-acetate (50:50, v/v). Chromatography was performed with an Agilent 1200 Series HPLC system coupled with a Diode Array Detector on a reverse phase column [Zorbax Eclipse Plus C18 (150 mm × 4.6 mm, 5 µm), Agilent Technologies] at room temperature using a 0.6 mL min^{-1} flow rate. The elution was performed with a linear gradient of solvent A [acetonitrile:methanol:0.1 M Tris buffer pH 8, 72:8:3 (v/v/v)] to solvent B [methanol:ethyl-acetate, 68:32 (v/v)] for 25 min, followed by 10 min in solvent B. For column equilibration, the mobile phase was returned to solvent A and maintained for 5 min. Carotenoids were identified at 440 nm by their order of elution and absorption spectra (Gupta et al., 2015) and co-migration with authentic standards (all-trans-lycopene, all-trans-β-carotene, lutein, violaxanthin, neoxanthin, zeaxanthin).

Soluble sugars and starch quantification

Ten milligrams of the freeze-dried samples from leaves and ripe fruits were five times extracted with 1.5 mL of 80% ethanol at 80 °C according to De Souza et al. (2013). Combined supernatants were dried under vacuum and then re-suspended in 1 mL of ultrapure water. To remove pigments, an extraction with 0.5 mL of chloroform was performed. Alcohol-soluble sugar identification and

quantification were done by a high performance anion exchange chromatography with pulsed amperometric detection (HPAEC/PAD) (Dionex-ICS3000, Dionex). Sugar separation was carried out on a CarboPac PA1 column using isocratic elution of 150 mM NaOH with a flow rate of 1 mL min^{-1}. The calibration curves were prepared using high purity standard solutions of glucose, fructose and sucrose with a concentration range from 50 to 200 µM.

For starch quantification, the dried insoluble material obtained after ethanol extraction was treated with α-amylase (120 U mL^{-1}, MEGAZYME) from *Bacillus licheniformis* and amyloglucosidase (30 U mL^{-1}, MEGAZYME) from *Aspergillus niger* according to Amaral et al. (2008). The glucose content obtained after starch hydrolysis was determined from extract aliquots of 20 and 50 µL for leaves and fruits, respectively, after an incubation with glucose oxidase/peroxidase and D-4-aminoantipirine (GOD/POD) (Labtest®, Brazil). Absorbance of quinoneimine dye, which is directly proportional to glucose concentration, was measured spectrophotometrically using an ELISA-type microplate reader at 490 nm. A standard curve was prepared using high purity glucose solution (SIGMA) ranging from 2.5 to 12.5 µg mL^{-1}.

Trolox equivalent antioxidant capacity (TEAC) assay

The TEAC assay was used to estimate antioxidant capacity of lipophilic extracts of tomato ripe fruits. The assay is based upon measuring the capacity of an extract to scavenge and detoxify the 2,2'-azin-obis-(3-ethylbenzothiazoline-6-sulfonic acid) ($ABTS^{\cdot+}$) radical. The antioxidant capacity of non-polar fruit extracts was assayed as previously described (Re et al., 1999), with minor modifications. The pre-formed radical $ABTS^{\cdot+}$ was produced by oxidation of 7 mM ABTS with potassium persulphate (2.45 mM final concentration) dissolved in ultrapure water. The mixture was incubated in the dark at room temperature for 12–16 h before use. The $ABTS^{\cdot+}$ solution was diluted with ethanol and adjusted to 0.70 ± 0.02 absorbance units at 734 nm.

Fifty microliters of diluted extract or Trolox standard was mixed with 150 µL of diluted $ABTS^{\cdot+}$ solution, and the absorbance was read at 734 nm after 10 min at 30ºC. The $ABTS^{\cdot+}$ antioxidant capacity was reported as µmol of TEAC per gram of sample on a dry weight basis calculated by comparing with a Trolox standard curve (0.015-0.50 mM). Analyses were run in triplicate at two dilutions for a total of six assays per sample.

Transmission electron microscopy

Leaf segments were fixed at 4 °C in Karnovsky's solution (2.5 % glutaraldehyde, 2 % (v/v) paraformaldehyde in 0.1 M sodium phosphate buffer pH 7.2) for 24 h. After washing in buffer, the samples were postfixed in buffered 1 % (w/v) osmium tetroxide, washed, dehydrated in a graded

series of acetone, and embedded in Spurr resin. The resin was polymerized at 60ºC. Ultrathin sections were stained with saturated uranyl acetate (Watson, 1958) and lead citrate (Reynolds, 1963) and observed using a Zeiss EM 900 transmission electron microscope.

Data analyses

Statistical analyses were performed using R statistical software (www.r-project.org). To determine significant differences between the transgenic lines and the control, data were analyzed by *t*-test or one-way analysis of variance (ANOVA) followed by a Dunnett's multiple comparison test with the level of significance set to 0.05.

SUPPLEMENTAL DATA

The following materials are available in the online version of this article.

Supplemental Fig. S1. Expression of *SlVTE5* and *SlFOLK* genes.

Supplemental Fig. S2. Downregulation of *SlVTE5* expression and fruit phenotype in transgenic lines.

Supplemental Fig. S3. Analysis of *folk-1* mutation.

Supplemental Fig. S4. Plastoquinone (PQ-9) and plastochromanol (PC-8) levels in *SlVTE5*-knockdown tomato plants.

Supplemental Fig. S5. Chloroplast ultrastructure resulting from *SlVTE5* downregulation.

Supplemental Table S1: Tocopherol content and composition of *SlVTE5*-knockdown tomato plants.

Supplemental Table S2. Moles of prenyllipids found in *SlVTE5*-knockdown tomato plants.

Supplemental Table S3. Transcriptional profile of genes encoding isoprenoid metabolism-related enzymes.

Supplemental Table S4. Changes in fatty acid-derived lipids in leaves of *SlVTE5*-knockdown lines compared with wild-type.

Supplemental Table S5. Primer used for each experiment.

ACKNOWLEDGEMENTS

We thank Silvia Blanco for technical assistant with transgenic plants and Waldir Caldeira for confocal microscopy imaging. FK thanks the University de Neuchâtel.

FIGURE LEGENDS

Figure 1. Phylogenetic analysis and subcellular localization of VTE5 and FOLK proteins. (A) Neighbor-joining phylogeny of VTE5 and FOLK homologs in flowering plants, which were identified by Blastp searches using AtVTE5 as the query against the Phytozome database (http://www.phytozome.net). Br, *Brassica rapa;* Bd, *Brachypodium distachyon*; Cc, *Citrus clementina*; Cs, *Citrus sinensis*; Pt, *Populus trichocarpa;* Nb, *Nicotiana benthamiana*; St, *Solanum tuberosum;* Sb, *Sorghum bicolor;* Zm, *Zea mays;* Os, *Oryza sativa;* Vv, *Vitis vinifera;* Rc, *Ricinus communis.* Gene numbers following names are based on those listed at Phytozome, with the exception of Arabidopsis ID. (B) Transient expression of SlVTE5-GFP and SlFOLK-GFP fusion proteins in foliar tobacco epidermal and mesophyll cells, respectively, indicate chloroplast targeting by confocal microscopy. Scale bars correspond to 10 μm and 20 μm for SlVTE5-GFP and SlFOLK-GFP images, respectively.

Figure 2. Total tocopherol content in *SlVTE5*-knockdown lines and *folk-1* mutant. Total tocopherol was measured in leaves, mature green and ripe fruits of *SlVTE5*-RNAi lines (A) and *folk-1* mutant (B). Data represent the mean ± SD of five biological replicates. Asterisk denotes significant differences between the wild-type (WT) and the transgenic lines (ANOVA/Dunnett's test, $P < 0.05$). DW, dry weight.

Figure 3. Free phytol content in leaves and ripe fruits of the *SlVTE5*-knockdown tomato plants. Data represent the mean ± SD of at least three biological replicates. Asterisk denotes significant differences between the wild-type (WT) and the transgenic lines (ANOVA/Dunnett's test, $P < 0.05$). DW, dry weight.

Figure 4. Total fatty acid phytyl ester (FAPE) content in *SlVTE5*-knockdown tomato plants. Data represent the mean ± SD of at least three biological replicates. Asterisk denotes significant differences between the wild-type (WT) and the transgenic lines (ANOVA/Dunnett's test, $P < 0.05$). DW, dry weight.

Figure 5. Molecular species composition of fatty acid phytyl esters (FAPEs) in *SlVTE5*-knockdown tomato plants. FAPEs were measured in leaves (A), mature green (B) and ripe fruits (C). Data represent the mean ± SD of at least three biological replicates.

Figure 6. Chlorophyll (Chl) and pheophytin *a* (Phein *a*) content in *SlVTE5*-knockdown tomato plants. Quantification of Chl and Phein *a* in leaves (A, C) and in fruits (B, D) at mature green (MG), breaker+1 (B+1) and breaker+3 (B+3) stage. Data represent the mean ± SD of at least three

biological replicates. No significant differences were observed (ANOVA/Dunnett's test, $P > 0.05$). FW, fresh weight.

Figure 7. Trolox equivalent antioxidant capacity (TEAC) in leaves and fruits of *SlVTE5*-knockdown tomato plants. Data represent the mean ± SD of five biological replicates. Measurements are from three technical replicates. Asterisk denotes significant differences between the wild-type (WT) and the transgenic lines (ANOVA/Dunnett's test, $P < 0.05$). DW, dry weight.

Figure 8. Changes in gene expression levels of some key isoprenoid-metabolism related genes resulting from *SlVTE5* downregulation in both leaves and fruits. (A) Pathway steps, for which the amount of mRNA of the gene encoding enzymes was measured, are indicated by gene abbreviations. The genes are the following: 1-deoxy-D-xylulose-5-P synthase (DXS); geranylgeranyl diphosphate reductase (GGDR); 4-hydroxyphenylpyruvate dioxygenase (HPPD); homogentisate phytyl transferase (VTE2); 2,3-dimethyl-5-phytylquinol methyltransferase (VTE3); tocopherol cyclase (VTE1); γ-tocopherol-C-methyl transferase (VTE4); phytoene synthase (PSY); phytoene desaturase (PDS); chloroplast-specific β-lycopene cyclase (LCYβ); chromoplast-specific β-lycopene cyclase (CYCβ); chlorophyll synthase (CHLG); staygreen 1 (SGR1); pheophytinase (PPH); pheophorbide a oxygenase (PAO); phytol kinase (VTE5); farnesol kinase (FOLK); homogentisate solanesyl transferase (HST); solanesyl-diphosphate synthase (SPS). Abbreviated intermediate metabolites are: glyceraldehyde 3-phosphate (GA3-P); 1-deoxy-D-xylulose-5-P (DXP); isopentenyl diphosphate (IDP); dimethylallyl diphosphate (DMADP); geranylgeranyl-diphosphate (GGDP); hydroxyphenylpyruvate (HPP); homogentisate (HGA); chlorophyllide a (Chlide a); chlorophyll a (Chl a); chlorophyll b (Chl b); pheophytin a (Phein a); pheophorbide a (Pheide a); red chlorophyll catabolite (RCC); 2-methyl-6-geranylgeranylbenzoquinol (MPBQ); 2,3-dimethyl-6-geranylgeranylbenzoquinol (DMBQ); 2-methyl-6-solanyl-1,4-benzoquinol (MSBQ); plastoquinol-9 (PQH2-9); plastochromanol-8 (PC-8). (B) Expression data are means ± SEM of three biological replicates of log2-fold changes compared to the corresponding organ of the wild-type control. Only genes that showed significantly different mRNA levels in SlVTE5-knockdown lines are shown (permutation test, $P < 0.05$). For simplicity, solely data from SlVTE5-RNAi#7 were represented. The complete data set is available in Supplemental Table S3.

Figure 9. Starch and soluble sugar levels in source leaves in *SlVTE5*-knockdown tomato plants. First-fully expanded leaves were harvested from 5-week-old plants at the middle of the light cycle. Starch is given in µg glucose equivalents. Data are means ± SD of five biological replicates. Asterisk denotes significant differences between the wild-type (WT) and the transgenic lines (ANOVA/Dunnett's test, $P < 0.05$). DW, dry weight.

Figure 10. Gas-exchange and PSII efficiency parameters in *SlVTE5*-knockdown tomato plants. The response of carbon assimilation (A) to light intensity (A); leaf stomatal conductance (g_s) (B); leaf dark respiration (R_d) (C); light-adapted PSII maximum quantum efficiency (F'_v/F'_m) (D) and PSII operating efficiency (Φ_{PSII}) (E). Data correspond to measurements in the first fully expanded leaf of 5-week-old plants and represent the means ± SD of 5 biological replicates. Asterisk denotes significant differences between the wild-type (WT) and the transgenic lines (ANOVA/Dunnett's test, $P < 0.05$).

Table I. Changes in prenyllipids contents in leaves and fruits of *SlVTE5*-knockdown lines compared with wild-type.

Prenyllipids (relative amounts)	WT	*SlVTE5*-RNAi #1	*SlVTE5*-RNAi #7	*SlVTE5*-RNAi #11
Leaf				
α-TQ	1.00 ± 0.18	**0.23 ± 0.03**	**0.22 ± 0.08**	**0.24 ± 0.01**
PC-8	1.00 ± 0.30	**0.52 ± 0.19**	**0.54 ± 0.19**	**0.36 ± 0.07**
PQ-9	1.00 ± 0.18	0.83 ± 0.15	0.87 ± 0.20	**0.63 ± 0.12**
PQH_2-9	1.00 ± 0.66	1.27 ± 0.59	1.02 ± 0.43	0.86 ± 0.37
PC-OH	1.00 ± 0.21	**0.65 ± 0.18**	0.72 ± 0.24	**0.51 ± 0.11**
PQ-OH	1.00 ± 0.20	1.01 ± 0.26	1.04 ± 0.27	0.70 ± 0.19
UQ-10	1.00 ± 0.24	0.83 ± 0.23	0.81 ± 0.12	0.81 ± 0.10
phylloquinone	1.00 ± 0.16	0.87 ± 0.12	0.84 ± 0.12	0.81 ± 0.12
β-carotene	1.00 ± 0.07	0.89 ± 0.04	0.91 ± 0.02	0.91 ± 0.07
lutein	1.00 ± 0.07	0.97 ± 0.06	0.96 ± 0.03	0.95 ± 0.03
violaxanthin/neoxanthin	1.00 ± 0.06	0.97 ± 0.06	1.00 ± 0.02	0.99 ± 0.06
Mature green fruit				
α-TQ	1.00 ± 0.15	1.11 ± 0.48	1.20 ± 0.47	1.13 ± 0.10
PC-8	1.00 ± 0.15	**1.89 ± 0.26**	**1.78 ± 0.05**	**1.88 ± 0.19**
PQ-9	1.00 ± 0.15	**2.11 ± 0.46**	**2.22 ± 0.42**	**2.22 ± 0.26**
PQH_2-9	1.00 ± 0.30	0.77 ± 0.23	1.24 ± 0.36	1.16 ± 0.36
PC-OH	1.00 ± 0.42	0.89 ± 0.34	1.10 ± 0.30	1.02 ± 0.29
PQ-OH	1.00 ± 0.26	1.31 ± 0.49	**1.74 ± 0.47**	1.52 ± 0.32
UQ-10	1.00 ± 0.13	**2.13 ± 0.24**	**1.76 ± 0.28**	**1.93 ± 0.34**
phylloquinone	1.00 ± 0.27	1.23 ± 0.18	1.25 ± 0.32	1.32 ± 0.16
β-carotene	1.0 ± 0.22	1.0 ± 0.16	0.9 ± 0.15	1.0 ± 0.16
lutein	1.0 ± 0.22	1.0 ± 0.10	1.1 ± 0.11	**1.3 ± 0.15**
violaxanthin/neoxanthin	1.0 ± 0.34	0.8 ± 0.16	0.8 ± 0.07	1.3 ± 0.20
Ripe fruit				
α-TQ	1.00 ± 0.25	**0.54 ± 0.04**	**0.64 ± 0.17**	**0.64 ± 0.15**
PC-8	1.00 ± 0.15	**2.29 ± 0.34**	**1.67 ± 0.20**	**2.07 ± 0.50**
PQ-9	1.00 ± 0.17	**2.40 ± 0.54**	**2.24 ± 0.20**	**1.76 ± 0.26**
PQH_2-9	1.00 ± 0.29	1.55 ± 0.39	1.77 ± 0.55	1.92 ± 1.06
PC-OH	1.00 ± 0.27	1.26 ± 0.51	1.35 ± 0.46	0.99 ± 0.42
PQ-OH	1.00 ± 0.07	2.27 ± 1.03	2.24 ± 0.80	2.10 ± 0.94
UQ-10	1.00 ± 0.14	**2.40 ± 0.38**	**1.96 ± 0.53**	**2.13 ± 0.24**
phylloquinone	1.00 ± 0.18	1.11 ± 0.18	1.32 ± 0.50	1.41 ± 0.50
phytoene	1.0 ± 0.09	**0.7 ± 0.11**	**0.7 ± 0.19**	**0.6 ± 0.10**
phytofluene	1.0 ± 0.14	**0.7 ± 0.13**	**0.7 ± 0.14**	**0.6 ± 0.08**
neurosporene	1.0 ± 0.22	0.7 ± 0.24	1.0 ± 0.18	**0.6 ± 0.20**
ζ-carotene	1.0 ± 0.20	**0.4 ± 0.17**	**0.3 ± 0.19**	**0.4 ± 0.18**
lycopene	1.0 ± 0.06	**0.8 ± 0.14**	**0.7 ± 0.08**	**0.7 ± 0.13**
β-carotene	1.0 ± 0.06	0.9 ± 0.20	0.9 ± 0.16	0.9 ± 0.14
lutein	1.0 ± 0.13	1.1 ± 0.13	1.0 ± 0.09	1.2 ± 0.25

Data were normalized to sample dry weight and expressed relative to wild type (WT) in each tissue. Values are represented as means ± SD. Terms in bold indicate a statistically significant difference by ANOVA/Dunnett's test ($P < 0.05$). α-tocopherolquinone (α-TQ), plastoquinone-9 (PQ-9), plastoquinol-9 (PQH_2-9), hydroxy-plastoquinone (PQ-OH), plastochromanol-8 (PC-8), hydroxy-plastochromanol (PC-OH), ubiquinone-10 (UQ-10).

Table II. Yield associated-traits of tocopherol-deficient tomato plants.

Trait	WT	*SlVTE5*-RNAi #1	*SlVTE5*-RNAi #7	*SlVTE5*-RNAi #11
Number of total fruits	36.2 ± 5.8	37.4 ± 4.7	40.8 ± 4.3	35.8 ± 1.5
Frequency red fruits (%)	63.9 ± 6.9	**49.6 ± 7.8**	54.0 ± 11.5	53.3 ± 8.8
Frequency green fruits (%)	37.3 ± 6.9	**50.4 ± 7.8**	46.0 ± 11.5	46.7 ± 8.8
Vegetative plant weight (g FW)	30.0 ± 8.3	34.3 ± 8.0	39.4 ± 6.9	34.0 ± 7.3
Total yield per plant (g FW)	114.4 ± 17.2	115.9 ± 11.3	125.9 ± 28.8	101.6 ± 16.9
Harvest index	0.79 ± 0.02	0.77 ± 0.04	**0.76 ± 0.02**	**0.75 ± 0.03**
Red yield /aerial biomass ratio	0.57 ± 0.08	**0.47 ± 0.11**	**0.50 ± 0.09**	0.52 ± 0.15

Vegetative plant weight was determined by weighing only the vegetative tissue (after harvesting the fruits) without the root. Harvest index was calculated as the ratio between total fresh yield per plant (red and green fruit mass) and aerial biomass (total yield + vegetative plant weight). Values indicate the mean ± SD of phenotypic values (n=5) determined for 15-week-old plants. Statistically significant differences between the wild-type (WT) control and transgenic lines are indicated in bold (*t*-test, $P < 0.05$). FW, fresh weight.

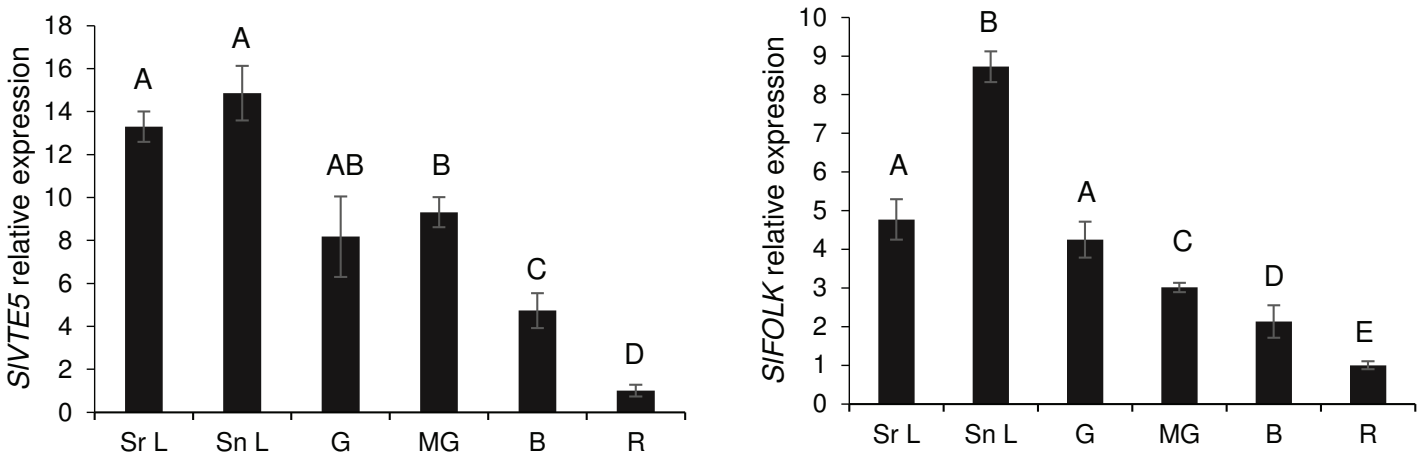

Supplemental Figure S1. Expression of *SlVTE5* and *SlFOLK*. (A) Relative *SlVTE5 and SlFOLK* expression were measured by qPCR in source (SrL) and sink (SnL) leaves, and green (G), mature green (MG), breaker (B) and ripe (R) fruits in at least three biological replicates. The means were calculated from two technical replicates and normalized against R fruit samples. Statistically significant differences ($P < 0.05$) are indicated with different letters according to permutation test.

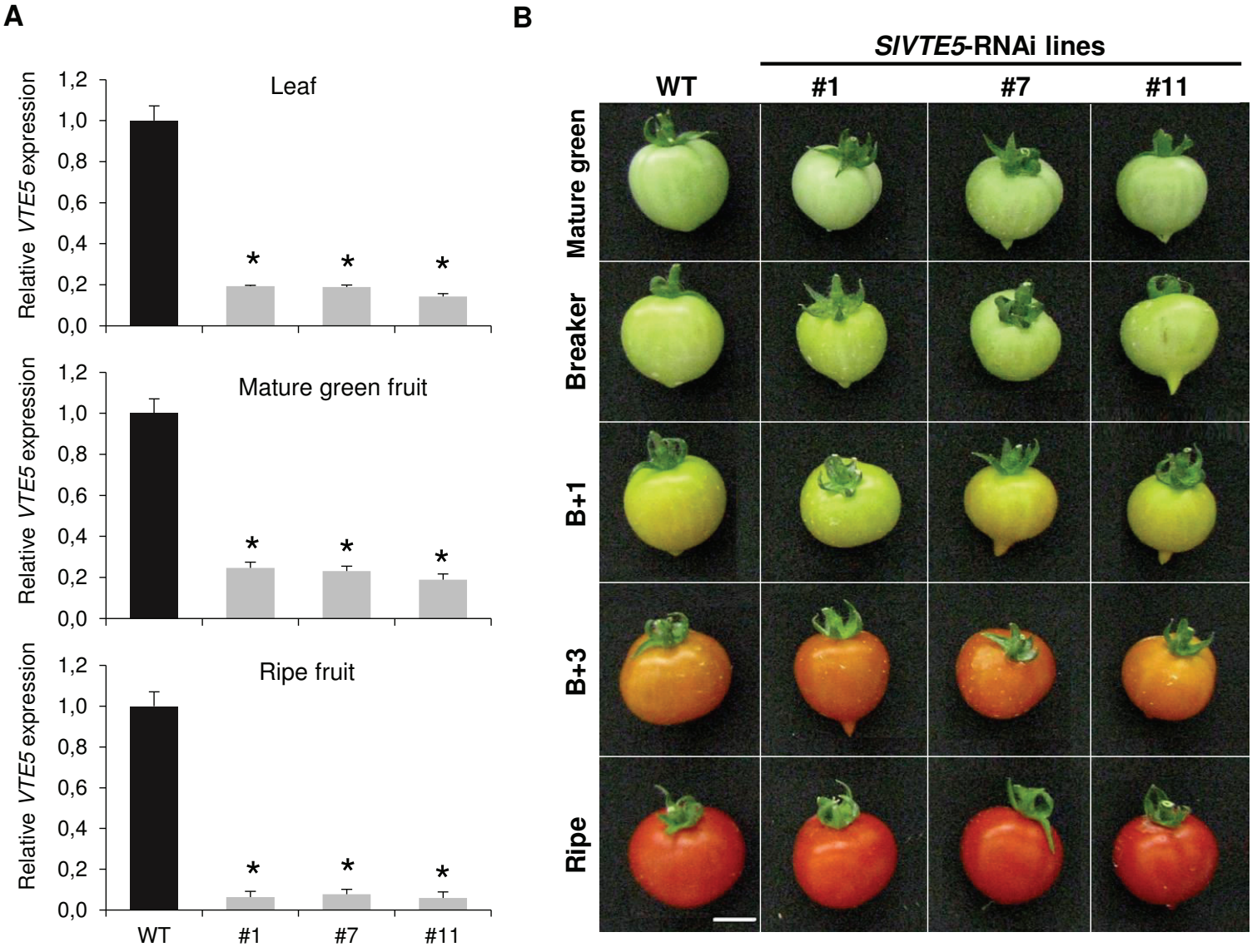

Supplemental Figure S2. Downregulation of *SlVTE5* expression and fruit phenotype in transgenic lines. (A) Relative expression of *SlVTE5* gene in wild type (WT) and *SlVTE5*-knockdown transgenic lines (#1, #7, and #11). Data are means ± SEM of five biological replicates. Asterisk denotes statistically significant differences (permutation test, $P < 0.05$). (B) Fruit phenotype at mature green, breaker, one day after breaker (B+1), three days after breaker (B+3) and ripe stages. Scale bar = 1cm.

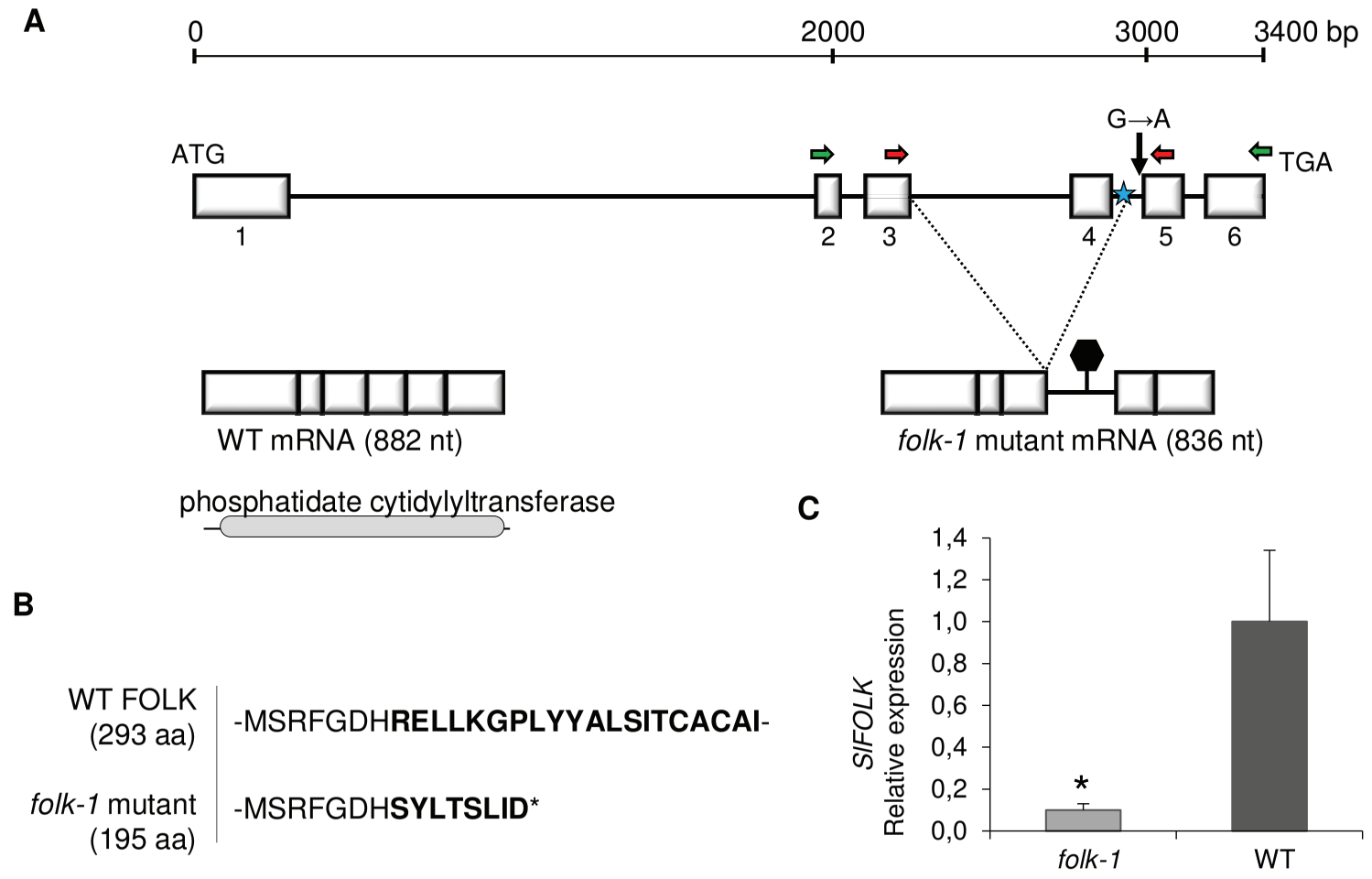

Supplemental Figure S3. Analysis of *folk-1* mutation**.** (A) Schematic diagram of *SlFOLK* (Solyc09g018510) splicing pattern showing the wild type (WT) and *folk-1* mutant mRNAs. The open boxes and solid lines represent exons and introns, respectively. The green arrows indicate the position of the primers used for TILLING screening and the red arrows indicate intron-flanking primers used for qPCR assay. The position of the G to A substitution (G2976A) is indicated in the 3' consensus splicing site of intron 4. The star denotes the 3' cryptic splicing site. The *folk-1* mutant mRNA generates a premature stop codon indicated by a black hexagon, which presumably affects the phosphatidate cytidylyltransferase domain. (B) Partial amino acid sequences deduced from WT and aberrant cryptic site transcripts. Frameshift in predicted amino acid sequence is indicated in bold. (C) qPCR analysis of *SlFOLK* expression in leaves of WT and *folk-1* mutant. Data are means ± SEM of three biological replicates. Asterisk denotes statistically significant differences (permutation test, $P < 0.05$). nt, nucleotide; bp, base pair; aa, amino acid.

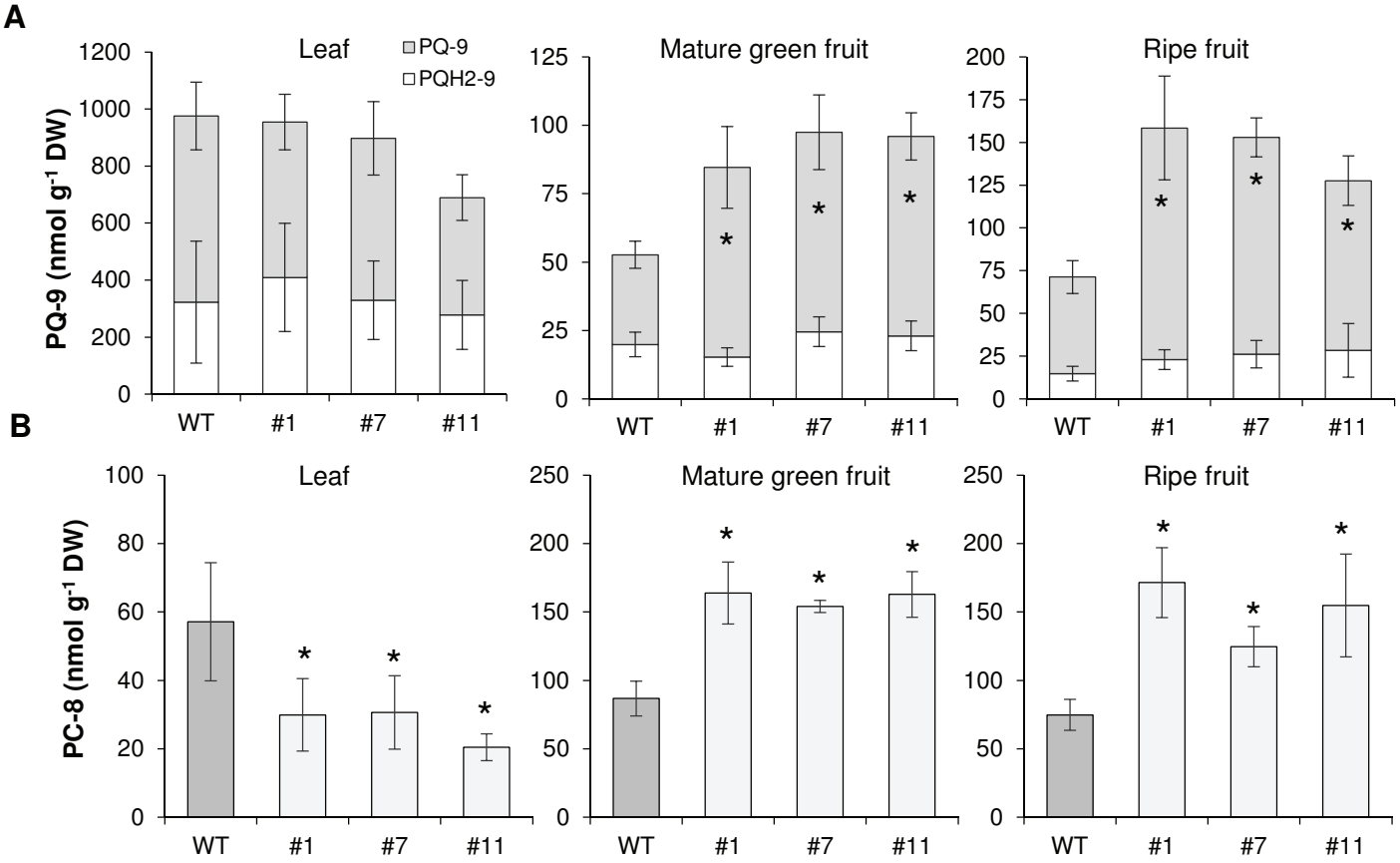

Supplemental Figure S4. Plastoquinone (PQ-9) and plastochromanol (PC-8) levels in *SlVTE5*-knockdown tomato plants. Prenylquinone were measured in leaves, mature green and ripe fruits of *SlVTE5*-RNAi lines. (A) Total PQ-9 content; bars indicate the fraction of oxidized (PQ-9) and reduced (PQH_2-9) forms. (C) PC-8 content. Data represent the mean ± SD of five biological replicates. Asterisk denotes significant differences between the wild-type (WT) and the transgenic lines (ANOVA/Dunnett's test, $P < 0.05$). DW, dry weight.

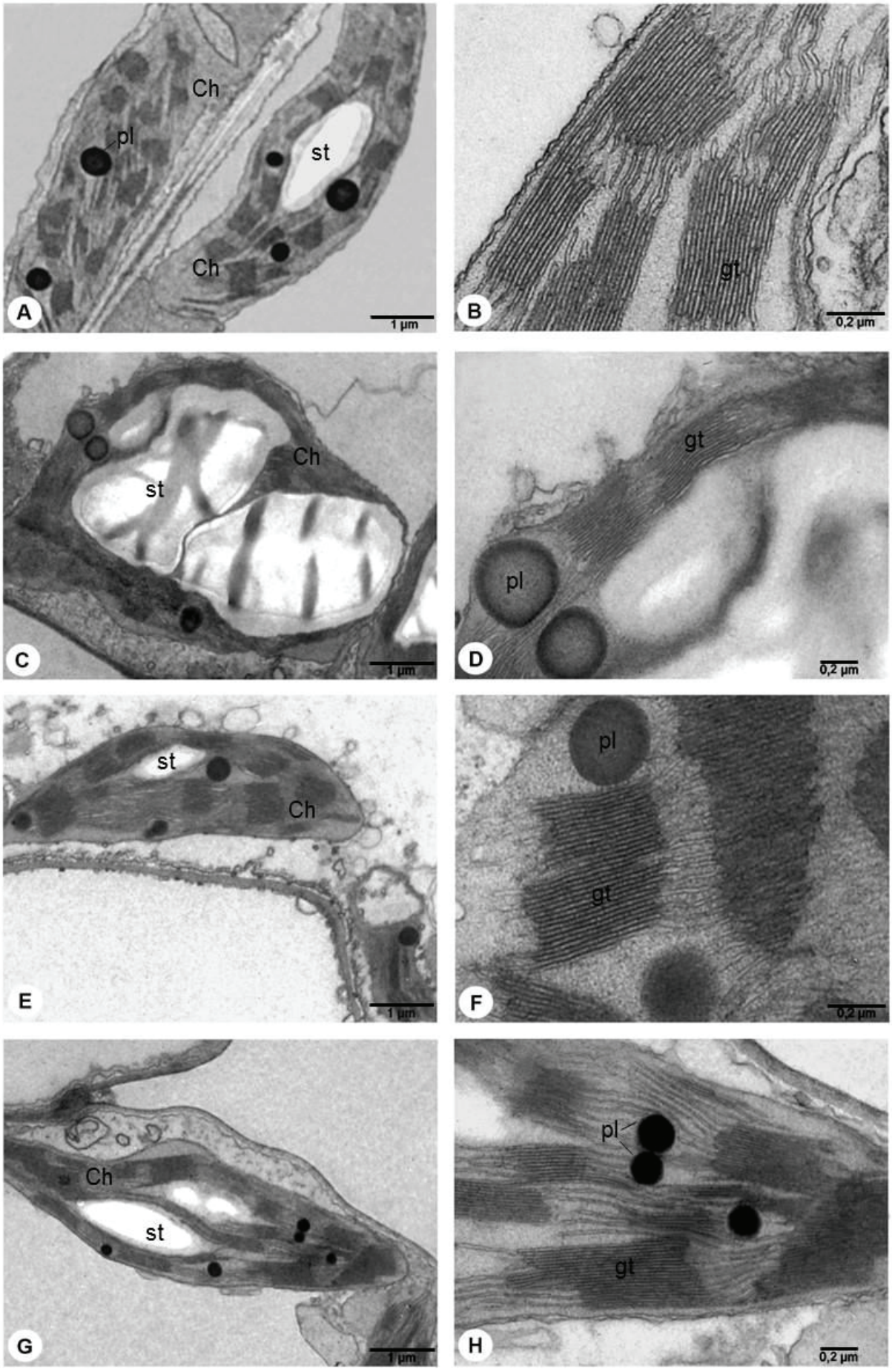

Supplemental Figure S5. Chloroplast ultrastructure resulting from *SlVTE5* downregulation. Transmission electron micrographs of the first leaflet from the first fully expanded leaf at the middle of day-light (16-week-old plant). (A,B) wild-type, (C,D) *SlVTE5*-RNAi#1, (E,F) *SlVTE5*-RNAi#7 and (G,H) *SlVTE5*-RNAi#11. Ch: chloroplast; st: starch granule; pl: plastoglobule; gt: grana thylakoids.

Supplemental Table S1. Tocopherol content and composition of *SlVTE5*-knockdown tomato plants.

	α-tocopherol (nmol g^{-1} DW)	β-/γ-tocopherol (nmol g^{-1} DW)	δ-tocopherol (nmol g^{-1} DW)	Total tocopherol (nmol g^{-1} DW)
leaf				
WT	176.1 ± 51.4	24.9 ± 2.8	nd	201 ± 52.6
SlVTE5-RNAi#1	**28.7 ± 12.5**	**2.0 ± 1.9**	nd	**30.7 ± 12.1**
SlVTE5-RNAi#7	**21.2 ± 9.1**	**4.2 ± 1.7**	nd	**25.5 ± 10.7**
SlVTE5-RNAi#11	**22.1 ± 9.5**	**4.5 ± 1.5**	nd	**26.6 ± 10.9**
Mature green fruit				
WT	53.6 ± 7.3	18.2 ± 4.1	nd	71.8 ± 10.1
SlVTE5-RNAi#1	**2.2 ± 3.4**	**11.0 ± 6.0**	nd	**13.1 ± 5.7**
SlVTE5-RNAi#7	**20.5 ± 6.2**	**2.5 ± 2.4**	nd	**23.0 ± 4.4**
SlVTE5-RNAi#11	**6.5 ± 7.3**	**3.7 ± 0.6**	nd	**10.3 ± 7.8**
Ripe fruit				
WT	44.6 ± 25.3	43.8 ± 17.8	2.4 ± 2	90.8 ± 34.7
SlVTE5-RNAi#1	**3.2 ± 1.9**	**0.7 ± 1.5**	nd	**3.9 ± 3.2**
SlVTE5-RNAi#7	**3.3 ± 1.1**	**1.9 ± 3.3**	**0.2 ± 0.4**	**5.3 ± 4.7**
SlVTE5-RNAi#11	**6.3 ± 5.4**	**3.0 ± 5.1**	**0.3 ± 0.6**	**9.6 ± 7.6**

Statistically significant differences between the wild-type (WT) and transgenic lines are indicated in bold terms (ANOVA/Dunnett's test, $P < 0.05$). DW, dry weight; nd, not detected.

Supplemental Table S2. Moles of prenyllipids found in *SlVTE5*-knockdown tomato plants.

		Prenyllipid (nmol g^{-1} DW)					
		PC-8	PQ-9	PQH_2-9	tocopherol	FAPE	free phytol
Leaf	WT	57	653	322	200	290	90
	SlVTE5-RNAi [a]	**27**	508	339	**25**	**3000**	**400**
Mature green	WT	87	33	20	71	350	nm
	SlVTE5-RNAi [a]	**160**	**72**	21	**15**	450	nm
Ripe	WT	75	56	15	90	260	193
	SlVTE5-RNAi [a]	**150**	**120**	26	**6**	460	**1095**

[a] Mean value obtained from three transgenic lines. Significant differences between wild-type (WT) and transgenic lines are indicated in bold (ANOVA/Dunnett's test, $P < 0.05$). nm, not measured.

Supplemental Table S3. Transcriptional profile of genes encoding isoprenoid metabolism-related enzymes.

	Leaf				Mature green fruits				Ripe fruits			
	WT	*SlVTE5*-RNAi#1	*SlVTE5*-RNAi#7	*SlVTE5*-RNAi#11	WT	*SlVTE5*-RNAi#1	*SlVTE5*-RNAi#7	*SlVTE5*-RNAi#11	WT	*SlVTE5*-RNAi#1	*SlVTE5*-RNAi#7	*SlVTE5*-RNAi#11
DXS(1)	1.00 ± 0.06	1.14 ± 0.15	1.12 ± 0.05	**1.53 ± 0.15**	1.00 ± 0.09	0.87 ± 0.09	0.87 ± 0.09	**0.58 ± 0.06**	1.00 ± 0.13	0.94 ± 0.18	**0.70 ± 0.07**	0.68 ± 0.14
GGPS(2)	1.00 ± 0.14	0.75 ± 0.08	1.06 ± 0.07	**1.80 ± 0.34**	1.00 ± 0.08	**1.43 ± 0.07**	1.23 ± 0.24	1.07 ± 0.07	1.00 ± 0.09	0.99 ± 0.06	**1.67 ± 0.22**	1.10 ± 0.17
GGDR	1.00 ± 0.07	0.84 ± 0.07	0.91 ± 0.04	**1.48 ± 0.20**	1.00 ± 0.17	0.96 ± 0.02	1.09 ± 0.14	**0.66 ± 0.06**	1.00 ± 0.27	1.21 ± 0.18	1.16 ± 0.16	0.68 ± 0.22
SPS	1.00 ± 0.12	**0.59 ± 0.06**	0.90 ± 0.04	0.92 ± 0.09	1.00 ± 0.10	**0.61 ± 0.02**	0.86 ± 0.13	**0.53 ± 0.05**	1.00 ± 0.11	1.20 ± 0.15	**1.36 ± 0.11**	1.17 ± 0.24
HST	1.00 ± 0.01	1.14 ± 0.12	1.03 ± 0.06	**1.37 ± 0.08**	1.00 ± 0.09	0.91 ± 0.09	1.20 ± 0.09	**0.75 ± 0.08**	1.00 ± 0.22	0.93 ± 0.12	**2.10 ± 0.26**	0.83 ± 0.13
HPPD(1)	1.00 ± 0.08	**0.70 ± 0.08**	**0.79 ± 0.01**	1.08 ± 0.05	1.00 ± 0.03	**1.28 ± 0.03**	**1.36 ± 0.13**	**1.09 ± 0.01**	1.00 ± 0.10	**1.38 ± 0.17**	**2.10 ± 0.37**	1.03 ± 0.17
HPPD(2)	1.00 ± 0.14	**0.52 ± 0.08**	0.80 ± 0.05	1.16 ± 0.05	1.00 ± 0.06	**1.74 ± 0.28**	**1.73 ± 0.18**	**1.25 ± 0.04**	1.00 ± 0.11	**1.55 ± 0.19**	**1.75 ± 0.37**	1.22 ± 0.21
VTE1	1.00 ± 0.06	1.06 ± 0.07	1.06 ± 0.03	**1.22 ± 0.02**	1.00 ± 0.10	0.98 ± 0.09	1.00 ± 0.03	**0.77 ± 0.05**	1.00 ± 0.19	1.11 ± 0.10	**1.57 ± 0.11**	0.98 ± 0.07
VTE2	1.00 ± 0.02	1.08 ± 0.06	**1.14 ± 0.07**	**1.28 ± 0.04**	1.00 ± 0.02	0.91 ± 0.10	**1.05 ± 0.02**	**0.83 ± 0.02**	1.00 ± 0.20	0.97 ± 0.10	1.26 ± 0.12	0.86 ± 0.08
VTE3(1)	1.00 ± 0.02	0.91 ± 0.07	**0.85 ± 0.02**	**0.96 ± 0.00**	1.00 ± 0.07	0.99 ± 0.04	1.08 ± 0.08	0.90 ± 0.02	1.00 ± 0.11	**1.23 ± 0.08**	**1.58 ± 0.16**	**1.39 ± 0.13**
VTE3(2)	1.00 ± 0.03	**0.73 ± 0.04**	**0.80 ± 0.03**	1.00 ± 0.02	1.00 ± 0.04	**0.84 ± 0.04**	1.01 ± 0.05	**0.71 ± 0.03**	1.00 ± 0.15	1.09 ± 0.03	**1.70 ± 0.27**	1.13 ± 0.10
VTE4	1.00 ± 0.09	0.86 ± 0.08	**0.71 ± 0.03**	**0.83 ± 0.02**	1.00 ± 0.10	0.86 ± 0.06	1.04 ± 0.09	**0.70 ± 0.02**	1.00 ± 0.10	0.89 ± 0.06	1.01 ± 0.10	1.10 ± 0.09
VTE5	1.00 ± 0.07	**0.19 ± 0.00**	**0.19 ± 0.01**	**0.14 ± 0.01**	1.00 ± 0.07	**0.25 ± 0.03**	**0.23 ± 0.02**	**0.19 ± 0.03**	1.00 ± 0.04	**0.06 ± 0.02**	**0.08 ± 0.01**	**0.06 ± 0.00**
FOLK	1.00 ± 0.09	0.92 ± 0.10	0.91 ± 0.04	1.07 ± 0.04	1.00 ± 0.07	0.86 ± 0.07	1.00 ± 0.07	**0.72 ± 0.04**	1.00 ± 0.14	**1.34 ± 0.11**	**1.93 ± 0.31**	1.28 ± 0.12
SGR1	1.00 ± 0.42	**0.56 ± 0.09**	**0.73 ± 0.29**	**0.54 ± 0.14**	1.00 ± 0.29	**1.83 ± 0.25**	**1.98 ± 0.16**	1.14 ± 0.10	1.00 ± 0.05	**1.55 ± 0.08**	**1.54 ± 0.25**	1.27 ± 0.15
CHLG	1.00 ± 0.01	**0.86 ± 0.04**	0.90 ± 0.07	**1.11 ± 0.04**	1.00 ± 0.02	0.97 ± 0.09	**1.17 ± 0.07**	**0.75 ± 0.05**	1.00 ± 0.12	1.16 ± 0.12	**1.88 ± 0.22**	1.04 ± 0.13
PAO	1.00 ± 0.04	0.77 ± 0.17	**0.90 ± 0.02**	**0.75 ± 0.07**	1.00 ± 0.12	**1.37 ± 0.09**	1.23 ± 0.11	0.97 ± 0.03	1.00 ± 0.01	1.04 ± 0.10	1.13 ± 0.07	1.04 ± 0.03
PPH	1.00 ± 0.06	0.79 ± 0.16	0.90 ± 0.02	0.84 ± 0.09	1.00 ± 0.05	1.07 ± 0.11	0.81 ± 0.09	**0.71 ± 0.03**	1.00 ± 0.17	**1.39 ± 0.07**	**1.78 ± 0.43**	1.20 ± 0.28
PYP/PES(1)	1.00 ± 0.10	**1.48 ± 0.21**	**1.56 ± 0.05**	**1.92 ± 0.05**	1.00 ± 0.14	0.96 ± 0.08	1.06 ± 0.15	**0.66 ± 0.05**	1.00 ± 0.11	1.50 ± 0.33	1.11 ± 0.01	0.92 ± 0.17
PES(2)	1.00 ± 0.11	1.11 ± 0.14	1.16 ± 0.10	1.09 ± 0.06	1.00 ± 0.01	1.14 ± 0.08	**1.25 ± 0.09**	1.02 ± 0.05	1.00 ± 0.12	1.02 ± 0.10	1.20 ± 0.08	1.09 ± 0.13
PSY(1)	1.00 ± 0.10	**0.37 ± 0.04**	**0.58 ± 0.07**	1.19 ± 0.12	1.00 ± 0.12	**1.89 ± 0.31**	**2.13 ± 0.37**	**1.30 ± 0.07**	1.00 ± 0.06	**1.41 ± 0.15**	**0.79 ± 0.08**	1.12 ± 0.13
PSY(2)	1.00 ± 0.03	**0.44 ± 0.05**	**0.58 ± 0.02**	1.10 ± 0.13	1.00 ± 0.04	**0.84 ± 0.05**	0.92 ± 0.07	0.87 ± 0.15	1.00 ± 0.07	**1.45 ± 0.21**	1.07 ± 0.08	1.07 ± 0.27
PDS	1.00 ± 0.08	**1.22 ± 0.05**	**1.29 ± 0.10**	**1.37 ± 0.02**	1.00 ± 0.06	**0.79 ± 0.04**	0.90 ± 0.04	**0.72 ± 0.05**	1.00 ± 0.05	1.01 ± 0.15	0.84 ± 0.22	1.09 ± 0.08
LCY-β	1.00 ± 0.06	**0.65 ± 0.03**	**0.70 ± 0.04**	1.00 ± 0.07	1.00 ± 0.05	1.00 ± 0.03	1.12 ± 0.12	**0.86 ± 0.06**	1.00 ± 0.05	1.16 ± 0.11	**0.85 ± 0.06**	0.81 ± 0.11
CYC-β	1.00 ± 0.09	**2.22 ± 0.27**	**1.57 ± 0.08**	**2.61 ± 0.29**	1.00 ± 0.08	**0.54 ± 0.08**	**0.70 ± 0.13**	**0.79 ± 0.06**	1.00 ± 0.05	**1.34 ± 0.14**	**1.54 ± 0.16**	**1.61 ± 0.16**

Values represent means from at least three biological replicates. The expression data shown represent fold-change compared to control wild-type (WT) in the respective organ. Significant differences were determined according to a permutation test ($P<0.05$) and indicate in bold.

Supplemental Table S4. Changes in fatty acid-derived lipids in leaves of *SlVTE5*-knockdown lines compared with wild-type.

		SlVTE5-RNAi		
Relative amounts	WT	# 1	#7	#11
MGDG-18:3/16:3	1.00 ± 0.06	0.92 ± 0.07	0.93 ± 0.03	0.96 ± 0.03
MGDG-18:3/18:3	1.00 ± 0.05	0.93 ± 0.08	**0.91 ± 0.02**	0.97 ± 0.03
DGDG-18:3/18:3	1.00 ± 0.05	**0.90 ± 0.07**	**0.89 ± 0.03**	**0.91 ± 0.04**
DGDG-18:3/16:0	1.00 ± 0.04	**0.90 ± 0.09**	**0.89 ± 0.06**	0.96 ± 0.03
DGDG-18:2/16:0	1.00 ± 0.08	1.09 ± 0.13	1.00 ± 0.07	0.92 ± 0.03
MGDG-18:2/18:3	1.00 ± 0.05	0.99 ± 0.13	0.91 ± 0.09	0.88 ± 0.01
DGDG-18:3/16:3	1.00 ± 0.07	**0.84 ± 0.09**	**0.88 ± 0.06**	**0.88 ± 0.05**
MGDG-18:3/16:1	1.00 ± 0.10	0.98 ± 0.14	0.95 ± 0.10	0.99 ± 0.09
DGDG-18:1/18:3	1.00 ± 0.02	0.93 ± 0.06	0.92 ± 0.05	**0.85 ± 0.06**
DGDG-18:3/20:3	1.00 ± 0.15	0.78 ± 0.21	0.81 ± 0.11	**0.76 ± 0.04**
DGDG-18:0/18:3	1.00 ± 0.11	0.85 ± 0.12	0.85 ± 0.16	**0.75 ± 0.06**
PE-18:2/16:0	1.00 ± 0.08	1.08 ± 0.04	1.07 ± 0.08	1.10 ± 0.10
PE-18:3/16:0	1.00 ± 0.06	0.92 ± 0.13	0.92 ± 0.20	0.92 ± 0.11
PE-18:2/18:2	1.00 ± 0.27	1.19 ± 0.17	1.11 ± 0.18	**1.38 ± 0.20**
DAG-18:0/18:0	1.00 ± 0.17	0.93 ± 0.25	0.79 ± 0.10	0.82 ± 0.22
DAG-18:0/16:0	1.00 ± 0.16	0.93 ± 0.26	0.77 ± 0.09	0.83 ± 0.23
DAG	1.00 ± 0.17	0.93 ± 0.25	0.79 ± 0.09	0.82 ± 0.22

Data were normalized to sample dry weight and expressed relative to wild type (WT) in each tissue. Values are represented as means ± SD. Terms in bold indicate a statistically significant difference by ANOVA/Dunnett's test ($P < 0.05$). Monogalactosyldiacylglycerol (MGDG); digalactosyldiacylglycerol (DGDG); phosphotidylethanolamine (PE); diacylglycerol (DAG).

Supplemental Table S5. Primers used for each experiment.

Experiment	Primer name	Primer Sequence (Foward/Reverse)
qPCR	DXS(1)	CAGGACTGGTGTGGTTTCAG
		GGGATAGTTCACAGTGTCC
	GGPS(2)	GTTGATTCATGGGGTCAAGC
		CAAATCGCCTTTTCAGCTACG
	GGDR	CAGAGACGCTCGCTAAGG
		GCTTCAGAGTCTGTCCGATATC
	HPPD(1)	CCAGGGCAGGGGATATACTG
		CTCCTTCCTCGTTTTTCAGC
	HPPD(2)	CCAGGCGTGTGAAGAATTG
		CGATCTAAACAGCTCAGAG
	VTE2	CAATTCCAGTTCCTGCTGAG
		CCTCCAACATGCTCTTGCGTG
	VTE3(1)	CTTGACCAATCTCCTCATC
		GCACGCCTTTCCTCCAGG
	VTE3(2)	GCTAAGGCTAGGCAGAAGGAG
		CAGGCAACCCCACCTATGG
	VTE1	CGAACTCCTCATAGCGGGTATC
		CACGCCAGTAAACCGAGGC
	VTE4	CAGATCATCGTGCTGCTCAG
		CCTCTCTGCTTGTACAGGAC
	VTE5	CGTATCAGGACGGGCTCGC
		TCACCACCACACATCATTGCTAATG
	FOLK	CTATGAGCCGATTTGGAGACC
		GAACCTCCTGCCAACAATGTC
	HST	GCTGCTAACTTGGTGCTC
		GATCCTAGCACAGTCCCACG
	CHLG	CCAATTCCTTCAGGTGCGGT
		CCCACCAAGGCAAGCTGATA
	PPH	TATGGAGGGAGCAAGTACGC
		TGGAGGGCAGAGGAAAAGTAC
	PAO	TCAGAAGTGGGTGATATGGA
		TATCCCCGTCATACACCTTA
	PSY(1)	CGATGGTGCTTTGTCCGATAC
		CTCATCAACCCAACCGTACC
	PSY(2)	GCATCACACATAACTCCACAAGC
		CGCATTCCTTCAACCATATCTCTG
	LCYβ	GCACCCACATCAAAGCCAGAG
		GCCACATGGAGAGTGGTGAAG
	CYCβ	TTGACTTAGAACCTCGTTATTGG
		AACAGTTCCCTTTGTCATTATCT
	PDS	CGTTCCGTGCTTCTCCGC
		CTAGAACATCCCTTGCCTCCAG
	SPS	GTGGTTGCGGATGACCTACTTA
	PYP/PES(1)	CTTCTGTGATTTGTGGTGAGTTCC
		ACAGGACACAACTCCAACC
	PES(2)	TAACCATCGCCATCTTCAGTG
		CGAAGAGAGGGAAAAATGCCTGTG
	SGR1	GCTGCCATCCTGACAAATTCAGAC
		GCAAAGAACTCCCTGTGGTT
	CAC	CCCACCAGAAGAAGATGAGG
		CCTCCGTTGTGATGTAACTGG
		ATTGGTGGAAAGTAACATCATCG
	EXPRESSED	GCTAAGAACGCTGGACCTAATG
		TGGGTGTGCCTTTCTGAATG
Subcellular localization (GFP-fusion construct)	FUS-FOLK-F	CACCATGGCTCTCTTTGCTTCTTCTG
	FUS-FOLK-R	AACAAGACTGCCAACCAGCAC
	FUS-VTE5-F	CACCATGCAAGCTTTGGTGTGTG
	FUS-VTE5-R	AGCCAATGATGCTACAACCATGC
SlVTE5-RNAi fragment	RNAi-VTE5-F	CACCATGCAAGCTTTGGTGTGTG
	RNAi-VTE5-R	CTAATAAGCAAAAGCCAATGATGCTAC
TILLING SlFOLK screening	external	TCATCTTTTAGAAGTGATATCCTAACC
		ACACAATCCTGTGTTAGACTAACACAT
	internal	GAACAGAAAGCTTGTTCATATTAGCAT
		ACATTGCCCATTTTCAGTAAGCATTTT

LITERATURE CITED

Abbasi AR, Hajirezaei M, Hofius D, Sonnewald U, Voll LM (2007) Specific roles of α- and γ-tocopherol in abiotic stress responses of transgenic tobacco. Plant Physiology 143: 1720–1738.

Adams WW, Muller O, Cohu CM, Demmig-Adams B (2013) May photoinhibition be a consequence, rather than a cause, of limited plant productivity? Photosynth Res 117: 31–44.

Almeida J, Quadrana L, Asís R, Setta N, De Godoy F, Bermúdez L, Otaiza SN, Corrêa da Silva JV, Fernie AR, et al (2011) Genetic dissection of vitamin E biosynthesis in tomato. J Exp Bot 62: 3781-3798.

Almeida J, Asís R, Molineri VN, Sestari I, Lira BS, Carrari F, Peres LE, Rossi M (2015) Fruits from ripening impaired, chlorophyll degraded and jasmonate insensitive tomato mutants have altered tocopherol content and composition. Phytochemistry 111: 72–83.

Amaral LIV, Gaspar M, Costa PF, Aidar MPM, Buckeridge MS (2008) Novo método enzimático rápido e sensível de extração e dosagem de amido em materiais vegetais. Hoehnea 34: 425-431.

Araújo WL, Ishizaki K, Nunes-Nesi A, Tohge T, Larson TR, Krahnert I, Balbo I, Witt S, Dörmann P, et al (2011) Analysis of a range of catabolic mutants provides evidence that phytanoyl-coenzyme A does not act as a substrate of the electron-transfer flavoprotein/electron-transfer flavoprotein:ubiquinone oxidoreductase complex in Arabidopsis during dark-induced senescence. Plant Physiol 157: 55-69.

Ariizumi T, Kishimoto S, Kakami R, Maoka T, Hirakawa H, Suzuki Y, Ozeki Y, Shirasawa K, Bernillon S, et al (2014) Identification of the carotenoid modifying gene PALE YELLOW PETAL 1 as an essential factor in xanthophyll esterification and yellow flower pigmentation in tomato (*Solanum lycopersicum*). Plant J *79*: 453–465.

Asensi-Fabado MA, Ammon A, Sonnewald U, Munné-Bosch S, Voll LM (2014) Tocopherol deficiency reduces sucrose export from salt-stressed potato leaves independently of oxidative stress and symplastic obstruction by callose. J Exp Bot 66: 957–971.

Botella-Pavía P, Besumbes O, Phillips MA, Carretero-Paulet L, Boronat A, Rodriguez-Concepcion M (2004) Regulation of carotenoid biosynthesis in plants: evidence for a key role of hydroxymethylbutenyl diphosphate reductase in controlling the supply of plastidial isoprenoid precursors. Plant J 40: 188–199.

Chen LQ, Qu XQ, Hou BH, Sosso D, Osorio S, Fernie AR, Frommer WB (2012) Sucrose efflux mediated by SWEET proteins as a key step for phloem transport. Science 335: 207–211.

Chun J, Lee J, Ye L, Exler J, Eitenmiller RR (2006) Tocopherol and tocotrienol contents of raw and processed fruits and vegetables in the United States diet. J Food Compos Anal 19: 196–204.

De Godoy F, Bermúdez L, Lira BS, De Souza AP, Elbl P, Demarco D, Alseekh S, Insani M, Buckeridge M, et al (2013) Galacturonosyltransferase 4 silencing alters pectin composition and carbon partitioning in tomato. J Exp Bot 64: 2449-2466.

DellaPenna D, Pogson BJ (2006) Vitamin synthesis in plants: tocopherols and carotenoids. Annu Rev Plant Biol 57: 711–738.

DellaPenna D, Mène-Saffrané L (2011) Vitamin E. In JC Kader, M Delseny, eds, Advances in Botanical Research, Vol 59. Academic Press, London, pp 179–227.

Demmig-Adams B, Stewart JJ, Adams, WW (2014) Multiple feedbacks between chloroplast and whole plant in the context of plant adaptation and acclimation to the environment. Philos Trans R Soc Lond B Biol Sci 369: 20130244.

De Souza AP, Arundale RA, Dohleman FG, Long SP, Buckeridge MS (2013) Will the exceptional productivity of *Miscanthus x giganteus* increase further under rising atmospheric CO_2? Agr Forest Meteorol 171-172: 82-92

Di Mascio P, Devasagayam TP, Kaiser S, Sies H (1990) Carotenoids, tocopherols and thiols as biological singlet molecular oxygen quenchers. Biochem Soc Trans 18: 1054–1056.

Di Rienzo JA (2009) Statistical software for the analysis of experiments of functional genomics. RDNDA, Argentina. http://sites.google.com/site/fgStatistics/.

Edreva A (2005) Generation and scavenging of reactive oxygen species in chloroplasts: a submolecular approach. Agr Ecosyst Environ 106: 119-133.

Eugeni-Piller L, Glauser G, Kessler F, Besagni C (2014) Role of plastoglobules in metabolite repair in the tocopherol redox cycle. Front Plant Sci 5:298

Fitzpatrick AH, Bhandari J, Crowell DN (2011) Farnesol kinase is involved in farnesol metabolism, ABA signaling and flower development in Arabidopsis. Plant J 66: 1078–88.

Fitzpatrick TB, Basset GJC, Borel P, Carrari F, DellaPenna D, Fraser PD, Hellmann H, Osorio S, Rothan C, et al (2012) Vitamin deficiencies in humans: can plant science help? Plant Cell 24: 395–414.

Foyer CH, Noctor G (2005) Redox homeostasis and antioxidant signaling: a metabolic interface between stress perception and physiological responses. Plant Cell 17: 1866–1875.

Fukuzawa K, Matsuura K, Tokumura A, Suzuki A, Terao J (1997) Kinetics and dynamics of singlet oxygen scavenging by alpha-tocopherol in phospholipid model membranes. Free Rad Biol Med 22: 923–930.

Gaude N, Bréhélin C, Tischendorf G, Kessler F, Dörmann, P (2007) Nitrogen deficiency in Arabidopsis affects galactolipid composition and gene expression and results in accumulation of fatty acid phytyl esters. Plant J 49: 729–739.

Genty B, Briantais JM, Baker NR (1989) The relationship between quantum yield of photosynthetic electron transport and quenching of chlorophyll fluorescence. Biochim Biophys Acta 990: 87-92.

Grusak MA, DellaPenna D (1999). Improving the nutrient composition of plants to enhance human nutrition and health1. Annu Rev Plant Physiol Plant Mol Biol 50: 133–161.

Gupta P, Sreelakshmi, Y, Sharma R (2015) A rapid and sensitive method for determination of carotenoids in plant tissues by high performance liquid chromatography. Plant Methods 11:5.

Havaux M, Eymery F, Porfirova S, Rey P, Dörmann P (2005) Vitamin E protects against photoinhibition and photooxidative stress in Arabidopsis thaliana. Plant Cell 17: 3451-3469.

Hemmerlin A, Bach TJ (2000) Farnesol-induced cell death and stimulation of 3-hydroxy-3-methylglutaryl-coenzyme A reductase activity in tobacco cv bright yellow-2 cells. Plant Physiol 123: 1257-1268.

Hemmerlin A, Harwood JL, Bach TJ (2012) A raison d'etre for two distinct pathways in the early steps of plant isoprenoid biosynthesis? Prog Lipid Res 51: 95–148.

Hofius D, Hajirezaei MR, Geiger M, Tschiersch H, Melzer M, Sonnewald U (2004) RNAi-mediated tocopherol deficiency impairs photoassimilate export in transgenic potato plants. Plant Physiol 135: 1256–1268.

Hortensteiner S (2009) Stay-green regulates chlorophyll and chlorophyll- binding protein degradation during senescence. Trends Plant Sci 14: 155–162.

Ischebeck T, Zbierzak AM, Kanwischer M, Dörmann P (2006) A salvage pathway for phytol metabolism in Arabidopsis. J Biol Chem 281: 2470–2477.

Jones MO, Perez-Fons L, Robertson FP, Bramley PM, Fraser PD (2013). Functional characterization of long-chain prenyl diphosphate synthases from tomato. Biochem J 449: 729–740.

Just D, Garcia V, Fernandez L, Bres C, Mauxion JP, Petit J, Jorly J, Assali J, Bournonville C, et al (2013) Micro-Tom mutants for functional analysis of target genes and discovery of new alleles in tomato. Plant Biotech 30*:* 225–231.

Kaiser S, Di Mascio P, Murphy ME, Sies H (1990) Physical and chemical scavenging of singlet molecular oxygen by tocopherols. Arch Biochem Biophys 277: 101–108.

Kamal-Eldin A, Appelqvist LA (1996) The chemistry and antioxidant properties of tocopherols and tocotrienols. Lipids 31: 671–701.

Karimi M, Inzé D, Depicker A (2002) GATEWAY vectors for Agrobacterium-mediated plant transformation. Trends Plant Sci 7:193-195.

Kim SH, Koroleva OA, Lewandowska D, Pendle AF, Clark GP, Simpson CG, Shaw PJ, Brown JW (2009) Aberrant mRNA transcripts and the nonsense-mediated decay proteins UPF2 and UPF3 are enriched in the Arabidopsis nucleolus. Plant Cell 21: 2045–2057.

Kruk J, Trebst A (2008) Plastoquinol as a singlet oxygen scavenger in photosystem II. Biochim Biophys Acta 1777: 154–162.

Kruk J, Szymańska R, Cela J, Munné-Bosch S (2014) Plastochromanol-8: Fifty years of research. Phytochemistry 108: 9–16.

Langmeier M, Ginsburg S, Matile P (1993) Chlorophyll breakdown in senescent leaves: demonstration of Mg-dechelatase activity. Physiol Plant 89: 347–353.

Lippold F, vom Dorp K, Abraham M, Hölzl G, Wewer V, Yilmaz JL, Lager I, Montandon C, Besagni C, et al (2012) Fatty acid phytyl ester synthesis in chloroplasts of Arabidopsis. Plant Cell 24: 2001–2014.

Lira B, Setta N, Rosado D, Almeida J, Freschi L, Rossi M (2014) Plant degreening: evolution and expression of tomato (*Solanum lycopersicum*) dephytylation enzymes. Gene 546: 359-366.

Lohmann A, Schöttler MA, Bréhélin C, Kessler F, Bock R, Cahoon EB, Dörmann P (2006) Deficiency in phylloquinone (vitamin K1) methylation affects prenyl quinone distribution, photosystem I abundance, and anthocyanin accumulation in the Arabidopsis AtmenG mutant. J Biol Chem 281: 40461-40472.

Loyola J, Verdugo I, González E, Casaretto JA, Ruiz-Lara S (2012) Plastidic isoprenoid biosynthesis in tomato: physiological and molecular analysis in genotypes resistant and sensitive to drought stress. Plant Biol (Stuttg) 14:149-156.

Luo Z, Zhang J, Li J, Yang C, Wang T, Ouyang B, Li H, Giovannoni J, Ye Z (2013) A STAY-GREEN protein SlSGR1 regulates lycopene and β-carotene accumulation by interacting directly with SlPSY1 during ripening processes in tomato. New Phytol 198: 442–452.

Maeda H, Song W, Sage TL, DellaPenna D (2006). Tocopherols play a crucial role in low-temperature adaptation and Phloem loading in Arabidopsis. Plant Cell 18: 2710–2732.

Maeda H, Sage TL, Isaac G, Welti R, Dellapenna D (2008) Tocopherols modulate extraplastidic polyunsaturated fatty acid metabolism in Arabidopsis at low temperature. Plant Cell 20: 452–470.

Maeda H, Song W, Sage T, DellaPenna D (2014) Role of callose synthases in transfer cell wall development in tocopherol deficient mutants. Front Plant Sci 5:46.

Martinis J, Glauser G, Valimareanu S, Kessler F (2013) A chloroplast ABC1-like kinase regulates Vitamin E metabolism in Arabidopsis thaliana. Plant Physiol 162: 652-662.

Martinis J, Glauser G, Valimareanu S, Stettler M, Zeeman S, Yamamoto H, Shikanai T, Kessler F (2014) ABC1K1/PGR6 kinase: a regulatory link between photosynthetic activity and chloroplast metabolism. Plant J 77: 268–283.

Mène-Saffrané L, Jones AD, DellaPenna D (2010) Plastochromanol-8 and tocopherols are essential lipid-soluble antioxidants during seed desiccation and quiescence in Arabidopsis. Proc Natl Acad Sci USA 107: 17815-17820.

Miret JA, Munné-Bosch S (2015) Redox signaling and stress tolerance in plants: a focus on vitamin E. Ann N Y Acad Sci 1340:29-38.

Muller O, Cohu CM, Stewart JJ, Protheroe JA, Demmig-Adams B, Adams WW (2014) Association between photosynthesis and contrastingfeatures of minor veins in leaves of summer annuals loadingphloem via symplastic versus apoplastic routes. Physiol Plantarum 152: 174-183.

Munné-Bosch S (2005) The role of a-tocopherol in plant stress tolerance. J Plant Physiol 162: 743–748.

Ng PC, Henikoff S (2003) SIFT: predicting amino acid changes that affect protein function. Nucleic Acids Res 31: 3812-3814.

Nowicka B, Gruszka J, Kruk J (2013) Function of plastochromanol and other biological prenyllipids in the inhibition of lipid peroxidation-A comparative study in model systems. Biochim Biophys Acta 1828: 233–240.

Okabe Y, Asamizu E, Saito T, Matsukura C, Ariizumi T, Brès C, Rothan C, Mizoguchi T, Ezura H (2011) Tomato TILLING technology: development of a reverse genetics tool for the efficient isolation of mutantsfrom Micro-Tom mutant libraries. Plant Cell Physiol 52: 1994–2005.

Pfaffl MW, Horgan GW, Dempfle L (2002) Relative expression software tool (REST) for group-wise comparison and statistical analysis of relative expression results in real-time PCR. Nucleic Acids Res 30: e36.

Pino LE, Lombardi-Crestana S, Azevedo MS, Scotton DC, Borgo L, Quecini V, Figueira A, Peres LE (2010) The Rg1 allele as a valuable tool for genetic transformation of the tomato 'Micro-Tom' model system. Plant Methods 6: 23.

Quadrana L, Almeida J, Otaiza SN, Duffy T, Corrêa da Silva JV, de Godoy F, Asís R, Bermúdez L, Fernie AR, et al (2013) Transcriptional regulation of tocopherol biosynthesis in tomato. Plant Mol Biol 81: 309–325.

Quadrana L, Almeida J, Asís R, Duffy T, Dominguez PG, Bermúdez L, Conti G, da Silva JVC, Colot V, et al (2014) Natural occurring epialleles determine vitamin E accumulation in tomato fruits. Nat Comm 5:3027.

Rastogi A, Yadav DK, Szymanska R, Kruk J, Sedlárová M, Pospíšil P (2014) Singlet oxygen scavenging activity of tocopherol and plastochromanol in *Arabidopsis thaliana*: relevance to photooxidative stress. Plant Cell Environ 37: 392–401.

Re R, Pellegrini N, Proteggente A, Pannala A, Yang A, Rice-Evans C (1999) Antioxidant activity applying an improved ABTS radical cation decolorization assay. Free Rad Biol Med 26: 1231-1237.

Reynolds ES (1963) The use of lead citrate at high pH as an electron-opaque stain in electron microscopy. J Cell Biol 17: 208–212.

Ruijter JM, Ramakers C, Hoogaars WM, Karlen Y, Bakker O, van den Hoff MJ, Moorman AFM (2009) Amplification efficiency: linking baseline and bias in the analysis of quantitative PCR data. Nucleic Acids Res 37: e45.

Sattler SE, Gilliland LU, Magallanes-Lundback M, Pollard M, Dellapenna D (2004). Vitamin E is essential for seed longevity and for preventing lipid peroxidation during germination. Plant Cell 16: 1419–1432.

Schelbert S, Aubry S, Burla B, Agne B, Kessler F, Krupinska K, Hörtensteiner S (2009) Pheophytin pheophorbide hydrolase (pheophytinase) is involved in chlorophyll breakdown during leaf senescence in Arabidopsis. Plant Cell 21: 767-785.

Serbinova E, Kagan V, Han D, Packer L (1991) Free radical recycling and intramembrane mobility in the antioxidant properties of alpha-tocopherol and alpha-tocotrienol. Free Radical Biol Med 10: 263–275.

Seymour GB, Østergaard L, Chapman NH, Knapp S, Martin C (2013) Fruit development and ripening. Annu Rev Plant Biol 64: 219–241.

Song W, Maeda H, Dellapenna D (2010) Mutations of the ER to plastid lipid transporters TGD1, 2, 3 and 4 and the ER oleate desaturase FAD2 suppress the low temperature-induced phenotype of Arabidopsis tocopherol-deficient mutant *vte2*. Plant J 62: 1004–1018.

Tamura K, Dudley J, Nei M, Kumar S (2007) MEGA4: Molecular Evolutionary Genetics Analysis (MEGA) software version 4.0. Mol Biol Evol 24: 1596–1599.

Taylor NE, Greene EA (2003) PARSESNP: A tool for the analysis of nucleotide polymorphisms. Nucleic Acids Res 31:3808-3811.

Thai L, Rush JS, Maul JE, Devarenne T, Rodgers DL, Chappell J, Waechter CJ (1999) Farnesol is utilized for isoprenoid biosynthesis in plant cells via farnesyl pyrophosphate formed by successive monophosphorylation reactions. Proc Natl Acad Sci U S A 96: 13080-13085.

Traber MG, Atkinson J (2008) Vitamin E, antioxidant and nothing more. Free Radic Biol Med 43: 4-15.

Till BJ, Reynolds SH, Greene EA, Codomo CA, Enns LC, Johnson JE, Burtner C, Odden AR, Young K, et al (2003) Large-scale discovery of induced point mutations with high-throughput TILLING. Genome Res 13: 524–530.

Triantaphylidès C, Havaux M (2009) Singlet oxygen in plants: production, detoxification and signaling. Trends Plant Sci 14: 219–228.

Valentin HE, Lincoln K, Moshiri F, Jensen PK, Qi Q, Venkatesh TV, Karunanandaa B, Baszis SR, Norris SR, et al (2006) The Arabidopsis vitamin E pathway gene5-1 mutant reveals a critical role for phytol kinase in seed tocopherol biosynthesis. Plant Cell 18: 212–224.

Vicente, MH, Zsögön A, Sá AFL, Ribeiro RV, Peres LEP (2015) Semi-determinate growth habit adjusts the vegetative-to-reproductive balance and increases productivity and water-use efficiency in tomato (*Solanum lycopersicum*). J Plant Physiol 177: 11-19. Watson ML (1958) Staining of tissue sections for electron microscopy with heavy metals. J Biophys Biochem Cytol 4: 475–478.

Watson ML (1958) Staining of tissue sections for electron microscopy with heavy metals. J Biophys Biochem Cytol 4: 475–478.

Welti R, Li W, Li M, Sang Y, Biesiada H, Zhou, HE, Rajashekar CB, Williams TD, Wang X (2002) Profiling membrane lipids in plant stress responses. Role of phospholipase D alpha in freezing-induced lipid changes in Arabidopsis. J Biol Chem 277: 31994–32002.

Yang W, Cahoon RE, Hunter SC, Zhang C, Han J, Borgschulte T, Cahoon EB (2011) Vitamin E biosynthesis: functional characterization of the monocot homogentisate geranylgeranyl transferase. Plant J 65: 206-217.

Zbierzak AM, Kanwischer M, Wille C, Vidi PA, Giavalisco P, Lohmann A, Briesen I, Porfirova S, Bréhélin C, et al (2010) Intersection of the tocopherol and plastoquinol metabolic pathways at the plastoglobule. Biochem J 425: 389–399.

Zhang C, Cahoon RE, Hunter SC, Chen M, Han J, Cahoon EB (2013) Genetic and biochemical basis for alternative routes of tocotrienol biosynthesis for enhanced vitamin E antioxidant production. Plant J 73: 628–639.

Zhang W, Liu T, Ren G, Hörtensteiner S, Zhou Y, Cahoon EB, Zhang C (2014) Chlorophyll degradation: the tocopherol biosynthesis related phytol hydrolase in Arabidopsis seeds is still missing. Plant Physiol 166:70-79.

CONSIDERAÇÕES FINAIS

O presente trabalho teve como propósito aprofundar o conhecimento sobre a regulação da rota biossintética de vitamina E em tomateiro. Os resultados apresentados estabelecem inúmeras relações entre tocoferóis e o restante do metabolismo vegetal e assinalam os muitos aspectos ainda por serem resolvidos que estão sob foco de pesquisa atual. Todavia, os esforços realizados ao longo dos seis capítulos ampliam não só a compreensão dos mecanismos regulatórios centrados na transcrição e sua resposta ao desenvolvimento e a perturbações causadas pela presença de variantes alélicas, mas também do controle do metabolismo celular. Consequentemente, tal constatação implica que as mudanças nos níveis de tocoferóis podem ser percebidas pelo organismo vegetal e disparam mecanismos adaptativos nas células.

Sob a perspectiva metodológica, primeiramente, fez-se necessário o estabelecimento de uma plataforma analítica para avaliação do perfil transcricional dos genes envolvidos na biossíntese de tocoferóis, o *array* de qPCR para VTE. O ponto de partida foi a sistemática caracterização *in silico* desses genes realizada anteriormente pelo nosso grupo (Almeida *et al.*, 2011). De fato, a eficiência dessa plataforma, alcançada pelo criterioso desenho experimental implementado, possibilitou a análise de perfis transcricionais, completos ou parciais, em todas as situações experimentais apresentadas (Capítulo I a VI). Os dados de expressão gênica juntamente com os perfis de tocoferóis e outros metabólitos foram analisados, nos Capítulos I e IV, à luz de métodos de inferência de redes regulatórias, as quais resultaram muito informativas e expuseram pontos chaves do metabolismo. Em segundo lugar, destaca-se a diversidade de genótipos de tomateiro utilizados aqui como material vegetal, incluindo desde a planta cultivada "selvagem" ao longo de diferentes estádios do desenvolvimento, passando por linhagens introgredidas, por mutantes naturais monogênicos - deficientes no amadurecimento, na degradação de clorofila e na percepção ao ácido jasmônico – e oriundos de população mutageneizada com EMS, até linhagens transgênicas silenciadas. Essa abordagem permitiu observar recorrências e especifidades da regulação da biossíntese de VTE nos diferentes tipos celulares/teciduais. O segundo ponto, por conseguinte, entrelaça-se com o terceiro: esta tese valeu-se da riqueza de métodos e recursos disponíveis para a espécie modelo *S. lycopersicum*. Nos Capítulos IV, V e VI, as linhagens transgênicas e os mutantes analisados estão em fundo genético da variedade anã Micro-Tom, que apresenta vantagens de tamanho reduzido e ciclo de vida curto. Para manipulação genética, fez-se uso tanto da técnica de VIGS - opção para análise do silenciamento gênico transiente e circunscrito ao fruto - quanto da transformação genética estável sob controle do promotor 35S, nesse caso, para avaliar o efeito no organismo como um todo. Por fim,

o genoma completo de tomateiro teve papel decisivo em tornar completo o cenário referente a VTE5 e CLH, identificando os respectivos parálogos.

Convém mencionar, diante da relevância das vias metabólicas abordadas – MEP, SK, clorofila, prenilquinonas, carotenóides, ésteres de fitol – no contexto da Biologia Vegetal, que os sucessivos avanços dos últimos anos foram gradativamente incorporados nas análises realizadas. Em particular, salientam-se as descobertas reportadas na literatura para as etapas iniciais da degradação da clorofila, incluindo as informações referentes às proteínas STAYGREEN (SGR) e FEOFITINASE (PPH). Especificamente, durante a elaboração dessa tese, destacam-se as publicações que reavaliaram a função defitiladora das CLH *in planta*, especialmente em *Arabidopsis*: na homeostase da clorofila (Lin *et al.*, 2014), no desverdecimento das sementes e subsequente suprimento para tocoferol (Zhang *et al.*, 2015), e na degradação da clorofila que ocorre durante o colapso celular frente à situação de herbivoria (Hu *et al.*, 2015). Apenas para este último fenômeno houve evidências contundentes sobre a participação da CLH, sobretudo como componente de um sistema de defesa contra herbivoria. Por conseguinte, em *Arabidopsis*, CLH não participa da quebra da clorofila em tecidos íntegros. Do mesmo modo, considerando os resultados aqui obtidos (Capítulo III e V), em contrapartida ao amadurecimento induzido por etileno em flavedo de *Citrus*, CLH(1) parece não contribuir para a degradação de clorofila em pericarpo de frutos de tomate. Com efeito, não se pode descartar por completo o papel das demais CLHs codificadas pelos genes parálogos. Perante esses resultados, parece pouco provável que esse gene tenha influência direta na determinação do QTL para VTE descrito na IL6-1 (Capítulo II), ainda que o *e*QTL$_{CLH(1)}$ tenha sido identificado. Entretanto, considerando a localização extra-plastidial das CLHs e os perfis de expressão dos genes *CLH* (Lira *et al.*, 2014), uma hipótese a ser testada seria seu envolvimento na degradação de clorofila presente no parênquima gelatinoso dentro da cavidade locular do fruto de tomate, uma vez que esse tecido sofre degeneração ao longo do amadurecimento. Para tanto, seria interessante obter plantas deficientes para os dois genes parálogos com expressão relevante em fruto, *CLH(1)* e *CLH(4).* Por outro lado, se as CLHs estão envolvidas no sistema de defesa contra herbivoria em folhas de tomateiro, também necessita ser demonstrado.

O uso da diversidade natural e da transgênese para supressão da ativação do fitol oriundo da degradação da clorofila revelaram importantes pontos regulatórios: (i) como a transcrição pode responder a perturbações nos metabólitos da via; e (ii) como a alteração na alocação de precursores modulam os influxos de intermediários entre as vias biossintéticas (*i.e.* nos mutantes *rin*, *nor*, *greenflesh* e *lutescent;* nas linhagens transgênicas *SlVTE5-RNAi*), sendo os resultados, por sua vez, dependente do órgão analisado.

Uma das conclusões centrais dessa tese é que a síntese de tocoferol em tomateiro é altamente dependente do fitol liberado da clorofila, tanto durante o *turnover* nos tecidos fotossinteticamente ativos quanto em frutos durante a degradação da clorofila no decorrer do amadurecimento. Esses dados contrastam com o cenário proposto para *Arabidopsis*, na qual a via dependente de VTE5 seria predominante em sementes e, em menor grau, em folhas. Além disso, os resultados obtidos com as linhagens transgênicas *SlVTE5-RNAi* nos permitem revisitar algumas das proposições/observações feitas ao longo dessa tese. Uma delas refere-se aos mutantes *rin*, *nor* e *greenflesh*: a manutenção da síntese *de novo* de fitil-difosfato compensaria a falta do fitol proveniente da degradação de clorofila para produção de tocoferóis nos estádios finais do desenvolvimento do fruto (Capítulo IV). A relação, nesse caso, pode não ser direta. É plausível ponderar que, nesses mutantes que retêm clorofila, a sustentação da biossíntese de clorofila e seu constante *turnover* nos estágios finais do fruto produz fitol suficiente para manter os níveis de tocoferol similares às plantas selvagens. Por outro lado, à luz da importância da rota de ativação do fitol dependente de VTE5 para síntese de tocoferóis em frutos, os resultados obtidos com os experimentos de VIGS tanto para *VTE5* quanto para *FOLK* são intrigantes. Primeiro, os mutantes de *folk-1* não apresentaram a redução pequena, porém significativa, no conteúdo de tocoferóis observada no experimento de VIGS em fruto. Além disso, a ausência de atividade fitol quinase compensatória nas plantas *SlVTE5-RNAi,* contribui para descartar uma contribuição significativa, se alguma, de *FOLK* na ativação do fitol direcionado à síntese de tocoferóis. Vale mencionar que um efeito do *background* genético ocasionado pelo tratamento com EMS não pode ser desconsiderado, dado que não foram realizados retrocruzamentos sucessivos para sua eliminação nos mutantes. À parte dessa questão, o mutante *folk-1* identificado pela estratégia de TILLING constitui um material vegetal de grande valor para investigar o papel biológico da proteína FOLK em *S. lycopersicum*; a começar pela demonstração da atividade farnesol quinase. Se confirmada, uma explicação para a divergência dos resultados de localização subcelular poderia ser o duplo direcionamento ao qual esta proteína estaria submetida na célula, sendo alocada tanto nos cloroplastos quanto no retículo endoplasmático.

No caso da ausência de fenótipo nos frutos silenciados para *VTE5* por VIGS, a verificação da possibilidade de transporte de fitil difosfato entre os tecidos é reforçada, ainda que a ocorrência de compostos hidrofóbicos no ambiente aquoso do floema seja pouco conhecida. No entanto, os achados de lipídeos e proteínas ligantes de lipídeos nos exudados de floema de *Arabidopsis* demonstram a existência de um transporte de longa distância para lipídeos em plantas (Guelette *et al.*, 2012). Diante da heterogeneidade do silenciamento obtida nos experimentos de VIGS, esse sistema não resultou adequado para avaliação dessa hipótese. No entanto, a geração de plantas transgênicas silenciadas

para VTE5 sob controle específico de fruto pode fornecer informações oportunas sobre a existência de transporte da cadeia isoprênica.

Por fim, as plantas deficientes em tocoferol *SlVTE5-RNAi* representam um valioso material vegetal para investigação do papel de tocoferóis na fisiologia de tomateiro nas mais diferentes condições experimentais, pois, ao contrário da deficiência em enzimas da biossíntese como VTE1 e VTE3, não interfere no conteúdo de PQ-9 em folhas, preservando assim a cadeia de transporte de elétrons.

Referências bibliográficas

Almeida, J., Quadrana, L., Asis, R., Setta, N., de Godoy, F., Bermudez, L., Otaiza, S., *et al.* (2011) Genetic dissection of vitamin E biosynthesis in tomato. *Journal of Experimental Botany,* 62, 3781–3798.

Guelette, B. S., Benning, U. F., Hoffmann-Benning, S. (2012) Identification of lipids and lipid-binding proteins in phloem exudates from *Arabidopsis thaliana*. *Journal of Experimental Botany*, 63, 3603–3616.

Hu, X., Makita, S., Schelbert, S., Sano, S., Ochiai, M., Tsuchiya, T., Hasegawa, S.F., *et al.* (2015) Re-examination of chlorophyllase function implies its involvement in defense against chewing herbivores. *Plant Physiology*, 167, 660-670.

Lin, Y. P., Lee, T., Tanaka, A., Charng, Y. (2014) Analysis of an *Arabidopsis* heat-sensitive mutant reveals that chlorophyll synthase is involved in reutilization of chlorophyllide during chlorophyll turnover. *The Plant Journal*, 80, 14–26.

Lira, B. S., de Setta, N., Rosado, D., Almeida, J., Freschi, L., Rossi, M. (2014) Plant degreening: evolution and expression of tomato (Solanum lycopersicum) dephytylation enzymes. *Gene*, 546, 359-366.

Zhang, W., Liu, T., Ren, G., Hörtensteiner, S., Zhou, Y., Cahoon, E. B., Zhang, C. (2014) Chlorophyll degradation: the tocopherol biosynthesis-related phytol hydrolase in arabidopsis seeds is still missing. *Plant Physiology*, 166, 70–79.

ARTIGOS PUBLICADOS

Decorrentes da publicação de capítulos da tese

Capítulo I

Quadrana, L.*, **Almeida, J.***, Otaiza, S., Duffy, T., Correa-Silva, J. V., de Godoy, F., Asís, R., Bermudez, L., Fernie, A., Carrari, F., Rossi, M. (2013). Transcriptional regulation of vitamin E biosynthesis in tomato. *Plant Molecular Biology*, 81, 309-325. * *Contribuição equivalente*.

Capítulo IV

Almeida, J., Asís, R., Molineri, V. N., Sestari, I., Lira, B. S., Carrari, F., Peres, L. E. P., Rossi, M. (2015). Fruits from ripening impaired, chlorophyll degraded and jasmonate insensitive tomato mutants have altered tocopherol content and composition. *Phytochemistry*, *111*, 72–83.

Capítulo VI

Almeida, J., Azevedo, M. S., Spicher L., Glauser, G., vom Dorp, K., Guyer, L., Carranza, A. V., Asis, R., de Souza, A. P., Buckeridge, M., Demarco, D., Bres, C., Rothan, C., Peres, L. E. P., Hörtensteiner, S., Kessler, F., Dörmann, P., Carrari, F., Rossi, M. Tocopherol content is highly dependent on *PHYTOL KINASE* in tomato (submetido).

Decorrentes de resultados da tese, mas que não formam parte dela:

Capítulo II

Quadrana, L., **Almeida, J.**, Asís, R., Duffy, T., Dominguez, P. G., Bermúdez, L., Conti, G., Correa-Silva, J. V., Peralta, I., Colot, V., Sebastian, A., Fernie, A., Rossi, M., Carrari, F. (2014). Natural occurring epialleles determine vitamin E accumulation in tomato fruits. *Nature Communications*, 5, 3027.

Decorrentes de colaboração com outros projetos do grupo de pesquisa:

Lira, B. S., de Setta, N., Rosado, D., **Almeida, J**., Freschi, L., Rossi, M. (2014). Plant degreening: evolution and expression of tomato (Solanum lycopersicum) dephytylation enzymes. *Gene*, 546, 359-366.

Bermúdez, L., de Godoy, F., Baldet, P., Demarco, D., Osorio, S., Quadrana, L., **Almeida, J.**, Asis, R., Gibon, Y., Fernie, A.R., Rossi, M., Carrari, F. (2014) Silencing of the tomato sugar partitioning affecting protein (SPA) modifies sink strength through a shift in leaf sugar metabolism. *The Plant Journal*, 77, 676-687.

de Godoy, F., Bermúdez, L., Lira, B. S., de Souza, A.P., Elbl, P., Demarco, D., Alseekh, S., Insani, M., Buckeridge, M., **Almeida, J.**, Grigioni, G., Fernie, A.R., Carrari, F., Rossi, M. (2013) Galacturonosyltransferase 4 silencing alters pectin composition and carbon partitioning in tomato. *Journal of Experimental Botany*, 64, 2449-2466.

ANEXO I

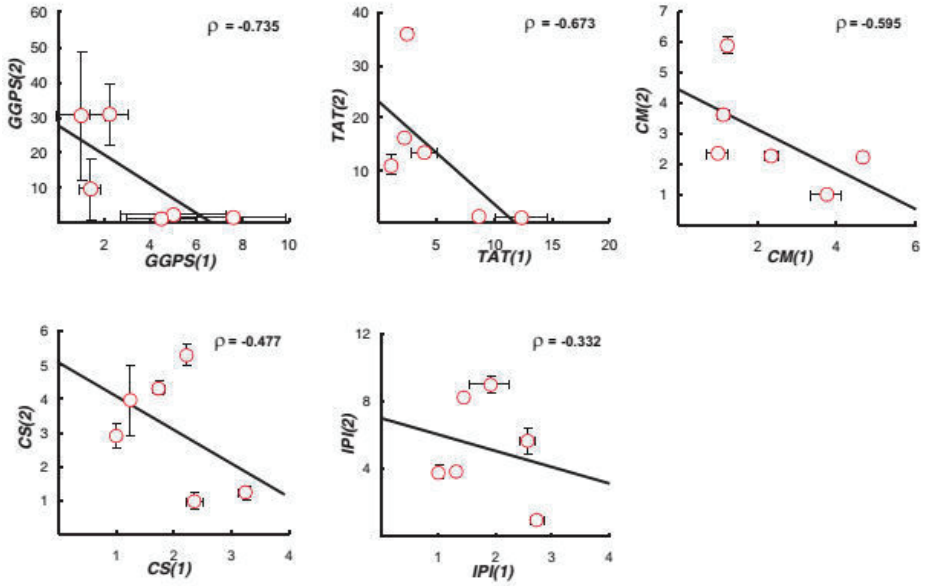

Supplementary Figure 1. Pearson´s correlation analysis performed with expression data from pairs of paralogous genes. The graphs show the expression of paralogous genes in the different tissues analyzed. Black line corresponds to a linear regression and the ρ parameter indicates the correlation coefficient.All correlations were statistically significant (p<0.01)

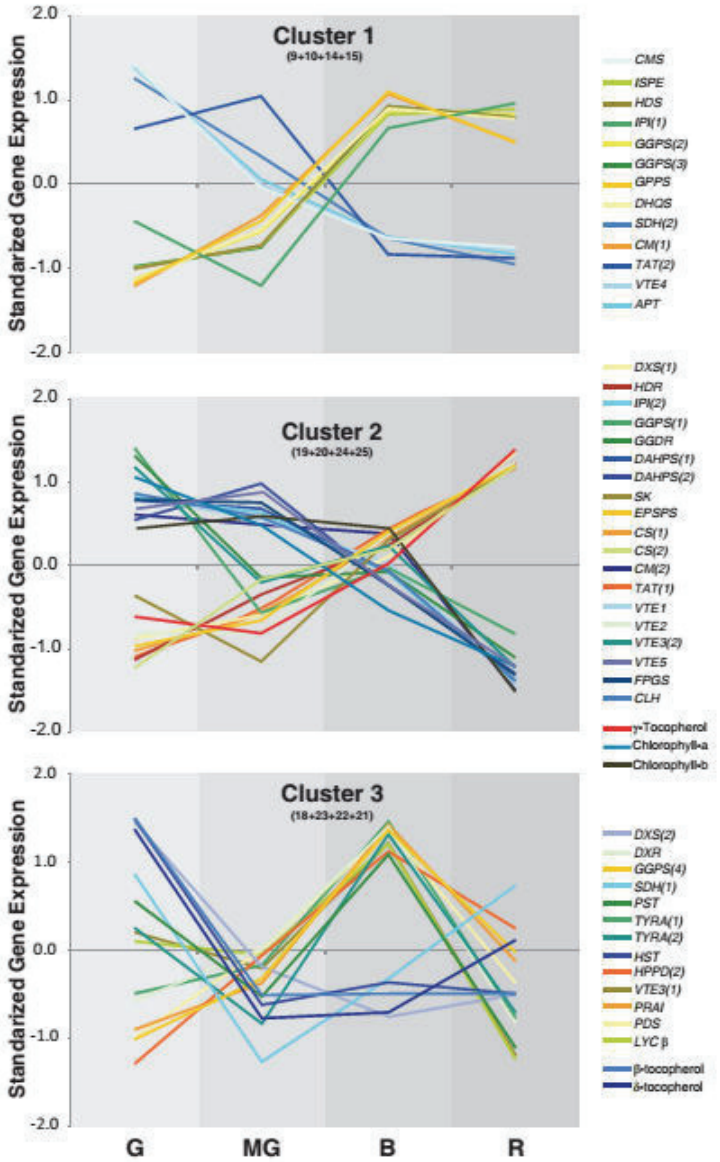

Supplementary Figure 2. Co-variation patterns by a neural network analysis. Three profiles of normalized gene expression and tocopherol variation levels along fruit ripening were identified: cluster 1 composed of neighbor neurons 9, 10, 14, 15; cluster 2 composed of neighbor neurons 19, 20, 24, 25; and cluster 3 composed of neighbor neurons 18, 23, 22, 21.Analysis was performed by applying the *omeSOM software (Milone et al., 2010).

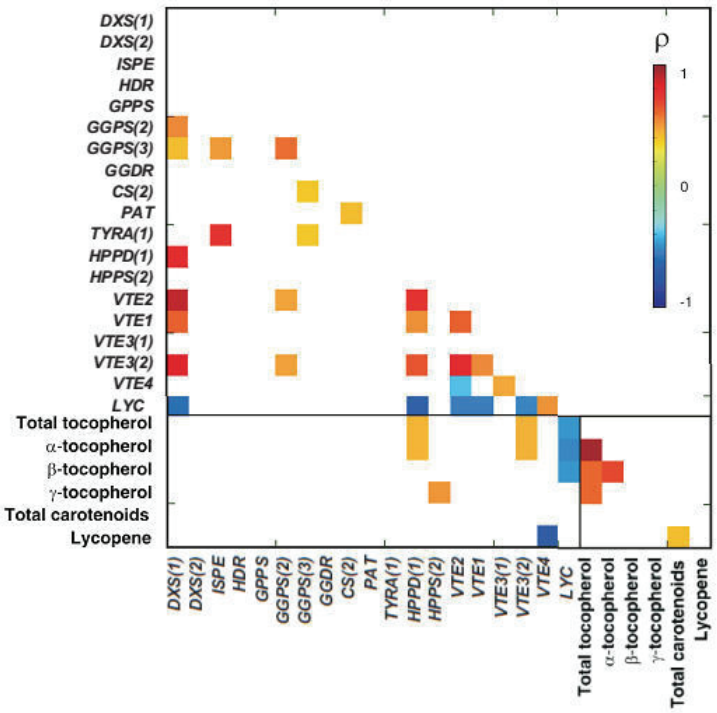

Supplementary Figure 3. Correlation between gene expression and metabolite data from ripe fruits of Andean landraces cultivars. Pearson´s correlation between metabolites and gene expression was performed. Each square represents statistical significant correlation ($p<0.01$) with a given r value indicated by the color scale.

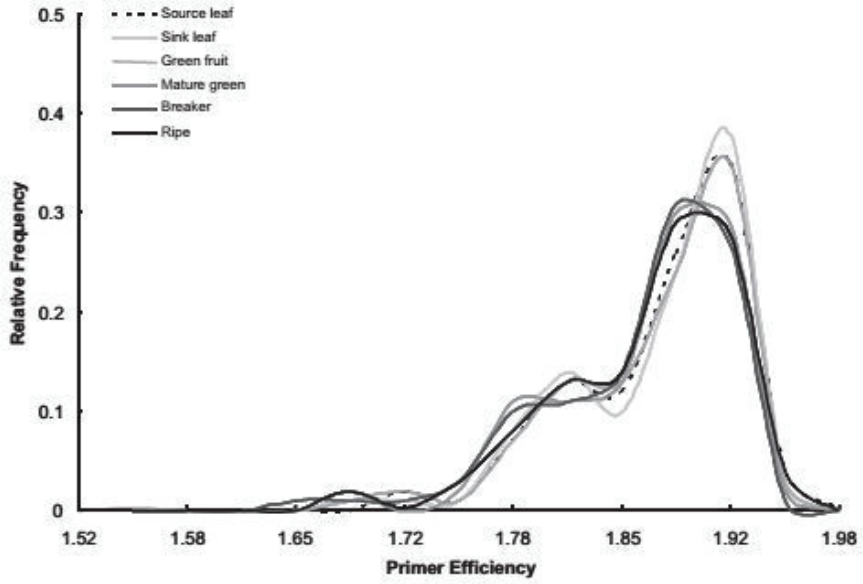

	Source leaf	Sink leaf	Green fruit	Mature green	Breaker	Ripe
Mean	1.86	1.87	1.87	1.87	1.87	1.87
Median	1.88	1.89	1.89	1.89	1.89	1.89

Supplementary Figure 4. qPCR efficiency. The histogram shows distribution of primer efficiency for all the genes and tissues analyzed. Means and medians are indicated below. No statistical differences were obtained (ANOVA, $p<0.05$) when comparing the sample efficiency distribution.

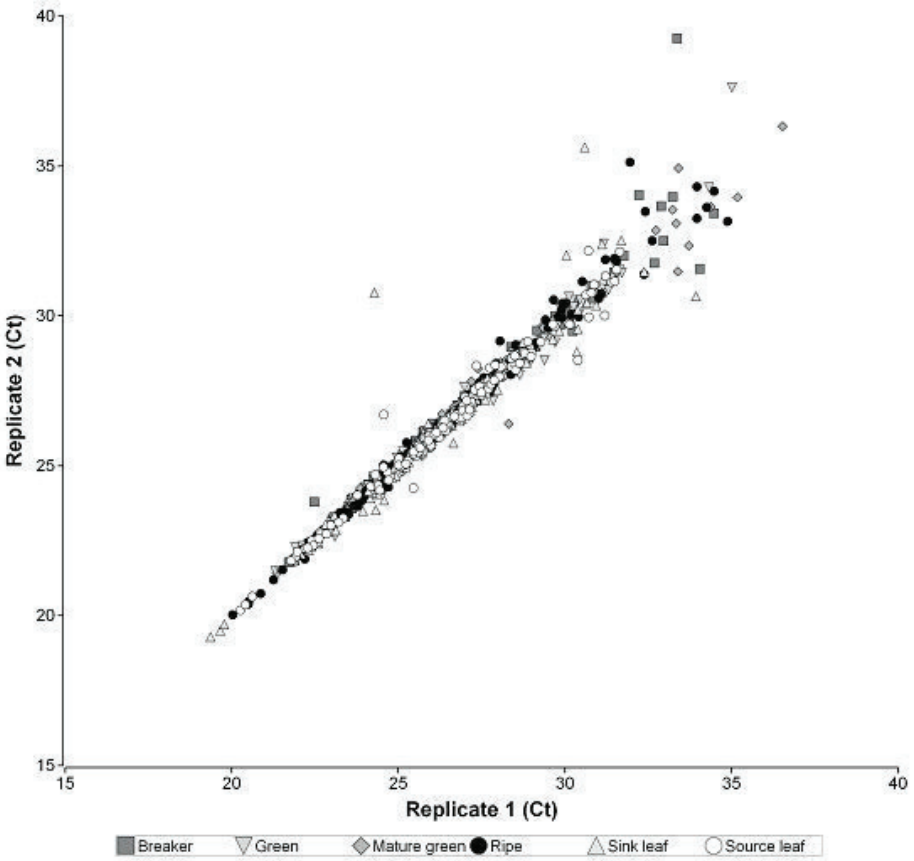

Supplementary Figure 5. Reproducibility of qRT-PCR. Results from the technical replicates for all the samples analyzed were plotted and R was calculated by linear regression.

Supplemental Table 1. Relative gene expression of tocopherol biosynthesis pathway genes in different tomato tissues.

	Source Leaf	Sink Leaf	Green	Mature Green	Breaker	Ripe
DXR	4.90 ± 0.35 [a]	3.01 ± 0.08 [b]	1.14 ± 0.20 [c,d]	1.49 ± 0.25 [c,d]	2.26 ± 0.43 [c]	1.00 ± 0.22 [d]
DXS(1)	1.30 ± 0.45 [a,b,c]	3.92 ± 0.16 [b]	1.00 ± 0.19 [a,c]	1.42 ± 0.28 [c]	2.49 ± 0.06 [a]	4.36 ± 1.26 [a,b]
DXS(2)	112 ± 29.1 [a]	272 ± 7.08 [b]	8.50 ± 4.41 [c]	2.20 ± 0.56 [c,d]	nd	1.00 ± 0.20 [d]
CMS	2.24 ± 0.14 [a]	3.25 ± 0.57 [b]	2.41 ± 0.84 [a,c,d]	1.46 ± 0.06 [c]	1.07 ± 0.09 [d]	1.00 ± 0.09 [d]
ISPE	1.49 ± 0.06 [a]	1.48 ± 0.28 [a]	1.00 ± 0.08 [b]	1.40 ± 0.22 [a,b]	3.84 ± 0.25 [c]	3.94 ± 0.53 [c]
ISPF	1.39 ± 0.04 [a]	1.31 ± 0.10 [a]	1.05 ± 0.22 [b]	1.01 ± 0.10 [b]	1.16 ± 0.10 [b]	1.00 ± 0.10 [b]
HDS	1.78 ± 0.04 [a]	1.31 ± 0.02 [b]	1.00 ± 0.14 [c]	1.07 ± 0.09 [c]	1.48 ± 0.02 [d]	1.44 ± 0.12 [b,d]
HDR	1.96 ± 0.07 [a]	1.58 ± 0.13 [b]	1.00 ± 0.06 [c]	1.39 ± 0.13 [b]	1.68 ± 0.07 [b]	2.18 ± 0.19 [a]
IPI(1)	1.00 ± 0.02 [a]	1.32 ± 0.07 [b]	1.91 ± 0.34 [b]	1.46 ± 0.07 [b]	2.56 ± 0.14 [c]	2.74 ± 0.12 [c]
IPI(2)	3.79 ± 0.42 [a]	3.85 ± 0.29 [a]	8.94 ± 0.48 [b]	8.25 ± 0.11 [b]	5.65 ± 0.75 [c]	1.00 ± 0.17 [d]
GPPS	1.39 ± 0.03 [a]	1.00 ± 0.04 [b]	1.17 ± 0.19 [a,b]	1.55 ± 0.08 [c]	2.34 ± 0.23 [d]	2.03 ± 0.02 [d]
GGPS(1)	7.58 ± 2.29 [a]	5.01 ± 2.29 [a,b]	4.49 ± 1.49 [b]	1.39 ± 0.42 [c]	2.23 ± 0.82 [c]	1.00 ± 1.06 [c]
GGPS(2)	1.55 ± 0.30 [a]	2.21 ± 0.90 [b]	1.00 ± 0.63 [a,b]	9.49 ± 8.77 [b,c]	30.8 ± 14.9 [c]	30.4 ± 18.2 [c]
GGPS(3)	1.84 ± 0.14 [a,b]	1.54 ± 0.13 [a]	1.00 ± 0.11 [c]	1.14 ± 0.19 [c]	2.15 ± 0.08 [d]	2.07 ± 0.01 [b,d]
GGPS(4)	1.13 ± 0.08 [a]	1.00 ± 0.14 [a]	1.04 ± 0.11 [a]	1.15 ± 0.05 [a]	1.40 ± 0.17 [b]	1.19 ± 0.06 [a]
GGDR	41.2 ± 4.11 [a]	59.7 ± 1.78 [b]	7.41 ± 0.68 [c]	3.53 ± 0.48 [d]	3.72 ± 0.74 [d]	1.00 ± 0.13 [e]
DAHPS(1)	4.89 ± 0.35 [a]	5.52 ± 0.64 [a]	3.87 ± 0.22 [b]	3.74 ± 0.19 [b]	2.74 ± 0.23 [b]	1.00 ± 0.19 [c]
DAHPS(2)	2.54 ± 0.26 [a]	2.60 ± 0.07 [a,b]	3.08 ± 0.38 [b]	3.57 ± 0.22 [b]	2.19 ± 0.11 [a,b]	1.00 ± 0.29 [c]
DHQS	2.19 ± 0.42 [a]	1.51 ± 0.10 [a]	1.00 ± 0.08 [b]	1.16 ± 0.10 [b]	1.54 ± 0.03 [a]	1.51 ± 0.17 [a]
SDH/DHQ(1)	1.00 ± 0.11 [a]	1.47 ± 0.44 [a,b]	1.61 ± 0.79 [b]	1.03 ± 0.12 [a]	1.29 ± 0.14 [a]	1.58 ± 0.17 [b]
SDH/DHQ(2)	14.4 ± 1.59 [a]	19.8 ± 0.29 [b]	15.8 ± 2.12 [a]	9.58 ± 2.64 [c]	3.06 ± 1.02 [d]	1.00 ± 0.15 [e]
SK	1.15 ± 0.14 [a,b]	1.11 ± 0.06 [a,b]	1.11 ± 0.39 [a,b]	1.00 ± 0.06 [a]	1.20 ± 0.12 [a,b]	1.32 ± 0.11 [b]
EPSPS	1.38 ± 0.17 [a,b]	1.11 ± 0.08 [a]	1.00 ± 0.41 [a]	1.10 ± 0.23 [a]	1.45 ± 0.06 [a]	1.72 ± 0.12 [c]
CS(1)	3.24 ± 0.10 [a]	2.36 ± 0.14 [b]	1.00 ± 0.01 [c]	1.25 ± 0.07 [d]	1.74 ± 0.11 [e]	2.21 ± 0.05 [a]
CS(2)	1.24 ± 0.20 [a]	1.00 ± 0.26 [a]	2.90 ± 0.38 [b]	3.95 ± 1.03 [b,c]	4.31 ± 0.21 [c]	5.28 ± 0.32 [d]
CM(1)	1.23 ± 0.12 [a]	1.15 ± 0.14 [a]	1.00 ± 0.25 [a]	2.35 ± 0.17 [b]	4.64 ± 0.10 [c]	3.74 ± 0.40 [d]
CM(2)	5.88 ± 0.27 [a]	3.60 ± 0.15 [b]	2.35 ± 0.07 [c]	2.28 ± 0.12 [c]	2.21 ± 0.01 [c]	1.00 ± 0.05 [d]
PAT	2.35 ± 0.11 [a]	1.88 ± 0.06 [b]	1.44 ± 0.21 [c]	1.15 ± 0.08 [c,d]	1.58 ± 0.07 [c]	1.00 ± 0.03 [d]
TYRA(1)	1.11 ± 0.33 [a]	1.88 ± 0.25 [b]	1.50 ± 0.40 [a,b]	2.09 ± 0.65 [b]	5.00 ± 0.87 [c]	1.00 ± 0.46 [a]
TYRA(2)	36.1 ± 8.48 [a]	7.23 ± 3.14 [b]	8.76 ± 3.30 [b]	nd	17.2 ± 6.74 [c]	1.00 ± 0.02 [d]
TAT(1)	2.39 ± 0.07 [a]	2.21 ± 0.04 [a]	1.00 ± 0.21 [b]	3.94 ± 1.18 [c]	8.67 ± 0.37 [d]	12.3 ± 2.22 [e]
TAT(2)	36.1 ± 0.90 [a]	16.2 ± 0.08 [b]	11.0 ± 1.90 [c]	13.48 ± 1.00 [c]	1.29 ± 0.28 [d]	1.00 ± 0.16 [d]
HPPD(1)	3.28 ± 0.17 [a]	1.92 ± 0.12 [b]	1.00 ± 0.16 [c]	1.08 ± 0.08 [c]	1.46 ± 0.03 [c]	1.37 ± 0.08 [c]
HPPD(2)	5.60 ± 0.48 [a]	3.09 ± 0.22 [b]	1.00 ± 0.99 [c]	4.96 ± 0.88 [a,b]	8.78 ± 0.43 [d]	5.95 ± 0.76 [a]
HST	4.21 ± 0.34 [a]	3.53 ± 0.97 [a,b]	1.83 ± 0.25 [b]	1.00 ± 0.11 [c]	1.10 ± 0.17 [c]	1.05 ± 0.11 [c]
VTE2	1.00 ± 0.06 [a]	1.19 ± 0.15 [a]	1.68 ± 0.04 [b]	1.69 ± 0.07 [b]	1.95 ± 0.21 [b,c]	2.14 ± 0.42 [c]
VTE3(1)	7.38 ± 0.13 [a]	9.39 ± 0.81 [b]	9.46 ± 4.17 [a,b,c]	7.02 ± 2.43 [c]	15.6 ± 2.40 [d]	1.00 ± 1.16 [e]
VTE3(2)	7.29 ± 0.55 [a]	7.30 ± 0.17 [a]	1.70 ± 0.22 [b]	1.29 ± 0.09 [c]	1.42 ± 0.08 [b,c]	1.00 ± 0.03 [d]
VTE1	1.58 ± 0.21 [a]	2.02 ± 0.06 [b]	2.40 ± 0.65 [b]	2.23 ± 0.29 [b]	1.91 ± 0.17 [b]	1.00 ± 0.08 [a]
VTE4	3.81 ± 0.78 [a]	2.76 ± 0.09 [a]	2.27 ± 0.06 [b]	1.45 ± 0.20 [c]	1.08 ± 0.12 [d]	1.00 ± 0.12 [d]
VTE5	13.29 ± 0.71 [a]	14.85 ± 1.26 [a]	8.18 ± 1.86 [b]	9.31 ± 0.70 [b]	4.73 ± 0.80 [c]	1.00 ± 0.27 [d]
APT	18.7 ± 2.83 [a]	18.6 ± 3.02 [a]	14.3 ± 6.63 [a,b]	6.40 ± 0.89 [b]	2.27 ± 0.94 [c]	1.00 ± 0.30 [d]
PRAI	1.00 ± 0.22 [a]	1.42 ± 0.35 [a]	2.04 ± 0.13 [b]	2.87 ± 1.05 [b]	5.71 ± 0.18 [c]	3.26 ± 0.88 [b]
FPGS	3.15 ± 0.41 [a]	2.31 ± 0.12 [b]	1.79 ± 0.44 [b,c]	1.78 ± 0.08 [c]	1.40 ± 0.23 [c,d]	1.00 ± 0.06 [d]
CHL	51.8 ± 8.21 [a]	16.9 ± 1.58 [b]	9.17 ± 0.41 [c]	8.15 ± 2.02 [c,d]	5.78 ± 0.46 [d]	1.00 ± 0.07 [e]
LYCB	1.00 ± 0.37 [a]	1.21 ± 0.58 [a]	5.97 ± 0.14 [b]	5.70 ± 1.74 [b]	7.96 ± 1.50 [c]	3.55 ± 0.12 [d]
PDS	1.42 ± 0.13 [a]	1.33 ± 0.19 [a]	1.00 ± 0.04 [b]	1.62 ± 0.32 [a]	2.47 ± 0.55 [c]	1.39 ± 0.32 [a]

Samples were obtained from 4-6 plants and pooled in three replicates. Values represent medians ± SE from three replicates. The medians were calculated from means of two technical replicates and normalized against the sample with the lowest relative expression. Statistically significant differences ($p<0.05$) between samples are indicated with different letters according to a permutation test, that lack of sample distribution assumptions (Pfaffl et al . 2002). nd: not detected.

Supplemental Table 2. Interconnections between genes and metabolites.

	Total	Gene-gene	Gene-metabolites	Metabolites-metabolites
VTE3(2)	20	15	5	-
CHL-a	20	-	16	4
CHL-b	19	-	15	4
CM(2)	19	14	5	-
DXR	13	9	4	-
CLH	9	6	3	-
TAT(2)	9	6	3	-
T-T	8	-	5	3
VTE4	7	5	2	-
GGDR	7	2	5	-
α-T	7	-	4	3
PAT	7	4	3	-
FPGS	6	4	2	-
HPPD(1)	6	4	2	-
GGPS(1)	6	4	2	-
HST	5	3	2	-
APT	5	3	2	-
VTE5	4	2	2	-
δ-T	4	-	2	2
DXS(2)	4	2	2	-
DAHPS(1)	4	2	2	-
T-Carotene	3	-	3	0
ISPF	2	1	1	-
SDH(2)	1	1	0	-
Lycopene	1	-	1	0

Supplemental Table 4. Relative gene expression of selected tocopherol biosynthetic pathway genes in ripe fruit pericarp of Andean landrace genotypes.

	LA407	C352	CZBU	TOPA	C169	C273	C369	C237	C525	ALGR	LA1589	CHMI	CMP	STUF	C526	GPEA	M82
DXS(1)	nd	0.89 ± 0.17	0.99 ± 0.27	1.16 ± 0.04	0.52 ± 0.25	**1.74 ± 0.19**	**0.53 ± 0.08**	**1.88 ± 0.38**	0.60 ± 0.07	1.09 ± 0.20	**1.85 ± 0.06**	1.12 ± 0.07	**0.60 ± 0.06**	1.35 ± 0.28	**0.78 ± 0.11**	**1.53 ± 0.06**	1.00 ± 0.12
DXS(2)	**28.0 ± 5.78**	1.98 ± 0.58	2.52 ± 0.74	**2.80 ± 0.00**	2.04 ± 0.92	**19.6 ± 4.28**	1.30 ± 0.00	2.55 ± 1.54	nd	0.96 ± 0.60	**16.9 ± 3.72**	1.15 ± 0.00	**2.34 ± 0.45**	**3.06 ± 1.01**	**2.75 ± 0.79**	**3.40 ± 0.76**	1.00 ± 0.00
ISPE	1.32 ± 0.09	0.82 ± 0.25	0.60 ± 0.22	1.98 ± 0.54	1.20 ± 0.54	**2.83 ± 0.28**	0.87 ± 0.17	**2.23 ± 0.22**	0.92 ± 0.30	1.17 ± 0.49	1.91 ± 0.46	1.67 ± 0.77	**0.58 ± 0.13**	**2.08 ± 0.08**	0.81 ± 0.31	1.96 ± 0.10	1.00 ± 0.14
HDR	3.57 ± 0.50	2.03 ± 0.16	1.88 ± 0.82	1.39 ± 0.47	**1.83 ± 0.24**	**2.99 ± 0.89**	1.57 ± 0.53	1.78 ± 0.39	1.24 ± 0.29	1.92 ± 0.25	1.86 ± 0.63	1.69 ± 1.22	0.87 ± 0.45	**2.16 ± 0.26**	1.56 ± 0.30	**4.67 ± 2.48**	1.00 ± 0.37
GPPS	0.43 ± 0.10	0.39 ± 0.07	0.56 ± 0.03	0.50 ± 0.04	0.42 ± 0.02	0.50 ± 0.02	0.50 ± 0.12	0.53 ± 0.06	0.67 ± 0.11	0.55 ± 0.12	0.70 ± 0.11	0.33 ± 0.05	**0.54 ± 0.02**	0.56 ± 0.03	0.33 ± 0.03	0.40 ± 0.10	1.00 ± 0.25
GGPS(2)	**0.13 ± 0.01**	0.94 ± 0.09	**0.48 ± 0.40**	**3.55 ± 0.79**	0.22 ± 0.63	**3.03 ± 1.74**	0.22 ± 0.07	0.77 ± 1.20	**0.35 ± 0.14**	1.08 ± 0.30	**2.59 ± 0.41**	0.27 ± 0.67	**0.29 ± 0.03**	1.20 ± 1.03	**0.27 ± 0.07**	**2.44 ± 0.20**	1.00 ± 0.06
GGPS(3)	0.61 ± 0.10	1.05 ± 0.27	0.73 ± 0.35	1.52 ± 0.07	0.62 ± 0.04	1.25 ± 0.18	0.59 ± 0.05	0.85 ± 0.09	0.75 ± 0.11	1.05 ± 0.18	0.88 ± 0.02	**0.45 ± 0.12**	0.60 ± 0.14	1.10 ± 0.07	1.16 ± 0.26	0.98 ± 0.04	1.00 ± 0.22
GGDR	28.9 ± 15.2	0.25 ± 0.44	2.49 ± 1.85	**6.52 ± 2.85**	0.19 ± 0.75	**3.03 ± 0.89**	2.58 ± 0.76	2.15 ± 1.35	1.38 ± 1.22	1.30 ± 0.51	1.71 ± 0.46	**5.30 ± 0.61**	**3.22 ± 0.83**	0.79 ± 0.38	1.91 ± 0.60	1.44 ± 0.85	1.00 ± 0.57
CS(2)	1.67 ± 0.34	1.11 ± 0.08	**2.39 ± 0.45**	**4.56 ± 0.66**	**2.03 ± 0.33**	**2.53 ± 0.65**	1.19 ± 0.29	**2.75 ± 0.52**	1.26 ± 0.10	1.52 ± 0.27	**2.67 ± 0.50**	1.61 ± 0.48	1.11 ± 0.48	1.56 ± 0.19	1.28 ± 0.31	1.33 ± 0.08	1.00 ± 0.29
PAT	0.91 ± 0.15	0.72 ± 0.08	0.67 ± 0.14	1.11 ± 0.15	0.82 ± 0.23	0.70 ± 0.10	0.75 ± 0.15	1.01 ± 0.12	0.94 ± 0.15	1.06 ± 0.24	0.80 ± 0.02	1.06 ± 0.22	0.73 ± 0.04	0.81 ± 0.11	0.47 ± 0.13	0.86 ± 0.07	1.00 ± 0.18
TYRA(1)	0.19 ± 0.03	0.73 ± 0.30	0.62 ± 0.16	1.43 ± 0.14	1.06 ± 0.78	0.50 ± 1.02	**3.18 ± 0.71**	**2.01 ± 1.07**	**2.07 ± 0.56**	1.38 ± 0.23	1.94 ± 0.63	1.25 ± 0.52	0.60 ± 0.13	**2.04 ± 0.67**	0.91 ± 0.09	1.02 ± 0.37	1.00 ± 0.25
HPPD(1)	**0.01 ± 0.00**	**0.09 ± 0.45**	1.26 ± 0.41	1.27 ± 0.45	0.40 ± 0.94	1.41 ± 0.32	0.48 ± 0.20	**1.40 ± 1.38**	1.61 ± 0.38	1.00 ± 0.45	**1.50 ± 0.28**	2.17 ± 1.79	0.84 ± 0.41	1.03 ± 0.18	0.65 ± 0.23	0.96 ± 0.61	1.00 ± 0.17
HPPD(2)	1.13 ± 0.48	**1.92 ± 0.06**	2.01 ± 0.79	1.31 ± 0.24	0.94 ± 1.07	**2.41 ± 0.42**	1.02 ± 0.20	**2.60 ± 0.48**	1.49 ± 0.20	1.77 ± 0.16	**4.35 ± 0.86**	**3.31 ± 0.70**	**3.01 ± 0.34**	**2.35 ± 0.19**	1.42 ± 0.47	**1.81 ± 0.08**	1.00 ± 0.19
VTE2	nd	0.97 ± 0.05	1.65 ± 0.84	**1.86 ± 0.28**	**1.14 ± 0.63**	**2.06 ± 0.48**	1.13 ± 0.09	**1.63 ± 0.63**	**0.74 ± 0.16**	**0.59 ± 0.07**	**2.26 ± 0.20**	**2.63 ± 0.84**	0.75 ± 0.21	1.26 ± 0.35	1.43 ± 0.04	**2.02 ± 0.06**	1.00 ± 0.03
VTE1	nd	0.62 ± 0.04	nd	0.87 ± 0.09	0.69 ± 0.22	0.82 ± 0.07	0.75 ± 0.10	1.14 ± 0.11	0.69 ± 0.10	**0.53 ± 0.09**	0.94 ± 0.11	1.15 ± 0.03	0.57 ± 0.07	0.65 ± 0.06	0.61 ± 0.12	0.91 ± 0.04	1.00 ± 0.15
VTE3(1)	**2.67 ± 0.23**	0.73 ± 0.12	**0.27 ± 0.23**	1.16 ± 0.20	**1.42 ± 0.44**	0.41 ± 0.55	1.02 ± 0.11	1.21 ± 0.38	0.61 ± 0.16	**0.70 ± 0.01**	**2.53 ± 0.75**	**2.36 ± 0.48**	**0.49 ± 0.29**	1.10 ± 0.10	0.83 ± 0.19	**1.66 ± 0.26**	1.00 ± 0.03
VTE3(2)	**0.08 ± 0.01**	1.07 ± 0.12	1.53 ± 0.49	1.85 ± 0.23	1.02 ± 0.43	**4.68 ± 1.06**	1.00 ± 0.17	**1.40 ± 0.44**	0.81 ± 0.20	**1.39 ± 0.13**	**2.12 ± 0.17**	**2.31 ± 0.42**	**1.73 ± 0.17**	**1.64 ± 2.71**	**2.86 ± 0.89**	**1.22 ± 0.10**	1.00 ± 0.04
VTE4	**16.1 ± 3.59**	1.79 ± 0.51	0.87 ± 0.24	**2.68 ± 1.31**	0.98 ± 0.37	**5.62 ± 2.01**	0.96 ± 0.10	**1.99 ± 0.52**	0.92 ± 0.21	**2.71 ± 0.89**	1.52 ± 0.31	**5.82 ± 1.62**	**2.47 ± 0.31**	**2.44 ± 0.57**	1.02 ± 0.21	**5.29 ± 0.60**	1.00 ± 0.31
LYCB	**23.7 ± 3.21**	1.45 ± 0.23	1.85 ± 0.30	**5.02 ± 0.60**	1.38 ± 0.32	2.95 ± 1.79	1.46 ± 0.35	0.97 ± 0.06	0.77 ± 0.20	1.46 ± 0.12	**1.91 ± 0.20**	0.68 ± 0.24	**0.67 ± 0.07**	1.16 ± 0.11	1.23 ± 0.23	1.26 ± 0.07	1.00 ± 0.29

Values represent medians ± SE from the three replicates. The medians were calculated from means of two technical replicates and normalized against M82 value. Statistically significant differences ($p < 0.05$) against M82 according to a permutation test, that lack of sample distribution assumptions (Pfaffl et al ., 2002), are highlighted in bold. nd: not detected

Supplemental Table 5. MIQE form, qPCR and samples information.

Experimental design		**Tocopherol array information**
Definition of experimental and control groups	E	*Solanum lycopersicum* (cv. M82): source leaves (Sr), sink leaves (Sn), green fruits (G), mature green fruits (MG), breaker fruits (B), ripe fruits (R) *S. lycopersicum* land-races cultivars: C352; CZBU1; TOPA; C169; C273; C369; C237; C525; CHMI; CMP; C526; *S. lycopersicum* commercial cultivars: GPEA; STUF; ALGR. *Solanum habroichates* (LA407); *Solanum pimpinellifolium* (LA1589)
Number within each group	E	All samples were obtained up to six independent plants and were pooled in three replicates.
Assay carried out by the core or investigator's laboratory?	D	yes
Acknowledgment of authors' contributions	D	-
Sample		
Description	E	*Solanum lycopersicum* (cv. M82): source (SL) and sink leaf (Sn); stages of fruit development (G, green, 30 days after anthesis; MG - mature green, 45 days after anthesis; B - breaker, 50 days after anthesis; R - ripe, 60 days after anthesis) ripe fruit of *Solanum lycopersicum* land-races cultivars (approximately 60-65 days after anthesis)
Volume/mass of sample processed	D	see sample information sheet on this file
Microdissection or macrodissection	E	macrodissection
Processing procedure	E	Freeze-dried material tissues were ground to a fine powder in liquid nitrogen
If frozen, how and how quickly?	E	tissue were harvested and immediately frozen into liquid nitrogen
If fixed, with what and how quickly?	E	-
Sample storage conditions and duration (especially for FFPE[2]samples)	E	–80 C until use
Nucleic acid extraction		
Procedure and/or instrumentation	E	Total RNA from 50 and 100 mg of leaf and fruit tissue respectively was isolated using Trizol reagent
Name of kit and details of any modifications	E	Trizol (Invitrogen)
Source of additional reagents used	D	-
Details of DNase or RNase treatment	E	DNA traces were removed by treatment with amplification-grade DNAse I (Invitrogen) following the manufacturer instructions
Contamination assessment (DNA or RNA)	E	The suitability of each cDNA for PCR reaction and DNA contamination were checked using an intron-flanking pair of primers of the vte1 gene
Nucleic acid quantification	E	see sample information sheet on this file
Instrument and method	E	NanoDrop spectrophotometer
Purity (A_{260}/A_{280})	D	in general, high-quality samples with OD ratios of at least 1,8 (260/280 nm) and 1,9 (260/230 nm) were used for further analysis; for exceptions see sample information
Yield	D	see sample information sheet on this file
RNA integrity: method/instrument	E	agarose-gel electrophoresis
RIN/RQI or C_q of 3' and 5' transcripts	E	analysis not performed
Electrophoresis traces	D	analysis not performed
Inhibition testing (C_q dilutions, spike, or other)	E	analysis not performed
Reverse transcription		
Complete reaction conditions	E	cDNA was synthesised from 1µg of total RNA using Superscript III reverse transcriptase (Invitrogen) according to the manufacturer instructions.
Amount of RNA and reaction volume	E	1 ug in 20 ul
Priming oligonucleotide (if using GSP) and concentration	E	random primers
Reverse transcriptase and concentration	E	SuperScript III enzyme (Invitrogen) according to manufacturer instructions
Temperature and time	E	according to manufacturer instructions
Manufacturer of reagents and catalogue numbers	D	Invitrogen
C_qs with and without reverse transcription	D[3]	The suitability of each cDNA for PCR reaction and DNA contamination were checked using an intron-flanking pair of primers of the vte1 gene
Storage conditions of cDNA	D	–20 ºC
qPCR target information		
Gene symbol	E	see primer and amplicon information sheet on this file
Sequence accession number	E	see primer and amplicon information sheet on this file
Location of amplicon	D	data not shown
Amplicon length	E	see primer and amplicon information sheet on this file
In silico specificity screen (BLAST, and so on)	E	blast against SGN (http://solgenomics.net/) unigene database
Pseudogenes, retropseudogenes, or other homologs?	D	-
Sequence alignment	D	data not shown

Secondary structure analysis of amplicon	D	not done
Location of each primer by exon or intron (if applicable)	E	intron-spanning primers (except GGPS paralogs and LYCB)
What splice variants are targeted?	E	the existance of alternative splicing is known.
qPCR oligonucleotides		**Tocopherol array information**
Primer sequences	E	see primer and amplicon information sheet on this file
RTPrimerDB identification number	D	-
Probe sequences	D[4]	none
Location and identity of any modifications	E	none
Manufacturer of oligonucleotides	D	Invitrogen
Purification method	D	none
qPCR protocol		
Complete reaction conditions	E	20 µl reaction contained optimized concentration of forward and reverse primer, 10 ul of SYBR mix, cDNA quantity corresponding to 10 or 20 ng of total RNA reverse-transcribed
Reaction volume and amount of cDNA/DNA	E	cDNA samples were 10X diluted to a final concentration of 10 ng reverse-transcribed RNA/ul; 2 or 4 ul were used per reaction (see primer and amplicon information)
Primer, (probe), Mg^{2+}, and dNTP concentrations	E	see primer and amplicon information sheet on this file
Polymerase identity and concentration	E	
Buffer/kit identity and manufacturer	E	2X SYBR Green Master Mix (Applied Biosystems)
Exact chemical composition of the buffer	D	-
Additives (SYBR Green I, DMSO, and so forth)	E	-
Manufacturer of plates/tubes and catalog number	D	-
Complete thermocycling parameters	E	10 min at 95oC, followed by 40 cycles of 15 s at 95oC, 30 s at 55 / 60oC, and 30 s at 72 oC. The amplification process was followed by a melting curve analysis
Reaction setup (manual/robotic)	D	manual
Manufacturer of qPCR instrument	E	Applied Biosystems 7500 Real Time PCR System
qPCR validation		
Evidence of optimization (from gradients)	D	Optimal concentration of PCR primer pair was selected in a 100–800 nM range based on: lowest Ct values and primer dimer formation
Specificity (gel, sequence, melt, or digest)	E	Specifity was validate by electrophoresis agarose gel and melt curve analysis
For SYBR Green I, C_q of the NTC	E	Ct undected or with more than 5 Cts of diference for the lowest concentration unknown
Calibration curves with slope and *y* intercept	E	-
PCR efficiency calculated from slope	E	The mean PCR efficiency was calculated based on the starting point of the exponential phase of amplification using LinReg PCR program from raw normalized fluorescence as input data (see primer and amplicon information)
CIs for PCR efficiency or SE	D	-
r^2 of calibration curve	E	NA
Linear dynamic range	E	Ct20 to Ct34
C_q variation at LOD	E	NA
CIs throughout range	D	-
Evidence for LOD	E	-
If multiplex, efficiency and LOD of each assay	E	-
Data analysis		
qPCR analysis program (source, version)	E	LinRegPCR (Ramakers *et al.*, 2003)
Method of C_q determination	E	The fluorescence threshold for determining Cq values is automatically set at 1 cycle below the upper limit of the window of linearity
Outlier identification and disposition	E	data not shown
Results for NTCs	E	Ct undected or with more than 5 Cts of diference for the lowest concentration unknown
Justification of number and choice of reference genes	E	Tomato reference genes described by Exposito-Rodriguez *et al.* (2008) were tested. Analyses performed indicated that the most stable genes were EXPRESSED and TIP41 as shown in Table S2
Description of normalization method	E	Normalized gene expression ratios (R) were calculated by the ΔΔCt method with the improvements proposed by Hellemans *et al.* (2007). This algorithm allows using several reference genes at the same time leading to a more accurate relative expression data according to the following equation: $$R = \frac{E_{goi}^{\Delta Ct,goi}}{\sqrt[f]{\prod_{0}^{f} E_{ref_0}^{\Delta Ct,ref_0}}}$$

Number and concordance of biological replicates	D	three
Number and stage (reverse transcription or qPCR) of technical replicates	E	For each biological replicate, qPCR dual replicates were run
Repeatability (intraassay variation)	E	see Figure S2
Reproducibility (interassay variation, CV)	D	-
Power analysis	D	-
Statistical methods for results significance	E	A permutation test, that lack of sample distribution assumptions (Pfaffl *et al*., 2002), was used to detect statistical (p<0.01) differences between tissues and land-races cultivars
Software (source, version)	E	algorithms incorporated to the fgStatistics software (Di Rienzo, 2009)
C_q or raw data submission with RDML		-

E: essential information; D: desirable information.

Supplemental Table 5. qPCR primers.

Gene name	Gene symbol [a]	UNIGENE or Genomic ID [b]	Primer Sequence (Foward/ Reverse)	cDNA amplicon lenght (bp)	Anneling Temperature (ºC)	cDNA quantity (ng/µl)	Primer concentration [nM]	Mean PCR eficciency
1-deoxy-D-xylulose-5-P synthase (DXS) EC 2.2.1.7	*DXS(1)*	SGN-U567647	CAGGACTGGTGTGGTTTCAG GGGATAGTTCACAGTGTCC	208	60	10	200	1.805
	DXS(2)	SGN-U316204	CTAAACAGCATTTTGGATGGACCC TCGATCCGTAGAACCTTATAGCC	210	60	10	200	1.891
2-C-methyl-D-erythritol 4-phosphate synthase (DXR) EC 1.1.1.267	*DXR*	SGN-U585813	GCTCACTACCTTTTCGGAGCTG AAGCCGAGGCCAAGTAATCTC	198	60	10	200	1.881
2-C-methyl-D-erythritol 4-phosphate cytidylyltransferase (CMS) EC 2.7.7.60	*CMS*	SGN-U566797	CCCAAGAATGTATTGCCTTC CCCCTTTCCTCCAGCAAG	207	60	10	400	1.914
4-(cytidine 5'-diphospho)-2-C-methyl-D-erythritol kinase (ISPE) EC 2.7.1.148	*ISPE*	SGN-U583224	GTAATGCTGCAACAACTC GGCTTTATGAGGACCATTGG	208	60	10	400	1.779
2-C-methyl-D-erythritol 2,4-cyclodiphosphate synthase (ISPF) EC 4.6.1.12	*ISPF*	SGN-U568497	CCACTCCGTTGAAGTCTC CAATATCAGGAAGCCCCAGAGC	195	60	10	400	1.904
4-hydroxy-3-methylbut-2-enyl-diphosphate synthase (HDS) EC 1.17.7.1	*HDS*	SGN-U567167	GAAGTATGGACGTGCAATGC CGATACGCCTGAACCATAAC	198	60	10	400	1.921
4-hydroxy-3-methylbut-2-enyl-diphosphate reductase (HDR) EC 1.17.1.2	*HDR*	SGN-U580658	GAGCGTGCAGTTCAGATTGC CATTTCATCAACAGCAGCC	219	60	10	400	1.906
isopentenyl diphosphate d-isomerase (IPI) EC 5.3.3.2	*IPI(1)*	SGN-U577516	CTTCTCATTCTTCACTCCG CATGGTCATTCTCATCCACC	207	55	10	200	1.913
	IPI(2)	SGN-U569721	CTGATGGAAAGTGGGGAG GGATGGTCCCCTTCTCAAC	240	60	10	800	1.909
geranyl pyrophosphate synthase (GPPS-SSU) non-catalytic small subunit	*GPPS* [former *GGPS(4)*]	SGN-U575882	CACTGCCTGTGCCTTAGAG GGGAACGAGATCACTTGG	202	60	10	400	1.908
Decaprenyl pyrophosphate synthase (DPS) EC 2.5.1.	*DPS* (former *GPPS*)	SGN-U573523	CAACTGCATTGAACGTACAG GAACCTATCCCACGTCTTG	178	55	10	400	1.890
Geranylgeranyl pyrophosphate synthase (GGPS) EC 2.5.1.29	*GGPS(1)*	SGN-U574849	CACCAAGCCAATCTTACAG GGTATTGCTTCATCTAGTGC	196	55	20	150	1.899
	GGPS(2)	SGN-U571085	GTTGATTCATGGGGTCAAGC CAAATCGCCTTTTCAGCTACG	227	60	10	400	1.906
	GGPS(3)	SGN-U573348	GTGTATAGCTGCTTGTGAG GTGCTCAAAGGCTAATGC	220	55	10	400	1.858
Geranylgeranyl reductase (GGDR) EC:1.3.1.83	*GGDR*	SGN-U564571	CAGAGACGCTCGCTAAGG GCTTCAGAGTCTGTCCGATATC	201	60	10	800	1.813
3-deoxy-D-arabino-heptulosonate-7-P synthase	*DAHPS(1)*	SGN-U581552	GGGAGACTGTGCTGAGAG	200	55	10	100	1.844

(DAHPS)			GTAACTTGGTAGCTTCACTC					
EC 2.5.1.54	*DAHPS(2)*	SGN-U566921	GTGCTGTTCTTATGTTTGGTG GATCAGCCTCTGAGGGTC	191	60	10	400	1.924
3-dehydroquinate synthase (DHQS) EC 4.2.3.4	*DHQS*	SGN-U568781	CACGATTGAAGGTGTTGG GTAACGACAAGGACTCTC	196	55	10	400	1.903
shikimate dehydrogenase (SDH)/3-dehydroquinate dehydratase (DHQ)	*SDH/DHQ(1)*	SGN-U570855	GAGGATCTTGGCAATCTAG GACAAAGTATCCGAGACATC	181	55	10	800	1.911
EC 4.2.3.4/ EC 4.2.1.10	*SDH/DHQ(2)*	SGN-U570070	GTATTAGTTGGGGCAGGTG GATCAGACTTTGGCTGCATG	223	60	20	400	1.900
shikimate kinase (SK) EC 2.7.1.71	*SK*	SGN-U582040	GCCTTCAGTTGTCCTCATG GATGCAGAGAAACATCCTG	229	60	10	200	1.894
5-enolpyruvylshikimate-3-P synthase (EPSPS) EC 2.5.1.19	*EPSPS*	SGN-U577580	CGTATTCTCCTTCTTGCTG GTTCCTGCATTTCCAAGG	224	55	10	800	1.833
chorismate synthase (CS)	*CS(1)*	SGN-U563165	CTGTGACAAGAGACAAACACG GCTGATTCAGGTGATGAC	202	55	10	800	1.798
EC 4.2.3.5	*CS(2)*	SGN-U563163	CCATCCAAGCTCTGTTCTTC CTCTGAGAGTGGGAGTCG	186	55	10	800	1.819
chorismate mutase (CM)	*CM(1)*	SGN-U575627	CAAACAACAATTACCTCCTTCTTCC TGTGCATTTGGTAAGTGGTATGA	169	60	10	400	1.895
EC 5.4.99.5	*CM(2)*	SGN-U585231	GCTCAGTACTGTTTCAATGCGGA CTTTGGATACTGCATGGGTGGC	202	60	10	400	1.894
prephenate aminotransferase (PAT) EC 2.6.1.57	*PAT*	SGN-U567172	CGGAGTAGAGGTTGATGGATTTG GTCGAAAGCGATGCTGCATA	150	60	10	800	1.903
arogenate dehydrogenase (ADH/TYRA)	*ADH(1)/ TYRA(1)*	SGN-U567861	CTCTGTCTCTTCTCCGTC GTTCTTGAATGAGCCAAC	225	60	10	800	1.889
EC 1.3.1.78	*ADH(2)/ TYRA(2)*	SGN-U570951	CGTGCCCAAAATAGCGACTTAAC AGCTTGTTATTGGAACATAAGAGGG	161	60	25	400	1.912
tyrosine aminotransferase (TAT)	*TAT(1)*	SGN-U577103	CTACTGTGGGACTTCCTC CGATGTTTCTAAATGCAGCAC	216	55	10	200	1.800
EC 2.6.1.5	*TAT(2)*	SGN-U563404	GCATCCTTCCTGCTAGAC CCTCCCACTCCTTCTCTG	249	60	20	400	1.854
4-hydroxyphenylpyruvate dioxygenase (HPPD)	*HPPD(1)*	SGN-U580457	CCAGGGCAGGGGATATACTG CTCCTTCCTCGTTTTTCAGC	209	60	20	400	1.887
EC 1.13.11.27	*HPPD(2)*	SGN-U578997	CCAGGCGTGTGAAGAATTG CGATCTAAACAGCTCAGAG	214	55	10	800	1.872
homogentisate solanesyl transferase (HST) EC 2.5.1.-	*HST*	SGN-U585005	GCTGCTAACTTGGTGCTC GATCCTAGCACAGTCCCACG	230	55	10	150	1.694
homogentisate phytyl transferase (VTE2) EC 2.5.1.-	*VTE2*	SGN-U327540	CAATTCCAGTTCCTGCTGAG CCTCCAACATGCTCTTGCGTG	154	60	10	400	1.796
2-methyl-6-solanyl-1,4-quinol methyltransferase /	*VTE3(1)*	SGN-U578249	CTTGACCAATCTCCTCATC	210	60	20	400	1.850

2-methyl-6-phytyl-1,4-quinol methyltransferase (VTE3) EC 2.1.1.-			GCACGCCTTTCCTCCAGG					
	VTE3(2)	SGN-U581492	GCTAAGGCTAGGCAGAAGGAG CAGGCAACCCCACCTATGG	185	60	10	200	1.851
tocopherol cyclase (VTE1) EC 5.3.-.-	*VTE1*	SGN-U570602	CGAACTCCTCATAGCGGGTATC CACGCCAGTAAACCGAGGC	189	60	20	200	1.824
γ-tocopherol C-methyl transferase (VTE4) EC 2.1.1.95	*VTE4*	SGN-U584511	CAGATCATCGTGCTGCTCAG CCTCTCTGCTTGTACAGGAC	194	60	20	200	1.758
phytol kinase (VTE5) EC 2.7.-.-	*VTE5*	SGN-U576753	CGTATCAGGACGGGCTCGC TCACCACCACACATCATTGCTAATG	246	60	10	200	1.902
anthranilate phosphoribosyltransferase (APT) EC 2.4.2.18	*APT*	SGN-U566340	CCAGTTCATCCGCTTGTG CAAGATGTTGAACACCGTC	197	60	10	800	1.911
phosphoribosylanthranilate isomerase (PAI/PRAI) EC 5.3.1.24	*PAI/ PRAI*	SGN-U564371	GCCTCTGATGCAGCAAAC GGCCTCCCTCTTCATCTG	202	55	10	400	1.788
dihydrofolate synthetase (DHFS)/ folylpolyglutamate synthase (FPGS) EC 6.3.2.17	*DHFS/ FPGS*	SGN-U581922	CAGACTATCAGGGAACGC CCACAACTGCAATTTCAG	202	55	10	200	1.817
chlorophyllase (CLH) EC 3.1.1.14	*CLH(1)/ CHL*	SGN-U574853	CATGGCTTCATTGTTGTTGCTCC GCCTGCTAGTCCAAGTTTCGTC	165	60	20	800	1.901
Chromoplastic lycopene β-cyclase (LYCB) EC 5.5.1.-	*CYCB/ LYCB*	SGN-U570109	GCACCCACATCAAAGCCAGAG GCCACATGGAGAGTGGTGAAG	184	60	10	400	1.907
phytoene desaturase (PDS) EC 1.14.99.-	*PDS*	SGN-U565586	CGTTCCGTGCTTCTCCGC CTAGAACATCCCTTGCCTCCAG	240	60	10	200	1.897
clathrin adaptor complexes medium subunit (CAC)	*CAC*	SGN-U314154	CCTCCGTTGTGATGTAACTGG ATTGGTGGAAAGTAACATCATCG	173	60	10	600	1.923
TIP41-like family protein (TIP41)	*TIP41*	SGN-U321250	ATGGAGTTTTTGAGTCTTCTGC GCTGCGTTTCTGGCTTAGG	235	60	10	400	1.905
Expressed unknown protein (EXPRESSED)	*EXPRESSED*	SGN-U346908	GCTAAGAACGCTGGACCTAATG TGGGTGTGCCTTTCTGAATG	183	60	10	200	1.890
Elongation factor 1-α (EF-1α)	*EF-1α*	SGN-U314885	ATTGGAAACGGATATGCTCCA TCCTTACCTGAACGCCTGTCA	102	60	10	200	1.864
chlorophyllase (CLH) EC 3.1.1.14	*CLH(2)*	Solyc09g065620	GGCTTCATGCTCCAACCTAG CGGCAGTACGGATTTGAGG	162	60	20	200	1.902
	CLH(4)	Solyc12g005300	ATTCCGCCTCCAACCCGACT GCAGCACAGAGTTGAGCTTCTTAGC	167	60	20	200	1.872
farnesol kinase (FOLK) EC 2.7.-.-	*FOLK*	Solyc09g018510	CTATGAGCCGATTTGGAGACC GAACCTCCTGCCAACAATGTC	170	60	10	400	1.904
Pheophytinase (PPH)	*PPH*	Solyc01g088090	TATGGAGGGAGCAAGTACGC TGGAGGGCAGAGGAAAAGTAC	236	60	20	200	1.898
Pheophorbide a oxygenase (PaO) EC 1.14.12.20	*PAO*	Solyc11g066440	TCAGAAGTGGGTGATATGGA TATCCCCGTCATACACCTTA	179	55	10	150	1.881
Chlorophyll synthase (CLHG)	*CHLG*	Solyc09g014760	CCAATTCCTTCAGGTGCGGT	250	60	10	200	1.884

EC 2.5.1.-			CCCACCAAGGCAAGCTGATA					
STAY-GREEN (SGR1)	*SGR1*	Solyc08g080090	GCAAAGAACTCCCTGTGGTT CCCACCAGAAGAAGATGAGG	185	60	10	200	1.883
Chloroplastic lycopene β-cyclase (LCYB) EC 5.5.1.-	*LCYB*	Solyc04g040190	TTGACTTAGAACCTCGTTATTGG AACAGTTCCCTTTGTCATTATCT	137	55	20	200	1.902
Phytoene synthase (PSY) EC 2.5.1.32	*PSY(1)*	Solyc03g031860	CGATGGTGCTTTGTCCGATAC CTCATCAACCCAACCGTACC	165	60	10	200	1.906
	PSY(2)	Solyc02g081330	GCATCACACATAACTCCACAAGC CGCATTCCTTCAACCATATCTCTG	161	60	10	200	1.886
solanesyl diphosphate biosynthesis (SPS) EC 2.5.1.33	*SPS*	Solyc07g061990	GTGGTTGCGGATGACCTACTTA CTTCTGTGATTTGTGGTGAGTTCC	197	60	10	200	1.859
Phytyl ester synthase (PES) EC 2.3.1.-	*PYP/ PES(1)*	Solyc01g098110	ACAGGACACAACTCCAACC TAACCATCGCCATCTTCAGTG	120	60	10	200	1.916
	PES(2)	Solyc02g094430	CGAAGAGAGGGAAAAATGCCTGTG GCTGCCATCCTGACAAATTCAGAC	212	60	10	200	1.870

[a] For some genes the annotation proposed by Almeida et al. (2011) was updated. The current gene annotation was underlined.
[b] UNIGENE or *locus* ID according to Solanaceae Genomics Network (http://solgenomics.net).
Genes highlighted in gray were not evaluated in Quadrana et al. (2013), but they were included in the further transcriptional profile analyses.

Supplemental Table 6. Evaluation of the suitability of housekeeping genes.

	EF1α	*CAC*	*EXPRESSED*	*TIP41*
NormFinder[a]	0.85	0.51	0.38	0.28
GeNorm[b]	0.86	0.68	0.61	0.58
BestKeeper[c]	0.23	0.69	0.72	0.74

[a] Gene ranking is based on the algorithm described in Lindbjerg et al. (2004), where the lowest number indicates the most stable housekeeping gene.

[b] Values represent the average expression stability as described in Vandesompele et al. (2002), where the lowest number indicates the most stable house-keeping gene.

[c] Values indicate the correlation for each house keeping gene to the Best Keeper index as described by Pfaffl et al. (2004), where the most stable housekeeping gene shows the highest correlation. Selected housekeeping genes with the best behavior for our experimental conditions are highlighted.

ANEXO II

nature COMMUNICATIONS

ARTICLE

Received 18 Mar 2014 | Accepted 2 May 2014 | Published 26 Jun 2014

DOI: 10.1038/ncomms5027

Natural occurring epialleles determine vitamin E accumulation in tomato fruits

Leandro Quadrana[1,2], Juliana Almeida[3], Ramon Asís[4], Tomás Duffy[1], Pia Guadalupe Dominguez[1], Luisa Bermúdez[1,5], Gabriela Conti[1,5], Junia V. Corrêa da Silva[3], Iris E. Peralta[6], Vincent Colot[2], Sebastian Asurmendi[1], Alisdair R. Fernie[7], Magdalena Rossi[3] & Fernando Carrari[1,5]

Vitamin E (VTE) content is a low heritability nutritional trait for which the genetic determinants are poorly understood. Here, we focus on a previously detected major tomato VTE quantitative trait loci (QTL; $mQTL_{9\text{-}2\text{-}6}$) and identify the causal gene as one encoding a 2-methyl-6-phytylquinol methyltransferase (namely *VTE3*(1)) that catalyses one of the final steps in the biosynthesis of γ- and α-tocopherols, which are the main forms of VTE. By reverse genetic approaches, expression analyses, siRNA profiling and DNA methylation assays, we demonstrate that $mQTL_{9\text{-}2\text{-}6}$ is an expression QTL associated with differential methylation of a SINE retrotransposon located in the promoter region of *VTE3*(1). Promoter DNA methylation can be spontaneously reverted leading to different epialleles affecting *VTE3*(1) expression and VTE content in fruits. These findings indicate therefore that naturally occurring epialleles are responsible for regulation of a nutritionally important metabolic QTL and provide direct evidence of a role for epigenetics in the determination of agronomic traits.

[1] Instituto de Biotecnología, Instituto Nacional de Tecnología Agropecuaria and Consejo Nacional de Investigaciones Científicas y Técnicas, Dr. N. Repetto y Los Reseros s/n CP 1686, Hurlingham, Buenos Aires, Argentina. [2] Ecole Normale Supérieure, Institut de Biologie (IBENS), Centre National de la Recherche Scientifique (CNRS), UMR 8197, Institut National de la Santé et de la Recherche Médicale (INSERM) U 1024, F-75005 Paris, France. [3] Departamento de Botânica Instituto de Biociências, Universidade de São Paulo, Rua do Matão 277, 05508-900 São Paulo, Brazil. [4] CIBICI, Facultad de Ciencias Químicas, Universidad Nacional de Córdoba, Córdoba CC 5000, Argentina. [5] Cátedra de Genética Agrícola. Facultad de Agronomía, Universidad de Buenos Aires, Avenida San Martín 4453, CABA 1417 Buenos Aires, Argentina. [6] Cátedra de Botánica Agrícola. Facultad de Agronomía, Universidad Nacional del Cuyo, Almirante Brown 500, Chacras de Coria & IADIZA-CCT CONICET, 5505 Mendoza, Argentina. [7] Max Planck Institute for Molecular Plant Physiology, Wissenschaftspark Gölm, Am Mühlenberg 1, D-14476 Potsdam-Golm, Germany. Correspondence and requests for materials should be addressed to F.C. (email: fcarrari@cnia.inta.gov.ar).

© 2014 Macmillan Publishers Limited. All rights reserved.

Genetic determinants of nutritional quality have long been studied in many important crops[1–5]. However, mechanisms linking the few identified genetic determinants to the end phenotypes are largely unknown. This is true for tocochromanols, a group of compounds exclusively produced in photosynthetic organisms[6,7] and that includes tocopherols and tocotrienols (termed vitamin E-VTE-), which have high nutritional value in the human diet. Tocopherols are the molecules that show the highest VTE activity[8]. These compounds consist of a polar chromanol head group (derived from homogentisate) and a prenyl lipophilic side chain, products of the plastidial shikimate and methylerythritol phosphate pathways, respectively. The first step for tocopherol synthesis is catalysed by homogentisate phytyl transferase (VTE2, EC 2.5. 1.-), which condenses phytyl 2P and homogentisate to yield 2-methyl-6-phytylquinol. From this precursor, the four naturally occurring forms are synthesized. While γ- and α-tocopherol are produced by the sequential activities of dimethyl-phytylquinol methyl transferase (VTE3, EC 2.1.1.-), tocopherol cyclase (VTE1, EC 5.3.-.-) and tocopherol C-methyl transferase (VTE4, EC 2.1.1.95); δ- and β-tocopherol synthesis, do not require VTE3 activity being formed merely by the action of the latter two enzymes (Fig. 1a)[9]. The role of tocopherols as lipid-soluble antioxidants is well documented for plants and humans and occurs by two mechanisms: (i) donation of a hydrogen atom to a highly reactive polyunsaturated fatty acid peroxyl radical thus preventing a chain reaction of lipid peroxidation and (ii) physically or chemically quenching singlet oxygen species, which damage many biological molecules including proteins, DNA, carbohydrates and polyunsaturated fatty acids[10]. Given that photosynthesis is a major source of singlet oxygen, this quenching mechanism plays an important role in the functional regulation of photosystem II with important implications in physiological responses to high light conditions, low temperature and osmotic stress[11].

The importance of tocopherol for both producer and consumer organisms has led to survey for quantitative trait loci (QTL) determining VTE content[3,12–15]. In tomato, we revealed the existence of four metabolic QTL (mQTL) affecting total tocopherol levels in fruits[9]. These four mQTL map onto chromosomes 6, 8 and 9. However, given the very low heritability (H^2) of VTE content in tomato[16] it will be difficult to breed fruit with elevated VTE contents until the genetic determinants and mechanisms underlying these QTL are fully understood.

In this work, we report the fine mapping of the major VTE mQTL ($mQTL_{9\text{-}2\text{-}6}$) in tomato to a locus encoding a VTE3 enzyme. We show that *VTE3(1)* alleles are differentially expressed and that these differences correlate with differences in DNA methylation of the promoter sequences and in the accumulation of matching short interfering RNA (siRNAs). Consistent with $mQTL_{9\text{-}2\text{-}6}$ being of an epigenetic nature, we find that DNA methylation at *VTE3(1)* varies considerably among natural

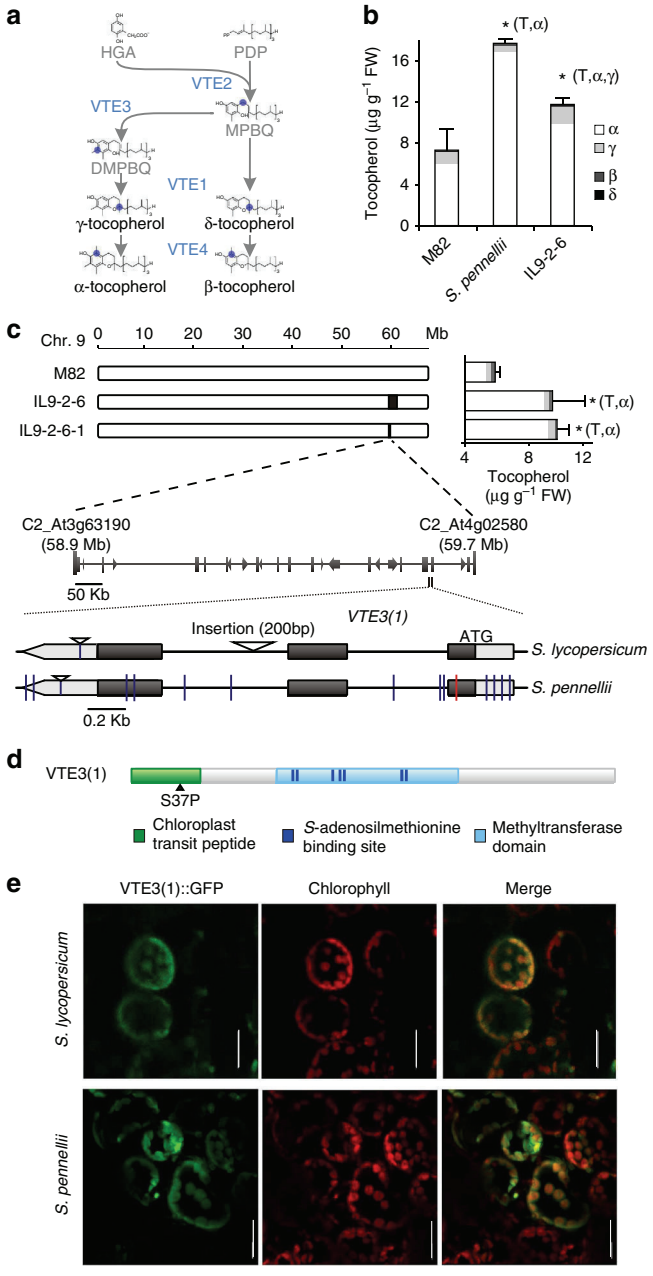

Figure 1 | Fine mapping of tocopherol $QTL_{9\text{-}2\text{-}6}$. (**a**) The tocopherol core pathway in plants. Biosynthetic enzymes, homogentisate phytyl transferase (VTE2), dimethyl-phytylquinol methyl transferase (VTE3), tocopherol cyclase (VTE1) and γ-tocopherol C-methyl transferase (VTE4) are in blue types. Precursors and intermediates are: homogentisate (HGA), phytyl 2P (PDP), methyl-phytylquinol (MPBQ) and dimethyl-phytylquinol (DMPBQ). (**b**) Composition and total tocopherol contents (mean ± s.e.m, $n=4$) in ripe tomato fruits from the two parental species; *S. lycopersicum* (cv. M82) and *S. pennellii* (LA716), and the IL9-2-6 that shows the mapped QTL. (**c**) Fine mapping of the $QTL_{9\text{-}2\text{-}6}$ to a centromeric region of chromosome 9 harbouring the wild allele of *VTE3*(1) gene. Through the analysis of 190 F2 and 50 F3 plants, derived from a cross between the *S. lycopersicum* (cv. M82) and the IL9-2-6, a recombinant subline (IL9-2-6-1) was obtained. Tocopherol contents (mean ± s.e.m, $n=6$) in ripe tomato fruits from these lines are shown on the right side of this panel. Genomic structure of the introgression contained in this line is shown below with black arrows indicating transcriptionally active genes. A magnified view of *S. lycopersicum* and *S. pennellii* alleles of *VTE3*(1) gene shows synonymous (blue bars) and non-synonymous (red bar) polymorphisms and insertions in the second intron and in the 3′UTR. Black and grey boxes represent exons and, 5′ and 3′ UTR, respectively. (**d**) Protein structure of the tomato VTE3(1) enzyme indicating the amino acid substitution (S37P). (**e**) Transient expression of both alleles of VTE3(1)::GFP fusion protein in mesophyll cells of *N. benthamiana* leaves indicates chloroplast targeting under confocal microscopy examination. Asterisks in panels **b** and **c** denote statistically significant differences for total tocopherol (T) and the indicated tocopherol forms (*t*-test $P<0.05$). Scheme of chromosome 9 is based on physical distances calculated according to version SL2.4 of the tomato genome (www.solgenomics.net). White bar in **e** indicates 25 μm.

© 2014 Macmillan Publishers Limited. All rights reserved.

tomato populations and that *VTE3(1)* can spontaneously revert from methylated to unmethylated forms, with an impact on VTE contents in fruits.

Results

Fine mapping of a major tocopherol mQTL in tomato fruits. We set out to identify the causal gene(s) harboured by the fruit-specific mQTL for total- and α-tocopherol contents that had previously been mapped to chromosome 9 ($mQTL_{9\text{-}2\text{-}6}$)[9] (Fig. 1b and Supplementary Fig. 1a). To this end, fine mapping was carried out using an F2 population of 190 individuals, derived from a cross between the parental *S. lycopersicum* line (cv. M82) and the introgressed line 9-2-6 (IL9-2-6) (spanning approximately 3 Mb and containing in excess of approximately 300 genes). The molecular markers C2_At3g63190 (58.9 Mb), VTE3(1)INDEL (59.6 Mb), C2_At4g02580 (60 Mb), 1531800 (61.0 Mb) and C2_At2g47890 (61.8 Mb) (Supplementary Fig. 1b) were used for screening and the introgressed fragment segregated 2:1:1 (*S.lyc*/*S.pen*:*S.lyc*/*S.lyc*:*S.pen*/*S.pen*, $\chi^2 = 0.98$). A single recombinant line between C2_At4g02580 and 1531800 markers was identified and selfed to give rise to recombinant IL9-6-2-1, which harbours only 769 Kb of the original introgressed fragment. VTE quantification demonstrated that the total tocopherol mQTL was maintained in this recombinant IL (Fig. 1c). Out of the 56 putative Open reading frames (ORFs) present in this 789 Kb interval (www.solgenomics.net) 13 ORFs are not supported by any available expression data (expressed-sequence-tags or RNA-seq reads) and only 36 show detectable expression levels in tomato fruits. A MapMan[17] functional annotation analysis revealed that out of these 36, only a single gene (*VTE3*(1)-Solyc09g065730 locus-), belongs to the Secondary Metabolism category (Supplementary Table 1). This gene displayed high similarity (~85%) to a dimethyl-phytylquinol methyl transferase from *Arabidopsis* (EC 2.1.1.-; Supplementary Fig. 1c,d) that catalyses the conversion of 2-methyl-6-phytylquinol to 2,3-dimethyl-5-phytylquinol, the immediate precursor of γ-tocopherol (Fig. 1a)[18]. This gene is duplicated in several eudicot species including *S. lycopersicum* (Supplementary Fig. 1c). The tomato VTE3(1) has 339 amino acids and contains the two characteristic functional domains found in the *Arabidopsis* protein as well as a putative chloroplast transit peptide. When comparing the allelic divergence between the *S. lycopersicum* and *S. pennellii* proteins, a single amino acid polymorphism located within a lowly conserved region of the chloroplast transit peptide was found (Fig. 1d and Supplementary Fig. 1d). Transient subcellular localization assays performed with *S. lycopersicum* and *S. pennellii* alleles fused to GFP indicated that both VTE3(1) alleles are targeted to the chloroplast where tocopherol biosynthesis takes place (Fig. 1e). Taken together, these results suggest that *VTE3*(1) is a major determinant of the $mQTL_{9\text{-}2\text{-}6\text{-}1}$ for fruit tocopherol content but that the causal polymorphism(s) are unlikely to reside within the coding sequence.

***VTE3*(1) mRNA levels modulate VTE contents in tomato fruits.** In order to demonstrate the involvement of *VTE3*(1) in the determination of fruit tocopherol contents, we specifically silenced this gene in fruits by means of an established virus-induced gene silencing protocol, which relies on GFP fluorescence as a visual marker[19]. For this purpose a 380 bp fragment of the *GFP* coding region was fused to a 349 bp fragmentinsp of the *VTE3*(1) tomato gene for cosilencing. Following the infiltration of inflorescent peduncles, fruit *GFP*-silenced sectors were monitored *in planta* across development and mature green (MG) and ripe tomatoes were harvested 42 and 60 days after infiltration, respectively. Sectors lacking fluorescence were dissected (Fig. 2a) and the levels of *VTE3*(1) mRNA were measured by quantitative PCR (qPCR). Reductions of approximately 60% were observed in the *GFP*-silenced pericarp sectors with respect to fruits set from plants infiltrated with pTRV2-GFP alone (Fig. 2b). We next assayed the effect of *VTE3*(1) silencing on fruit tocopherol metabolism. VTE3-dependent tocopherol forms (γ and α) showed significant reductions in both developmental stages, while VTE3-independent forms (δ and β) were increased more than twofold. Moreover, absolute levels of α- and γ-tocopherol were significantly reduced in *VTE3*(1) silenced ripe fruits (Fig. 2c). These alterations in tocopherol metabolism were specifically related to *VTE3*(1) silencing since mRNA levels of the other genes of the tocopherol core biosynthetic pathway (*VTE1*, *VTE3*(2) and *VTE4*) were unaltered in this experiment (Supplementary Fig. 2a). Furthermore, a metabolic profiling analysis of the silenced tissues revealed no major alterations suggesting that this enzyme does not affect primary metabolism. However, increases in lycopene and α-carotene were detected in ripe fruits in which *VTE3*(1) gene had been silenced (Supplementary Fig. 2b) and these changes were accompanied by an increased antioxidant capacity (Supplementary Fig. 2c). These data thus demonstrate that the alteration of *VTE3*(1) mRNA levels directly affects tocopherol content and composition in tomato fruit and furthermore supports earlier hypotheses that fruit redox status is balanced by mechanisms which impact the metabolic pathways associated with both tocopherol and carotenoid metabolism[20–22].

Specific *VTE3*(1) alleles expression determines $mQTL_{9\text{-}2\text{-}6}$. Having demonstrated that *VTE3*(1) expression determines tocopherol levels both at MG and ripe stages, we next compared the expression of the cultivated and wild alleles. In agreement with the tocopherol content profiles (Fig. 1b), the wild allele displayed significantly higher mRNA levels in ripe fruits from both introgression lines (IL9-2-6 and 9-2-6-1) in comparison with the recipient parental control. In other words, $QTL_{9\text{-}2\text{-}6}$ is an expression QTL (eQTL; Fig. 3a). The higher mRNA accumulation of *VTE3*(1) following introgression of the wild allele into the *S. lycopersicum* background was not restricted to mature fruits but was also observed in leaves and across fruit development (Fig. 3b). Moreover, these differences in *VTE3*(1) expression are not accompanied by changes in the expression level of any of the other genes encoding the enzymes involved in the tocopherol biosynthetic pathway (Fig. 3c). Furthermore, evaluation of expression levels of 19 other ORFs present in the introgressed IL9-2-6-1 segment by qPCR showed similar results as those deposited in public data bases (ted.bti.cornell.edu), except for three ORFs. However, none of these three ORFs are known to be related to the VTE metabolism pathways and their expression does not correlate with tocopherol levels in tomato fruit. Also, the three *A. thaliana* orthologs are not coexpressed with any gene involved in the tocopherol biosynthesis[23]. Taken together, these results further confirm that *VTE3(1)* is the causal gene harboured by $mQTL_{9\text{-}2\text{-}6}$.

To further unravel the nature of the *VTE3*(1) eQTL, its transgenerational stability was analysed in ripe fruits from the F1 hybrid and F2 segregating lines with the three possible allele combinations determined by an allele-specific expression assay. In the F1 hybrid, the total *VTE3*(1) mRNA level is equivalent to that measured in IL9-2-6 as a consequence of the dominance of the wild allele. Similarly, *VTE3*(1) expression displays the same pattern in the derived F2 recombinant lines (Fig. 3d). Moreover, the total tocopherol content follows the same profile as that of the *VTE3*(1) mRNA levels (Fig. 3e), suggesting that the $mQTL_{9\text{-}2\text{-}6}$ and the *VTE3*(1) eQTL are tightly and stably coupled across generations.

© 2014 Macmillan Publishers Limited. All rights reserved.

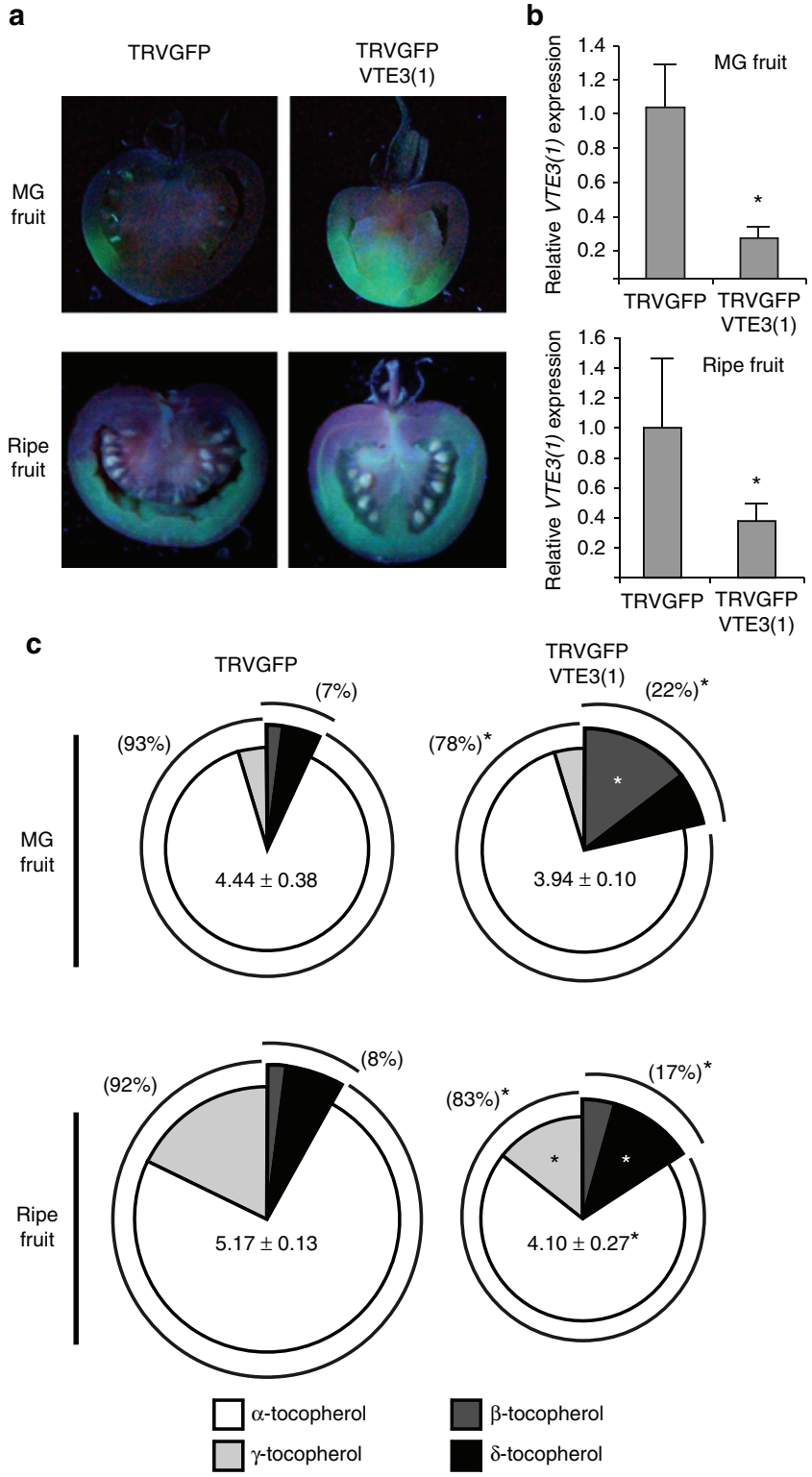

Figure 2 | Tocopherol contents in *VTE3*(1) transiently silenced tomato fruits. (**a**) *GFP* (control) and *GFP-VTE3*(1) silenced MG and ripe fruits harvested from virus-induced gene silencing agroinfiltrated inflorescent peduncles of GFP-expressing tomato plants (*S. lycopersicum* cv. Moneymaker). (**b**) Relative levels of *VTE3*(1) mRNA in *GFP* (control) and *GFP-VTE3*(1) silenced fruits (mean ± s.e.m, $n=6$). (**c**) Tocopherol contents ($\mu g\, g^{-1}$ FW ± s.e.m, $n=6$), relative tocopherol composition and proportion of VTE3-dependent and VTE3-independent tocopherol forms from the same silenced fruits showed in **a** are indicated by numbers, pie charts and semicircles, respectively. Note that sizes of pie charts are proportional to the mean total tocopherol content. Asterisks denote statistically significant differences (*t*-test $P<0.05$).

Revealing the molecular mechanism of the tocopherol QTL$_{9\text{-}2\text{-}6}$. The higher *VTE3*(1) mRNA levels in IL9-2-6 and IL9-2-6-1 could be the result of differences in the transcriptional promoter activities between the domesticated and wild alleles. Therefore, we analysed the promoter regions of these alleles by a *de novo* search for *cis*-regulatory elements (CREs)[24]. The *S. lycopersicum*

© 2014 Macmillan Publishers Limited. All rights reserved.

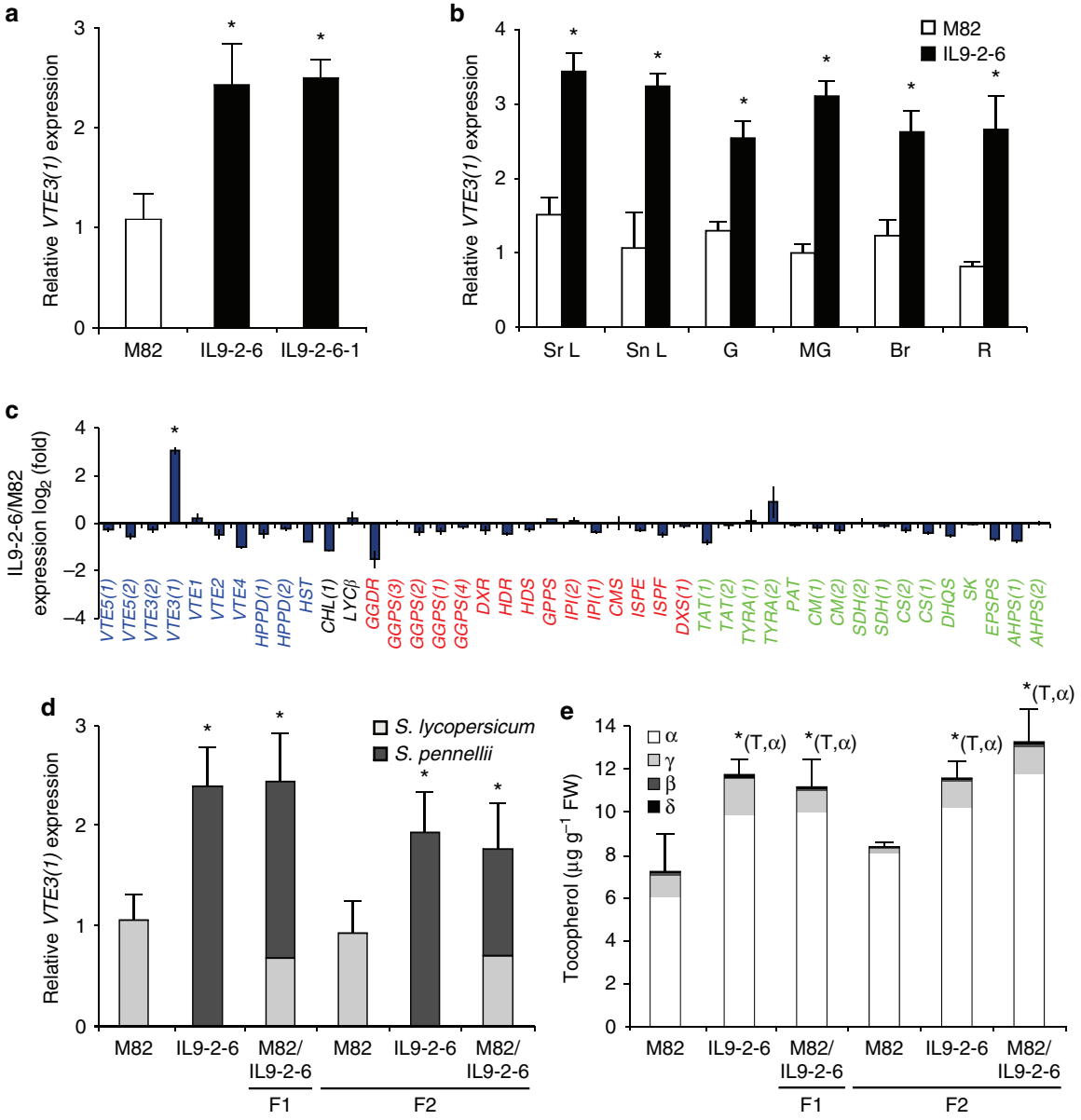

Figure 3 | An eQTL of *VTE3*(1) is revealed in the tocopherol QTL$_{9\text{-}2\text{-}6}$. (**a**) *VTE3*(1) mRNA levels in ripe fruits from the parental lines *S. lycopersicum* (cv. M82) and IL9-2-6 and the resulting recombinant IL9-2-6-1 (mean ± s.e.m, $n=5$). (**b**) *VTE3(1)* mRNA levels in source (Sr L) and sink leaves (Sn L) and along fruit development (green-G, mature green-MG, breaker-Br and ripe-R fruits) harvested from the parental lines *S. lycopersicum* (cv. M82) and IL9-2-6 (mean ± s.e.m, $n=6$). (**c**) mRNA levels quantified in ripe fruits from the parental lines *S. lycopersicum* (cv. M82) and IL9-2-6 of all genes encoding enzymes involved in tomato tocopherol metabolism according to[24] (mean ± s.e.m, $n=3$). Genes belonging to tocopherol core, associated, methylerythritol phosphate and shikimate pathways are indicated in blue, black, red and green, respectively. (**d**,**e**) *VTE3*(1) mRNA, tocopherol composition and total levels measured in *VTE3*(1) homozygous and heterozygous lines for two generations (F1 and F2) derived from a cross between *S. lycopersicum* (cv. M82) and IL9-2-6 (mean ± s.e.m, $n=5$). The contribution of each *VTE3*(1) allele (*S. lycopersicum* and *S. pennellii*) was quantified by allele-specific quantitative reverse transcriptase-PCR and indicated by light and dark grey bars, respectively. Asterisks in **a**,**b**,**c** and **d** denote statistically significant differences, (randomization test $P<0.05$ corrected by false discovery rate in case of multiple testing). Asterisks in **e** denote statistically significant differences for total tocopherol (T) and the indicated tocopherol forms (*t*-test $P<0.05$).

VTE3(1) gene promoter contains seven statistically over-represented CREs, while the *S. pennellii* one contains four. Two of these elements are common to the *S. lycopersicum*, *S. pennellii* and *S. phureja VTE3*(1) promoter regions (Supplementary Fig. 3a). Further comparisons between the promoter regions of *S. lycopersicum*, *S. pimpinellifolium*, *S. pennellii* and *S. phureja* revealed distinct patterns of transposable element (TE) insertions. While two copies of the *Tc1-IS630-Pogo* family of DNA transposons[25] are common between all four analysed species, indicating that they were present in the common ancestral, a retrotransposon element of the SINE family[26] is exclusively found in the closest species *S. lycopersicum* and *S. pimpinellifolium*, suggesting a later specific insertion in the tomato lineage (section Lycopersicon; Supplementary Fig. 3b). Furthermore, the genomic region spanning this SINE is highly methylated in fruits from *S. lycopersicum* (cv Ailsa Craig) (http://ted.bti.cornell.edu/epigenome/), mainly at CHH sites, which is a hallmark of

© 2014 Macmillan Publishers Limited. All rights reserved.

RNA-directed DNA methylation (RdDM)[27]. In order to address whether the RdDM machinery may be involved in the establishment and maintenance of the DNA methylation in this region, we next generated siRNA-seq profiles from ripe fruits of *S. lycopersicum*, *S. pennellii* and the IL9-2-6-1. We found that a considerable number of 21-24 nt-siRNAs species (sense and antisense) matches the TE sequences located in the promoter of *S. lycopersicum* (Fig. 4a,b), but none in *S. pennellii* nor in the IL9-2-6-1. By means of McrBC enzyme digestion and allele-specific semiquantitative PCR, we assessed the methylation status of three different fragments of *VTE3*(1) gene: two on the promoter region (I and II) and one on the coding sequence (III). The results revealed that the proximal promoter region of *S. lycopersicum* allele harbouring the *SINE* TE is hypermethylated, whilst the wild one, either in its own background (*S. pennellii*) or in the M82 background (IL9-2-6 and IL9-2-6-1), showed low levels of DNA methylation (Fig. 4c). To better characterize these epialleles, we investigated DNA methylation at single-nucleotide resolution, using bisulphite treatment of genomic DNA followed by targeted sequencing. Results confirmed hypermethylation of the proximal *VTE3*(1) promoter region (II) of the *S. lycopersicum* allele in the three genomic contexts (Fig. 4d). Since siRNAs seem to be involved in the establishment of the hyper-methylated epiallele of *VTE3*(1), we tested the existence of allelic interactions such as paramutation[28]. To determine whether this is the case or not, we next analysed the allele-specific DNA

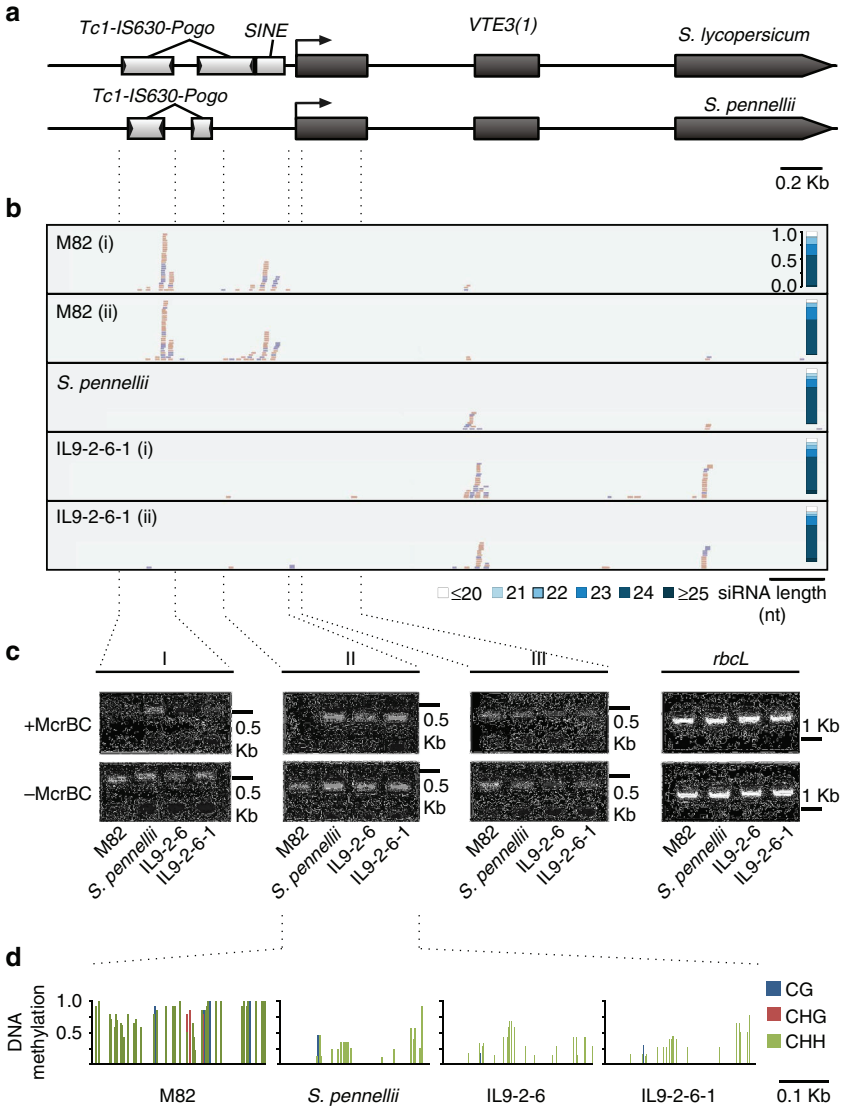

Figure 4 | siRNA profile and methylation status of the wild and cultivated alleles of *VTE3*(1) gene. (**a**) *VTE3*(1) gene and promoter structure (4 Kb window) showing exons (black boxes) and TE insertions (light grey boxes). (**b**) Locus-specific siRNA profiles of the *VTE3(1)*. Tracks show mapping position of sense (red) and antisense (blue) unique siRNA obtained from ripe fruits of *S. lycopersicum* (cv. M82), *S. pennellii* (LA716) and IL9-2-6-1. The length distribution of the mapped siRNAs is represented on the right of each track. siRNA from *S. lycopersicum* (cv. M82) and IL9-2-6-1 were extracted and analysed from two pools of fruits harvested from independent plants (indicated by i and ii), while from *S. pennellii* (LA716) were extracted and analysed from a pool of five fruits. (**c**) DNA methylation status assayed by a McrBC methylation-sensitive endonuclease DNA treatment followed by PCR amplification in two regions of the *VTE3*(1) promoter (I: distal and II: proximal), in the first exon of the gene (III) and on a coding region of the Rubisco LS chloroplast gene (*rbcL*) as a control. DNA was extracted from at least four ripe fruits of the *S. lycopersicum* (cv. M82), *S. pennellii* (LA716), IL9-2-6 and IL9-2-6-1 genotypes. (**d**) Methylation of cytosine residues in CG, CHG and CHH sites (blue, red and green lines, respectively) assayed by bisulphite sequencing of the proximal promoter region (region II in c) in DNA extracted from ripe fruits of the *S. lycopersicum* (cv. M82), *S. pennellii* (LA716), IL9-2-6 and IL9-2-6-1 genotypes.

© 2014 Macmillan Publishers Limited. All rights reserved.

methylation in the F1 hybrids and F2 heterozygous. In line with the expression results (Fig. 3d), we found that the epigenetic status of each allele remains unaltered in the hybrids, demonstrating that they are not targets of paramutation (Supplementary Fig. 4).

In order to evaluate whether the methylation-dependent regulation of the *S. lycopersicum VTE3*(1) allele is an M82-specific mechanism or rather one that can be extended to other genetic backgrounds, we further analysed the expression of *VTE3*(1) and DNA methylation across an allelic series of tomato Andean landraces, three commercial reference cultivars and one closely (*S. pimpinellifolium* -LA1589) and one distantly related wild species (*S. habrochaites* -LA407). These accessions were collected from different geographical locations and assayed under the same field conditions. Previously published results demonstrated that they differ in tocopherol and carotenoid contents[24]. We found that both *VTE3*(1) expression and methylation of its proximal promoter region vary among the different genotypes. Furthermore, *VTE3*(1) mRNA abundance inversely correlates with the methylation levels of the proximal promoter region (Fig. 5a and Supplementary Fig. 5a). Accordingly, the cultivars with higher *VTE3*(1) mRNA levels accumulate more γ-tocopherol in mature fruits (Supplementary Fig. 5b). Sequence analysis of a 850 bp interval encompassing the promoter of *VTE3*(1) gene from the 13 genotypes studied here revealed the presence of single-nucleotide polymorphisms and small InDels, but these do not correlate with differences in expression level or DNA methylation (Supplementary Figs 5a and 6).

Finally, we found that the number of siRNAs targeting the SINE element and the methylation status of the *VTE3*(1) promoter reverted when the reference cultivar M82 (the recurrent parental line of the ILs) was grown under field conditions (Fig. 5b,c). This epiallelic conversion was accompanied by an increase in the level of *VTE3*(1) mRNA as well as in the levels of tocopherol in ripe fruits (Fig. 5d,e). These results provide therefore conclusive evidence of the epigenetic nature of $mQTL_{9\text{-}2\text{-}6}$. Moreover, when the transcriptional activity of the two de-methylated promoters was tested in a transient expression assay no differences were detected (Fig. 5f), demonstrating that the difference in *VTE3*(1) expression of both alleles results from the specific epigenetic silencing of the *S. lycopersicum* variant. When taken in combination, the sum results presented here demonstrate that *S. pennellii* and *S. lycopersicum VTE3*(1) are epialleles and strongly hint that their differential behaviour is determined by the presence of TE insertions within the promoter region.

Discussion

Identification of genes that impact on the nutritional quality of domesticated fruits and vegetables has been a major goal of modern breeding programs. Cultivated tomato is one of the most consumed vegetables in the world and because of the relatively high levels of tocopherol found in tomato fruits, this vegetable is an important source of VTE in the human diet[7]. However, it has been documented that VTE content is a low heritability trait[16], therefore a more comprehensive knowledge of the genetic factors underlying this trait is a prerequisite for nutritional quality improvement. In this work, we focused on a major mQTL for total tocopherol, which maps to the introgressed region of the *S. pennellii* IL9-2-6 and explains about 50% of the variation in VTE between the parental genotypes. By means of a fine mapping approach we were able to restrict the genetic determinant of the $mQTL_{9\text{-}2\text{-}6}$ to a pericentromeric region of chromosome 9 harbouring the *VTE3*(1) locus. This gene encodes a 2-methyl-6-phytylquinol methyl transferase which is a central enzyme for α-tocopherol and γ-tocopherol synthesis (Fig. 1a). *VTE3* was the subject of an ancient duplication event that, according to the substitution rate calculated for tomato[29], we estimated took place 152 ± 24 Myr ago, following the radiation between eudicots and monocots.

Comparison of the *VTE3*(1) coding regions from *S. pennellii* and *S. lycopersicum* revealed a single non-synonymous substitution in a non-conserved region within the chloroplast transit peptide (Fig. 1d and Supplementary Fig. 1d), which does not impact protein targeting as indicated by GFP fusion experiments (Fig. 1e). Moreover, the virus-mediated transient silencing assay demonstrated that the alteration of *VTE3*(1) mRNA levels directly affects tocopherol contents and composition in tomato fruit (Fig. 2) and that this effect is likely due to a redirection of carbon flow from the α- and γ-tocopherol branch to the β- and δ-tocopherol branch of the pathway (Fig. 1a). Reductions in VTE3(1) activity would also likely result in an increase in the availability of geranylgeranyl 2P, a precursor of carotenoid biosynthesis. Accordingly, fruit tissues silenced for *VTE3*(1) showed significant increments in lycopene and α-carotene levels and in the antioxidant capacity.

The wild allele of *VTE3*(1) displayed significantly higher mRNA levels in all tested organs and developmental stages, indicating the existence of an eQTL (Fig. 3a,b). Additional examination of hybrids (F1 and F2) derived from a cross between *S. lycopersicum* (cv. M82) and IL9-2-6, demonstrated that the wild allele is dominant and stable through generations. Moreover, the $mQTL_{9\text{-}2\text{-}6}$ co-varies with *VTE3*(1) expression, suggesting that this eQTL determines VTE levels (Fig. 3d,e). Furthermore, *VTE3*(1) upregulation in IL9-2-6 and IL9-2-6-1 favour carbon flow to α-tocopherol (Fig. 1c), supporting *VTE3*(1) as the causal gene of the $mQTL_{9\text{-}2\text{-}6}$. However, the absolute levels of the other tocopherol forms did not show significant differences. Because a second *VTE3* gene copy is present in tomato (like in other higher plant species Supplementary Fig. 1c) and many factors (for example, oxidative stress status) can significantly affect tocopherol content, either epistatic or pleiotropic effects cannot be discarded and should be considered for further studies.

Several reports have linked eQTLs to phenotypic variation in plants[30]; however, in tomato only a few has been proposed[31–33]. Further experimentation allowed us to uncover that *VTE3*(1) eQTL is determined by differential methylation level of the wild and cultivated alleles. In addition, this differential epigenetic regulation is associated with a specific fragment within the regulatory region of *VTE3*(1) that harbours a SINE TE that is present in only some species of the *Lycopersicon* section (Supplementary Figs 3b and 6). Moreover, this TE insertion is predominantly methylated at CHH sites and matches with a considerable number of siRNAs (Figs 4 and 5), suggesting the involvement of the RdDM machinery in the establishment and maintenance of DNA methylation at this locus[27]. Accordingly, the promoter of *VTE3(1)* lacks the SINE insertion and is unmethylated in *S. pennellii*. On the other hand, this SINE insertion is not always methylated when present in the promoter of *VTE3(1)* and conversion from the methylated to the unmethylated state was observed in some cases (Fig. 5 and Supplementary Fig. 5). These results demonstrate that the $mQTL_{9\text{-}2\text{-}6}$ is of an epigenetic nature and that variation in caused by the differential methylation of the TE sequence located in the promoter region of the *VTE3*(1) gene. To our knowledge, this is the first report unravelling an epigenetic QTL for a highly valuable nutritional trait.

A small number of genes with natural epialleles leading to different phenotypes have been described in plants, which determine floral symmetry in *Linaria vulgaris*[34], sex determination in melon[35] or plant stature in rice[36]. In tomato, epigenetic regulation has already been reported for the *cnr*

© 2014 Macmillan Publishers Limited. All rights reserved.

(colourless non-ripening) *locus* encoding a SBP-box transcription factor, which results in ripening defective fruits. Interestingly, revertant 'ripening' sectors have been reported[37,38]. In this sense, epialelle reversion has been seen to be a common phenomenon in plants[39–41]. In addition, several epigenetic QTL for flowering time and root length have been mapped using an experimental population of isogenic *A. thaliana* that segregates induced DNA methylation changes[42]. Our results extend these findings by providing direct evidence for the existence of epigenetic QTL (QTL^{epi}) in natural populations.

The existence of a second *VTE3* copy in tomato might have been important for the establishment of the epiallelic variation at *VTE3*(1), since the spontaneous downregulation of *VTE3*(1) by methylation in *S. lycopersicum* could be compensated by the second copy, avoiding the deleterious phenotype of tocopherol reduction on seed longevity and stress response[11]. This situation is analogous to that underlying a case of genetic incompatibility in *Arabidopsis*[43].

Epigenetic-dependent gene expression regulation associated with the presence of TEs insertions has also been described. This is the case of *FWA* gene in *Arabidopsis* for which the transcription level depends on the methylation status of a SINE element contained in the promoter region[44]. Moreover, a genome wide study revealed that methylated TE insertions are frequently associated with reduced expression of adjacent genes, therefore being subject of purifying selection[45]. In this line, the presence of a SINE TE insertion on the promoter region of *VTE3*(1) gene, which enables the existence of several epialleles in natural populations of tomatoes, determines tocopherol accumulation in fruit (Fig. 5a). Furthermore, the epigenetic regulation of tocopherol levels documented here might be suggesting a role of naturally occurring epialleles in heritable environmental adaptation. Probably because of their sessile nature, plants have extensively enhanced genetic and epigenetic strategies for coping with different environmental conditions. The tocopherol mQTL determined by epialleles allow us to extend this phenomenon to the tuning of antioxidant potential that might provide adaptation advantages.

In light of the results presented here, the low heritability of the tocopherol content trait[16] can now be reinterpreted due to the epigenetic and reversible nature of $mQTL_{9\text{-}2\text{-}6}$, where the instability of epialleles produce phenotypic dynamics that cannot be predicted from strictly Mendelian models of inheritance. Further studies aiming to understand the genetic determinants of other natural and low heritability traits will allow the development of a population

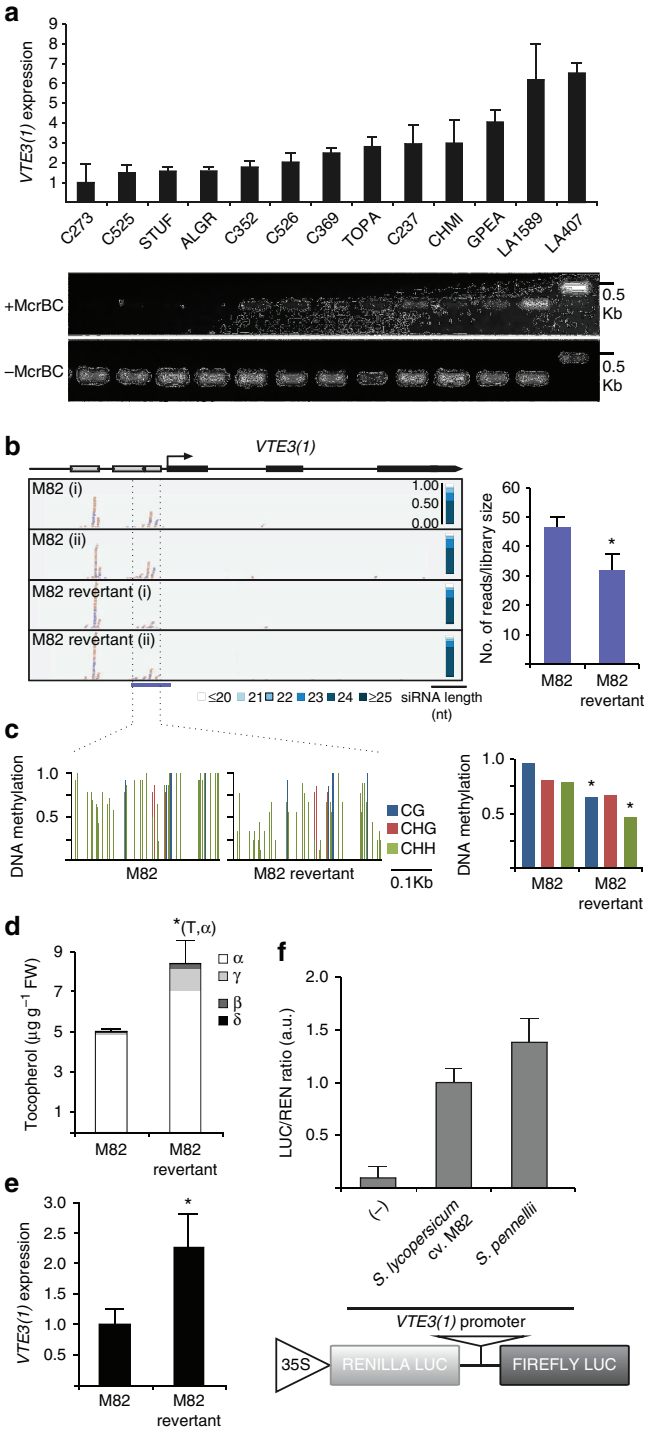

Figure 5 | Natural occurring epiallele regulates *VTE3*(1) gene expression and tocopherol levels. (**a**) *VTE3*(1) mRNA levels (mean ± s.e.m, $n=3$) and DNA methylation status assayed by a McrBC methylation-sensitive endonuclease DNA treatment, followed by PCR amplification of the proximal promotor region (analysed in Fig. 4d) in ripe fruits from eight tomato Andean landrace (*S. lycopersicum*), three commercial reference cultivars and the wild species *S. pimpinellifolium* (LA1589) and *S. habrochaites* (LA407). (**b**) Locus-specific siRNAs profiles of *VTE3(1)*. Tracks show mapping position of sense (red) and antisense (blue) unique siRNA from ripe fruits harvested from *S. lycopersicum* (cv. M82) cultivated under greenhouse conditions and from a field trial performed in Mendoza (Argentina, 32° 50′S, 68° 52′W and 900 masl). The length distribution of the mapped siRNAs is represented on a box at the right of each track. The bar plot on the right panel shows the normalized number (± s.e.m, $n=2$) of siRNAs mapped on the proximal promoter region of *VTE3(1)* (indicated by a blue line below the tracks panel). siRNAs were extracted and analysed from two pools of fruits harvested from independent plants each (indicated by i and ii) (**c**) Methylation of cytosine residues in CG, CHG and CHH sites (blue, red and green lines, respectively) assayed by targeted bisulphite sequencing of the proximal promoter region (analysed in Fig. 4d) from DNA extracted from a pool of the same samples as in **b**. The bar plot on the right panel shows the quantification of DNA methylation for each context. (**d**,**e**) Tocopherol composition and *VTE3*(1) mRNA levels (mean ± s.e.m, $n=3$) from the same samples as in **b** and **c**. (**e**) Transcriptional activity of wild and cultivated allele promoters measured by a transient assay using the pGreenII 0800-LUC vector as described in the Methods (± s.e.m, $n\geq6$). Asterisk in panel **b**,**c** and **e** denotes statistically significant differences (*t*-test, Fisher test and randomization test, respectively; $P<0.05$). Asterisk in **d** denotes statistically significant differences for total tocopherol (T) and the indicated tocopherol forms (*t*-test $P<0.05$).

© 2014 Macmillan Publishers Limited. All rights reserved.

genetics theory which will incorporate the epigenetic information and therefore be capable to predict plants phenotypes and their stabilities in a more accurate manner.

Methods

Plant materials and growth conditions. Tomato seeds from *S. lycopersicum* cv. M82 (LA3475), *S. pennelli* (LA716), IL9-2-6 (LA4083), were obtained from the Tomato Genetic Resource Center (http://tgrc.ucdavis.edu). *S. lycopersicum* cv. MoneyMaker-GFP#6 were obtained from ref. 19. *Nicotiana benthamiana* seeds were obtained from Dr Roger Beachy (Stanford University, CA, USA). Tomato and *N. benthamiana* plants were grown in 20 l pots under greenhouse conditions: 16/8 h photoperiod, 24 ± 3 °C, 60% humidity, and 300 ± 100 μmol $m^{-2} s^{-1}$ incident photoirradiance. Source (Sr L) and sink (Sn L) leaves were collected from 8-week-old plants. Fruits at green (G), MG, breaker (B) and ripe (R) stage were harvested 30, 45, 50 and 60 days after anthesis, respectively. Seeds of the eight Andean landrace cultivars, commercial reference cultivars (GPEA, ALGR and STUF) and the two wild species; *S. pimpinellifolium* (LA1589) and *S. habrochaites* (LA407), were obtained from the germoplasm bank of the EEA-INTA-La Consulta (Argentina). The last two accessions were reproduced from seeds originally sent by the Tomato Genetic Resource Center. Seedlings were grown until four true leaves in 150 ml pots and transplanted to soil under field-production conditions in the Campo Experimental del Instituto de Horticultura, Universidad Nacional de Cuyo, Mendoza, Argentina, 32° 50′S, 68° 52′W and 900 masl. The field experiment was conducted from October 2008 to March 2009 in a randomized design of three replicates with three plants each. The experiment was protected with an antihail mesh and crop irrigation was applied to keep soil available water content constant. At ripe stage, two fruits per plant were harvested approximately 60–65 days after anthesis and immediately frozen in liquid N_2 and kept at −80 °C until use.

Tocopherol quantification by high-performance liquid chromatography. Tocopherol extraction and quantification was performed exactly as previously described[9]. Briefly, tomato fruits were ground to a fine powder in liquid nitrogen and 500 mg of material was extracted with 1.5 ml methanol and, after vortex mixing, 1 ml chloroform was added. Following 5 min of sonication, 1 ml of Tris buffer (Tris (pH 7.5, 50 mM), NaCl 1 M) was added. The chloroform phase was recovered and the methanol phase (remaining pellet) was reextracted with chloroform (2 ml). Chloroform extracts were pooled and adjusted to a final volume of 4 ml. Two ml were dried under nitrogen gas and resuspended in 0.2 ml of 99.5:0.5 hexane:isopropanol. The tocopherol content was determined using a Hewlett-Packard series 1100 HPLC system coupled with a fluorescence detector (Agilent Technologies series 1200). Separation was carried out on a normal-phase column Metasil Si (250 mm × 4.6 mm, 5 μm, Varian, Metachem, Torrance, CA) maintained at room temperature using a isocratic solvent system (mobile phase) consisting of 99.5:0.5 hexane/isopropanol with a flow rate at 1 ml min^{-1}. Eluting compounds were detected and quantified by fluorescence with excitation at 296 nm and emission at 340 nm. Identification and quantification of tocopherol compounds was achieved by comparison with the retention times and peaks areas of standards purchased from Merck (tocopherol set Calbiochem #613424). A daily calibration curve was carried out using a tocopherol solution with a concentration range between 0.31 and 5 μg ml^{-1} for each isoform.

Fine mapping of the tocopherol $QTL_{9\text{-}2\text{-}6}$. Flowering plants from the *S. lycopersicum* cv. M82 and from the IL9-2-6 were crossed. F1 hybrid was selfed and 190 F2 and 50 F3 plants were screened with five codominants molecular markers distributed along the introgression: PCR-markers C2_At3g63190 and C2_At2g47890, and the CAP-marker C2_At4g02580 were obtained from http://solgenomics.net. VTE3(1)INDEL (Chr.9: 59.6 Mb) and 1531800 (Chr.9: 61.0 Mb) markers were designed based on InDels identified between *S. lycopersicum* and *S. pennellii VTE3*(1) allele's sequences and a flanking region, respectively. An F2 plant recombinant between C2_At4g02580 and 1531800 markers was selfed and the homozygous lines IL9-2-6-1 was selected from the F3 population. Primer sequences are listed in Supplementary Table 2.

***VTE3*(1) subcellular localization.** The full lenght cDNA of both alleles of *VTE3*(1) was amplified by PCR using Taq Platinum Pfx DNA polymerase (Invitrogen) and cloned into the binary vector pK7FWG2 by recombination using LR clonase (Invitrogen) resulting in a C-terminal green fluorescent protein (GFP) fusion protein (pK7FWG2-VTE3(1)). Primer sequences are listed in Supplementary Table 2. Transient expression via *Agrobacterium tumefaciens* and confocal microscopy examination were performed as has been previously described[46].

Virus-induced gene silencing of *VTE3*(1). Construct, infiltration and fruit harvesting procedures were performed as has been previously described[19]. Briefly, a 349-bp fragment of the *VTE3(1)* gene (Solyc09g065730) was amplified from tomato leaves cDNA (primer sequences are listed in Supplementary Table 2) and cloned into the pTOPO 2.1 vector (Invitrogen) giving rise to the pTOPO-VTE3.1 vector. pTOPO-*gfp*380 (ref. 19) and pTOPO-VTE3.1 vectors were digested with EcoRI restriction enzyme (NEB) and ligated at room temparature for 2 h using 0.4 unit of T4 DNA Ligase (NEB). Ligation products were subsequently amplified by PCR and a 729 bp PCR product were inserted into the pCR8/GW/TOPO vector (Invitrogen). The resulting vectors were recombined into the pTRV2-GW vector[19]. pTRV1, pTRV2-GFP[19] and pTRV2-GFP-VTE3(1) were introduced into *Agrobacterium tumefaciens* strain GV3101. A 5-ml culture was grown overnight at 28 °C in 50 mg l^{-1} gentamycin and 50 mg l^{-1} kanamycin in LB medium and used to inoculate 50 ml of LB medium containing the same antibiotics. After an overnight culture at 28 °C, cells were harvested by centrifugation and resuspended in infiltration media (10 mM $MgCl_2$, 10 mM MES and 200 mM acetosyringone), adjusted to an OD600 of 1.0, and left at room temperature for 4 h. Equivalent aliquots of GV3101-pTRV1 and -pTRV2 were mixed immediately before inoculation. One week preanthesis inflorescence peduncles of 8-week-old tomato plants were wounded with a needle (27 G ½ inches) and approximately 40 μl of the *Agrobacterium* suspension was delivered. Pericarp tissue from MG and ripe fruits were harvested 42 and 60 days after infiltration, respectively. All samples were immediately frozen in liquid N_2 and stored at −80 °C until use.

RNA isolation and qPCR analysis. Total RNA was extracted from 50 mg and 100 mg of frozen leaves and fruit pericarps, respectively, with TRIZOL reagent (Invitrogen) according to the manufacturer's instructions. DNA traces were removed by treatment with amplification-grade DNAse I (Invitrogen) following the manufacturer's instructions. cDNA was synthesized from 1 μg of total RNA using random primers and the SuperScript III enzyme (Invitrogen) in a final volume of 20 μl. Reactions were carried out in duplicate using 2X SYBR Green Master Mix reagent (Applied Biosystems) in a 20 μl final volume and a 7500 real-time PCR system (Applied Biosystems). Primers used for gene expression analysis of *VTE3*(1) and the 19 selected ORFs spanning on the IL9-2-6-1 introgressed fragment are listed in Supplementary Table 2. Primer sequences for VTE biosynthetic pathway enzymes encoding genes were as previously described[24] and are included in Supplementary Table 2.

Gas chromatography-mass spectrometry. Metabolites extraction and quantification was performed exactly as described before[19]. Briefly, tomato frozen tissues (~ 250 mg) were extracted with 2000 μl of methanol and 120 μl of internal standard (0.2 mg ml^{-1} water of ribitol) was added for quantification. The mixture was extracted for 15 min at 70 °C, mixed vigorously with one volume of water, centrifuged at 2,200 *g* and subsequently reduced to dryness under vacuum. The residue was redissolved and derivatized for 120 min at 37 °C (in 60 μl of 30 mg ml^{-1} methoxyamine hydrochloride in pyridine) followed by a 30-min treatment at 37 °C with 120 μl of *N*-methyl-*N*-[trimethylsilyl] trifluoroacetamide. Sample volumes of 1 μl were then injected in splitless and split modes, using a hot needle technique. The gas chromatography–time-of-flight–mass spectrometry (GC-tof-MS) system was composed of an AS 2000 autosampler, a GC 6890N gas chromatographer (Agilent Technologies, USA), and a Pegasus III time-of-flight mass spectrometer (LECO Instruments, USA). Mass spectra were recorded at 20 scans s^{-1} with a scanning range of 70 to 600 m/z. Both chromatograms and mass spectra were evaluated using ChromaTOF chromatography processing and mass spectral deconvolution software, version 3.00 (LECO Instruments, USA). Identification and quantification of the compounds were performed with TagFinder 4.0 software[47] and the mass spectra were cross referenced with those in the Golm Metabolome Database[48,49]. Six biological replicates were used for this analysis.

Promoter sequence analyses. *In silico* CRE identification was performed as indicated[24]. TEs were identified by WU-BLAST (v4.0.3 version) with RepeatMasker[50] against the Solanacea database.

McrBC-based methylation assay. Genomic DNA was extracted from 100 mg of tomato fruits by PhytoPure kit (GE Healthcare). A quantity of 1 μg of DNA was digested for 3 h with 10 U of McrBC enzyme (NEB) in parallel with a mock reaction. 50 ng of digested DNA was further used for 28 cycles PCR amplifications in 1X reaction buffer with 0.75 mM MgCl2, 0.1 μM dNTPs, 0.4 μM primer concentration and 1 unit of Platinum TAQ DNA polymerase (Invitrogen). Cycling conditions were: 15 s 94 °C, 1 min 55 °C and 1 min 72 °C. Primer sequences are listed in Supplementary Table 2.

Bisulphite analysis. Bisulphite treatment was performed on 200 ng of genomic DNA using the EZ DNA Methylation-Gold Kit (Zymo Reseacrh). The treated DNA was amplified by nested PCR using the primers listed in the Supplementary Table 2. Amplified fragments were cloned into pGEM-T vector (Promega) for sequencing. At least nine clones of each genotype were sequenced. The bisulphite conversion efficiency was calculated by analysing a chloroplast loci[51] indicating a conversion rate greater than 99%.

siRNA analysis. Small RNAs from ripe fruits were extracted using mirVana Kit (Ambion) according to the manufacturer's instructions. RNA libraries were multiplexed and sequenced on a HiSeq2500 system (Illumina) obtaining

© 2014 Macmillan Publishers Limited. All rights reserved.

~12 million of high quality reads per library. After clipping with fastx_clipper (FASTX-Toolkit), reads were mapped without mismatches to the reference sequences of *S. lycopersicum* and *S. pennellii VTE3*(1) *loci* using bowtie2 software[52]. Mapping visualization were carried on using Integrative Genomics Viewer (IGV)[53]. Small RNA sequence information is provided in Supplementary Table 3.

***VTE3(1)* promoter activity assay.** A promoter region of approximately 1000 bp from the two *VTE3(1)* alleles was cloned into the MCS upstream of the firefly luciferase (LUC) in the vector pGreenII 0800-LUC harbouring the *Renilla* luciferase (REN) gene under the control of the 35S promoter[54], transformed into *Agrobacterium tumefaciens* cells (GV3101 strain) and infiltrated in fully expanded leaves of *Nicotiana benthamiana* adult plants. After 2 days, leaves were harvested and measured for LUC and REN activities by using the Dual-Luciferase Reporter Assay System (Promega).

References

1. Fridman, E., Carrari, F., Liu, Y.-S., Fernie, A. R. & Zamir, D. Zooming in on a quantitative trait for tomato yield using interspecific introgressions. *Science* **305,** 1786–1789 (2004).
2. Fernie, A. R., Tadmor, Y. & Zamir, D. Natural genetic variation for improving crop quality. *Curr. Opin. Plant Biol.* **9,** 196–202 (2006).
3. Gilliland, L. U. *et al.* Genetic basis for natural variation in seed vitamin E levels in *Arabidopsis thaliana*. *Proc. Natl Acad. Sci. USA* **103,** 18834–18841 (2006).
4. Klee, H. J. & Giovannoni, J. J. Genetics and control of tomato fruit ripening and quality attributes. *Annu. Rev. Genet.* **45,** 41–59 (2011).
5. Moose, S. P., Dudley, J. W. & Rocheford, T. R. Maize selection passes the century mark: a unique resource for 21st century genomics. *Trends Plant Sci.* **9,** 358–364 (2004).
6. Mène-Saffrané, L. & DellaPenna, D. Biosynthesis, regulation and functions of tocochromanols in plants. *Plant Physiol. Biochem.* **48,** 301–309 (2010).
7. Fitzpatrick, T. B. *et al.* Vitamin deficiencies in humans: can plant science help? *Plant Cell* **24,** 395–414 (2012).
8. DellaPenna, D. & Pogson, B. J. Vitamin synthesis in plants: tocopherols and carotenoids. *Annu. Rev. Plant Biol.* **57,** 711–738 (2006).
9. Almeida, J. *et al.* Genetic dissection of vitamin E biosynthesis in tomato. *J. Exp. Bot.* **62,** 3781–3798 (2011).
10. Sattler, S. E. *et al.* Nonenzymatic lipid peroxidation reprograms gene expression and activates defense markers in *Arabidopsis* tocopherol-deficient mutants. *Plant Cell* **18,** 3706–3720 (2006).
11. Maeda, H. & DellaPenna, D. Tocopherol functions in photosynthetic organisms. *Curr. Opin. Plant Biol.* **10,** 260–265 (2007).
12. Chander, S. *et al.* Genetic dissection of tocopherol content and composition in maize grain using quantitative trait loci analysis and the candidate gene approach. *Mol. Breed* **22,** 353–365 (2008).
13. Tang, S., Hass, C. G. & Knapp, S. J. Ty3/gypsy-like retrotransposon knockout of a 2-methyl-6-phytyl-1,4-benzoquinone methyltransferase is non-lethal, uncovers a cryptic paralogous mutation, and produces novel tocopherol (vitamin E) profiles in sunflower. *Theor. Appl. Genet.* **113,** 783–799 (2006).
14. Shutu, X. *et al.* Dissecting tocopherols content in maize (Zea mays L.), using two segregating populations and high-density single nucleotide polymorphism markers. *BMC Plant Biol.* **12,** 201 (2012).
15. Li, H. *et al.* Identification of QTL underlying vitamin E contents in soybean seed among multiple environments. *Theor. Appl. Genet.* **120,** 1405–1413 (2010).
16. Schauer, N. *et al.* Mode of inheritance of primary metabolic traits in tomato. *Plant Cell* **20,** 509–523 (2008).
17. Thimm, O. *et al.* MAPMAN: a user-driven tool to display genomics data sets onto diagrams of metabolic pathways and other biological processes. *Plant J.* **37,** 914–939 (2004).
18. Cheng, Z. *et al.* Highly divergent methyltransferases catalyze a conserved reaction in tocopherol and plastoquinone synthesis in cyanobacteria and photosynthetic eukaryotes. *Plant Cell* **15,** 2343–2356 (2003).
19. Quadrana, L. *et al.* Coupling virus-induced gene silencing to exogenous green fluorescence protein expression provides a highly efficient system for functional genomics in *Arabidopsis* and across all stages of tomato fruit development. *Plant Physiol.* **156,** 1278–1291 (2011).
20. Baroli, I. & Niyogi, K. K. Molecular genetics of xanthophyll-dependent photoprotection in green algae and plants. *Philos. Trans. R. Soc. London* **355,** 1385–1394 (2000).
21. Woitsch, S. & Römer, S. Impact and interaction of lipophilic antioxidants in mutants and transgenic plants. *J. Plant Physiol.* **162,** 1197–1209 (2005).
22. Demmig-Adams, B. & Adams, W. W. Antioxidants in photosynthesis and human nutrition. *Science* **298,** 2149–2153 (2002).
23. Obayashi, T., Hayashi, S., Saeki, M., Ohta, H. & Kinoshita, K. ATTED-II provides coexpressed gene networks for *Arabidopsis*. *Nucleic Acids Res.* **37,** D987–D991 (2009).
24. Quadrana, L. *et al.* Transcriptional regulation of tocopherol biosynthesis in tomato. *Plant Mol. Biol.* **81,** 309–325 (2013).
25. The Potato Consortium. Genome sequence and analysis of the tuber crop potato. *Nature* **475,** 189–195 (2011).
26. Shankar, R. & Jurjka, J. A SINE consensus sequence from *Solanum demissum*. *Repbase Reports* **6,** 506–506 (2006).
27. Zhang, H. & Zhu, J. RNA-directed DNA methylation. *Curr. Opin. Plant Biol.* **14,** 142–147 (2011).
28. Arteaga-vazquez, M., Sidorenko, L., Rabanal, F. A., Shrivistava, R. & Nobuta, K. RNA-mediated trans -communication can establish paramutation at the b1 locus in maize. *Proc. Natl Acad. Sci. USA* **107,** 12986–12991 (2010).
29. Kamenetzky, L. *et al.* Genomic analysis of wild tomato introgressions determining metabolism- and yield-associated traits. *Plant Physiol.* **152,** 1772–1786 (2010).
30. Cubillos, F. A., Coustham, V. & Loudet, O. Lessons from eQTL mapping studies: non-coding regions and their role behind natural phenotypic variation in plants. *Curr. Opin. Plant Biol.* **15,** 192–198 (2012).
31. Ronen, G., Carmel-goren, L., Zamir, D. & Hirschberg, J. An alternative pathway to b-carotene formation in plant chromoplasts discovered by map-based cloning of Beta and old-gold color mutations in tomato. *Proc. Natl Acad. Sci. USA* **97,** 11102–11107 (2000).
32. Chapman, N. H. *et al.* High-resolution mapping of a fruit firmness-related quantitative trait locus in tomato reveals epistatic interactions associated with a complex combinatorial locus. *Plant Physiol.* **159,** 1644–1657 (2012).
33. Goulet, C. *et al.* Role of an esterase in flavor volatile variation within the tomato clade. *Proc. Natl Acad. Sci. USA* **109,** 19009–19014 (2012).
34. Cubas, P., Vincent, C. & Coen, E. An epigenetic mutation responsible for natural variation in floral symmetry. *Nature* **401,** 157–161 (1999).
35. Martin, A. *et al.* A transposon-induced epigenetic change leads to sex determination in melon. *Nature* **461,** 1135–1138 (2009).
36. Miura, K. *et al.* A metastable DWARF1 epigenetic mutant affecting plant stature in rice. *Proc. Natl Acad. Sci. USA* **106,** 11218–11223 (2009).
37. Manning, K. *et al.* A naturally occurring epigenetic mutation in a gene encoding an SBP-box transcription factor inhibits tomato fruit ripening. *Nat. Genet.* **38,** 948–952 (2006).
38. Zhong, S. *et al.* Single-base resolution methylomes of tomato fruit development reveal epigenome modifications associated with ripening. *Nat. Biotechnol.* **31,** 154–159 (2013).
39. Becker, C. *et al.* Spontaneous epigenetic variation in the *Arabidopsis thaliana* methylome. *Nature* **480,** 245–252 (2011).
40. Schmitz, R. J. *et al.* Transgenerational epigenetic instability is a source of novel methylation variants. *Science* **334,** 369–373 (2011).
41. Silveira, A. B. *et al.* Extensive natural epigenetic variation at a de novo originated gene. *PLoS Genet.* **9,** e1003437 (2013).
42. Cortijo, S. *et al.* Mapping the epigenetic basis of complex traits. *Science* **343,** 1145–1148 (2014).
43. Durand, S., Bouché, N., Perez Strand, E., Loudet, O. & Camilleri, C. Rapid establishment of genetic incompatibility through natural epigenetic variation. *Curr. Biol.* **22,** 326–331 (2012).
44. Fujimoto, R. *et al.* Evolution and control of imprinted FWA genes in the genus Arabidopsis. *PLoS Genet.* **4,** e1000048 (2008).
45. Wang, X., Weigel, D. & Smith, L. M. Transposon variants and their effects on gene expression in *Arabidopsis*. *PLoS Genet.* **9,** e1003255 (2013).
46. De Godoy, F. *et al.* Galacturonosyltransferase 4 silencing alters pectin composition and carbon partitioning in tomato. *J. Exp. Bot.* **64,** 2449–2466 (2013).
47. Luedemann, A., Strassburg, K., Erban, A. & Kopka, J. TagFinder for the quantitative analysis of gas chromatography-mass spectrometry (GC–MS)-based metabolite profiling experiments. *Bioinformatics* **24,** 732–737 (2008).
48. Kopka, J. *et al.* GMD@CSB.DB: the Golm Metabolome Database. *Bioinformatics* **21,** 1635–1638 (2005).
49. Schauer, N. *et al.* GC–MS libraries for the rapid identification of metabolites in complex biological samples. *FEBS Lett.* **579,** 1332–1337 (2005).
50. Tarailo-Graovac, M. & Chen, N. Using RepeatMasker to identify repetitive elements in genomic sequences. *Curr. Protoc. Bioinformatics* **25,** 1–14 (2009).
51. Catoni, M., Lucioli, A., Doblas-Ibáñez, P., Accotto, G. & Vaira, A. From immunity to susceptibility: virus resistance induced in tomato by a silenced transgene is lost as TGS overcomes PTGS. *Plant J.* **75,** 941–953 (2013).
52. Langmead, B. & Salzberg, S. L. Fast gapped-read alignment with Bowtie 2. *Nat. Methods* **9,** 357–359 (2012).
53. Robinson, J. T. *et al.* Integrative genomics viewer. *Nat. Biotechnol.* **29,** 24–26 (2011).
54. Hellens, R. P. *et al.* Transient expression vectors for functional genomics, quantification of promoter activity and RNA silencing in plants. *Plant Methods* **1,** 1–14 (2005).

Acknowledgements

L.Q. was recipient of a fellowship of Agencia Nacional de Promoción Científica y Tecnológica and Consejo Nacional de Investigaciones Científicas y Técnicas in Argentina

© 2014 Macmillan Publishers Limited. All rights reserved.

and supported by a postdoctral fellowship from Investissements d'Avenir ANR-10-LABX-54 MEMO LIFE in France. J.A. and L.B. were recipients of a fellowship of Fundação à Amparo da Pesquisa do Estado de São Paulo (Brazil). J.V.C.d.S. was recipient of a fellowship of Conselho Nacional de Desenvolvimento Científico e Tecnológico (Brazil). R.A., L.B. and F.C. are members of Consejo Nacional de Investigaciones Científicas y Técnicas (Argentina). This work was carried out in compliance with current laws governing genetic experimentation in Brazil and in Argentina. This work was supported with grants from Instituto Nacional de Tecnologia Agropecuária, Consejo Nacional de Investigaciones Científicas y Técnicas and Agencia Nacional de Promoción Científica y Tecnológica (Argentina), Fundação à Amparo da Pesquisa do Estado de São Paulo, Conselho Nacional de Desenvolvimento Científico e Tecnológico and Universidade de São Paulo (Brazil); Max Planck Society (Germany); the Agence Nationale de la Recherche (Investissements d'Avenir ANR-10-LABX-54 MEMO LIFE and ANR-11-IDEX-0001-02 PSL* Research University to V.C.); and the European Union (EpiGeneSys FP7 Network of Excellence number 257082 to V.C. and the European Solanaceae Integrated Project FOOD-CT-2006-016214 to F.C., M.R. and A.R.F.).

Author contributions

L.Q. designed and performed experiments, analysed data and wrote the paper. J.A. performed experiments and analysed data. T.D. performed *in silico* analyses. R.A., P.G.D., L.B., G.C. and J.V.C.d.S participated with technical tasks. I.E.P. conducted field trials. S.A. and V.C. discussed the results. A.R.F discussed the results and wrote the paper. M.R. and F.C. supervised the project, designed experiments and wrote the paper.

Additional information

Accession codes. The siRNA sequencing data have been deposited in the ENA short read archive under project number PRJEB6247 and accessions codes ERR493820 to 93826.

Supplementary Information accompanies this paper at http://www.nature.com/naturecommunications

Competing financial interests: The authors declare no competing financial interests.

Reprints and permission information is available online at http://npg.nature.com/reprintsandpermissions/

How to cite this article: Quadrana, L. *et al.* Natural occurring epialleles determine vitamin E accumulation in tomato fruits. *Nat. Commun.* 5:4027 doi: 10.1038/ncomms5027 (2014).

© 2014 **Macmillan Publishers Limited. All rights reserved.**

ANEXO III

Anexo III – Primers utilizados nos estudos funcionais.

Experimento	Iniciador	Direto (5'→3') Reverso (5'→3')	Temperatura ºC	Fragmento pb
Síntese de cDNA	ActinaUp ActinaLow	TGGCATCATACCTTTTACAA TCCGGGCATCTGAACCCTCT	55	812 (gDNA) 521 (cDNA)
Sequenciamento vetor TOPO	M13F M13R	GTAAAACGACGGCCAG CAGGAAACAGCTATGAC	55	-
VIGS	TRVF TRVR	ATGTTCAGGCGGTTCTTGTGTG ATGTCAATCTCGTAGGTTTA	55	-
VIGS	VIGS-CLH(1)-F VIGS-CLH(1)-R	GGTAGACTTGCTAGTGACCTG ACATTCGTTGTAGAAATCGC	57	240
VIGS	VIGS-FOLK-F VIGS-FOLK-R	GATCCCTATCGTCTCTTCTCCA CAGCAGAGCATGAAGACTAGC	60	275
VIGS	VIGS-VTE5-F VIGS-VTE5-R	GAAGAAGGTTTGGGTCCAC CAGAAATGTTATCGTCTACCATTCC	56	237
VIGS	GFP-F	GGTAAAGGAGAAGAACTT	55	-
Localização subcelular	FUS-CLH(1)F FUS-CLH(1)R	CACCATGGTCATAACTAGTACTTCCTCTG GACAAGAAAATCAATATCTTGGAGC	53	936
RNAi	RNAi-CLH(1)F RNAi-CLH(1)R	CACCGGTAGACTTGCTAGTGACCTG CAATACTGGGAAGTTTCCTGC	53,5	168
Localização Subcellular/ RNAi	35SRight 35SLeft	5'-CCCACTATCCTTCGCAAG-3' 5'-GCAGGTCACTGGATTTTGG-3'	55	-
Localização Subcellular	Egfp	5'-CTTGTGGCCGTTTACGTCGC-3'	55	-

ANEXO IV

Table S1. Expression profile of genes involved in the methyl erythritol phosphate (red), shikimate (green), tocopherol biosynthetic (blue), carotenoid biosynthetic (orange), chlorophyll metabolic (grey) and phytol recycling (white) pathways.

	Mature green						Ripe					
	MT	MT-*nor*	MT-*rin*	MT-*gf*	MT-*l*	MT-*jai*	MT	MT-*nor*	MT-*rin*	MT-*gf*	MT-*l*	MT-*jai*
DXS(1)	1.00 ± 0.05 a	0.79 ± 0.09 *a	0.69 ± 0.05 *a	0.54 ± 0.06 *a	1.23 ± 0.12 *a	0.93 ± 0.07 a	1.42 ± 0.27 b	1.03 ± 0.1 b	0.71 ± 0.06 *a	1.16 ± 0.13 b	2.01 ± 0.30 b	1.84 ± 0.37 b
ISPE	1.00 ± 0.14 a	0.79 ± 0.05 a	0.70 ± 0.28 a	0.94 ± 0.05 a	1.26 ± 0.12 a	0.45 ± 0.06 *a	1.23 ± 0.15 a	0.33 ± 0.2 *b	0.31 ± 0.04 *a	1.27 ± 0.14 b	1.24 ± 0.33 a	1.43 ± 0.16 b
GGDR	1.00 ± 0.06 a	0.83 ± 0.11 *a	0.59 ± 0.12 *a	0.58 ± 0.08 *a	1.16 ± 0.11 a	1.10 ± 0.09 a	0.45 ± 0.10 b	1.28 ± 0.3 *a	1.29 ± 0.21 *b	1.07 ± 0.24 *b	0.30 ± 0.04 b	0.57 ± 0.10 b
ADH(1)	1.00 ± 0.17 a	1.87 ± 0.18 *a	1.00 ± 0.02 a	1.22 ± 0.15 a	1.32 ± 0.37 a	1.34 ± 0.16 a	0.67 ± 0.11 a	0.97 ± 0.2 b	1.01 ± 0.13 *a	0.67 ± 0.05 b	0.61 ± 0.11 b	0.85 ± 0.25 b
ADH(2)	1.00 ± 0.10 a	7.01 ± 0.03 *a	3.49 ± 0.08 *a	1.56 ± 0.07 a	0.37 ± 0.16 a	1.45 ± 0.07 a	0.36 ± 0.03 b	1.38 ± 0.1 *b	0.54 ± 0.08 b	0.11 ± 0.04 *b	0.25 ± 0.05 a	0.51 ± 0.07 b
TAT(1)	1.00 ± 0.39 a	0.56 ± 0.13 a	0.73 ± 0.16 a	0.35 ± 0.06 *a	1.31 ± 0.42 a	2.39 ± 0.53 *a	9.43 ± 2.05 b	4.72 ± 1.8 b	2.68 ± 0.11 *b	7.01 ± 0.45 b	5.54 ± 0.37 b	16.70 ± 3.87 b
TAT(2)	1.00 ± 0.21 a	1.04 ± 0.04 a	0.75 ± 0.02 a	0.61 ± 0.12 a	0.98 ± 0.18 a	0.60 ± 0.14 a	0.07 ± 0.01 b	0.14 ± 0.0 *b	0.15 ± 0.02 *b	0.10 ± 0.03 b	0.05 ± 0.01 b	0.07 ± 0.01 b
HPPD(1)	1.00 ± 0.07 a	0.61 ± 0.06 *a	0.70 ± 0.01 *a	0.83 ± 0.05 *a	1.03 ± 0.12 a	0.95 ± 0.02 a	0.71 ± 0.06 b	0.60 ± 0.1 a	0.50 ± 0.05 *b	0.75 ± 0.04 a	0.64 ± 0.03 b	0.78 ± 0.07 b
HPPD(2)	1.00 ± 0.09 a	0.37 ± 0.06 *a	0.52 ± 0.02 *a	0.93 ± 0.05 a	0.99 ± 0.18 a	1.00 ± 0.18 a	0.51 ± 0.09 b	0.26 ± 0.0 *a	0.63 ± 0.10 a	0.37 ± 0.01 b	0.50 ± 0.08 b	0.44 ± 0.07 b
VTE1	1.00 ± 0.03 a	0.89 ± 0.05 a	0.83 ± 0.05 *a	0.82 ± 0.09 a	1.02 ± 0.07 a	1.17 ± 0.06 *a	0.55 ± 0.06 b	0.94 ± 0.0 *a	0.60 ± 0.01 b	0.88 ± 0.07 *a	0.65 ± 0.04 b	0.65 ± 0.04 b
VTE2	1.00 ± 0.10 a	0.74 ± 0.05 a	0.85 ± 0.05 a	0.85 ± 0.03 a	1.08 ± 0.07 a	1.36 ± 0.16 a	1.40 ± 0.17 a	1.19 ± 0.1 b	0.51 ± 0.04 *b	1.32 ± 0.05 b	1.61 ± 0.21 b	1.14 ± 0.12 a
VTE3(1)	1.00 ± 0.05 a	0.96 ± 0.06 a	0.79 ± 0.01 *a	0.83 ± 0.10 *a	1.06 ± 0.06 a	1.01 ± 0.04 a	0.55 ± 0.05 b	0.52 ± 0.0 b	0.52 ± 0.07 b	0.61 ± 0.06 b	0.49 ± 0.04 b	0.58 ± 0.03 b
VTE3(2)	1.00 ± 0.04 a	0.93 ± 0.03 a	0.85 ± 0.03 *a	0.76 ± 0.06 *a	1.13 ± 0.04 *a	1.03 ± 0.04 a	0.59 ± 0.07 b	0.94 ± 0.1 *a	0.70 ± 0.05 b	0.74 ± 0.08 a	0.50 ± 0.04 b	0.71 ± 0.04 b
VTE4	1.00 ± 0.09 a	0.66 ± 0.01 *a	1.00 ± 0.06 a	0.91 ± 0.08 a	1.15 ± 0.06 a	0.81 ± 0.05 a	0.28 ± 0.03 b	0.37 ± 0.0 b	0.48 ± 0.07 *b	0.74 ± 0.09 *a	0.28 ± 0.02 b	0.44 ± 0.04 *b
PDS	1.00 ± 0.05 a	0.66 ± 0.04 *a	0.59 ± 0.13 *a	0.59 ± 0.03 *a	1.24 ± 0.07 *a	0.79 ± 0.07 a	2.39 ± 0.25 b	1.54 ± 0.2 *b	1.48 ± 0.20 *b	2.43 ± 0.13 b	2.16 ± 0.14 b	3.34 ± 0.46 b
PSY(1)	1.00 ± 0.47 a	0.35 ± 0.03 *a	0.54 ± 0.03 a	0.77 ± 0.14 a	0.71 ± 0.32 a	0.67 ± 0.14 a	11.30 ± 0.78 b	1.86 ± 0.2 *b	0.90 ± 0.19 *b	10.06 ± 0.74 b	12.64 ± 1.54 b	13.02 ± 3.66 b
PSY(2)	1.00 ± 0.16 a	0.60 ± 0.02 *a	0.68 ± 0.09 *a	0.92 ± 0.03 a	1.28 ± 0.09 a	1.04 ± 0.13 a	0.90 ± 0.10 a	0.68 ± 0.1 a	1.23 ± 0.12 *b	0.95 ± 0.05 a	0.81 ± 0.10 b	1.09 ± 0.11 a
CYCβ	1.00 ± 0.15 a	1.26 ± 0.02 a	1.12 ± 0.16 a	0.94 ± 0.04 a	1.28 ± 0.23 a	1.61 ± 0.14 *a	0.69 ± 0.11 b	1.05 ± 0.1 *a	2.28 ± 0.37 *b	0.69 ± 0.14 b	1.03 ± 0.13 *a	0.67 ± 0.17 b
LCYβ	1.00 ± 0.10 a	0.80 ± 0.03 a	0.62 ± 0.08 *a	0.68 ± 0.07 *a	1.07 ± 0.16 a	0.93 ± 0.07 a	0.27 ± 0.03 b	0.57 ± 0.1 *b	0.40 ± 0.08 *b	0.32 ± 0.04 b	0.24 ± 0.05 b	0.35 ± 0.07 b
CHLG	1.00 ± 0.04 a	0.79 ± 0.01 *a	0.67 ± 0.03 *a	0.61 ± 0.02 *a	1.13 ± 0.15 a	1.09 ± 0.03 a	0.90 ± 0.10 a	0.74 ± 0.0 a	0.51 ± 0.02 *b	1.22 ± 0.14 *b	0.83 ± 0.09 a	0.94 ± 0.05 b
CLH(1)	1.00 ± 0.12 a	1.09 ± 0.20 a	1.22 ± 0.06 *a	1.28 ± 0.13 a	1.40 ± 0.17 *a	1.42 ± 0.10 *a	0.12 ± 0.03 b	0.43 ± 0.1 *b	1.19 ± 0.23 *a	0.27 ± 0.03 *b	0.12 ± 0.01 b	0.20 ± 0.03 *b
CLH(4)	1.00 ± 0.39 a	1.04 ± 0.10 a	0.77 ± 0.04 a	0.72 ± 0.07 a	1.58 ± 0.30 a	1.14 ± 0.26 a	3.07 ± 0.61 b	1.96 ± 0.8 a	0.53 ± 0.08 *b	1.96 ± 0.12 *b	1.55 ± 0.15 *a	1.90 ± 0.50 *a
PPH	1.00 ± 0.08 a	0.82 ± 0.09 a	0.83 ± 0.04 *a	0.78 ± 0.06 *a	1.47 ± 0.12 *a	0.80 ± 0.08 *a	2.56 ± 0.42 b	2.14 ± 0.5 b	1.55 ± 0.18 *b	2.90 ± 0.22 b	2.02 ± 0.09 b	3.52 ± 0.56 b
PAO	1.00 ± 0.16 a	0.65 ± 0.06 *a	0.95 ± 0.10 a	0.82 ± 0.05 a	1.61 ± 0.24 *a	1.17 ± 0.10 a	2.33 ± 0.12 b	1.30 ± 0.1 *b	1.47 ± 0.13 *b	2.36 ± 0.08 b	2.54 ± 0.06 b	2.32 ± 0.06 b
VTE5	1.00 ± 0.08 a	0.71 ± 0.10 *a	0.73 ± 0.09 *a	0.74 ± 0.10 *a	1.25 ± 0.14 a	0.95 ± 0.09 a	0.32 ± 0.01 b	0.42 ± 0.1 *b	0.39 ± 0.03 *b	0.27 ± 0.04 b	0.30 ± 0.02 b	0.34 ± 0.05 b

Values represent means from at least three biological replicates. Relative expression was calculated from means of two technical replicates and normalized against mature green sample from the MT wild type genotype. Statistically significant differences were determined according to a permutation test lacking assumptions of sample distribution (Pfaffl *et al.*, 2002). Different letters indicate significant differences between the two stages in the same genotype ($p < 0.05$). Asterisks denote significant differences from the corresponding stage of the MT wild type control genotype ($p < 0.05$).

Table S2. Expression ratio between ripe and mature green stages.

	MT	MT-*nor*	MT-*rin*	MT-*gf*	MT-*l*	MT-*jai*
DXS(1)	1.4	1.3	1.0	2.1	1.6	2.0
ISPE	1.0	0.4	1.0	1.3	1.0	3.2
GGDR	0.5	1.0	2.2	1.9	0.3	0.5
ADH(1)	1.0	0.5	1.0	0.5	0.5	0.6
ADH(2)	0.4	0.2	0.2	0.1	1.0	0.4
TAT(1)	9.4	8.4	3.7	19.9	4.2	7.0
TAT(2)	0.1	0.1	0.2	0.2	0.1	0.1
HPPD(1)	0.7	1.0	0.7	1.0	0.6	0.8
HPPD(2)	0.5	1.0	1.0	0.4	0.5	0.4
VTE1	0.5	1.0	0.7	1.0	0.6	0.6
VTE2	1.0	1.6	0.6	1.6	1.5	1.0
VTE3(1)	0.6	0.5	0.7	0.7	0.5	0.6
VTE3(2)	0.6	1.0	0.8	1.0	0.4	0.7
VTE4	0.3	0.6	0.5	1.0	0.2	0.5
PDS	2.4	2.3	2.5	4.1	1.7	4.2
PSY(1)	11.3	5.4	1.7	13.1	17.8	19.5
PSY(2)	1.0	1.0	1.8	1.0	0.6	1.0
CYCβ	0.7	1.0	2.0	0.7	1.0	0.4
LCYβ	0.3	0.7	0.6	0.5	0.2	0.4
CHLG	1.0	1.0	0.8	2.0	1.0	0.9
CLH(1)	0.1	0.4	1.0	0.2	0.1	0.1
CLH(4)	3.1	1.9	0.7	2.7	1.0	1.7
PPH	2.6	2.6	1.9	3.7	1.4	4.4
PAO	2.3	2.0	1.6	2.9	1.6	2.0
VTE5	0.3	0.6	0.5	0.4	0.2	0.4

Genes involved in the methyl erythritol phosphate, shikimate, tocopherol biosynthetic, carotenoid biosynthetic, chlorophyll metabolic and phytol recycling pathways are highlighted in red, green, blue, orange, grey and white, respectively. Value 1.0 represents non differences between mature green and ripe fruits stages ($p > 0.05$).

Table S3. Primers used for qPCR

Gene name	Gene symbol	Locus	Primer Sequence (Foward/Reverse)
1-deoxy-D-xylulose-5-P synthase	*DXS(1)*	Solyc01g067890	CAGGACTGGTGTGGTTTCAG GGGATAGTTCACAGTGTCC
4-(cytidine 5'-diphospho)-2-C-methyl-D-erythritol kinase	*ISPE*	Solyc01g009010	GTAATGCTGCAACAACTC GGCTTTATGAGGACCATTGG
Geranylgeranyl reductase	*GGDR*	Solyc03g115980	CAGAGACGCTCGCTAAGG GCTTCAGAGTCTGTCCGATATC
Arogenate dehydrogenase	*ADH(1)*	Solyc07g007590	CTCTGTCTCTTCTCCGTC GTTCTTGAATGAGCCAAC
	ADH(2)	Solyc09g011870	CGTGCCCAAAATAGCGACTTAAC AGCTTGTTATTGGAACATAAGAGGG
Tyrosine aminotransferase	*TAT(1)*	Solyc10g007110	CTACTGTGGGACTTCCTC CGATGTTTCTAAATGCAGCAC
	TAT(2)	Solyc07g053720	GCATCCTTCCTGCTAGAC CCTCCCACTCCTTCTCTG
4-Hydroxyphenylpyruvate dioxygenase	*HPPD(1)*	Solyc07g045050	CCAGGGCAGGGGATATACTG CTCCTTCCTCGTTTTTCAGC
	HPPD(2)	Solyc05g041200	CCAGGCGTGTGAAGAATTG CGATCTAAACAGCTCAGAG
Homogentisate phytyl transferase	*VTE2*	Solyc07g017770	CAATTCCAGTTCCTGCTGAG CCTCCAACATGCTCTTGCGTG
2-Methyl-6-phytyl-1,4-benzoquinol methyltransferase	*VTE3(1)*	Solyc09g065730	CTTGACCAATCTCCTCATC GCACGCCTTTCCTCCAGG
	VTE3(2)	Solyc03g005230	GCTAAGGCTAGGCAGAAGGAG CAGGCAACCCCACCTATGG
Tocopherol cyclase	*VTE1*	Solyc08g068570	CGAACTCCTCATAGCGGGTATC CACGCCAGTAAACCGAGGC
γ-Tocopherol C-methyl transferase	*VTE4*	Solyc08g076360	CAGATCATCGTGCTGCTCAG CCTCTCTGCTTGTACAGGAC
Phytol quinase	*VTE5*	Solyc03g071720	CGTATCAGGACGGGCTCGC TCACCACCACACATCATTGCTAATG
Chlorophyll synthase	*CHLG*	Solyc09g014760	CCAATTCCTTCAGGTGCGGT CCCACCAAGGCAAGCTGATA
Chlorophyllase	*CLH(1)*	Solyc06g053980	CATGGCTTCATTGTTGTTGCTCC GCCTGCTAGTCCAAGTTTCGTC
	CLH(4)	Solyc12g005300	ATTCCGCCTCCAACCCGACT GCAGCACAGAGTTGAGCTTCTTAGC
Pheophytinase	*PPH*	Solyc01g088090	TATGGAGGGAGCAAGTACGC TGGAGGGCAGAGGAAAAGTAC
Pheophorbide a oxygenase	*PAO*	Solyc11g066440	TCAGAAGTGGGTGATATGGA TATCCCCGTCATACACCTTA
Phytoene synthase	*PSY(1)*	Solyc03g031860	CGATGGTGCTTTGTCCGATAC CTCATCAACCCAACCGTACC
	PSY(2)	Solyc02g081330	GCATCACACATAACTCCACAAGC CGCATTCCTTCAACCATATCTCTG
Lycopene β-cyclase	*CYCβ*	Solyc06g074240	GCACCCACATCAAAGCCAGAG GCCACATGGAGAGTGGTGAAG
	LCY6	Solyc04g040190	TTGACTTAGAACCTCGTTATTGG AACAGTTCCCTTTGTCATTATCT
Phytoene desaturase	*PDS*	Solyc03g123760	CGTTCCGTGCTTCTCCGC CTAGAACATCCCTTGCCTCCAG
Clathrin adaptor complexes medium subunit	*CAC*	Solyc06g061150	CCTCCGTTGTGATGTAACTGG ATTGGTGGAAAGTAACATCATCG
Expressed unknown protein	*EXPRESSED*	Solyc07g025390	GCTAAGAACGCTGGACCTAATG TGGGTGTGCCTTTCTGAATG

Figure S1

MT

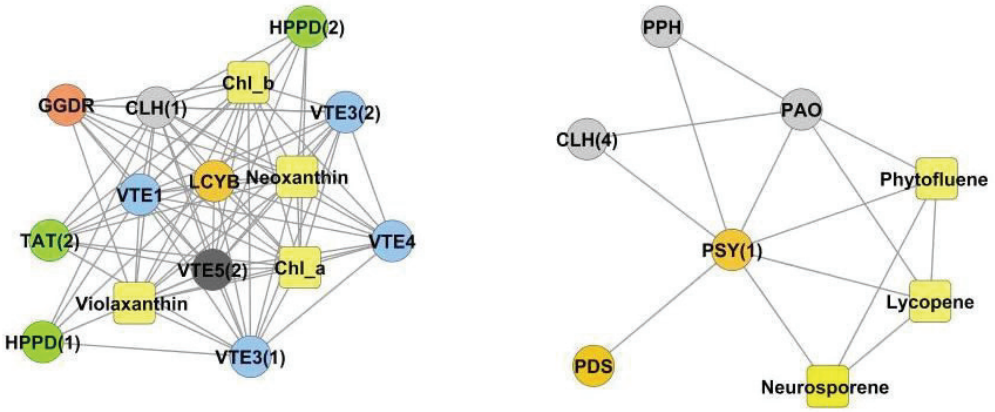

MT-*rin*

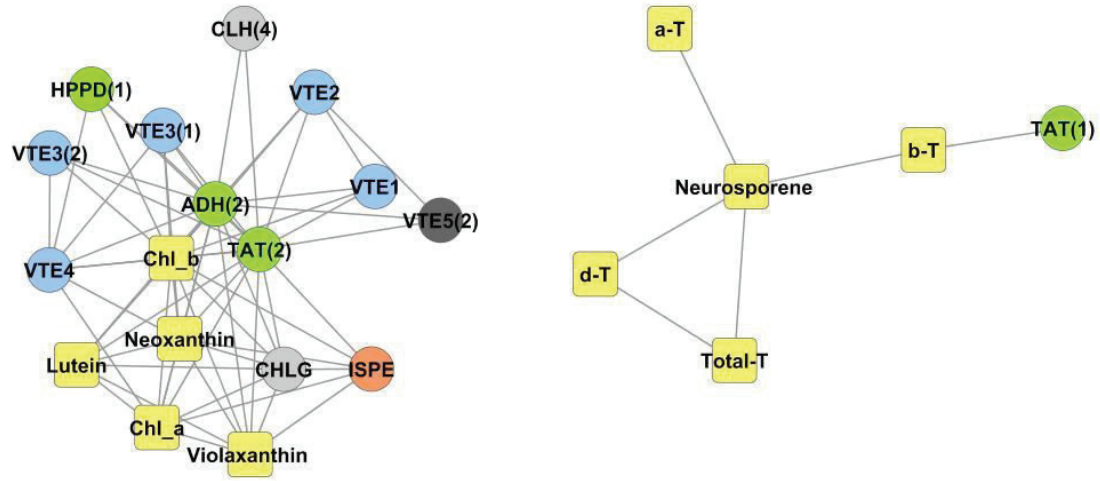

MT-*nor*

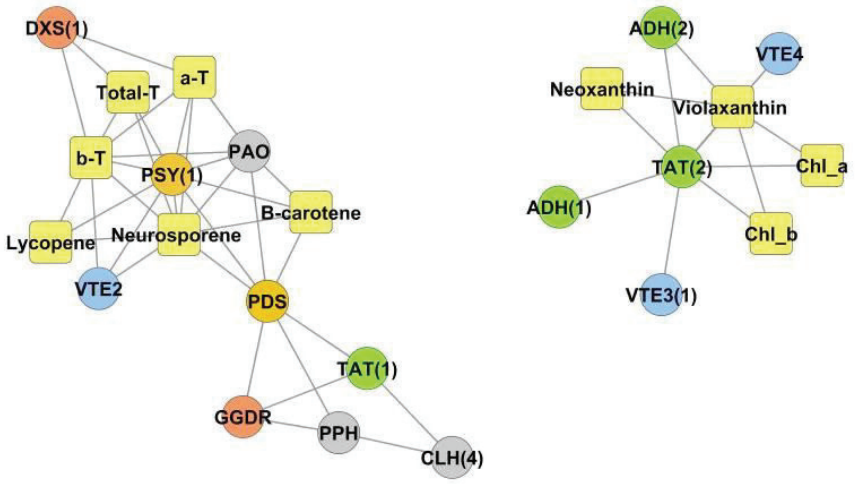

Figure S1 – *continued*

MT-*gf*

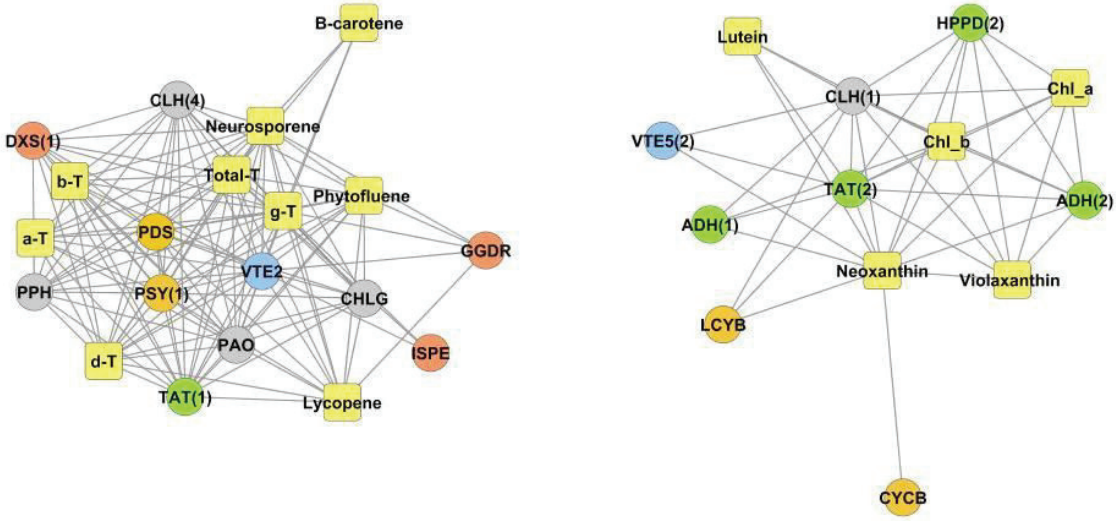

MT-*l*

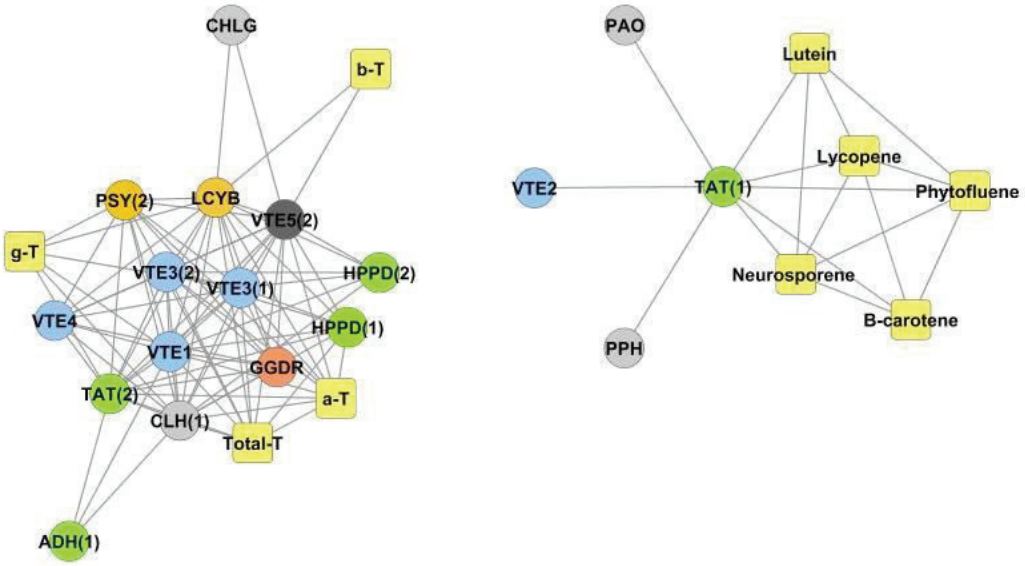
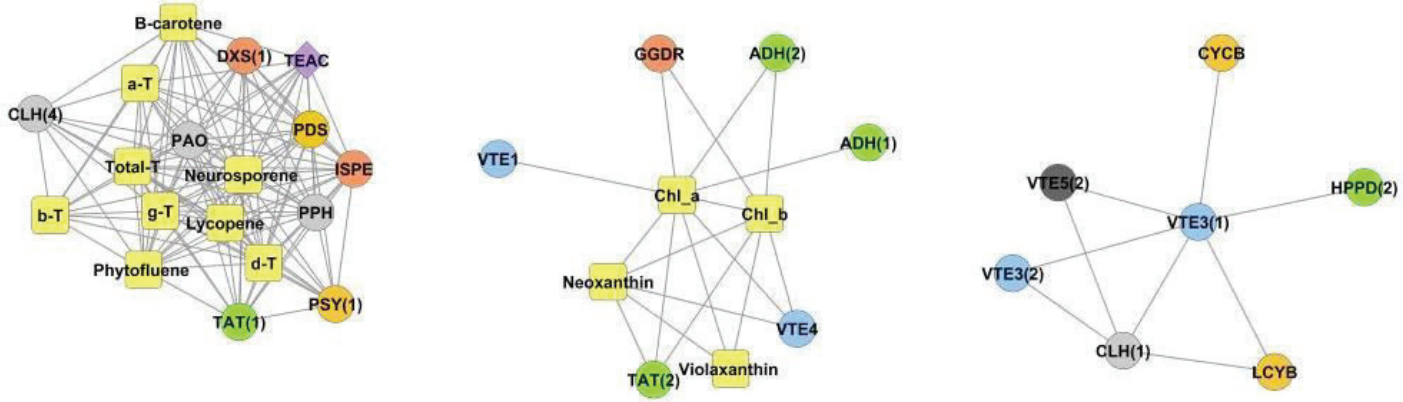
MT-*jai*